

AD/A-001 604

EVALUATION OF THE RELIABILITY AND SENSITIVITY OF  
NDT METHODS FOR TITANIUM ALLOYS

McDONNELL AIRCRAFT COMPANY

PREPARED FOR  
AIR FORCE MATERIALS LABORATORY

JUNE 1974

DISTRIBUTED BY:

**NTIS**

National Technical Information Service  
U. S. DEPARTMENT OF COMMERCE



Unclassified

Security Classification

AD/A-001604

DOCUMENT CONTROL DATA - R & D

(Security classification of title, body of abstract and indexing annotation must be entered when the overall report is classified)

1. ORIGINATING ACTIVITY (Corporate author) McDonnell Aircraft Co. St. Louis, Mo. 63166		2a. REPORT SECURITY CLASSIFICATION Unclassified	
		2b. GROUP	
3. REPORT TITLE Evaluation of the Reliability and Sensitivity of NDT Methods for Titanium Alloys			
4. DESCRIPTIVE NOTES (Type of report and inclusive dates) Final Report, 1 May 1972 to 31 January 1974			
5. AUTHOR(S) (First name, middle initial, last name) Robert J. Lord			
6. REPORT DATE June 1974		7a. TOTAL NO. OF PAGES 375	7b. NO. OF REFS 3
8a. CONTRACT OR GRANT NO. F33615-72-C-1203		9a. ORIGINATOR'S REPORT NUMBER(S) AFML-TR-73-107 Vol II	
b. PROJECT NO. 7351		9b. OTHER REPORT NO(S) (Any other numbers that may be assigned this report)	
c.			
d.			
10. DISTRIBUTION STATEMENT Approved for public release; distribution unlimited <b>PRICES SUBJECT TO CHANGE</b>			
11. SUPPLEMENTARY NOTES		12. SPONSORING MILITARY ACTIVITY Air Force Materials Laboratory Wright-Patterson AFB, Ohio 45433	
13. ABSTRACT The program objectives were to improve and to measure the detection capability of the penetrant, ultrasonic, x-ray and eddy current methods. Several penetrant inspection parameters were investigated. The minimum penetrant dwell time required to detect a variety of discontinuities was found to be 10 minutes for water washable fluorescent penetrant and 20 minutes for post-emulsifiable fluorescent penetrant. The minimum penetrant bleed-out time was 5 minutes for each. Either dry powder and nonaqueous wet developer was found to be most effective. In ultrasonic inspection, contour sound entry surfaces significantly affected inspection for radii of curvature up to 4 inches. Near surface resolution was found to be affected by test frequency and sound entry surface condition. It was also found that a significant difference in sound transmission characteristics can exist between the part to be inspected and the reference standard used when inspecting titanium bar, plate, and forgings. In radiography, penetrameters do not provide for a consistent indication of the quality of a particular radiograph with the present thickness tolerances. During the detection capability portion of the program, it was determined that surface cracks with lengths of approximately 0.050 to 0.10 inch can be detected with a high probability in a production penetrant inspection. The probability of detection can be substantially increased by following a production penetrant inspection with a production surface wave and angle beam inspection. Also, the effectiveness of ultrasonic inspection of titanium ingot, billet, and forgings can be increased by using the shear wave as well as the longitudinal wave mode. The ultrasonic method was effective in detecting Type I alpha stabilized defects in titanium ingot and billet as well as bar, plate, and forgings.			

DD FORM 1 NOV 65 1473

Security Classification

Reproduced by  
NATIONAL TECHNICAL  
INFORMATION SERVICE  
U.S. Department of Commerce  
Springfield, VA 22151

Unclassified

Security Classification

14. KEY WORDS	LINK A		LINK B		LINK C	
	ROLE	WT	ROLE	WT	ROLE	WT
Nondestructive Testing Titanium Alloys Structural and Engine Components Reliability						

ja

Security Classification

**EVALUATION OF THE RELIABILITY AND SENSITIVITY OF  
NDT METHODS FOR TITANIUM ALLOYS**

Robert J. Lord

Approved for public release; distribution unlimited

16

## FOREWORD

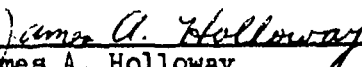
This Final Technical Report covers work performed under Contract F33615-72-C-1203 from 1 May 1972 to 31 January 1974. The work performed during the period 1 May 1972 to 28 February 1973 has previously been documented in AFML-TR-73-107. The work was performed under the direction of the Air Force Materials Laboratory, Wright-Patterson Air Force Base, Ohio, with Mr. James Holloway (AFML/LLP) as Project Engineer.

The work was performed by the McDonnell Aircraft Company, McDonnell Douglas Corporation, St. Louis, Missouri, with the Aircraft Engine Group of the General Electric Company, Evendale, Ohio, acting as major subcontractor for the program. Mr. R. J. Juergens of McDonnell Aircraft Company is the Program Manager. Mr. R. J. Lord of McDonnell Aircraft Company is the Principal Investigator of the program and Mr. H. Truscott of General Electric Company is the Principal Investigator for the engine portion of the program.

All of the items compared in this report were commercial items that were not developed or manufactured to meet Government specifications, to withstand the tests to which they were subjected, or to operate as applied during this study. Any failure to meet the objectives of this study is no reflection on any of the commercial items discussed herein or on any manufacturer.

This report was submitted by the author in March 1974.

This technical report has been reviewed and is approved for publication.

  
James A. Holloway  
Project Engineer, Mechanical Physics Branch  
Metals and Ceramics Division  
Air Force Materials Laboratory

Dr. H. M. Burte  
Chief, Metals and Ceramics Division  
Air Force Materials Laboratory

## ABSTRACT

This report describes the work conducted on a program designed to improve nondestructive testing techniques and, then, to evaluate the capability and reproducibility of the improved nondestructive testing techniques for the evaluation of discontinuities occurring in titanium. Reported are penetrant dwell times, penetrant bleed-out times, developer types, emulsification times, and water washing parameters required to effectively penetrant inspect parts which may contain a variety of crack sizes and porosity. Both post-emulsifiable and water washable fluorescent penetrants were investigated. The effect of kilovoltage on radiographic contrast sensitivity is discussed. Ultrasonic inspection of contour surfaces is reported and methods for improving near-surface resolution are documented. Methods for ultrasonic inspection of thin machined parts are reported. A full scale Ti-6Al-4V ingot was melted in a manner to intentionally produce stabilized alpha defects. Documented are the details of the ingot melting and conversion to billet, bar, and plate. Results of ultrasonic and radiographic inspections of the ingot and billets are reported. A study to determine the detection capability of various nondestructive testing methods was carried out. The capability of penetrant, ultrasonic, radiographic, and eddy current inspections to detect surface cracks, internal cracks, porosity, and alpha stabilized defects are documented.

TABLE OF CONTENTS

Section	Page
I SUMMARY . . . . .	1
II INTRODUCTION . . . . .	2
III IMPROVEMENT OF NONDESTRUCTIVE TESTING TECHNIQUES . . . . .	3
1. Penetrant Method . . . . .	3
a. Penetrant Systems . . . . .	4
b. Specimen Fabrication . . . . .	4
(1) Specimens With Tight Cracks . . . . .	5
(2) Specimens With Gross Cracks . . . . .	5
(3) Porosity Specimens . . . . .	7
c. Pre-Penetrant Drying . . . . .	8
(1) Water Washable Penetrant System . . . . .	8
(2) Post-Emulsifiable Penetrant System . . . . .	11
d. Penetrant Bleed-Out Time . . . . .	11
(1) Post-Emulsifiable Penetrant System . . . . .	12
(2) Water Washable Penetrant System . . . . .	15
e. Penetrant Dwell Time . . . . .	18
(1) Post-Emulsifiable Penetrant System . . . . .	20
(2) Water Washable Penetrant System . . . . .	23
f. Developer Effectiveness . . . . .	25
(1) Post-Emulsifiable Penetrant System . . . . .	25
(2) Water Washable Penetrant System . . . . .	28
g. Emulsification Time . . . . .	30
h. Water Washing Techniques . . . . .	35
(1) Post-Emulsifiable Penetrant System . . . . .	35
(2) Water Washable Penetrant System . . . . .	39
i. Viewing Light Intensity . . . . .	46
(1) Test Procedure . . . . .	46

Section	Page
j. Effect of Mechanical Processing Prior To Penetrant Inspection . . . . .	54
k. Penetrant System Effectiveness . . . . .	62
2. Radiographic Method . . . . .	64
a. Fabrication of Step Wedges . . . . .	64
b. Testing . . . . .	66
3. Ultrasonic Method . . . . .	77
a. Surface Curvature Compensation . . . . .	77
b. Near Surface Resolution . . . . .	103
(1) Specimen Fabrication . . . . .	103
(2) Testing of As-Received Material. . . . .	108
(3) Testing of Machined Material . . . . .	111
c. Sound Transmission Characteristics . . . . .	116
d. Effect of Surface Condition . . . . .	119
(1) Angle Beam Inspection-As-Rolled Plate . . . . .	119
(2) Straight Beam Inspection-Extrusion . . . . .	129
e. Inspection of Thin, Machined Parts . . . . .	130
(1) Pulse-Echo . . . . .	130
(2) Reflector Plate Method . . . . .	132
(3) Ringing Method . . . . .	140
(4) Pitch-Catch . . . . .	140
f. Angle Beam Immersion Testing of Plate . . . . .	142
IV PROCESSING OF INGOT . . . . .	153
1. Ingot Melting . . . . .	154
2. Ingot Conversion to Billet, Bar, Plate and Forgings . . . . .	158
3. Inspection of Ingot . . . . .	170
a. Radiography . . . . .	170
b. Ultrasonic Inspection . . . . .	170

Section	Page
4. Inspection of 9 Inch Diameter Billet . . . . .	183
a. Radiography . . . . .	183
b. Ultrasonic Inspection . . . . .	183
c. Macroetching and Anodic Etch . . . . .	189
5. Inspection of 6 Inch Diameter Billet . . . . .	195
a. Ultrasonic Inspection . . . . .	195
b. Radiographic Inspection . . . . .	198
6. Correlation of Inspection Results . . . . .	203
7. Summary of NDT Results . . . . .	203
V NDT Capability . . . . .	205
1. Surface Connected Cracks . . . . .	205
a. Tension - Tension Fatigue Specimen Fabrication . . . . .	205
b. Liquid Penetrant Testing of Tension - Tension Fatigue Specimens . . . . .	207
(1) Laboratory Inspection . . . . .	207
(2) Production Inspection . . . . .	210
(3) Overhaul Inspection . . . . .	212
c. Ultrasonic Surface Wave Testing . . . . .	215
(1) Production Inspection . . . . .	215
(2) Laboratory Inspection . . . . .	224
d. Ultrasonic Contact Angle Beam Testing . . . . .	226
(1) Production Inspection . . . . .	226
e. Overall Production NDT Capability . . . . .	231
f. Laboratory Eddy Current Inspection . . . . .	232
g. Radiographic Inspection of Surface Cracks . . . . .	237
h. Bending Fatigue Specimen Fabrication . . . . .	238
i. Liquid Penetrant Testing of Bending Fatigue Specimens . . . . .	238
j. Radioactive Penetrant Testing . . . . .	242

Section	Page
k. Eddy current Inspection of Fastener Holes . . . . .	244
l. Verification of Surface Crack Size . . . . .	259
2. Porosity . . . . .	259
a. Ultrasonic Method . . . . .	259
b. Radiographic Method . . . . .	266
c. Penetrant Method . . . . .	266
3. Internal Cracks . . . . .	268
a. Specimen Fabrication . . . . .	268
b. Ultrasonic Testing . . . . .	270
c. Verification of Internal Crack Size . . . . .	282
4. Segregates - Jet Engine Disk Forgings . . . . .	284
a. Radiographic Inspection . . . . .	284
b. Penetrant Inspection . . . . .	286
c. Ultrasonic Inspection . . . . .	286
5. Segregates - Plate . . . . .	298
a. Ultrasonic Inspection . . . . .	298
b. Radiographic Inspection . . . . .	305
6. Segregates - Bar . . . . .	306
a. Ultrasonic Inspection . . . . .	306
b. Radiographic Inspection . . . . .	324
7. Segregates - Airframe Forgings . . . . .	324
a. Ultrasonic Inspection . . . . .	324
8. Metallographic Examination of Segregates In Bar, Plate, and Forgings . . . . .	329
VI CONCLUSIONS . . . . .	348
VII RECOMMENDATIONS . . . . .	350
VIII REFERENCES . . . . .	351

LIST OF ILLUSTRATIONS

<u>Figure</u>	<u>Title</u>	<u>Page</u>
1	Fixture for Stressing Specimens . . . . .	5
2	Shaker Table Test Set-Up . . . . .	6
3	Porosity in Hand Forged Billets . . . . .	7
4	Photomicrographs of Stress Corrosion Cracks and Shaker Table Produced Cracks . . . . .	8
5	Photomicrographs of Porosity . . . . .	9
6	Pre-penetrant Drying Test Program . . . . .	10
7	Test Plan for Penetrant Bleed-out Time Study (Post- emulsifiable Penetrant System) . . . . .	13
8	Effectiveness of Vapor Degreasing Between Penetrant Inspections . . . . .	14
9	Effect of Penetrant Bleed-out Time (Post-emulsifiable Penetrant System with Dry Powder Developed) . . . . .	17
10	Effect of Penetrant Dwell Time (Post-emulsifiable Penetrant - 15 Minute Bleed-out Time) . . . . .	21
11	Effect of Penetrant Dwell Time (Water Washable Penetrant) . . . . .	24
12	Relative Effectiveness of Developer on Small Crack Indications (Post-emulsifiable Penetrant - 20 Minutes Dwell Time - 15 Minutes Bleed-out Time) . . . . .	26
13	Relative Effectiveness of Developer for Detection of Gross Cracks (Post-emulsifiable Penetrant - 20 Minutes Dwell Time - 15 Minutes Bleed-out Time) . . . . .	27
14	Relative Effectiveness of Developer for Detection of Smaller, Tighter Cracks (Water Washable Penetrant) . . . . .	29
15	Test Plan for Emulsification Time Study . . . . .	31
16	Effect of Emulsification Time (Post-emulsification Penetrant System - 20 Minutes Penetrant Dwell Time and 15 Minute Penetrant Bleed-out Time) . . . . .	33
17	Degradation in Penetrant Indications Due to Overwashing (Post-emulsifiable Penetrant System) . . . . .	38

LIST OF ILLUSTRATIONS (Continued)

<u>Figure</u>	<u>Title</u>	<u>Page</u>
18	Degradation in Penetrant Indications Due to Overwashing (Water Washable Penetrant System) . . . . .	41
19	Effect of Water Washing Time (Spray Washing - 40 PSI/ 70°F) . . . . .	43
20	Luminosity Curves . . . . .	47
21	Brightness Ratio as a Function of Visible Light and Ultraviolet Light Intensity . . . . .	49
22	Penetrant Indications Under Various Levels of Visible Light (Ultraviolet Light Level is 1000 Microwatts per cm <sup>2</sup> ) . . . . .	50
23	Penetrant Indications Under Various Levels of Visible Light (Ultraviolet Light Level is 2000 Microwatts per cm <sup>2</sup> ) . . . . .	51
24	Brightness Ratio as a Function of Visible Light and Ultraviolet Light Intensity (Fatigue Crack) . . . . .	55
25	Representative Test Procedure . . . . .	57
26	Effect of Mechanical Processing Upon Penetrant Indications of Tight Cracks . . . . .	59
27	Effect of Mechanical Processing Upon Penetrant Indications of Gross Cracks . . . . .	60
28	Radiographic Test Specimens . . . . .	65
29	Test Specimens Arrangement . . . . .	67
30	Step Wedges with MIL-STD-453 Penetrimeters . . . . .	69
31	Log Relative Exposure Used to Evaluate the Data . . . . .	72
32	Convex Curvature Reference Standards . . . . .	78
33	Concave Curvature Reference Standards . . . . .	79
34	Concave Ultrasonic Specimens . . . . .	80
35	Flat Surface Reference Standard . . . . .	81
36	Tests to Establish Difference in Sound Transmission Characteristics . . . . .	84

LIST OF ILLUSTRATIONS (Continued)

<u>Figure</u>	<u>Title</u>	<u>Page</u>
37	Typical Curves for Contour Surface Effect . . . . .	96
38	Variation in dB Difference as a Function of Search Unit and Ultrasonic Instrument (Titanium Specimens - 3/64 Inch Diameter Flat Bottom Hole - 3/4 Inch Metal Travel). . . . .	97
39	Focal Distance Versus Concave Radius of Curvature . . . . .	100
40	Decibel Difference Between Flat Surface Response and Curved Surface Response as a Function of Radius and Metal Travel (3/4 Inch Diameter, 5 MHz, SIL Search Unit). . .	101
41	Die Forging Used for Near Surface Resolution Study . . . . .	108
42	Near Surface Resolution Specimens - As-Rolled Plate . . . . .	104
43	Near Surface Resolution Specimen Configuration . . . . .	105
44	Near Surface Resolution Specimens . . . . .	107
45	Response from 3/64 Inch Diameter Flat Bottom Hole in 4 Inch Plate As-Rolled (3/4 Inch Diameter, 5 MHz, SIL Search Unit with 9 Inch Water Path) . . . . .	112
46	Relative Response Vs Metal Travel . . . . .	120
47	Relative Response Vs Metal Travel . . . . .	121
48	Angle Beam Test Specimen . . . . .	127
49	Test Specimen Configuration . . . . .	131
50	Definition of Near Surface Resolution and Back Surface Resolution . . . . .	133
51	Typical Cathode Ray Tube Displays for Pulse Echo Tests . . .	135
52	Increase in Resolution With 25 MHz Test Frequency (3/64 Inch Diameter Hole, .094 Inch Metal Travel) . . . . .	136
53	Increased Resolution of Back Surface With Increased Test Frequency . . . . .	137
54	Reflection Plate Method . . . . .	138
55	Test Setup for Reflector Plate Tests . . . . .	138
56	Sound Entry Positions . . . . .	143
57	First Melt Ingot . . . . .	154
58	Seeds Used to Intentionally Produce Alpha Segregation . . . .	156
59	Pattern for Seeding First Melt . . . . .	157

LIST OF ILLUSTRATIONS (Continued)

<u>Figure</u>	<u>Title</u>	<u>Page</u>
60	Final Melt Ingot . . . . .	155
61	Expected Ingot Defects After Second Melt . . . . .	159
62	Conversion of Ingot to 9 Inch Round Billet . . . . .	160
63	Conversion of 9 Inch Billet From ingot Top . . . . .	161
64	Conversion of 9 Inch Billet From Ingot Middle . . . . .	162
65	Conversion of 9 Inch Billet From Ingot Bottom . . . . .	162
66	Two Pieces of One and One-half Inch Thick Plate . . . . .	163
67	Two-Inch Square Bar . . . . .	164
68	Airframe Forging . . . . .	165
69	Jet Engine Disk Forgings . . . . .	166
70	Cross Section View of Jet Engine Disk Forging . . . . .	166
71	Test Forging Simulating Airframe Component . . . . .	167
72	Schematic Showing Exposure Layout for Radiographic Inspection of Ingot . . . . .	171
73	Arrangement for Radiographic Inspection of Ingot . . . . .	171
74	Schematic Showing Axial and Circumferential Dimensions . . .	173
75	Ultrasonic Inspection of Ingot . . . . .	175
76	Scan Plan for Ingot . . . . .	174
77	Search Unit Acoustical Analysis . . . . .	177
78	Sound Beam Path . . . . .	178
79	Ultrasonic Reference Standards for Ingot Inspection . . . .	179
80	Schematic Showing Exposure Layout for Radiographic Inspection of 9 Inch Billet . . . . .	184
81	Spiral Scan During Ultrasonic Inspection of 9 Inch Diameter Billet . . . . .	186
82	Ultrasonic Reference Standards for 9 Inch Billet Inspection . . . . .	188

LIST OF ILLUSTRATIONS (Continued)

<u>Figure</u>	<u>Title</u>	<u>Page</u>
83	Typical Macroetched Billet Surface From Seeded Ingot . . . .	191
84	Typical Macroetched Surface in Commercial 9 Inch Billet . .	192
85	Discontinuity in 9 Inch Billet (1-2B) . . . . .	193
86	Ultrasonic Inspection Set-Up . . . . .	196
87	Ultrasonic Reference Standards for 6 Inch Billet Inspection . . . . .	199
88	Schematic Showing Exposure Layout for Radiographic Inspection of 6 Inch Billet . . . . .	198
89	Summary of NDT Results . . . . .	204
90	Fatigue Specimen . . . . .	206
91	Surface Wave Scanning . . . . .	218
92	Distance-Amplitude Correction (DAC) Curves for 3 Representative Technicians . . . . .	219
93	Test Set-Up Used to Measure Sound Transmission Differences .	227
94	Procedure for Distance - Amplitude Correction Curve . . . .	229
95	Scan Plan for Contact Angle Beam Testing . . . . .	228
96	Eddy Current Sensitivity Standard . . . . .	233
97	Configuration of Bending Fatigue Cracked Specimens . . . . .	239
98	Specimen for 0.250 Diameter Holes . . . . .	245
99	Specimen for 0.375 Diameter Holes . . . . .	246
100	Specimen for 0.750 Diameter Holes . . . . .	247
101	Secondary Cracks in Fastener Hole . . . . .	248
102	Titanium Eddy Current Sensitivity Standard . . . . .	250
103	Scan Index Used During Eddy Current Inspection . . . . .	249
104	Photograph of Typical Fracture Surfaces . . . . .	252

LIST OF ILLUSTRATIONS (Continued)

<u>Figure</u>	<u>Title</u>	<u>Page</u>
105	Cathode Ray Tube Presentation of Crack Response . . . . .	258
106	Photographs of Fracture Surface of Surface Cracks . . . . .	261
107	Typical Porosity In Hand Forged Billets . . . . .	264
108	Penetrant Indications of Porosity . . . . .	267
109	Diffusion Bonding of Internally Cracked Specimens . . . . .	269
110	Reference Standard . . . . .	272
111	Sound Beam Angle for Jet Engine Inspection of Internal Cracks (Laboratory) . . . . .	273
112	Setup for Straight Beam Immersion Testing of Internally Cracked Specimens . . . . .	278
113	Typical Responses from Internal Cracks During Straight Beam Immersion Tests . . . . .	281
114	Photographs of Fracture Surface of Internal Cracks . . . . .	283
115	Radiography of Disk Forgings . . . . .	285
116	Areas Machined on Disk Forging . . . . .	287
117	Sound Beam Directions for Disk Forging Inspection . . . . .	289
118	Circumferential Shear Inspection . . . . .	290
119	Defect Location Summary for Engine Inspector A . . . . .	292
120	Defect Location Summary for Engine Inspector B . . . . .	293
121	Total Ultrasonic Indications From Engine Production Inspections of Disk Forgings . . . . .	294
122	Total Ultrasonic Indications from AFML Inspections of Disk Forgings . . . . .	297
123	High Noise Level In Plate After Subtraction of 19 dB . . . . .	299
124	High Noise Level In Plate After Subtraction of 7 dB . . . . .	299
125	Scan Plan for Plate . . . . .	301
126	Typical Response from Discontinuity in Plate . . . . .	302

LIST OF ILLUSTRATIONS (Continued)

<u>Figure</u>	<u>Title</u>	<u>Page</u>
127	Location of Defects in Plate A . . . . .	304
128	Photographs of Cathode Ray Tube Presentation of Back Surface Response and Noise in Bar at Several Gain Levels . .	307
129	Scan Plan for Bar . . . . .	308
130	Data Presentation . . . . .	310
131	Layout of Bars for Ultrasonic Inspection . . . . .	310
132	Location of Defects in Bar . . . . .	311
133	Sound Entry Points Used to Establish the DAC Curve . . . . .	325
134	Scan Plan for Airframe Forgings . . . . .	327
135	Ultrasonic Indications in Airframe Forgings . . . . .	328
136	Photomicrographs of Segregate in Plate A, Section 3 (Response was Greater Than No. 5 Flat Bottom Hole) . . . . .	331
137	Photomicrographs of Segregates in Plate A, Section 17 (Response was Equal to a No. 2 Flat Bottom Hole) . . . . .	333
138	Photomicrographs of Segregate in Plate A, Section 18 (Response was Equal to No. 2 Flat Bottom Hole) . . . . .	334
139	Photomicrographs of Segregate in Bar 1-2A2B, Section 1 (Response was Less Than No. 2 Flat Bottom Hole) . . . . .	336
140	Photomicrographs of Segregate in Bar 1-2A2B, Section 6 (Response was Equal to No. 2 Flat Bottom Hole) . . . . .	337
141	Photomicrographs of Segregate in Bar 1-2A2E, Section 4 (Response was Greater Than No. 5 Flat Bottom Hole) . . . . .	338
142	Photomicrograph of Segregate in Bar 1-2A2E, Section 5 (Response was Equal to No. 2 Flat Bottom Hole) . . . . .	339
143	Typical Airframe Forging Microstructure . . . . .	340
144	Location of Metallographic Cross Sections in Disk Forgings . . . . .	345
145	Discontinuities in Disk Forgings . . . . .	346
146	Photomicrograph of Discontinuity M in Disk Forging 7 (See Table 98) . . . . .	347

LIST OF TABLES

<u>Table</u>		<u>Page</u>
1	Minimum Bleed-out Time for Post-emulsifiable System . . . . .	16
2	Minimum Bleed-out Time for Water Washable Penetrant System . . . . .	19
3	Minimum Penetrant Dwell Time (Post-emulsifiable Penetrant System) . . . . .	20
4	Minimum Penetrant Dwell Time (High Sensitivity Water Washable Penetrant System) . . . . .	24
5	Relative Effectiveness of Developer Types (Post-emulsifiable Penetrant) . . . . .	25
6	Relative Effectiveness of Developer Types (Water Washable Penetrant) . . . . .	28
7	Effective Emulsification Range . . . . .	32
8	Water Washing Parameters . . . . .	36
9	Acceptable Washing Conditions (Post-emulsifiable Penetrant System) . . . . .	37
10	Acceptable Washing Conditions (Water Washable Penetrant System) . . . . .	40
11	Washing Parameters . . . . .	44
12	Effect of Remover Concentration on Indication Brightness . . . . .	52
13	Effect of Wash Time on Indication Brightness . . . . .	52
14	Brightness Measurements Made on Fatigue Crack . . . . .	53
15	Effect of Mechanical Processing Prior to Penetrant Inspection . . . . .	58
16	Relative Effectiveness of Penetrant Systems . . . . .	63
17	Exposure Conditions . . . . .	68
18	Contrast and Resolution as a Function of Kilovoltage and Thickness . . . . .	71
19	Comparison of Film Densities for Exposures Under Same Conditions Using Isovolt 400 and PG 300 X-Ray Machines . . . . .	74
20	Variation In Determination in Radiographic Quality . . . . .	76

LIST OF TABLES (Continued)

<u>Table</u>	<u>Page</u>
21	Ultrasonic Instruments and Transducers Used for Curved Surface Study . . . . . 83
22	Response Ratio of Flat Surface Response ( $I_F$ ) to Curved Surface Response ( $I_C$ ) - Titanium Specimens . . . . . 86
23	Response Ratio of Flat Surface Response ( $I_F$ ) to Curved Surface Response ( $I_C$ ) - Aluminum Specimens . . . . . 93
24	Metal Travels Used for Near Surface Resolution Study . . . . . 106
25	Near Surface Resolution of As-Received Specimens (3/64 Inch Diameter Flat Bottom Hole Response) . . . . . 110
26	Near Surface Resolution of As-Received Specimens (5/64 Inch Diameter Flat Bottom Hole Response) . . . . . 110
27	Near Surface Resolution of Machined Specimens (3/64 Inch Diameter Flat Bottom Hole Response) . . . . . 114
28	Near Surface Resolution of Machined Specimens (5/64 Inch Diameter Flat Bottom Hole Response) . . . . . 115
29	Maximum Scan Index for Machined Sound Entry Surface (Metal Travels Are Indicated In Parenthesis) . . . . . 127
30	Difference in Response Between Plate and Forging And ASTM - Type Reference Standards . . . . . 128
31	Immersion Pulse Echo Testing . . . . . 134
32	Test Results for Reflector Plate Testing . . . . . 139
33	Results of Pitch-Catch Tests . . . . . 141
34	Ultrasonic Noise During Angle Beam Immersion Testing of 2 Inch As-Rolled Plate . . . . . 144
35	Ultrasonic Noise During Angle Beam Immersion Testing of 2 Inch Plate -125 RMS . . . . . 145
36	Ultrasonic Noise During Angle Beam Immersion Testing of 2 Inch Plate - 63 RMS . . . . . 146
37	Ultrasonic Noise During Angle Beam Immersion Testing of 1 1/2 Inch As-Rolled Plate . . . . . 147
38	Ultrasonic Noise During Angle Beam Immersion Testing of 1 1/2 Inch Plate - 125 RMS . . . . . 148

LIST OF TABLES (Continued)

<u>Table</u>	<u>Page</u>
39	Ultrasonic Noise During Angle Beam Immersion Testing of 1 1/2 Inch Plate - 63 RMS . . . . . 149
40	Ultrasonic Noise During Angle Beam Immersion Testing of 1 Inch Plate - As-Rolled . . . . . 150
41	Ultrasonic Noise During Angle Beam Immersion Testing of 1 Inch Plate - 125 RMS . . . . . 151
42	Ultrasonic Noise During Angle Beam Immersion Testing of 1 Inch Plate - 63 RMS . . . . . 152
43	Ingot Inventory List . . . . . 168
44	Comparison of Ingot Processing With Standard Practice . . . . . 169
45	Results of Radiographic Inspection of Ingot . . . . . 172
46	Equipment Used for Ingot Inspection . . . . . 180
47	Number of Ultrasonic Indications in Ingot . . . . . 182
48	Results of Radiographic Inspection of 9 Inch Billet . . . . . 185
49	Equipment Used for 9 Inch Billet Inspection . . . . . 186
50	Number of Ultrasonic Indications in 9 Inch Diameter Billet . . . . . 190
51	Equipment Used to Ultrasonically Inspect 6 Inch Billet . . . . . 197
52	Number of Ultrasonic Indications in 6 Inch Diameter Billet . . . . . 200
53	Results of Radiographic Inspection of 6 Inch Billet 1-2A6 . . . . . 201
54	Comparison of Radiographic and Ultrasonic Indications in 6 Inch Billet 1-2A6 . . . . . 202
55	Summary of Inspection Methods Used for Detection of Surface Cracks . . . . . 205
56	Parameters for Surface Connected Cracks (Stress Ratio = 0.1) . . . . . 208
57	Results of Laboratory Penetrant Inspection of Surface Cracks . . . . . 211
58	Results of Production Penetrant Inspection of Surface Cracks . . . . . 213

LIST OF TABLES (Continued)

<u>Table</u>		<u>Page</u>
59	Number of False Indications Production Penetrant Inspection . . . . .	214
60	Comparison of Production Penetrant Inspectors . . . . .	214
61	Results of Overhaul Penetrant Inspection . . . . .	216
62	Number of False Indications - Overhaul Penetrant Inspection . . .	217
63	Results of Production Surface Wave Ultrasonic Inspection . . . . .	220
64	Comparison of Penetrant and Surface Wave Test Results . . . . .	221
65	Summary of Crack Detection Capability of Surface Wave Ultrasonics By Operator . . . . .	222
66	Cracks Detected from Both Sides of Specimen By Surface Wave Ultrasonics (Summation of 5 Operators) . . . . .	223
67	Summary of False Indications - Ultrasonic Surface Wave . . . . .	224
68	Results of Laboratory Surface Wave Inspection . . . . .	225
69	Results of Production Contact Angle Beam Inspection . . . . .	228
70	Cracks Detected From Both Sides of Specimens By Contact Angle Beam Ultrasonics (Summation of 2 Inspectors) . . . . .	230
71	Eddy Current Test Results . . . . .	235
72	Summary of Crack Detection Capability-Laboratory Eddy Current . . . . .	236
73	Parameters for Surface Connected Cracks Made By Bending Fatigue . . . . .	238
74	Results of Engine Laboratory Penetrant Testing of Surface Cracked Specimens (Results for Inspector B Shown In Parenthesis) . . . . .	241
75	Results of Engine Production Penetrant Inspection of Surface Cracked Specimens . . . . .	241
76	Results of Airframe Production Penetrant Inspection of Surface Cracked Specimens . . . . .	243

LIST OF TABLES (Continued)

<u>Table</u>	<u>Page</u>
77	Results of AFML Penetrant Inspection of Bending Fatigue Surface Cracked Specimens . . . . . 243
78	Results of Radioactive Penetrant Testing . . . . . 244
79	Results of Eddy Current Inspection of Fastener Holes . . . . . 253
80	Summary of Eddy Current Response Versus Maximum Crack Depth . . . . . 254
81	Eddy Current Crack Response . . . . . 256
82	Actual Size of Surface Cracks . . . . . 260
83	Porosity Diameters . . . . . 267
84	Crack Lengths Before Bonding in Internally Cracked Specimens . . . . . 268
85	Summary of Ultrasonic Testing of Internally Cracked Specimens . . . . . 271
86	Jet Engine Ultrasonic Inspection (laboratory) Results for Internal Cracks . . . . . 271
87	Results of Engine Production Straight Beam Immersion Tests . . . 275
88	Results of Engine Immersion Angle Beam Tests . . . . . 276
89	Results of AFML Ultrasonic Inspections . . . . . 277
90	Ultrasonic Inspection Results (Airframe) for Internal Cracks . . 280
91	Jet Engine Manufacturer Laboratory Disk X-Ray Inspection Parameters . . . . . 285
92	Summary of Ultrasonic Inspections of Disk Forgings . . . . . 289
93	Comparison of Total G.E. Ultrasonic Indications With Total AFML Ultrasonic Indications . . . . . 296
94	Summary of Straight Beam Testing of Plate From Ingot Bottom (Surface "A" Was the Sound Entry Surface) . . . . . 303
95	Summary of Straight Beam Testing of Plate From Ingot Bottom (Surface "B" Was the Sound Entry Surface) . . . . . 304
96	Variation in Average Sound Transmission Characteristics Between Bar and Reference Standards for 5MHz Straight Beam Testing . . . . . 306

LIST OF TABLES (Continued)

<u>Table</u>		<u>Page</u>
97	Dimensions of Type I Alpha Stabilized Defects . . . . .	330
98	Comparison of three Methods Used in Finding Defects for Evaluation (Disk No. 6) . . . . .	342
99	Comparison of Manual and Analog Scans for Disk No. 7 . . . . .	344

## SECTION I

### SUMMARY

The results of the testing reported herein have emphasized the importance of controlling the significant parameters which make up each nondestructive testing (NDT) method. In order to effectively inspect titanium by penetrant inspection, the penetrant dwell time, development time, water washing conditions, and inspection light intensity must all be chosen to effectively enhance the defect detection capability of this method. Ultrasonic inspection of titanium was found to be affected by the internal structure and the physical configuration of the particular component undergoing inspection. Characteristics of the component such as surface finish, surface contour, section thickness, and internal structure can all affect the ultrasonic inspection.

The capability of the NDT methods for detecting flaws which occur in titanium was found to vary as a function of the chosen inspection method, the inspector, and the flaw size. Exceedingly small surface cracks could be detected with production ultrasonic and penetrant inspections but not to a high degree of reliability. The capability of the ultrasonic method for detecting internal cracks in thick sections was found to be highly dependent upon the orientation of the crack with respect to the sound beam. Small cracks oriented perpendicular to the sound beam can be detected, but, if the crack is oriented 45 degrees to the sound beam, large cracks can go undetected. With this knowledge, production parts can be more effectively inspected, knowing the likely orientation of expected flaws and the most critical flaw orientations. For thin sections, the orientation of the flaw was found to have less effect.

Titanium melt defects, such as Type I alpha stabilized areas, are detectable using production ultrasonic techniques, but, radiography seems to be ineffective.

## SECTION II

### INTRODUCTION

The performance demands placed upon present day military aircraft are stringent. Advancements in the area of nondestructive testing (NDT) which parallel new developments in manufacturing technology can result in significant payoff. Improvements in the detection and evaluation of titanium defects by NDT can be made which can result in improved integrity and reliability of airframe and engine components.

The primary objectives of the program, then, were to improve nondestructive testing techniques which is discussed in Section III and to measure the capability and reproducibility of the improved nondestructive testing techniques for the evaluation of discontinuities occurring in titanium which is discussed in Section V of this report. In addition, it was intended to document NDT techniques presently used in industry and their shortcomings.

The program was conducted using NDT methods and discontinuity types encountered in inspection of airframe and jet engine components. The NDT methods used were ultrasonics, penetrant, X-ray, and eddy current. Discontinuities which might occur in titanium components originate from two general sources. One source is associated with raw materials and ingot melting and includes discontinuities such as ingot pipe and alpha stabilized areas. Another source is component fabrication and includes discontinuities such as surface cracks, internal cracks, and porosity. All of the above discontinuities were utilized throughout the program.

The penetrant, radiographic, and ultrasonic methods were improved as discussed in subsections 1, 2 and 3 of Section III of this report. After the NDT improvement portion of the program was completed, the capability and reproducibility of the NDT methods were measured with respect to surface cracks, porosity, internal cracks, and segregates as reported in subsections 1, 2, 3, 4, 5, 6, and 7 of Section V of this report. The evaluation was divided into airframe and jet engine inspections with laboratory, production, and overhaul inspections being included. Product forms inspected included bar, plate, and airframe and jet engine forgings. Following the nondestructive testing, the actual size of the discontinuities was measured using selected destructive techniques such as metallography. (See subsection 8 of Section V).

## SECTION III

### IMPROVEMENT OF NONDESTRUCTIVE TESTING TECHNIQUES

A great deal needs to be learned about the variables of conventional NDT methods with regard to inspection of titanium hardware. The effect of several factors, such as complex shapes encountered, is not sufficiently understood at this time. Also, the effect of surface structure upon an effective inspection needs investigation. The NDT methods commonly used for inspection of titanium hardware are ultrasonics, penetrant, X-ray, and eddy current. Although these NDT methods are considered established only limited work has been performed in investigating the production process variables of the NDT methods as relate' to detection of discontinuities in real components.

#### 1. PENETRANT METHOD

Penetrant inspection is heavily relied upon in the aircraft industry for the detection of surface connected discontinuities. For many aircraft components, penetrant inspection is the last inspection method used on the finish machined part prior to its installation in the aircraft. In some cases, it is the only inspection method used. Consequently, penetrant inspection is the final means used to guarantee that the subject component is "defect free". The penetrant method is of major importance in ensuring the integrity of titanium components.

In general, a penetrant inspection consists of:

- (1) Preparation of the surfaces to be inspected
- (2) Drying of the inspection surface
- (3) Application of the penetrant
- (4) Removal of excess penetrant
- (5) Examination of the inspection surface.

The effectiveness of the penetrant inspection is entirely dependent upon the penetrant entering the discontinuities and re-emerging for visual inspection. Any pre-penetrant process or any penetrant inspection variable which reduces penetration and re-emergence of the penetrant can potentially reduce the effectiveness of the inspection. Some of the factors which can affect the reliability and resolution limits of the inspection are:

- (1) The effectiveness of the drying procedure prior to application of penetrant.
- (2) The use or non-use of a developer
- (3) The dwell time of the penetrant, emulsifier, and developer (if used).

- (4) Viewing ultraviolet light intensity versus ambient white light intensity.
- (5) The type of developer used (dry, nonaqueous wet, or aqueous wet)
- (6) The technique used to remove excess penetrant
- (7) Mechanical processing, such as shot peening, performed upon the inspection surface prior to the penetrant inspection.
- (8) The proficiency of the inspector

A test program was conducted in order to study several of the penetrant inspection variables. Both gross cracks and small cracks were used in the program to measure the effect of such variables as penetrant dwell time and developer type.

#### a. Penetrant Systems

A large number of penetrant material systems are presently marketed and used throughout the airframe and engine industries. These systems are characterized as color contrast (visible) dye penetrants (solvent removable and water washable) of several sensitivities, and fluorescent penetrants (solvent removable, water washable, and post-emulsifiable) of several sensitivities. The scope of the program to improve the penetrant method encompassed two penetrant systems which are considered representative of the systems in common use today. The chosen systems are:

<u>Penetrant Type</u>	<u>Sensitivity</u>	<u>Manufacturer's Designation</u>
Fluorescent Post-Emulsifiable	MIL-I-25135, Group V when used with developer	Magnaflux ZL-2A penetrant, ZE-3 emulsifier, ZPX-437 non- aqueous wet developer, ZP-4 dry powder developer, and ZP-13 aqueous developer
Fluorescent Water Washable	Equivalent to MIL-I- 25135, Group VI pene- trant when used with a developer	Tracer-Tech P-133 penetrant, D499C nonaqueous wet developer, D493A dry developer, D492C aqueous developer

#### b. Specimen Fabrication

In a typical production penetrant inspection facility, a variety of crack sizes are encountered. Consequently, if a program is to be conducted on penetrant inspection variables, a variety of crack sizes should be used. Both gross cracks and small cracks were used in the study reported here.

(1) Specimens with Tight Cracks

Ti-6Al-4V blanks,  $1/4 \times 2 \times 5$  inches, were cut to size and ground on one side. The blanks were ground to approximately 32 rms using a 60 grit wheel (12 inch diameter x 1 inch wide), 2,000 rpm wheel speed, .002 to .003 inch downfeed, and approximately .100 inch crossfeed per pass. The workpiece was flooded with coolant during the process. After grinding, the specimens were bent in a fixture, as shown in Figure 1, to approximately 25% yield strength. The bent specimens were wetted with methanol and NaCl was applied such that NaCl adhered to the specimen surface. The stressed specimens were lowered into an anhydrous methanol-NaCl solution and remained immersed until cracking occurred in a few hours.

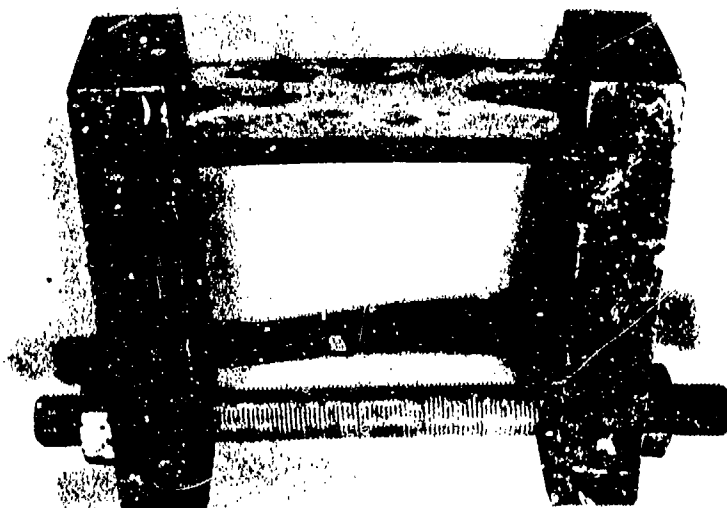
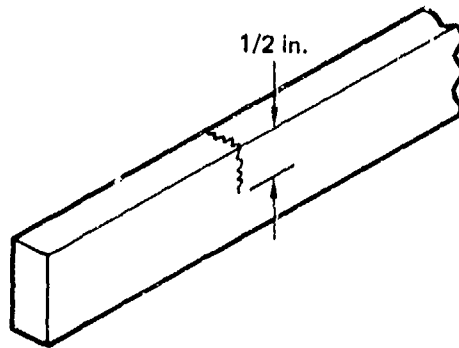
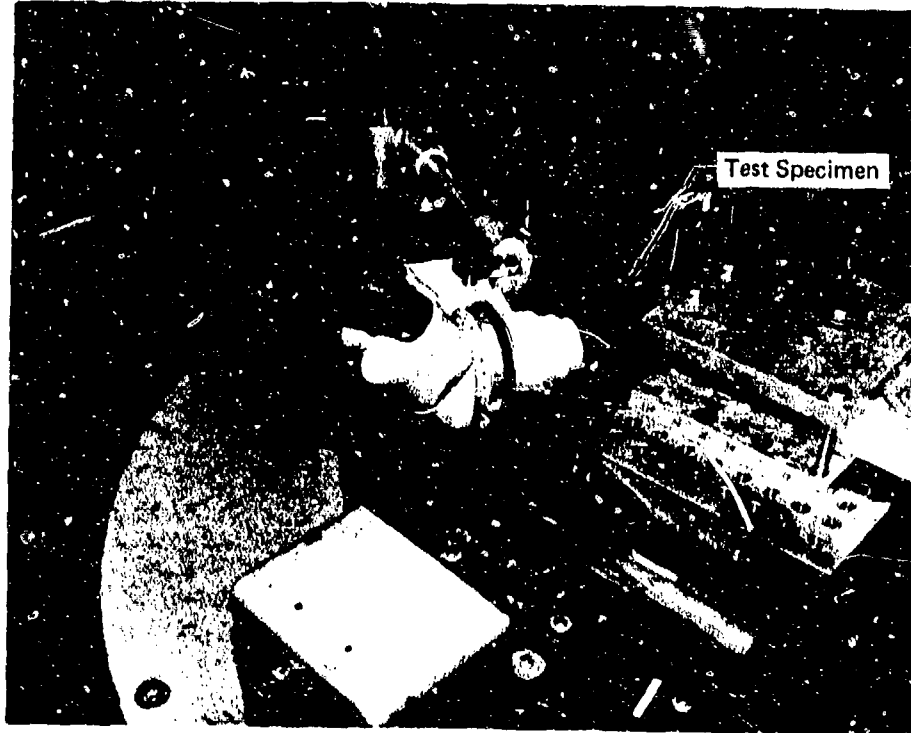


FIGURE 1  
FIXTURE FOR STRESSING SPECIMENS

GP74 0117 14B

(2) Specimens with Gross Cracks

Blanks,  $1/4 \times 1 \times 6$  inches, were cut from Ti-6Al-4V and a saw-cut notch was put into the  $1/4 \times 6$  inch face to serve as a crack initiation site. Each specimen was cantilevered in a shaker table with a mass of 239 grams added near the free end and was vibrated at its resonant frequency (approximately 550 Hz). The crack growth was monitored optically until the desired crack length ( $1/4$  to  $1/2$  inch) was obtained. The test set-up is shown in Figure 2. The resulting cracks were propagated through the  $1/4$  inch thickness and  $1/4$  to  $1/2$  inch into the  $1 \times 6$  face (see Figure 2). The surface finish on the specimens was approximately 32 rms.



GP73-0284-41

**FIGURE 2**  
**SHAKER TABLE TEST SET-UP**

### (3) Porosity Specimens

Several hand forged billets (Ti-6Al-6V-2Sn) containing porosity have been collected during past internal programs. The porosity is depicted in Figure 3. Sections 1/4 inch thick were cut from the billets, ground flat and etched, for use in the penetrant investigation.

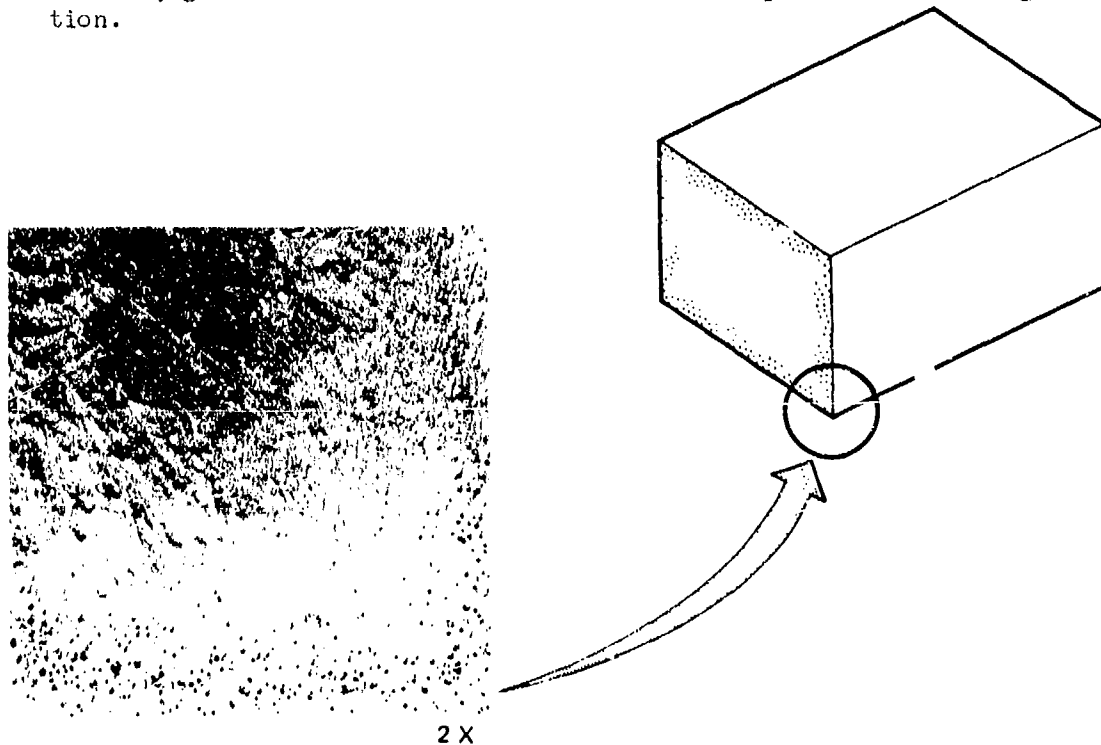


**FIGURE 3**  
**POROSITY IN HAND FORGED BILLETS**

GP74-0117 146

Photomicrographs of typical tight cracks, gross cracks, and porosity are shown in Figures 4 and 5. As can be seen in Figure 4, a wide range of crack sizes are represented by the tight cracks and gross cracks. The gross cracks had widths at the surface of approximately .001 inch and depths of 0.25 and 0.50 inch. Cracks of this size are among those which have been encountered in production processes. For example, rolling cracks have been encountered with widths of approximately .001 inch. The width of the tight cracks (at the surface) varied from .00016 to .0002 inch and the crack depth varied from .007 to .060 inch. Cracks this size have also been encountered in production processes such as forming. As shown in Figure 5, the porosity size varied considerably. The diameter of several pores was measured at high magnification and found to vary from .0005 to .0075 inch; the depths varied from .002 to .015 inch.

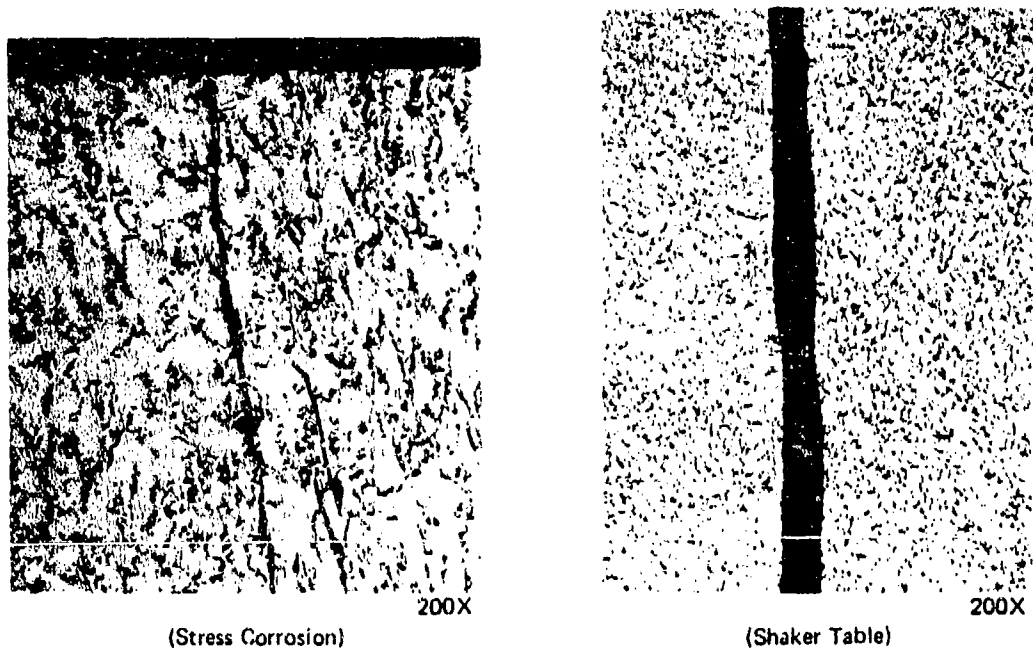


**FIGURE 4**  
**PHOTOMICROGRAPHS OF STRESS CORROSION CRACKS AND**  
**SHAKER TABLE PRODUCED CRACKS**

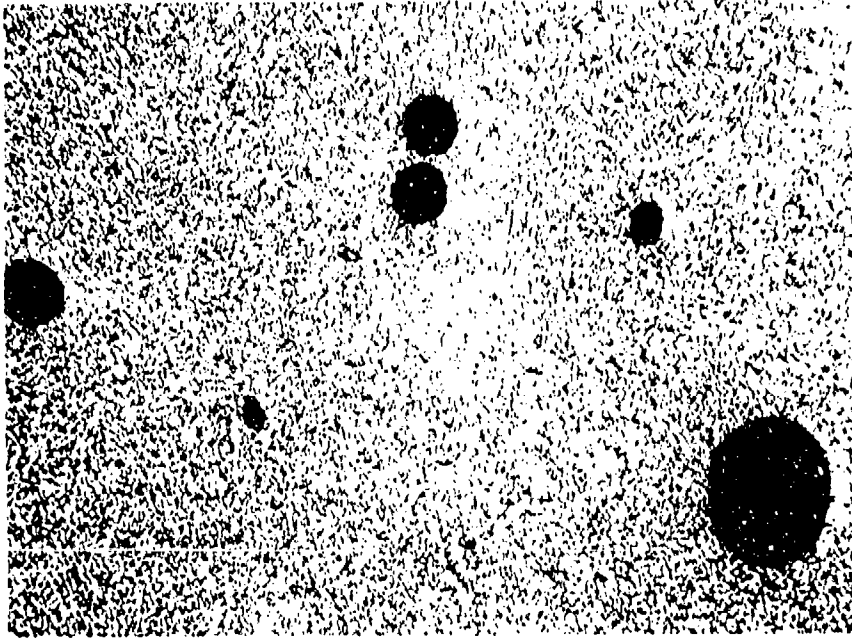
c. Pre-Penetrant Drying

In the normal penetrant inspection sequence, the inspection surface is cleaned and dried prior to applying the penetrant. The purpose of the drying operation is to remove residual water and cleaning solution which may have become entrapped in the discontinuities. A number of drying procedures are commonly used in industrial production penetrant inspection systems.

Several drying methods were evaluated and compared to oven drying for 10 minutes at 225°F which was chosen as a typical adequate drying procedure. A flow chart is shown in Figure 6 to summarize the test program. It should be noted that the same production cleaning method was used throughout the drying study.

(1) Water Washable Penetrant System

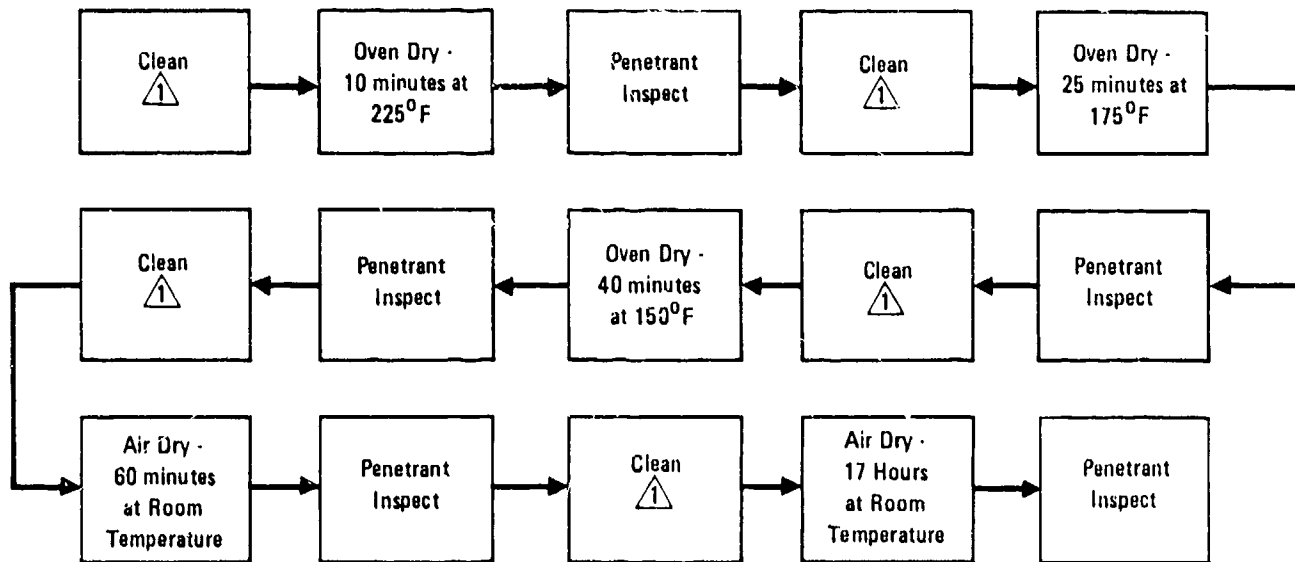
A high sensitivity fluorescent water washable penetrant was chosen for the investigation. Tracer-Tech P-133 penetrant, equivalent in sensitivity to a MIL-I-25135, Group V penetrant, was used along with Tracer-Tech D499C nonaqueous wet developer.



100X

GP77-0117-144

FIGURE 5  
PHOTOMICROGRAPH OF POROSITY



⚠ Vapor degrease for 16 hours to remove residual penetrant followed by normal production cleaning (alkaline clean followed by acid pickle to remove 0.00005 inch and water rinse).

**FIGURE 6**  
**PRE-PENETRANT DRYING TEST PROGRAM**

GP74 0117 143

Seven gross cracks (approximately .001 inch wide x .25 inch long) were used to study each drying condition. The specimens were completely immersed during penetrant dwell (10 minutes). Excess penetrant was washed from the specimens using a water spray nozzle; the wash water temperature was approximately 90°F and the wash water pressure was approximately 40 psi. Each specimen was washed until the specimen surface was visually clean under 200 microwatts per cm<sup>2</sup> of ultraviolet light (approximately 15 seconds). Next, the specimens were placed in a circulating air oven at 170°F and dried until visually dry (15-20 minutes). Nonaqueous wet developer was applied to the cracks. After a development time of 15 minutes, the penetrant indications were photographed using the following parameters: approximately 1,000 microwatts per cm<sup>2</sup> of ultraviolet light, 25 second exposure at f9, Royal Fan Film, Tiffen Yellow No. 2 filter. An Ultraviolet Products, Inc. spot ultraviolet light was used to produce the ultraviolet light. Each drying procedure was compared to oven drying at 225°F for 10 minutes by directly comparing the photographs of the penetrant indications. The ultraviolet light intensity was measured with an Ultraviolet Products, Inc. UV Black-Ray meter, Model J221.

There appeared to be little difference between the various pre-penetrant drying methods used on the gross cracks. Presumably, these cracks were so large that entrapment of small quantities of water or cleaning solution did not effectively reduce the penetration of the penetrant into the cracks.

#### (2) Post-Emulsifiable Penetrant System

The effect of pre-penetrant drying was also investigated for a post-emulsifiable penetrant system. A MIL-I-25135, Group V fluorescent penetrant system was chosen for the investigation. Specifically, Magnaflux ZL-2A penetrant was used with Magnaflux ZPX-457 nonaqueous wet developer. The excess penetrant was removed using Magnaflux ZR-10 remover at a concentration of 0.5 volume percent. The ZR-10 was metered into the water stream with a FMI Lab Pump, Model RRP.

As for the water washable system, gross cracks (approximately .001 inch wide x .25 inch long) were used as discontinuities. The specimens were alkaline cleaned, acid etched, and water rinsed followed by the applicable pre-penetrant drying method. The following drying methods were investigated: oven dry at 225°F for 10 minutes, 175°F for 25 minutes, and 150°F for 40 minutes and air dry at room temperature for 60 minutes. The penetrant dwell time was 20 minutes and the development time was 15 minutes. All other inspection parameters were as for the water washable penetrant.

The three oven dry schedules appeared to be more effective than did air drying at room temperature for 60 minutes. However, the crack indications were all visible for all the conditions. There was little difference in the effectiveness of the 3 oven drying methods.

#### d. Penetrant Bleed-Out Time

An important variable in the penetrant inspection process is the length of time that the penetrant is allowed to bleed out of the discontinuity after the excess penetrant has been removed and prior to the actual inspection. If the penetrant is not given enough time to bleed out of the discontinuity, the subsequent penetrant indication may not attain maximum brilliance. In order to investigate penetrant bleed-out times, an investigation was carried out for both a water washable fluorescent penetrant system and a post-emulsifiable fluorescent penetrant system.

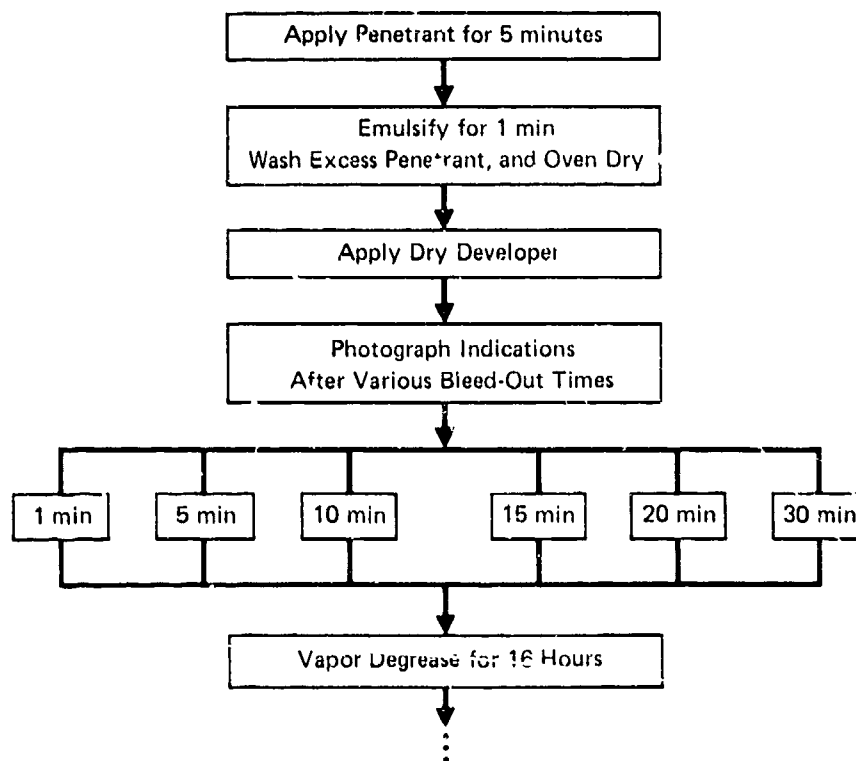
(1) Post-Emulsifiable Penetrant System

A MIL-I-25135, Group V fluorescent penetrant system was chosen for the investigation. Specifically, Magnaflux ZL-2A penetrant was used with Magnaflux ZE-3 emulsifier. The penetrant was used with Magnaflux ZPX-437 nonaqueous wet developer, with Magnaflux ZP-4 dry developer, and with Magnaflux ZP-13 aqueous wet developer in order to determine the effect of various developer types on the results. In addition, the penetrant was used without a developer although this system was not a MIL-I-25135, Group V system.

As can be seen from the Figure 7 test plan, the penetrant bleed-out times were evaluated by photographing the penetrant indications after the penetrant was allowed to bleed out of the discontinuities for 1, 5, 10, 15, 20, and 30 minutes. Then the photographs were visually compared to determine the penetrant bleed-out time required for the indications to achieve their maximum brilliance. After the completion of the test plan shown in Figure 7, the entire program was repeated for penetrant dwell times of 10, 20, and 30 minutes and for nonaqueous wet developer, aqueous developer, and no developer. The dwell times were chosen based on the MIL-I-6866B dwell time requirement of 20 to 30 minutes for post-emulsifiable penetrants.

As shown in Figure 8, it was decided to clean the residual penetrant from the specimens between tests by trichlorethylene vapor degreasing for 16 hours. In order to demonstrate the effectiveness of vapor degreasing between penetrant inspections, a specimen with tight cracks and a specimen with a gross crack were penetrant inspected, vapor degreased for 16 hours, and developer was applied to the surface. As shown in Figure 8, no penetrant indications were visible after 6 hours of development time. Trichlorethylene vapor degreasing is not normally recommended for cleaning titanium production parts because the presence of residual chlorine can cause cracking under the stresses and elevated temperatures a part encounters during service. Since the cracked panels used in this investigation were not subjected to stress, no further cracking of the panels was expected.

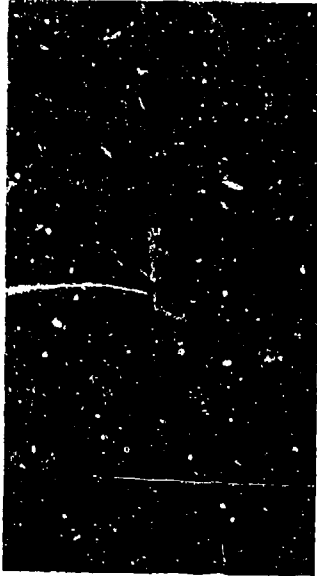
Specimens containing gross cracks (approximately .001 inch wide x .25 inch long) and small cracks (approximately .0002 inch wide x .007 to .060 inch long) were used in the evaluation as well as porosity specimens. The specimens were completely immersed in the penetrant during the applicable penetrant dwell. Excess penetrant was washed from the specimens using a Tri-Con 400501 water spray nozzle after emulsification for 1 minute; the wash water temperature was approximately 90°F and the wash water pressure was approximately 40 psi. Each specimen was washed until the specimen surface was visually clean under 200 microwatts/cm<sup>2</sup> of ultraviolet light (approximately 15 seconds). Next, the specimens were dried until visually dry (10-15 minutes) in a circulating air oven at 170°F. The concentration of the aqueous wet developer, when used, was 1/2 pound per



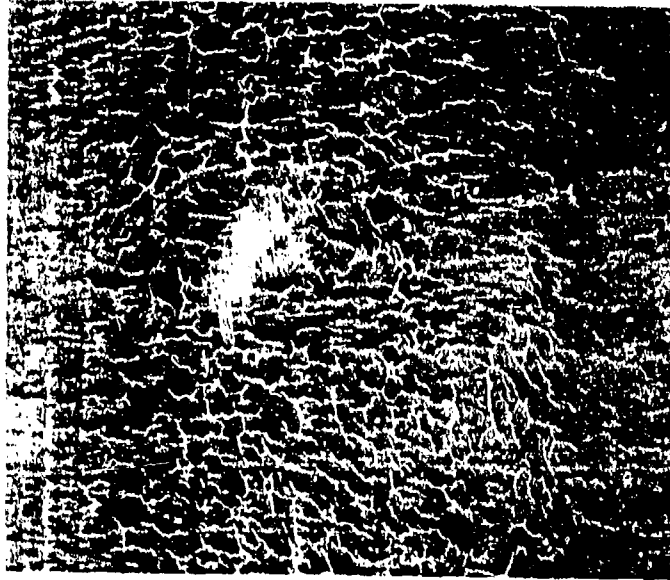
Note: This process was repeated for penetrant dwell times of 10, 20, and 30 minutes and for nonaqueous wet developer, aqueous developer, and no developer

**FIGURE 7**  
**TEST PLAN FOR PENETRANT BLEED-OUT TIME STUDY**

QP74-0117-149

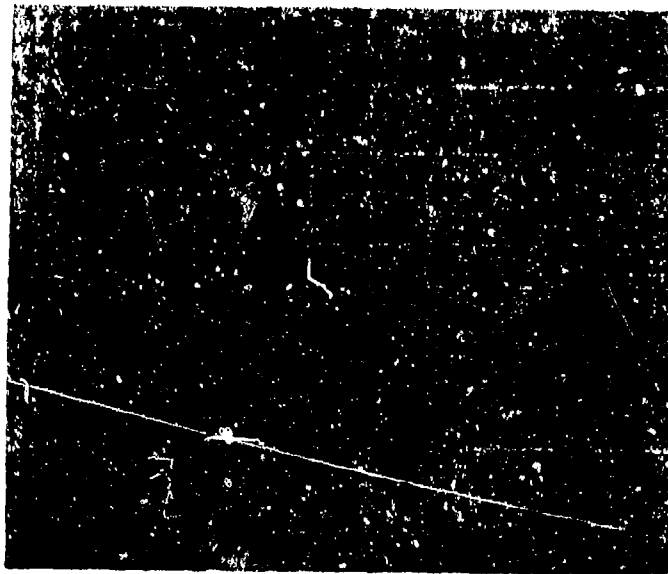
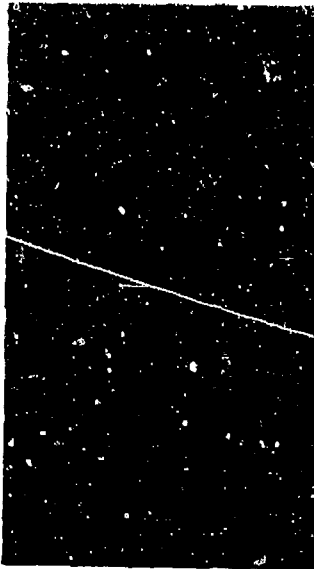


Gross Crack



Tight Cracks

Initial Penetrant Indications



After 16 Hour Degreasing  
(6 Hours Development Time)

GP/4 0117 142

**FIGURE 8**  
**EFFECTIVENESS OF VAPOR DEGREASING BETWEEN PENETRANT INSPECTIONS**

gallon. After the appropriate bleed-out times, the penetrant indications were photographed using the following parameters: approximately 1000 microwatts per cm<sup>2</sup> of ultraviolet light, 25 second exposure at f9, Royal Pan Film, Tiffen yellow No. 2 filter.

The results of the penetrant bleed-out time study as a function of discontinuity type, developer type, and penetrant dwell time are summarized in Table I and demonstrated in Figure 9. For the gross cracks and the porosity, no improvement in the penetrant indications was realized by increasing the penetrant bleed-out time above 1 minute. For several smaller, tighter cracks, the minimum penetrant bleed-out time varied from 1 to 15 minutes depending upon the developer used and the penetrant dwell time chosen.

Table 1 indicates that the penetrant bleed-out time should be at least 1 minute for the most effective penetrant inspection except for small, tight cracks where at least 15 minutes is necessary. Of course, the penetrant/developer combinations listed in Table 1 are not equivalent in effectiveness even when the penetrant bleed-out times are numerically equivalent.

As previously mentioned, the study was performed on 2 penetrant systems and 3 discontinuity types. Consequently, this data on penetrant bleed-out time should be considered as only a guide to choosing adequate bleed-out times in a production inspection environment. For example, a longer bleed-out time might be necessary if the test parts to be inspected contain tighter, smaller cracks than those investigated in this program or if the test parts are not as clean as those investigated in the program.

## (2) Water Washable Penetrant System

A high-sensitivity fluorescent water washable penetrant was chosen for the investigation. Specifically, Tracer-Tech P-133 penetrant was used, which is equivalent in sensitivity to a MIL-I-25135, Group V penetrant when used without developer. The penetrant was used without a developer, with Tracer-Tech D499C nonaqueous wet developer, with Tracer-Tech D493A dry developer, and with Tracer-Tech D492C aqueous wet developer (1/2 pound per gallon) in order to determine the effect of various developer types on the results. The use of a developer increases the sensitivity of the system to that of a Group VI system.

Specimens containing tight and gross cracks were used in the evaluation as well as porosity specimens. The specimens were completely immersed in the penetrant during the applicable penetrant dwell. Excess penetrant was washed from the specimens using a Tri-Con 400501 water spray nozzle; the wash water temperature was approximately 90°F and the wash water pressure was approximately

**TABLE 1**  
**MINIMUM BLEED-OUT TIME FOR POST-EMULSIFIABLE SYSTEM** 

Gross Cracks

Developer	Minimum Bleed-Out Time (Min)		
	Penetrant Dwell Time		
	5 Min	10 Min	20 Min
None	1	1	1
Nonaqueous Wet	1	1	1
Dry	1	1	1
Aqueous Wet	1	1	1

Porosity

Developer	Minimum Bleed-Out Time (Min)		
	Penetrant Dwell Time		
	5 Min	10 Min	20 Min
None	1	1	1
Nonaqueous Wet	1	1	1
Dry	1	1	1
Aqueous Wet	1	1	1

Smaller, Tighter Cracks

Developer	Minimum Bleed-Out Time (Min)		
	Penetrant Dwell Time		
	5 Min	10 Min	20 Min
None	1	1	1
Nonaqueous Wet	1	1	1
Dry	1-15 	1-15 	1-5 
Aqueous Wet	1	1	1

 MIL-1-25135, Group V post-emulsifiable penetrant, 1 minute emulsification time

 One minute bleed-out was sufficient for most cracks but a longer time was required for a few small cracks

GP74 0117 1B1

Penetrant Dwell Time = 10 min  
Specimen 195C



1 min Bleed-Out Time



15 min Bleed-Out Time

GP 74 0117 150

**FIGURE 9**  
**EFFECT OF PENETRANT BLEED-OUT TIME**  
Post-Emulsifiable Penetrant System with Dry Powder Developer

40 psi. Each specimen was washed until the specimen surface was visually clean under 200 microwatts/cm<sup>2</sup> of ultraviolet light (approximately 15 seconds). Next, the specimens were dried until visually dry (10-15 minutes) in a circulating air oven at 170°F. After the appropriate bleed-out times, the penetrant indications were photographed using the following parameters: approximately 1000 microwatts per cm<sup>2</sup> of ultraviolet light, 25 second exposure at f9, Royal Pan Film, Tiffen yellow No. 2 filter.

The test plan was similar to that used for the post-emulsifiable penetrant (Figure 7) except that the penetrant dwell times were 1, 5, and 20 minutes. Specific values for penetrant dwell time for high-sensitivity water washable penetrants are not specified in MIL-I-6866B. Consequently, the dwell times were based upon McDonnell Aircraft Company experience in production penetrant inspection. The penetrant bleed-out times were evaluated by photographing the penetrant indications after the penetrant was allowed to bleed out of the discontinuities for 1, 5, 10, 15, 20, and 30 minutes. Then the photographs were visually compared to determine the penetrant bleed-out time required for the indications to achieve their maximum brilliance.

The results of the penetrant bleed-out time study for the water washable penetrant are summarized in Table 2 as a function of developer type and discontinuity type. As in the case of the post-emulsifiable penetrant system, a penetrant bleed-out time of 1 minute was required for full development of the penetrant indications from the more open discontinuities such as the porosity and gross cracks. However, no improvement in the penetrant indications occurred by using a longer penetrant bleed-out time. For several smaller, tighter cracks, as much as 5 minutes was required to fully develop the penetrant indications depending upon the developer type used.

It should be noted that Table 2 in no way indicates the relative effectiveness of various developer types or the effect of varying penetrant dwell times. For example, a shorter minimum bleed-out time for aqueous wet developer versus dry developer does not indicate that aqueous wet developer was more effective. These effects are covered in later sections of this report.

As in the case of the post-emulsifiable penetrant system work, this investigation was performed with one penetrant system. Consequently, these minimum penetrant bleed-out times should be regarded only as guidelines for production penetrant inspection.

#### e. Penetrant Dwell Time

An important variable in the penetrant inspection process is the dwell time of the penetrant. The dwell time of the penetrant should be long enough to allow the penetrant to enter any discontinuity; however, if the penetrant dwell time is too long, the penetrant can dry making it difficult to remove excess penetrant. Also, the minimum penetrant dwell time may vary as the size of the discontinuity varies.

**TABLE 2  
MINIMUM PENETRANT BLEED- OUT TIME FOR  
WATER WASHABLE PENETRANT SYSTEM**

Gross Cracks

Developer	Minimum Bleed-Out Time (Min)		
	Penetrant Dwell Time		
	1 Min	5 Min	20 Min
None	1	1	1
Nonaqueous Wet	1	1	1
Dry	1	1	1
Aqueous Wet	1	1	1

Porosity

Developer	Minimum Bleed-Out Time (Min)		
	Penetrant Dwell Time		
	1 Min	5 Min	20 Min
None	1	1	1
Nonaqueous Wet	1	1	1
Dry	1	1	1
Aqueous Wet	1	1	1

Smaller, Tighter Cracks

Developer	Minimum Bleed-Out Time (Min)		
	Penetrant Dwell Time		
	1 Min	5 Min	20 Min
None	1	1	1
Nonaqueous Wet	1 to 5	1 to 5	1 to 5
Dry	1 to 5	1 to 5	1 to 5
Aqueous Wet	1	1	1

GP74 011 / 152

Consequently, this important aspect of penetrant testing was investigated for both a water washable fluorescent penetrant system and a post-emulsifiable fluorescent penetrant system.

(1) Post-Emulsifiable Penetrant System

The photographs of the penetrant indications taken during the bleed-out time study were used to study the effect of penetrant dwell time.

The penetrant bleed-out time study indicated that under no circumstances was more than 15 minutes bleed-out time required to achieve maximum brilliance of the penetrant indications. Consequently, the penetrant dwell times were compared for a penetrant bleed-out time of 15 minutes.

The results of the penetrant dwell time study as a function of discontinuity type and developer type are summarized in Table 3 and demonstrated in Figure 10.

**TABLE 3**  
**MINIMUM PENETRANT DWELL TIME**  
(Post-Emulsifiable Penetrant System)

Developer	Minimum Penetrant Dwell Time (Min) <sup>△1</sup>		
	Gross Cracks	Porosity	Smaller, Tighter Cracks
None	20	20	20
Nonaqueous Wet	10	20	20
Dry	5	20	5 and 20 <sup>△2</sup>
Aqueous Wet	5	10	20

<sup>△1</sup> A 1 min emulsification time was used

<sup>△2</sup> 5 min was sufficient for most cracks but 20 min was required for several small cracks

GP 74 0117 154

The test results indicate that the minimum penetrant dwell time varies as a function of discontinuity type and developer type. The longest required penetrant dwell time was 20 minutes. If it is assumed that it is necessary to detect all three discontinuity types (gross cracks, small cracks, and porosity) in a penetrant inspection process, then, for all cases, at least a 20 minute penetrant dwell time would be necessary. These data support the present MIL-I-6866B dwell time requirement of 20 to 30 minutes. It should be noted that Table 3 in no way indicates the relative effectiveness of various developer types. For example, a shorter required dwell time,

Gross Cracks Specimen 33C  
Nonaqueous Wet Developer

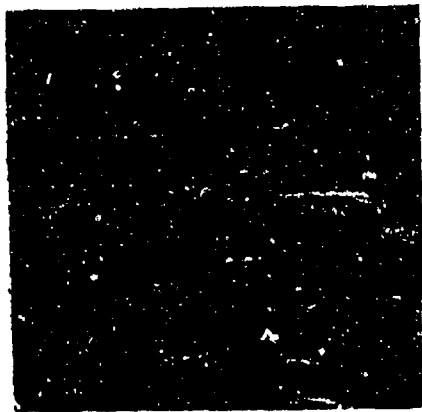


5 min  
Dwell Time



10 min  
Dwell Time

Smaller, Tighter Cracks, Specimen 15SC  
No Developer



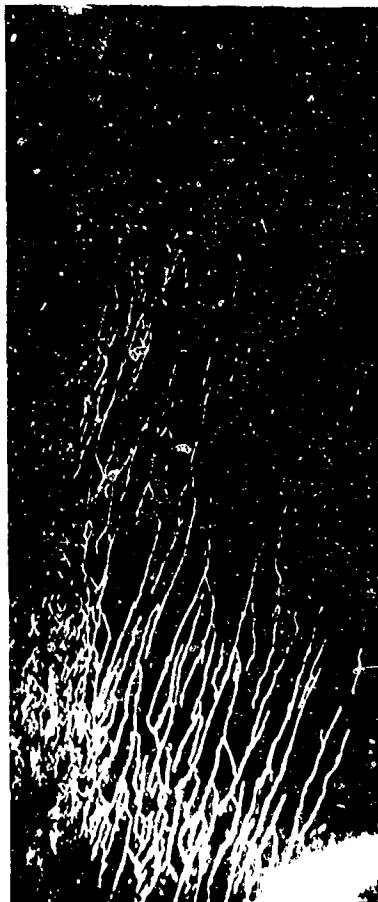
5 min  
Dwell Time



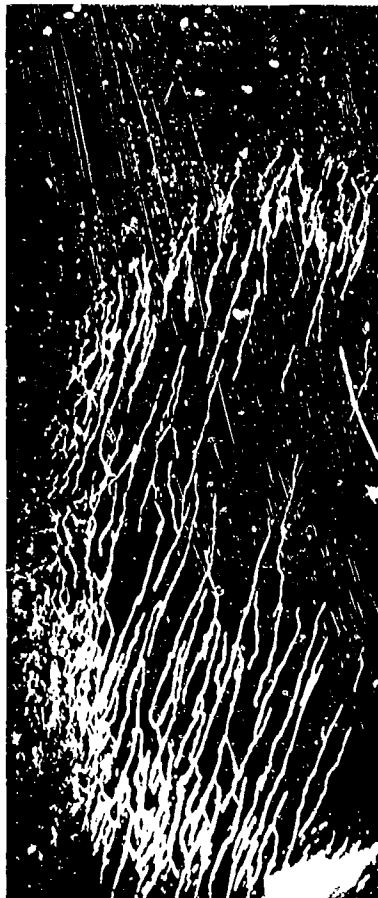
20 min  
Dwell Time

GP/4 0117 :35

**FIGURE 10**  
**EFFECT OF PENETRANT DWELL TIME**  
(Post-Emulsifiable Penetrant - 15 Min Bleed-Out Time)



10 min Penetrant  
Dwell Time



20 min Penetrant  
Dwell Time



30 min Penetrant  
Dwell Time

GP74 011 - 211

**FIGURE 10 (Continued)**  
**EFFECT OF PENETRANT DWELL TIME**  
(Post-Emulsifiable Penetrant - 15 Min Bleed-Out Time)

when using dry developer on gross cracks versus nonaqueous wet developer, did not necessarily indicate that the dry developer was more effective. These effects are covered in later sections of this report.

## (2) Water Washable Penetrant System

As with the post-emulsifiable penetrant system, the photographs of the penetrant indications taken during the bleed-out time study were used to study the effect of penetrant dwell time. The photographs of the penetrant indications were visually compared to determine the penetrant dwell time necessary for maximum penetrant indication brilliance.

Since the penetrant bleed-out time study indicated that under no circumstances was more than 5 minutes bleed-out time required to achieve maximum brilliance of the penetrant indications, the penetrant dwell times were compared using a penetrant bleed-out time of 5 minutes.

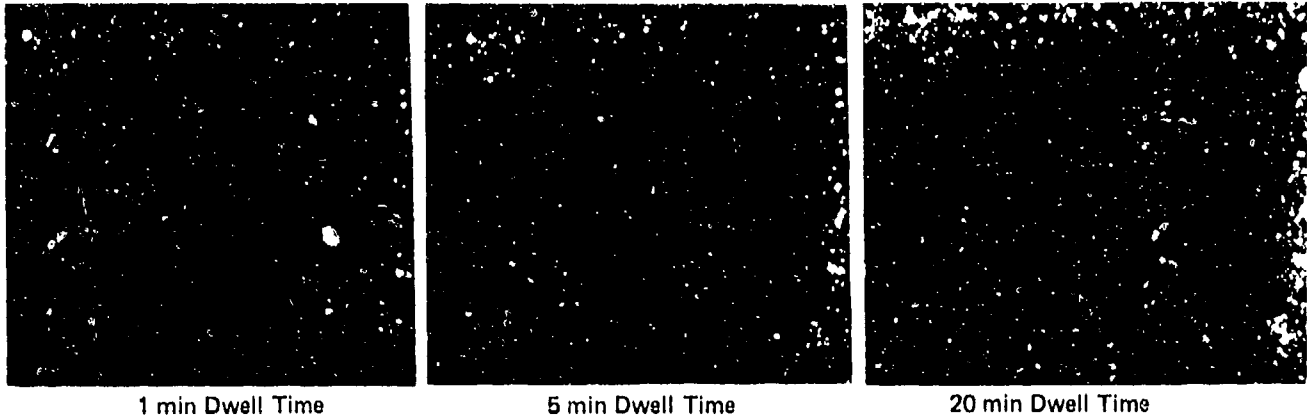
The results of the penetrant dwell time study as a function of discontinuity type and developer type are summarized in Table 4 and demonstrated in Figure 11.

As seen in Table 4, the required penetrant dwell time varied as a function of discontinuity type and developer type. The required penetrant dwell time was 5 minutes for the gross cracks, irrespective of the developer type used. A variation in the required penetrant dwell time was noted for the smaller tighter cracks depending upon the type of developer used. When no developer was used, the majority of the crack indications were present when the dwell time was 5 minutes. However, 20 minutes dwell time was required for several of the small, tight cracks. When nonaqueous wet developer or dry developer was used, a 5 minute penetrant dwell time was sufficient. For aqueous wet developer, a 1 minute dwell time is indicated, which indicates that the strengths of the indications were not improved by longer bleed-out times. However, this developer was totally ineffective as very few of the smaller, tighter crack indications were visible, no matter what penetrant dwell time was used.

In summary, for the most effective penetrant inspection, at least 20 minutes dwell time should be used for a system without developer or with aqueous developer, and at least 10 minutes dwell time should be used for systems employing a nonaqueous wet or dry developer. Of course, these penetrant/developer combinations are not equivalent in effectiveness even if the required penetrant dwell times are numerically equivalent. The relative effectiveness of the systems are discussed in Section 1-k of this report.

It should be kept in mind that the penetrant dwell time study was performed on 2 penetrant types. Other Group V penetrant systems may require greater or lesser dwell times. Most likely, the required penetrant dwell times would be different if a higher sensitivity penetrant were used or if a different type of discontinuity

Nonaqueous Wet Developer  
Porosity Specimen - 4P-1



1 min Dwell Time

5 min Dwell Time

20 min Dwell Time

**FIGURE 11**  
**EFFECT OF PENETRANT DWELL TIME**  
(Water Washable Penetrant)

GP74-0117-157

**TABLE 4**  
**MINIMUM PENETRANT DWELL TIME**  
(High Sensitivity Water Washable Penetrant System)

Developer	Penetrant Dwell Time (Min) <sup>1</sup>		
	Gross Cracks	Porosity	Smaller, Tighter Cracks
None	5	10	5 and 20 <sup>2</sup>
Nonaqueous Wet	5	10	5
Dry	5	10	5
Aqueous Wet	5	20	1 <sup>3</sup>

<sup>1</sup> The bleed-out time exceeded the minimum effective bleed-out time

<sup>2</sup> 5 min was required for most cracks but 20 min was required for several small cracks

<sup>3</sup> Few crack indications were visible when using aqueous wet developer

GP74 0117 156

were to be detected. Also, the test specimens used for this laboratory investigation were very carefully cleaned for the investigation. Production parts cleaned prior to a production penetrant inspection may not attain this degree of cleanliness and therefore, a longer penetrant dwell might be necessary. However, the penetrant dwell time data developed in this program can be used as a guideline for selecting adequate penetrant dwell times in a production penetrant inspection.

f. Developer Effectiveness

The purpose of a developer in penetrant inspection is to increase the visibility of the penetrant available at a discontinuity by spreading it and drawing more of it from the discontinuity and to provide a background from which to view the penetrant indications. Several types of developers are currently in use: nonaqueous wet, dry, and aqueous wet. Consequently, a program was undertaken to evaluate the relative effectiveness of these developer types in comparison with no developer.

(1) Post-Emulsifiable Penetrant System

The photographs of the penetrant indications taken during the bleed-out time study were used to study the relative effectiveness of developer types. Previously mentioned studies indicated that no improvement in penetrant indications was noted for penetrant dwell times greater than 20 minutes and for penetrant bleed-out times greater than 15 minutes. Consequently, the developer effectiveness was compared by evaluating the photographs of penetrant indications resulting from a penetrant dwell time of 20 minutes and a penetrant bleed-out of 15 minutes. A 1 minute emulsification time was used.

The results of the developer effectiveness study are summarized in Table 5 and shown in Figures 12 and 13.

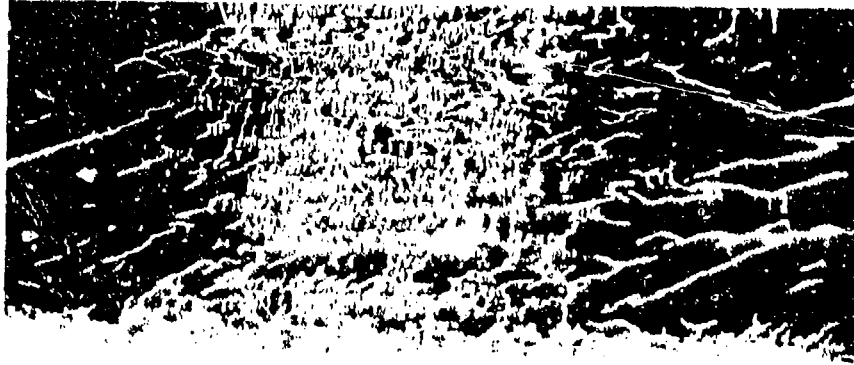
**TABLE 5**  
**RELATIVE EFFECTIVENESS OF DEVELOPER TYPES**

Post-Emulsifiable Penetrant	
Gross Cracks	(1) Nonaqueous Wet, Dry and Aqueous - Equally Effective (2) No Developer
Porosity	(1) Dry (2) Nonaqueous Wet (Slightly Less) (3) No Developer (4) Aqueous
Smaller, Tighter Cracks	(1) Nonaqueous Wet and Dry - Equally Effective (2) No Developer (Slightly Less Effective) (3) Aqueous

GP74 0117 158



Aqueous  
Developer



Dry  
Developer



Nonaqueous Wet  
Developer

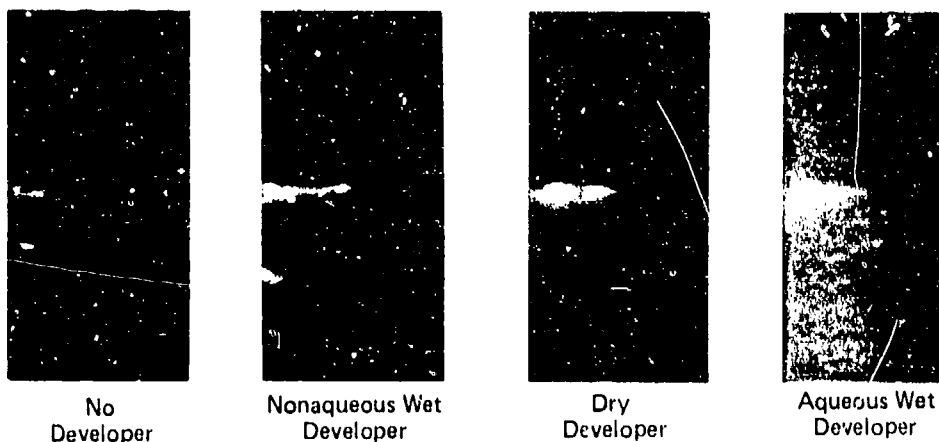


No  
Developer

GP74-0117 159

**FIGURE 12**  
**RELATIVE EFFECTIVENESS OF DEVELOPER ON**  
**SMALL CRACK INDICATIONS**  
(Post-Emulsifiable Penetrant - 20 Min Dwell Time -  
15 Min Bleed-Out Time)

Specimen No. 34C



GP74-0117-160

**FIGURE 13**  
**RELATIVE EFFECTIVENESS OF DEVELOPER FOR**  
**DETECTION OF GROSS CRACKS**  
(Post-Emulsifiable Penetrant - 20 Min Dwell Time -  
15 Min Bleed-Out Time)

The gross cracks (approximately .001 inch wide x .25 inch long) were all visible for each of the four conditions (no developer, nonaqueous developer, dry developer, and aqueous wet developer); however, the indications were brighter when a developer was used. The three developer types were essentially equally effective on the gross cracks. As shown in Figure 12, aqueous wet developer was least effective for the tight cracks. For the detection of the smaller, tighter cracks (approximately .0002 inch wide x .060 inch long) nonaqueous and dry developers were most effective with no developer being slightly less effective. Aqueous developer was the least effective. For the detection of porosity, dry developer was the most effective with nonaqueous slightly less effective. No developer was next effective while aqueous developer was the least effective of all.

Based on these test results, then, there is a definite difference in the effectiveness of the various developer types depending on the discontinuity that is of interest and for a production penetrant inspection to be most effective these considerations should be kept in mind.

(2) Water Washable Penetrant System

Specimens containing tight and gross cracks were used in the evaluation as well as porosity specimens. The specimens were penetrant inspected using Tracer-Tech P-133 high sensitivity water washable penetrant, equivalent in sensitivity to MIL-I-25135 Group V penetrant when used without a developer. Tracer-Tech D-499C nonaqueous wet developer, Tracer-Tech D493A dry developer, and Tracer-Tech D492C aqueous wet developer were used in the investigation as well as no developer. The use of a developer increases the sensitivity of the system to that of a Group VI system. The penetrant dwell times and developer bleed-out times used exceeded the minimum effective times established in the previously discussed dwell time study. The penetrant inspection parameters were the same as used in the dwell time study.

The test results are summarized in Table 6. The penetrant indications of the gross cracks (approximately .001 inch wide x .25 inch long) were essentially equivalent when any of the three developers were used, but the crack indications without developer were less effective. Because of the large crack area involved, a large reservoir is available for the penetrant. Consequently, the difference between developers is probably reduced due to the large volume of penetrant within the cracks.

The effectiveness of the developers on smaller, tighter cracks (approximately .0002 inch wide x .060 inch long) is demonstrated in Figure 14. Aqueous wet developer was nearly totally ineffective when used with the water washable penetrant to detect the smaller, tighter cracks, as very few of the crack indications were evident. Many crack indications were evident when no developer

TABLE 6  
RELATIVE EFFECTIVENESS OF DEVELOPER TYPES

Water Washable Penetrant	
Gross Cracks	(1) Nonaqueous Wet, Dry and Aqueous - Equally Effective (2) No Developer
Porosity	All Types Equally Effective
Smaller, Tighter, Cracks	(1) Nonaqueous Wet and Dry - Equally Effective (2) No Developer (3) Aqueous

GP/4 011 / 101

Specimen 4SC



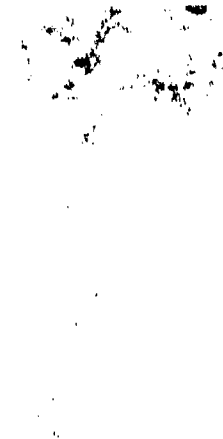
No Developer



Nonaqueous Wet Developer



Dry Developer



Aqueous Wet Developer

GP74 0117 162

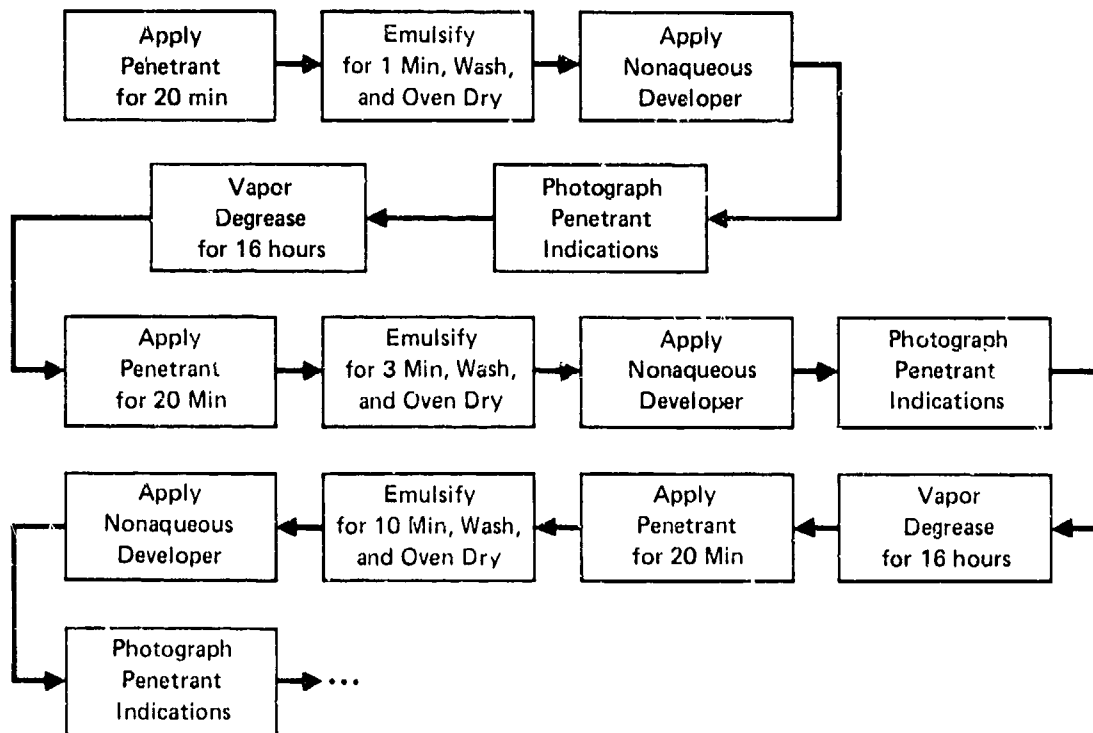
**FIGURE 14**  
**RELATIVE EFFECTIVENESS OF DEVELOPER FOR**  
**DETECTION OF SMALLER, TIGHTER CRACKS**  
(Water Washable Penetrant)

was used but these indications were enhanced when either dry or nonaqueous wet developer was applied. Nonaqueous wet and dry developers were the most effective. Except for a few isolated cases, the nonaqueous wet and dry developers were equivalent in effectiveness.

All three developer types, as well as no developer, were equally effective on porosity indications. As in the case of the gross cracks, the porosity probably holds a relatively large volume of penetrant compared with the smaller, tighter cracks, lessening the difference between developers. It should be noted, however, that the aqueous wet developer tends to make the porosity indications indistinct.

#### g. Emulsification Time

In a post-emulsification penetrant system, the emulsifier is applied in a separate step prior to washing excess penetrant from the test part surface. The time that the emulsifier remains in contact with the part must be long enough so that the excess penetrant can be effectively removed from the part surface but not so long as to cause penetrant to be removed from discontinuities. This aspect of penetrant testing was studied for the MIL-I-25135, Group V fluorescent penetrant (Magnaflux ZL-2A) used with Magnaflux ZPX-437 nonaqueous developer, Magnaflux ZP-4 dry developer Magnaflux ZP-13 aqueous wet developer, and without a developer. Magnaflux ZE-3 emulsifier was used and emulsification times of 1, 3, and 10 minutes were evaluated. Based on the previous results, a penetrant dwell time of 20 minutes was used along with a penetrant bleed-out time of 15 minutes. As before, specimens containing tight and gross cracks were used as well as as porosity specimens. A summary of the testing is shown in Figure 15.



Note: This process was repeated for dry developer, aqueous developer, and no developer

GP74-0117-153

**FIGURE 15**  
**TEST PLAN FOR EMULSIFICATION TIME STUDY**

The specimens were completely immersed in the penetrant during the applicable penetrant dwell time. Excess penetrant was washed from the specimens after the appropriate emulsification time using a Tri-Con 400501 water spray nozzle; the wash water temperature was approximately 90°F and the wash water pressure was approximately 40 psi. Each specimen was washed until the specimen surface was visually clean under 200 microwatts/cm<sup>2</sup> of ultraviolet light (approximately 15 seconds). Next, the specimens were dried until visually dry (10-15 minutes) in a circulating air oven at 170°F. The concentration of the aqueous wet developer, when used, was 1/2 pound per gallon. After the 15 minute bleed-out time, the penetrant indications were photographed using the following parameters: approximately 1000 microwatts per cm<sup>2</sup> of ultraviolet light, 25 second exposure at f9, Royal Pan Film, Tiffen yellow No. 2 filter. The effect of emulsification time was evaluated by directly comparing the photographs of the penetrant indications resulting from 1, 3, and 10 minutes emulsification time.

The results of the emulsification time study are summarized in Table 7. An emulsification time of 1 minute was adequate for effective removal of excess penetrant in all cases. For the gross cracks as much as 10 minutes emulsification time could be used without reducing the effectiveness of the penetrant test (Figure 16). However, for smaller, tighter discontinuities, the emulsification time had to be kept at 3 minutes or less to avoid a reduction in the brilliance of the penetrant indications. Based on these results, then, an emulsification time of less than 3 minutes should be used in order to effectively detect a wide variety of crack and porosity sizes using a MIL-I-25135, Group V post-emulsifiable penetrant system.

By necessity, the emulsification study was limited in scope. Only a few emulsification times and one surface condition (as-machined) was investigated. Consequently, these results should be used only as guidelines to the selection of emulsification times for alternate surface conditions such as as-cast or as-forged surfaces.

TABLE 7  
EFFECTIVE EMULSIFICATION RANGE

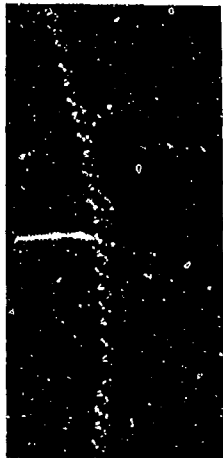
Developer	Effective Emulsification Range (Min) <sup>1</sup>		
	Gross Cracks	Porosity	Smaller, Tighter Cracks
None	1 to 10	1 to Less Than 3	1 to Less Than 3
Nonaqueous Wet	1 to 10	1 to Less Than 3	1 to 3 <sup>2</sup>
Dry	1 to 10	1 to 3	1 to Less Than 3 <sup>2</sup>
Aqueous Wet	1 to 10	1 to 3	1 to Less Than 3

<sup>1</sup> Penetrant bleed-out time (15 min) and penetrant dwell time (20 min) exceeded the minimum required

<sup>2</sup> 10 min emulsification time was acceptable for most cracks but was too long for several small cracks

GP 74 011 163

Gross Cracks - Specimen 30C  
Dry Developer



1 min  
Emulsification  
Time



10 min  
Emulsification  
Time

**FIGURE 16**  
**EFFECT OF EMULSIFICATION TIME**  
(Post-Emulsifiable Penetrant System - 20 Min Penetrant Dwell Time  
and 15 Min Penetrant Bleed-Out Time)

GP74-0117-165

Smaller, Tighter Cracks - Specimen 19SC  
Nonaqueous Wet Developer



1 min  
Emulsification  
Time



3 min  
Emulsification  
Time



10 min  
Emulsification  
Time

**FIGURE 16 (Continued)**  
**EFFECT OF EMULSIFICATION TIME**  
(Post-Emulsifiable Penetrant System - 20 Min Penetrant Dwell Time  
and 15 Min Penetrant Bleed-Out Time)

GP74 0117 166

#### h. Water Washing Techniques

The removal of the excess penetrant prior to examination is an important step in the penetrant inspection process. The purpose of removing the excess penetrant is to remove any confusing background or false indications which may interfere with the indications of discontinuities. At the same time, the cleaning operation must not remove penetrant from discontinuities themselves.

Several types of cleaning operations can be used to remove excess penetrant. Wiping the surface with cloths, either dry or moistened with solvent, has been done but has the disadvantage of being too slow for quantity production inspection. When cleaning by spraying with solvents, it can be difficult to avoid removal of penetrant from discontinuities. Probably the most important and widely-used cleaning technique is washing with water; this can be accomplished either by using penetrant with an incorporated emulsifier or by application of the emulsifier as a separate step. Because of the emphasis upon water washing in production penetrant inspections, this portion of the program concentrated on the variables involved in water washing. Hand held sprayers were used for this portion of the program; therefore, the angle of water impingement varied throughout the entire washing operation.

##### (1) Post-Emulsifiable Penetrant

An investigation was performed to establish acceptable water washing parameters for removal of excess penetrant using a post-emulsifiable penetrant system.

Magnaflux ZL-2A penetrant (MIL-I-25135, Group V fluorescent penetrant) was used along with Magnaflux ZE-3 emulsifier and Magnaflux ZPX-437 nonaqueous developer. The penetrant dwell time was 20 minutes, the emulsification time was 1 minute, and the penetrant bleed-out time was 15 minutes; these choices were based upon the results of the previous testing

Specimens containing tight and gross cracks were used in the evaluation as well as porosity specimens. The specimens were completely immersed in the penetrant during the applicable penetrant dwell. After emulsification, excess penetrant was washed from the specimens using the applicable washing parameters shown in Table 8. Each specimen was washed until the specimen surface was visually clean under 200 microwatts/cm<sup>2</sup> of ultraviolet light.

**TABLE 8  
WATER WASHING PARAMETERS**

Water Removal Method	Water Temp (°F)	Water Pressure (psi)
Water Spray (Nozzle) 	70	40
		60
		90
	100	40
		60
		90
	145	40
		60
		90
Immersion	70	—
	100	—
	145	—

 Tri-Con-400 501 Nozzle

QP74-0117-167

A Tri-Con 400501 heavy duty spray wash gun was used for the spray wash portion of the program. The spray gun was held 8 inches from the specimen surface during the washing. Initial testing indicated that approximately 7 seconds washing time was required to remove all the excess penetrant from the specimens; consequently, a 7 second washing time was used throughout the program for consistency.

The immersion wash tests were carried out using a 10 x 16 inch container, 6 inches deep. The water in the container was air agitated using a stainless steel tube (3/8 inch I.D. x 12 inches long) which had 44 holes drilled in it for air passage. The stainless steel tube was directly connected to a 90 psi air line. It was found that a time of 2 minutes was required to wash excess penetrant from each specimen using this apparatus and, consequently, a two minute wash time was used throughout the program. The specimens were dried after washing until visually dry (10-15 min.) in a circulating air oven at 170° and after the appropriate bleed-out times, the penetrant indications were photographed using the following parameters: approximately 1000 microwatts per cm<sup>2</sup> of ultraviolet light, 25 second exposure at f9, Royal Pan Film, Tiffen yellow No. 2 filter. Next, specimens were vapor degreased for 16 hours in order to remove residual penetrant and the testing was repeated using another set of washing parameters.

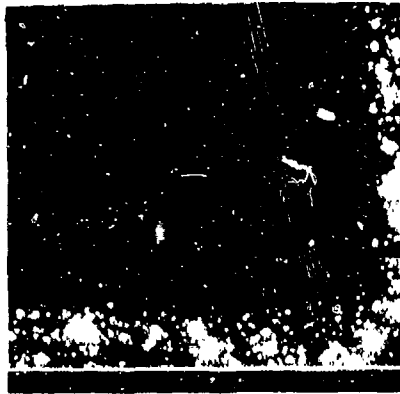
The water washing parameters were evaluated by visually comparing the photographs of the penetrant indications resulting from each test condition. Since it was found initially that the excess penetrant could be adequately removed by washing for 7 seconds at 40 psi and 70°F, the photographs of the penetrant indications resulting from the other washing conditions were compared to the 40 psi/70°F indications to determine if any overwashing occurred at the higher pressures and temperatures. The results of the investigation indicated that the specimens containing gross cracks could be washed using water pressures up to 90 psi and water temperatures up to 145°F without reducing the strength of the penetrant indications by overwashing (see Table 9).

The more open discontinuities, such as porosity, could be effectively washed without overwashing as long as the spray water was either 40 psi/70°F or 40 psi/100°F. Increasing the water pressure to 60 psi or the water temperature to 145°F reduced the strength of the penetrant indications as demonstrated in Figure 17.

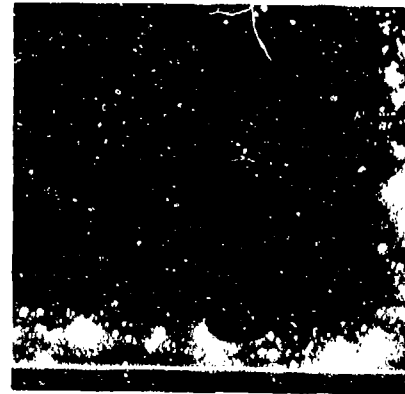
**TABLE 9**  
**ACCEPTABLE WASHING CONDITIONS**  
Post-Emulsifiable Penetrant System

Removal Method	Discontinuity Type	Acceptable Conditions
Spray Nozzle (Tri-Con-400501) for 7 Sec	Gross Cracks	40 psi - 70°F to 145°F 60 psi - 70°F to 145°F 90 psi - 70°F to 145°F
	Porosity	< 60 psi - 70°F to > 100°F but < 145°F
	Smaller, Tighter Cracks	40 psi - 70°F to 145°F 60 psi - 70°F to 145°F < 90 psi - 70°F to > 100°F but < 145°F
Immersion For 2 Min	Gross Cracks	70°F to 145°F
	Porosity	70°F to 145°F
	Smaller, Tighter Cracks	< 60 psi - 70°F to > 100°F but < 145°F

GP74-0117 168



40 psi - 70°F



90 psi - 145°F

GP/4 0117-109

**FIGURE 17**  
**DEGRADATION IN PFNETRANT INDICATIONS DUE TO**  
**OVER WASHING**  
(Post-Emulsifiable Penetrant System)

The specimens containing smaller, tighter cracks could be washed at all water pressure/water temperature combinations except 90 psi/145°F without overwashing.

Overwashing of small discontinuities was less of a problem with the immersion method than with the water spray method. There was no reduction in the penetrant effectiveness for porosity at 145°F compared with 70°F. In addition, the porosity penetrant indications were larger and more distinct after immersion washing as compared with spray washing. Presumably, the mechanical scrubbing action of the water spray removes some of the penetrant from the pores while the immersion method does not.

All of the specimens were washed for 2 minutes during the immersion tests in order to evaluate the water temperatures under equivalent washing times. However, it was found that the time required to wash excess penetrant from the specimen surfaces was a function of water temperature. At 70°F, 2 minutes were required; at 100°F, 45 seconds were required; and at 145°F, 30 seconds were required.

These test results bear out the importance of controlling the water washing parameters, even with a post-emulsifiable penetrant system. For example, if a production penetrant inspection were to be performed with the intent being to detect open, shallow discontinuities, such as porosity, the spray wash should be performed at a maximum water pressure which lies between 40 psi and 60 psi and at a maximum water temperature which lies between 100°F and 145°F.

(2) Water Washable Penetrant

An investigation was made of the effect of wash water pressure and temperature for the water washable penetrant system.

Tracer-Tech P-133 penetrant was used, which is equivalent in sensitivity to a MIL-I-25135, Group V penetrant. The penetrant was used with Tracer-Tech D499C nonaqueous wet developer. Based on the previous results, a penetrant dwell time of 20 minutes was used along with a penetrant bleed-out time of 15 minutes.

Specimens containing tight and gross cracks were used in the evaluation as well as porosity specimens. The penetrant testing was performed using the same equipment and techniques described above for the post-emulsifiable penetrant system.

As in the case of the post-emulsifiable penetrant system, the excess penetrant was adequately removed by washing for 7 seconds at 40 psi and 70°F. Consequently the photographs of the penetrant indications resulting from the other washing conditions were compared to the 40 psi/70°F indications to determine if any overwashing occurred at higher pressures and temperatures.

The results indicated that the specimens containing gross cracks could be washed using water pressures up to 90 psi and water temperatures up to 145°F without reducing the strength of the penetrant indications by overwashing (see Table 10).

**TABLE 10**  
**ACCEPTABLE WASHING CONDITIONS**  
(Water Washable Penetrant System)

Removal Method	Discontinuity Type	Acceptable Conditions
Spray Nozzle (Tri-Con-400501) for 7 Sec	Gross Cracks	40 psi - 70°F to 145°F 60 psi - 70°F to 145°F 90 psi - 70°F to 145°F
	Porosity	< 40 psi - 70°F to < 100°F
	Smaller, Tighter Cracks	40 psi - 70°F to 145°F 60 psi - 70°F to 145°F 90 psi - 70°F to 145°F <sup>△</sup>
Immersion For 2 Min	Porosity	70°F to < 100°F
	Gross Cracks	70°F to < 100°F
	Smaller, Tighter Cracks	70°F to < 100°F

<sup>△</sup> 145°F was acceptable for most cracks but for a few cracks 70°F was the maximum acceptable temperature

QP74 011 / 170

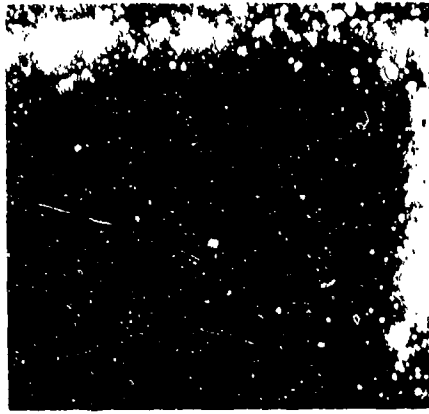
However, as might be expected, the porosity was much more susceptible to overwashing. Overwashing occurred when the water pressure was increased from 40 psi to 60 psi or when the water temperature was increased from 70°F to 100°F. The smaller, tighter cracks could be washed at water pressures of up to 90 psi and water temperatures of up to 145°F (in most cases) without overwashing occurring. Typical photographs of the results are shown in Figure 18.

The water washable penetrant system was quite sensitive to water temperature when the immersion technique was used. If the water temperature was increased from 70°F to 100°F, the excess penetrant was very difficult to remove, even with extended washing times. Several penetrant manufacturers were contacted concerning this situation and it was learned that most high sensitivity water washable penetrants are formulated such that washing at higher water temperatures is difficult. Apparently, this is overcome by scrubbing action during water spray removal.

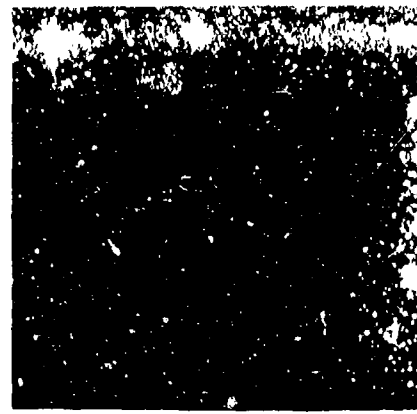
An investigation was made of the effect of washing time on subsequent penetrant indications. A few of the test panels containing the smaller, tighter cracks were spray washed as shown below:

<u>Specimen No.</u>	<u>Wash Water Pressure (psi)</u>	<u>Wash Water Temp. (°F)</u>	<u>Washing Time</u>
A	40	70	7 seconds
	40	70	60 seconds
B	40	70	7 seconds
	40	70	2 minutes
C	40	70	7 seconds
	40	70	3 minutes

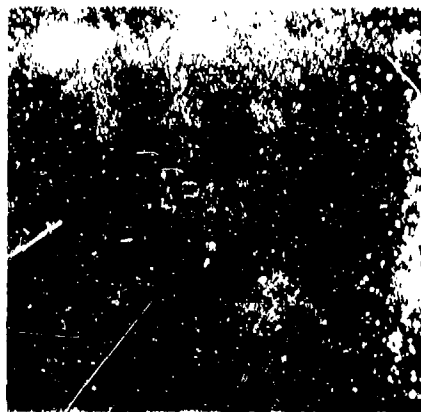
The cursory examination of the effect of washing time revealed that the smaller, tighter cracks could be washed for as long as 3 minutes at a water pressure of 40 psi and a water temperature of 70°F without any degradation in the strength of the penetrant indications (see Figure 19). However, extrapolation of these results to other discontinuity types should be done with caution. More open discontinuities, such as porosity, most surely would be more sensitive to washing time.



40 psi - 70°F



60 psi - 70°F



40 psi - 145°F

**FIGURE 18**  
**DEGRADATION IN PENETRANT INDICATIONS DUE TO**  
**OVER WASHING**  
(Water Washable Penetrant System)

GP74 0117 1/1

A separate test program was conducted in cooperation with and through the courtesy of the Magnaflux Corporation, Chicago, Illinois, in order to further study water washing parameters. The specimen types used for this study were four specimens with gross cracks, four specimens with tight cracks, and two specimens containing porosity. A MIL-I-25135, Group V fluorescent penetrant system was chosen for the investigation. Specifically, Magnaflux ZL-2A penetrant was used with Magnaflux ZP-9 nonaqueous wet developer. Limited additional work was done using Magnaflux ZP-4 dry powder developer and Magnaflux ZP-13A aqueous wet developer. The excess penetrant was removed in all cases with Magnaflux ZR-10 remover. A summary of the test parameters is shown in Table 11.

Initially, all specimens were vapor degreased for 16 hours as a cleaning method. Next, the specimens were immersed in the penetrant bath and allowed to dwell immersed for 5 minutes. Excess penetrant was removed by spraying ZR-10 remove solution onto the specimen surface at 70°F. In practice, the specimens were hand-held by clamps and oscillated up and down and from side-to-side in a spraying area which directed two remover/water streams at the front and rear of the specimens. The ZR-10 remover concentration was controlled by metering the remover into the wash water stream with a calibrated piston pump. After washing for the specified time, the specimens were dipped into clean water and immediately blown with compressed air to remove residual ZR-10 remover. Next, the specimens were force air dried for 3 minutes at 175°F before application of the developer. The ZP-9 nonaqueous wet developer was applied by aerosol can. Three or four passes were made over each surface. The development time was 10 minutes. The effect of varying the washing parameters was determined by measuring the brightness of selected penetrant indications with a Spectra Spot Meter, Model UB 1/4, manufactured by the Photo Research Division of Kollmorgen. The Spectra Spot Meter was used with the visual brightness filter supplied with the instrument in order to make the light meter closely follow the sensitivity of the eye. The brightness measurements were made while the specimens were illuminated with 3000 microwatts per cm<sup>2</sup> of ultraviolet light at the specimen surface as measured with the Ultraviolet Light Products Model J-221 light meter. The Spectra Spot Meter measures the visible



7 sec Wash Time



3 min Wash Time

**FIGURE 19**  
**EFFECT OF WATER WASHING TIME**  
(Spray Washing - 40 PSI/70°F)

GP/4 0117 1/2

**TABLE 11  
WASHING PARAMETERS**

Wash Time (sec)	Water Pressure (psi)	ZR-10 Remover Concentration (Volume %)
15	10	0.29 0.43
	25	0.00 0.10 0.29
	35	0.35 1.07
	40	0.29
60	10	0.29 0.43
	25	0.00 0.10 0.29
	35	0.35 1.07
	40	0.29
120	10	0.29 0.43
	25	0.00 0.10 0.29
	35	0.35 1.07
	40	0.29
300	10	0.29 0.43
	25	0.00 0.10 0.29
	35	0.35 1.07
	40	0.29

GP 74 0117 265

brightness of an area 1/60 inch in diameter. For the network of tight cracks, brightness measurements were made at the junction between cracks where the developed indications occupied approximately 10 to 25 percent of the viewing area. Approximately 16 measurements were made for each specimen and the readings were averaged. The gross crack indications occupied the entire viewing area and the porosity indications occupied from 50 to 100 percent of the viewing area. Approximately 6 measurements were made for each gross crack and the readings were averaged.

After the brightness measurements were made, the specimens were cleaned to remove all residual penetrant materials so that the specimens could be reprocessed using another set of washing parameters. The specimens were cleaned by perchlorethylene vapor degreasing for 30 minutes followed by ultrasonic cleaning with perchlorethylene for 10 minutes.

An examination of the indication brightness as a function of water pressure indicated that there was no significant overwashing for water pressures up to 40 psi. For the purposes of these tests a significant change in indication brightness is considered at least 20 percent change since this is approximately the smallest change which can be detected by the eye.

The effect of ZR-10 remover concentration on the indication brightness is shown in Table 12 for a 60 second wash time and 25 psi water pressure. The indication brightness decreased significantly where the remover concentration was increased from 0.35 volume percent to 1.07 volume percent. It should also be noted that the background fluorescence was easily removed with a concentration as low as 0.1 volume percent. These results indicate that machined parts can be properly processed with ZR-10 remover without overwashing but that the concentration of the ZR-10 remover is a factor that should be controlled.

The effect of spray time on indication brightness is demonstrated in Table 13. Each indication brightness value was arrived at by using a total of 4 specimens containing small cracks and 4 specimens containing gross cracks. For each of the 4 specimens containing small cracks, approximately 16 indication brightness measurements were made and an average for each specimen was computed. For each of the 4 specimens containing gross cracks, approximately 4 brightness measurements were made and an average was computed for each. Finally, a single value of indication brightness for that particular spray wash time was arrived at by adding the 8 average brightness values. It is this summation value that appears in Table 13. It can be seen that for the parameters chosen, the wash time did not appear to reduce the strength of the penetrant indications significantly.

i. Viewing Light Intensity

During inspection using fluorescent penetrant, the piece to be inspected is illuminated with ultraviolet light. The fluorescent dye in the discontinuities absorbs the black light and re-emits the energy in the visible light range. Consequently, the brilliance of the discontinuity indication varies with the intensity of the black light at the inspection area.

In order to study the effects of ultraviolet light versus background white light, tests were conducted in cooperation with and through the courtesy of the Magnaflux Corporation, Chicago, Illinois.

(1) Test Procedure

A test specimen containing porosity was used. The penetrant indications were produced by penetrant testing with Magnaflux ZL-2A post-emulsifiable fluorescent penetrant which is a MIL-I-25135, Group V penetrant. The porosity specimen was dipped into the penetrant and allowed to drain in air for 5 minutes. Excess penetrant was removed using Magnaflux ZR-10 remover injected into a water stream at a concentration of .29 volume percent, a water temperature of 170°F, and a wash water pressure of 25 psi. The ZR-10 remover was metered into the wash water stream by a calibrated piston pump. The wash time was 60 seconds and the water spray was approximately 90 degrees to the specimen surface. After spray washing, the specimen was dipped into clean water to remove excess ZR-10 and excess water was removed with compressed air. Next, the specimen was force air dried for three minutes at 175°F and Magnaflux ZP-9 nonaqueous wet developer was applied. After a development time of 10 minutes, brightness measurements were made.

The brightness measurements were made using a Spectra Spot Meter, Model UB 1/4, manufactured by the Photo Research Division of Kollmorgen. The Spectra Spot Meter was used with the visual brightness filter supplied with the instrument in order to make the meter light response closely follow the sensitivity of the eye (see Figure 20). Brightness measurements in the visible range were made on one of the penetrant indications under the following lighting conditions:

Background Visible Light (Foot Candles) 	Ultraviolet Light (Microwatts/cm <sup>2</sup> )	
Near Zero	1000	2000
3	1000	2000
6	1000	2000
14	1000	2000
20	1000	2000

 Includes the visible light from the ultraviolet lamp.

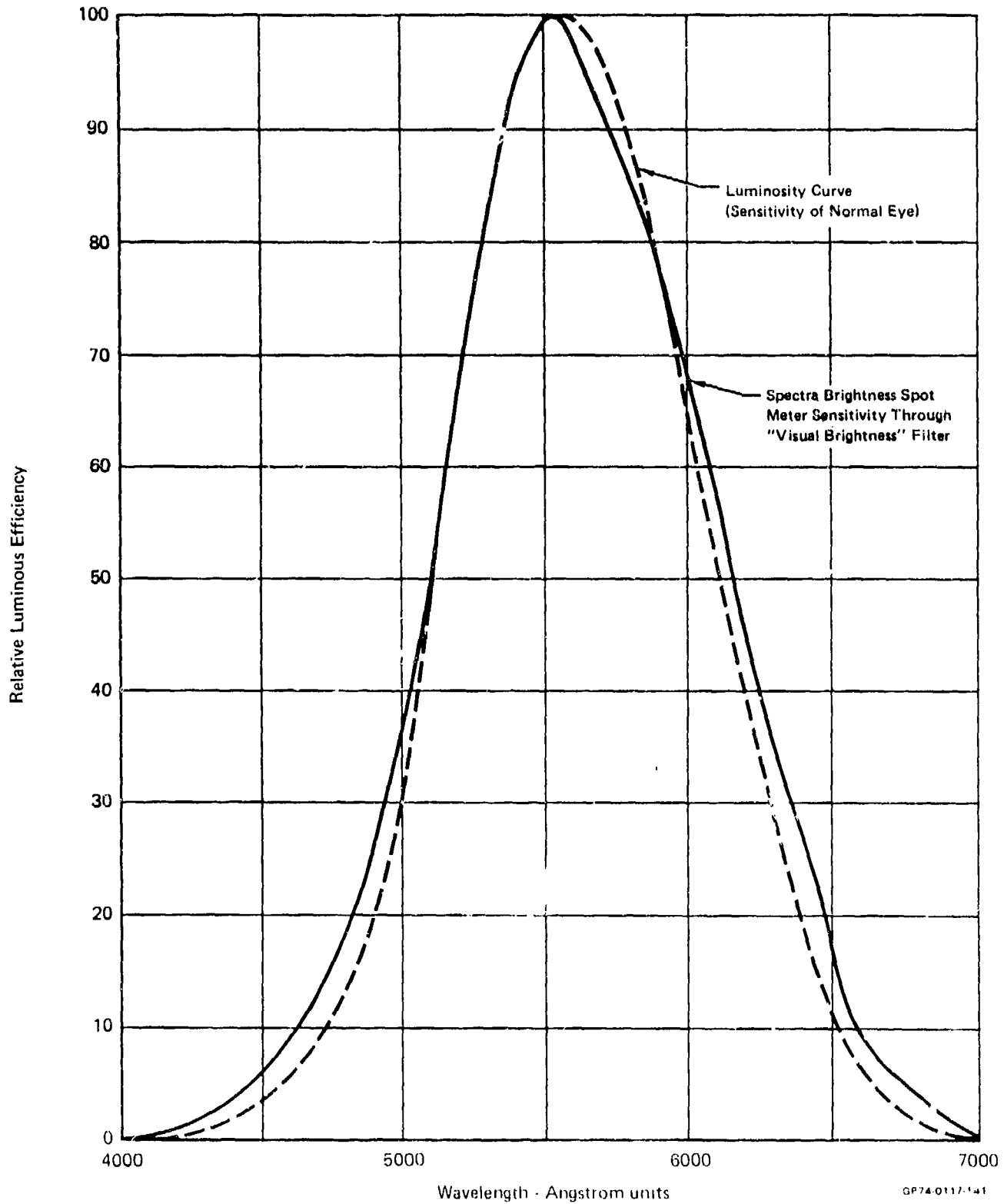


**FIGURE 20**  
LUMINOSITY CURVES

The background visible light level was increased or decreased by adding or removing lamps. The background light level was measured with the Spectra Spot Meter in conjunction with a magnesium oxide reflector plate. The ultraviolet light intensity was varied by changing the distance between the test specimen and the 100 watt mercury arc lamp. The ultraviolet light intensity was measured with an Ultraviolet Light Products Model J221 light meter. The Model J221 measures both the ultraviolet and infrared components of the light emitted by the mercury arc lamp. The infrared component was measured independently and was found to comprise approximately 5 percent of the total J221 reading at 15 inches from a 100 watt mercury arc lamp.

The measurements of the indication brightness were made by focusing the Spectra Spot Meter on a single indication. The actual area measured was 1/60 inch in diameter and the penetrant indication filled approximately 50% of the measured area. After measuring the indication brightness, the field of view was moved to an adjacent area away from any penetrant indication and the brightness of the developer background was measured. From this data, the ratio of indication brightness to background brightness was calculated. Obviously, high brightness ratios are desired.

The test results are plotted in Figure 21 and photographically demonstrated in Figures 22 and 23. It should be noted that, in Figures 22 and 23, the lines are scratches on the negative and are not penetrant indications. The importance of inspecting parts in a relatively dark inspection booth (less than 3 foot candles) is demonstrated. For a constant ultraviolet light intensity, the brightness ratio is reduced from approximately 65 to approximately 2.5 when the visible light level is increased from nearly zero to 3 foot candles. The visible light level has a much greater effect on the brightness ratio than does the ultraviolet light level. For example, at a constant visible light level of near zero increasing the ultraviolet light level from 1,000 to 2,000 microwatts only increases the brightness ratio from 62.1 to 68.6. However, at a constant 2,000 microwatts/cm<sup>2</sup> of ultraviolet light, decreasing the visible light level from 3 foot candles to nearly zero causes the brightness ratio to go from 2.8 to 68.6.

After the above testing was performed, similar experiments were conducted using a fatigue crack as a discontinuity. Magnaflux ZL-2 penetrant was again used and the specimen was dipped in the penetrant and allowed to drain in air for 10 minutes. Magnaflux ZE-3 emulsifier was applied for 30 seconds and excess penetrant was washed from the specimen using a Magnaflux P/N 3070 water spray nozzle. The water temperature was approximately 50°F and the water pressure was 30-40 psi. The specimen was dried for 2 minutes at 175°F in a circulating air oven. Finally, Magnaflux ZP-9 nonaqueous

Light Meter - Spectra Spot Meter, Model UB-1/4  
 Penetrant Indication Filled Approximately 50% of Measured Area

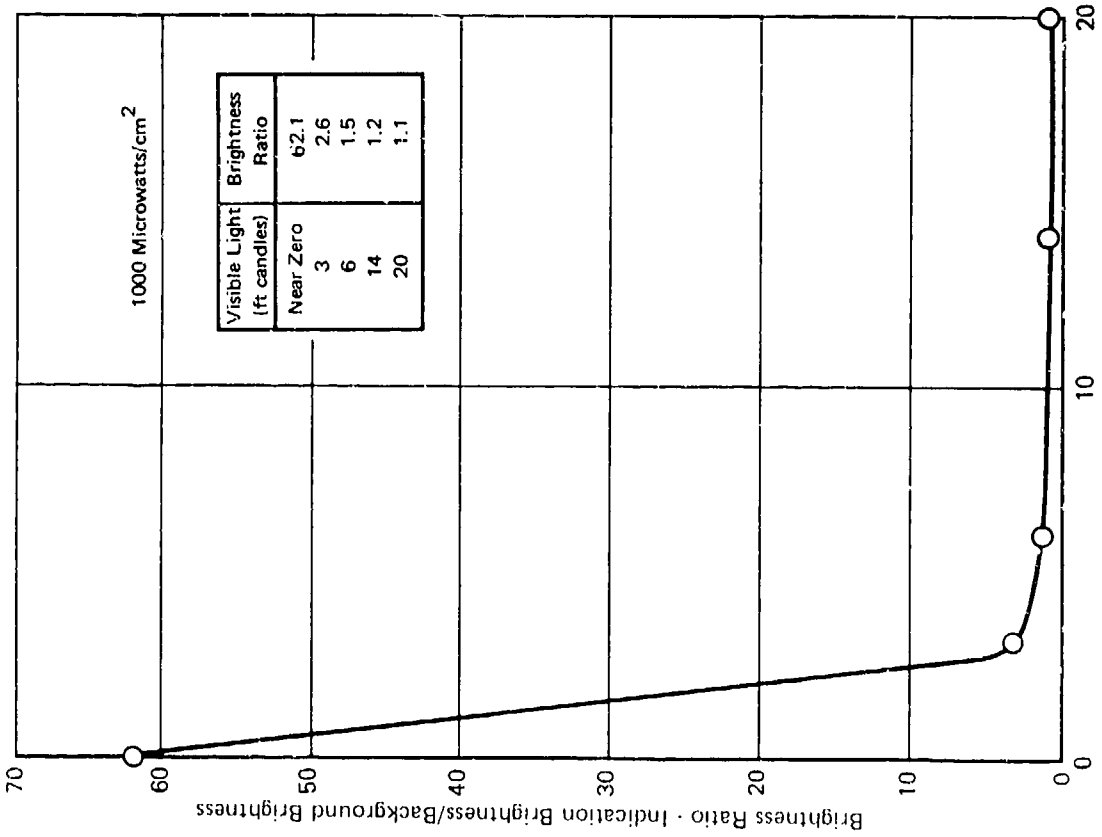
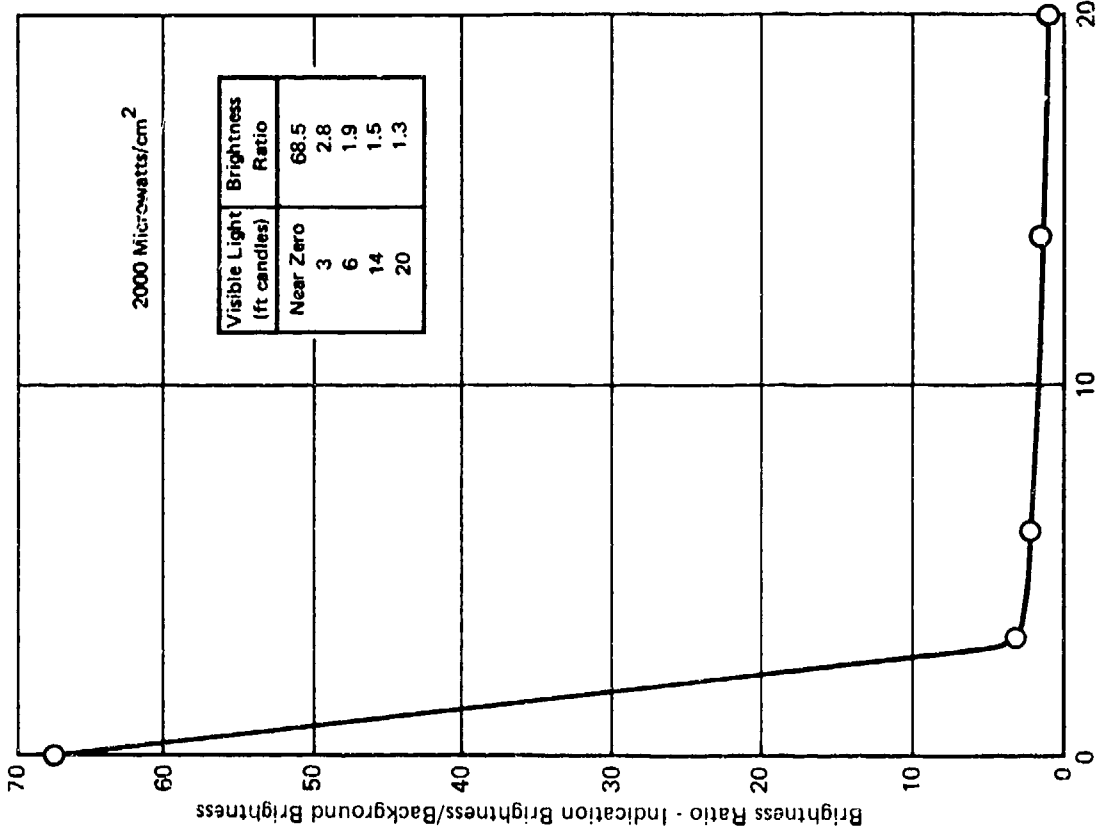
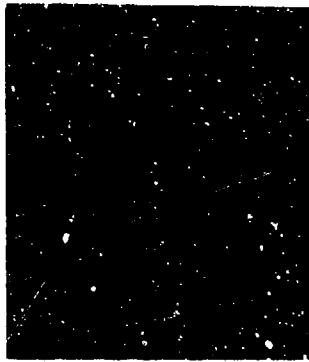
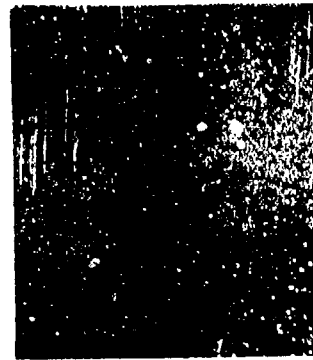


FIGURE 21

BRIGHTNESS RATIO AS A FUNCTION OF VISIBLE LIGHT AND ULTRAVIOLET LIGHT INTENSITY



Near Zero ft Candles



3 ft Candles



6 ft Candles

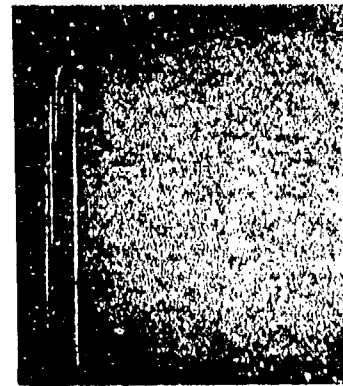
20 ft Candles

**FIGURE 22**  
**PENTRANT INDICATIONS UNDER VARIOUS LEVELS OF VISIBLE LIGHT**  
(Ultraviolet Light Level is 1000 Microwatts Per  $\text{cm}^2$ )

GP74-C 17-139



Near Zero ft Candles



3 ft Candles



6 ft Candles



20 ft Candles

**FIGURE 23**  
**PENETRANT INDICATIONS UNDER VARIOUS LEVELS OF VISIBLE LIGHT**  
(Ultraviolet Light Level is 1,000 Microwatts Per  $\text{cm}^2$ )

QP74-0117-138

**TABLE 12**  
**EFFECT OF REMOVER CONCENTRATION ON INDICATION BRIGHTNESS**

Flaw Type	Specimen No.	Indication Brightness (foot-lamberts)				
		0%	0.10%	0.29%	0.35%	1.07%
Gross Cracks	39	15.5	19.4	13.8	23.2	11.2
	40	36.8	36.6	44.2	33.0	16.1
	41	20.0	21.4	17.2	19.4	11.8
	42	38.0	34.8	36.7	27.1	15.7
Small Cracks	SC 29	10.4	8.2	8.9	13.6	4.3
	SC 32	10.0	7.4	6.4	11.5	2.6
	SC 33	10.0	8.6	7.5	12.6	4.5
	SC 34	14.0	11.8	10.9	14.3	3.9
Porosity	17P1	5.8	4.2	5.1	2.5	4.6
	17P2	39.0	37.4	37.2	32.0	5.6

GP74 0117-257

**TABLE 13**  
**EFFECT OF WASH TIME IN INDICATION BRIGHTNESS (FOOT-LAMBERTS)**

Penetrant	Developer	Water Pressure (psi)	Remover Concentration (Vol %)	Wash Time (sec)				
				15	60	120	300	
ZL-2A	ZP-9	25	0.01	127	148	155	111	
			0.29	179	201	188	177	
		10	0.43	156	202	124	146	
			1.07	76	70	67	63	
	ZP-4	25	0.29	78	90	63	55	
		ZP-13	25	0.29	39	43	42	36
		ZP-13A	25	0.29	24	20	23	22
ZL-22A	ZP-9	25	0.29	218	280	228	264	

GP74 0117-256

**TABLE 14**  
**BRIGHTNESS MEASUREMENTS MADE ON FATIGUE CRACK**

Ultraviolet Light Intensity (microwatts per cm <sup>2</sup> )		Ambient Light Intensity (foot candles)		
		0	2 1/2	5
500	A	1.62	3.8	5.9
	B	0.115	1.7	5.3
	C	14.1	2.2	1.1
920	A	3.0	4.9	6.9
	B	0.21	2.0	5.5
	C	14.3	2.5	1.25
1300	A	4.2	6.1	8.1
	B	0.30	2.1	5.6
	C	14.4	1.9	1.4
3500	A	11.2	12.1	13.2
	B	0.8	2.3	6.1
	C	14.0	5.3	2.2
6450	A	19.0	19.7	20.5
	B	1.15	2.5	6.5
	C	16.5	7.9	3.1
7900	A	20.0	21.8	23.5
	B	1.3	2.7	6.8
	C	15.5	8.0	3.5

- A - Brightness of crack indication in foot-Lamberts
- B - Brightness of background in foot candles
- C - Ratio of indication brightness and background brightness

GP74-0117 114

wet developer was applied. After a 10 minute development time, brightness measurements were made.

The Spectra Spot Meter was used to take the brightness measurements at several ultraviolet and background visible light values. The crack indication filled about 1/16 of the measured area. For these tests, a single brightness measurement was made for each condition. The results are shown in Table 14 and plotted in Figure 24. As before, the importance of low background light levels is demonstrated. The data in Table 14 also demonstrates that by increasing the amount of ultraviolet light a greater amount of ambient white light intensity can be tolerated without any loss in brightness ratio.

#### j. Effect of Mechanical Processing Prior to Penetrant Inspection

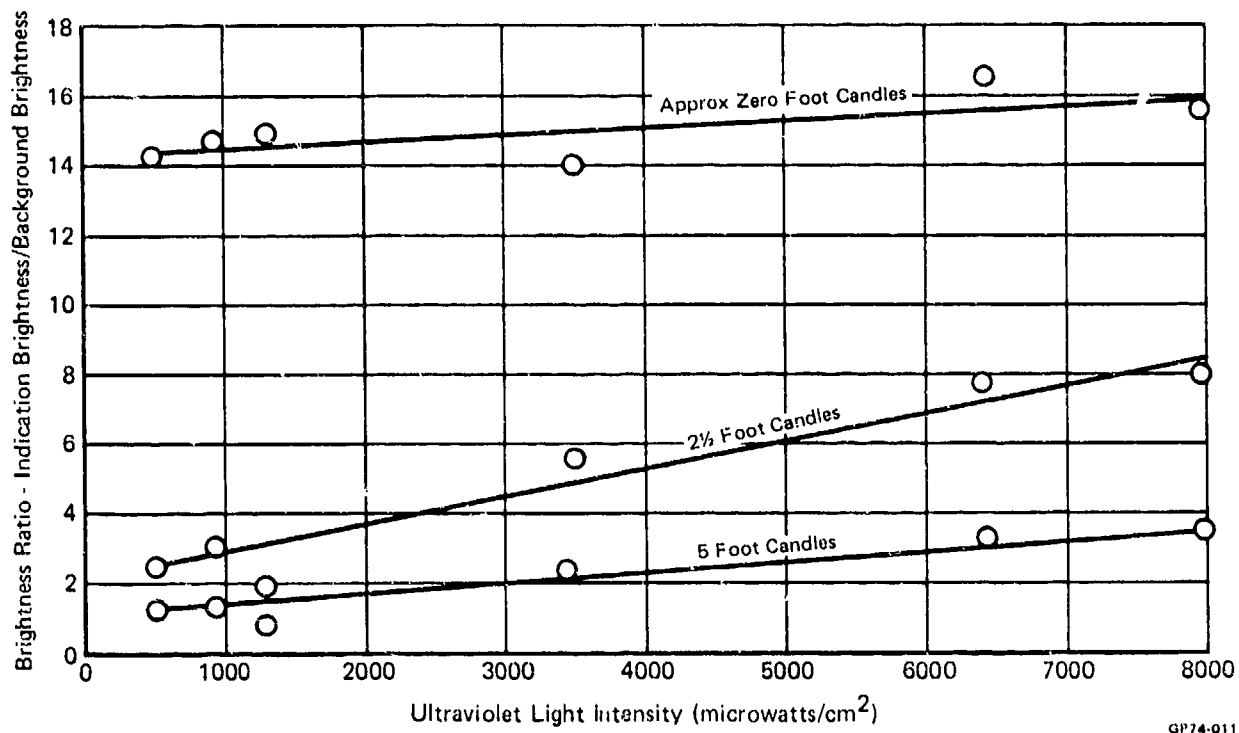
Penetrant inspection can be an effective inspection method only if the discontinuities are open to the surface so that penetrant can enter the discontinuity. Any process which closes the discontinuity can destroy the reliability and resolution limits of the subsequent penetrant inspection; such "masked" discontinuities may go completely undetected. Some mechanical processing operations performed prior to penetrant inspection may mask discontinuities by causing surface material to plastically deform, flow over and seal discontinuities. Consequently, a program was conducted to identify several of the detrimental processes.

The mechanical processes investigated were glass bead peening, grinding, face milling, rotary filing, disc sanding, and shot peening. The glass bead peening was performed using MIL-G-9954, Size 13 glass beads. A nozzle pressure of 70 psi was used and each specimen was peened for 30 seconds.

The grinding was performed on a production surface grinder. The 1 inch wide, 9 inch diameter silicon carbide grinding wheel was 60 grit with J hardness. The work piece was flooded with Macco 472 coolant (1 to 30 mixture). The test specimens were ground using a wheel speed of approximately 4,200 surface feet per minute. Initially, three passes were made to remove 0.0005 inch per pass and, finally, several passes were made to remove 0.0002 inch per pass such that a total of 0.003 inch was ground from the surface.

Face milling was performed with a 5 inch diameter carbide insert face mill. The cuts were made perpendicular to the cracks in the specimens. Macco 472 coolant was used at a mixture of 1 to 30.

Rotary filing was accomplished using a 3/4 inch diameter x 1 inch long high speed steel cutter at approximately 8000 rpm to remove approximately 0.001 inch of material.



GP74-0117-115

**FIGURE 24**  
**BRIGHTNESS RATIO AS A FUNCTION OF VISIBLE LIGHT AND**  
**ULTRAVIOLET LIGHT INTENSITY (FATIGUE CRACK)**

The disc sanding was performed with 80 grit, 2 inch diameter aluminum oxide sanding discs at 1200 to 1500 rpm.

Shot peening was performed using No. 330 steel shot and a nozzle pressure of 20 psi. Each specimen was shot peened for approximately 30 seconds.

The specimen types used to study each process are indicated below.

<u>Process</u>	<u>Specimen Type</u>	<u>Number of Specimens</u>
Face Milling	Gross cracks	7
Glass Bead Peening	Gross cracks	7
	Tight cracks	7
Grinding	Gross cracks	7
Rotary Filing	Gross cracks	7
Disc Sanding	Gross cracks	7
Shot Peening	Gross cracks	7
	Tight cracks	7

These crack types are the same as those previously described in Section 1-6.

The schematic shown in Figure 25 is representative of the test procedure used to investigate the effect of each process. The photographs of the penetrant indications were compared both before and after the mechanical process. If the strength of the penetrant indications were reduced by the particular mechanical process, the specimens were pickled to remove surface metal and re-penetrant inspected. This was repeated until the penetrant indications returned to full strength.

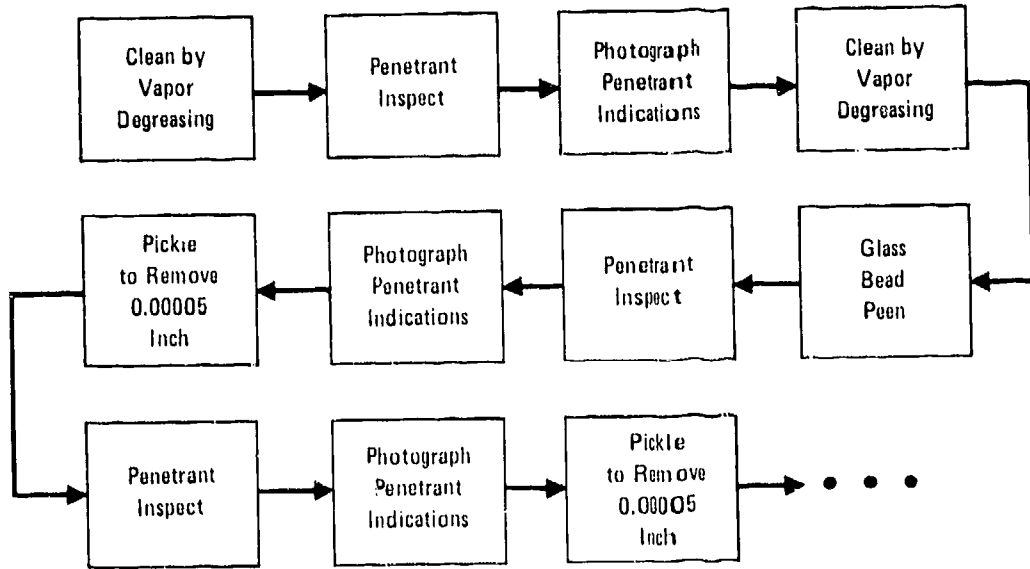


**FIGURE 25**  
**REPRESENTATIVE TEST PROCEDURE**

GP74-0117-137

Each penetrant inspection was performed using Tracer-Tech P-133 fluorescent penetrant, equivalent in sensitivity to a MIL-I-25135, Group V penetrant. The developer used was Tracer-Tech D499C nonaqueous wet developer. Based on the previous program results, a penetrant dwell time of 20 minutes was used and a developer dwell time of 15 minutes was used. The specimens were completely immersed in the penetrant during the applicable penetrant dwell. Excess penetrant was washed from the specimens using a Tri-Con 400501 water spray nozzle; the wash water temperature was approximately 40 psi. Each specimen was washed until the specimen surface was visually clean under 200 microwatts/cm<sup>2</sup> of ultraviolet light (approximately 3200 to 3800 Angstrom units in wavelength) which took approximately 15 seconds. Next, the specimens were dried until visually dry (10-15 minutes) in a circulating air oven at 170°F. After the bleed-out time, the penetrant indications were photographed using the following parameters: approximately 1000 microwatts per cm<sup>2</sup> of ultraviolet light, 25 second exposure at f9, Royal Pan Film, Tiffen Yellow No. 2 filter.

The results of the investigation are tabulated in Table 15 and demonstrated in Figures 26 and 27. As might be expected, the effect of mechanical processing varied as a function of the process and crack size. The most detrimental processes were glass bead and shot peening. Nearly all the penetrant indications were obliterated by these two processes. Face milling, grinding, and rotary filing were much less severe; but, even so, the strength of the penetrant indications were reduced. It should be kept in mind that these processes were used only on gross cracks. Disc sanding had no effect on the gross cracks (tight cracks were not used to evaluate disc sanding).

The test results also demonstrate that the detrimental effects of certain processes performed prior to penetrant inspection can be alleviated by chemical etching. The amount of material that need be removed by etching varied from 0.0002 inch to more than 0.0017 inch, depending upon the process (see Table 15). Based upon these results, production parts which have undergone processing such as grit blasting should be etched prior to penetrant inspection.

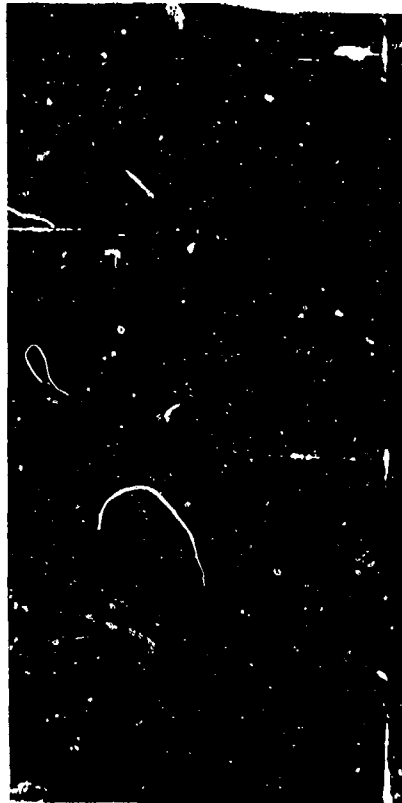
TABLE 15  
EFFECT OF MECHANICAL PROCESSING PRIOR TO PENETRANT INSPECTION

Mechanical Process	Etching Required to Restore Indications (In.)	
	Gross Cracks	Small Cracks
Disc Sanding	No Effect	--
Face Milling Grinding Rotary Filing	0.0002	
Glass Bead Peening	0.0007 $\triangle$	More than 0.0012 $\triangle$
Shot Peening	0.0007 $\triangle$	More than 0.0017 $\triangle$

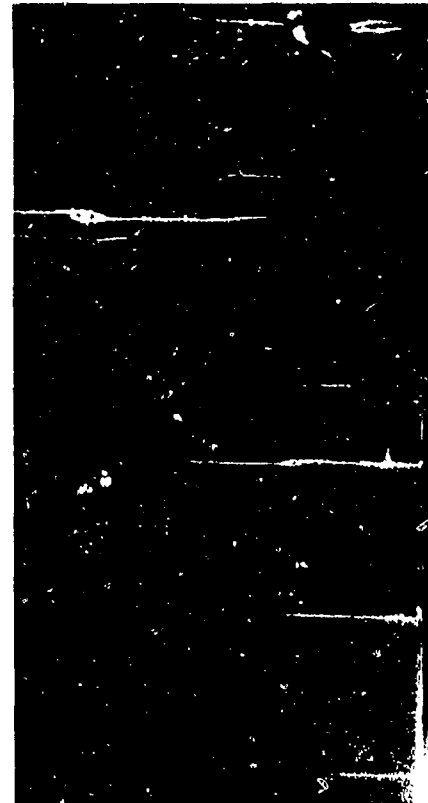
$\triangle$  All penetrant indications were totally obliterated  
 $\triangle$  Most penetrant indications were obliterated



Initial  
Indications



After  
Shot Peening



After  
Etching 0.0017

**FIGURE 26**  
**EFFECT OF MECHANICAL PROCESSING UPON PENETRANT INDICATIONS**  
**OF TIGHT CRACKS**

GP/4 0117 136



Initial  
Indication



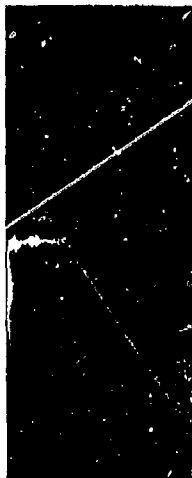
After  
Peening



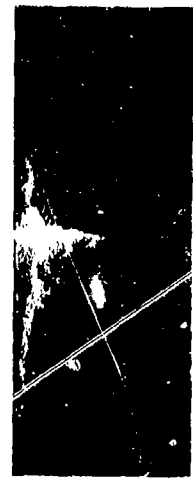
After  
Etching 0.0007



Initial  
Indication



After  
Grinding



After  
Etching 0.0002

**FIGURE 27**  
**EFFECT OF MECHANICAL PROCESSING UPON PENETRANT INDICATIONS**  
**OF GROSS CRACKS**

GP74 0117 1:34



Initial  
Indication



After  
Milling



After  
Etching 0.0002



Initial  
Indication



After  
Rotary Filing



After  
Etching 0.0002

**FIGURE 27 (Continued)**  
**EFFECT OF MECHANICAL PROCESSING UPON PENETRANT INDICATIONS**  
**OF GROSS CRACKS**

CP74 0117 133

#### k. Penetrant System Effectiveness

A summation of the overall relative effectiveness of the various penetrant systems is presented in Table 16. The ranking of systems is based upon the studies of penetrant bleed-out times, penetrant dwell times, emulsification times, developer effectiveness, and water washing techniques discussed previously. These summaries are predicted on the assumption that it is desirable to be able to detect gross cracks, smaller cracks, and porosity in the same penetrant inspection. For example, if a MIL-I-25135, Group V sensitivity post-emulsifiable penetrant was chosen for a typical production penetrant inspection in which a variety of discontinuities has to be detected, then, for the most effective inspection, either a nonaqueous wet or a dry powder developer should be used, the penetrant dwell time should be at least 20 minutes, and the penetrant bleed-out time should be at least 5 minutes (see Table 16).

No effort was made during this investigative program to compare the effectiveness of a post-emulsifiable penetrant system with that of a water washable penetrant system and Table 16 should not be used to this end. It was felt that in order to make a comparison, a large number of systems would have to be compared and this was outside the scope and intent of the program.

**TABLE 16  
RELATIVE EFFECTIVENESS OF PENETRANT SYSTEMS**

<b>High Sensitivity Water Washable System</b>	
<b>Best</b>	Nonaqueous or Dry Developer * Penetrant Dwell Time = 10 min Spray Washing - Maximum Water Pressure Between 40 and 60 psi Maximum Water Temperature Between 70 and 100°F Immersion Washing Maximum Water Temperature - Between 70 and 100°F * Penetrant Bleed-Out Time = 5 min
<b>Second Best</b>	No Developer * Penetrant Dwell Time = 20 min * Penetrant Bleed-Out Time = 1 min
<b>Third Best</b>	Aqueous Developer * Penetrant Dwell Time = 20 min * Penetrant Bleed-Out Time = 1 min
<b>Post-Emulsifiable System</b>	
<b>Best</b>	Nonaqueous or Dry Developer * Penetrant Dwell Time = 20 min Emulsification Time = Less than 3 min Spray Washing - Maximum Water Pressure - Between 40 and 60 psi Maximum Water Temperature - Between 100 and 145°F Immersion Washing Maximum Water Temperature - Between 100 and 145°F * Penetrant Bleed-Out Time = 5 min
<b>Second Best</b>	No Developer * Penetrant Dwell Time = 20 min * Penetrant Bleed-Out Time = 1 min
<b>Third Best</b>	Aqueous Developer * Penetrant Dwell Time = 20 min * Penetrant Bleed-Out Time = 1 min

\* Specified times are recommended minimum times

QP74 0117 1/3

## 2. RADIOGRAPHIC METHOD

Two of the most important parameters in the radiographic method are the choice of kilovoltage and beam spectrum. There is a wide range of kilovoltages that can be selected to yield the same apparent test sensitivity when the image quality is evaluated by the use of penetrameters such as the plaque type shown in MIL-STD-453. However, if the selected kilovoltage is too high, the subject contrast may be so low as to render the test ineffective, even though the MIL-STD-453 penetrameter indicates that the quality of the radiograph is acceptable. Consequently, data are necessary to aid in the establishment of maximum acceptable kilovoltages as a function of material thickness and subject contrast and definition quality.

A test program has been conducted to determine the kilovoltages required to obtain varying levels of contrast sensitivity. The effect of beam spectrum was investigated by using three types of X-ray machines (full wave rectified, self-rectified, and constant potential) with varying inherent filtration.

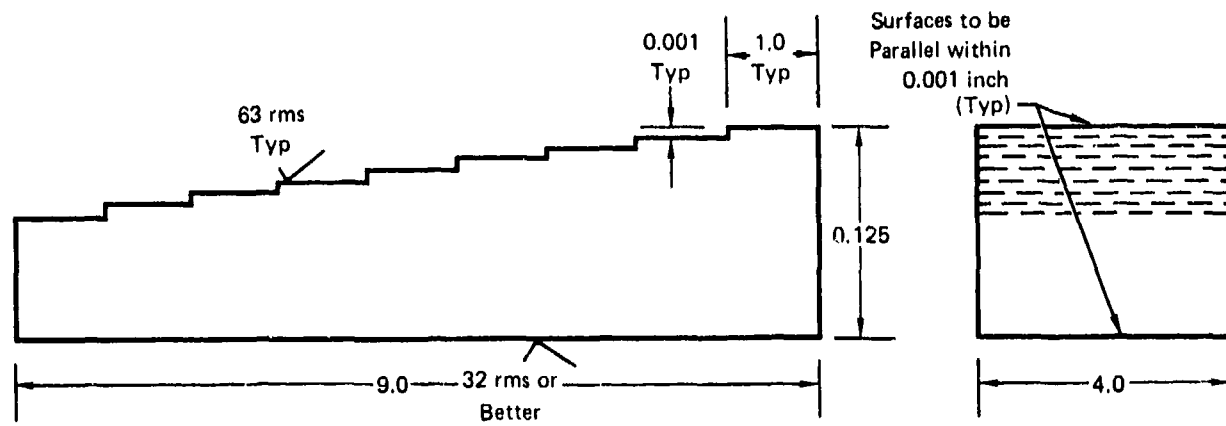
### a. Fabrication of Step Wedges

Nine step wedges were fabricated from Ti-6Al-4V plate for use in the program. The step wedges were designed to represent a 1/2%, 1%, and 2% thickness change for a total thickness of .125, .50, 1.00, 2.00, and 4.00 inches. The configuration of these specimens is shown in Figure 28. As can be seen below, the effect of surface finish was also taken into account.

<u>Configuration</u>	<u>Thickness</u>	<u>Surface Finish</u>
A	0.125	63 RMS
B	0.25	125 RMS
B	0.50	63 RMS
B	0.50	125 RMS
B	1.00	63 RMS
B	1.00	125 RMS
B	2.00	63 RMS
B	2.00	125 RMS
C	4.00*	63 RMS

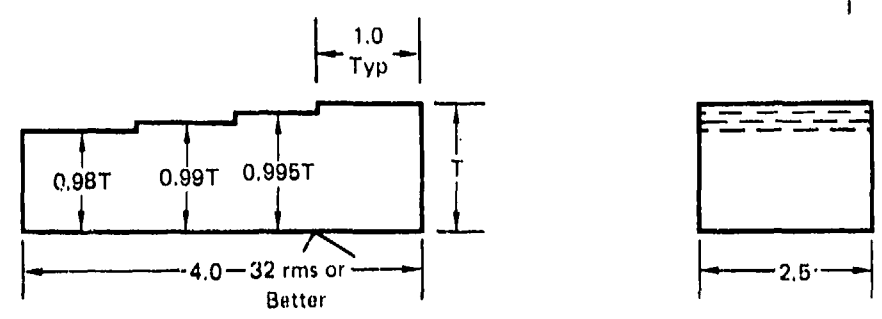
\* Two inch specimen used with a 2 inch thick shim.

The thickness changes of 1/2%, 1%, and 2% were chosen because contrast sensitivities of 1% and 2% are commonly used in radiographic inspection of airframe components. A 1/2% thickness change was included to determine if a greater than normal contrast sensitivity could be achieved. The width of the step wedges was chosen to reduce the effect of undercutting at the edges during the exposures. A density gradient across the steps could occur on the film if the step wedge width was too small.

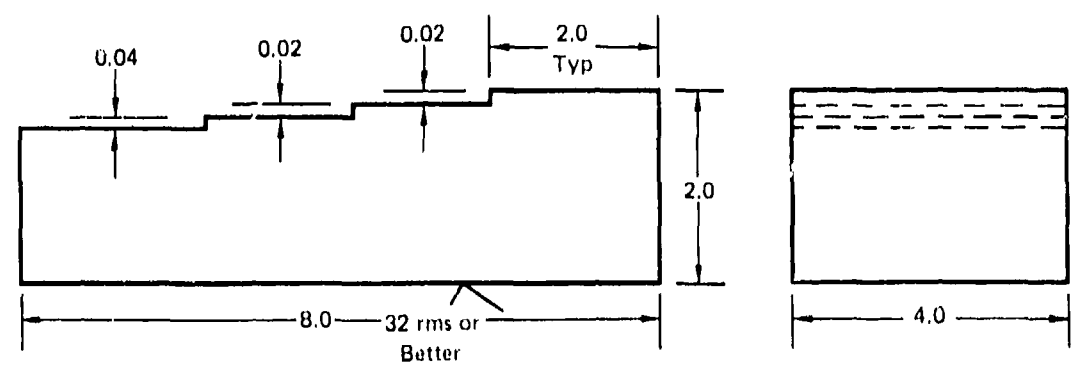


Configuration A.

	T
63 rms	0.50, 1.00, 2.00
125 rms	0.50, 1.00, 2.00



Configuration B



Note: Each step must be parallel to the other steps within 0.0005 inch.

Configuration C

QP74 0117 132

**FIGURE 28**  
**RADIOGRAPHIC TEST SPECIMENS**

The step wedges were machined in a lathe. The wedges were rotated in a slow rate and the cutting tool was held stationary. Initially, the work was attempted on a milling machine but the cutting tool was dulled by the back tracking of the tool over the surface to be cut causing the step to be out of tolerance in terms of surface finish.

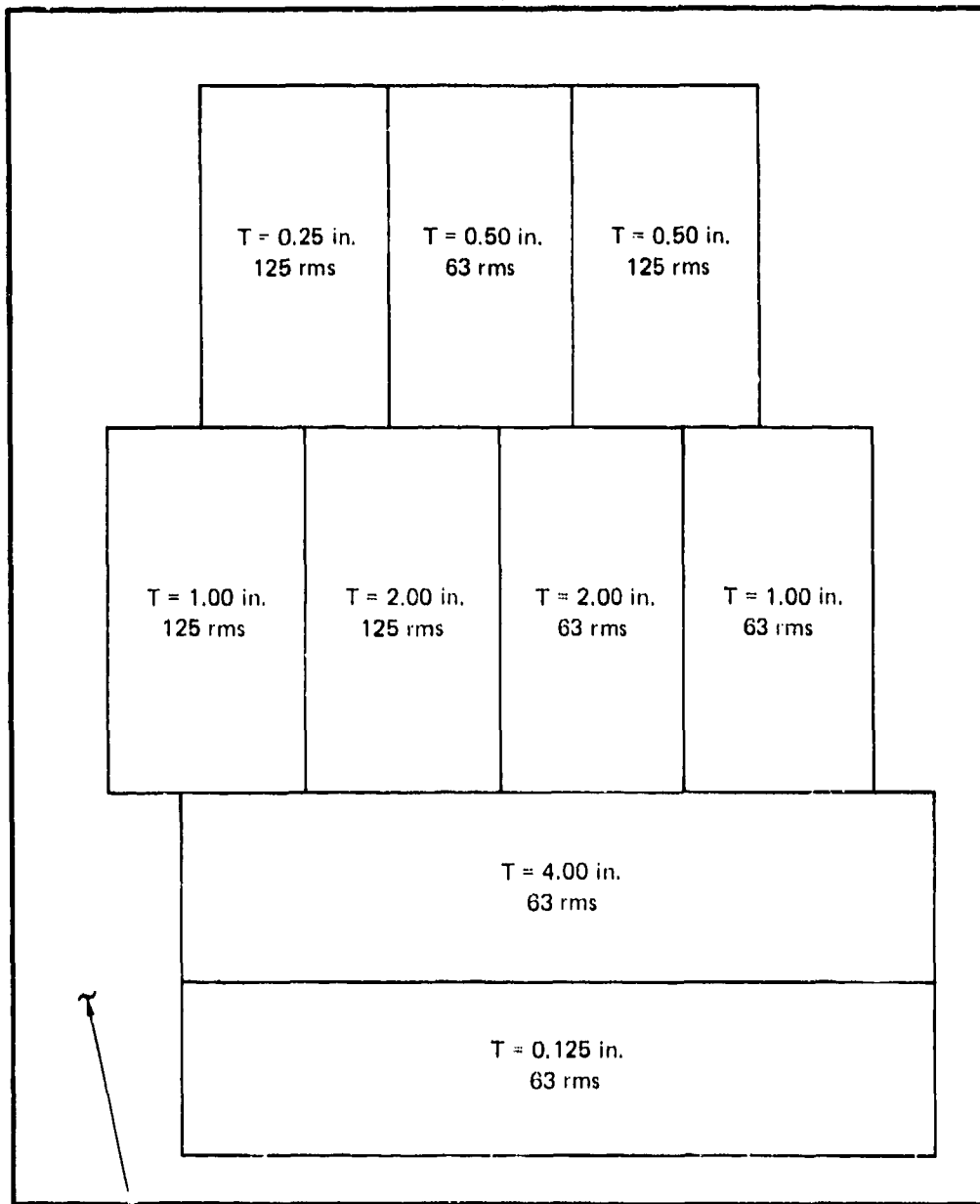
b. Testing

The 9 step wedges were set up for each exposure on the film cassette as shown in Figure 29. A plumb line was used to locate the focal spot directly over the center of the set-up. Cardboard cassettes were used for exposures made at voltages over 50 KV and blackened exposed film was used as film cassettes for those exposures made at voltages of 50 KV and lower. Blackened exposed film was used below 50 KV because previous experience has indicated that mottling of the image can occur at these voltages when paper or cardboard cassettes are used. A lead sheet, 1/8 inch thick, was used to back up the film cassette. Gevaert D7 (ASTM Class II) film was used for all the exposures. Since it is known that the intensity of the X-ray beam varies from one side of the beam cone to the other, the heel side of the beam cone was positioned the same for each exposure. Lead screens were used, depending upon the voltage, as described below:

<u>KV</u>	<u>Front Screen Thickness (Inches)</u>	<u>Back Screen Thickness (Inches)</u>
Up to 100 KV	None	0.010
100 KV to 200 KV	0.005	0.010
200KV to 300 KV	0.010	0.010
300 KV and greater	0.010	0.020

These screen combinations are typical for a production radiographic inspection. Prior to exposure, titanium 2% penetrameters (MIL-STD-453) were placed on each step of the test specimens (Figure 30). A focal spot-to-film distance of 72 inches was used for each exposure. This resulted in a geometric unsharpness of .005 inch or less for all the radiographs except at the 4 inch step wedge for exposures made with the Isovolt 400 where the geometric unsharpness is .0088 inch. Exposures were made using the kilovoltage/milliamp-minute combinations shown in Table 17. Exposures of 16 and 64 milliamp-minutes were chosen in order to yield a sufficient number of section thicknesses with film density between 0.5 and 3.5 H&D for evaluation. For the lower kilovoltages, longer exposures (96 and 240 milliamp-minutes) were also investigated to help determine if the increase in contrast warrants the longer exposure times and to determine the upper titanium thickness limits which exist for each kilovoltage. To ensure reproducibility, the chosen exposure time was never less than 1 minute. One minute exposures compensated for transient line voltage fluctuations as well as variations in the rate of increase of the X-ray beam to full power from one exposure to the next. Each exposed film was processed automatically in a Kodak Model B X-OMAT using Gevaert G135N developer and G334N fixer.

Heel of X-Ray Beam Here



14 x 17 in. Gevaert D7 Film (ASTM Class II)

GP74-0117 131

**FIGURE 29**  
**TEST SPECIMEN ARRANGEMENT**

**TABLE 17**  
**EXPOSURE CONDITIONS**

**G.E. OX 140**  
(Full Wave Rectified)  
2.5 mm Focal Spot)  
Inherent Filtration  
Pyrex Plus Oil  
(Equivalent to 0.06 mm Cu)

KVP	MA	Time	MAM
30	10	1 min 36 sec	16
30	10	6 min 24 sec	64
40 $\Delta$	10	25 min	250
50	10	1 min 36 sec	16
50	10	6 min 24 sec	64
70	10	1 min 36 sec	16
70	10	6 min 24 sec	64
100 $\Delta$	3	1 min	3
100	8	2 min	16
100	8	8 min	64
120 $\Delta$	1	45 sec	3/4
120	5	3 min 12 sec	16
120	5	12 min 48 sec	64

**Phillips PG-300**  
(Self Rectified  
2.3 mm Focal Spot)  
Inherent Filtration - 0.3 mm  
Cu Plus 3 mm Al  
(Equivalent to 0.4 mm Cu)

KVP	MA	Time	MAM
70	3	5 min 18 sec	16
70	3	21 min 18 sec	64
90	3	5 min 18 sec	16
90	3	21 min 18 sec	64
140	4	4 min	16
140	4	16 min	64
160	4	4 min	16
160	4	16 min	64
180	4	4 min	16
180	4	16 min	64
200	4	4 min	16
200	4	16 min	64
250	4	4 min	16
250	4	16 min	64

**Siefert Isovolt 400**  
(Constant Potential  
4.0 mm Focal Spot)  
Inherent Filtration  
4.5 mm Cu

KVP	MA	Time	MAM
100 $\Delta$	8	5 min	40
100 $\Delta$	8	12 min	96
100 $\Delta$	8	30 min	240
120	8	2 min	16
120	8	8 min	64
140	8	2 min	16
140	8	8 min	64
160	8	2 min	16
160	8	8 min	64
180	8	2 min	16
180	8	8 min	64
200	10	1 min 36 sec	16
200	10	6 min 24 sec	64
250	10	1 min 36 sec	16
250	10	6 min 24 sec	64
300	10	1 min 36 sec	16
300	10	6 min 24 sec	64
350	10	1 min 36 sec	16
350	10	6 min 24 sec	64
380	8	2 min	16
380	8	8 min	64

$\Delta$  Both D4 and D7 film was used.

GP74-0117-120



GP/4 0117 130

**FIGURE 30**  
**STEP WEDGES WITH MIL-STD-453 PENETRAMEters**

Prior to processing any lot of film, one unexposed film was run through the automatic processor and the film density was subsequently measured in order to check that the processor was operating properly and that the radiographic film was not outdated or exposed due to improper storage facilities. Records were made of the time of day and date of each exposure to check any effect of line voltage fluctuations due to the plant workload. Also, the temperature of the processing solutions was recorded.

For each radiograph where the density was between 0.5 and 3.5 H&D, the density was measured in the center of the penetrometer image and in the center of the step image adjacent to the penetrometer. The measurements were made in these locations to avoid the effects of undercutting at the edges of the step wedges on the film. Density measurements were made with a Meebold Quantalog Densitometer, Model TD 100A calibrated with film density strips provided by Gevort. This instrument has an accuracy of  $\pm .02$  H&D.

In order to determine the effect of kilovoltage on contrast sensitivity, the density data for a particular thickness change were normalized to an overall film density of 2.00 by using the characteristic curve to arrive at the log relative exposure (LRE). A film density of approximately 2.00 H&D is usually used in industrial radiography since the X-ray film characteristic curves are linear in this density range and the film behavior is quite predictable. Also, X-ray film illuminators have sufficient intensity such that viewing of films with density of approximately 1.0 to 3.0 H&D can be accomplished.

The LRE for each film density was determined from the characteristic film curve and the difference in LRE for various thickness changes were calculated. By applying this difference in LRE to the LRE for a 2.0 H&D density, the LRE differences are normalized and the true exposure change and/or contrast can be determined. Thus it was not necessary for each film to have the same nominal density in order to make comparisons.

An example of the use of log relative exposure is shown in Figure 31. For this hypothetical example, the difference in the log relative exposure was .021 for 160 KV and .025 for 120 KV. Since the difference in log relative exposure is greater for the lower kilovoltage, it could be concluded from this data that greater subject contrast was attained with the lower kilovoltage. The data, however, did seem to substantiate the use of lower kilovoltage/higher contrast techniques. Table 18 is a list of penetrameter contrast and the minimum detectable hole size for that penetrameter for all data points falling in a film density range of 1.5 to 2.5 H&D. No differentiation was made between instruments or specimen surface finish as in the collection of these data points. It can be seen that

- (1) In general, as the kilovoltage becomes lower for a given thickness, the hole resolution increases and the contrast is increased.
- (2) It is far easier to achieve a 2-1T image quality in large section thicknesses and therefore the penetrameter's role as an image quality indicator diminishes.
- (3) Data of this type could be used to plot 1T or 2T or 4T resolution as a function of kilovoltage and section thickness.
- (4) Apparent differences in penetrameter thicknesses or material types exist. As an example, the hole resolution for .50 inch thick sections was as expected for the 100, 120, and 140 kilovoltage exposures but was not as expected at the 160 kilovoltage. This could be explained by an inadvertent exchange of one penetrameter with another - each having the same identification as to type and material.

**TABLE 18  
CONTRAST AND RESOLUTION AS A FUNCTION OF  
KILOVOLTAGE AND THICKNESS**

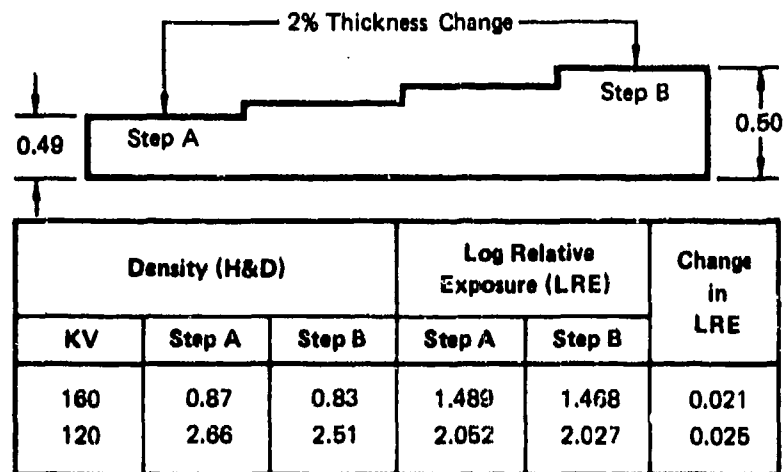
Kilovoltage	Thickness (in.)					
	0.12	0.25	0.50	1.0	2.0	4.0
70	1/0.08 1/0.11 1/0.10	1/0.10				
90	2/0.06	2/0.05				
100	2/0.06 2/0.04 2/0.05	2/0.06 2/0.04	1/0.10 1/0.10			
120		2/0.04 4/0.02	2/0.10 2/0.02 2/0.02 2/0.08			
140			4/0.03 4/0.02	2/0.07 2/0.07 2/0.04		
160			2/0.04 2/0.04	1/0.08 1/0.14		
180				2/0.09 2/0.03 2/0.04		
200				2/0.02 2/0.01 2/0.04		
250					1/0.10	
300					1/0.08 1/0.08	1/0.10
350						1/0.12
380						1/0.10

Code X/Y

X = Smallest penetrometer hole resolved.

Y = Difference in density between penetrometer and adjacent area.

GP74 011/316



GP74-0117-292

**FIGURE 31**  
**LOG RELATIVE EXPOSURE USED TO EVALUATE THE DATA**

Analysis of the actual data taken in the program indicated that the data were inconclusive in terms of arriving at the relationship between contrast and kilovoltage. The chosen thickness changes (1/2%, 1%, and 2%) were so small that the density differences were in the range of scatter of the densitometer instrument measurements.

Although it was not known at the time of these tests, variations in penetrameter thickness may have also contributed to the data scatter.

A small internal program has revealed a problem with using the plaque-type penetrameter as an image quality indicator. It has been found that there can be a significant effect of the difference in penetrameter thickness for MIL-STD-453 penetrameters. A titanium weld assembly was radiographed using a certain MIL-STD-453 penetrameter. It was subsequently necessary to radiograph the part again and a second MIL-STD-453 penetrameter was used. A difference was noted in the radiographic quality of the two radiographs even though the exposure conditions were the same.

In one radiograph the 1T hole was easily resolvable, however, in the second radiograph the 1T hole was not detectable. In addition, the penetrameter contrast was much lower in the second radiograph. Consequently, the two penetrameters were exposed side-by-side simultaneously on the same film so that the exposure conditions were identical and the film densities were measured. These densities were as follows:

	<u>Minimum Resolvable Hole</u>	<u>Density At Penetrameter (H&amp;D)</u>	<u>Density Adjacent To Penetrameter (H&amp;D)</u>
Penetrameter A	1T	2.78	3.06
Penetrameter B	2T	3.10	3.12

Next, the thicknesses of the penetrameters were measured and found to be .007 and .0085 inch. The MIL-STD-453 thickness requirement for a .37 penetrameter is .0063 to .0077 inch. It can be seen that one of the penetrameters exceeds the MIL-STD-453 tolerances even though it was marked by the manufacturers as conforming to MIL-STD-453. The penetrameter which exceeded the tolerance requirement was close enough to the maximum allowable thickness to suggest that the MIL-STD-453 thickness range may result in a density spread which is quite significant. It is possible that the MIL-STD-453 tolerances are too large.

Based on these results, it would appear that MIL-STD-453 penetrameters do not provide for a consistent indication of the quality of a particular radiograph with the present thickness tolerances. MIL-STD-00453 presently requires that a minimum of .02 H&D density units between the penetrameter image and the image adjacent to the penetrameter be obtained for a 2-1T radiographic quality. Based on the difficulties of measuring small density differences and on the variation in penetrameter thicknesses, it is questionable if this is a workable requirement no matter how desirable.

It is also possible that tighter tolerances on material types might have to be imposed since X-ray transmission/absorption varies directly with both thickness and density.

It should also be noted that there are no penetrameters manufactured for use with thicknesses less than 1/4 inch. Since the current 1/4 inch penetrometer is inadequate for defining contrast or detail for thin section thicknesses, special penetrameters would be of great use for thin section radiography.

The test program highlighted some information which is of practical use for industrial radiography. One such example concerns the output of constant potential X-ray machines when compared to self-rectified and full wave rectified X-ray machines. Based on the electrical circuitry, the output from a constant potential circuit to that from a self-rectified circuit is significantly higher.

Halmshaw indicates in "Physics of Industrial Radiology" that self-rectified circuits emit X-rays with a maximum output at photon energies corresponding to about 60% of the peak voltage applied to the tube and constant potential circuits emit X-rays with a maximum output corresponding to about 76% of the peak applied voltage. Thus it would appear that the maximum emission from a self-rectified unit would be about 79% as high as that from a constant potential unit. However, it was found that, in practice, this relationship may be hidden because of factors such as the effect of different target materials and different inherent filtration due to tube windows, the cooling medium around the tube and different ports. An example of this is shown in Table 19 where, for several step wedges and kilovoltages, the resultant film density is greater for the self-rectified X-ray machine than for the constant potential X-ray machine under the same exposure conditions.

TABLE 19  
COMPARISON OF FILM DENSITIES FOR EXPOSURES UNDER THE SAME  
CONDITIONS WITH ISOVOLT 400 AND PG300 X-RAY MACHINES

Thickness of Step Wedge (in.)	kV	Exposure (MAM)	Film Density	
			Isovolt 400 (Constant Potential)	PG300 (Self-Rectified)
1/2	120	16	0.58	0.84
	140	16	1.26	1.64
	160	16	2.20	2.51
1/4	120	16	1.50	2.03
	140	16	2.96	3.47
1/8	120	16	2.66	3.31

GP74 0117 291

The common practice today is to express the radiographic quality level in terms of the visibility of a penetrameter image on the film and in terms of the smallest visible penetrameter hole on the film. For example, a 2-1T quality level indicator that a penetrameter whose maximum thickness is 2% of the test part thickness is visible on the film and that the penetrameter hole with a diameter equal to the penetrameter thickness is also visible on the film. It is left up to the radiographic interpreter to judge whether or not the penetrameter image and penetrameter hole is visible on the film and hence, the desired quality level has been achieved.

Sixteen radiographs of the step wedges were selected to measure the variation in judgment from one inspector to another as to the smallest discernible hole in a penetrameter image on a radiograph. One of the observers used was a laboratory technician whereas the remaining two observers were production radiographic interpreters. All three people have been qualified technically to Supplement A of SNT-TC-1A, Level II. Each man was instructed to record the smallest hole which he could see in each penetrameter.

The radiographic films were viewed with an illuminator equipped with a variable controlled light source capable of reading a film density up to 3.5. The illuminator had a minimum brightness capability of 30,000 candelas per square meter at the illuminator opal glass. For the actual viewing of the films, the background illuminator adjacent to the illuminator was approximately the same as the image on the film.

A total of 162 penetrameter images were examined by each man. Of these, all 3 men recorded the same hole in 127 of the penetrameters. The variation for the remaining 35 penetrameters is shown in Table 20

The data in Table 20 were examined to see if any individual consistently interpreted the hole image more conservatively than others. It was found that Inspector A, the laboratory technician, chose a hole diameter larger than that chosen by the other two people 43% of the time. These percentages were 29% and 3% for the other two people.

Since acuity is a relative phenomenon, there can be no judgements as to who is right or who is wrong. However, the subject was presented to illustrate one of the possible differences which can result in two evaluations of the same material even with optimum technique conditions.

The variation shown in Table 20 has a particular significance when it is considered that it is also a suggestion of the variation to be expected when actual radiographs of production parts are interpreted. One man could conceivably reject a condition where another man would accept it purely on a difference in visual acuity and judgement.

The data were examined to determine if the smaller penetrameter holes were visible more often if the surface finish was 63 RMS as compared to 125 RMS. The data indicated that the surface finish was not a significant factor for the two finishes evaluated.

In conclusion, there are many radiographic factors which need to be controlled for reproducible radiographs. If penetrameter contrast measurements are to be used to properly control radiographic image contrast, tighter tolerances may be necessary on the penetrameter thickness. Also, penetrameters for use with section thicknesses less than .25 inch are needed for thin section radiography. Kilovoltage and beam spectrum must also be controlled in order to control radiographic image contrast.

A choice of kilovoltage as a function of thickness can produce different results from one X-ray machine to another. For example, the actual potential across the electron emitter and target is not directly measured by the voltmeter on the machine. Voltmeter accuracy must be checked on a periodic basis to ensure reproducibility. Also, variations in inherent filtration between X-ray tubes should be taken into consideration. Fluctuations in line voltage due to plant workload can also have an effect.

TABLE 20  
VARIATION IN DETERMINATION IN RADIOGRAPHIC QUALITY 

Smallest Detectable Hole			Smallest Detectable Hole		
Inspector A	Inspector B	Inspector C	Inspector A	Inspector B	Inspector C
1T	2T	1T	2T	1T	1T
4T	2T	2T	2T	4T	2T
4T	2T	2T	2T	4T	2T
1T	1T	2T	4T	2T	2T
2T	1T	1T	4T	2T	2T
2T	2T	1T	4T	2T	2T
2T	2T	1T	2T	4T	2T
2T	1T	1T	2T	4T	2T
2T	1T	1T	2T	4T	2T
2T	2T	1T	2T	4T	2T
2T	2T	1T	2T	4T	2T
2T	1T	1T	2T	4T	2T
2T	2T	1T	2T	4T	2T
2T	1T	1T	2T	4T	4T
2T	1T	1T	2T	2T	1T
2T	1T	1T	2T	1T	1T
2T	1T	2T	2T	1T	1T
2T	1T	2T	2T	1T	1T

 The 3 inspectors detected the same hole in 127 penetrameters.

GP 74 0117 290

### 3. ULTRASONIC METHOD

Several ultrasonic inspection parameters were investigated during the program. These include the effect of surface curvature, the detection of discontinuities located near the surface of the test article, and the effect of variations in sound transmission characteristics of the reference standard vs. those of the material to be tested. Also, an investigation was made to improve ultrasonic inspection of titanium plate and thin section machined parts.

#### a. Surface Curvature Compensation

Many titanium die forgings which must be ultrasonically tested possess curved surfaces. Also, round bars and billets are frequently ultrasonic tested. However, if the commonly used flat surface reference standards are used, compensation for the curved surface must be necessary or erroneous results may be obtained. Without correction, a discontinuity in a production part may appear to be smaller or larger than it actually is and a rejectable part may be accepted or vice versa.

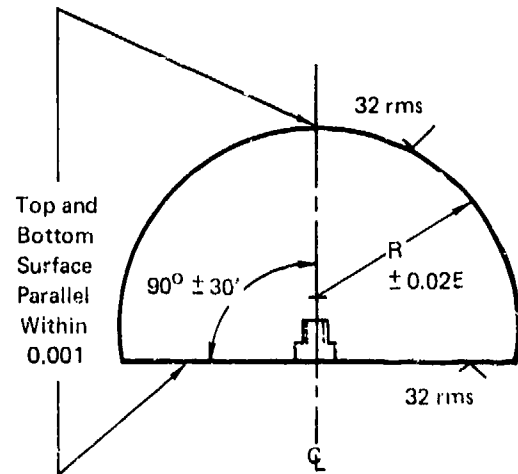
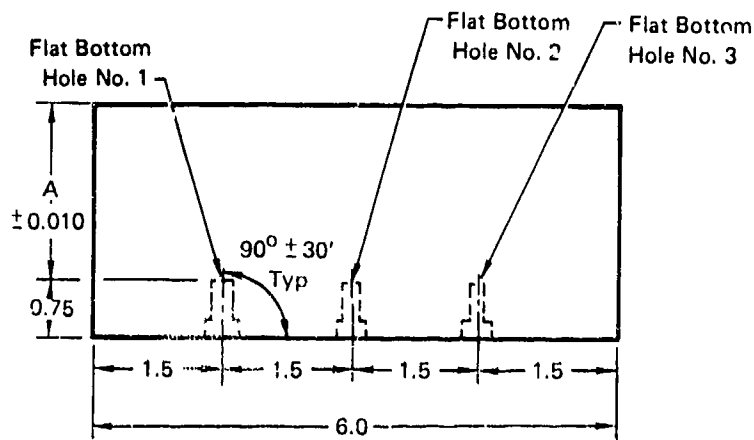
Consequently, a test program has been undertaken to study the effect of convex and concave sound entry surfaces.

Twenty-seven convex and thirty concave ultrasonic test specimens have been fabricated to the Figure 32 and 33 configuration. Several radii of curvature and metal travel distances were used. The convex specimens were sectioned from round stock of the appropriate diameter prior to machining. The concave specimens were sectioned from 3 inch thick plate with the 3 inch specimen dimension parallel to the 3 inch plate thickness. After the convex and concave specimens were machined and drilled, the hole depth, hole diameter, and metal travel were measured to establish that they were within tolerance. The hole orientation and location were measured on several selected specimens to ensure that the drilling set-up had been correct. The flatness of the hole bottom was checked optically.

A number of the larger diameter reference standards were fabricated from aluminum. Testing was performed with these in order to determine if aluminum contour blocks can be used for inspecting titanium. Obviously, fabricating a set of aluminum contour surface reference standards would be less expensive than fabricating titanium standards due to lower material cost and machining costs.

A photograph of several concave specimens is presented in Figure 34.

Flat surface reference standards, fabricated from 2-1/8 inch diameter Ti-6Al-4V bar, were used in conjunction with the curved specimens to compare responses from the flat bottom hole (Figure 35). This configuration was used to conform to the ASTM E127 configuration. Prior to drilling the flat bottom holes to a depth of  $0.5 \pm .050$  inch, the bar was cut into several 7" long sections and the 2-1/8 inch diameter faces were machined flat and to a 63 rms or better finish.



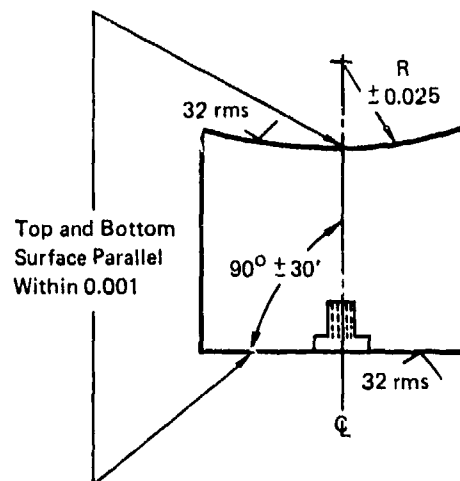
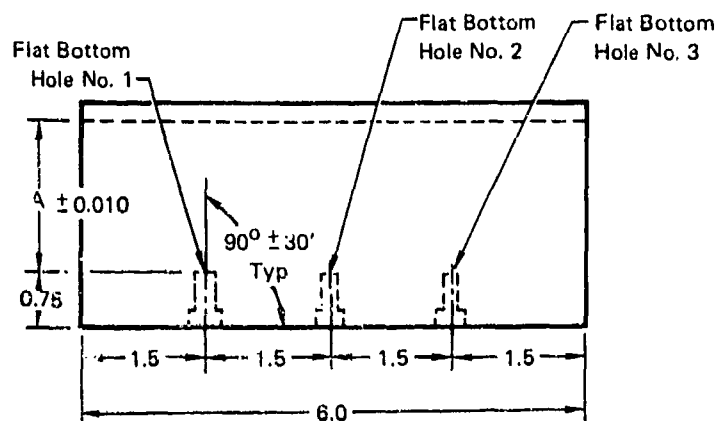
Hole Bottom Must be Flat Within 0.001 in./1/8 In. and Located Within 0.015 In. of Radial Axis

Material	Radius, R (Inches)	A (Inches)	Hole No. 1 (±0.001)	Hole No. 2 (±0.0005)	Hole No. 3 (±0.001)
Ti-6Al-4V	0.5	0.5	5/64	3/64	1/8
	0.5	0.75	5/64	3/64	1/8
	1.0	0.5	5/64	3/64	—
	1.0	0.75	5/64	3/64	—
	1.5	0.5	5/64	3/64	—
	1.5	0.75	5/64	3/64	—
	1.5	1.25	5/64	3/64	—
	2.0	0.5	5/64	3/64	1/8
	2.0	0.75	5/64	3/64	1/8
2024 Aluminum	2.0	0.5	5/64	3/64	—
	2.0	2.5	5/64	3/64	—
	2.5	0.5	5/64	3/64	—
	2.5	1.00	5/64	3/64	—
	2.5	1.5	5/64	3/64	—
	2.5	2.5	5/64	3/64	—
	2.5	4.0	5/64	3/64	—
	3.0	0.5	5/64	3/64	—
	3.0	1.0	5/64	3/64	—
	3.0	1.5	5/64	3/63	—
	3.0	2.5	5/64	3/64	—
	3.0	4.0	5/64	1/64	—
	4.0	0.5	5/64	3/64	—
	4.0	1.0	5/54	3/64	—
	4.0	1.5	5/64	3/64	—
4.0	2.5	5/64	3/64	—	
4.0	4.0	5/64	3/64	—	

FIGURE 32

GP74 011 / 265

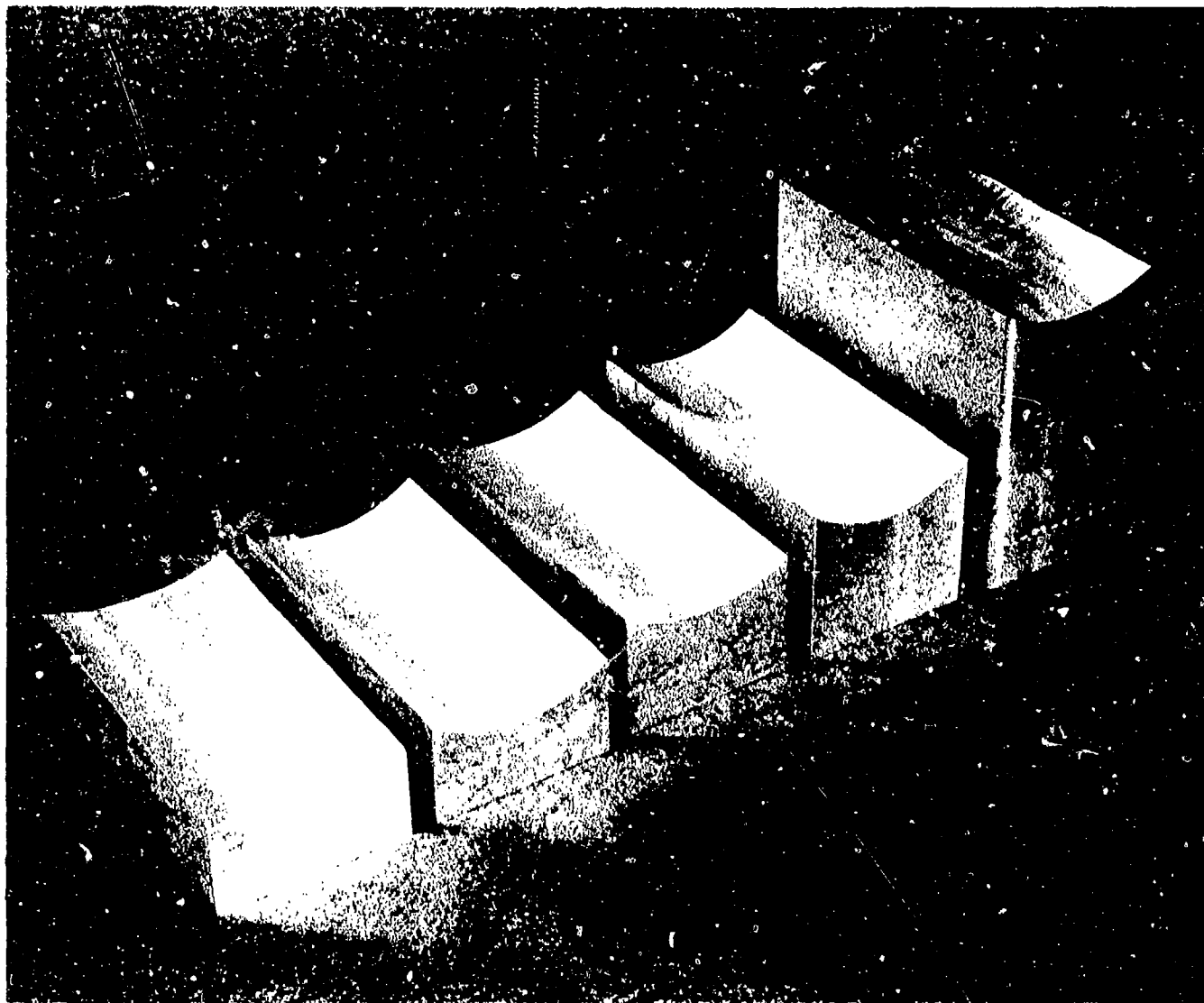
CONVEX CURVATURE REFERENCE STANDARDS



Hole Bottom Must be Flat Within 0.001 In./1/8 In. and Located Within 0.015 In. of Radial Axis

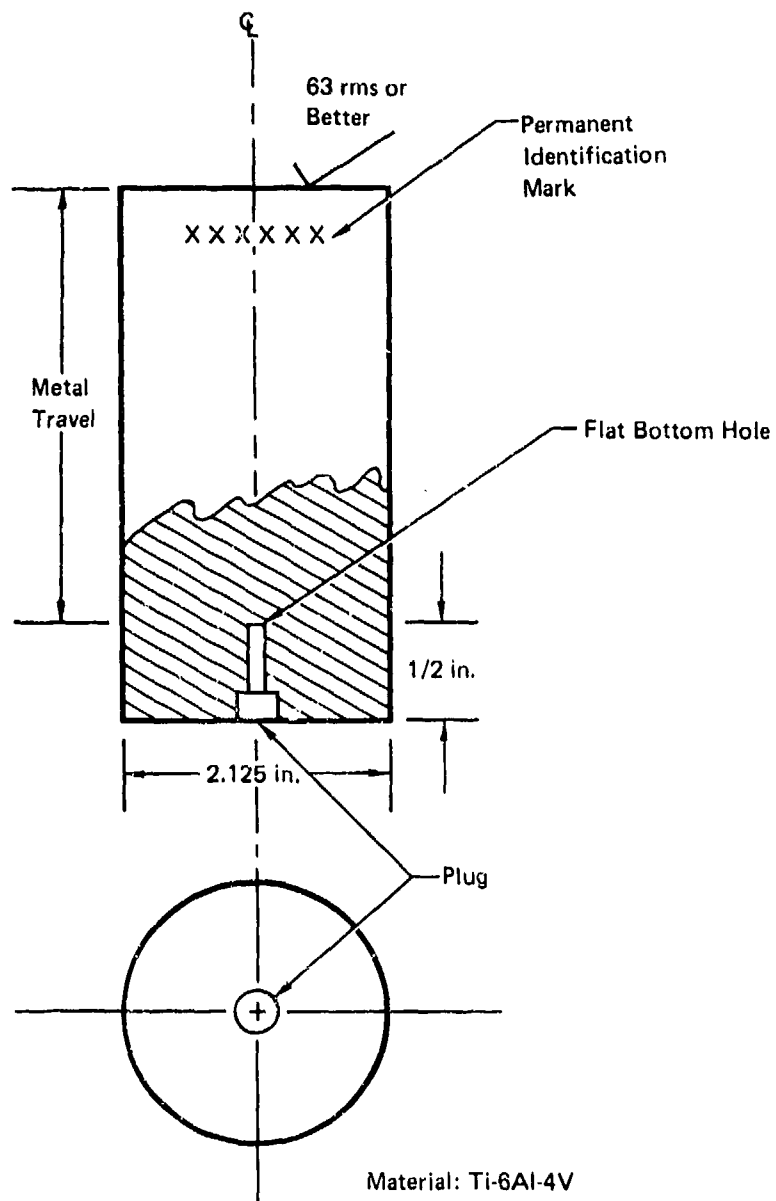
Material	Radius, R (Inches)	A (Inches)	Hole No. 1 (±0.001)	Hole No. 2 (±0.0005)	Hole No. 3 (±0.001)
Ti-6Al-4V	1/2	0.50	5/64	3/64	8/64
	1/2	0.75	5/64	3/64	8/64
	1	0.50	5/64	3/64	—
	1	0.75	5/64	3/64	—
	1	1.25	5/64	3/64	—
	1-1/2	0.50	5/64	3/64	—
	1-1/2	0.75	5/64	3/64	—
	1-1/2	1.25	5/64	3/64	—
	1-1/2	2.25	5/64	3/64	—
	2	0.50	5/64	3/64	8/64
2024 Aluminum	2	0.75	5/64	3/64	8/64
	2	2.25	5/64	3/64	8/64
	2	3.25	5/64	3/64	8/64
	2	0.50	5/64	3/64	—
	2	2.50	5/64	3/64	—
	2-1/2	0.5	5/64	3/64	—
	2-1/2	1.00	5/64	3/64	—
	2-1/2	1.50	5/64	3/64	—
	2-1/2	2.50	5/64	3/64	—
	2-1/2	4.00	5/64	3/64	—
	3	0.50	5/64	3/64	—
	3	1.00	5/64	3/64	—
	3	1.50	5/64	3/64	—
	3	2.50	5/64	3/64	—
3	4.00	5/64	3/64	—	
4	0.50	5/64	3/64	—	
4	1.00	5/64	3/64	—	
4	1.50	5/64	3/64	—	
4	2.50	5/64	3/64	—	
4	4.00	5/64	3/64	—	

FIGURE 33  
CONCAVE CURVATURE REFERENCE STANDARDS



GPJ4 0117 267

FIGURE 34  
CONCAVE ULTRASONIC SPECIMENS



GP74-0117 268

**FIGURE 35**  
**FLAT SURFACE REFERENCE STANDARD**

In order to select pieces which were closely matched acoustically, immersion straight beam through-transmission tests were performed on each piece by sending the sound beam parallel to the 7 inch axis. A 3/4 inch diameter, 5 MHz SLZ search unit was used as a receiver. During these tests, it was noticed that, in some pieces, the sound was attenuated more in one direction than in the other. For the majority of the specimens, the difference was on the order of 2dB but, for a few, the difference was as much as 6dB. This difference in attenuation with direction may be due to such factors as a preferential grain pattern and the prior working history of the bar. This data serves to emphasize the sound transmission differences that can occur between, say, the reference standard and the part to be inspected during a normal production ultrasonic inspection, and also between different sets of reference standards. Obviously, correction for these differences is desirable.

The curved surface testing was performed using straight beam immersion techniques. Initially, a flat surface reference standard was placed in the water and the immersion search unit was adjusted to a 3 inch water path. A 3 inch water path was selected because it represents a common industry water path used for production ultrasonic inspection. The choice of the 3 inch water path caused all the testing to be performed in the near field. Testing was performed with the reject control and the damping control off. Next, the search unit was positioned and angulated to maximize the response from the 3/64 diameter flat bottom hole in the flat surface standard and the instrument gain was adjusted to bring the response from the flat bottom hole to 80% of saturation. The dB setting at this point was recorded. Then the search unit was positioned over a curved surface specimen containing a 3/64 inch diameter flat bottom hole at the same metal travel distance and the gain was changed in order to bring the hole response to 80% of saturation. The dB required to bring the response to 80% of saturation was recorded. From the data recorded, the decibel difference between the responses and the response ratio (flat surface/curved surface) were calculated.

The ultrasonic instruments and search units used for the investigation are listed in Table 21.

The data developed during the above testing was given an adjustment for any differences in sound transmission characteristics between the titanium flat surface reference standard and the titanium curved surface test specimens. These differences might result from differences in grain structure, prior working history, surface finish, and heat treatment. As shown in Figure 36, a piece was removed from that concave specimen with a 2-inch radius and 3.25-inch metal travel. The response from the flat bottom hole was maximized and adjusted to 80% of full saturation. Next, the search unit was moved to the flat surface reference standard with an identical metal travel and the dB required to bring the response to 80% of full saturation was measured. The dB difference between the two responses was measured

**TABLE 21**  
**ULTRASONIC INSTRUMENTS AND TRANSDUCERS USED FOR**  
**CURVED SURFACE STUDY**

Ultrasonic Instrument	Transducer
Branson 600	3/4 in. Dia, 5 MHz, Aerotech $\alpha$ 1/2 in. Dia, 5 MHz, Aerotech $\alpha$ 1/2 in. Dia, 5 MHz, SIZ (S/N 18268) 3/4 in. Dia, 2-1/4 MHz, $\gamma$ (S/N 10595) 3/4 in. Dia, 5 MHz, SIL (S/N 21263) 3/4 in. Dia, 5 MHz, SIZ (S/N 21269)
Sperry UM-715	1/2 in. Dia, 5 MHz, SIZ (S/N 18268) 3/4 in. Dia, 5 MHz, SIZ (S/N 21269) 3/4 in. Dia, 5 MHz, SIL (S/N 21263)

GP 74-0117-254

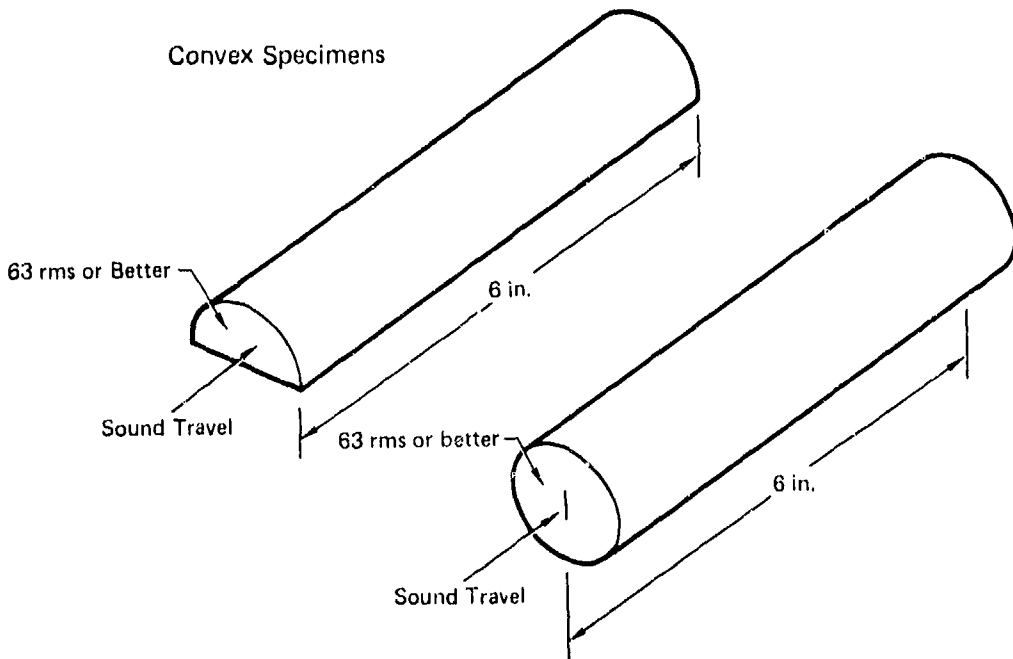
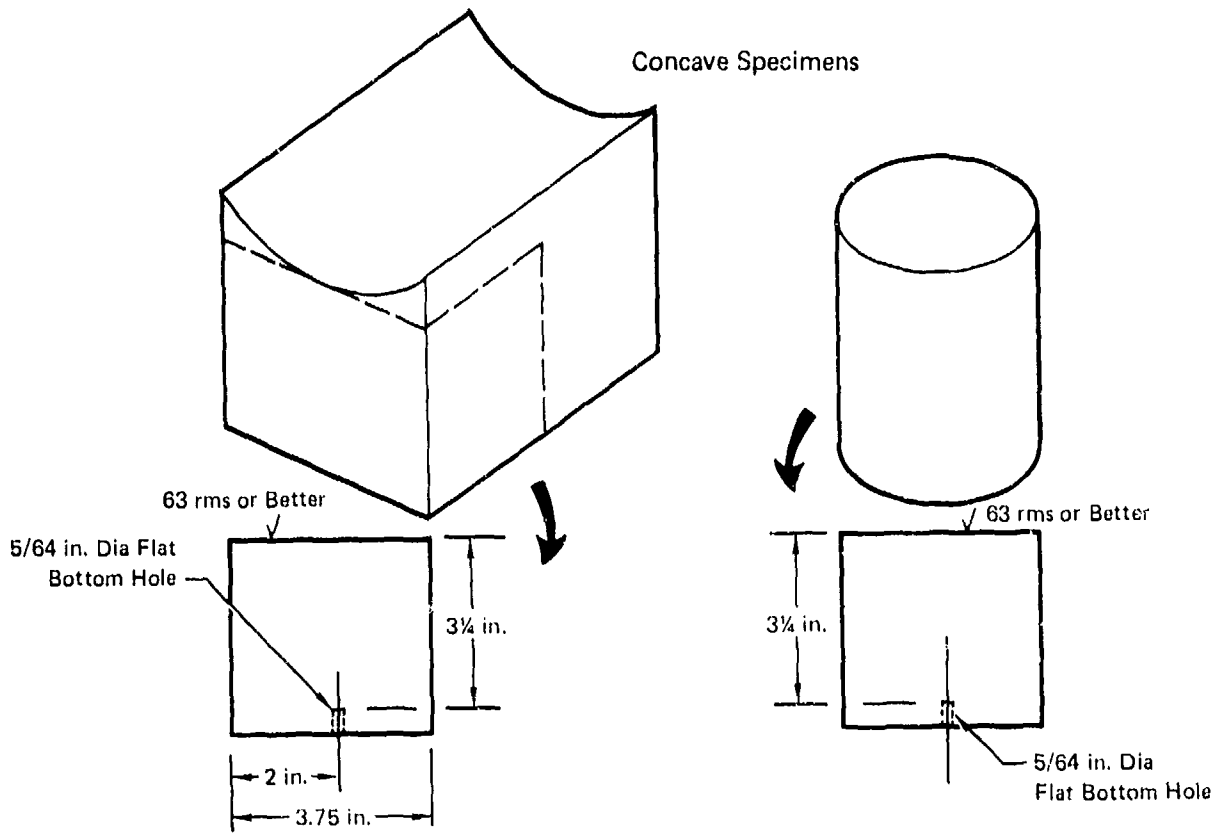


FIGURE 36  
TESTS TO ESTABLISH DIFFERENCE IN SOUND TRANSMISSION  
CHARACTERISTICS

GP 74 0117 260

to be 7 dB. Since all the concave specimens were fabricated from one piece of 2 inch thick plate, the data for the concave specimens were corrected by 2.15 dB per inch of metal travel.

Correction for convex specimens were made by adjusting the back reflection through a 6 inch long flat surface reference standard to 80% of full saturation and noting the dB required to bring the back surface response in the convex specimen to 80% of full saturation (see Figure 36). It was found that dB difference was so small that data correction was unnecessary for the convex specimens.

The results of the testing are shown in Tables 22 and 23. The general shapes of the plots of decibel difference as a function of radius of curvature for concave and convex surfaces are shown in Figure 37. It should be pointed out that decibel measurements were made because of the difficulty in accurately measuring small amplitude heights directly off a cathode ray tube screen.

As can be seen from the test data, the response from the flat bottom hole was always less with a convex sound entry surface than with a flat sound entry surface; that is, the decibel difference was always positive. Consequently, during a normal production ultrasonic inspection, a discontinuity will appear smaller than it actually is due to the influences of a convex sound entry surface. The data presented indicates that the amplitude of the response due to the convex entry surface can be as small as 10% of the response with a flat sound entry surface over a metal travel range of 1/2 to 3-1/4 inches.

It is significant that the decibel difference varies as a function of radius and metal travel for this implies that a total correction for curvature can only be made after the discontinuity is located. Consequently, an ultrasonic inspection of a production part in the areas with a curved surface of a particular radius should be conducted at a scanning gain high enough to ensure the detection of all discontinuities at that radius regardless of their depth location. Then, a second evaluation should be made using the appropriate scanning gain corrections as a function of the metal travel to determine the true size of the discontinuity.

The hole responses from specimens with concave sound entry surfaces were sometimes less and greater than those specimens with flat entry surfaces depending upon the concave radius and metal travel distance. The sound beam converges after passing through the concave water/metal interface. The maximum response from a reference reflector within the metal would occur at a metal travel equivalent to the focal distance.

Typical variations in decibel difference as a function of search unit are shown in Figure 38. Two ultrasonic instruments are also represented. The curves in Figure 38 were all for the response from a 3/64 inch diameter hole at a 3/4 inch metal travel. As can

**TABLE 22**  
**RESPONSE RATIO OF FLAT SURFACE RESPONSE ( $I_f$ ) TO CURVED SURFACE**  
**RESPONSE ( $I_c$ ) - TITANIUM SPECIMENS**  
 Ultrasonic Instrument - Branson 600  
 Reflector - 3/64 In. Dia Flat Bottom Hole  
 3/4 In. Dia, 5MHz, Aerotech  $\alpha$

Concave				Convex			
Metal Travel (in.)	Radius of Curvature (in.)	$I_f - I_c$ (dB)	$\frac{I_f}{I_c}$	Metal Travel (in.)	Radius of Curvature (in.)	$I_f - I_c$ (dB)	$\frac{I_f}{I_c}$
1/2	1/4	13	4.50	1/2	1/2	9	4.50
	1	-3	0.70		1	8	2.50
	1 1/2	-18	0.13		1 1/2	4	1.60
	2	-2	0.80		2	3	1.40
3/4	1/2	$\triangle$	$\triangle$	3/4	1/2	9	2.80
	1	12	4		1	13	4.50
	1 1/2	3	1.40		1 1/2	11	3.50
	2	-7	0.45		2	1	3.50
1 1/4	1	18	8.00	1 1/4	1	-	-
	1 1/2	7	2.20		1 1/2	15	5.50
2 1/4	1 1/2	11	3.50	2 1/4	1 1/2	-	-
	2	7	2.20		2	-	-

$\triangle$  Response from flat bottom hole could not be separated from spurious indications.

GP74 0117 296

**TABLE 22 (Continued)**  
**RESPONSE RATIO OF FLAT SURFACE RESPONSE ( $I_f$ ) TO CURVED SURFACE**  
**RESPONSE ( $I_c$ ) - TITANIUM SPECIMENS**  
 1/2 In. Dia, 5MHz, Aerotech  $\alpha$

Concave				Convex			
Metal Travel (in.)	Radius of Curvature (in.)	$I_f - I_c$ (dB)	$\frac{I_f}{I_c}$	Metal Travel (in.)	Radius of Curvature (in.)	$I_f - I_c$ (dB)	$\frac{I_f}{I_c}$
1/2	1/2	15	5.50	1/2	1/2	17	7.00
	1	3	1.40		1	10	3.20
	1 1/2	-6	0.50		1 1/2	7	2.20
	2	-2	0.80		2	5	1.80
3/4	1/2	$\triangle$	$\triangle$	3/4	1/2	21	11.00
	1	13	4.50		1	15	5.50
	1 1/2	8	2.50		1 1/2	12	4.00
	2	2	1.25		2	10	3.20
1 1/4	1	15	5.50	1 1/4	1	-	-
	1 1/2	11	3.50		1 1/2	16	6.30
2 1/4	1 1/2	17	7.00	2 1/4	1 1/2		
	2	13	4.50		2		

$\triangle$  Response from flat bottom hole could not be separated from spurious signals.

GP74 0117-294

**TABLE 22 (Continued)**  
**RESPONSE RATIO OF FLAT SURFACE RESPONSE ( $I_F$ ) TO CURVED SURFACE**  
**RESPONSE ( $I_C$ ) - TITANIUM SPECIMENS**  
 1/2 In. Dia 5MHz Lead Zirconate Titanate Search Unit (S/N 18268)

Concave				Convex			
Metal Travel (in.)	Radius of Curvature (in.)	$I_F - I_C$ (dB)	$I_F / I_C$	Metal Travel (in.)	Radius of Curvature (in.)	$I_F - I_C$ (dB)	$I_F / I_C$
1/2	1/2	10	3.2	1/2	1/2	13	4.5
	1	2	1.25		1	9	2.8
	1-1/2	-10	0.32		1-1/2	6	2.0
	2	-4	0.63		2	4	1.6
3/4	1/2	△	△	1/2	1/2	15	5.5
	1	10	3.2		1	13	4.5
	1-1/2	1	1.1		1-1/2	9	2.8
	2	-6	0.5		2	7	2.2
1-1/4	1	16	6.3	1-1/4	1-1/2	14	5.0
	1-1/2	8	2.5				
2-1/4	1-1/2	12	4.0				
	2	8	2.5				

GP74 0117 288

△ Response from flat bottom hole could not be separated from spurious indications

3/4 In. Dia 2-1/4 MHz Ceramic Search Unit (S/N 10595)

Concave				Convex			
Metal Travel (in.)	Radius of Curvature (in.)	$I_F - I_C$ (dB)	$I_F / I_C$	Metal Travel (in.)	Radius of Curvature (in.)	$I_F - I_C$ (dB)	$I_F / I_C$
1/2	1/2	9	2.80	1/2	1/2	7	2.20
	1	2	0.80		1	3	1.40
	1-1/2	-8	0.40		1-1/2	6	2.00
	2	-5	0.56		2	6	2.00
3/4	1/2	△	△	3/4	1/2	△	△
	1	4	1.60		1	8	2.50
	1-1/2	0	1.00		1-1/2	9	2.80
	2	5	0.56		2	7	2.20
1-1/2	1	11	3.50	1-1/4	1-1/2	12	4.00
	1-1/2	3	1.4				

GP74 0117 289

Notes:

$I_F$  Flat surface response  
 $I_C$  Curved surface response

△ Response from flat bottom hole could not be separated from spurious indications

**TABLE 22 (Continued)**  
**RESPONSE RATIO OF FLAT SURFACE RESPONSE ( $I_f$ ) TO CURVED SURFACE**  
**RESPONSE ( $I_c$ ) - TITANIUM SPECIMENS**  
**3/4 In. Dia 5MHz LiSO<sub>4</sub> Search Unit (S/N 21263)**

Concave				Convex			
Metal Travel (in.)	Radius of Curvature (in.)	$I_F - I_C$ (dB)	$I_F/I_C$	Metal Travel (in.)	Radius of Curvature (in.)	$I_F - I_C$ (dB)	$I_F/I_C$
1/2	1/2	5	1.80	1/2	1/2	7	2.2
	1	-5	0.56		1	7	2.2
	1-1/2	-16	0.16		1-1/2	5	1.8
	2	-10	0.32		2	4	1.6
3/4	1/2	△	△	3/4	1/2	△	△
	1	7	2.20		1	8	2.5
	1-1/2	2	1.25		1-1/2	9	2.8
	2	-6	0.50		2	5	1.8

Notes:

GP74 0117 280

$I_F$  = Flat surface response  
 $I_C$  = Curved surface response

△ Response from flat bottom hole could not be separated from spurious indications

**3/4 In. Dia 5MHz Lead Zirconate Titanate Search Unit (S/N 21269)**

Concave				Convex			
Metal Travel (in.)	Radius of Curvature (in.)	$I_F - I_C$ (dB)	$I_F/I_C$	Metal Travel (in.)	Radius of Curvature (in.)	$I_F - I_C$ (dB)	$I_F/I_C$
1/2	1/2	8	2.50	1/2	1/2	9	2.80
	1	-1.5	0.85		1	8	2.50
	1-1/2	-16	0.14		1-1/2	4.5	1.70
	2	-15	0.18		2	4	1.60
3/4	1/2	△	△	3/4	1/2	18	8.00
	1	15	5.60		1	10	3.20
	1-1/2	2	1.30		1-1/2	11	3.50
	2	-5	0.56		2	8	2.50
1-1/4	1	20	10.00	1-1/4	1-1/2	19.5	9.50
	1-1/2	11	3.50				
2-1/4	1-1/2	12	4.00				
	2	0	1.00				
3-1/4	2	7.5	2.40				

Notes:

GP74 0117 287

$I_F$  = Flat surface response  
 $I_C$  = Curved surface response

△ Response from flat bottom hole could not be separated from spurious indications

**TABLE 22 (Continued)**  
**RESPONSE RATIO OF FLAT SURFACE RESPONSE ( $I_f$ ) TO CURVED SURFACE**  
**RESPONSE ( $I_c$ ) - TITANIUM SPECIMENS**  
 Ultrasonic Instrument - Sperry UM-715  
 Reflector - 3/64 In. Dia Flat Bottom Hole  
 1/2 In. Dia, 5MHz, SIZ (S/N 18268)

Concave				Convex			
Metal Travel (in.)	Radius of Curvature (in.)	$I_f - I_c$ (dB)	$\frac{I_f}{I_c}$	Metal Travel (in.)	Radius of Curvature (in.)	$I_f - I_c$ (dB)	$\frac{I_f}{I_c}$
1/2	1/2	7	2.20	1/2	1/2	11	3.50
	1	-1	0.90		1	8	2.50
	1 1/2	-9	0.35		1 1/2	5	1.80
	2	-1	0.90		2	5	1.80
3/4	1/2	23	10.40	3/4	1/2	14	5.00
	1	9	2.80		1	10	3.20
	1 1/2	1	1.10		1 1/2	9	2.80
	2	-5	0.56		2	6	2.00
1 1/4	1	15	5.60	1 1/4	1	-	-
	1 1/2	9	2.80		1 1/2	13	4.50
2 1/4	1 1/2	10	3.20				
	2	7	2.20				
3 1/4	2	6	2.00				

GP74 0117 29R

**TABLE 22 (Continued)**  
**RESPONSE RATIO OF FLAT SURFACE RESPONSE ( $I_f$ ) TO CURVED SURFACE**  
**RESPONSE ( $I_c$ ) - TITANIUM SPECIMENS**  
**3/4 In. Dia, 5MHz, SIZ (S/N 21269)**

Concave				Convex			
Metal Travel (in.)	Radius of Curvature (in.)	$I_f - I_c$ (dB)	$\frac{I_f}{I_c}$	Metal Travel (in.)	Radius of Curvature (in.)	$I_f - I_c$ (dB)	$\frac{I_f}{I_c}$
1/4	1/2	10	3.3	1/4	1/2	10	3.2
	1	-3	0.7		1	6	2.0
	1 1/2	-12	0.25		1 1/2	5	1.8
	2	-7	0.45		2	3	1.4
3/8	1/2	△	△	3/8	1/2	16	6.3
	1	9	2.8		1	12	4.0
	1 1/2	2	1.25		1 1/2	12	4.0
	2	-1	0.9		2	10	3.2
1/2	1	16	6.3	1/2	1	-	-
	1 1/2	9	2.8		1 1/2	16	6.3
2/4	1 1/2	18	8.0	2/4	1 1/2	-	-
	2	19	9.0		2	-	-
3/4	2	9	2.8	-	-	-	-

△ Response from flat bottom hole could not be separated from spurious indications.

GP74 0117 30u

TABLE 22 (Continued)  
 RESPONSE RATIO OF FLAT SURFACE RESPONSE ( $I_f$ ) TO CURVED SURFACE  
 RESPONSE ( $I_c$ ) - TITANIUM SPECIMENS  
 3/4 In. Dia, 5 MHz, SIL (S/N 21263)

Concave				Convex			
Metal Travel (in.)	Radius of Curvature (in.)	$I_f - I_c$ (dB)	$\frac{I_f}{I_c}$	Metal Travel (in.)	Radius of Curvature (in.)	$I_f - I_c$ (dB)	$\frac{I_f}{I_c}$
1/4	1/2	9	2.80	1/4	1/2	7	2.2
	1	-2	0.80		1	7	2.2
	1 1/2	-13	0.22		1 1/2	5	1.8
	2	-1	0.90		2	4	1.6
3/4	1/2	△	△	3/4	1/2	8	2.5
	1	7	2.20		1	9	2.8
	1 1/2	3	1.40		1 1/2	8	2.5
	2	-7	0.45		2	7	2.2
1 1/4	1	15	5.60	1 1/4	1	-	-
	1 1/2	13	4.50		1 1/2	19	9.0

△ Response from flat bottom hole could not be separated from spurious signals.

GP 74 0117 209

**TABLE 23**  
**RESPONSE RATIO OF FLAT SURFACE RESPONSE ( $I_f$ ) TO CURVED SURFACE**  
**RESPONSE ( $I_c$ ) - ALUMINUM SPECIMENS**

Ultrasonic Instrument - Branson 600  
 Reflector - 3/64 In. Dia Flat Bottom Hole  
 3/4 In. Dia, 5MHz, SIL (S/N 21263)

Concave				Convex			
Metal Travel (in.)	Radius of Curvature (in.)	$I_f - I_c$ (dB)	$\frac{I_f}{I_c}$	Metal Travel (in.)	Radius of Curvature (in.)	$I_f - I_c$ (dB)	$\frac{I_f}{I_c}$
1/2	2	-11	0.28	1/2	2	7	2.2
	2 1/2	-8	0.40		2 1/2	5	1.8
	3	-7	0.45		3	6	2.0
	4	-3	0.70		4	3	1.4
1	2 1/2	1	1.10	1	2 1/2	11	3.5
	3	-4	0.61		3	10	3.2
	4	-5	0.55		4	8	2.5
1 1/2	2 1/2	6.5	2.10	1 1/2	2 1/2	11.5	3.7
	3	5.5	1.90		3	11.5	3.7
	4	-0.5	0.95		4	8.5	2.7
2 1/2	2	13		2 1/2	2	15	5.5
	2 1/2	10	3.20		2 1/2	11	3.5
	3	10	3.20		3	11	3.5
	4	7	2.20		4	10	3.3
4	2 1/2	12	4.00	4	2 1/2	12	4.0
	3	10	3.20		3	12	4.0
	4	10	3.20		4	11	3.5

QP74 0117 297

**TABLE 23 (Continued)**  
**RESPONSE RATIO OF FLAT SURFACE RESPONSE ( $I_f$ ) TO CURVED SURFACE**  
**RESPONSE ( $I_c$ ) - ALUMINUM SPECIMENS**  
 Ultrasonic Instrument - Branson 600  
 Reflector - 3/64 In. Dia Flat Bottom Hole  
 3/4 In. Dia, 5MHz, SIZ (S/N 21269)

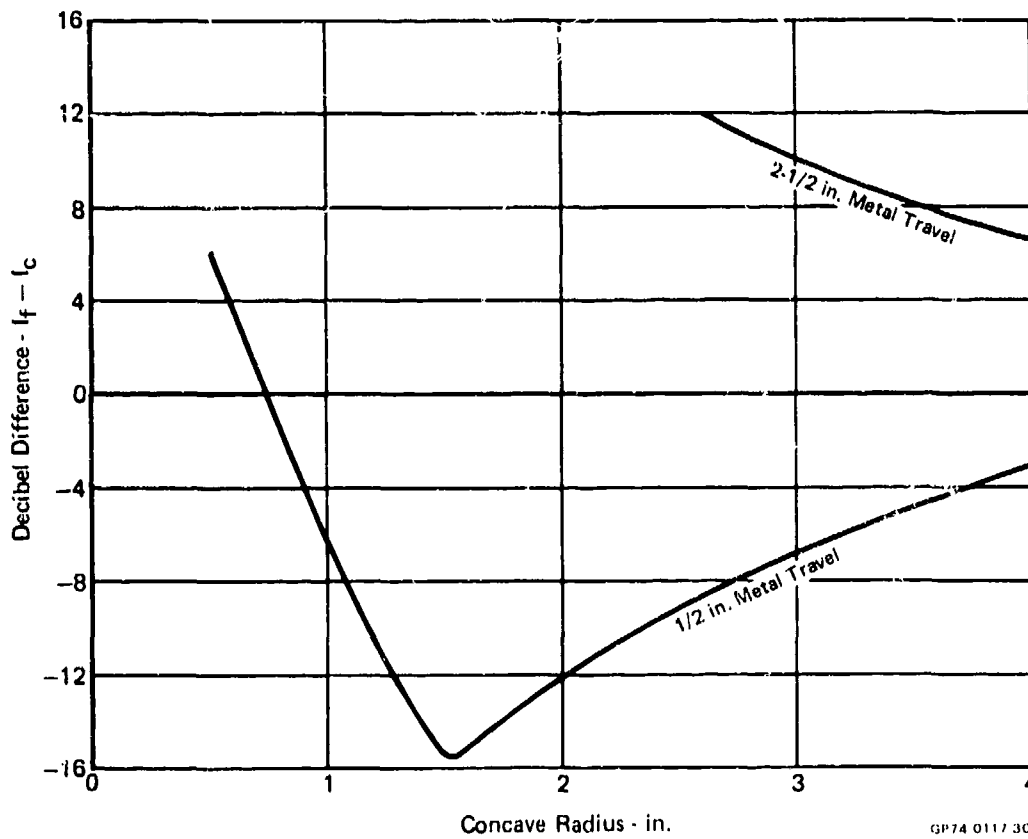
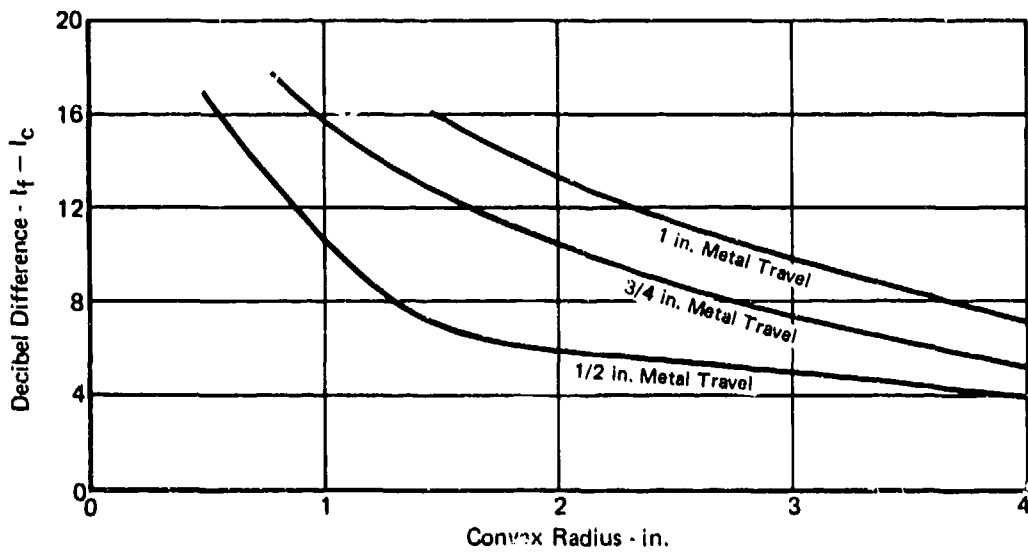
Concave				Convex			
Metal Travel (in.)	Radius of Curvature (in.)	$I_f - I_c$ (dB)	$\frac{I_f}{I_c}$	Metal Travel (in.)	Radius of Curvature (in.)	$I_f - I_c$ (dB)	$\frac{I_f}{I_c}$
1/2	2	-10	0.32	1/2	2	5.5	1.90
	2 1/2	-8	0.40		2 1/2	4.5	1.70
	3	-6	0.50		3	3.5	1.50
	4	-3	0.70		4	3	1.40
1	2 1/2	-2.5	0.75	1	2 1/2	7.5	2.30
	3	-6	0.50		3	6.5	2.10
	4	-7	0.45		4	5	1.80
1 1/2	2 1/2	6	2.00	1 1/2	2 1/2	12	4.00
	3	4	1.60		3	11	3.50
	4	-2.5	0.75		4	8	2.50
2 1/2	2	12.5	4.20	2 1/2	2	13.5	4.70
	2 1/2	11.5	3.70		2 1/2	11.5	3.70
	3	10	3.20		3	11	3.50
	4	7.5	2.40		4	10.5	3.30
4	2 1/2	12	4.00	4	2 1/2	13.5	4.70
	3	11	3.50		3	11.5	3.70
	4	10	3.20		4	11	3.50

GP74 0117 206

**TABLE 23 (Continued)**  
**RESPONSE RATIO OF FLAT SURFACE RESPONSE ( $I_f$ ) TO CURVED SURFACE**  
**RESPONSE ( $I_c$ ) - ALUMINUM SPECIMENS**  
 Ultrasonic Instrument - Branson 600  
 Reflector - 3/64 In. Dia Flat Bottom Hole  
 1/2 In. Dia, 5MHz Aerotech  $\alpha$

Concave				Convex			
Metal Travel (in.)	Radius of Curvature (in.)	$I_f - I_c$ (dB)	$\frac{I_f}{I_c}$	Metal Travel (in.)	Radius of Curvature (in.)	$I_f - I_c$ (dB)	$\frac{I_f}{I_c}$
1/2	2	-7	0.45	1/2	2	7	2.20
	2 1/2	-5	0.56		2 1/2	5	1.80
	3	-4.5	0.60		3	4.5	1.70
	4	-4	0.64		4	4	1.60
1	2 1/2	-2	0.80	1	2 1/2	11	3.50
	3	-3	0.70		3	9	2.80
	4	-3	0.70		4	7.5	2.30
1 1/2	2 1/2	6	2.00	1 1/2	2 1/2	9	2.80
	3	6	2.00		3	9.5	3.00
	4	-1	0.90		4	7	2.20
2 1/2	2	13.5	4.70	2 1/2	2	12	4.00
	2 1/2	9	2.80		2 1/2	11	3.50
	3	9	2.80		3	10	3.20
	4	6	2.00		4	9	2.80
4	2 1/2	10	3.20	4	2 1/2	11	3.50
	3	9	2.80		3	9	2.80
	4	10	3.20		4	9	2.80

QP74 0117 203



GP74 0117 302

**FIGURE 37**  
**TYPICAL CURVES FOR CONTOUR SURFACE EFFECT**

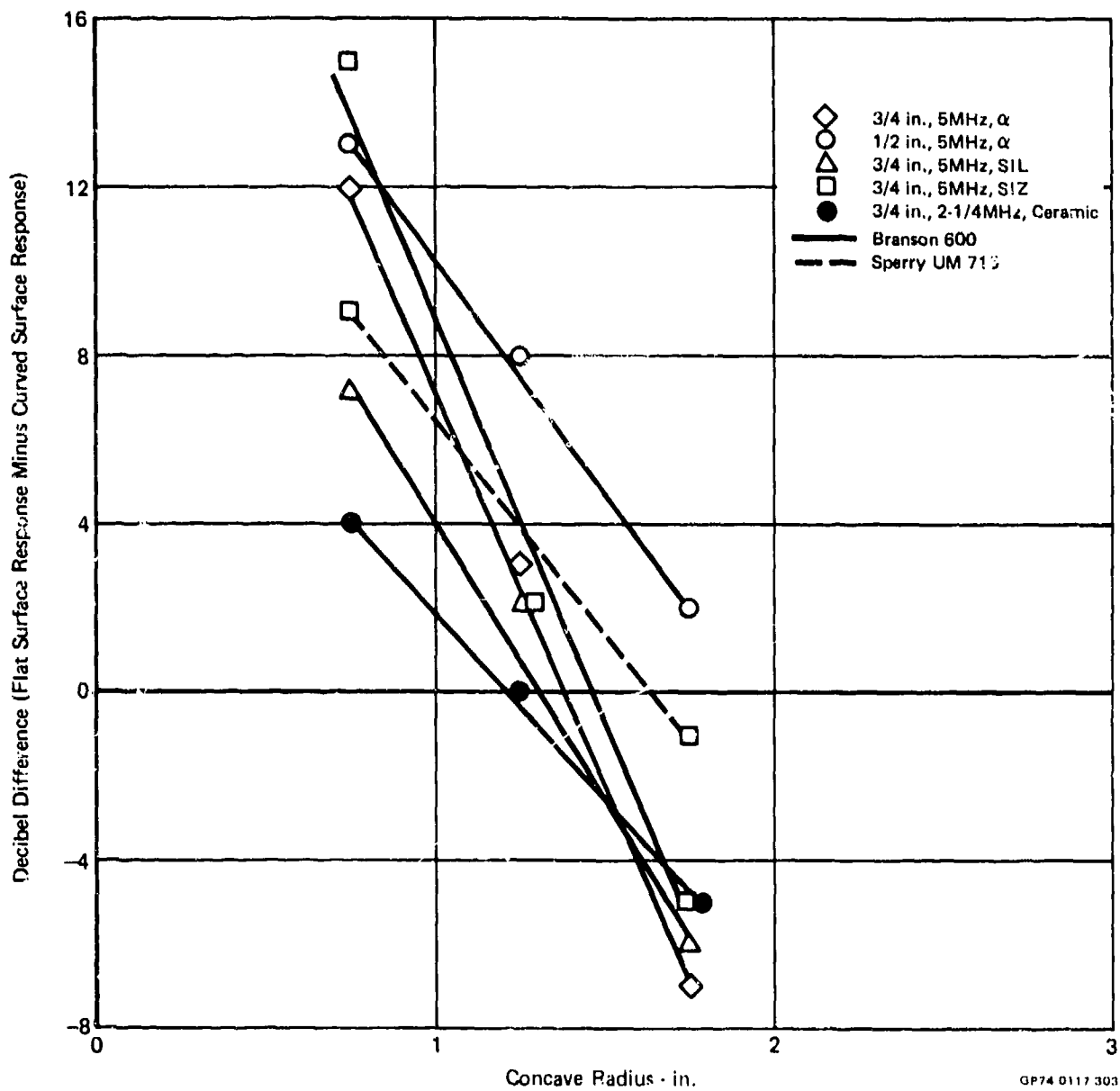


**FIGURE 38**  
**VARIATION IN dB DIFFERENCE AS A FUNCTION OF SEARCH UNIT AND**  
**ULTRASONIC INSTRUMENT (TITANIUM SPECIMENS - 3/64 IN. DIAMETER**  
**FLAT BOTTOM HOLE - 3/4 IN. METAL TRAVEL)**

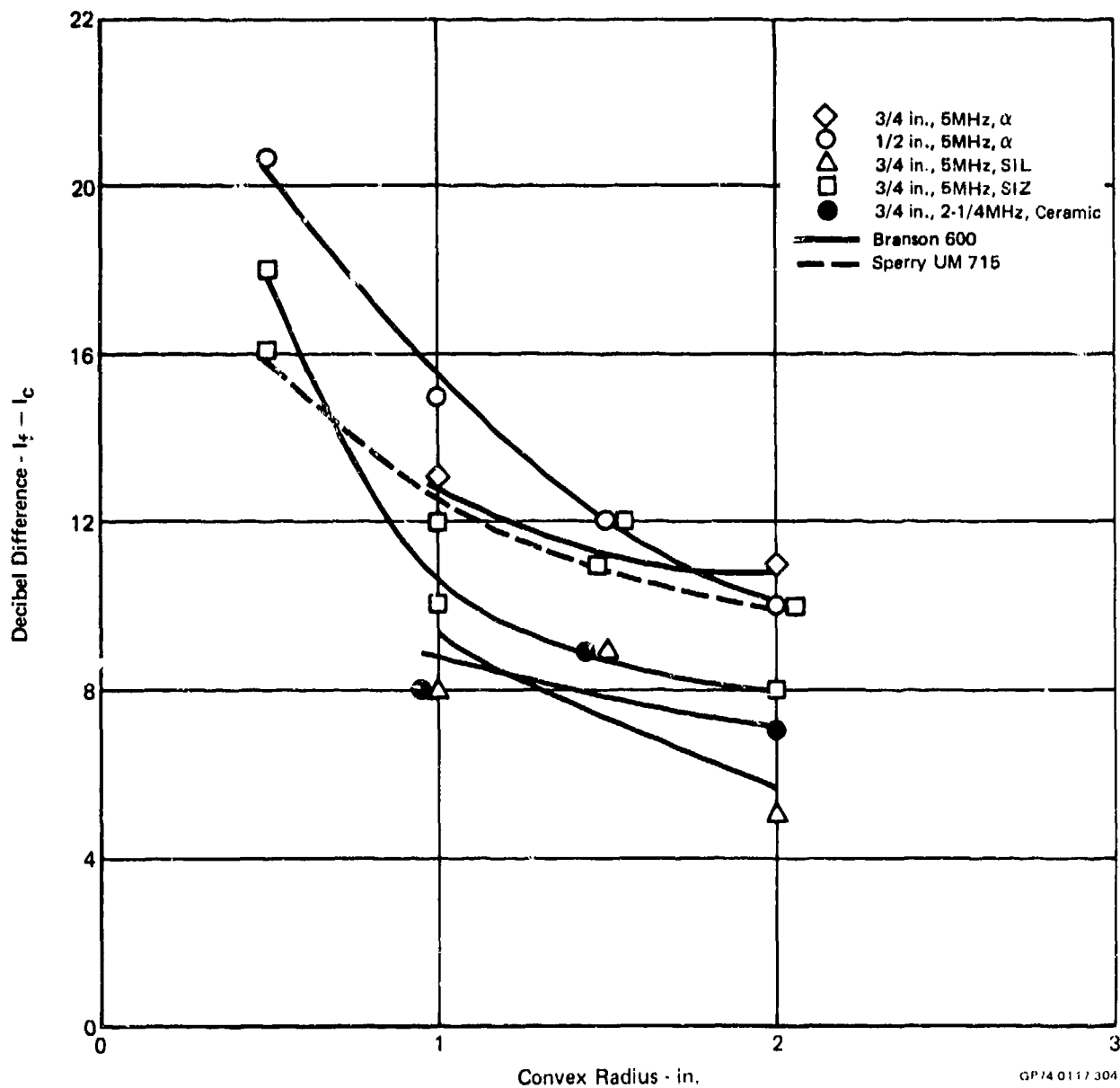


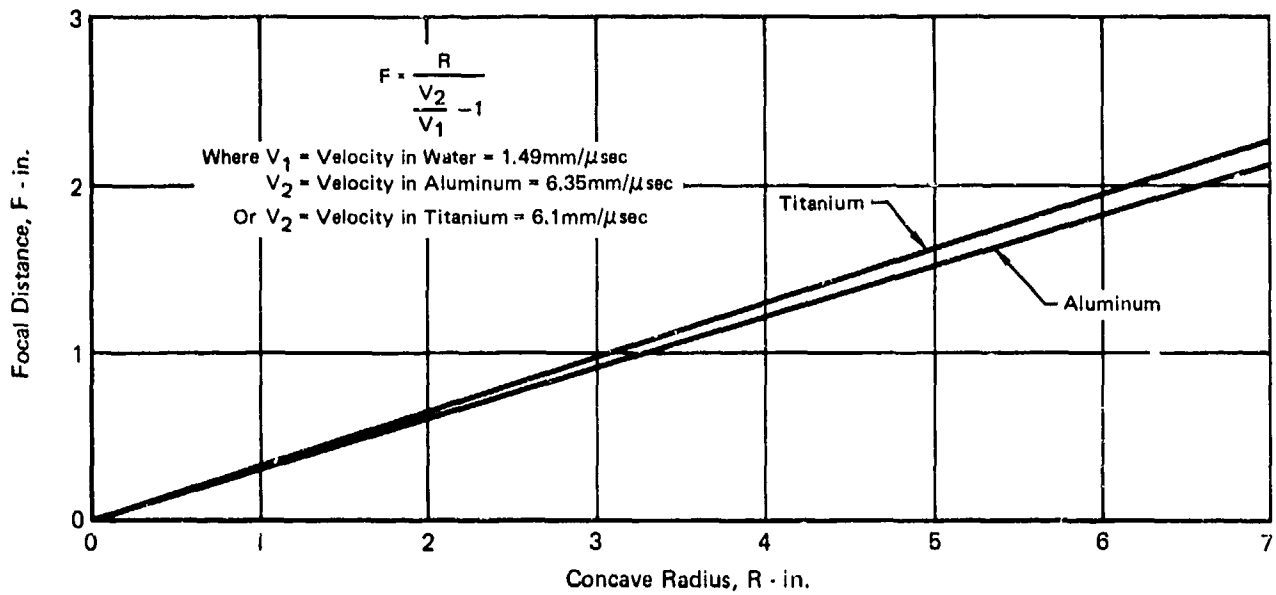
FIGURE 38 (Continued)  
 VARIATION IN dB DIFFERENCE AS A FUNCTION OF SEARCH UNIT AND  
 ULTRASONIC INSTRUMENT (TITANIUM SPECIMENS - 3/64 IN. DIAMETER  
 FLAT BOTTOM HOLE - 3/4 IN. METAL TRAVEL)

be seen, the variation is quite large at several of the radius values. For example, there is an 8 dB difference in correction between the 1/2 inch diameter, 5 MHz, Alpha search unit and the 3/4 inch diameter, 5 MHz, SIL search unit for a convex radius of 1 inch. The variation in slope as a function of search unit is probably due to beam spread variations. The large variation in correction values for contour surfaces as a function of search unit and ultrasonic instruments suggests that development of correction curves may be difficult. It appears that a new set of correction curves would be required for each selection of equipment. A more reasonable approach might be the direct use of curved surface reference standards during the actual ultrasonic inspection of production parts.

As mentioned previously, both aluminum and titanium convex and concave blocks were fabricated with a 2 inch radius of curvature and a 1/2 inch metal travel. In order to study the feasibility of using aluminum contour blocks in the ultrasonic inspection of titanium, the following tests were performed. The titanium and aluminum contour blocks, along with titanium and aluminum flat surface ASTM-type reference standards, were placed in the immersion tank. All six pieces contained a 3/64 inch diameter flat bottom hole at a 1/2 inch metal travel. In each of the six blocks, the hole response was adjusted to 80 percent of saturation and the dB setting was recorded. These tests were repeated for 4 search units. In all cases, the decibel difference between the aluminum flat surface response and the aluminum curved surface response was within 2 dB of the decibel difference for titanium. These results indicate that the material difference (aluminum versus titanium) does not affect the sound beam refraction sufficiently to invalidate the use of aluminum standards when inspecting titanium providing adjustment is made for surface finish differences. Further, evidence to support this conclusion can be derived from a theoretical plot of the focal distance as a function of radius of curvature for concave surfaces in aluminum and titanium (see Figure 39). There is little difference between the focal distance for aluminum and titanium which indicates that the sound beam is affected in essentially the same way by the concave surface in both aluminum and titanium.

Typical curves for one search unit and radii from 1/2 to 4 inches are shown in Figure 40. As can be seen, the effect of the concave and convex surfaces are still quite evident at a radius of 4 inches. Obviously, the radius of curvature at which correction is no longer necessary is greater than 4 inches.

An examination of the data can be of use in designing a set of contour surface reference standards for use in a production ultrasonic inspection. It appears that it is not necessary to fabricate a set which contains all the radii and metal travels which are to be encountered. For example, with a 1/2, 5 MHz, Alpha search unit, there is very little variation in dB difference for convex radii of 2-1/2, 3, and 4 inches at a metal travel of 1/2 inch. Consequently, a convex



GP74-0117 306

**FIGURE 39**  
**FOCAL DISTANCE vs CONCAVE RADIUS OF CURVATURE**

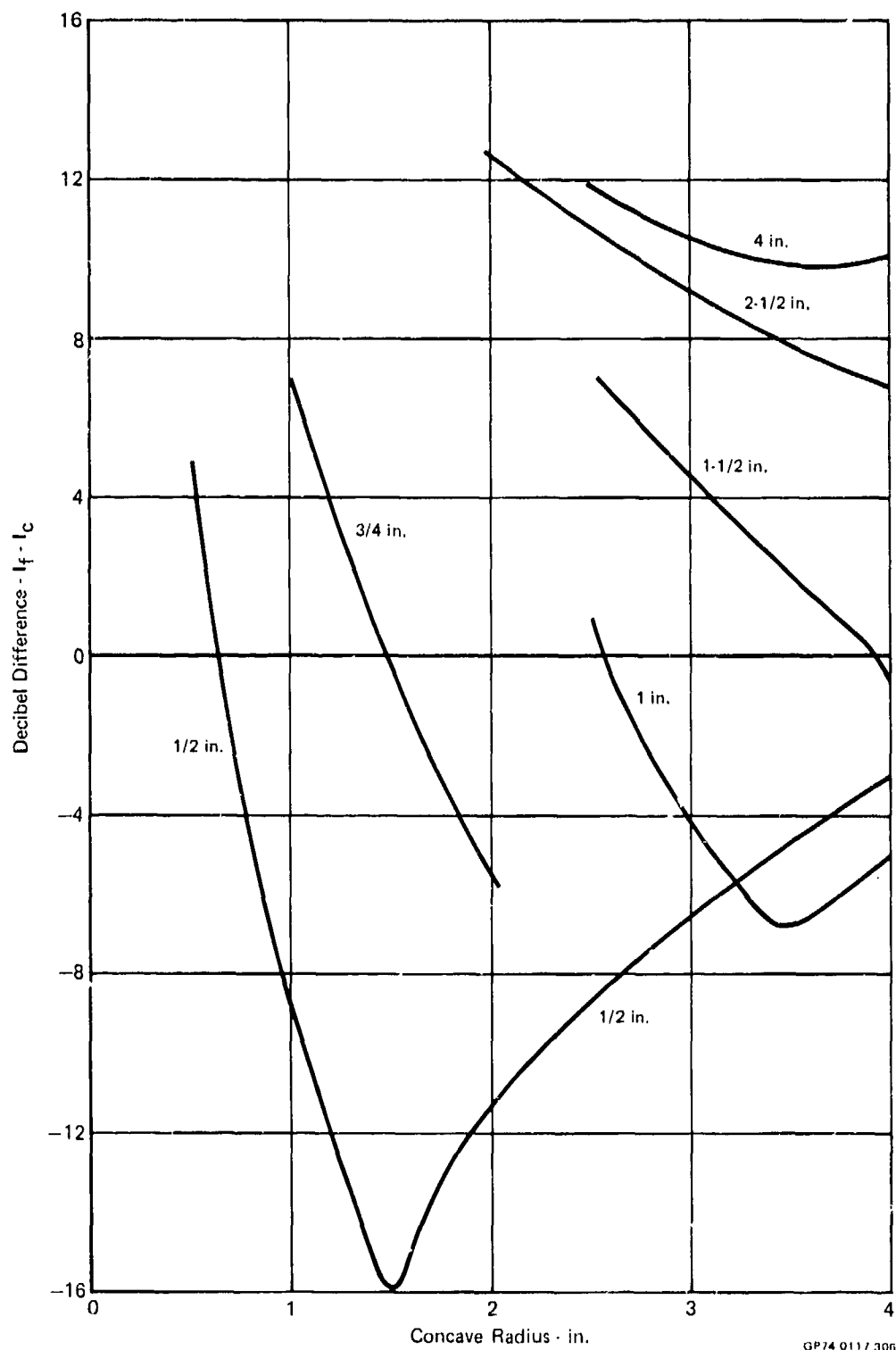
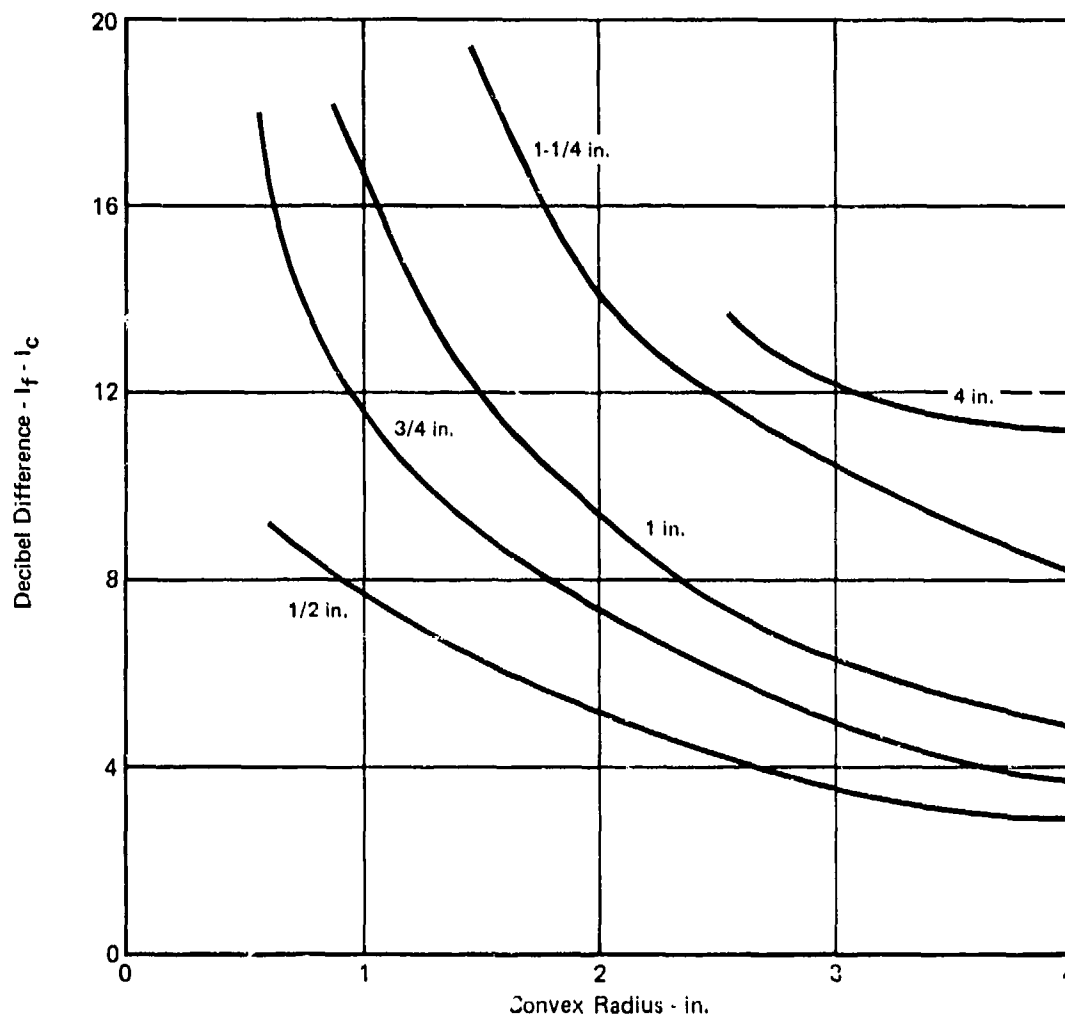


**FIGURE 40**  
**DECIBEL DIFFERENCE BETWEEN FLAT SURFACE RESPONSE AND CURVED**  
**SURFACE RESPONSE AS A FUNCTION OF RADIUS AND METAL TRAVEL**  
**(3/4 IN. DIAMETER, 5MHz, SIL SEARCH UNIT)**



GP74 0117 307

**FIGURE 40 (Continued)**  
**DECIBEL DIFFERENCE BETWEEN FLAT SURFACE RESPONSE AND CURVED**  
**SURFACE RESPONSE AS A FUNCTION OF RADIUS AND METAL TRAVEL**  
**(3/4 IN. DIAMETER, 5MHz, SIL SEARCH UNIT)**

entry surface reference standard with a 3 inch radius and 1/2 inch metal travel could be used to inspect all radii from 2-1/2 to 4 inches of a 1/2 inch metal travel. Of particular interest, and concern, are those combinations of concave radii and metal travels which result in negative decibel differences. Here the differences can change very rapidly with small variations in either radius or metal travel. Differences between search units, even of similar type, are likely to be large as well.

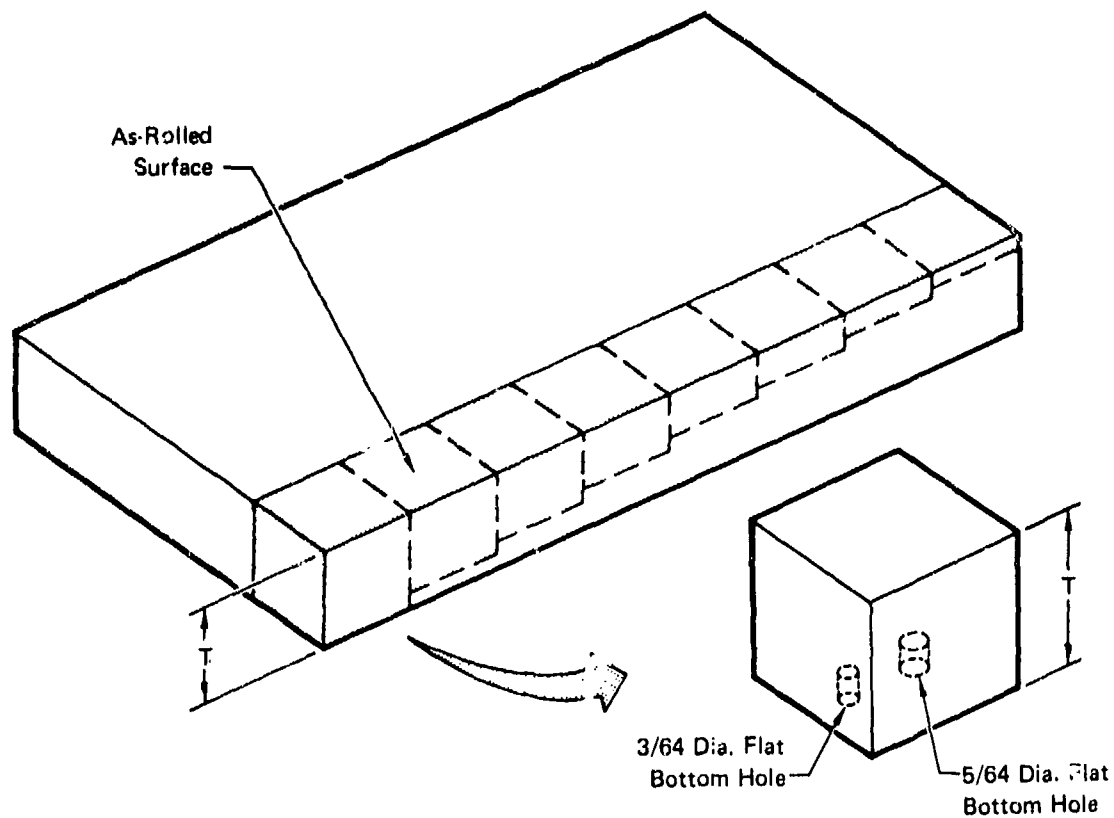
#### b. Near Surface Resolution

The resolution of discontinuities near the sound entry surface is a factor that should be considered during straight beam immersion ultrasonic inspection. Resolution is sometimes difficult or impossible due to the magnitude of the response from the water/metal interface. Variation of test parameters, such as test frequency, can result in improved near surface resolution. (A higher frequency results in a narrower water/metal interface spike on the cathode ray tube (CRT)). Other considerations, however, must be taken into account. For example, it may not be possible to test through the entire thickness of the part due to increased attenuation. Also, surface finish and mill product form may have a significant effect on the problem.

In order to gain a better understanding of the near surface resolution capabilities of the straight beam immersion test, a program was conducted to determine the effects of product form, surface finish, and test frequency on near surface defect resolution.

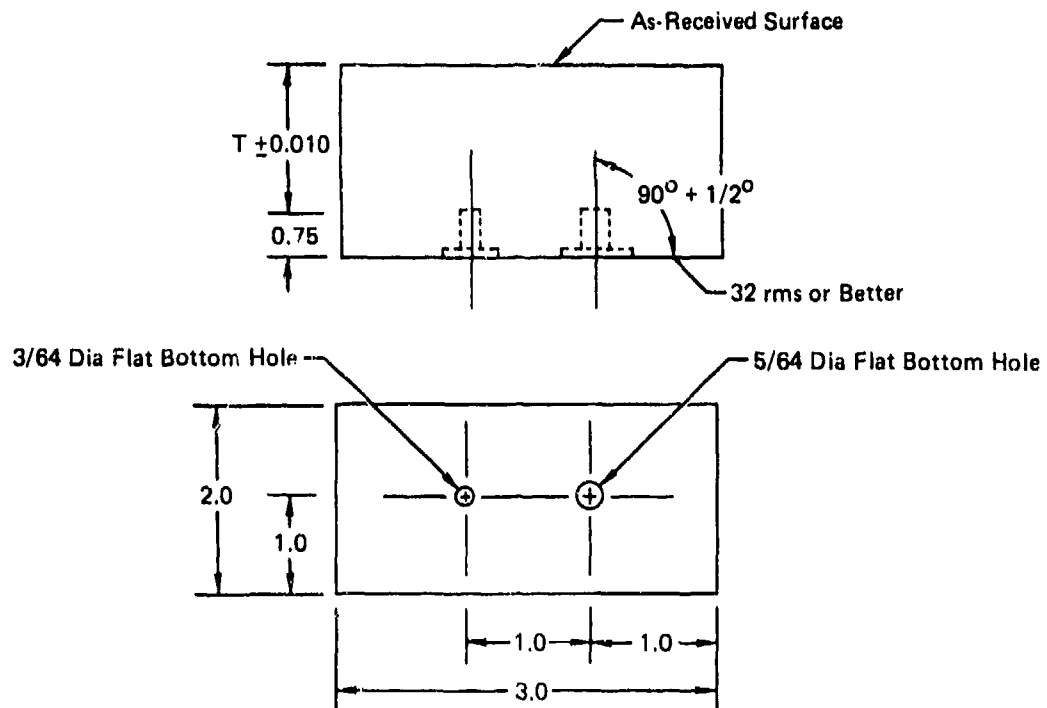
##### (1) Specimen Fabrication

Ultrasonic test specimens were fabricated from 2 and 4 inch thick as-rolled Ti-6Al-4V plate, 5 inch thick Ti-6Al-4V die forging. The forged pieces were sawcut from a production die forging (see Figure 41). Several sections were sawcut from each as shown for the plate in Figure 42. The as-received surfaces were kept intact and ultrasonic specimens were fabricated according to the Figure 43 configuration. The sound metal travel distances were as shown in Table 24. Photographs of the specimens are shown in Figure 44. After the testing was performed upon the as-received specimens, the as-received surfaces were machined to a 125 rms or better finish on several of the specimens. Further testing was performed to study the near surface resolution capability in final machined parts.



QP74-0117 262

**FIGURE 42**  
**NEAR SURFACE RESOLUTION SPECIMENS - AS-ROLLED PLATE**



Notes:

1. Hole dia tolerance is  $\pm 0.0005$  in.
2. Hole bottom must be flat within 0.001 in. per 1/8 in.
3. Hole must be straight and perpendicular to entry surface within  $1/2^\circ$  and located within 0.010 in. of longitudinal axis

GP74-0117 263

**FIGURE 43**  
**NEAR SURFACE RESOLUTION SPECIMEN CONFIGURATION**

**TABLE 24**  
**METAL TRAVELS USED FOR NEAR SURFACE RESOLUTION STUDY**

Product Form	Specimen No.	Metal Travel (in.)	
		As-Received Surface <sup>1</sup>	Machined Surface <sup>3</sup>
As-Rolled 4 in. Plate	1-4	3.35 <sup>2</sup>	3.31
	2-4	2.00	-
	3-4	1.00	-
	4-4	0.60	-
	5-4	0.40	0.37
	6-4	0.25	0.17
	7-4	0.125	0.08
As-Rolled 2 in. Plate	1-2	1.25 <sup>2</sup>	1.19
	2-2	1.00	-
	3-2	0.50	0.49
	4-2	0.40	0.38
	5-2	0.25	0.20
	6-2	0.125	0.11
As-Forged Die Forged	F-3-5	4.35 <sup>2</sup>	4.27
	2½-F-3-5	2.50	-
	08-F-3-5	0.80	0.41
	06-F-3-5	0.60	0.21
	04-F-3-5	0.40	0.15
	02-F-3-5	0.20	-
	0125-F-3-5	0.125	0.10

- <sup>1</sup> Dimensions are approximate.
- <sup>2</sup> Both the sound entry surface and the surface opposite are in the as-received condition.
- <sup>3</sup> Both surfaces were machined.

GP74-0117 113



Die Forging



4 Inch Plate



2 Inch Plate

FIGURE 44  
NEAR SURFACE RESOLUTION SPECIMENS

SP24-0117-264

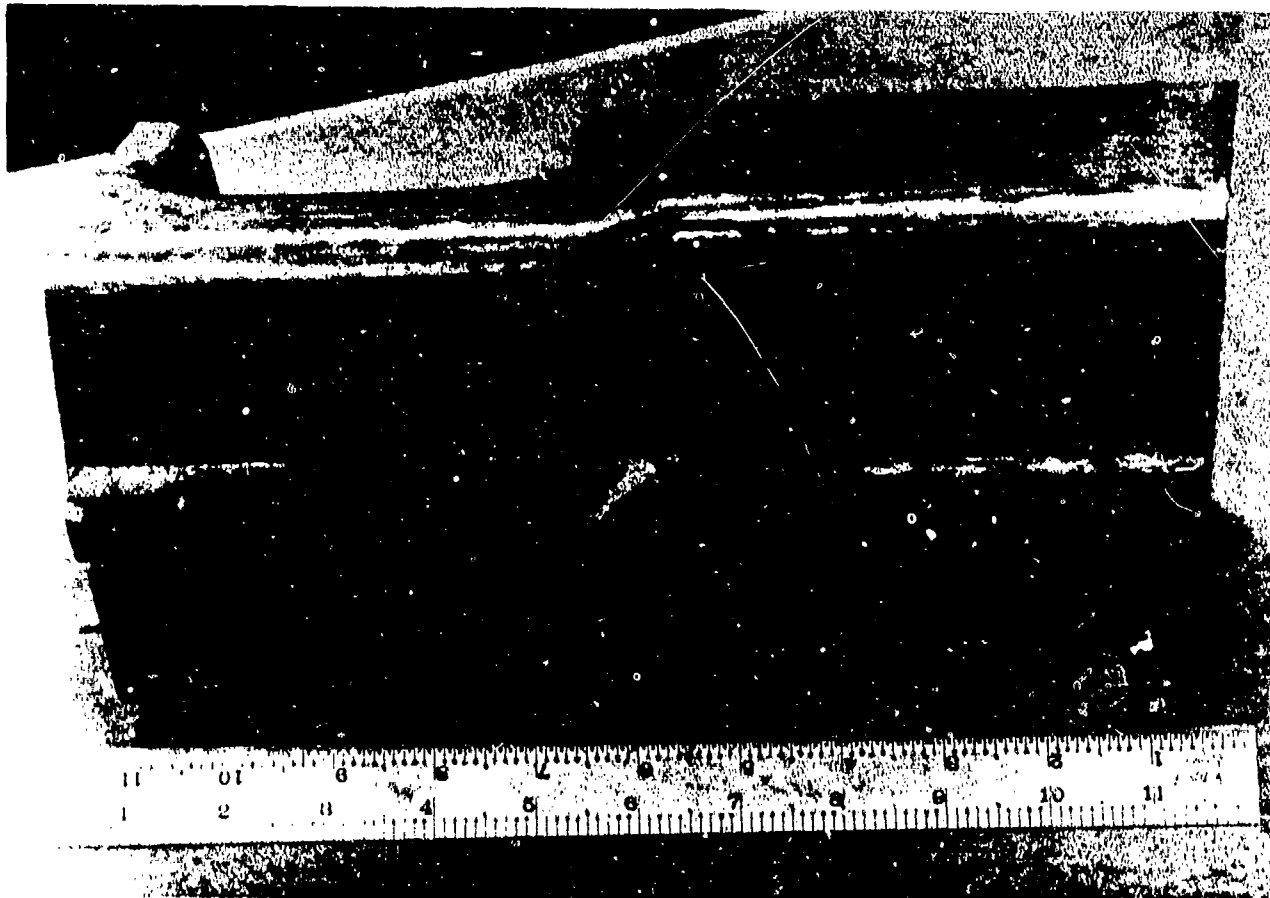


FIGURE 41  
DIE FORGING USED FOR NEAR SURFACE RESOLUTION STUDY

SP7A 0117 261

#### (c) Testing of As-received Material

The test specimens with as-rolled and as-forged surfaces were tested with 4 separate flat transducers. These were: (1) 3/4 inch diameter, 5 MHz, 31b, (2) 1/2 inch diameter, 5 MHz, a, (3) 3/8 inch, 15 MHz, 31b, and (4) 3/4 inch, 5 MHz, 31b. The 3/4 inch, 5 MHz, 31b transducer was chosen as being representative of the transducers used to inspect raw forgings and plate by the suppliers. The other transducers were chosen for comparative purposes to measure the effect of diameter, frequency, and material type on near surface resolution. Two ultrasonic instruments which are commonly used in industry were used for comparative purposes. These were the Branson 600 and the Sperry UM-715.

Prior to any testing, the vertical and horizontal linearity of the systems were determined according to ASTM E317-68. The upper linearity limit was greater than 95 percent of the vertical limit, the lower linearity limit was less than 10 percent of the vertical limit, and the horizontal linearity range was greater than 85 percent of the horizontal limit as best can be measured with the ASTM E317-68 method. The search unit profile data, obtained upon purchase of the search units, were examined to confirm that the peak radiated frequency was within  $\pm 10$  percent of the specified frequency.

The testing performed on the specimens from the 4 inch thick plate was typical of the testing performed on the other pieces. Initially, all seven of the 4 inch plate test specimens were placed into the immersion tank. The search unit was adjusted to the chosen water path and angulated to maximize the response from the  $3/64$  inch diameter flat bottom hole. A 3 inch water path was used for the majority of the testing since this is commonly used in industry. A 9 inch water path was also investigated in order to see if the near surface resolution could be improved by testing the holes outside the near field of the sound beam. The testing was performed using the distance - amplitude correction (DAC) curve method which is often used in the ultrasonic inspection of airframe components. The test specimen in the set of seven which exhibited the maximum response was selected. The response from that hole was adjusted to 80% of saturation. Then, without changing the gain, the search unit was moved to each of the other specimens and the near surface resolution was determined by noting the minimum distance between the sound entry surface and the flat bottom hole that produced a first-echo indication whose leading edge met the horizontal sweep line. The amplitude of the response at each metal travel was also recorded. It is recognized that, in actual practice, that first echo indications can sometimes be resolved even if they do not meet the horizontal sweep line. However, in order to perform a reproducible test, the designated convention was chosen.

The testing was then repeated using a  $5/64$  inch diameter flat bottom hole in each specimen.

The near surface resolution capability as a function of product form, instrument, and search unit is summarized in Tables 25 and 26. For these test purposes, the near surface resolution must be expressed as a range since the metal travels investigated were varied in only a few increments. For example, a near surface resolution of .125 to .25 inch would result from a test where the flat bottom hole was resolvable at .25 inch but not at .125 inch.

An examination of the data presented in Tables 25 and 26 reveals several important points. In several cases, the near surface resolution was improved by lengthening the water path from 3 inches to 9 inches when testing with the  $3/4$  inch diameter, 5 MHz STZ search unit. The hole was located in the far field of the sound beam with a 9 inch water path, and, presumably, this improved the near surface resolution capability since the sound beam is more coherent and interference-free in the far field.

**TABLE 25**  
**NEAR SURFACE RESOLUTION OF AS-RECEIVED SPECIMENS (3/64**  
**INCH DIA FLAT BOTTOM HOLE RESPONSE)**

Product Form	Branson 800				Sperry UM-715
	3/4 in., 5 MHz, SIZ, (3 in. Water Path)	3/4 in., 5 MHz, SIZ, (9 in. Water Path)	1/2 in., 10 MHz, SIZ, (9 in. Water Path)	3/8 in., 15 MHz SIL, (3 in. Water Path)	3/4 in., 5 MHz, SIL, (3 in. Water Path)
4 in. Plate	0.25 to 0.40	0.125 to 0.25	0.125 to 0.25 ⚠	0.125 to 0.25 ⚠	0.25 to 0.40
2 in. Plate	0.25 to 0.40	0.25 to 0.40	0.125 to 0.25	0.125 to 0.25	0.25 to 0.40
Die Forging	0.20 to 0.40 ⚠	0.20 to 0.40 ⚠	0.125 to 0.20 ⚠	Less than 0.125 ⚠	0.20 to 0.40 ⚠

⚠ Response from largest metal travel was less than 10% of saturation

GP74-0117-112

**TABLE 26**  
**NEAR SURFACE RESOLUTION OF AS-RECEIVED SPECIMENS (5/64**  
**INCH DIA FLAT BOTTOM HOLE RESPONSE)**

Product Form	Branson 600				Sperry UM-715
	3/4 in., 5 MHz, SIZ, (3 in. Water Path)	3/4 in., 5 MHz, SIZ, (9 in. Water Path)	1/2 in., 10 MHz, SIZ, (9 in. Water Path)	3/8 in. 15 MHz SIL (3 in. Water Path)	3/4 in., 5 MHz, SIL, (3 in. Water Path)
4 in. Plate	0.25 to 0.40	0.125 to 0.25 ⚠	0.125 to 0.25 ⚠	Less than 0.125 ⚠	0.125 to 0.25
2 in. Plate	0.25 to 0.40	0.125 to 0.25	0.125 to 0.25	Less than 0.125	0.125 to 0.25
Die Forging	0.20 to 0.40 ⚠	0.20 to 0.40 ⚠	0.125 to 0.20 ⚠	Less than 0.125 ⚠	0.20 to 0.40 ⚠

⚠ Response from largest metal travel was less than 10% of saturation

GP74-0117-111

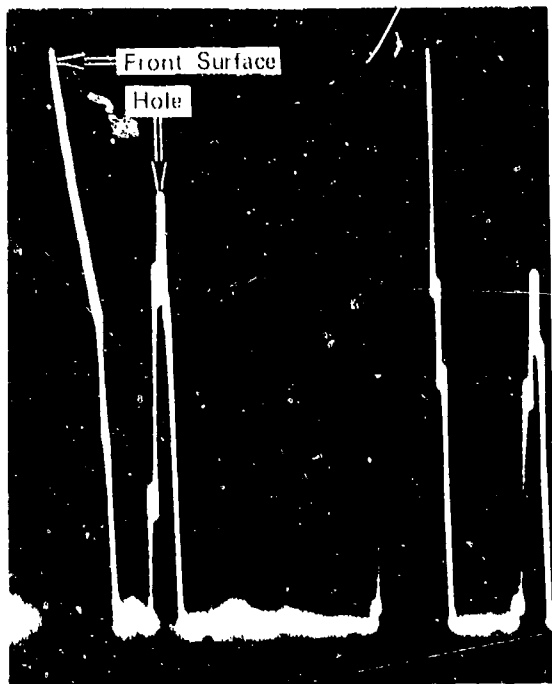
As might be expected, the use of higher test frequencies also improved the near surface resolution capability since the water/metal interface spike is narrowed with higher frequencies. However, in several cases the response from the flat bottom hole at the greatest metal travel in the set was less than 10 percent of full saturation. This would indicate that if, during a normal inspection, the scanning gain is established by adjusting the response from the flat bottom hole exhibiting the maximum response to 80% full saturation, it would not be possible to detect the same size defects throughout the full thickness of the part. This situation was found to occur in both the die forging and 4 inch thick plate. In order to properly test these pieces for defects using the above mentioned techniques, either a second inspection would have to be performed from the opposite side or scanning from one side would have to be performed at two scanning gains with metal travel overlap. Typical CRT photographs demonstrating the above effects are shown in Figure 45. Here it can be seen that the hole is resolvable at .40 inch but not at .25 inch and that it is not possible to test through the material in this case.

MIL-I-8950B, "Inspection, Ultrasonic, Wrought Metals, Process For", specifies that the near surface resolution capability must be 10 percent of the thickness or 0.125 inches, whichever is greater. Consequently, a near surface resolution capability of 0.4 inch, 0.2 inch, and 0.5 inch is required for the 4 inch, 2 inch, and 5 inch thick material tested under this program. From the data in Tables 25 and 26, it can be seen that this capability can be met for the 4 inch thick plate and 5 inch thick die forging. However, it was not possible to meet this requirement for the 2 inch thick plate when using the 5 MHz test frequency.

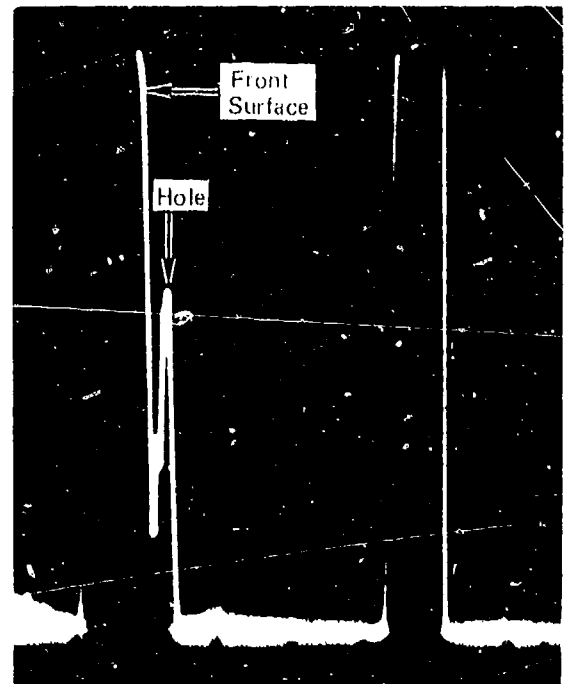
### (3) Testing of Machined Material

After testing the pieces in the as-rolled and as-forged condition, the as-received surfaces were machined to a 125 rms or better finish, leaving them with the metal travels shown in Table 24. These specimens were then tested using 4 separate flat transducers. These were: (1) 3/4 inch, 5 MHz, SIL; (2) 1/2 inch, 5 MHz, ; (3) 3/8 inch, 15 MHz, SIL; and (4) 3/4 inch, 5 MHz, SIL. The water path was 3 inches in all cases. Again, the Branson 600 and Sperry UM-715 ultrasonic instruments were used.

The test procedure was identical to that used for the as-received material. Following those tests, a second series of tests was performed in which the gain was established by adjusting the minimum response from each set of specimens to 80 percent of saturation. This method is also commonly used in industry for ultrasonic inspection.

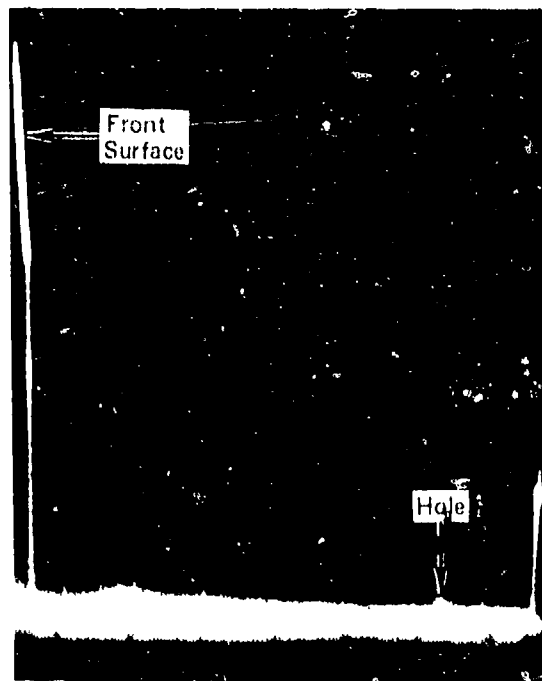


Metal Travel = 0.40 in.  
Hole is Resolved



Metal Travel = 0.25 in.  
Hole is not Resolved

GP74 0117 110



Metal Travel = 3.35 in.  
Hole Response is Less than 10% of Saturation

**FIGURE 45**  
RESPONSES FROM 3/64 INCH DIA FLAT BOTTOM HOLE IN 4 INCH  
PLATE AS-ROLLED (3/4 INCH DIA, 5MHz, 51Z TRANSDUCER WITH  
9 INCH WATER PATH)

GP74 0117 109

The near surface resolution capability as a function of product form, instrument, and search unit is summarized in Tables 27 and 28.

An examination of the data, indicates that the near surface resolution was again improved by increasing the test frequency. For example, with Test A, the near surface resolution in 4 inch plate was .17 to .37 inches with the 3/4 inch, 5 MHz, SIZ search unit but was .08 to .17 inches with the 3/8 inch, 15 MHz, SIL.

As in the case of the as-received material tests, there were several instances where, during Tests B, the hole response at the largest metal travel was less than 10 percent of saturation. Hence, it would not be possible to inspect through the total thickness of the 4 inch plate and 5 inch die forging under those conditions. It should be noted that by choosing the lower frequency (3/4 inch, 5 MHz, SIZ) it was possible to test through the total thickness of the material at the expense of reducing the near surface resolution capability.

It is interesting to compare the results from the two test methods. Obviously, using Test Method A, where the minimum response is adjusted to 80 percent of saturation, there is no difficulty in testing through the total thickness as was the case several times when testing with Test Method B. It might be thought that the near surface resolution would be less with Test Method A since the higher scan gain required, compared with Test Method B, would tend to broaden the water/metal interface response. It was found that in most cases, however, that the near surface resolution capability of Test Method A was not less than that of Test Method B. Only in one case, in fact, was it less; that being for the 3/8 inch, 15 MHz, SIL search unit. It would seem from these results, that, if it were imperative to inspect material from one side only, it could be done so using Test Method A without any effect upon the near surface resolution capability. However, the increased ultrasonic noise level may at least partially offset the gains obtained by inspecting at higher sensitivity.

A comparison of the near surface resolution data for the as-received material and the machined material was made. In a few cases, the near surface resolution was improved after machining. For example, for a 3/4 inch, 5 MHz, SIZ search unit the 3/64 inch diameter hole in the die forging was resolved at a metal travel of .20 inch after machining, whereas it was not resolved when the sound entry surface was in the as-forged condition. Improvement was made due to machining in the following cases:

- (a) die forging - 3/4 inch, 5 MHz, SIZ with Branson 600
- (b) die forging - 3/4 inch, 5 MHz, SIL with Sperry UM-715

**TABLE 27**  
**NEAR SURFACE RESOLUTION OF MACHINED SPECIMENS**  
**(3/64 In. Dia meter Flat Bottom Hole Response)**

Product Form	△ <sub>1</sub> Test A			
	Branson 600			Sperry UM-715
	3/4 in., 5 MHz SIZ	1/2 in., 5 MHz α	3/8 in., 15 MHz SIL	3/4 in., 5 MHz SII
4 in. Plate	0.17 to 0.37	0.08 to 0.17	0.08 to 0.17	0.17 to 0.37
2 in. Plate	0.10 to 0.20	0.10 to 0.20	0.10 to 0.20	0.20 to 0.38
Die Forging	0.15 to 0.21	0.15 to 0.21	0.10 to 0.15	0.15 to 0.21

Product Form	△ <sub>2</sub> Test B			
	Branson 600			Sperry UM-715
	3/4 in., 5 MHz SIZ	1/2 in., 5 MHz α	3/8 in., 15 MHz SIL	3/4 in., 5 MHz SIL
4 in. Plate	0.17 to 0.37	0.08 to 0.17 △ <sub>3</sub>	0.08 to 0.17 △ <sub>3</sub>	0.17 to 0.37
2 in. Plate	0.10 to 0.20	0.10 to 0.20	0.10 to 0.20	0.20 to 0.38
Die Forging	0.15 to 0.21	0.15 to 0.21 △ <sub>3</sub>	0.15 to 0.21 △ <sub>3</sub>	0.15 to 0.21

- △<sub>1</sub> Test A was performed by setting the minimum response to 80% of saturation.
- △<sub>2</sub> Test B was performed by adjusting the maximum response to 80% of saturation.
- △<sub>3</sub> Response from largest metal travel was less than 10% of saturation.

GP74 0117 107

**TABLE 28**  
**NEAR SURFACE RESOLUTION OF MACHINED SPECIMENS**  
**(5/64 In. Diameter Flat Bottom Hole Response)**

Product Form	1 Test A			
	Branson 600			Sperry JIM-715
	3/4 in., 5 MHz SIZ	1/2 in., 5 MHz $\alpha$	3/8 in., 15 MHz SIL	3/4 in., 5 MHz SIL
4 in. Plate	0.17 to 0.37	0.08 to 0.17	0.08 to 0.17	0.17 to 0.37
2 in. Plate	0.10 to 0.20	Less Than 0.08C	Less Than 0.10	0.20 to 0.38
Die Forging	0.15 to 0.21	0.15 to 0.21	0.10 to 0.15	0.15 to 0.21

Product Form	2 Test B			
	Branson 600			Sperry UM-715
	3/4 in., 5 MHz SIZ	1/2 in., 5 MHz $\alpha$	3/8 in., 15 MHz SIL	3/4 in., 5 MHz SIL
4 in. Plate.	0.17 to 0.37	0.08 to 0.17 3	0.08 to 0.17 3	0.17 to 0.37
2 in. Plate.	0.10 to 0.20	0.10 to 0.20	Less Than 0.10	0.20 to 0.38
Die Forging	0.15 to 0.21	0.15 to 0.21	Less Than 0.10 3	0.15 to 0.21

- 1 Test A was performed by setting the minimum response to 80% of saturation.
- 2 Test B was performed by setting the maximum response to 80% of saturation.
- 3 Response from largest metal travel was less than 10% of saturation.

GP74-0117-108

In each case the near surface resolution went from .20 - .40 inch to .15 - .21 inch.

Upon completion of the near surface resolution study, the machined specimens were used to investigate scan index. During an ultrasonic inspection of production parts, one of the parameters which must be selected is the scan index. It is important that the scan index be small enough to ensure 100 percent inspection of the parts. During a typical ultrasonic inspection all discontinuities whose amplitude exceeded 50 percent of the distance-amplitude curve would be marked for further evaluation since the response may not be maximized on the discontinuity. The final evaluation would be made by positioning the search unit for maximum response from the discontinuity and, if the response exceeded the distance - amplitude curve, the discontinuity would be considered rejectable. On this basis of testing, then, it is important to choose a scan index through which no less than 50% of the reference standard response is obtained.

Several tests were performed to determine the maximum scan index for the test specimens on hand. Initially, the search unit was positioned to maximize the response from the flat bottom hole with a 3 inch water path and then moved off centerline until response dropped to 50 percent of its initial amplitude. This, then, was considered one-half the maximum scan index. The results of the testing are shown in Table 29. In general, the maximum scan index increases with search unit diameter and with the reference reflector size.

#### c. Sound Transmission Characteristics

In many ultrasonic inspection situations, there exists a significant difference in sound transmission characteristics between the reference standard and the part to be inspected. In addition to attenuation differences, such things as surface finish variations, grain flow direction, and metallurgical variations can contribute to the difference. If corrections are not made for the differences, it is possible that rejectable defects can be accepted because they can appear smaller than they actually are based on their ultrasonic response.

A test program was conducted to quantitatively determine the magnitude of sound transmission differences for rolled plate and die forging material. The test specimens were those fabricated for the near surface resolution study described previously (see Figure 43 and Table 24). In addition to these specimens, a set of ASTM-type Ti-6Al-4V reference standards containing 3/64 inch diameter flat bottom holes were used to represent typical straight beam immersion reference standards (see Figure 35).

Initially, a distance-amplitude correction (DAC) curve was constructed using the ASTM-type reference standards with 3/64 inch diameter flat bottom holes and with metal travels varying from 1/2 to 5-1/2 inches. The ASTM-type standards were placed in the water, the search unit was

**TABLE 29**  
**MAXIMUM SCAN INDEX FOR MACHINED SOUND ENTRY SURFACE**  
(Metal Travels are Indicated in Parenthesis)

Search Unit	4 in. Plate		2 in. Plate		Die Forging	
	3/64 in. Hole	5/64 in. Hole	3/64 in. Hole	5/64 in. Hole	3/64 in. Hole	5/64 in. Hole
3/8 in. Dia 15 MHz, SIL (S/N 17205)	0.060 (0.17)	0.20 (0.08)	0.060 (0.20)	—	0.050 (0.15)	—
3/4 in. Dia 5 MHz, SIZ (S/N 21269)	0.18 (0.37)	—	—	—	0.20 (0.21)	—
1/2 in. Dia 5 MHz, Aerotech α	0.10 (0.37)	0.14 (0.08)	0.08 (0.20)	—	0.06 (0.21)	—
3/4 in. Dia 5 MHz, SIL (S/N 21263)	0.18 (0.37)	—	0.18 (0.38)	—	0.12 (0.21)	—

QP74-0117-100

adjusted to the selected water path, and the reference standard which exhibited the maximum response was located. Then, the amplitude of that response was adjusted to 80 percent of saturation. Without changing the gain, the amplitude responses from the other ASTM-type standards was recorded and distance-amplitude curves (DAC) were constructed.

These tests were performed using the following search unit and ultrasonic instrument combinations:

- (a) 3/4 inch diameter, 5 MHz, SIZ (S/N 21269) with the Branson 600
- (b) 1/2 inch diameter, 10 MHz, SIZ (S/N 15544) with Branson 600
- (c) 3/8 inch diameter, 15 MHz, SIL (S/N 17205) with Branson 600
- (d) 3/4 inch diameter, 5 MHz, SIL (S/N 21263) with Sperry UM-715

The testing was repeated 7 times using the same technician, the S/N 21269 search unit and a 3 inch water path. Also, the testing was repeated 4 times with the same technician, the S/N 21269 search unit and a 9 inch water path. These tests were repeated in order to measure the variation in response from one test to another. Each repeated test was initiated from the beginning with the placing of the reference standards made for the program in the water. The data was normalized prior to plotting the DAC curves by adjusting the maximum response in each test to an amplitude of 1 inch with the remaining amplitudes in the DAC curve adjusted accordingly. Typical plots of the relative amplitudes as a function of metal travel are shown in Figures 46 and 47. Also, shown are the positions of the near field in the metal as calculated from the search unit diameter, sound velocity, and test frequency. A decibel (dB) scale is included in each plot for reference.

When plotted logarithmically, the amplitude response versus metal travel for a constant flat bottom hole size, should follow a straight line. However, deviations from this straight line may occur in repeated tests since the holes may not be exactly of the same diameter and orientation. Also, there may be some variation in repeatability due to variations in search unit orientation with respect to the reference standard, etc.

The data was analyzed and it was found that one standard deviation for the response variation from the ideal straight line due to variation in hole preparation was approximately 1.7 dB. One standard deviation due to test repeatability was approximately 1.3 dB. For a 95 percent confidence level, then, a specific 3/64 inch diameter hole response was within  $\pm 3.5$  dB of the theoretical response. The test-retest repeatability of the operator, equipment, and setup combination was  $\pm 2.5$  dB. It should be noted that these specific values could be expected to vary with such factors as search unit size, test frequency, and hole preparation.

After the distance-amplitude curves were produced, testing was performed upon the as-rolled plate and as-forged die forging material containing flat bottom holes. These tests were performed using the same operator, and equipment as described above. The search unit was positioned over the particular piece and, with the gain setting the same as for the previously tested standard, the response from the flat bottom hole was recorded. Typical normalized responses are plotted in Figures 46 and 47.

Next, the plate and forging pieces were machined to a 125 rms or better surface finish and the testing was repeated. Typical normalized responses are plotted in Figures 46 and 47.

A comparison of the relative responses from the plate, forging and ASTM-type reference standards was made for those data points in the far field. This comparison is documented in Table 30. It should be recalled that the response variation was  $\pm 6$  dB due to the sum of the variations in hole geometry and test-retest repeatability. As shown in Table 30, the only case where the response difference exceeded  $\pm 6$  dB was for the 4 inch machined plate. The greater attenuation of the machined plate was expected due to the higher noise levels normally experienced in production machined part ultrasonic inspection whenever the ultrasonic beam is directed normal to the grain flow of the part.

A comparison of the distance-amplitude plots in the straight line region for the ASTM-type reference standards revealed that the slope of the straight line varied as a function of the search unit used. For the three SIZ search units the slope was approximately 6 dB per inch of metal travel, for the three SII search units the slope was approximately 3.5 dB per inch of metal travel and for the Aerotech Alpha search unit the slope was approximately 9.0 dB per inch.

The difference in peak amplitude positions from plot to plot was explainable by the end of the near field zone. It is significant, however, that the calculated near field length was too short in some cases indicating a difference in search unit frequency and/or diameter than indicated on the housing of the search unit. It is also significant to note that many parts are inspected completely in the near field zone.

#### d. Effect of Surface Condition

Several ultrasonic tests were performed to determine the effect of as-received and machined surfaces upon ultrasonic response during contact and immersion inspections.

##### (1) Angle Beam Inspection - As-rolled Plate

The test specimen shown in Figure 46 was used to determine if the ultrasonic response from a flat bottom hole is changed when an as-rolled surface is machined to a finish of 125 rms or better.

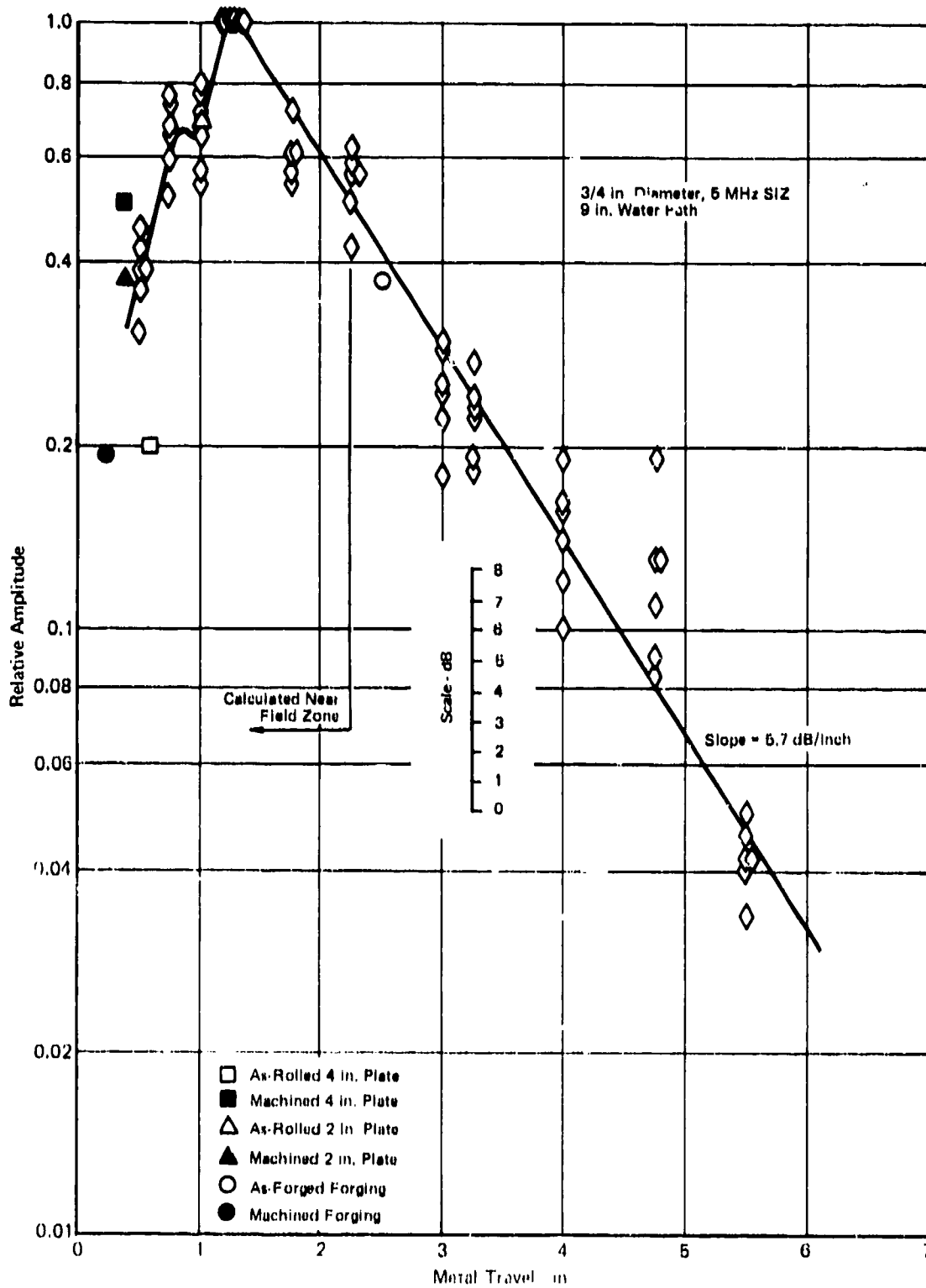


FIGURE 46  
RELATIVE RESPONSE vs METAL TRAVEL

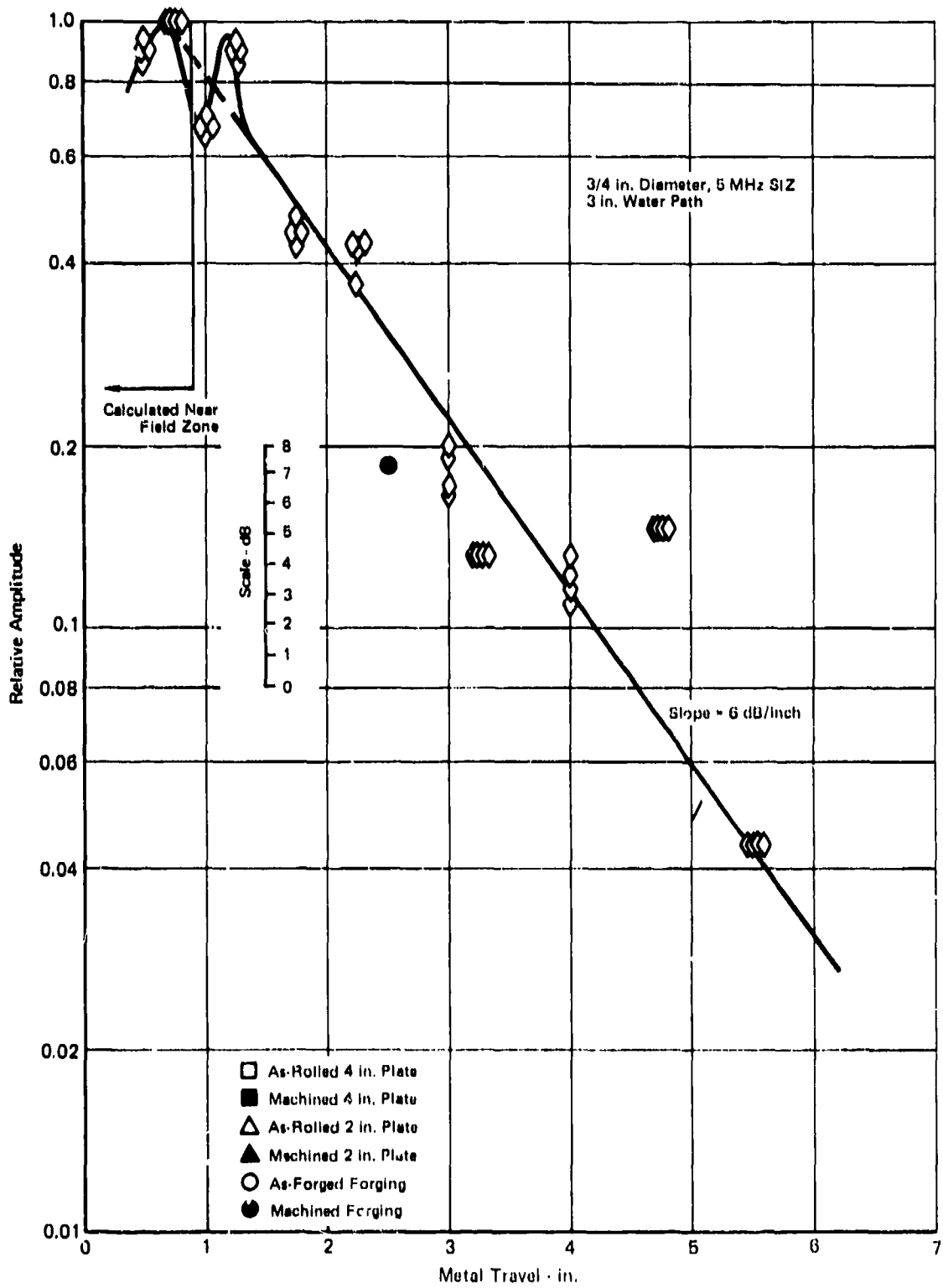


FIGURE 47  
RELATIVE RESPONSE vs METAL TRAVEL

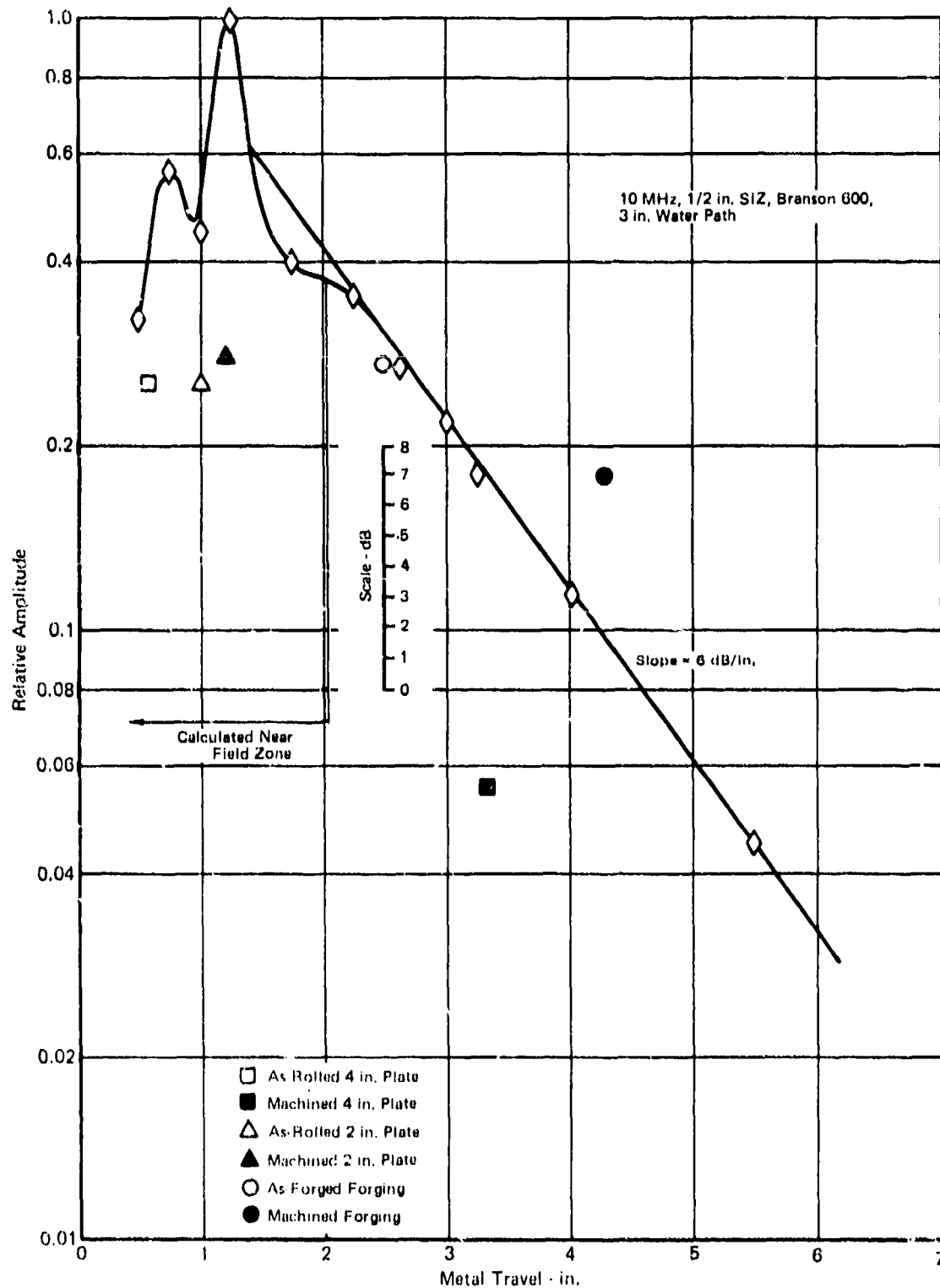


FIGURE 47 (Continued)  
RELATIVE RESPONSE vs METAL TRAVEL

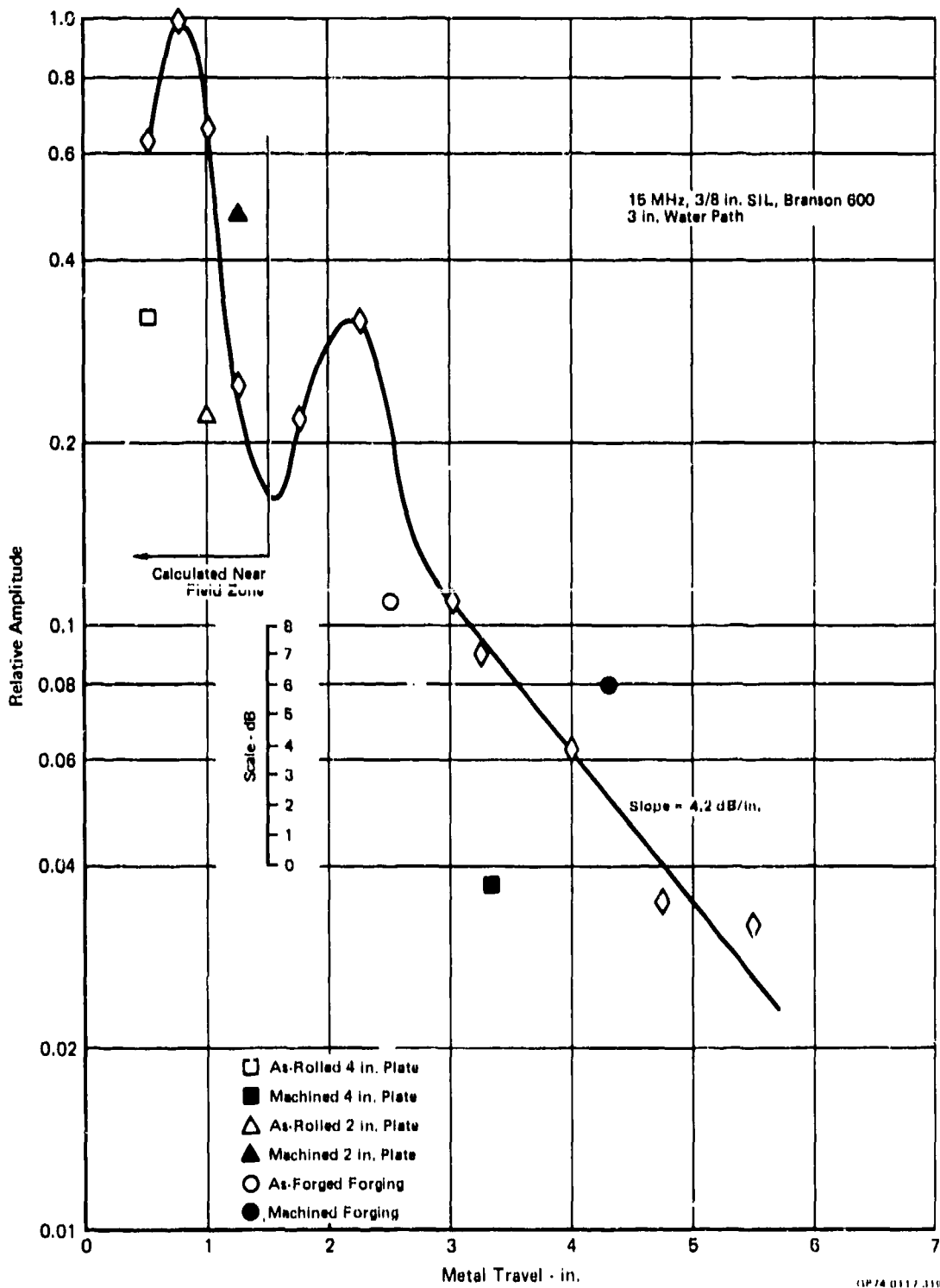


FIGURE 47 (Continued)  
RELATIVE RESPONSE vs METAL TRAVEL

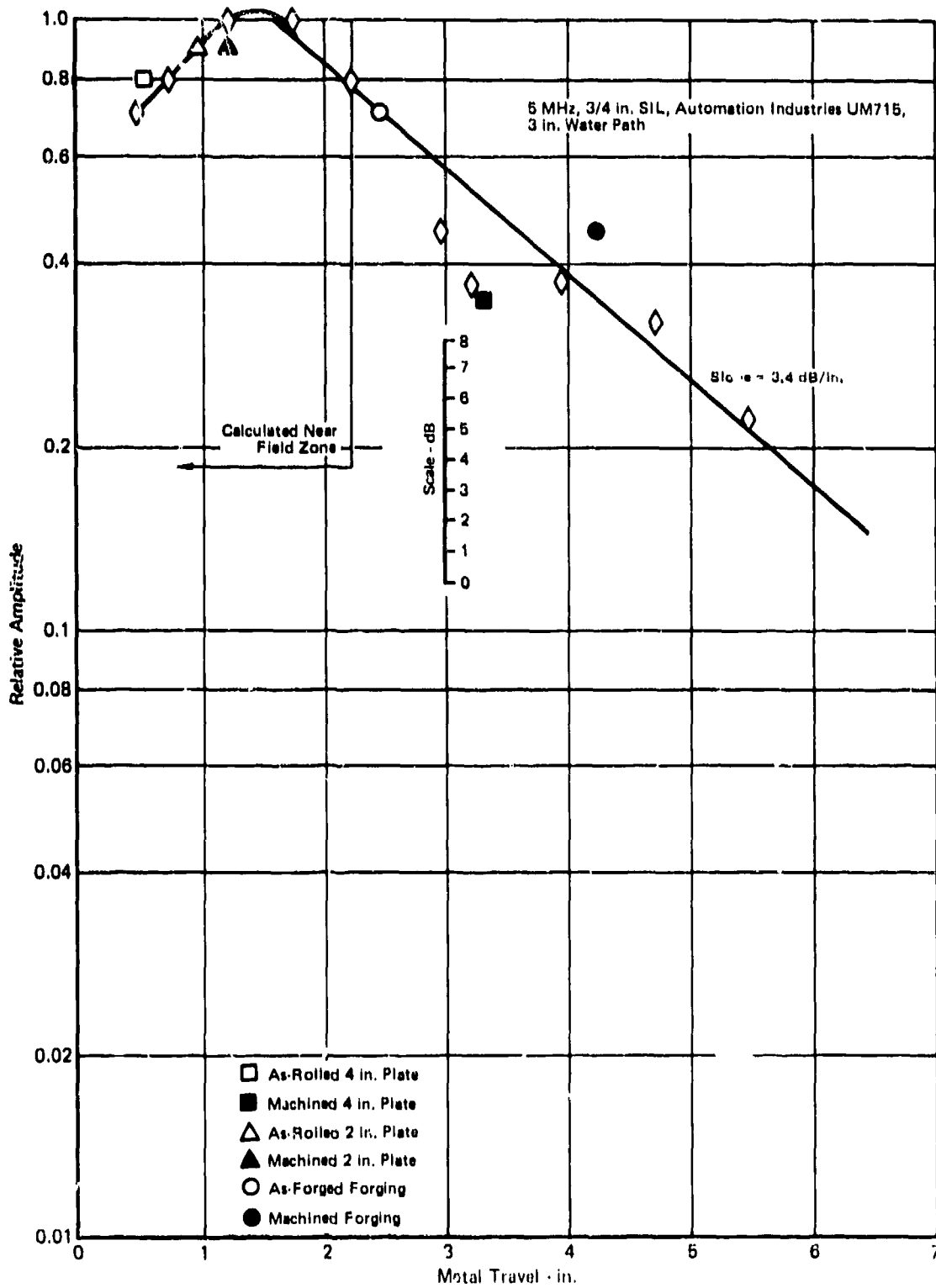


FIGURE 47 (Continued)  
RELATIVE RESPONSE vs METAL TRAVEL

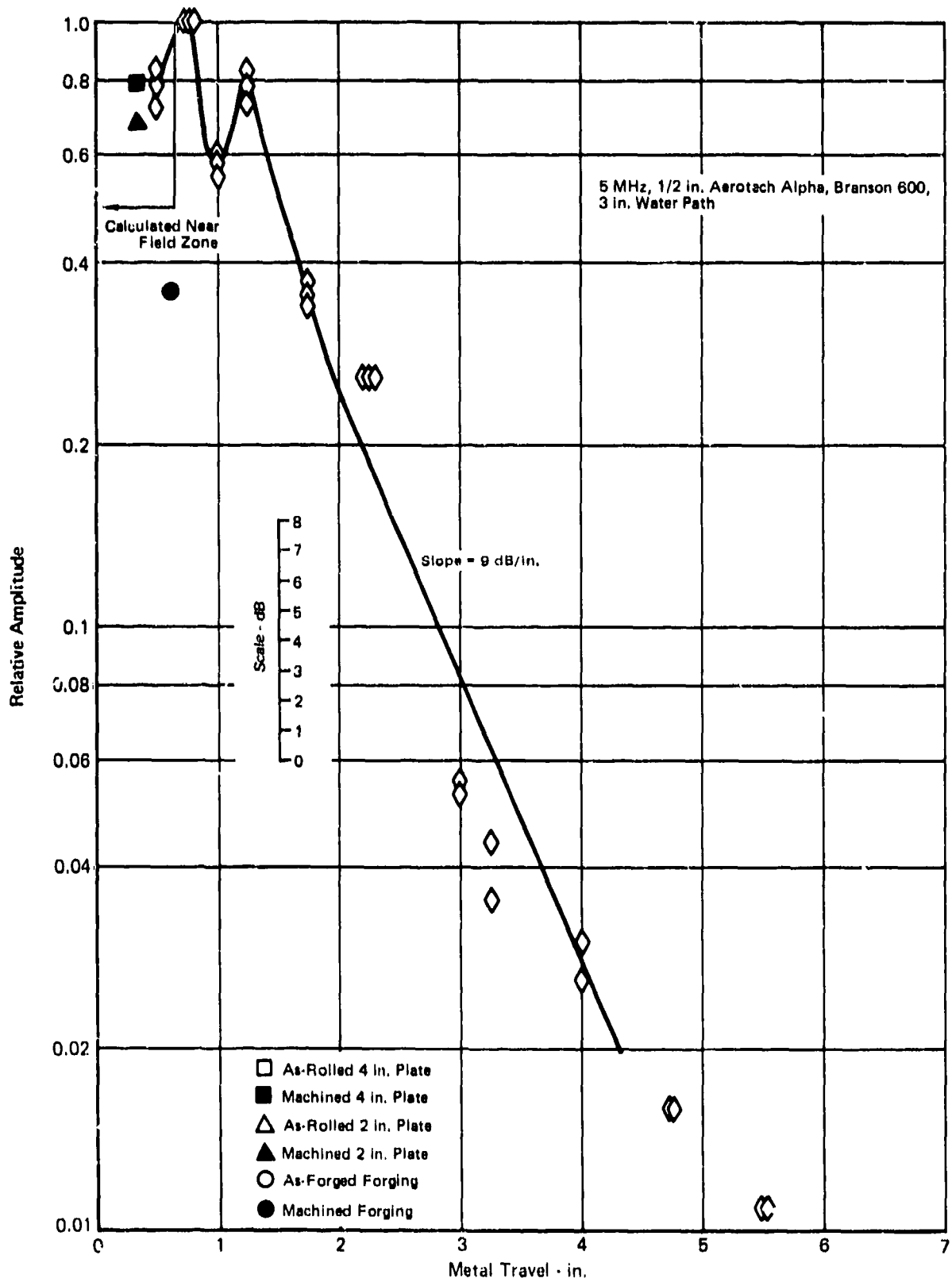


FIGURE 47 (Continued)  
RELATIVE RESPONSE vs METAL TRAVEL

GP74 0117 321

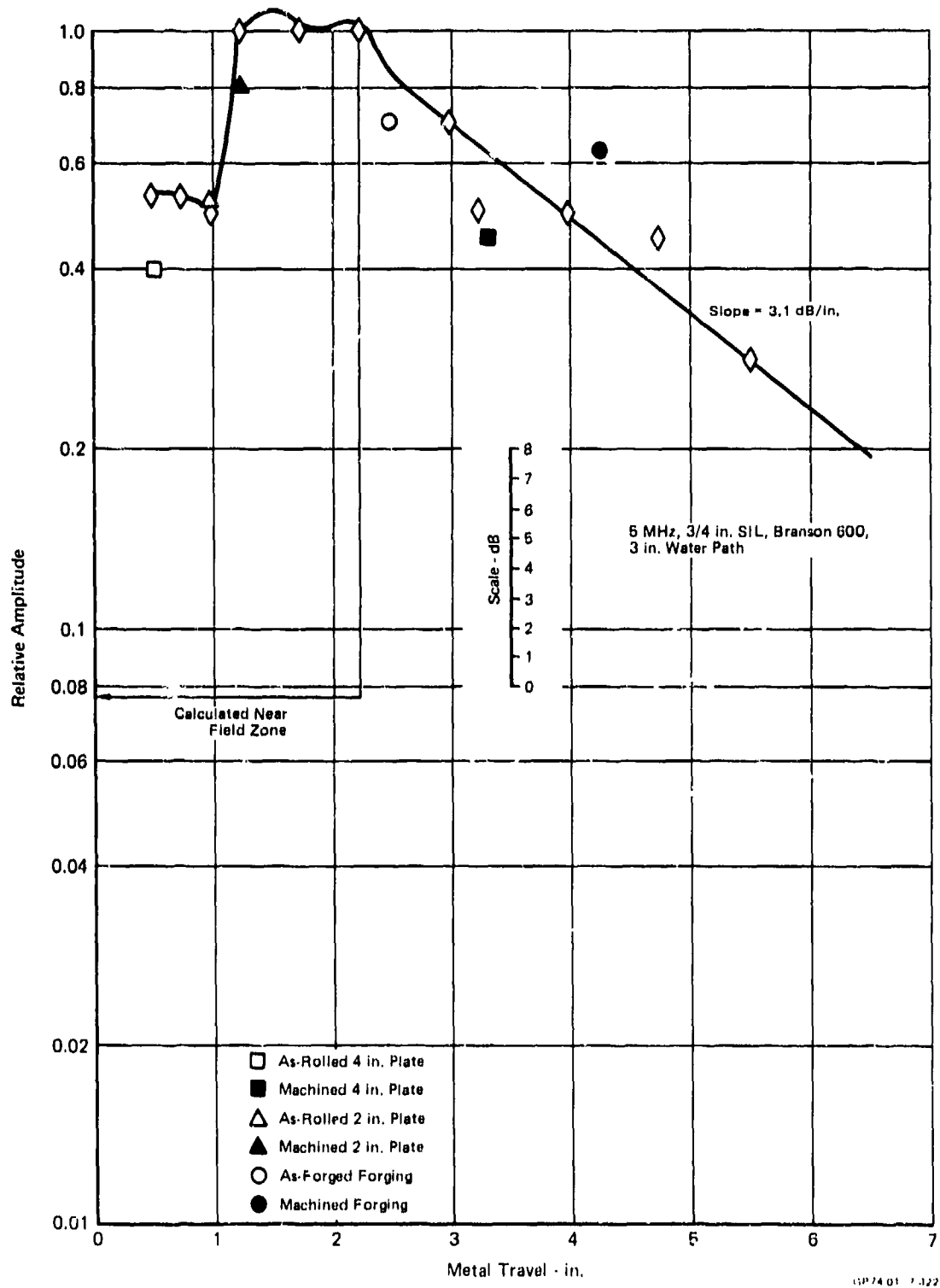
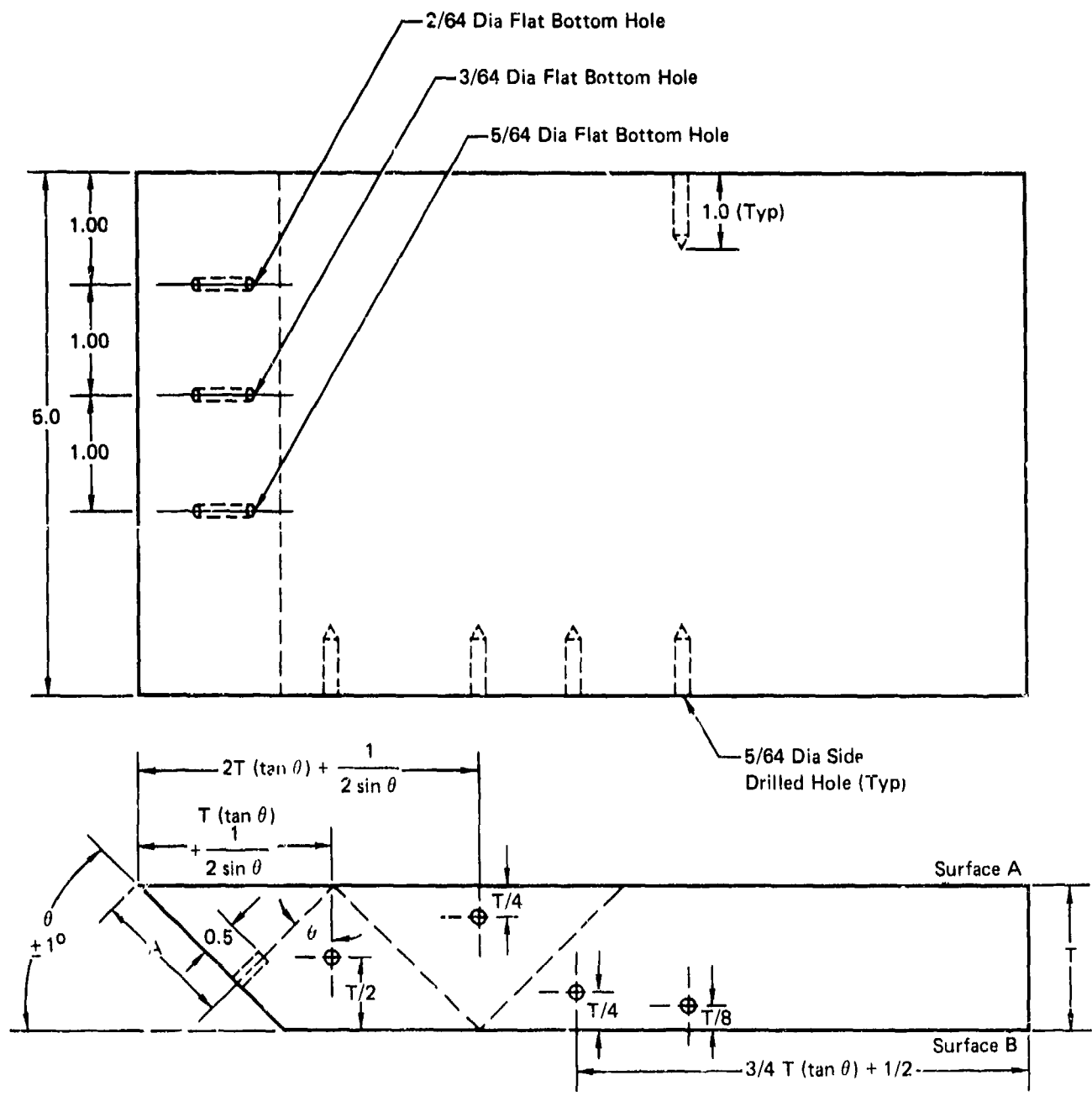


FIGURE 47 (Continued)  
RELATIVE RESPONSE vs METAL TRAVEL



Notes:

1. Surface A and Surface B must be flat and parallel within 0.001 inch.
2. All dimensions are  $\pm 0.03$  in, except for hole diameters which are  $\pm 3\%$  of the diameter specified.
3. Hole bottom must be flat within 0.001 in. per 1/8 in. diameter.

GP74-0117-82

FIGURE 48  
ANGLE BEAM TEST SPECIMEN

**TABLE 30**  
**DIFFERENCE IN RESPONSE BETWEEN PLATE AND FORGING AND**  
**ASTM - TYPE REFERENCE STANDARDS**

Search Unit	Response Variation (dB)			
	2 in. As-Rolled Plate	4 in. Machined Plate	As-Forged Forging	Machined Forging
3/4 in. Diameter, 5 MHz, SIZ	-2	-2.75	-1	+2.5
1/2 in. Diameter, 10 MHz, SIZ	-4	-8	-1	+3.5
3/8 in. Diameter, 15 MHz, SIL	-4	-8.5	-1	+3.5

GP74-0117-313

Initially, the 1-1/2 inch thick as-rolled plate specimen was positioned in the water tank and a 3/4 inch diameter, 5 MHz, SIZ search unit (S/N 21269) was adjusted to a 3 inch water path and a refracted sound beam angle in the metal of 45 degrees  $\pm$  5 degrees. A Branson 600 ultrasonic instrument was used for the testing. The response from the flat bottom hole was adjusted to 80 percent of saturation and the gain control setting and dB setting were recorded.

Next, the testing with an as-rolled sound entry surface was repeated for the contact angle beam method. A 5 MHz, 45 degree contact angle beam search unit was used along with "Lubri-plate" grease as a couplant. Again, the responses from the flat bottom holes were adjusted to 80 percent of saturation and the gain and dB setting were recorded.

After testing was completed with an as-rolled sound entry surface, the surfaces were machined to a finish of 125 rms or better. The previous testing was repeated by returning to the original gain setting, adjusting the hole response to 80 percent of saturation, and recording the dB setting. The results are shown below.

dB Difference In Response From As-Rolled and Machined Specimens			
Immersion		Contact	
3/64 Hole	5/64 Hole	3/64 Hole	5/64 Hole
1-1/2	1-1/2	0	0

As can be seen, the response difference between as-rolled and machined was insignificant for both the immersion and contact testing for the size reference holes used. This would appear to indicate that an as-rolled sound entry surface on a piece of plate would not reduce the inspectability of that plate as compared to a machined sound entry surface.

## (2) Straight Beam Inspection - Extrusion

In order to investigate the effect of an extruded sound entry surface, a 3/64 inch diameter flat bottom hole was drilled in a 1/2 inch thick piece of titanium extrusion. The hole was drilled to a depth of approximately 1/8 inch. With the as-extruded surface intact, a straight beam immersion test was performed at a water path of 3 inch using a 1/2 inch diameter, 10 MHz Aerotech Alpha search unit and again with a 1/2 inch, 5 MHz Aerotech Alpha search unit along with a Branson 600 instrument. The hole response was adjusted to 80 percent of saturation and the gain and dB setting were recorded.

After testing the as-extruded piece, the sound entry surface and back surface were machined to a finish of 125 rms or better. The testing was repeated at the original gain setting. The results are shown below.

dB Difference In Response From As-Extruded and Machined Specimens	
<u>10 MHz</u>	<u>5 MHz</u>
2	1/2

As can be seen, the response difference was insignificant for the immersion tests.

e. Inspection of Thin, Machined Parts

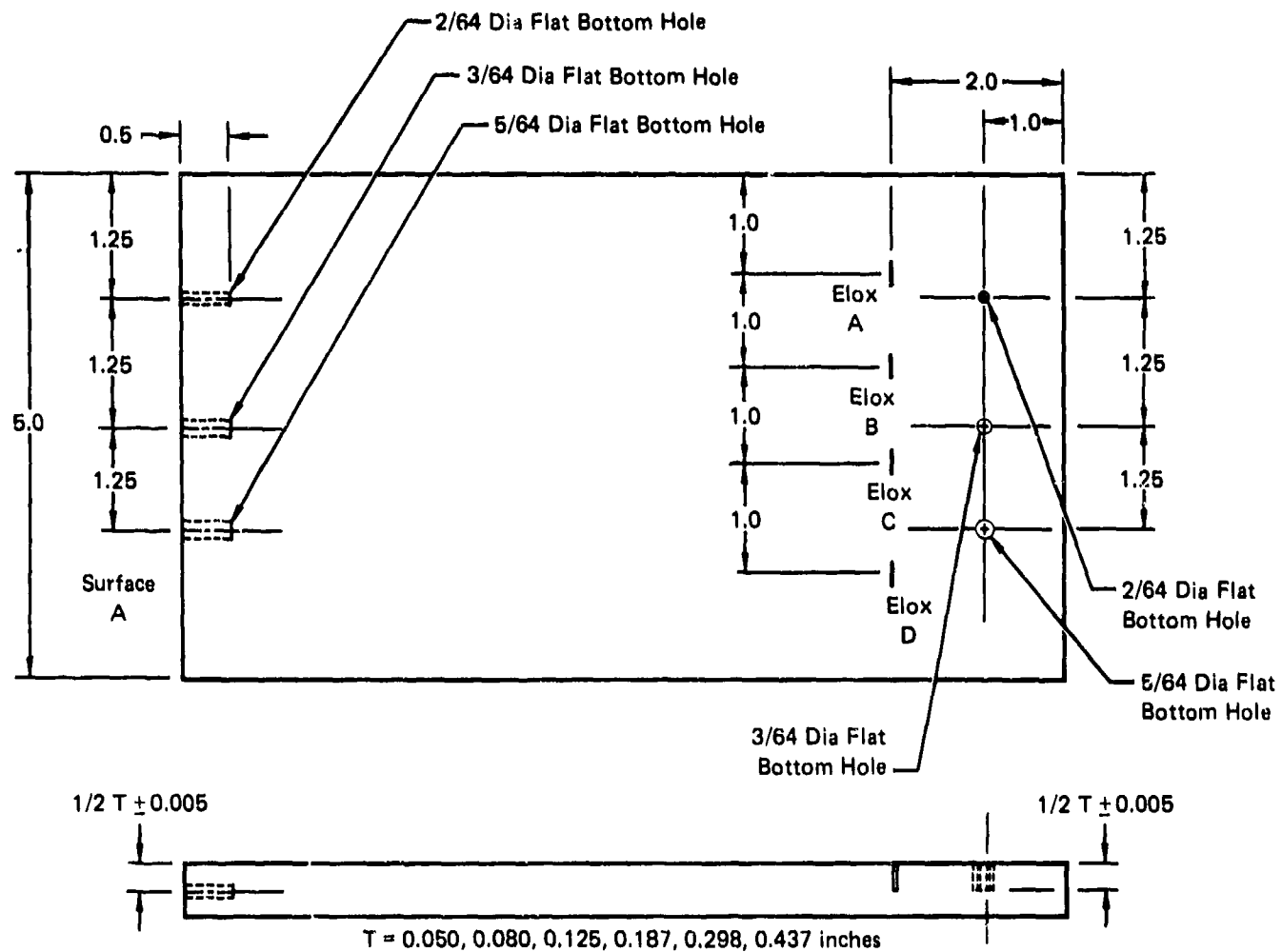
Some airframe manufacturer's employ ultrasonic inspection techniques on final machines parts particularly in thin sections including such areas as the webs of machined bulkheads. Testing performed during this program has demonstrated the value of such inspections. There are defects that can be detected in final machined parts that cannot be detected in thicker product forms such as raw forgings. As shown in Section 3 of the NDT capability portion of this report, the detectability of internal cracks with angle beam techniques can be quite low in thick section parts because of the part thickness and crack orientation. However, a large number of these cracks can be detected after final machining to a thinner section (see Table 69).

A program was conducted to investigate several ultrasonic techniques for application to ultrasonic inspection of thin areas.

(1) Pulse - Echo

Initially, pulse-echo immersion testing was examined with the intent being to establish the resolution capabilities of the methods for flaws lying parallel to the machined surface as a function of test frequency. Two search units were evaluated. These were a 1/2 inch diameter 10 MHz SIL long focus search unit (3.7 inch focal length in water) and a 5/16 inch diameter 25 MHz SIL focused search unit. Both search units were used in conjunction with a Branson 600 ultrasonic instrument and a 623 Ts pulser/receiver. Test specimens ranging in thickness from .050 to .437 inch were drilled with 2/64, 3/64, and 5/64 inch diameter flat bottom holes as shown in Figure 49. These flat bottom holes were designed to represent discontinuities in parts of various thickness.

The test specimens were placed in the water and the search unit was adjusted to bring the focal point to the front surface of the particular specimen being tested. Next, the search unit was moved to the 5/64 diameter hole and positioned to peak the response from the hole. The gain was adjusted to position the response to 80% of saturation on the cathode ray tube in order to simulate the scanning gain for an actual inspection where the minimum response is adjusted to 80% of saturation.



Notes:

1. Hole bottom must be flat within 0.001 in. per 1/8 dia.
2. All dimensions are  $\pm 0.03$  in. except for hole diameters which are  $\pm 3\%$  of the specified dia.
3. Plane of flat bottom holes and elox slots must be perpendicular to sound entry surface and parallel to 5 in. dimension within  $\pm 2$  degrees.
4. Side drilled flat bottom holes must be perpendicular to Surface A  $\pm 1$  degree in two directions 90 degrees opposed.

QP74-0117 7B

FIGURE 49  
TEST SPECIMEN CONFIGURATION

It was noted whether or not the hole response was resolvable from the water/metal interface and if the back surface was resolvable from the water/metal interface. Also, the noise level was measured on the CRT screen. For the purposes of this test, the hole and back surface response was considered resolvable if they came completely down to the baseline on the CRT (see Figure 50).

Next, the search unit was moved to the  $5/64$  inch diameter hole in the 0.298 inch thick piece and the hole response was adjusted to 80% of saturation. The dB required to adjust the hole response to 80% of saturation was measured. Again it was noted whether or not the hole response and the back surface were resolvable.

This test procedure was repeated for all the test specimens and all the flat bottom holes in an attempt to ascertain the best choice of search unit for inspection of flat thin parts using the pulse-echo technique.

A summary of the results is presented in Table 31. A series of photographs demonstrating typical CRT displays is shown in Figures 51 thru 53. It can be seen from Table 31 that an improvement in resolution was obtained by increasing the test frequency from 10 MHz to 25 MHz. For example, the  $3/64$  inch diameter hole was resolvable at a .063 inch metal travel with 25 MHz but not with 10 MHz (see Figure 52).

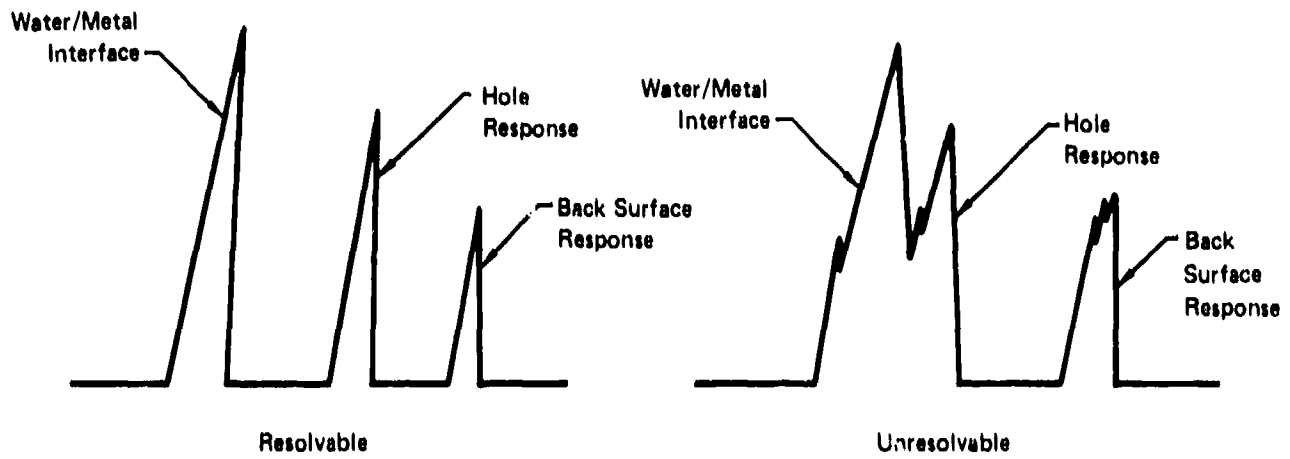
The ultrasonic noise from the test specimens was quite low; never exceeding 10% of saturation at the gain level required for a hole response of 80% of saturation.

Separation of the back surface response from the water/metal interface response was also improved by increasing the test frequency to 25 MHz from 10 MHz. An example of a CRT display is shown in Figure 53.

Based on these results, it appears that it is possible to resolve discontinuities equivalent to a  $2/64$  inch diameter flat bottom hole at metal travels as small as 0.094 inch.

## (2) Reflector Plate Method

Another potential technique for ultrasonic inspection of thin parts is the reflector plate technique demonstrated in Figure 54.



GP74-0117-76

**FIGURE 50**  
**DEFINITION OF NEAR SURFACE RESOLUTION AND BACK SURFACE RESOLUTION**

**TABLE 31**  
**IMMERSION PULSE ECHO TESTING**  
**5/64 in. Dia Flat Bottom Holes**

Metal Travel (in.)	dB for 80% Response		Back Surface Resolvable	
	10 MHz	25 MHz	10 MHz	25 MHz
0.218	21	9	Yes	Yes
0.149	21	10	Yes	Yes
0.094	18	14	Yes	Yes
0.083	△	△	Yes	Yes
0.040	△	△	No	Yes
0.025	△	△	No	No

**3/64 in. Dia Flat Bottom Holes**

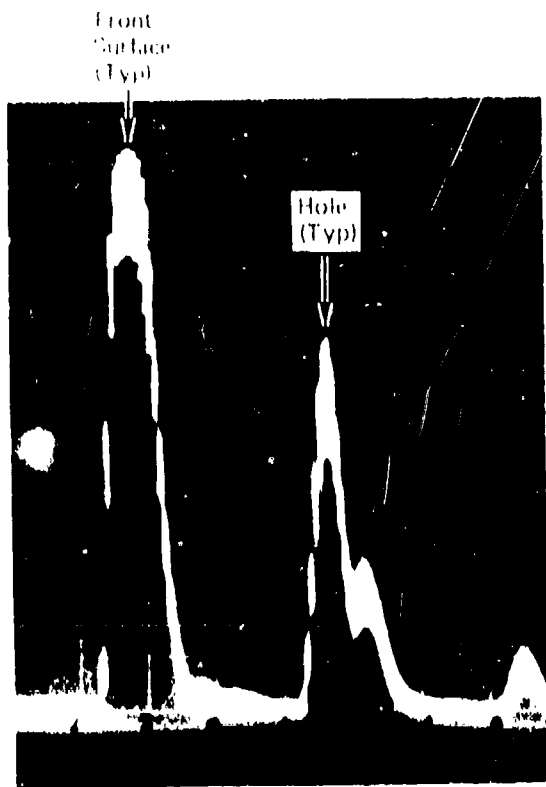
Metal Travel (in.)	dB for 80% Response		Back Surface Resolvable	
	10 MHz	25 MHz	10 MHz	25 MHz
0.218	15.5	7	Yes	Yes
0.149	14	10	Yes	Yes
0.094	△	12	No	Yes
0.083	△	12	No	Yes
0.040	△	△	No	Yes
0.025	△	△	No	No

**2/64 in. Dia Flat Bottom Holes**

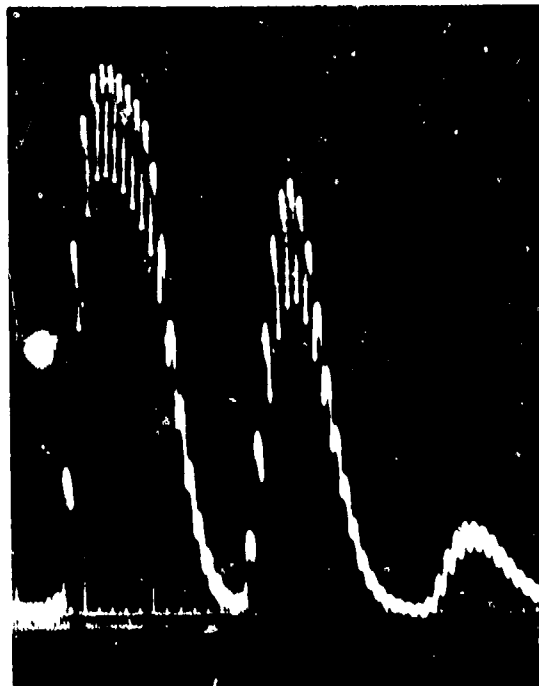
Metal Travel (in.)	dB for 80% Response		Back Surface Resolvable	
	10 MHz	25 MHz	10 MHz	25 MHz
0.218	10	2	Yes	Yes
0.149	15	5	Yes	Yes
0.094	△	10	No	Yes
0.083	△	△	No	Yes
0.040	△	△	No	Yes
0.025	△	△	No	Yes

△ Hole not Resolved

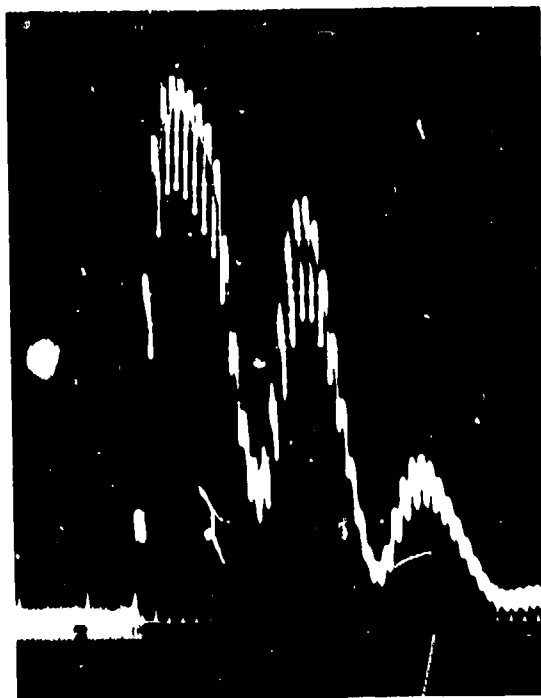
GP74 0117 77



0.149 in. Metal Travel



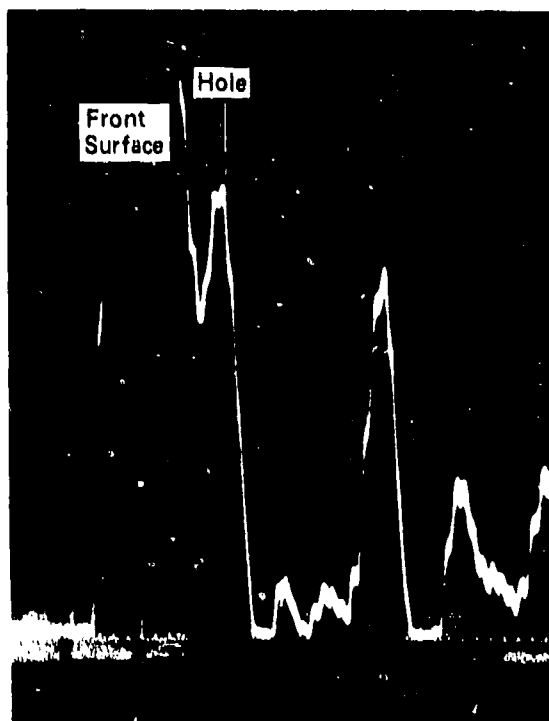
0.094 in. Metal Travel



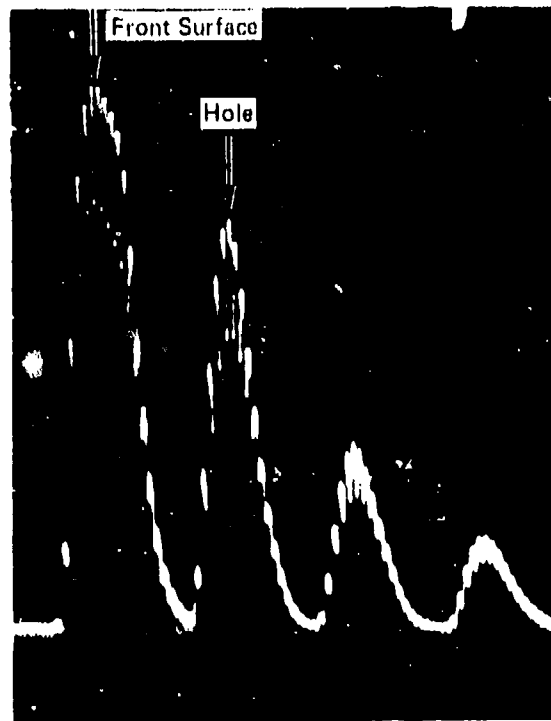
0.063 in. Metal Travel (Unresolved)

GE74-011-00

**FIGURE 51**  
**TYPICAL CRT DISPLAYS FOR PULSE ECHO TESTS**  
 2/64 In. Dia Flat Bottom Holes  
 5/16 In. Dia, 25 mHz SIL Search Unit



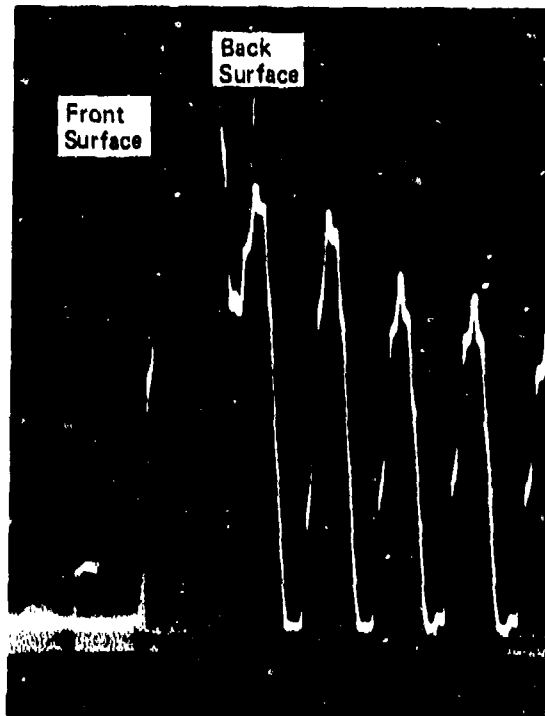
10 MHz (Unresolved)



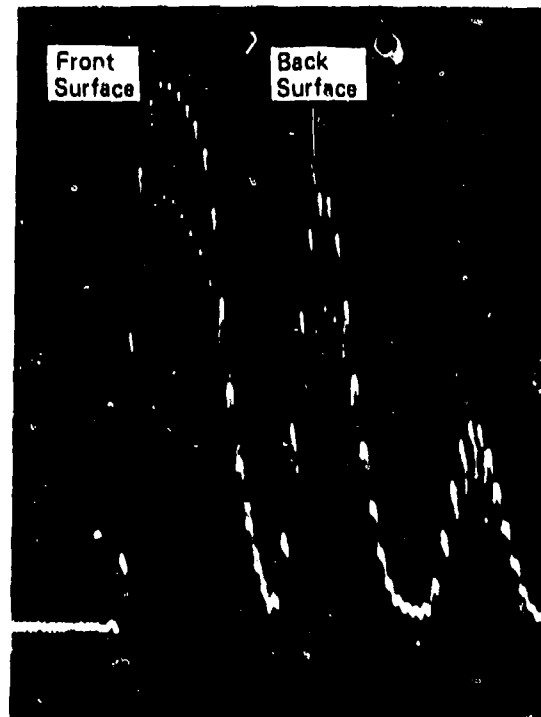
25 MHz (Resolved)

GP74-0117-MB

**FIGURE 52**  
**INCREASE IN RESOLUTION WITH 25 MHz TEST FREQUENCY (3/64 IN. DIA HOLE,**  
**0.094 IN. METAL TRAVEL)**



0.040 in. Metal Travel  
10 MHz (Unresolved)



0.040 in. Metal Travel  
25 MHz (Resolved)

FIGURE 53  
INCREASED RESOLUTION OF BACK SURFACE WITH INCREASED  
TEST FREQUENCY

GP74-0117-07

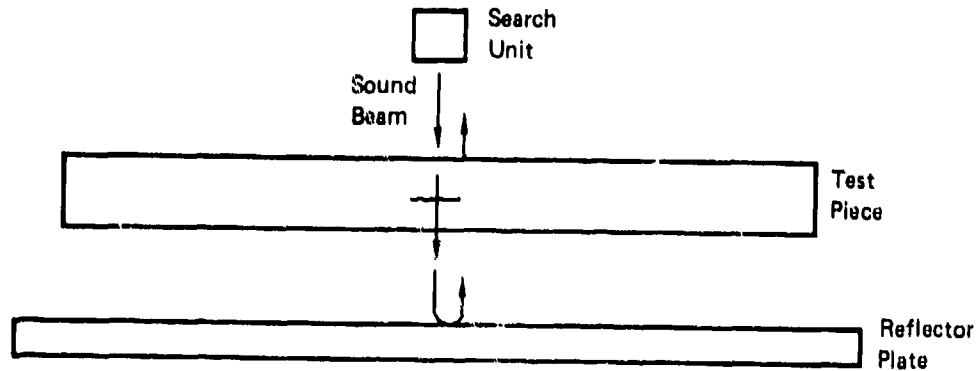


FIGURE 54  
REFLECTOR PLATE METHOD

QP74-0117-70

As can be seen, the sound beam is transmitted through the test piece, reflected from the reflector plate, transmitted back through the test piece and, finally, received by the search unit. Interruption of the sound beam by a discontinuity in the test piece reduces the amplitude of the reflector plate response. Resolution of discontinuities near the surface may be easier with the reflector plate method than pulse-echo because the response occurs further out in time and, hence, is less affected by the large water/metal interface response.

The test specimens, search units, and pulse receiver were the same as previously used in the pulse-echo tests. The fiber-phenolic reflector plate was 1 inch thick. Initially, the test specimens were immersed in the water and the search unit and reflector plate were positioned as shown in Figure 55.

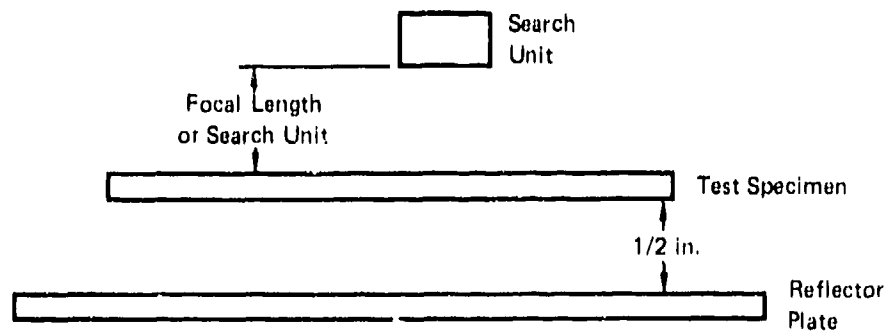


FIGURE 55  
TEST SETUP FOR REFLECTOR PLATE TESTS

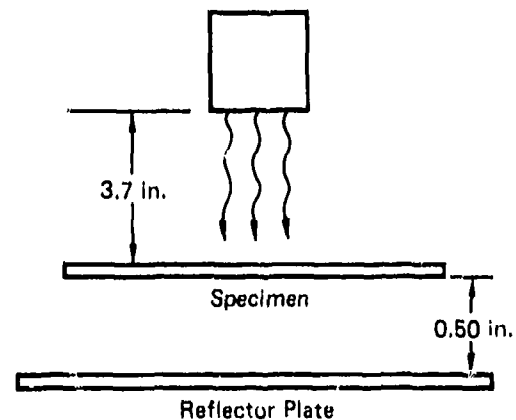
QP74 0117 70

The reflection from the reflector plate, through the test specimen, was adjusted to 80% of saturation in a non-hole area of the test specimen. Then, the search unit was moved over the 5/64 inch diameter hole in the specimen and the reduction in amplitude from the reflector plate was measured by recording the dB required to return the signal to 80% of saturation. This was repeated for all the holes in each of the specimens. In this way, the smallest detectable hole was identified as a function of the test piece thickness and test frequency. In order to measure the scanning noise level, the search unit was moved to a non-hole area, and with the reflector plate signal adjusted to 80% of saturation, the search unit was transversed back and forth over the reflector plate. Multiple exposure photographs were taken of the CRT display and the variation in amplitude of the reflector plate signal was noted to be 3 dB.

The results of the testing are shown in Table 32.

**TABLE 32**  
**TEST RESULTS FOR REFLECTOR PLATE TESTING**  
 10 MHz, 1/2 In. Dia S/L Search Unit

Plate Thickness (in.)	Metal Travel (in.)	Signal Reduction Due to Flat Bottom Hole (dB)		
		2/64	3/64	5/64
0.487	0.218	10	14	20
0.298	0.149	11	14	18
0.187	0.094	8	17	20
0.125	0.063	8	14	20
0.080	0.040	6	12	17
0.050	0.025	5	9	13



GP74-0117 80

It was found that at a test frequency of 25 MHz, there was not enough power to get a signal back from the reflector plate. This was true for all thicknesses except for 0.050 inch where a very low amplitude signal was received. As can be seen in Table 32, all the holes were detectable in all the specimens using 10 MHz. The scanning noise was found to be approximately 3 dB. Based upon these results, it appears that the reflector plate method is better than the pulse-echo method for locating flaws and evaluating their size in flat, thin machined parts.

### (3) Ringing Method

An ultrasonic ringing method was investigated for application to inspection of thin parts. This method is based upon the presence of sound reverberations within the part and the change in the reverberations. When the metal travel distance is changed the 10 MHz and 25 MHz focused search units and Branson 600 instrument used in the pulse-echo tests were used in the immersion ringing tests. The gate was adjusted to monitor changes in the width and amplitude of the water/metal interface echo. Initially, the water/metal interface response was adjusted to saturation in a non-hole area of the test specimen (see Figure 49 for specimen configuration) and the gate was adjusted to trigger at 30 percent of saturation on the right hand side of the response. The gate was adjusted to monitor the last 3 spikes without changing the gain; the search unit was positioned over each flat bottom hole in order to measure detectability of the holes.

The results of these tests indicated that the ringing method was ineffective. It was not possible to detect any of the flat bottom holes in any of the specimens.

### (4) Pitch-Catch

Contact pitch-catch tests were performed upon the test specimens using a 5 MHz Branson 1/4 inch fingertip probe with a Branson 600 ultrasonic instrument. The 2/64, 3/64, and 5/64 inch diameter flat bottom holes in the specimens shown in Figure 49 were used as artificial reflectors. The couplant was "Lubriplate" grease. The search unit was oriented to provide for maximum response from the chosen flat bottom hole and the hole response was adjusted to 80 percent of saturation. The dB setting at 80 percent of saturation was recorded and it was noted whether or not the hole response was resolvable from the back surface response. For the purposes of this testing, the trailing edge of the hole response had to meet the horizontal sweep line to be considered resolved from the back surface response.

Finally, the testing was repeated using a 10 MHz Branson 1/4 inch probe.

The test results are shown in Table 33. As can be seen, in every case, except for the 3/64 inch hole at 5 MHz, the hole was resolvable down to a test part thickness of .187 inch (.094 inch metal travel). Based on these results, it appears that thinner parts can be ultrasonically inspected with the 5 MHz or 10 MHz pitch-catch technique than with the 10 MHz pulse-echo technique. With the 10 MHz pulse-echo technique, it was not possible to resolve the hole response (2/64 and 3/64 inch diameter holes) for metal travels less than .149 inch. However, in comparing the pitch-catch and pulse-echo methods with the reflection plate method, it could be concluded that the reflector plate method is superior in that metal travels as small as .025 inch can be inspected.

**TABLE 33  
RESULTS OF PITCH-CATCH TESTS**

5 MHz

Plate Thickness	Metal Travel (in.)	dB for 80% of Saturation		
		2/64	3/64	5/64
0.437	0.218	26	32	39
0.298	0.149	24	34	41
0.187	0.094	24	33 $\triangle$	40
0.125	0.063	$\triangle$	$\triangle$	$\triangle$
0.080	0.040	$\triangle$	$\triangle$	$\triangle$
0.650	0.025	$\triangle$	$\triangle$	$\triangle$

10 MHz

Plate Thickness	Metal Travel (in.)	dB for 80% of Saturation		
		2/64	3/64	5/64
0.437	0.218	19	25	31
0.298	0.149	20	27	36
0.187	0.094	17	23	28
0.125	0.063	$\triangle$	$\triangle$	$\triangle$
0.080	0.040	$\triangle$	$\triangle$	$\triangle$
0.050	0.025	$\triangle$	$\triangle$	$\triangle$

$\triangle$  Hole response was not resolved from back surface response.

GP74-0117-81

f. Angle Beam Immersion Testing of Plate

A program was conducted to evaluate the effectiveness of various search units during angle beam immersion testing of specimens fabricated from plate. A total of 9 test specimens (Ti-6Al-4V) were fabricated to the Figure 48 configuration with the following dimensions:

<u>Thickness, T</u> <u>(Inches)</u>	<u>Surface Finish</u> <u>(RMS)</u>	<u>θ</u> <u>(Degrees)</u>	<u>A</u> <u>(Inches)</u>
1.00	63	30	1.44
1.00	125	30	1.44
1.00	as-rolled	30	1.44
1.50	63	45	1.55
1.50	125	45	1.55
1.50	as-rolled	45	1.55
2.00	63	45	1.91
2.00	125	45	1.91
2.00	as-rolled	45	1.91

As shown in Figure 48, flat bottom holes, having diameters of 2/64, 3.64, and 5/64 inch, were incorporated as artificial reflectors.

Five flat search units were compared. These were:

- (a) 3/4 inch diameter, 2-1/4 MHz, Aerotech Gamma
- (b) 3/4 inch diameter, 5 MHz, Aerotech Gamma
- (c) 3/4 inch, 2-1/4 MHz, SIZ
- (d) 3/4 inch, 5 MHz, SIZ
- (e) 3/4 inch, 5 MHz, SIL

A Branson 600 ultrasonic instrument was used along with a 622T pulser/receiver for each test. Each search unit was adjusted for a 3 inch water path and a refracted sound beam angle in the specimen of 45 degrees  $\pm$  5 degrees for the 1-1/2 and 2 inch thick specimens and 60 degrees  $\pm$  5 degrees for the 1 inch thick specimen. The sound entry point was adjusted to Position 1 (see Figure 56) and the flat bottom hole response was adjusted to 80 percent of saturation. The response-to-noise ratio was measured off the cathode ray tube. Next, the search unit was moved to Position 2 and the testing was repeated. A few selected tests were performed from Position 3.

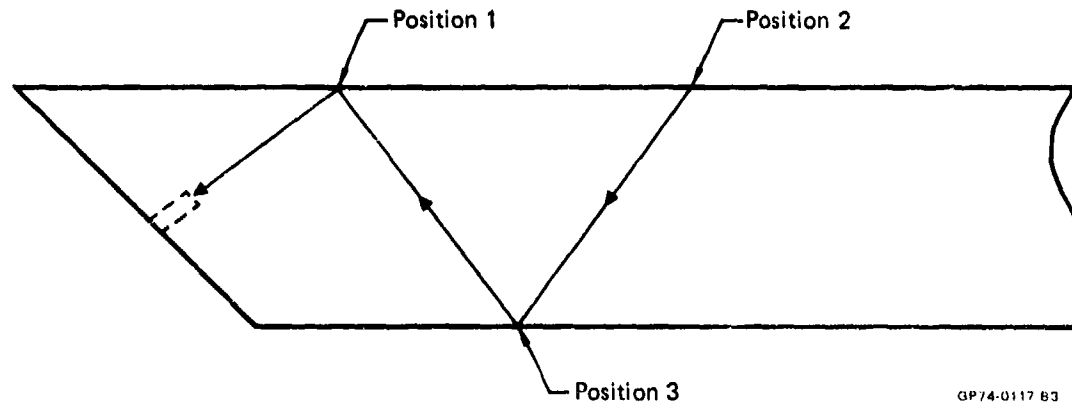


**FIGURE 56**  
**SOUND ENTRY POSITIONS**

The results of the tests are shown in Tables 34 through 42. With the sound entry point at Position 1 (1/4 skip), the 3 flat bottom holes were detectable in all cases. The ultrasonic noise amplitude varied from 0.05 to 1.6 inches with the hole response adjusted to 2.4 inches. In several cases, there was little difference between the signal-to-noise ratio for the 5 search units. In those cases where there was a difference, it was found that the SIZ search units produced the greatest signal-to-noise ratio.

It was not possible to detect any of the flat bottom holes at 1-1/4 skips (Position 2). At 3/4 skips (Position 3) it was possible to detect the holes in a few cases. These results indicate that angle beam immersion inspection of a plate 1/2 inch thick or greater should be confined to less than 3/4 skips.

It should be noted that it is not possible to determine the effect of machining upon ultrasonic response from this data since the pieces were removed from different plates. These effects were studied in a separate program which is described in Section 3-d.

**TABLE 34**  
**ULTRASONIC NOISE DURING ANGLE BEAM IMMERSION TESTING**  
**OF 2 INCH AS-ROLLED PLATE**  
**2/64 in. Dia Flat Bottom Holes**

Search Unit	Ultrasonic Signal-to-Noise Ratio <sup>1</sup>		
	Position 1	Position 2	Position 3
2-1/4 MHz, Gamma	2.4/0.3	<sup>2</sup>	<sup>3</sup>
5 MHz, Gamma	2.4/0.25	↓	<sup>2</sup>
2-1/4 MHz, SIZ	2.4/0.5		<sup>3</sup>
5 MHz, SIZ	2.4/0.2		<sup>2</sup>
5 MHz, SIL	2.4/0.7		<sup>3</sup>

**3/64 in. Dia Flat Bottom Holes**

Search Unit	Ultrasonic Noise Level <sup>1</sup>		
	Position 1	Position 2	Position 3
2-1/4 MHz, Gamma	2.4/0.1	<sup>2</sup>	<sup>3</sup>
5 MHz, Gamma	2.4/0.1	↓	0.2/0.1
2-1/4 MHz, SIZ	2.4/0.3		<sup>3</sup>
5 MHz, SIZ	2.4/0.05		<sup>2</sup>
5 MHz, SIL	2.4/0.15		<sup>3</sup>

**5/64 in. Dia Flat Bottom Holes**

Search Unit	Ultrasonic Noise Level <sup>1</sup>		
	Position 1	Position 2	Position 3
2-1/4 MHz, Gamma	2.4/0.1	<sup>2</sup>	<sup>3</sup>
5 MHz, Gamma	2.4/0.05	↓	0.6/0.05
2-1/4 MHz, SIZ	2.4/0.1		<sup>3</sup>
5 MHz, SIZ	2.4/0.01		<sup>2</sup>
5 MHz, SIL	2.4/0.1		<sup>3</sup>

- <sup>1</sup> Amplitude of the noise in inches when the hole response is adjusted to 80% of saturation.
- <sup>2</sup> No hole response
- <sup>3</sup> Testing not performed from Position 3.

GP74-0117-84

**TABLE 35**  
**ULTRASONIC NOISE DURING ANGLE BEAM IMMERSION TESTING**  
**OF 2 INCH PLATE - 125 RMS**  
**2/64 in. Dia Flat Bottom Holes**

Search Unit	Ultrasonic Signal-to-Noise Ratio <sup>1</sup>		
	Position 1	Position 2	Position 3
2-1/4 MHz, Gamma	2.4/1.0	<sup>2</sup>	<sup>3</sup>
5 MHz, Gamma	2.4/0.3	↓	<sup>2</sup>
2-1/4 MHz, SIZ	2.4/0.7		<sup>3</sup>
5 MHz, SIZ	2.4/0.5		<sup>2</sup>
5 MHz, SIL	2.4/0.1		<sup>3</sup>

**3/64 in. Dia Flat Bottom Holes**

Search Unit	Ultrasonic Noise Level <sup>1</sup>		
	Position 1	Position 2	Position
2-1/4 MHz, Gamma	2.4/0.25	<sup>2</sup>	<sup>3</sup>
5 MHz, Gamma	2.4/0.1	↓	<sup>2</sup>
2-1/4 MHz, SIZ	2.4/0.5		<sup>3</sup>
5 MHz, SIZ	2.4/0.2		<sup>2</sup>
5 MHz, SIL	2.4/0.4		<sup>3</sup>

**5/64 in. Dia Flat Bottom Holes**

Search Unit	Ultrasonic Noise Level <sup>1</sup>		
	Position 1	Position 2	Position 3
2-1/4 MHz, Gamma	2.4/0.12	<sup>2</sup>	<sup>3</sup>
5 MHz, Gamma	2.4/0.05	↓	<sup>2</sup>
2-1/4 MHz, SIZ	2.4/0.1		<sup>3</sup>
5 MHz, SIZ	2.4/0.01		<sup>2</sup>
5 MHz, SIL	2.4/0.15		<sup>3</sup>

- <sup>1</sup> Amplitude of the noise in inches when the hole response is adjusted to 80% of saturation.
- <sup>2</sup> No hole response
- <sup>3</sup> Testing not performed from Position 3.

GP74-0117 85

**TABLE 36**  
**ULTRASONIC NOISE DURING ANGLE BEAM IMMERSION TESTING**  
**OF 2 INCH PLATE - 63 RMS**  
**2/64 in. Dia Flat Bottom Holes**

Search Unit	Ultrasonic Noise Level 		
	Position 1	Position 2	Position 3
2-1/4 MHz, Gamma	2.4/1.1		
5 MHz, Gamma	2.4/0.9	↓	↓
2-1/4 MHz, SIZ	2.4/0.9	↓	↓
5 MHz, SIZ	2.4/1.0	↓	↓
5 MHz, SIL	2.4/1.2	↓	↓

3/64 in. Dia Flat Bottom Holes

Search Unit	Ultrasonic Noise Level 		
	Position 1	Position 2	Position 3
2-1/4 MHz, Gamma	2.4/0.3		
5 MHz, Gamma	2.4/0.15	↓	↓
2-1/4 MHz, SIZ	2.4/0.3	↓	↓
5 MHz, SIZ	2.4/0.2	↓	↓
5 MHz, SIL	2.4/0.3	↓	↓

5/64 in. Dia Flat Bottom Holes

Search Unit	Ultrasonic Noise Level 		
	Position 1	Position 2	Position 3
2-1/4 MHz, Gamma	2.4/0.08		
5 MHz, Gamma	2.4/0.02	↓	↓
2-1/4 MHz, SIZ	2.4/0.1	↓	↓
5 MHz, SIZ	2.4/0.02	↓	↓
5 MHz, SIL	2.4/0.1	↓	↓

-  Amplitude of the noise in inches when the hole response is adjusted to 80% of saturation.
-  No hole response
-  Testing not performed from Position 3.

GP74 0117 R6

**TABLE 37**  
**ULTRASONIC NOISE DURING ANGLE BEAM IMMERSION TESTING**  
**OF 1½ INCH AS-ROLLED PLATE**  
**2/64 In. Dia Flat Bottom Holes**

Search Unit	Ultrasonic Noise Level <sup>1</sup>		
	Position 1	Position 2	Position 3
2-1/4 MHz, Gamma	2.4/0.6	<sup>2</sup>	<sup>3</sup>
5 MHz, Gamma	2.4/0.3	<sup>2</sup>	0.6/0.35
2-1/4 MHz, SIZ	2.4/1.0	<sup>2</sup>	<sup>3</sup>
5 MHz, SIZ	2.4/0.5	<sup>2</sup>	<sup>3</sup>
5 MHz, SIL	2.4/1.6	<sup>2</sup>	<sup>3</sup>

3/64 In. Dia Flat Bottom Holes

Search Unit	Ultrasonic Noise Level <sup>1</sup>		
	Position 1	Position 2	Position 3
2-1/4 MHz, Gamma	2.4/0.3	<sup>2</sup>	<sup>3</sup>
5 MHz, Gamma	2.4/0.1	<sup>2</sup>	0.55/0.2
2-1/4 MHz, SIZ	2.4/0.15	<sup>2</sup>	<sup>3</sup>
5 MHz, SIZ	2.4/0.05	<sup>2</sup>	<sup>3</sup>
5 MHz, SIL	2.4/0.4	<sup>2</sup>	<sup>3</sup>

5/64 In. Dia Flat Bottom Holes

Search Unit	Ultrasonic Noise Level <sup>1</sup>		
	Position 1	Position 2	Position 3
2-1/4 MHz, Gamma	2.4/0.15	<sup>2</sup>	<sup>3</sup>
5 MHz, Gamma	2.4/0.05	<sup>2</sup>	0.8/0.1
2-1/4 MHz, SIZ	2.4/0.1	<sup>2</sup>	<sup>3</sup>
5 MHz, SIZ	2.4/0.01	<sup>2</sup>	0.25/0.01
5 MHz, SIL	2.4/0.2	<sup>2</sup>	<sup>3</sup>

- <sup>1</sup> Amplitude of the noise in inches when the hole response is adjusted to 80% of saturation.
- <sup>2</sup> No hole response
- <sup>3</sup> Testing not performed from Position 3.

GP74-0117 95

**TABLE 38**  
**ULTRASONIC NOISE DURING ANGLE BEAM IMMERSION TESTING**  
**OF 1½ INCH PLATE - 125 RMS**  
**2/64 In. Dia Flat Bottom Holes**

Search Unit	Ultrasonic Noise Level 		
	Position 1	Position 2	Position 3
2-1/4 MHz, Gamma	2.4/1.2		
5 MHz, Gamma	2.4/1.2		
2-1/4 MHz, SIZ	2.4/0.8		
5 MHz, SIZ	2.4/0.6		
5 MHz, SIL	2.4/1.5		

**3/64 In. Dia Flat Bottom Holes**

Search Unit	Ultrasonic Noise Level 		
	Position 1	Position 2	Position 3
2-1/4 MHz, Gamma	2.4/0.4		
5 MHz, Gamma	2.4/0.35		
2-1/4 MHz, SIZ	2.4/0.4		
5 MHz, SIZ	2.4/0.2		
5 MHz, SIL	2.4/0.6		

**5/64 In. Dia Flat Bottom Holes**

Search Unit	Ultrasonic Noise Level 		
	Position 1	Position 2	Position 3
2-1/4 MHz, Gamma	2.4/0.2		
5 MHz, Gamma	2.4/0.2		
2-1/4 MHz, SIZ	2.4/0.1		
5 MHz, SIZ	2.4/0.1		
5 MHz, SIL	2.4/0.2		

-  Amplitude of the noise in inches when the hole response is adjusted to 80% of saturation.
-  No hole response
-  Testing not performed from Position 3.

QP74-011/94

**TABLE 39**  
**ULTRASONIC NOISE DURING ANGLE BEAM IMMERSION TESTING**  
**OF 1½ INCH PLATE - 63 RMS**  
**2/64 In. Dia Flat Bottom Holes**

Search Unit	Ultrasonic Noise Level 		
	Position 1	Position 2	Position 3
2-1/4 MHz, Gamma	2.4/1.1		
5 MHz, Gamma	2.4/0.6		
2-1/4 MHz, SIZ	2.4/0.7		
5 MHz, SIZ	2.4/0.2		
5 MHz, SIL	2.4/1.0		

3/64 In. Dia Flat Bottom Holes

Search Unit	Ultrasonic Noise Level 		
	Position 1	Position 2	Position 3
2-1/4 MHz, Gamma	2.4/0.4		
5 MHz, Gamma	2.4/0.25		
2-1/4 MHz, SIZ	2.4/0.3		
5 MHz, SIZ	2.4/0.2		
5 MHz, SIL	2.4/0.4		

5/64 In. Dia Flat Bottom Holes

Search Unit	Ultrasonic Noise Level 		
	Position 1	Position 2	Position 3
2-1/4 MHz, Gamma	2.4/0.2		
5 MHz, Gamma	2.4/0.25		
2-1/4 MHz, SIZ	2.4/0.1		
5 MHz, SIZ	2.4/0.1		
5 MHz, SIL	2.4/0.2		

-  Amplitude of the noise in inches when the hole response is adjusted to 80% of saturation.
-  No hole response
-  Testing not performed from Position 3.

GP74-0117 93

**TABLE 40**  
**ULTRASONIC NOISE DURING ANGLE BEAM IMMERSION TESTING**  
**OF 1 INCH PLATE AS-ROLLED**  
**2/64 In. Dia Flat Bottom Holes**

Search Unit	Ultrasonic Noise Level 		
	Position 1	Position 2	Position 3
2-1/4 MHz, Gamma	2.4/0.3		
5 MHz, Gamma	2.4/0.1		
2-1/4 MHz, SIZ	2.4/0.1		
5 MHz, SIZ	2.4/0.6		
5 MHz, SIL	2.4/0.15		

3/64 in. Dia Flat Bottom Holes

Search Unit	Ultrasonic Noise Level 		
	Position 1	Position 2	Position 3
2-1/4 MHz, Gamma	2.4/0.3		
5 MHz, Gamma	2.4/0.1		
2-1/4 MHz, SIZ	2.4/0.1		
5 MHz, SIZ	2.4/0.7		
5 MHz, SIL	2.4/0.1		

5/64 In. Dia Flat Bottom Holes

Search Unit	Ultrasonic Noise Level 		
	Position 1	Position 2	Position 3
2-1/4 MHz, Gamma	2.4/0.12		
5 MHz, Gamma	2.4/0.05		
2-1/4 MHz, SIZ	2.4/0.1		
5 MHz, SIZ	2.4/0.8		
5 MHz, SIL	2.4/0.15		

-  Amplitude of the noise in inches when the hole response is adjusted to 80% of saturation.
-  No hole response
-  Testing not performed from Position 3

GP74 0117 92

**TABLE 41**  
**ULTRASONIC NOISE DURING ANGLE BEAM IMMERSION TESTING**  
**OF 1½ INCH PLATE - 125 RMS**  
**2/64 In. Dia Flat Bottom Holes**

Search Unit	Ultrasonic Noise Level <sup>①</sup>		
	Position 1	Position 2	Position 3
2-1/4 MHz, Gamma	2.4/0.4	<sup>②</sup>	<sup>③</sup>
5 MHz, Gamma	2.4/0.2	↓	↓
2-1/4 MHz, SIZ	2.4/0.2	↓	↓
5 MHz, SIZ	2.4/0.3	↓	↓
5 MHz, SIL	2.4/0.2	↓	↓

**3/64 In. Dia Flat Bottom Holes**

Search Unit	Ultrasonic Noise Level <sup>①</sup>		
	Position 1	Position 2	Position 3
2-1/4 MHz, Gamma	2.4/0.4	<sup>②</sup>	<sup>③</sup>
5 MHz, Gamma	2.4/0.3	↓	↓
2-1/4 MHz, SIZ	2.4/0.2	↓	↓
5 MHz, SIZ	2.4/0.3	↓	↓
5 MHz, SIL	2.4/0.2	↓	↓

**5/64 In. Dia Flat Bottom Holes**

Search Unit	Ultrasonic Noise Level <sup>①</sup>		
	Position 1	Position 2	Position 3
2-1/4 MHz, Gamma	2.4/0.4	<sup>②</sup>	<sup>③</sup>
5 MHz, Gamma	2.4/0.2	↓	↓
2-1/4 MHz, SIZ	2.4/0.3	↓	↓
5 MHz, SIZ	2.4/0.2	↓	↓
5 MHz, SIL	2.4/0.5	↓	↓

- <sup>①</sup> Amplitude of the noise in inches when the hole response is adjusted to 80% of saturation.
- <sup>②</sup> No hole response
- <sup>③</sup> Testing not performed from Position 3.

6074 011 01

**TABLE 42**  
**ULTRASONIC NOISE DURING ANGLE BEAM IMMERSION TESTING**  
**OF 1½ INCH PLATE - 63 RMS**  
**2/64 In. Dia Flat Bottom Holes**

Search Unit	Ultrasonic Noise Level 		
	Position 1	Position 2	Position 3
2-1/4 MHz, Gamma	2.4/0.15		
5 MHz, Gamma	2.4/0.3		
2-1/4 MHz, SIZ	2.4/0.1		
5 MHz, SIZ	2.4/0.4		
5 MHz, SIL	2.4/0.1		

3/64 In. Dia Flat Bottom Holes

Search Unit	Ultrasonic Noise Level 		
	Position 1	Position 2	Position 3
2-1/4 MHz, Gamma	2.4/0.2		
5 MHz, Gamma	2.4/0.1		
2-1/4 MHz, SIZ	2.4/0.2		
5 MHz, SIZ	2.4/0.3		
5 MHz, SIL	2.4/0.1		

5/64 In. Dia Flat Bottom Holes

Search Unit	Ultrasonic Noise Level 		
	Position 1	Position 2	Position 3
2-1/4 MHz, Gamma	2.4/0.2		
5 MHz, Gamma	2.4/0.2		
2-1/4 MHz, SIZ	2.4/0.1		
5 MHz, SIZ	2.4/0.6		
5 MHz, SIL	2.4/0.15		

-  Amplitude of the noise in inches when the hole response is adjusted to 90% of saturation.
-  No hole response
-  Testing not performed from Position 3.

GP74 0117 00

## SECTION IV

### PROCESSING OF INGOT

This program was concerned with the detection of typical discontinuities in titanium alloy components using nondestructive methods.

The sources of defects in components manufactured from titanium alloys include many of those which also are common to other metals. However, sponge reduction, consumable electrode fabrication, and arc melting processes present a number of problem sources which are unique to titanium alloys. These problems have been of particular concern since NDT methods were not always originally selected with the aim of finding these unusual types of defects. In addition, some of these defects were found to be of a size and character which necessitated the development of more sensitive and sophisticated NDT techniques.

A considerable effort has been expended over the past several years in an attempt to identify, and insofar as possible prevent, the sources of defects in titanium components. These sources may be divided into those associated with raw materials (sponge, alloying elements, etc.) and ingot melting conditions and those associated with thermo-mechanical processing of ingots to billet, bar, sheet, etc., and of mill products to finished components (forging, machining, forming, heat treating, etc.).

The defects associated with raw materials and melting are more or less peculiar to titanium metallurgy, while those associated with thermomechanical processing include defects which are also common to other materials. Discontinuities which might occur in titanium ingot include pipe in the top of the ingot, Type I and Type II alpha stabilized defects and general porosity. Type I alpha stabilized defects are characterized by high hardness, high thermal stability and an increased oxygen and nitrogen content compared with the matrix. Type II alpha stabilized defects are characterized by a lower hardness than Type I, a lower thermal stability, and an increased aluminum content compared with the matrix (Reference 3).

Mill products might include unhealed pipe and porosity, Type II alpha stabilized defects, unhealed porosity, and Type I alpha stabilized areas, with or without associated voids. Forgings might contain unhealed pipe and porosity, Type II alpha stabilized defects, unhealed porosity, and Type I alpha stabilized areas, with or without associated voids.

Consequently, a full size production ingot was melted using techniques to intentionally induce Type I and II alpha stabilized areas.

The ingot was converted to bar, plate, airframe forgings, and engine disk forgings, containing the discontinuities. The capability of appropriate NDT methods for the detection of the segregates was established.

## 1. INGOT MELTING

A full size double vacuum melted production Ti-6Al-4V ingot (24 inch diameter, 7,500 pounds) was produced for the program by Oregon Metallurgical Company (Oremet) in Albany, Oregon. The ingot raw material components were sponge, alloy, and revert chip. A photograph of the first melt ingot is shown in Figure 57.

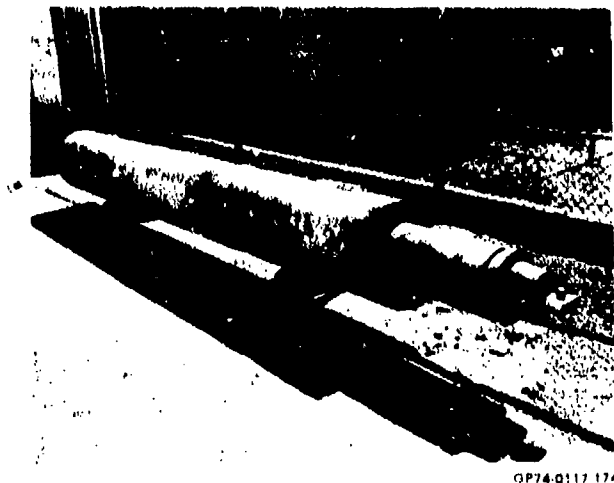


**FIGURE 57**  
**FIRST MELT INGOT**

In order to intentionally produce Type I alpha stabilized defects in the ingot, the first melt electrode was seeded with titanium nitride. This seeding technique has been successfully used in the past by the U. S. Bureau of mines, Albany Oregon Station, under Air Force sponsorship and has been found to produce defects which closely resemble those which have occasionally occurred in normal melting practice (**Reference 4**).

Two types of high nitrogen seeds, nitrided sponge and melted buttons, were prepared by Oremet for insertion onto the first melt ingot.

Initially, nitrided sponge was produced by placing approximately 10 pounds of good quality titanium sponge in thin layers in carbon steel trays. These trays were stacked vertically in a stainless steel pit furnace retort and tested to ensure a leak was not present which would allow a pressure rate of rise of more than 1 micron of Hg per hour. Terminal pressure was a little less than 1 micron of Hg. The system was heated in vacuum to 1000°C and back-filled with high purity nitrogen. A demand type regulator was held at 5 psig for 6 hours and the system was cooled to ambient temperature under nitrogen.

In order to increase the chances of inducing typical defects, two types of seeds were used for the ingot. The first type was the nitrided sponge itself. The second type was 15 to 25 gram (approximate) nonconsumable arc melted buttons made from randomly selected nitrided sponge. The buttons were broken with a hammer and seeds were selected from the pieces. Each of the seed types used were 1 to 4 grams as Oremet experience indicated this range of seed sizes would yield a range of segregate sizes. A total of 79 seeds were selected for use in the ingot.

Figure 58 is a photograph of typical seeds along with the chemical analysis data.

Holes, 1/2 inch diameter x 1 inch deep were drilled in 79 locations in the first melt ingot so that the seeds could be inserted. Hole locations for the first melt ingot were profiled in the form of a right hand spiral shown in Figure 59. Each hole was coded with proper identity to be certain correct seeds were inserted. The seeds were inserted and normal sponge particles inside. Care was taken not to break brittle seeds in this process.

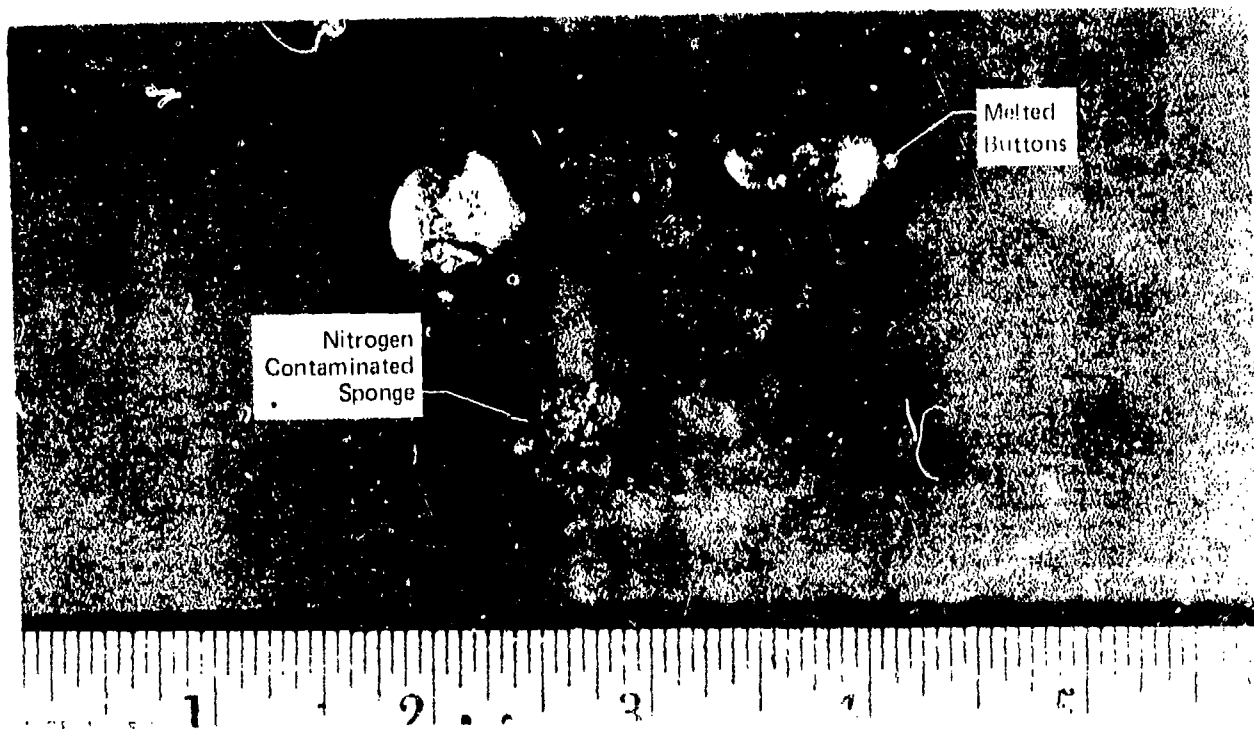
The second melt was made using the seeded first melt ingot as an electrode. Melting was accomplished according to standard practice. The melting was stopped 3 inches from the top. Power cutback on termination of remelt was purposely extremely rapid in comparison to normal practice in order to induce a large pipe and shrinkage zone in the ingot top with possible Type II alpha stabilized defects.

The second melt ingot, Figure 60, was chamfered on the top and bottom to break the sharp corners to minimize cracking during subsequent forging and was shipped to the Ladish Company for conversion to billet stock.

The chemical analysis of samples removed from the top and bottom of the ingot is as follows:

Ingot Chemical Composition (Heat No. RD2234)			
Element	% by Weight		Ingot Aim
	Top	Bottom	
Aluminum	6.20	6.40	6.2
Vanadium	4.03	4.10	4.0
Iron	0.166	0.164	0.16
Oxygen	0.15	0.14	0.16
Carbon	0.062	0.062	Low
Nitrogen	0.010	0.008	Low
Hydrogen	0.0019	0.0016	Low

GP74-0117 177



Chemical Analysis of Seed Material

Seed Type	Nitrogen Content (Weight Percent)
Sponge No. 1	8.4
Sponge No. 2	4.4
Sponge No. 3	8.0
Melted Button No. 1	8.8
Meltea Button No. 2	8.7

GP74 0.17 175

**FIGURE 58**  
**SEEDS USED TO INTENTIONALLY PRODUCE**  
**ALPHA SEGREGATION**

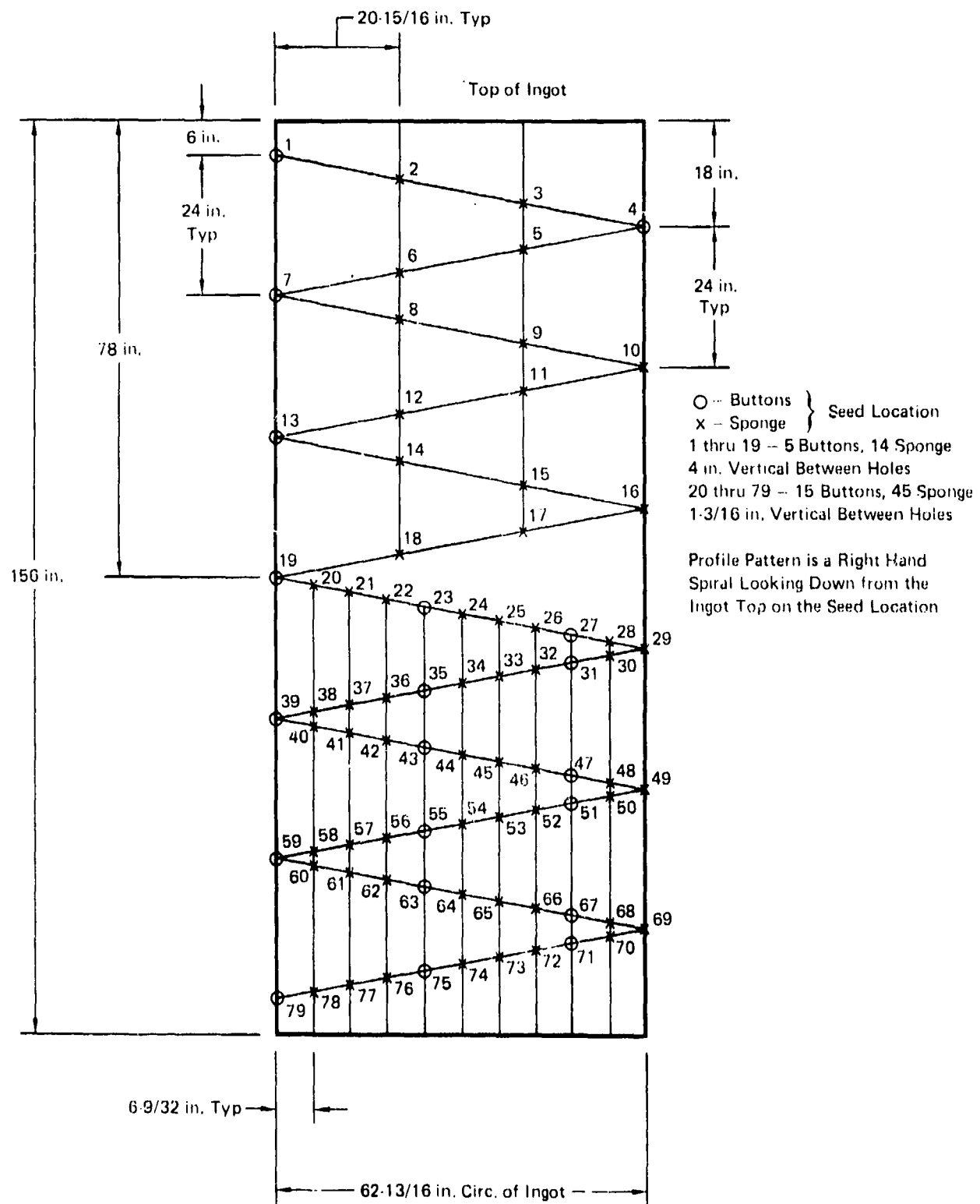


**FIGURE 59**  
**PATTERN FOR SEEDING FIRST MELT**

GP/4 0117 176



GP74-0117-178

**FIGURE 60**  
**FINAL MELT INGOT**

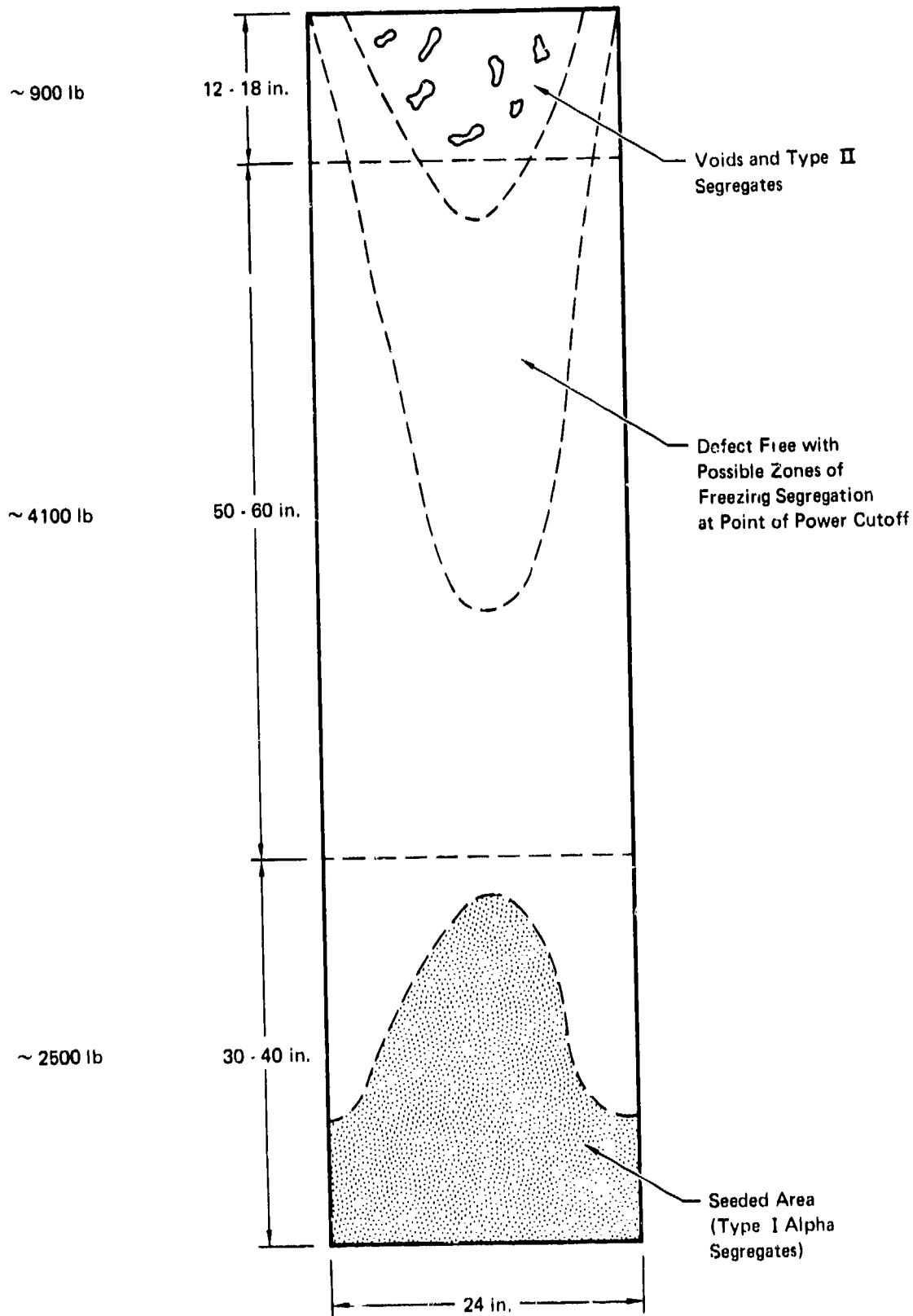
The defects expected to be present in the 24 inch diameter ingot included a void region with Type II alpha stabilized defects in the top 12-18 inches of the ingot (900-1300 pounds in weight). It was expected that the void area would be healed by diffusion bonding during the forging operations. However, it has been observed that these voids can be lined with an aluminum rich zone, and an attempt was made to preserve this segregation by using relatively low working temperatures and short heating times during the ingot conversion process. The initial ingot conversion took place at the Ladish Company. Ladish usually forges at 2050-2100°F for initial ingot breakdown but they used 1950°F for the subject ingot in order to retain the segregation. It is also possible that the relatively rapid freezing rate without hot-topping produced one or more zones of segregation in the top section of the ingot.

The bottom portion of the ingot was expected to contain the Type I segregation zones. Figure 61 shows the expected general locations of the various defects.

## 2. INGOT CONVERSION TO BILLET, BAR PLATE, AND FORGINGS

A schematic showing the steps taken to convert the ingot is shown in Figures 62, 63, 64, and 65. After having been lathe turned to a 125 rms surface finish and inspected, the ingot was heated to 1950°F and press forged by the Ladish Company to 18 inch round corner square (RCS) in one heat. Next, the 18 inch RCS was reheated to 1800°F and press forged to 14 inch RCS. The RCS was hot sheared to 3 lengths (101, 67 and 62 inches) with the section locations being based upon the discontinuity locations determined by the ultrasonic and radiographic inspections.

The three billets were heat treated according to a proprietary Ladish process. After reheating to 1750°F the three billets were press forged to 10 inch RCS. The 10 inch RCS from the middle and bottom portions of the ingot were hot sheared as shown in Figure 62. The 10 inch RCS from the top portion of the ingot was not hot sheared at this stage to avoid any possibility of cutting through the ingot pipe. If the ingot pipe was opened to the atmosphere at this stage, the surfaces of the pipe would oxidize preventing the pipe from healing upon subsequent forging.



GP74 0117-170

**FIGURE 61**  
**EXPECTED INGOT DEFECTS AFTER SECOND MELT**

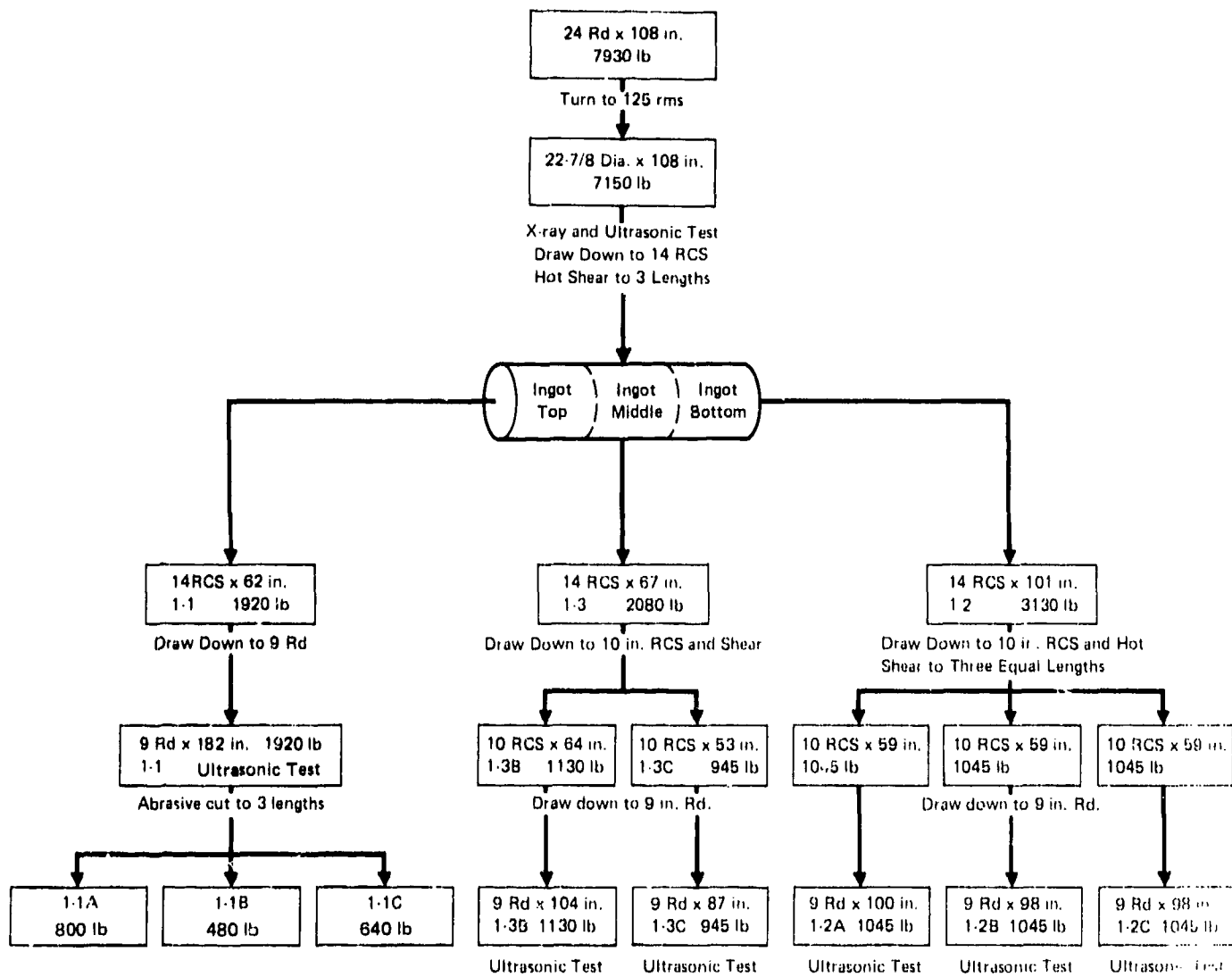
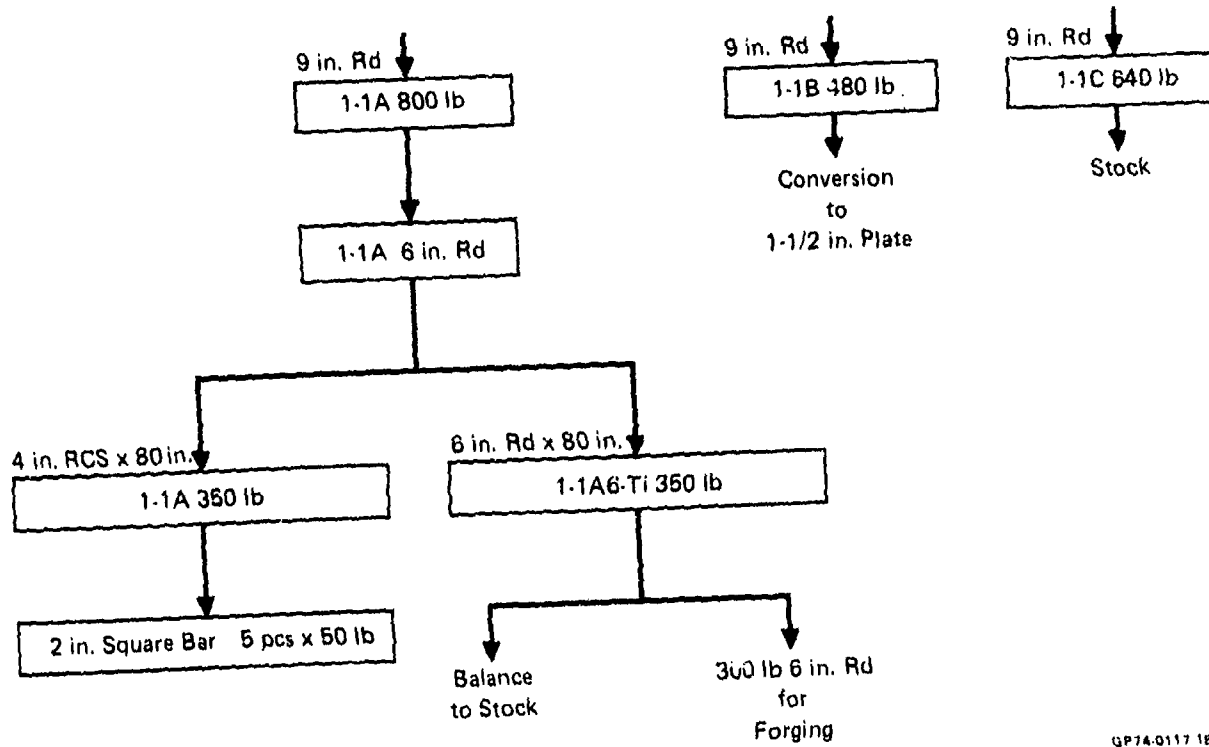
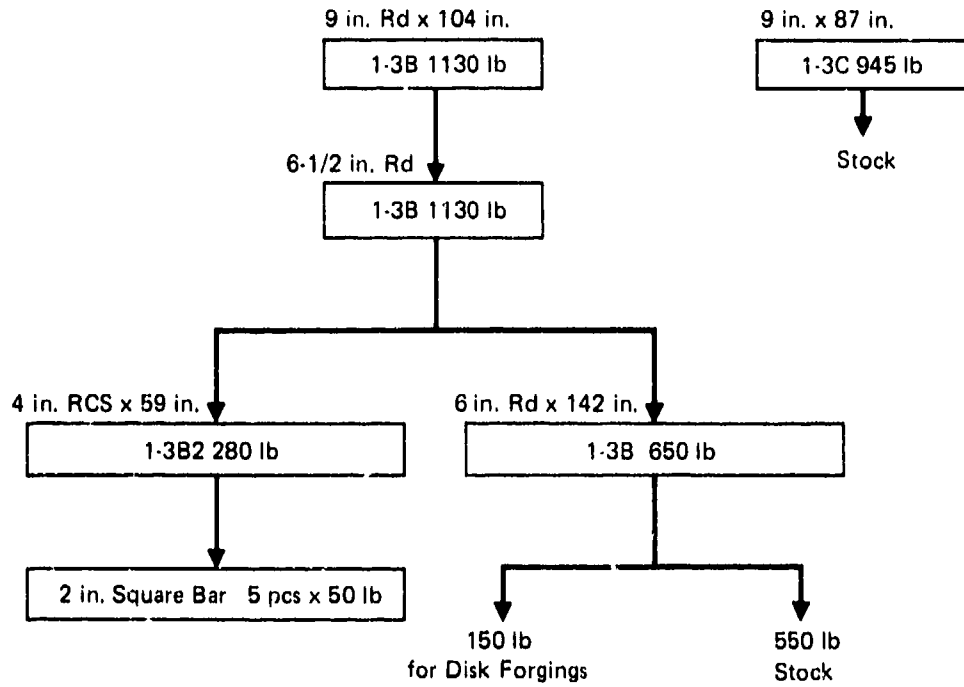


**FIGURE 62  
CONVERSION OF INGOT TO 9 INCH ROUND BILLET**



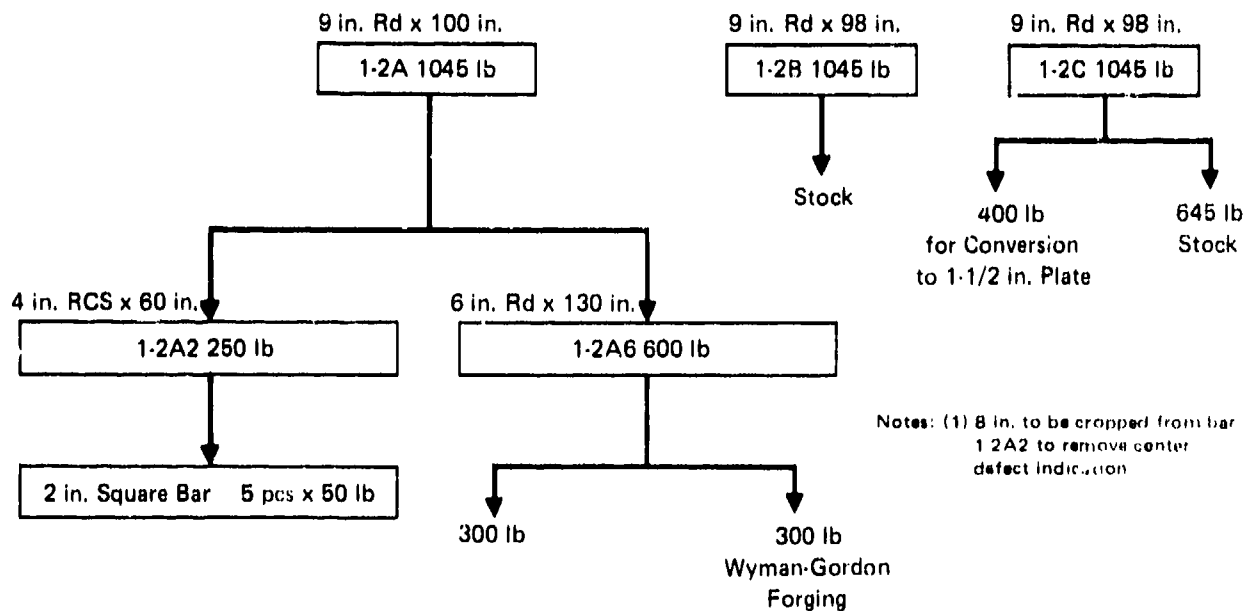
GP74-0117 181

**FIGURE 63**  
**CONVERSION OF 9 INCH BILLET FROM INGOT TOP**



GP74-0117-182

**FIGURE 64**  
**CONVERSION OF 9 INCH BILLET FROM INGOT MIDDLE**



Notes: (1) 8 in. to be cropped from bar 1-2A2 to remove center defect indication

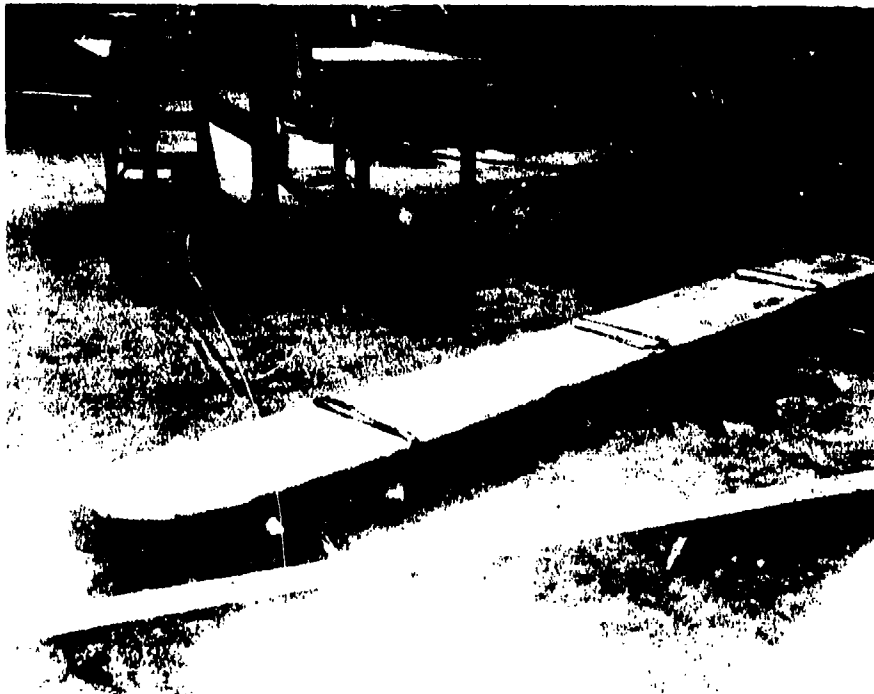
GP74-0117-183

**FIGURE 65**  
**CONVERSION OF 9 INCH BILLET FROM INGOT BOTTOM**

Next, each 10 inch RCS was heated to 1750°F and press forged to 9-1/4 inch rough round. The surfaces were Tysaman ground to 9 inch round with a 125 rms surface finish.

As shown in Figures 63, 64, and 65, one piece of 9 inch round from each of the three ingot sections was heated to 1750°F and press forged to 6 inch round by the Ladish Company. These pieces were then converted by the Ladish Company to 2 inch square bar and forging blanks. The 2 inch square bar was produced by open die hammer forging at 1750°F - 1800°F.

Plate, 1-1/2 inches thick, was produced from 9 inch round billets from the top and bottom of the ingot. The 9 inch diameter billets were initially flattened to 4-1/2 inches thick by cross die forging at 1950°F by RMI Company. Finally, the two pieces were rolled on a four-high rolling mill to 1-1/2 inches thick from a furnace temperature of 1875°F. The plate was rolled without reheating. A photograph of the two pieces of plate is shown in Figure 66.



GP74 0111 117

**FIGURE 66**  
**TWO PIECES OF ONE AND ONE-HALF INCH THICK PLATE**

Two inch square bar was produced from each of the three ingot sections. Six inch diameter billet was press forged at 1750°F - 1800°F to 4 inch square bar and then hammer forged at 1750°F - 1800°F to 2 inch square bars. Next, the 2 inch bars were annealed at 1300°F for 2 hours and air cooled. Processing was completed by grit blasting. A photograph of the 2 inch square bar is shown in Figure 67.



FIGURE 67  
TWO-INCH SQUARE BAR

CP74 010 118

Wyman-Gordon forged the airframe and jet engine disk forgings. Nine jet engine disk forgings were produced, each weighing 50 pounds; three of the forgings came from the top of the ingot where the Type II defects are expected, three came from the defect-free ingot center, and three came from the ingot bottom where the Type I defects are expected. To produce the disk forgings, the 6 inch diameter billets were upset at 1775°F to 6 inch thick pancakes, reheated to 1775°F and closed die press forged to the finished disk configuration. Finally, the forgings were annealed at 1300°F for 2 hours and air cooled.

Eight airframe forgings were produced, each weighing 25 pounds. Four of the forgings came from the ingot top and four came from the ingot bottom. The initial 6 inch diameter billets were shaped on open dies at 1775°F. After being reheated to 1775°F, the pieces were blocked to intermediate shape on a press and each blocked shape was cut in half to make two forgings. The pieces were reheated to 1775°F and closed die press forged to the finished part shape. Finally, the finished forgings were annealed at 1300°F for 2 hours and air cooled.

Prior to shipping, all the forgings were grit blasted and pickled to remove any alpha case. Photographs of the forgings are presented in Figures 68 and 69. Drawings of the forging configurations are shown in Figures 70 and 71.

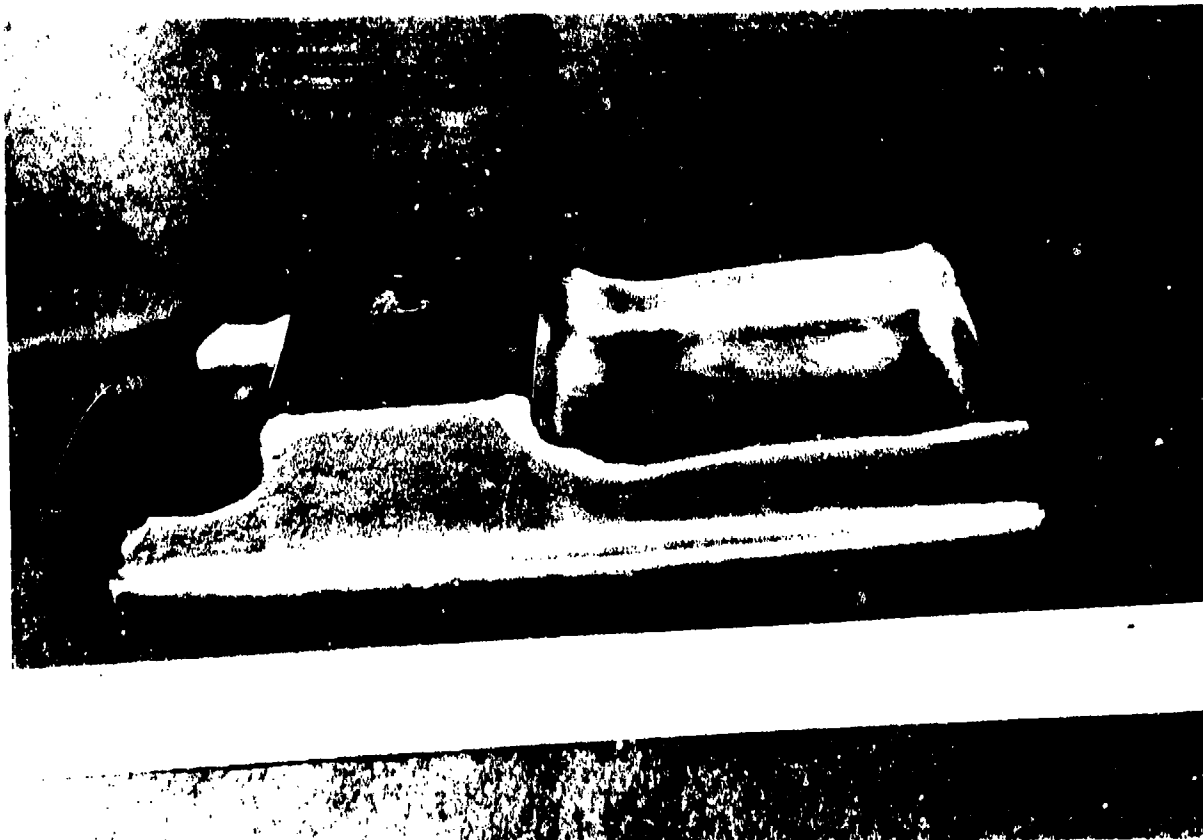
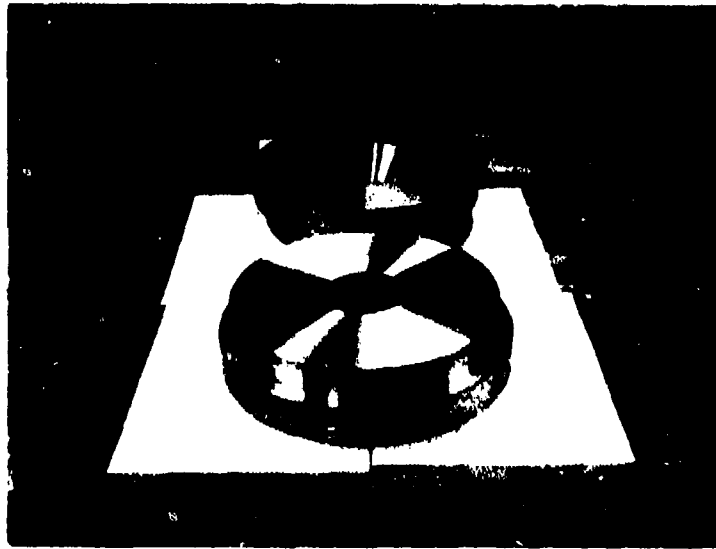


**FIGURE 68**  
**AIRFRAME FORGING**

GP74 011 118

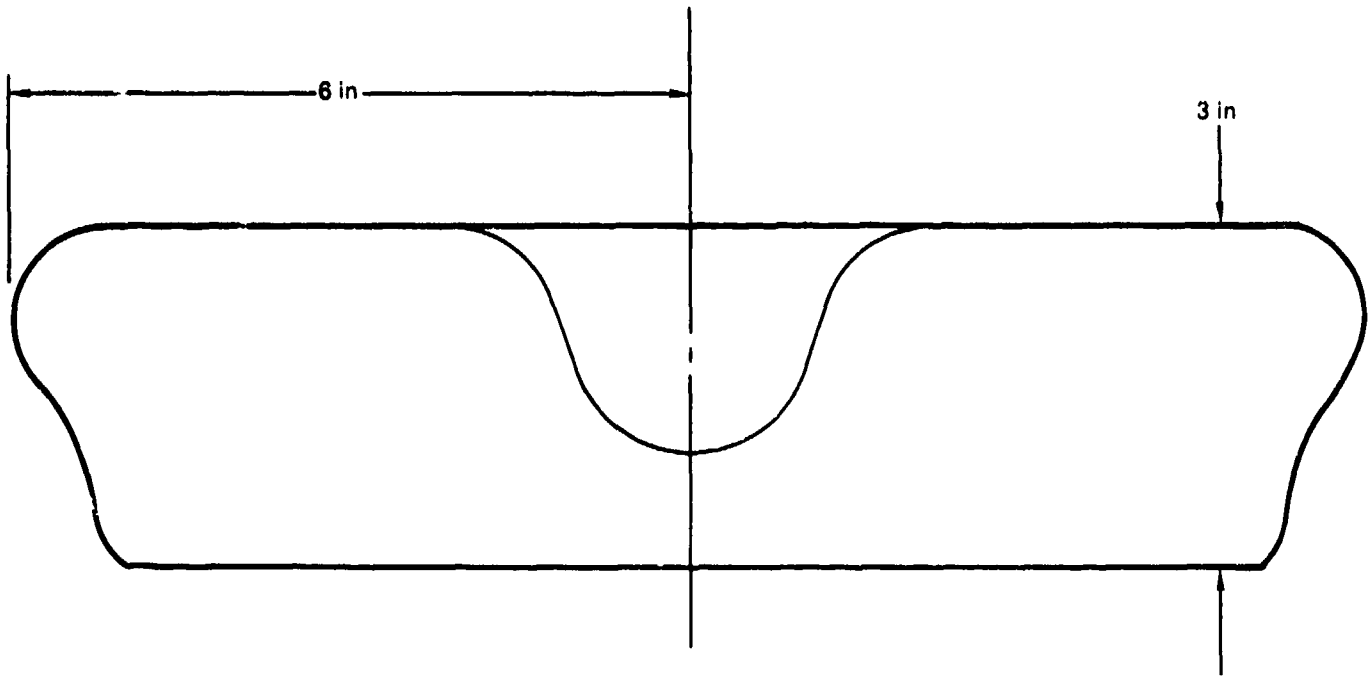
The melting of the ingot and subsequent conversion to billet was conducted in a manner to simulate an actual production ingot. A summary of the procedures used is shown in Table 44 along with the details of standard practice.

A summary of the conversion is shown in Table 43.



QP74-0117-120

**FIGURE 69**  
**JET ENGINE DISK FORGINGS**



QP74-0117-121

**FIGURE 70**  
**CROSS SECTION VIEW OF JET ENGINE DISK FORGING**



**TABLE 43  
INGOT INVENTORY LIST**

Form	Location in Original Ingot	Approx. Total Weight (lb)	Approximate Dimensions (in.)
4 Airframe Forgings	Top (Type II Segregates)	100	--
4 Airframe Forgings	Bottom (Type I Segregates)	100	--
3 Disk Forgings	Top (Type II Segregates)	150	--
3 Disk Forgings	Middle (Defect Free)	150	--
3 Disk Forgings	Bottom (Type I Segregates)	150	--
1-1/2 in. Plate	Top (Type II Segregates)	450	15 W x 131 L
1-1/2 in. Plate	Bottom (Type I Segregates)	405	15 W x 105 L
2 in. x 2 in. Bar	Top (Type II Segregates)	250	520 L
2 in. x 2 in. Bar	Middle (Defect Free)	250	430 L
2 in. x 2 in. Bar	Bottom (Type I Segregates)	250	420 L
9 in. Dia Billet	Top (Type II Segregates)	480	48 L
9 in. Dia Billet	Middle (Defect Free)	825	82 L
9 in. Dia Billet	Bottom (Type I Segregates)	1450	148 L
6 in. Dia Billet	Top (Type II Segregates)	56	12 L
6 in. Dia Billet	Middle (Defect Free)	330	72 L
6 in. Dia Billet	Bottom (Type I Segregates)	336	68 L

QP74 0117 118

**TABLE 44  
COMPARISON OF INGOT PROCESSING WITH STANDARD PRACTICE**

Item	Contract Ingot	Standard Ti-6Al-4V Ingot	Premium Ti-6Al-4V Ingot
Ingot Diameter	24 in.	24 in., 30 in., 34 in., 36 in.	30 in., 34 in., 36 in.
Ingot Weight	7500 lb	7500 lb - 14,000	9000 - 14,000
Melt Practice	Double Vac, Short Hot-Top	Double or Triple Vac or Argon, Long Hot-Top	Double or Triple Vac, Long Hot-Top
Ingot Breakdown to 18 in. Square	1950°F	1950 <sup>0</sup> -2150 <sup>0</sup> F	1950 <sup>0</sup> -2150 <sup>0</sup> F
Conversion to 14 in. Square Round	1900°F	1750 <sup>0</sup> -1850 <sup>0</sup> F	1750 <sup>0</sup> -1850 <sup>0</sup> F
Conversion to 9 in. Round & 6 in. Round	1750°F	1750 <sup>0</sup> -1830 <sup>0</sup> F	1750 <sup>0</sup> -1800 <sup>0</sup> F
Conversion 9 in. Round to 1½ in. Plate	1950 <sup>0</sup> -1875 <sup>0</sup> F	1900 <sup>0</sup> -1750 <sup>0</sup> F	-
Conversion 6 in. Round to 2 in. Square	1750 <sup>0</sup> -1800 <sup>0</sup> F	1750 <sup>0</sup> -1800 <sup>0</sup> F	-
Contour Forging	1750°F	1750°F	1750°F

GP74-0117-184

### 3. INSPECTION OF INGOT

The ingot was inspected both radiographically and ultrasonically. Since a previous Air Force program had been conducted to improve nondestructive testing for inspection of titanium alloy ingots, the inspection of the subject ingot was not developmental in nature (Reference 2). Many of the Allis Chalmers and Ladish Company established production inspection techniques were utilized since the primary objective of the ingot inspection was to select the locations for shearing the ingot after the first draw down. In addition, certain General Electric inspection techniques were used to increase the effectiveness of the inspections. However, the inspections were not intended to establish the minimum detectable defect size nor to precisely detail the location of each discontinuity in the ingot.

#### a. Radiography

The radiographic inspection of the ingot (125 rms surface finish) was carried out by Allis Chalmers in Milwaukee, Wisconsin. The inspection was performed using a 24 MeV Allis Chalmers betatron and an exposure of 1900 Roentgens. An ASTM E-142 No. 100 penetrameter was used as an image quality indicator. Front and back lead screens, 0.060 inch thick, were used and the back-up material was one inch thick lead. The Kodak AA film was processed manually. Figure 72 shows the plan for the exposures taken (6 circumferential positions for each of 10 axial positions). Twelve inch wide axial areas were exposed using 14 x 17 inch film providing for film overlap. A schematic of the ingot being radiographed is in Figure 73. During the exposures the film was flat as opposed to being curved around the ingot. The image of the IT hole and the outer edge of the penetrameter panel were visible on all the radiographs resulting in an equivalent penetrameter sensitivity of 0.29 percent. The density range of the radiographs was 1.5 to 3.0 H and D units.

The results of the radiographic inspection are shown in Table 45. The schematic in Figure 74 indicates the location of the axial and apparent circumferential dimensions listed in Table 45. As shown at the bottom of Figure 74, there are two possible circumferential locations for each indication since it is not possible to determine if the indication lies on the far side or near side of the ingot using the chosen techniques. The ingot pipe was found to start within 2 inches of the top of the ingot and to extend to a depth of 16 inches from the ingot top. Low density indications were evident throughout the length of the ingot. A total of 22 indications were located (not including the ingot pipe) varying in approximate size from .005 x .050 inch to .010 x .150 inch. The large accumulation of Type I segregates expected in the bottom of the ingot apparently was unresolvable by the radiographic inspection.

#### b. Ultrasonic Inspection

The ultrasonic inspection of the ingot was carried out at the Ladish Company in Milwaukee, Wisconsin. Prior to the inspection, the surface of the ingot was lathe turned to a 125 rms finish. For both

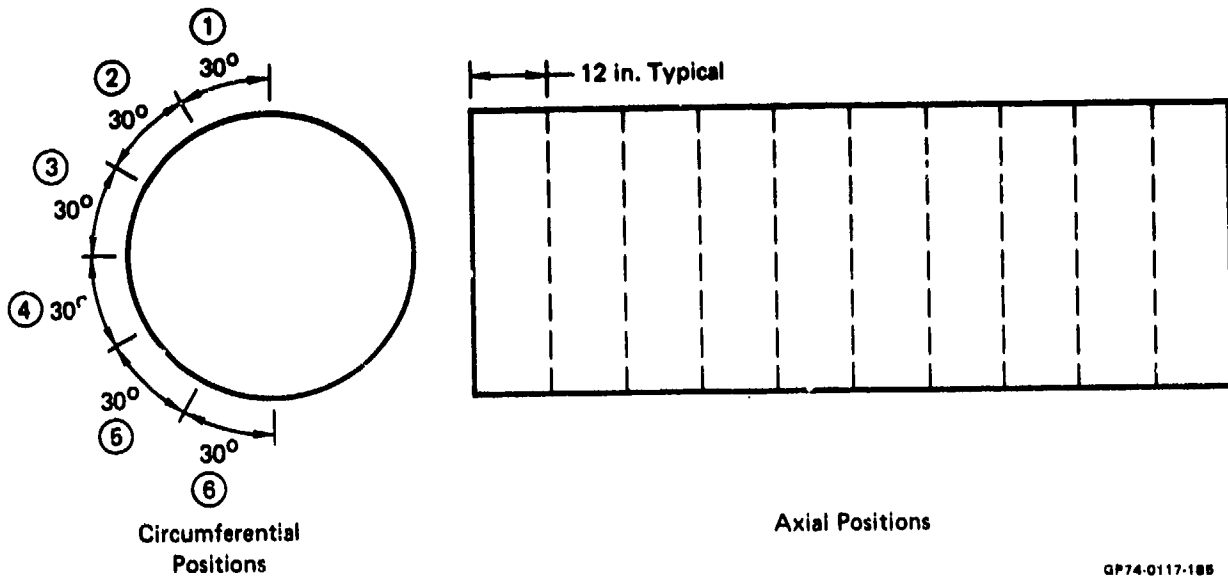


**FIGURE 72**  
**SCHEMATIC SHOWING EXPOSURE LAYOUT FOR RADIOGRAPHIC**  
**INSPECTION OF INGOT**

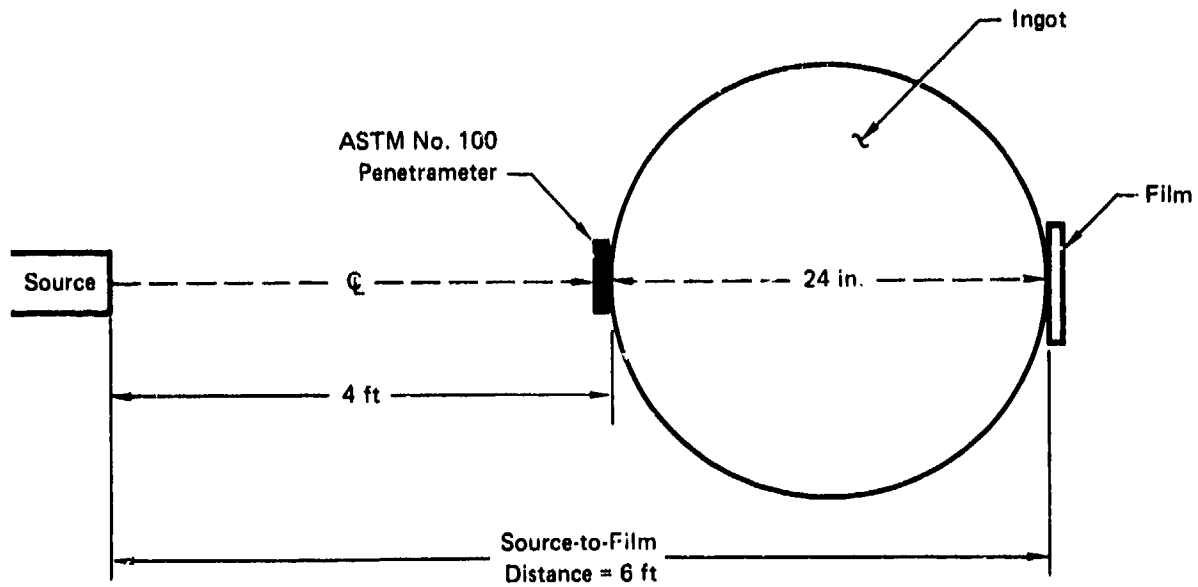


**FIGURE 73**  
**ARRANGEMENT FOR RADIOGRAPHIC INSPECTION OF INGOT**

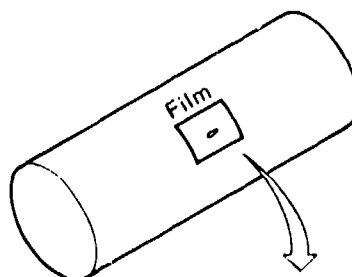
**TABLE 45**  
**RESULTS OF RADIOGRAPHIC INSPECTION OF INGOT**

Axial Reference Zero - edge of chamfer approximately 1.4 in. from bottom of ingot  
Circumferential Reference Zero - plug removed for property checks

Distance from Bottom (in.)	Distance from Circumferential Reference Zero (in.)	Approximate Dimensions Axial / Circumferential (mils)	Type 
8.7	28.5 or 64.7	10 x 100	Low Density
10.1	25 or 61.2	20 x 60	Low Density
11.5	25 or 61.2	80 x 30	Low Density
14.1	19.5 or 55.7	20 x 100	Low Density
26.4	16.5 or 52.7	30 x 50	Low Density
26.6	7 or 43	150 x 10	Minor Low Density
31.4	24.3 or 60.5	20 x 100	Low Density
35.1	31.4 or 67.6	30 x 50	Low Density
41.2	6 or 42	5 x 50	Minor Low Density
43.4	17 or 53	80 x 40	Low Density
53.2	0.5 or 36.8	20 x 40	Minor Low Density
54.0	0 or 36.2	50 x 2	Low Density
54.0	2.3 or 59.2	90 x 40	Low Density w/Depth
59.6	18.5 or 54.7	20 x 40(3)	Low Density
60.0	28 or 64.2	50 x 50(Round)	High Density
62.2	0 or 36.2	10 x 50	Low Density
62.4	25.2 or 61.2	20 x 120	Low Density
67	19.5 or 55.7	30 x 50	Low Density
76.4	19 or 55.2	10 x 100	Low Density
86	27.5 or 63.7	20 x 150	Low Density
86.2	26.8 or 63	60 x 30	Low Density w/Depth
87.1	18.1 or 54.3	10 x 50	Low Density
90.5 to 107	All	18 in. all Around	Void (Pipe) Tapers Outward to Perhaps 9 in. at Approx 104 in. from Bottom

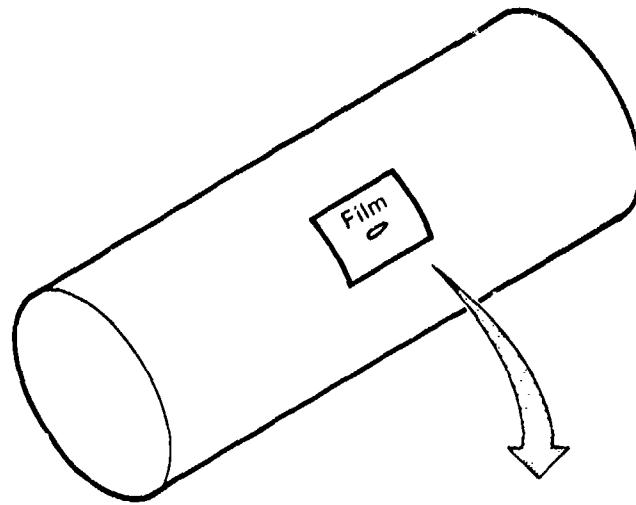
 Indications were visually judged to be low density or high density.

GP74 0117-187

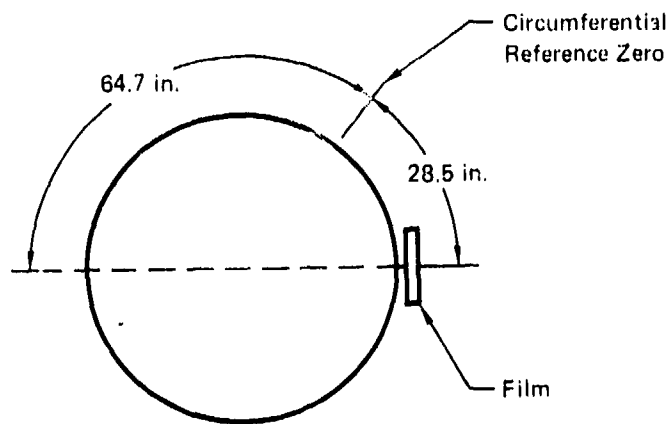
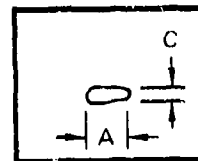


A = Axial Dimension  
C = Circumferential Dimension





A = Axial Dimension  
C = Circumferential Dimension



GP/4 0117 18B

**FIGURE 74**  
**SCHEMATIC SHOWING AXIAL AND CIRCUMFERENTIAL DIMENSIONS**

the longitudinal and shear inspection, two separate pulser/receivers (Sperry 10N and Sperry 5N) were used in conjunction with two Automation Industries unfocused transducers and two Sperry 721 oscilloscopes as shown in Figure 75. The vertical linearity of the electronic system had been checked by Ladish within 30 days of the ingot inspection. Each pulser/receiver was checked for noise and calibration response on the same reference standard; there was little difference in the response of each. As shown in Figure 76, the two transducers were positioned 4 inches apart and the scan direction was parallel to the longitudinal axis of the ingot.

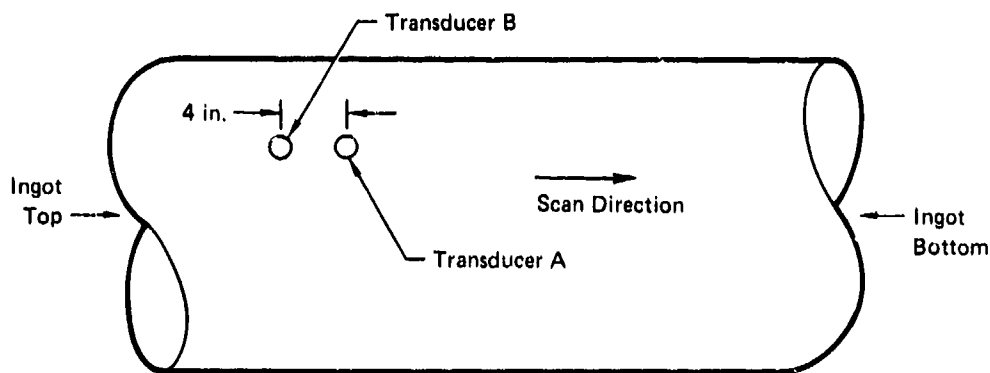


**FIGURE 76**  
**SCAN PLAN FOR INGOT**

GP74-0117 190

The scan rate was approximately 3 inches per second; prior to the actual ingot inspection, the scan rate was checked on the reference standard to ensure that the holes in the reference standard were detectable at that scan rate. After the transducers had scanned the full length of the ingot, the ingot was rotated less than 1/2 inch and the scanning was continued.

During the inspection, the automatic alarm was set to trigger at 50% of the response from a 3/64 inch diameter flat bottom hole, since the search unit may not be positioned for maximum response when it passed over each discontinuity. Therefore, prior to the inspection, the reference standard was checked to verify that with a 1/2 inch scan index the response was greater than 50% of the maximum response from the 3/64 inch diameter flat bottom hole in the reference standard. When an indication is found, in order to determine its actual size as compared to the reference standard, the search unit must be manipulated to maximize the signal response before making a value judgment.

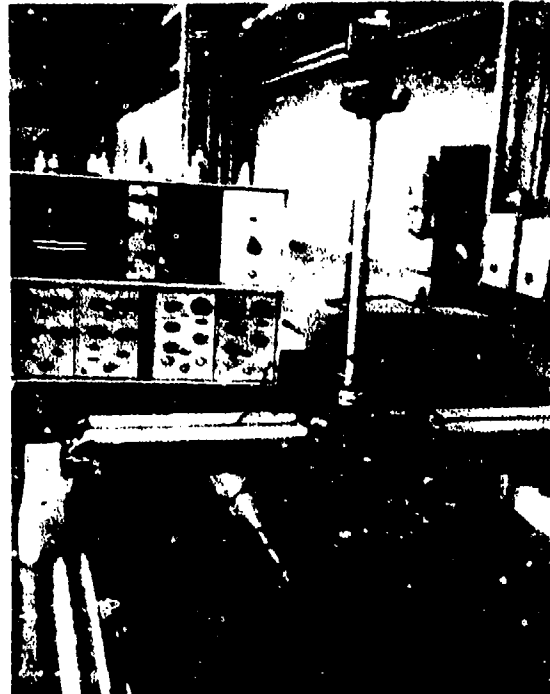


FIGURE 75  
ULTRASONIC INSPECTION OF INGOT

SIJ series ceramic transducers were obtained from Automation Industries for the ingot inspection. A group of transducers were tuned for use with the pulser/receiver to be used in the ingot inspection. From this group, several optimum transducers were selected by using the transducers on several Ti-6Al-4V test blocks containing both natural and artificial defects. The characteristics of a typical transducer used in the ingot inspection are shown in Figure 77.

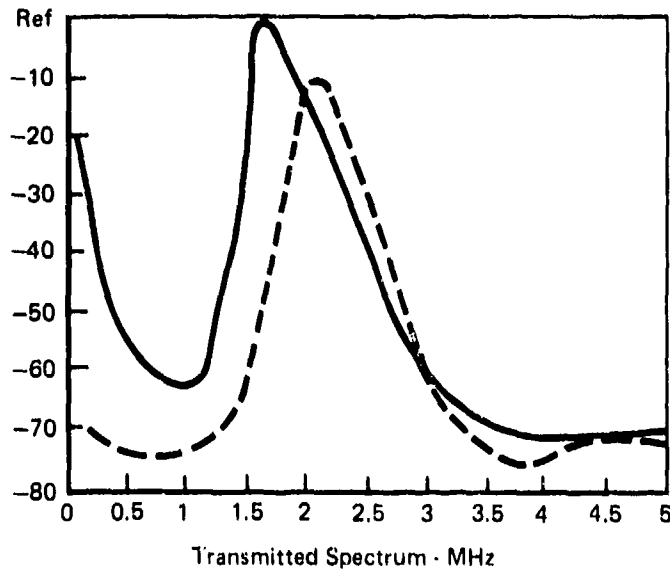
Figure 77 shows the spectrum analysis when the transducer was driven by a wide range pulser (Automation HRL) and also by the equipment used in the inspections. As can be seen, the peak radiated frequency using the 10N pulser was within  $\pm 10\%$  of the specified frequency.

Previous experience in inspecting jet engine disk forgings indicated that some discontinuities undetectable using longitudinal inspection are detectable using shear. Consequently, both longitudinal and shear wave immersion inspections were carried out on the ingot. The longitudinal inspection was performed using 1 inch diameter unfocused transducers and a frequency of 2.25 MHz and a 5-inch water path. A frequency of 2.25 MHz was necessary to inspect to the center of the 24-inch diameter ingot. The sound beam path was as shown in Figure 78. The reference standard used for the longitudinal inspection was a 14-inch diameter forged Ti-6Al-4V standard provided by the Ladish Company with  $3/64$  inch diameter flat bottom holes at metal travel distances of 6 and 7.5 inches (Figure 79). It would have been preferred to use a reference standard with the same diameter as the ingot (24 inches) but only a 14-inch diameter was available at Ladish. During the inspection, the automatic alarm system was set to trigger at 50% of the response from a  $3/64$  diameter flat bottom hole. As mentioned previously, two pulser/receiver-transducer arrangements were used. One channel was gated to inspect the first 6 inches in depth of ingot and the second channel was gated to inspect from a depth of 5 to 12 inches. The 5N pulser/receiver, which was affected least by noise, was used for the 5-12 inch inspection. A summary of the equipment used is presented in Table 46.

Both an axial and circumferential shear wave inspection were also performed. The same transducer and pulser/receiver arrangement was used as was with the longitudinal inspection. Again, a scan rate of approximately 3 inches per second was used and the scan index was less than  $1/2$  inch. The sound beam directions within the ingot are depicted in Figure 78. With circumferential shear wave, approximately the first 5 inches of the ingot was inspected, whereas, with axial shear, the ingot material from the surface to the center (12 inches) was inspected. Two  $3/4$  inch diameter unfocused transducers were used at a test frequency of 5 MHz. The sound beam angle in water was chosen such that the sound beam angle in the metal was 45 degrees. The water path was 4 inches. The reference standard used for circumferential shear was a 14.5-inch diameter forged Ti-6Al-4V standard provided by the Ladish

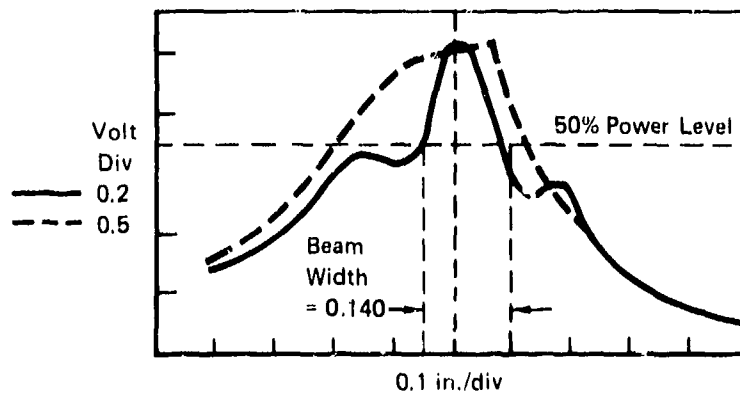
### Frequency Spectrum Analysis

— Wide Range Pulse (Automation HRL)  
 - - - Pulse With ION at 2.25 MHz



#### Beam Width

Water Path	Beam Width
7.5 in.	0.140
6.0 in.	0.340



Mfg - Automation      Serial No. - 22684      Size - 1 in.  
 Type - SIJ              Frequency - 2.25 MHz      Material - Ceramic  
 Reflection - 0.5 Dia Ball

GP74 0117 181

**FIGURE 77**  
**SEARCH UNIT ACOUSTICAL ANALYSIS**

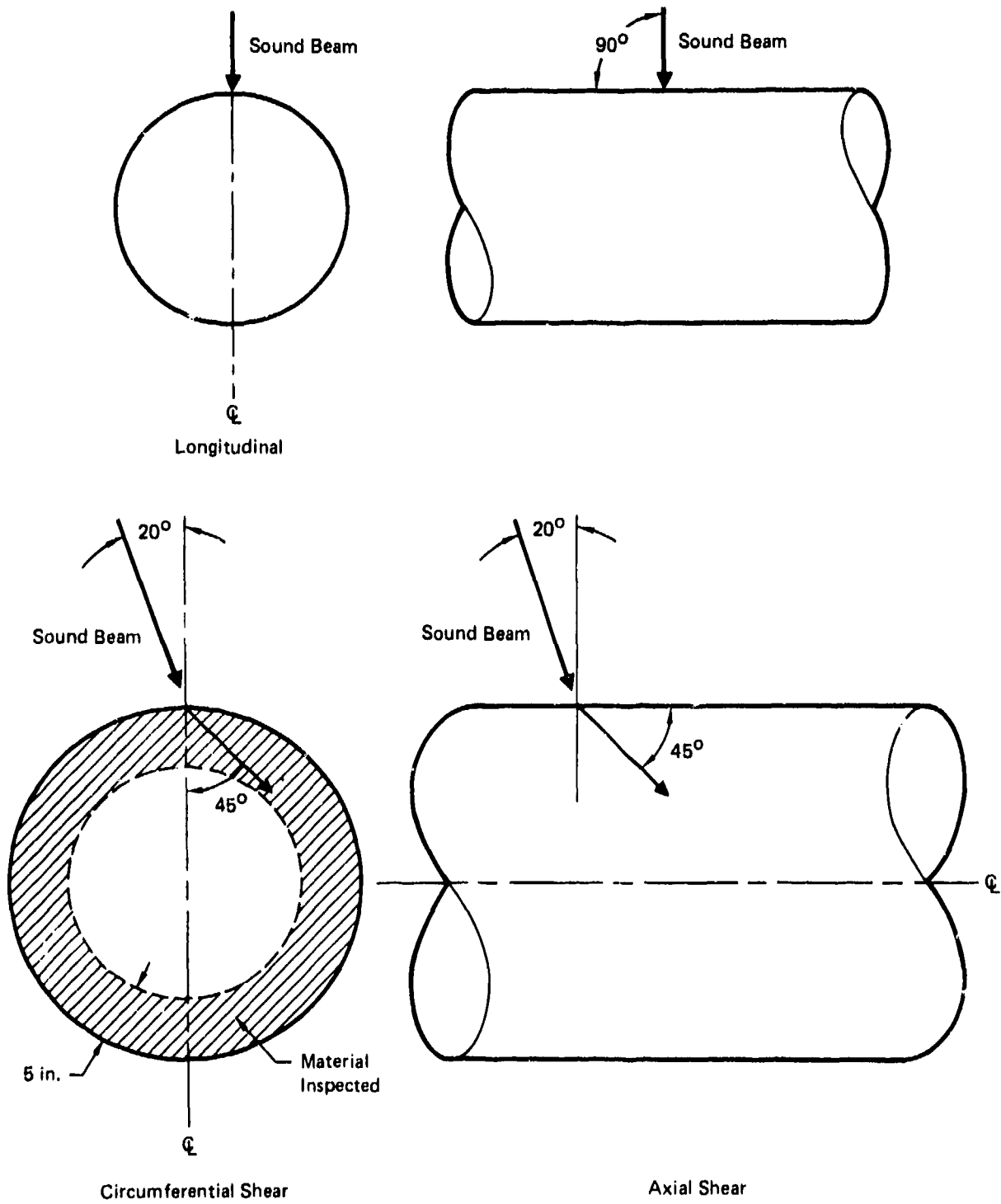


**FIGURE 78**  
**SOUND BEAM PATH**

GP74-0117 192

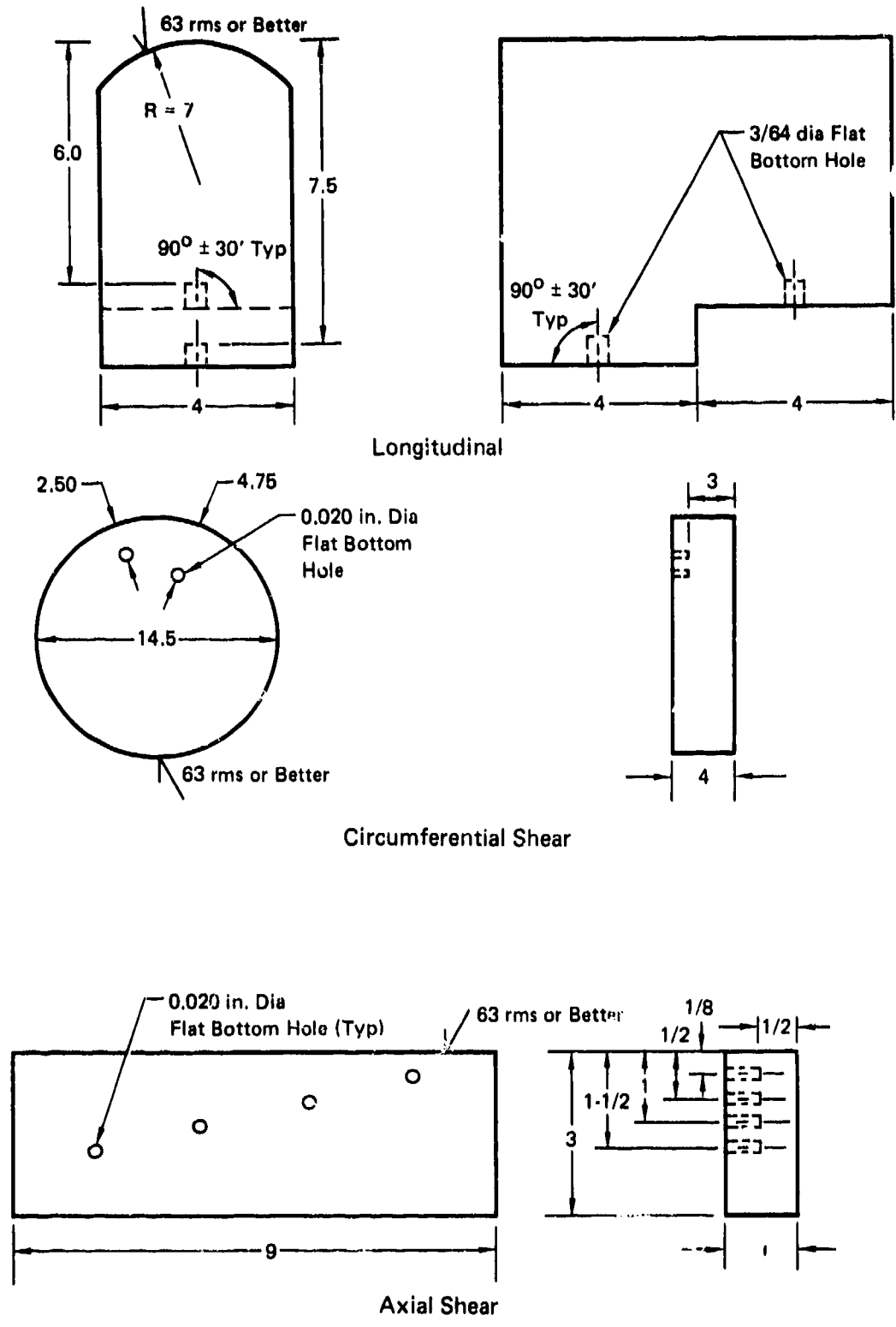


**FIGURE 79**  
**ULTRASONIC REFERENCE STANDARDS FOR INGOT INSPECTION**

GP74-0117-104

**TABLE 46  
EQUIPMENT USED FOR INGOT INSPECTION**

Display Units - Sperry 721  
Pulser Receivers - Sperry 10N (2 Units)  
Sperry 5N (2 Units)

Transducers								
Serial	Make	Size (in.)	Material	Focal Distance in Water (in.)		Spec Freq (MHz)	Water Path (in.)	Use
22684	Automation	1 Dia	SIJ Ceramic	>7.5	2.25	2.25	5	Longitudinal
26226 26227	Automation	3/4 Dia	SIJ Ceramic	6.5	5	5	4	Axial and Circumferential Shear

GP74-0117-103

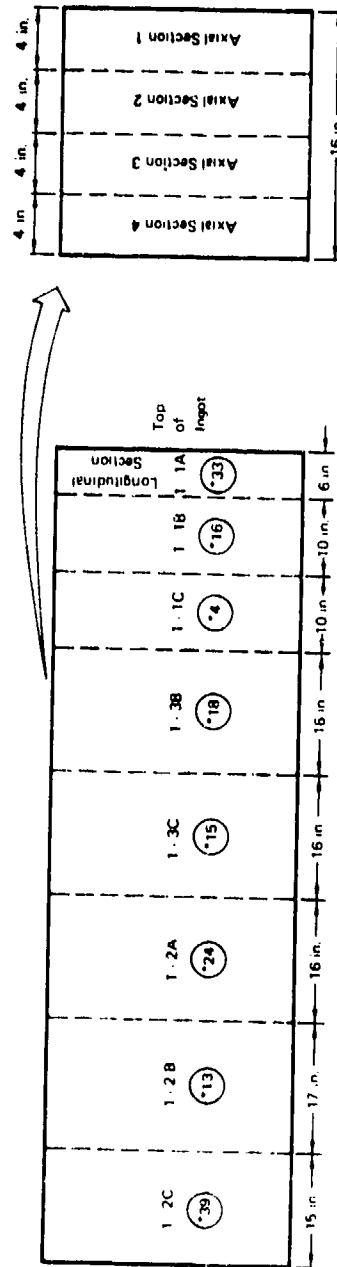
Company with 0.020 inch diameter side drilled holes drilled at metal travel distances of 2.50 and 4.75 inches (Figure 79). Again, a 24-inch diameter reference standard would have been preferred to match the ingot diameter; however, the 14-inch diameter was the largest available at Ladish. The reference standard for axial shear was as shown in Figure 79.

The results of the ultrasonic inspection are shown in Table 47. During the actual straight beam scanning of the ingot material, the background noise amplitude never exceeded 20 percent of full saturation. This was true for the inspection of the first 6 inches of ingot and, also, for the 5 to 12-inch depth scan. Each indication location was recorded with reference to the axial section, depth from the surface, and longitudinal section. The indications in the top 16 inches of the ingot (49 indications total) are probably due to the ingot pipe. It should also be noted that a large number of indications (76 total) are located in the bottom 48 inches of the ingot, where the Type I alpha segregates are expected. It is possible that several of the shear indications are from the same discontinuity as a longitudinal wave indication. In Sections 1-2A and 1-2B, it is apparent that several discontinuities that were detected using shear wave were not detected by longitudinal wave. In Section 1-2A, 11 axial shear wave indications were present with only 9 longitudinal wave indications. In Section 1-2B, there were 11 additional axial shear wave indications. These results are further proof that discontinuities can often be detected using the shear mode when they are undetectable using the longitudinal mode. This may be due to the orientation of the discontinuities. Also, since the wavelength of shear waves is less than that of longitudinal waves (for a constant frequency), the resolution capability with shear waves is probably greater than with longitudinal waves.

An analysis of the sound transmission characteristics indicates that there was a difference of at least 12 dB between the reference standards and the ingot material. Also, a variation of as much as 18 dB existed within small sections of the ingot itself.

Based upon these results of the ultrasonic inspection, the ingot was cut into the 8 longitudinal sections shown in Table 47 in preparation for further conversion to billet.

**TABLE 47**  
**NUMBER OF ULTRASONIC INDICATIONS IN INGOT**



Note: Each longitudinal section was divided into 6 equal length axial sections.

Longitudinal Section	Longitudinal Wave										Total Longitudinal Wave Indications	Axial Shear Wave						Total Axial Shear Indications	Circumferential Shear Wave						Total Circumferential Shear Indications	
	Axial Section			Depth from Surface (in.)			Axial Section			Depth from Surface (in.)			Axial Section			Depth from Surface (in.)										
	1	2	3	4	0-2	2-4	4-6	Over 6	1	2		3	4	0-2	2-4	4-6	Over 6		1	2	3	4	0-2	2-4		4-6
1-1A	11	11	4	7	-	-	-	33	-	-	-	-	-	-	-	-	-	-	-	-	-	-	-	-	-	0
1-1B	1	2	4	8	5	1	4	5	-	-	-	-	-	-	-	-	-	-	-	-	-	-	-	-	-	1
1-1C	-	-	1	2	3	-	-	3	-	-	-	-	-	-	-	-	-	-	-	-	-	-	-	-	-	1
1-3C	-	3	3	3	7	-	-	9	-	-	-	-	-	-	-	-	-	-	-	-	-	-	-	-	-	9
1-2A	2	2	3	1	-	6	-	8	-	-	-	-	-	-	-	-	-	-	-	-	-	-	-	-	-	5
1-2B	1	-	-	-	-	1	-	9	6	2	2	1	11	-	-	-	-	-	-	-	-	-	-	-	-	4
1-2C	29	7	2	-	-	17	10	2	2	6	4	1	1	-	-	-	-	-	-	-	-	-	-	-	-	0
								38																		0

GP74-0117-185

#### 4. INSPECTION OF 9 INCH DIAMETER BILLET

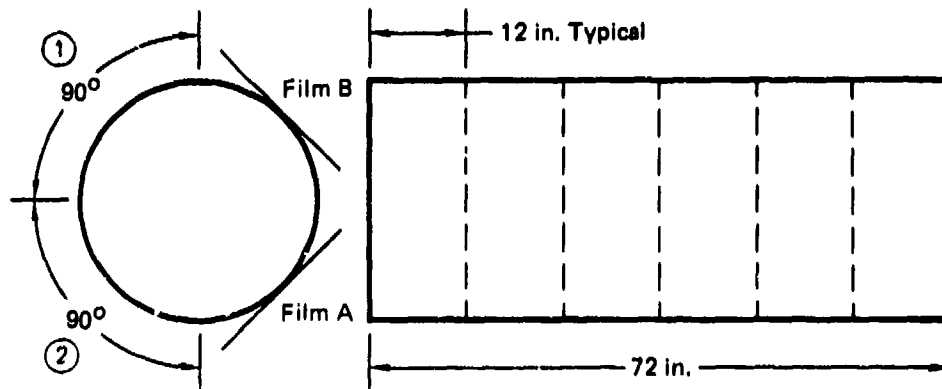
##### a. Radiography

The radiographic inspection of the billet Sections 1-1A, 1-2C, and 1-3B (see Table 47) was carried out by Allis Chalmers in Milwaukee, Wisconsin. The inspection was performed using a 24 MeV Allis Chalmers betatron and an exposure of 200 Roentgens. An ASTM No. 40 penetrometer was used as an image quality indicator and was placed on the source side of the billet. Front and back lead screens, 0.060 inch thick, were used and the back-up material was one inch thick lead. The source-to-film distance was 9 feet and the film (Kodak M) was placed directly against the billet material. The film was processed manually. Figure 80 shows the plan for the exposures taken. During each exposure the film was flat as opposed to being curved around the billet. Twelve inch wide axial areas were exposed using 14 x 17 inch film to provide for overlapping of exposures. The image of the IT hole and the outer edge of the penetrometer panel were visible on all the radiographs resulting in an equivalent penetrometer sensitivity of 0.31 percent. The film density ranged from 1.5 to 3.0 H&D units.

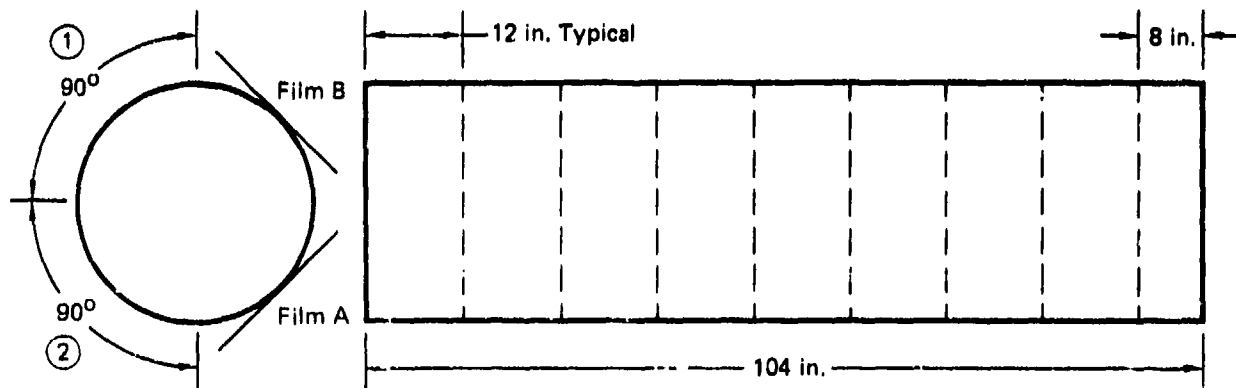
The results of the radiographic inspection are shown in Table 48. As with the ingot inspection, there are two possible circumferential locations for each indication since it is not possible to determine if the indication lies on the far side or the near side of the billet using the chosen techniques. In comparing these results with the results of the ingot inspection, it is clear that the ingot pipe healed during conversion to 9 inch billet. The pipe originally started within 2 inches of the ingot and extended to a depth of 16 inches.

##### b. Ultrasonic Inspection

The ultrasonic inspection of the 9 inch billet was carried out at the Ladish Company in Milwaukee, Wisconsin. Two separate pulser/receivers were used in conjunction with two long focused transducers and two Sperry 721 oscilloscopes. The vertical linearity of the electronic system had been checked by Ladish within 30 days of the inspection. Each pulser/receiver was checked for noise and calibration response on the same reference standard; there was little difference in the response of each. A summary of the equipment used is shown in Table 49. As shown in Figure 81, the two transducers were positioned 4 inches apart and the billet was rotated such that the scan was in a spiral. The scan rate was 2 inches per second; prior to the actual billet inspection, the scan rate was checked on the reference standard to ensure that the reference holes were detectable at a scan rate of 2 inches per second. The scan index was 1/4 inch per revolution. The scan index was checked on the reference standard to determine that with the chosen scan index, the response was greater than 50 percent of the maximum response from 3/64 diameter flat bottom hole in the reference standard.



Section 1-1A



Sections 1-2C and 1-3B

GP74-0117 198

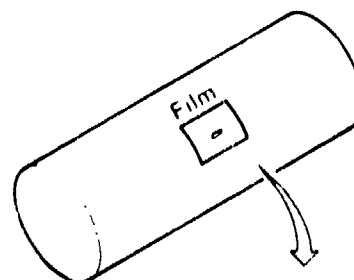
**FIGURE 80**  
**SCHEMATIC SHOWING EXPOSURE LAYOUT FOR RADIOGRAPHIC**  
**INSPECTION OF 9-INCH BILLET**

**TABLE 48**  
**RESULTS OF RADIOGRAPHIC INSPECTION OF 9 INCH BILLET**

Billet	Distance from Billet End (in.) <sup>1</sup>	Estimated Distance from Ingot Bottom (in.)	Distance from Circumferential Zero Location (in.)	Approximate Dimensions (Axial/Circumferential) (in.)	
				Film A <sup>3</sup>	Film B <sup>3</sup>
1-1A (Bar and Forgings from Ingot Top)	4	105	27.1 <sup>2</sup>	1-1/4 x 1/8	-
	27.5	100.5	15.6 or 29.0	3/8 x 1/2	1-1/4 x 1/8
	28.5	100	15.6 or 27.8	3/16 x 3/8	6 x 1/16
	29	99.8	15.2 <sup>2</sup>	1/8 x 1/4	-
1-3B (Bar and Forgings from Ingot Middle)	103.5	61	13.1 <sup>2</sup>	1/8 x 5/16	-
1-2C (Plate from Ingot Bottom)	34	10.8	27.9 <sup>2</sup>	1/8 x 3/8	-
	77	4.7	23.6 <sup>2</sup>	1/4 x 3/8	-
	79	4.35	23.6 <sup>2</sup>	3/16 x 3/8	-
	80	3.7	23.6 <sup>2</sup>	1/2 x 3/16	-
	90	2.1	17.9 <sup>2</sup>	1/2 x 3/16	-
	96	0.81	14.7 <sup>2</sup>	2-1/2 x 1/16	-
	99	0.65	14.7 or 25.5	4 x 1/8	3 x 1/8
	100	0.484	16.3 <sup>2</sup>	1-3/4 x 1/4	-
	103	-	17.9 <sup>2</sup>	1 x 1/4	-
	103	-	15.6 <sup>2</sup>	1 x 1/2	-

- <sup>1</sup> Billet end nearest ingot top.
- <sup>2</sup> The indication was not visible on second film.
- <sup>3</sup> See Figure 38 for film location.

UP740117 107



A = Axial Dimension  
C = Circumferential Dimension

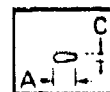
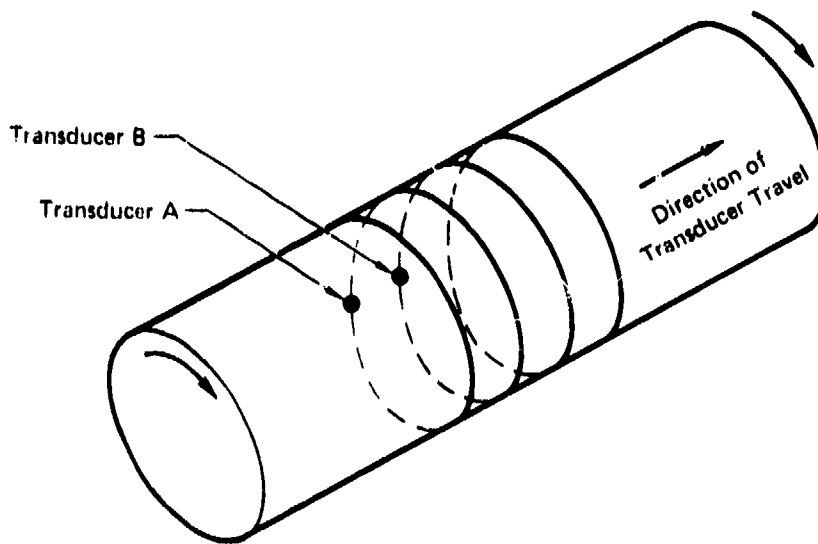


**TABLE 49  
EQUIPMENT USED FOR 9 INCH BILLET INSPECTION**

Display Units - Sperry 721  
Pulser Receivers - Sperry 10N (2 Units)  
Speiry 5N (2 Units)

Transducers								
Serial	Make	Size (in.)	Material	Focal Distance in Water (in.)	Spec Freq (MHz)	Spec Freq (MHz)	Water Path (in.)	Use
26226 26227	Automation	3/4 Dia	SIJ Ceramic	6.5	5	5	5	Axial and Circumferential Shear
FH3100 FH3102	Branson	3/4 Dia	Gamma Ceramic	9 Est	10	5	6	Longitudinal, Axial and Circumferential Shear

GP74 0117 198



GP74-0117 199

**FIGURE 81  
SPIRAL SCAN DURING ULTRASONIC INSPECTION OF 9 INCH DIAMETER BILLET**

Several transducers were obtained for the billet inspection. These transducers were focused, some with a focal length of approximately 9 inches in water and others with a focal length of approximately 6.5 inches in water. The transducers were optimized for the billet inspection using the methods described under the ingot inspection. The transducers were selected specifically for use with a specific pulser/receiver (either Sperry 5N or Sperry 10N, as applicable). Previous experience has indicated that some discontinuities that are not detectable using the longitudinal mode are detectable using a shear mode inspection. Consequently, both longitudinal and shear wave immersion inspections were carried out on the 9 inch diameter billet.

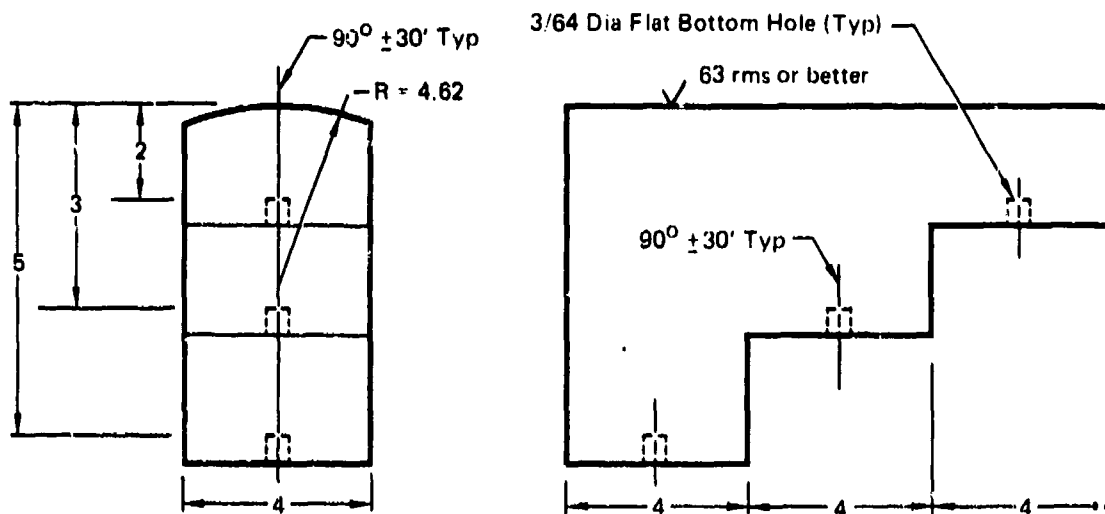
The longitudinal inspection was performed using a 3/4 inch diameter focused search unit pulsed at 5 MHz. Two Sperry 5N pulser/receivers were used. The sound beam angle is shown in Figure 78. A 6 inch water path was used. The reference standard used for the longitudinal inspection was a 9.25 inch round of forged Ti-6Al-4V supplied by Ladish Company with 3/64 inch diameter flat bottom holes at metal travel distances of 2, 3, and 5 inches (Figure 82).

As previously mentioned, the scan index was 1/4 inch per revolution of the billet and the scan rate was 2 inches per second. Both the scan rate and the index were checked on the reference standard prior to testing.

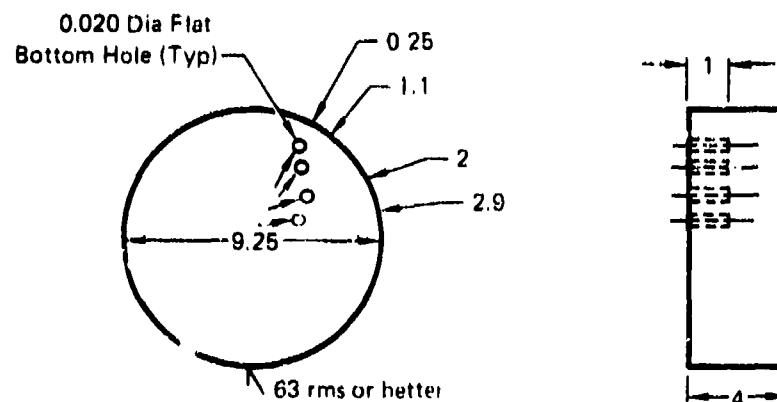
The difference in sound transmission characteristics between the reference standard and the 9 inch billet was checked using the 9 inch round circumferential shear reference standard and a representative piece of billet. The pieces were set-up for straight beam immersion testing and back-surface response through the reference standard was adjusted to 80 percent of saturation. Next, without changing the gain the back-surface response through the 9 inch billet was monitored. It was found that there was no more than 2 dB difference between the two. Since the circumferential shear reference standard and the longitudinal reference standard were machined out of the same piece of material, it was assumed that the circumferential shear standard could be substituted for the longitudinal standard to make these measurements.

The scanning gain was established by adjusting the response to the hole at 5 inches metal travel to 80 percent of saturation. All discontinuities whose amplitude exceeded 50 percent of saturation were evaluated further. The search unit was positioned over the discontinuity and the response was compared to that from the hole in the reference standard with a metal travel closest to that of the discontinuity.

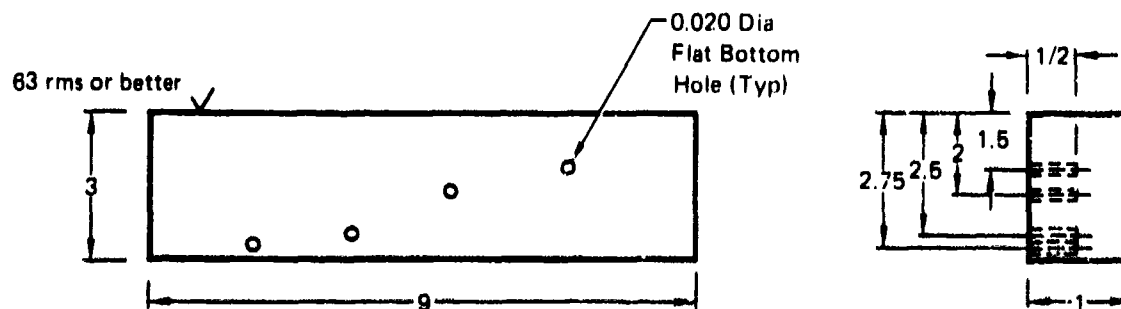
Both an axial and circumferential shear wave inspection were performed. The same test equipment arrangement was used as with the longitudinal inspection. Again, a scan rate of 2 inches per second was used with a scan index of 1/4 inch per revolution. Each were checked with the reference standard prior to testing.



Longitudinal



Circumferential Shear



Axial Shear

**FIGURE 82**  
**ULTRASONIC REFERENCE STANDARDS FOR 9 INCH BILLET INSPECTION**

QP74-0117 200

With circumferential shear wave, approximately the first 3 inches of the billet was inspected, whereas with axial shear, the billet material from surface to center (4-1/2 inches) was inspected. Billet Sections 1-1 and 1-2B were inspected using two Sperry 5N pulser/receivers, two long focused Branson transducers, 3/4 inch diameter, pulsed at 5 MHz. The sound beam angle is shown in Figure 78. The water path was 6 inches. Billet Sections 1-2A and 1-2C were inspected using two Sperry 10N pulser/receivers, two long focused Automation transducers, 3/4 inch in diameter, pulsed at 5 MHz. The sound beam angle is shown in Figure 78 and a water path of 5 inches was used. This arrangement was necessitated by the availability of equipment. The reference standard used for circumferential shear was a 9.25 inch diameter round of forged Ti-6Al-4V supplied by the Ladish Company with 0.020 inch diameter side drilled holes (Figure 82). The 9.25 inch diameter forged reference standard had been fabricated in a manner similar to the 9 inch diameter billet to be inspected resulting in little difference (less than 2 dB) in sound transmission characteristics between the two.

A reference standard with 0.020 inch diameter side drilled holes at metal travels of 1.5, 2, 2.5, and 2.75 inches was used for the axial shear inspection (Figure 82).

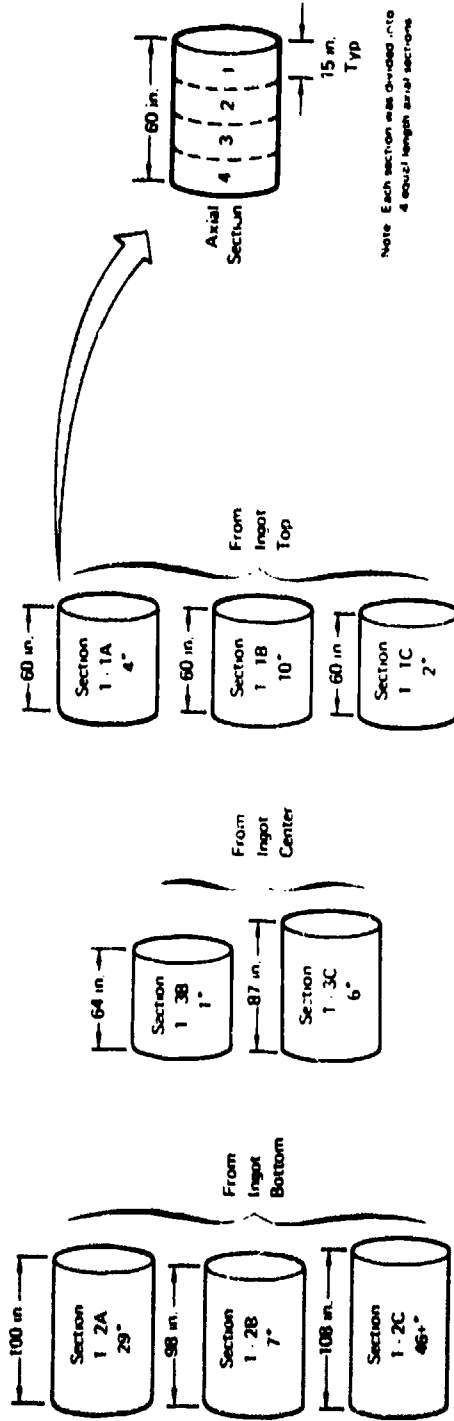
The results of the ultrasonic inspections are shown in Table 50. The indication found by longitudinal wave in Axial Section 1 in Longitudinal Section 1-1A was 1.3 inches long; it is suspected that this is a section of ingot pipe still remaining as is the 3 inch long indication found by longitudinal wave in Axial Section 4 in Longitudinal Section 1-1C.

In Section No. 1-2A, it is apparent that several discontinuities detected using circumferential shear wave were not detected using longitudinal wave. Specifically, there were 21 circumferential shear indications and only 8 longitudinal indications in the same volume of material. Obviously, the effectiveness of billet inspection can often be increased by supplementing the usual longitudinal wave inspection with a shear wave inspection due to defect orientation and the difference in resolution capability between longitudinal and shear waves.

#### c. Macroetching and Anodic Etch

A cross section was cut from each of the eight 9 inch diameter billets for etching evaluation. Prior to etching, the disks were machined flat. Macroetching was performed by the Ladish Company using a 15% HNO<sub>3</sub> - 5% HF - Balance H<sub>2</sub>O solution. The general appearance of the macroetched surfaces were similar to that of a typical commercial 9 inch round Ti-6Al-4V billet as shown in Figures 83 and 84. Examination of all the macroetched surfaces revealed only one discontinuity. That discontinuity was located in the disk cut from the bottom of the ingot; it was this area that had been intentionally seeded to produce Type I stabilized alpha. A photograph of the macroetched surface at the discontinuity is shown in Figure 85.

**TABLE 50  
NUMBER OF ULTRASONIC INDICATIONS IN 9 INCH DIAMETER BILLET**



Section	Longitudinal Wave						Total Longitudinal Wave Indications	Axial Shear Wave						Total Axial Indications	Circumferential Shear Wave						Total Circumferential Indications				
	Axial Section			Depth from Surface (in.)				Axial Section			Depth from Surface (in.)				Axial Section			Depth from Surface (in.)							
	1	2	3	4	0-2	2-4		4-6	Over 6	1	2	3	4		0-2	2-4	4-6	Over 6	1	2		3	4	0-2	2-4
1.1A	1	-	-	1	1	-	-	2	-	-	-	-	-	-	-	-	-	1	-	-	-	-	-	-	1
1.1B	-	-	-	1	1	-	-	1	-	-	-	-	-	-	-	-	-	-	-	-	-	-	-	-	1
1.1C	-	-	-	1	1	-	-	1	-	-	-	-	-	-	-	-	-	-	-	-	-	-	-	-	1
1.3A	-	-	-	3	2	6	-	6	-	-	-	-	-	-	-	-	-	-	-	-	-	-	-	-	-
1.2A	1	-	3	4	1	1	6	8	-	-	-	-	-	-	-	-	-	-	-	-	-	-	-	-	21
1.2B	1	1	1	4	1	4	2	7	-	-	-	-	-	-	-	-	-	-	-	-	-	-	-	-	-
1.2C**	11	10	4	3	11	6	5	28	3	1	4	-	4	4	-	-	-	8	4	1	-	-	-	-	10

\*\*Total ultrasonic indications  
\*\*Last 25 in not inspected in shear



FIGURE 83  
TYPICAL MACROETCHED BILLET SURFACE FROM SEDED INGOT

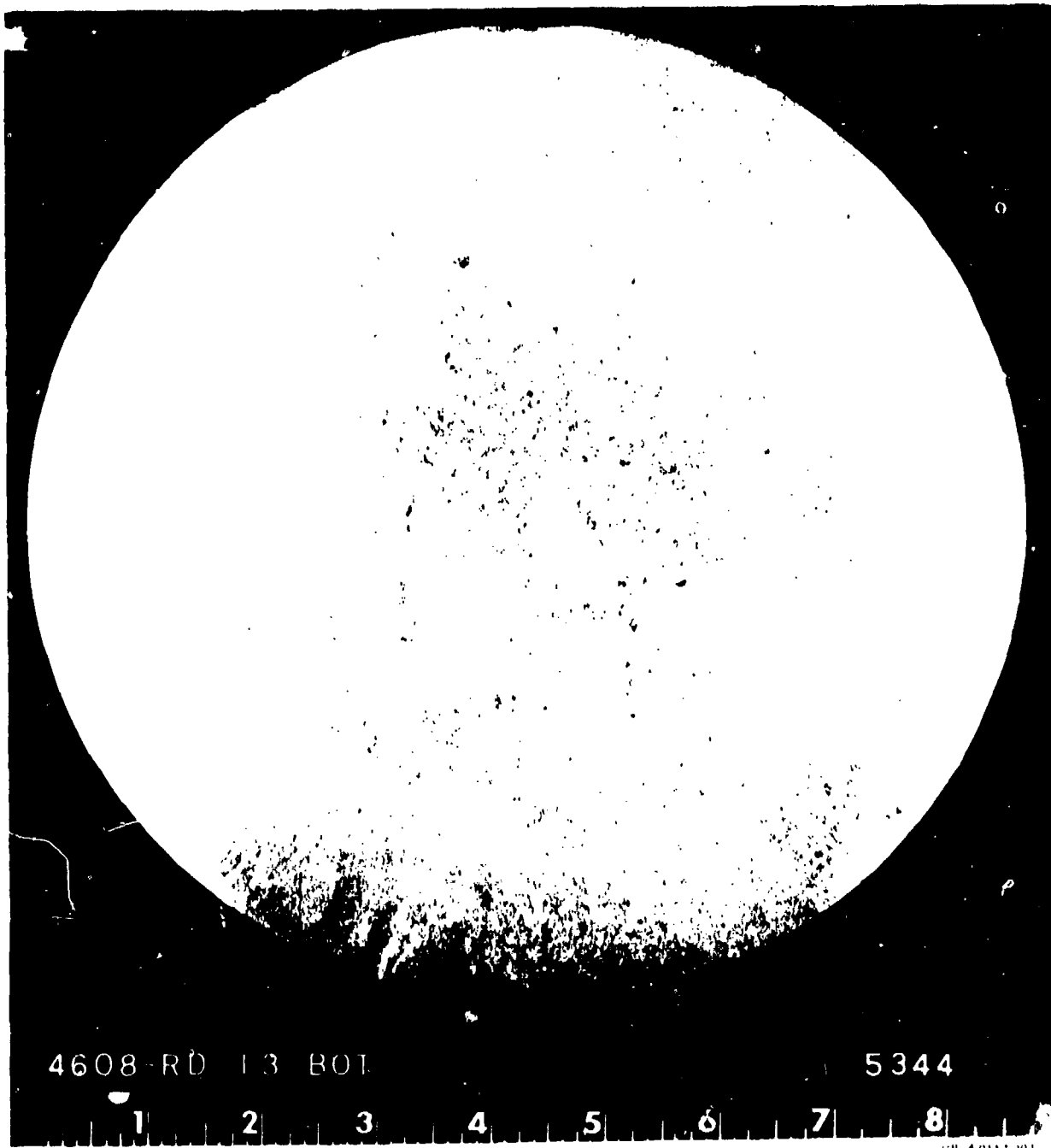
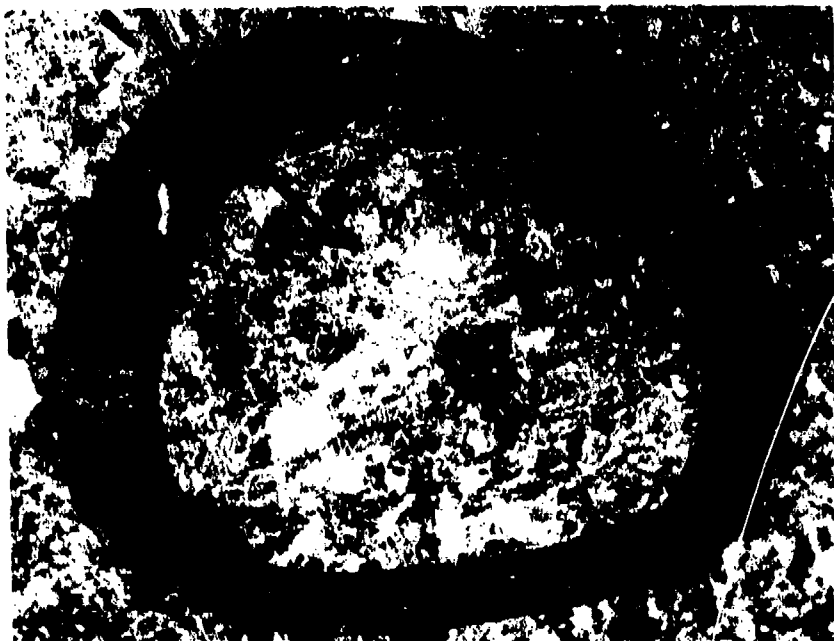
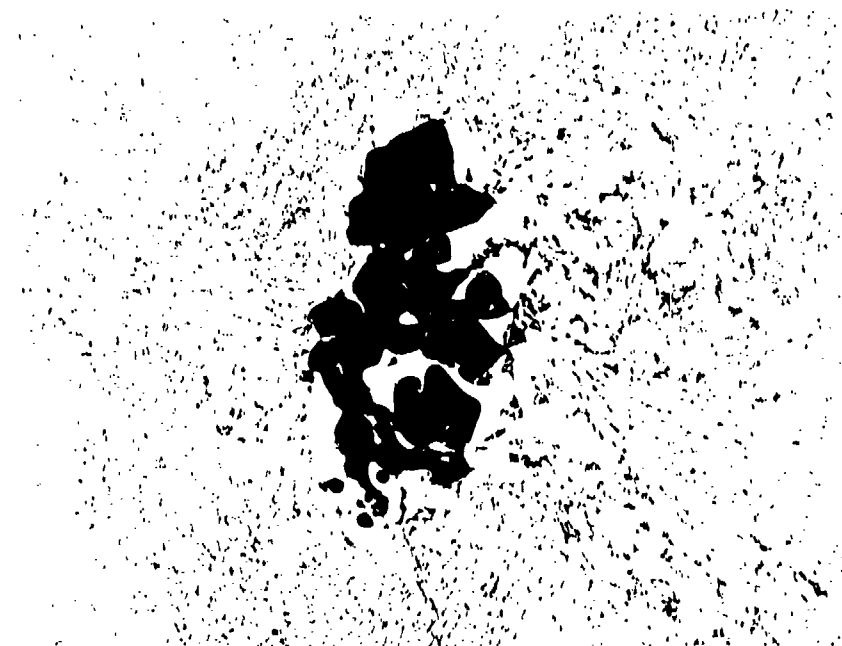


FIGURE 84  
TYPICAL MACROETCHED SURFACE IN COMMERCIAL 9 INCH BILLET



6 X



50 X

QP74 0117 204

**FIGURE 85**  
**DISCONTINUITY IN 9 INCH BILLET (1-2B)**

After macroetching, the disks were sent to Metals Testing Company in South Windsor, Connecticut to be anodically etched. The discontinuity detected during macroetching etched dark blue in this process. No other obvious defects were revealed. However, some of the disks from the top section of the ingot, Bar 1-1B in particular, showed patches of blue etching alpha of a deeper shade than surrounding areas. These areas did not have the typical "lightening streak," zig-zag, pattern of aluminum segregation found in Ti-6Al-4V forgings in the past.

Following the anodic etching, metallographic cross sections were taken through several of the disks. One cross section was taken through the discontinuity revealed by macroetching and anodic etching. In addition, a total of 12 metallographic cross sections were taken at random from several of the disks. The discontinuity previously detected by macroetching was found to be a typical Type I alpha stabilized void with cracking around the void (See Figure 85). No additional discontinuities were found in the random cross sections.

Since only one Type I alpha stabilized area was detected, it appears that macroetching and anodic etching of random billet sections are **ineffective** techniques for establishing the existence of Type I alpha stabilized areas. This conclusion is based upon the assumption that a large number of Type I discontinuities are present in the 9 inch billets as indicated by the ultrasonic indications.

The lack of macroetching indications in the billet sections from the top of the ingot suggests that the ingot pipe was completely healed during ingot conversion.

## 5. INSPECTION OF 6 INCH DIAMETER BILLET

### a. Ultrasonic Inspection

The 6 inch diameter billet sections to be converted to bar and forgings were ultrasonically inspected. Prior to ultrasonic inspection, the billet surfaces were Tysaman ground to a 125 rms or better surface finish.

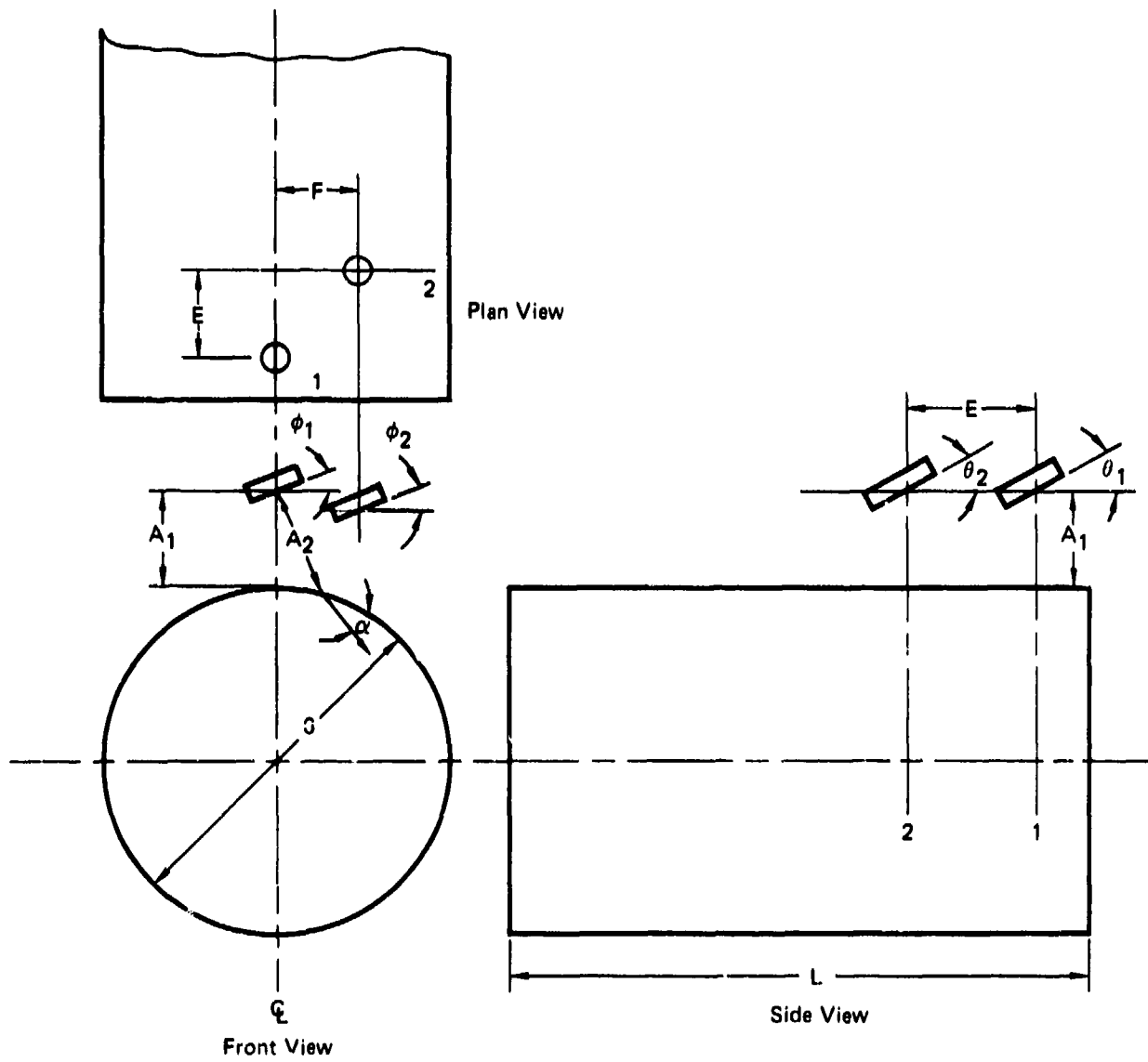
A summary of the equipment used during the inspection is shown in Table 51. The inspections were carried out by a variety of inspection personnel at several locations within the plant; hence, the large variety of equipment. Again, as with the ingot and 9 inch diameter billet inspections, two separate pulser/receivers were used in conjunction with two transducers and two Sperry 721 oscilloscopes. One pulser/receiver-transducer combination was used to inspect to a depth of 1.5 inches while the other was used from 1 to 3 inches. The vertical linearity of the electronic systems used had been checked by Ladish within 30 days of the inspection. Each pulser/receiver was checked for noise and calibration response on the same reference standard; there was little difference in the response of each.

The position of the transducers during inspection is shown in Figure 86. The 6 inch billet sections were rotated such that the scan was in a spiral. The scan rate was 3.9 inches per second; prior to the actual billet inspection, the scan rate was checked on the reference standard to ensure that the reference holes were detectable at a scan rate of 3.9 inches per second. The scan index was 0.1 inch per revolution. The scan index was checked on the reference standard to determine that with the chosen scan index the response was greater than 50 percent of the maximum response from the applicable flat bottom hole in the reference standard. Each billet section was examined through the half-section thickness.

The reference standards used for the inspections are shown in Figure 87. Prior to the inspections the difference in sound transmission between the longitudinal reference standard and the 6 inch billet and the axial shear reference standard and the 6 inch billet were measured. First, the 6 inch diameter circumferential shear and 6 inch diameter billet were placed in the water. The back surface reflection of a straight beam through the reference standard was adjusted to 69 percent of saturation. Next, without changing the gain, the back reflection through the 6 inch billet was noted to be 57 percent of saturation.

The axial shear reference standard and the 6 inch billet were checked next. In this case, the sound beam in the shear mode was reflected off a corner of the axial shear reference standard through 6 inches of metal. The response was adjusted to 60 percent of saturation. Then, without changing the gain, the sound beam in the shear mode was reflected off the far surface of the billet, and, this response was 75 percent of saturation.

It was decided, from these tests, that it was not necessary to compensate for sound transmission differences.



\*F Offset Both Channels

Type Inspection	$A_1$ or $A_2$ (in.)	E (in.)	$\alpha$ $0^\circ$	$\phi_1$ $\phi_2$	$\theta_1$ $\theta_2$	F* (in.)
Longitudinal	Water Path	7.5	$90^\circ$	$0^\circ$	$0^\circ$	0
Axial Shear	Water Path	7.5	$45^\circ$	$0^\circ$	$19^\circ$	0
Circum Shear	Water Path	7.5	$45^\circ$	$19^\circ$	$0^\circ$	0.4

GP74-0117-206

**FIGURE 86**  
**ULTRASONIC INSPECTION SETUP**

**TABLE 51**  
**EQUIPMENT USED TO ULTRASONICALLY INSPECT 6 INCH BILLET**

Display Units - Sperry 721 - 3 Units  
 Pulser-Receivers - Sperry 10N - 3 Units  
 Sperry 5N - 3 Units

Transducers																		
Serial No.	Make	Size (in.)	Material	Focal Distance in Water	Spec. Freq MHz	Freq Used MHz	Water Path (in.)	1-1A6 (Ingot Top)			1-3B6 (Ingot Middle)			1-2A6 (Ingot Bottom)			Top Middle Bottom	
								L	C	A	L	C	A	L	C	A		
26226	Automation	3/4 Dia	SiJ Ceramic	6.5	5	5	2						X			X	X	X
FH3100	Branson	3/4 Dia	Gamma Ceramic	9	10	5	4					X					X	X
A713	Automation	1/4 x 1	SiL Lithium Sulphate	Cyl	15	10(T Jack)	0.8	X			X				X	X		
A39	Automation	1/4 x 1	SiL Lithium Sulphate	Cyl	15	10(T Jack)	1.2	X			X				X	X		
A216	Automation	5/16 x 1-1/4	SiL Lithium Sulphate	Cyl	5	5(R Jack)	2			X					X	X		
A678	Automation	1/4 x 3/4	SiL Lithium Sulphate	Cyl	10	5(R Jack)	2			X					X	X		
A839	Automation	5/16 x 1	SiZ Ceramic	Cyl	10	5(T Jack)	0.8										X	

L - Longitudinal  
 C - Circumferential Shear  
 A - Axial Shear

GP74-0117-206

a. Ultrasonic Inspection (Continued)

The results of the ultrasonic inspections are shown in Table 52. As can be seen, there are a large number of indications in those pieces which were converted to 2 inch square bar and forgings.

b. Radiographic Inspection

The radiographic inspection of those 6 inch diameter billet portions to be converted into forgings was carried out at the General Electric Company in Evendale, Ohio. The inspection was performed using a 2MeV Vandergraf accelerator and an exposure of 650 Roentgens. A 0.015 inch thick MIL-STD-453 penetrameter was used as an image quality indicator and was placed on the source side of the billet. Front and back lead screens, 0.060 inch thick, were used and the back-up material was one inch thick lead. The source-to-film distance was 4 feet and the film (DuPont NDT 75) was placed directly against the billet material. The film was processed manually. Figure 88 shows the plan for the exposures taken. During each exposure, the film was held flat as opposed to being curved around the billet. Twelve inch wide axial areas were exposed using 14 x 17 inch film to provide the overlapping of exposures. The overall film density ranged from 1.5 to 3.0 H and D units. The IT penetrameter hole and the outer edge of the penetrameter panel were discernible in every radiograph resulting in an equivalent sensitivity of 0.18 percent.

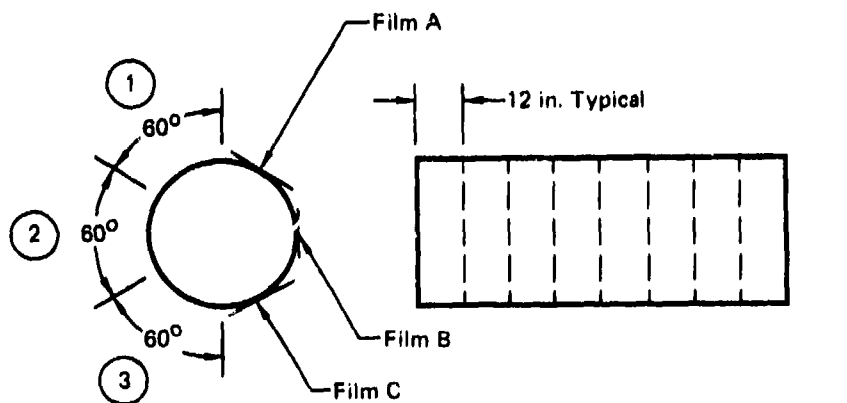


**FIGURE 88**  
**SCHEMATIC SHOWING EXPOSURE LAYOUT FOR RADIOGRAPHIC**  
**INSPECTION OF 6 IN. BILLET**

The results of the radiographic inspection are shown in Table 53 and a comparison of the radiographic indications with the results of the previous ultrasonic inspection is presented in Table 54. As can be seen from Table 54, many more indications were discovered with the ultrasonic method as opposed to the radiographic method.

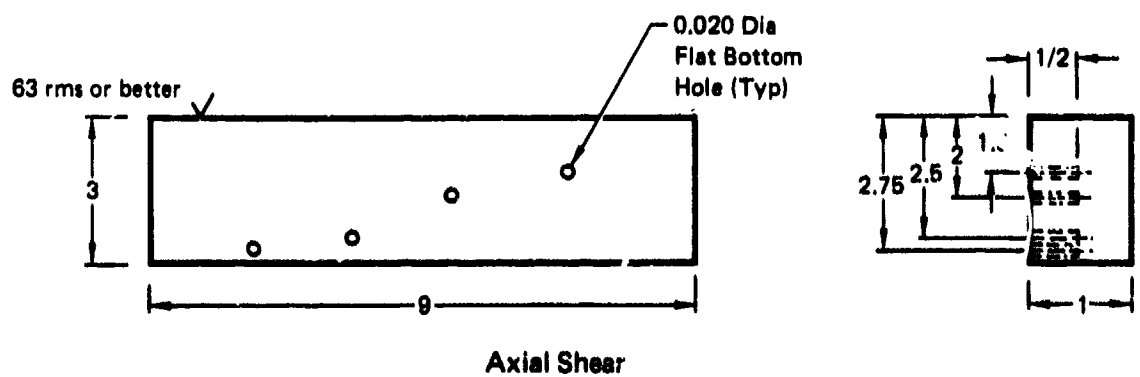
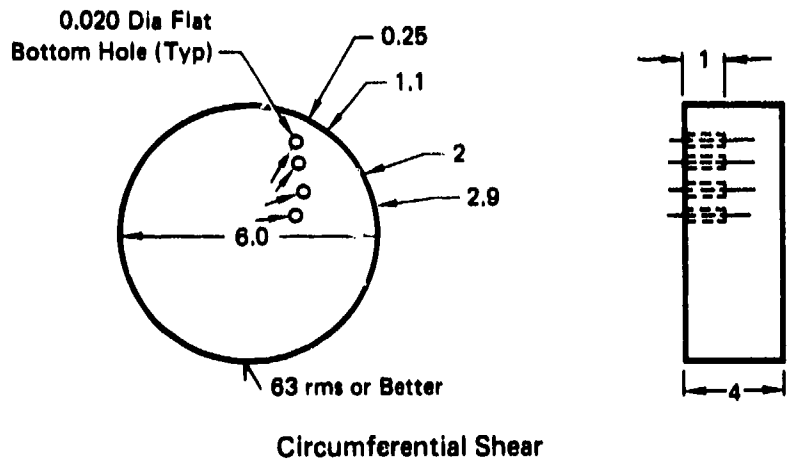
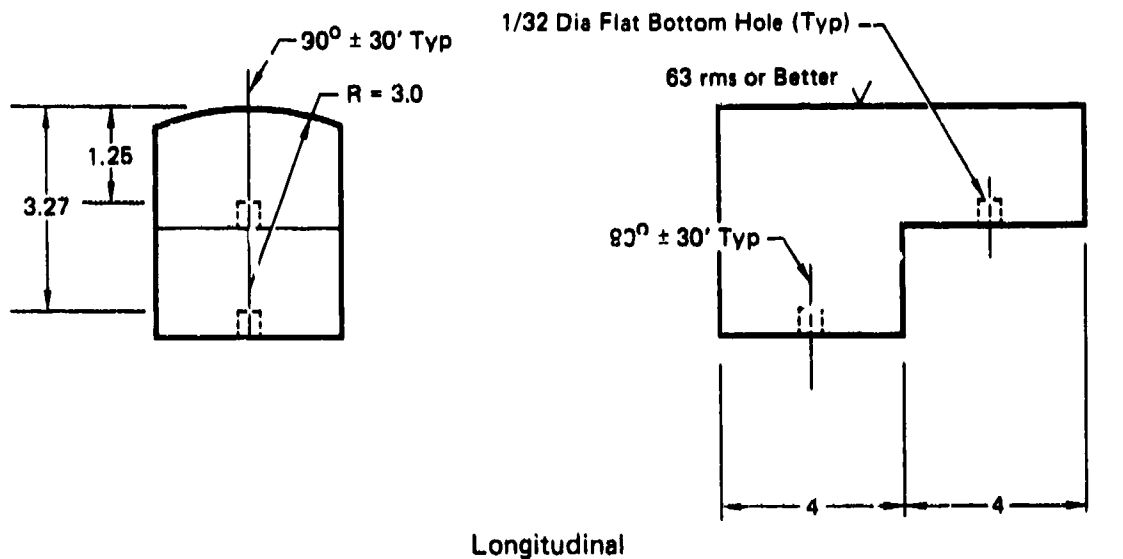
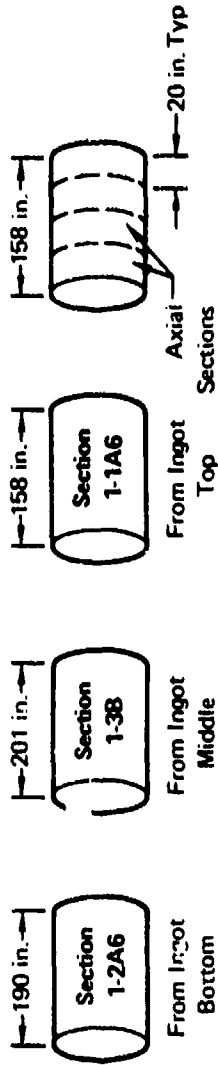


**FIGURE 87**  
**ULTRASONIC REFERENCE STANDARDS FOR 6 INCH BILLET INSPECTION**

QP74-0117-207

TABLE 52  
 NUMBER OF ULTRASONIC INDICATION IN 6 INCH DIA-METER BILLET



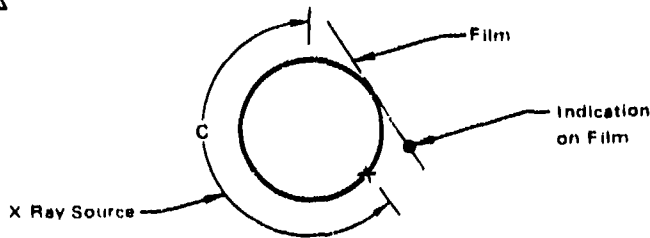
Section	Longitudinal Wave (0.031 in. Calib)							Axial Shear Wave (0.020 in. Calib)							Circumferential Shear (0.020 in. Calib)											
	Axial Section			Depth from Surface				Axial Section			Depth from Surface				Axial Section			Depth from Surface								
	1	2	3	4	0-1	1-2	2-3	Total	1	2	3	4	0-1	1-2	2-3	Total	1	2	3	4	0-1	1-2	2-3	Total		
1-1A (Bar and Forgings)	31	30	34	20	2	102	11	115	0	0	0	0	0	0	0	0	0	0	0	0	0	0	0	0	0	24
1-3B (Bar and Forgings)	54	19	26	2	4	81	16	101	1					1												7
1-2A (Bar and Forgings)	31	40	42	25	0	88	50	138	1	1						2										15

GP74 0117-208

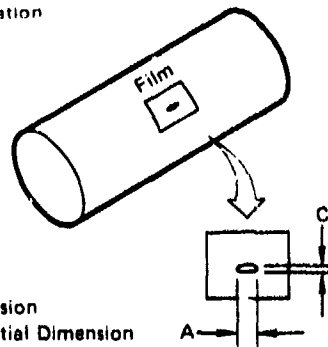
**TABLE 53**  
**RESULTS OF RADIOGRAPHIC INSPECTION OF 6 INCH BILLET 1-2A6**

Forging Blank	Forging No.	Distance from Blank End <sup>1</sup>	Distance from Circumferential Zero (C) <sup>2</sup>			Approximate Dimensions (Axial/Circumferential) (in.)		
			Film A <sup>3</sup>	Film B <sup>3</sup>	Film C <sup>3</sup>	Film A <sup>3</sup>	Film B <sup>3</sup>	Film C <sup>3</sup>
3	GE5	7	-	7.0	-	-	1/16 x 1/8	-
		7	-	2.3	-	-	1/16 Dia	-
		4-7/8	6.7	-	-	1/32 x 1 1/2	-	-
		1/2	6.7	-	-	0.025 Dia	-	-
		1/2	7.6	-	-	0.025 Dia	-	-
5	GE6	2-1/4	12.1	2.35	-	0.070 Dia	0.050	-
		1.5	-	-	16.3	-	0.040 Dia	-
1	GE4	0.2	16.6	13.4	7.2	0.15 <sup>4</sup>	0.15 <sup>4</sup>	0.4 <sup>4</sup>
		2.9	1.9	10.1	6.7	0.3 <sup>4</sup>	0.15 <sup>4</sup>	0.3 <sup>4</sup>
2	M-1,2	2.8	17.0	13.4	6.6	0.5 <sup>4</sup>	0.4 <sup>4</sup>	0.3 <sup>4</sup>
		8.0	0.2	11.6	7.0	-	0.2 <sup>4</sup>	0.3 <sup>4</sup>
		8.5	0.5	11.9	6.4	-	0.3 <sup>4</sup>	0.3 <sup>4</sup>
		9.7	1.3	11.7	6.2	0.5 <sup>4</sup>	0.25 <sup>4</sup>	0.3 <sup>4</sup>
4	M-3,4	4.0	0.5	13.1	5.0	0.15 <sup>4</sup>	-	0.3 Dia
		6.1	17.2	12.4	7.4	0.5 <sup>4</sup>	-	0.2 Dia
		9.8	1.1	13.2	4.4	0.4 <sup>4</sup>	-	0.15 Dia

<sup>1</sup> Forging Blank End Nearest Ingot Top  
<sup>2</sup>



<sup>3</sup> See Figure 43 for Film Location  
<sup>4</sup> Ellipse Length



A = Axial Dimension  
 C = Circumferential Dimension

**TABLE 54**  
**COMPARISON OF RADIOGRAPHIC AND ULTRASONIC INDICATIONS**  
**IN 6 INCH BILLET 1-2A6**

Forging No.	Billet Part No.	Forging Blank	Number of Indications		
			Ultrasonic Longitudinal	Ultrasonic Shear	Radiography
GF1	1-3B-6	7	2	0	—
GE2	1-3B-6	8	3	0	—
GE3	1-3B-6	9	4	0	—
GE4	1-2A-6	1	11	4	2
GE5	1-2A-6	3	9	0	5
GE6	1-2A-6	5	9	8	2
GE7	1-1A-6	10	9	2	—
GE8	1-1A-6	12	6	2	—
GE9	1-1A-6	14	7	5	—
MC1	1-2A-6	2	19	0	4
MC2	1-2A-6				
MC3	1-2A-6	4	9	5	3
MC4	1-2A-6				
MC5	1-1A-6	11	6	2	—
MC6					
MC7	1-1A-6	13	9	1	—
MC8					

GP74-0117 126

## 6. CORRELATION OF INSPECTION RESULTS

The ultrasonic inspection results for the ingot, 9 inch diameter billet and 6 inch diameter billet were analyzed to determine how many of the longitudinal and shear wave indications result from the same discontinuity. A total of 172 ultrasonic indications have been evaluated as to their location. Of these 172 indications, only a few were close enough together to consider the shear wave and longitudinal wave indications were from the same discontinuity. For example, there were a total of 138 indications detected by longitudinal wave and a total of 15 indications detected by circumferential shear wave in Section 1-2A of the 6 inch billet. Since none of these indications were in close proximity, it can be concluded that 15 discontinuities were detected by shear wave that were not detected by longitudinal wave. This may be due to the orientation of the discontinuities. Also, since the wavelength of shear waves is less than that of longitudinal waves (for a constant frequency), the resolution capability with shear waves is probably greater than with longitudinal waves.

## 7. SUMMARY OF NDT RESULTS

A summary of the ultrasonic and radiographic test results for the ingot, 9 inch billet, and 6 inch billet inspections is shown in Figure 89. From these results, it can be seen that the ingot pipe, which was intentionally exaggerated during melting, was healed during the conversion to 9 inch billet. The total number of longitudinal indications decreased from 57 to 3 when the total number of shear indications decreased from 11 to 2. Also, the pipe was not detected during the radiographic inspection of the 9 inch billet. As can be seen from the 6 inch billet results, a large number of indications are present in the material to be converted to bar and forgings indicating that a large number of segregates survived the conversion process.

As was previously mentioned, the ultrasonic and radiographic testing conducted on the ingot and billet material was not developmental in nature as a previous Air Force program had been conducted to improve nondestructive testing of ingot and billet material (Reference 2). The purpose of the inspections was to select the locations for shearing the material for subsequent conversion. It became clear during the program that several ultrasonic techniques still need to be implemented into ultrasonic inspection of ingot and billet as presently practiced by the industry. For example, reference standards should be used which have metal travels extending over the depth range to which the test part is to be inspected. Such reference standards were not available for the ultrasonic inspection of the ingot. The billet surfaces were prepared for ultrasonic inspection by Tysaman grinding and the reference standards had a machined surface of 63 rms or better. It was learned that no compensation is normally made for this difference in surface finish from reference standard to test part. Several other aspects of ultrasonic inspection do not seem to be adequately controlled through specifications. For example, inaccuracies were found in the decade switches on some of the pulser/receivers and these are not normally checked periodically. It was found that the search unit characteristics are not always required to be checked and compensation requirements for differences in sound transmission characteristics between the reference standard and the test part are not



SECTION V

NDT CAPABILITY

The capability of the improved penetrant, ultrasonic, eddy current, and radiographic methods for the detection of discontinuities was measured. Discontinuity types used were surface cracks, internal cracks, porosity, fatigue cracks in fastener holes, and Type I and Type II segregation in bar, plate, airframe forgings, and engine disk forgings. Many of the test specimens were inspected under laboratory, production, and overhaul inspection conditions by jet engine inspection personnel and airframe inspection personnel. The nondestructive testing techniques were intended to represent the present state-of-the-art; however, where possible, technique improvements developed earlier in the program were incorporated. Finally the actual size of several of the various discontinuities were measured.

1. SURFACE CONNECTED CRACKS

A program was carried out in order to measure the capability of penetrant, ultrasonic, radiographic, and eddy current testing for detection of surface cracks in titanium. A summary of the test program is presented in Table 55.

**TABLE 55  
SUMMARY OF INSPECTION METHODS USED  
FOR DETECTION OF SURFACE CRACKS**

Environment	Testing Group	Test Method
Laboratory	Airframe	Fluorescent Penetrant Eddy Current
Production	Airframe	Fluorescent Penetrant Surface Wave Ultrasonics Contact Angle Beam Ultrasonics Radiography
Overhaul	Airframe	Fluorescent Penetrant
Laboratory	Engine	Fluorescent Penetrant
Production	Engine	Fluorescent Penetrant
Laboratory	AFML	Fluorescent Penetrant

QP74-0117 1

a. Tension - Tension Fatigue Specimen Fabrication

Specimens containing surface connected cracks were produced by subjecting fatigue specimens (see Figure 90) to tension-tension fatigue using a 50,000 pound Sonntag fatigue machine. Electrical discharge machined (EDM) slots were incorporated at various locations to serve as

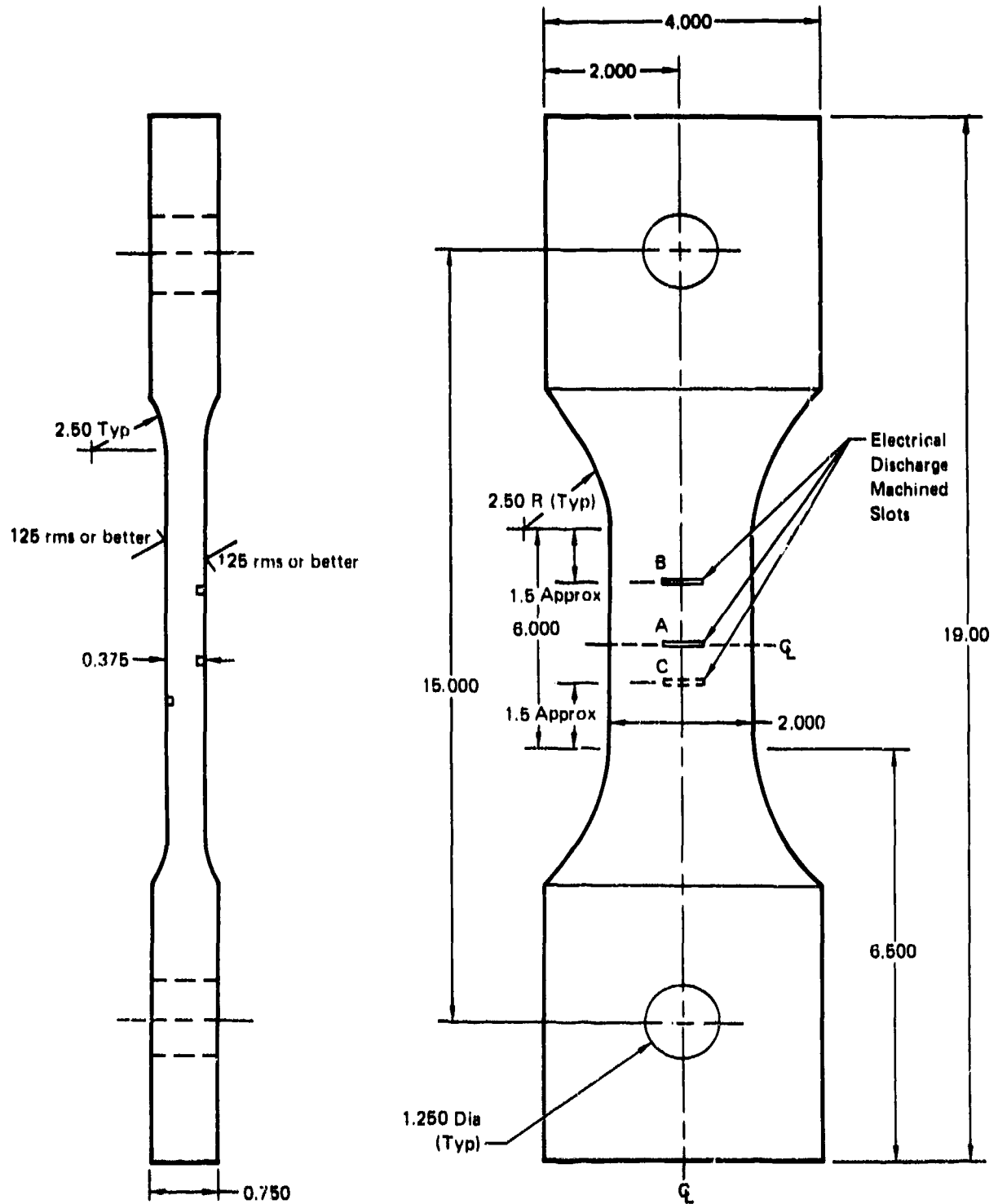


FIGURE 90  
FATIGUE SPECIMEN

QP74-0117-218

fatigue crack initiators (see Figure 90). During fatiguing a cyclic rate of 30 cycles per second was used. A summary of the fatigue parameters is shown in Table 56. As shown, more than one crack was produced in several specimens. Therefore, the same specimen number may appear in more than one location in Table 56. The fatigue cracks were grown to predetermined lengths by optically monitoring the crack growth. For those specimens which had more than one EDM slot, the crack in Position A was monitored. After the fatigue cracks were grown, the grip ends were cut off the specimens and the EDM slots were machined off. The surface finish after machining was better than 63 rms. A set of specimens were selected from the group such that ten cracks were available in each of the following crack length ranges:

less than .025 inch  
.025 to .050 inch  
.050 to .10 inch  
.10 to .25 inch  
.25 to .50 inch

#### b. Liquid Penetrant Testing of Tension-Tension Fatigue Specimens

##### (1) Laboratory Inspection

The test specimens described in Table 56 were all penetrant inspected under laboratory conditions using a high sensitivity fluorescent penetrant system. Tracer-Tech F-133 penetrant was used, along with Tracer-Tech D499C nonaqueous wet developer. This system is equivalent in sensitivity to a MIL-I-25135, Group VI system. A laboratory NDT specialist, with several years experience with penetrant inspection, performed the inspections using laboratory equipment. The technician did not know the location of the cracks in the specimens. The specimens were first alkaline cleaned, pickled to remove 0.0004 inch from each surface, and water rinsed. Next, the specimens were vapor degreased for 16 hours. Penetrant was applied by dipping. A penetrant dwell time of 10 minutes was used and the specimens were allowed to drain in air during that period of time. Excess penetrant was removed using a Tri-Con 400501 water spray nozzle; the wash water temperature was approximately 70°F and the wash water pressure was approximately 40 psi. The specimens were washed until clean under 200 microwatts per cm<sup>2</sup> of ultraviolet light. Next, the specimens were dried for 20 minutes in a circulating air oven at 170°F. After a bleed-out time of 5 minutes, the specimens were visually examined for crack indications. Prior to examining the specimens, the laboratory inspector allowed 5 minutes for his eyes to adapt to the darkness of the inspection booth. During the inspection, the ultraviolet light intensity at the specimen surface was greater than 6,000 microwatts per cm<sup>2</sup> as measured with the Ultraviolet Products BLAK RAY UV meter, Model J-221, and the visible light level in the inspection booth was less than 1/2 foot candle as measured with the Photo Research White-Spectra Illuminator Meter, Model FC-200A. The laboratory NDT specialist was instructed to mark linear indications. Rounded indications were not considered. The inspections were performed on 3 separate occasions. The first round consisted of inspecting approximately 60 pieces which included

**TABLE 56**  
**PARAMETERS FOR SURFACE CONNECTED CRACKS MADE BY TENSION - TENSION**  
**FATIGUE (STRESS RATIO = 0.1)**

Target Crack Length (in.)	Elox Size (in.)	Specimen Number	Load (lb)	Number of Cycles
Less Than 0.025	0.015 x 0.05 x 0.003	39	33,750	333,000 $\triangle_2$
		46	33,750	158,000 $\triangle_3$
		47	33,750/45,000	480,000/35,000 $\triangle_4$
		53	45,000 ↓	50,000 $\triangle_3$
		54		41,000 $\triangle_3$
		55		35,000 $\triangle_3$
		65		44,000 $\triangle_3$
		70		35,000 $\triangle_3$
		76		31,000 $\triangle_3$
		77		31,000 $\triangle_3$
		81		35,000 $\triangle_3$
0.025 to 0.050 $\triangle_1$	0.030 x 0.010 x 0.003	34		45,000
		13	45,000 ↓	12,000 $\triangle_3$
		14		18,000 $\triangle_3$
		57		28,000 $\triangle_3$
		57		38,000 $\triangle_3$
		64		24,000 $\triangle_3$
		66		37,000 $\triangle_3$
		72		55,000 $\triangle_3$
		73		35,000 $\triangle_3$
		75		34,000 $\triangle_3$
0.050 to 0.100	0.060 x 0.020 x 0.005	33	33,750 ↓	35,000
		35		44,000
		24		95,000
		38		84,000
		10		71,000
		49		55,000
		56		65,000
		14		32,000
		63		45,000
18	86,000			

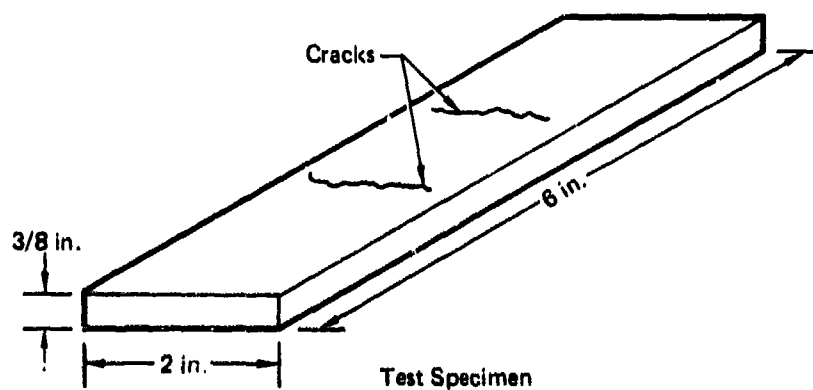
GP74-0117 219

**TABLE 56 (Continued)**  
**PARAMETERS FOR SURFACE CONNECTED CRACKS MADE BY TENSION - TENSION**  
**FATIGUE (STRESS RATIO = 0.1)**

Target Crack Length (in.)	Elox Size (in.)	Specimen Number	Load (lb)	Number of Cycles
0.100 to 0.25	0.060 x 0.020 x 0.005	3	33,750	104,000
		4		152,000
		9		138,000
		11		114,000
		13		81,000
		15		168,000
		19		148,000
		20		129,000
		25		146,000
		27		141,000
0.25 to 0.50	0.060 x 0.020 x 0.005	2	33,750	201,000
		8		132,000
		12		199,000
		21		135,000
		22		110,000
		23		122,000
		28		113,000
		29		115,000
		30		81,000
		31		123,000

- ① Target length was 0.050 in. Specimen surface was machined to reduce crack length to 0.025 to 0.050 in. range
- ② Salt was applied to the Elox after 320,000 cycles
- ③ Salt was applied initially
- ④ Fatigued for 480,000 cycles at 33,750 lb; then another 35,000 cycles at 45,000 lb

GP74-0117-220



25 uncracked "dummy" specimens. The second and third rounds were performed on approximately 12 pieces of which 4 were uncracked dummies. Each specimen was steel stamped with an identification number which was random and bore no relationship to the crack size in the specimen.

The results of the inspection are presented in Table 57.

The test data is binomial in that each flaw is either detected or not detected. Consequently, the data can be presented in terms of the probability of detection. The confidence of the test was established at 95 percent and it was desired to find the crack size range at which the probability of detection is greater than 90 percent. As can be seen from Table 57, for cracks .025 to .050 inch long, 30 out of 30 were detected. These results indicate that, 95 percent of the time, the probability of detecting cracks .025 to .050 inch long is at least 90 percent. If one considers the data for all cracks greater than .025 inch long, it can be said that, 95 percent of the time, at least 95 percent of the cracks will be detected.

During the entire laboratory testing, a total of two false indications were marked. A false indication, for the purposes of these tests, was considered an indication located where cracks were not intentionally grown. No measures were taken to determine the origin of the false indications (surface pits, scratches, etc.).

## (2) Production Inspection

The test specimens described above were penetrant inspected using production facilities and inspection personnel. The test specimens were initially vapor degreased for 16 hours after the laboratory inspection effort previously described had been completed. Penetrant inspection was performed using Tracer-Tech P-133A fluorescent penetrant and D499C nonaqueous wet developer. This system is equivalent in sensitivity to a MIL-I-25135, Group VI system. The specimens were immersed for 10 minutes in the penetrant and then excess penetrant was removed by water spray washing using a Tri-Con 400501 nozzle, a wash water pressure of 40 psi and a water temperature of 78°F. The specimens were washed until they appeared clean under 200 microwatts per cm<sup>2</sup> of ultraviolet light. After having been dried with forced air heated to 159°F, the specimens were sprayed with Tracer-Tech D499C nonaqueous wet developer. A Devilbiss Co. type MBC 715893 spray gun was used with a 1 quart type KR suction feed cup. After a 15 minute bleed-out time, the specimens were examined by a production penetrant inspector, designated Inspector A. All the production penetrant inspectors used for the program have been qualified to Level II of ASNT Recommended Practice No. SNT-TC-1A, Supplement D. The ultraviolet light intensity at the inspection surface was greater than 6,000 microwatts per cm<sup>2</sup> as measured with an Ultraviolet Products, Inc. BLAK-RAY UV meter, Model J-221, and the background white light level was less than 1 foot candle as measured with a Weston 703 meter. Prior to inspecting the specimens, the inspector allowed 5 minutes for dark adaptation. The specimens were inspected in batches of approximately 30 pieces of which approximately 10 pieces were uncracked "dummies". The inspectors and supervisors were not aware of the location of any of the

**TABLE 57  
RESULTS OF LABORATORY PENETRANT INSPECTION**

Crack Length Range (in.)	Crack Location	Specimen No.	Laboratory Penetrant Inspector					Total	Probability of Detection <sup>△</sup>
			A	B	C	D	E		
Less Than 0.025	C	35	1/1					6/10	
	A	53	1/1						
	A	54	1/1						
	A	55	0/1						
	A	63	1/1						
	C	63	1/1						
	B	65	0/1						
	A	70	0/1						
	A	76	1/1						
A	77	0/1							
0.025-0.050	A	33	3/3					30/30	At least 90%
	B	33	3/3						
	A	35	3/3						
	A	39	3/3						
	A	45	3/3						
	B	57	3/3						
	A	65	3/3						
	B	70	3/3						
	A	75	3/3						
A	81	3/3							
0.050-0.10	A	29	1/1					10/10	-
	A	34	1/1						
	A	38	1/1						
	B	39	1/1						
	A	47	1/1						
	A	49	1/1						
	B	56	1/1						
	B	57	1/1						
	A	59	1/1						
A	73	1/1							
0.10-0.25	A	3	1/1					10/10	-
	A	9	1/1						
	B	9	1/1						
	A	11	1/1						
	A	15	1/1						
	A	25	1/1						
	A	56	1/1						
	A	64	1/1						
	A	66	1/1						
A	72	1/1							
0.25-0.50	A	8	1/1					10/10	-
	A	12	1/1						
	A	21	1/1						
	A	22	1/1						
	A	23	1/1						
	A	28	1/1						
	C	29	1/1						
	A	30	1/1						
	B	30	1/1						
A	31	1/1							

<sup>△</sup> 95 percent confidence level

cracks from one inspection to another. During each inspection, the crack locations were marked with a china marker pencil and returned to an engineer for evaluation. After the data was recorded by the engineer, the specimens were vapor degreased for 16 hours to remove residual penetrant. A total of 6 production penetrant inspectors were used in the study. The results of the inspections of each specimen is shown in Table 58. The test results indicate that, 95 percent of the time (95 percent confidence level), the probability of detecting cracks .050 to .10 inch long is at least 88 percent. Obviously by choosing an NDT plan, the overall crack detection capability for a particular part can be increased. For example, the penetrant might be followed by surface wave and contact angle beam ultrasonic inspections. It also should be noted that these results are statistically relevant to the actual test including the penetrant materials, processing equipment, and inspectors actually used in these tests.

The number of false crack indications detected by Inspectors D, E, and F are shown in Table 59 as a function of the number of pieces examined, including uncracked dummies. For the purposes of these tests, a false indication was considered an indication in a location where a crack was not intentionally grown. No efforts were taken to determine the source of false indications (surface pits, scratches, etc.). As can be seen, quite a large number of false indication was recorded. There appears to be a difference between inspectors in this respect because Inspector D recorded approximately 1 false indication for every 2 pieces examined, Inspector E recorded approximately 1 false indication for every one piece examined, and Inspector F recorded approximately 1 false indication for every 3 pieces examined.

It was not possible to measure the number of false indications recorded by Inspectors A, B, and C since these 3 inspectors recorded all penetrant indications, be they rounded or linear indications.

A comparison of the detection capability of each inspector is shown in Table 60. For the larger crack sizes, there is little difference among the various inspectors. However, for the smaller cracks there appears to be a significant difference. For the cracks with lengths up to .050 inch, Inspector E detected only 2 of 34 cracks whereas Inspector D detected 47 of 81 and Inspector F detected 22 of 28.

Several of the cracks went undetected more often than others. The data for actual crack size (see Section 1-k) was examined to determine if the size of these cracks varied from the more "detectable" cracks within a crack size range but no correlation was found. For example, crack No. 65B was detected 7 of 12 times whereas crack No. 38A was detected 12 of 12 times. The actual size of each, however, was nearly the same (.080 x .020 inch versus .070 x .025 inch).

### (3) Overhaul Inspection

The test specimens described in Table 56 were penetrant inspected at a facility representative of a penetrant inspection at an overhaul facility. This facility is a converted overhaul inspection facility where

**TABLE 58  
RESULTS OF PRODUCTION PENETRANT INSPECTION**

Crack Length Range (in.)	Crack Location	Specimen No.	Production Penetrant Inspector						Total	Probability of Detection <sup>△</sup>
			A	B	C	D	E	F		
Less Than 0.025	C	35	0/1	—	—	4/7	0/1	2/3	37/95	At least 34%
	A	53	1/1	—	—	2/3	0/1	—		
	A	54	1/1	—	—	6/7	0/2	—		
	A	55	0/1	—	—	2/7	0/2	—		
	A	63	0/1	—	—	5/7	0/2	—		
	C	63	1/1	—	—	2/7	0/2	—		
	B	65	0/1	—	—	1/3	0/1	1/3		
	A	70	0/1	—	—	2/3	0/2	2/3		
	A	77	0/1	—	—	4/7	0/2	—		
0.025-0.050	A	33	0/1	—	—	3/3	1/2	3/3	45/68	At least 59%
	B	33	0/1	—	—	1/3	0/2	2/3		
	A	35	1/1	—	—	6/7	0/2	2/3		
	A	39	1/1	—	—	—	—	1/1		
	A	45	1/1	—	—	—	0/2	—		
	B	57	1/1	—	—	—	—	—		
	A	65	1/1	—	—	2/3	0/2	3/3		
	B	70	1/1	—	—	2/3	0/2	3/3		
	A	81	1/1	—	—	1/1	1/2	—		
0.050-0.10	A	29	5/5	2/3	1/1	2/3	—	—	110/119	At least 88%
	A	34	5/5	3/3	1/1	3/3	—	—		
	A	38	5/5	3/3	1/1	3/3	—	—		
	B	39	4/5	3/3	1/1	3/3	—	1/1		
	A	47	5/5	3/3	1/1	3/3	—	—		
	A	49	5/5	3/3	1/1	3/3	—	—		
	B	56	3/5	1/3	1/1	2/3	—	—		
	B	57	4/5	3/3	1/1	3/3	—	—		
	A	69	4/4	3/3	1/1	3/3	—	—		
0.10-0.25	A	3	3/3	3/3	1/1	5/5	—	—	101/103	At least 94%
	A	9	3/3	3/3	1/1	3/3	—	—		
	B	9	3/3	3/3	1/1	3/3	—	—		
	A	11	3/3	3/3	1/1	3/3	—	—		
	A	15	3/2	3/3	1/1	3/3	—	—		
	A	25	3/3	3/3	1/1	3/3	—	—		
	A	58	2/2	3/3	1/1	3/3	—	—		
	A	64	3/3	3/3	1/1	3/3	—	—		
	A	72	3/3	2/3	1/1	2/3	—	—		
0.25-0.50	A	8	1/1	—	—	6/6	2/2	—	87/89	At least 93%
	A	12	1/1	—	—	6/6	2/2	—		
	A	21	1/1	—	—	7/7	2/2	—		
	A	22	1/1	—	—	7/7	2/2	—		
	A	23	1/1	—	—	7/7	2/2	—		
	A	28	1/1	—	—	7/7	2/2	—		
	C	29	1/1	—	—	—	—	—		
	A	30	1/1	—	—	7/7	2/2	—		
	B	30	1/1	—	—	5/7	2/2	—		
A	31	1/1	—	—	7/7	2/2	—			

<sup>△</sup> 95 percent confidence level

**TABLE 59  
NUMBER OF FALSE INDICATIONS – PRODUCTION  
PENETRANT INSPECTION**

Inspector	Total Number of Pieces Inspected	Total Number of False Indications
D	249	138
E	56	69
F	22	7

QP74-0117-8

**TABLE 60  
COMPARISON OF PRODUCTIVE PENETRANT INSPECTORS**

Crack Length Range (in.)	Total Number of Cracks Detected					
	A	B	C	D	E	F
Less than 0.025	3 of 10	–	–	29 of 58	0 of 18	5 of 9
0.025 – 0.050	8 of 10	–	–	18 of 23	2 of 16	17 of 19
0.050 – 0.100	45 of 49	27 of 30	10 of 10	28 of 30	–	–
0.100 – 0.250	29 of 29	29 of 30	10 of 10	33 of 34	–	–
0.250 – 0.500	10 of 10	–	–	59 of 61	18 of 18	–

QP74-0117-9

production parts are now inspected. For this inspection, Sherwin HM-3 penetrant, a water washable fluorescent penetrant, was used along with Sherwin D-100 nonaqueous wet developer. This system is equivalent in sensitivity to a MIL-I-25135, Group VI system. Prior to penetrant inspection, the specimens were cleaned by trichlorethylene vapor degreasing for 16 hours. The specimens were immersed in the penetrant and allowed to drain in air for 10 minutes after which excess penetrant was spray washed off with a Magnaflux 3070 nozzle. The water pressure was 40 psi and the water temperature was 90°F. Next, the specimens were dried in an oven for 10 minutes at 140°F. The developer was applied and after a 5 minute development time the parts were inspected in a dark inspection booth. The two inspectors allowed for a dark adaptation time of 5 minutes and the ultraviolet light intensity at the test part surface was 4,300 microwatts/cm<sup>2</sup>. The white light intensity in the booth was less than 2 foot candles. During the inspection, the inspector marked all linear indications; rounded indications were not considered for this study.

The results of the overhaul inspection are presented in Table 61. These test results indicate that, 95 percent of the time, the probability of detecting cracks .025 to .050 inch long is at least 80 percent. For cracks .050 to .10 inch long, the probability increases to 94 percent.

The total number of false indications recorded by each inspector as a function of the number of pieces inspected, which includes uncracked dummies, is shown in Table 62. As in the case of the production penetrant inspections, there is a large variation in the number of false indications from one inspector to another.

From these results, it would seem that an overhaul penetrant inspection is more effective than a production penetrant inspection. Such generalizations can be misleading, however. For example, two different penetrant systems were used. Even though the two penetrant systems are both equivalent in sensitivity to a MIL-I-25135, Group VI penetrant there probably is a difference in sensitivity between the two since the MIL-I-25135 sensitivity test is qualitative in nature. Also, the work load in the inspection area at the time of testing can influence the results as this will affect the amount of time an inspector can spend examining a particular piece.

#### c. Ultrasonic Surface Wave Ultrasonic Inspection

##### (1) Production Inspection

The test specimens described in Table 56 were all ultrasonically inspected using contact surface wave techniques. The inspections were performed in a production ultrasonic inspection facility using production inspectors. A 1/4 x 1/4 inch, 2 1/4 MHz lead metaniobate search unit (S/N CF2764) was used along with a Sperry UM721 (S/N 59697) and a 10S dB pulser/receiver (S/N 3719-0). The couplant was 20W oil.

Several couplants were evaluated prior to selecting 20 W oil. Penetrant emulsifier, 20W oil, 90W oil, and 40-20W oil were all

**TABLE 61  
RESULTS OF OVERHAUL PENETRANT INSPECTION**

Crack Length Range (in.)	Crack Location	Specimen No.	Overhaul Penetrant Inspector					Total	Probability of Detection <sup>△</sup>
			A	B	C	D	E		
Less Than 0.025	C	35	1/2	—				8/15	—
	A	53	1/1	—					
	A	54	1/1	—					
	A	55	0/1	—					
	A	63	0/1	—					
	C	63	1/1	—					
	B	65	2/3	—					
	A	70	2/3	—					
	A	76	0/1	—					
A	77	0/1	—						
0.025-0.050	A	33	3/3	—				31/34	At least 80%
	B	33	1/3	—					
	A	35	2/3	—					
	A	39	3/3	2/2					
	A	45	3/3	—					
	B	57	3/3	2/2					
	A	65	3/3	—					
	B	70	3/3	—					
	A	75	3/3	—					
A	81	3/3	—						
0.050-0.10	A	29	3/3	2/2				50/50	At least 94%
	A	34	3/3	2/2					
	A	38	3/3	2/2					
	B	39	3/3	2/2					
	A	47	3/3	2/2					
	A	49	3/3	2/2					
	B	56	3/3	2/2					
	B	57	3/3	2/2					
	A	59	3/3	2/2					
A	73	3/3	2/2						
0.10-0.25	A	3	1/1	—				14/14	—
	A	9	1/1	—					
	B	9	1/1	—					
	A	11	1/1	—					
	A	15	1/1	—					
	A	25	1/1	—					
	A	56	3/3	2/2					
	A	64	1/1	—					
	A	66	1/1	—					
A	72	1/1	—						
0.25-0.50	A	8	1/1	—				14/14	—
	A	12	1/1	—					
	A	21	1/1	—					
	A	22	1/1	—					
	A	23	1/1	—					
	A	28	1/1	—					
	C	29	3/3	2/2					
	A	30	1/1	—					
	B	30	1/1	—					
A	31	1/1	—						

<sup>△</sup> 95 percent confidence level

**TABLE 62**  
**NUMBER OF FALSE INDICATIONS - OVERHAUL PENETRANT INSPECTION**

Inspector	Number of Pieces Examined	Number of False Indications
A	122	44
B	30	2

GP 74 0117 293

investigated. A 0.125 inch thick reference standard containing an EDM notch which is .010 inch wide, .029 inch deep and .057 inch long (equivalent in reflecting area to a 3/64 inch diameter flat bottom hole) was used in conjunction with the search unit. The couplant was applied to the surface and the signal from the EDM notch at a 4 inch metal travel was adjusted to 80 percent of saturation. The search unit was held steady and the variation in signal amplitude was observed. It was found that the 90 weight oil and the 20W oil provided a constant signal amplitude whereas the signal dropped 0.6 inch in a 15 second period with the 40-20W oil and 0.8 inch with the emulsifier.

The scanning gain was established with an Elox slot (.057 long x .029 deep x .010 wide) in a .125 inch thick piece of Ti-6Al-4V machined to 63 rms or better. The scanning gain was established by peaking the signal from the slot at the metal travel distance which yielded the maximum response and adjusting the signal to 80% of saturation. At that gain, a distance-amplitude correction (DAC) curve was constructed at metal travels of 1-1/2, 2, 2-1/2, 3, 3-1/2, and 4 inches by marking the amplitudes on the CRT and drawing a smooth curve through the points. Finally, the gain was increased by subtracting 19 dB of attenuation. This, then, is approximately equivalent to setting the response from an Elox slot .019 inch long x .0095 inch deep x .010 inch wide (equivalent in area to a 1/64 inch diameter flat bottom hole) to 80% of saturation on the CRT.

At that gain level, each 2 x 6 inch test specimen was hand scanned as shown in Figure 91. The search unit was swiveled from right to left, through an included angle of approximately 60 degrees during each scan. All indications with amplitudes equal to or greater than the DAC curve were marked on the surface of the specimen using a china marker pencil. No attempt was made to evaluate the size of the cracks. Although many of the cracks were detected, their amplitude did not exceed the DAC curve and were, therefore, not recorded as being detected.

Considerable difficulty was encountered in establishing a reproducible distance-amplitude curve during the surface wave testing. The amplitude of the response was very sensitive to variations in hand pressure on the search unit. In order to demonstrate this effect, 4 DAC

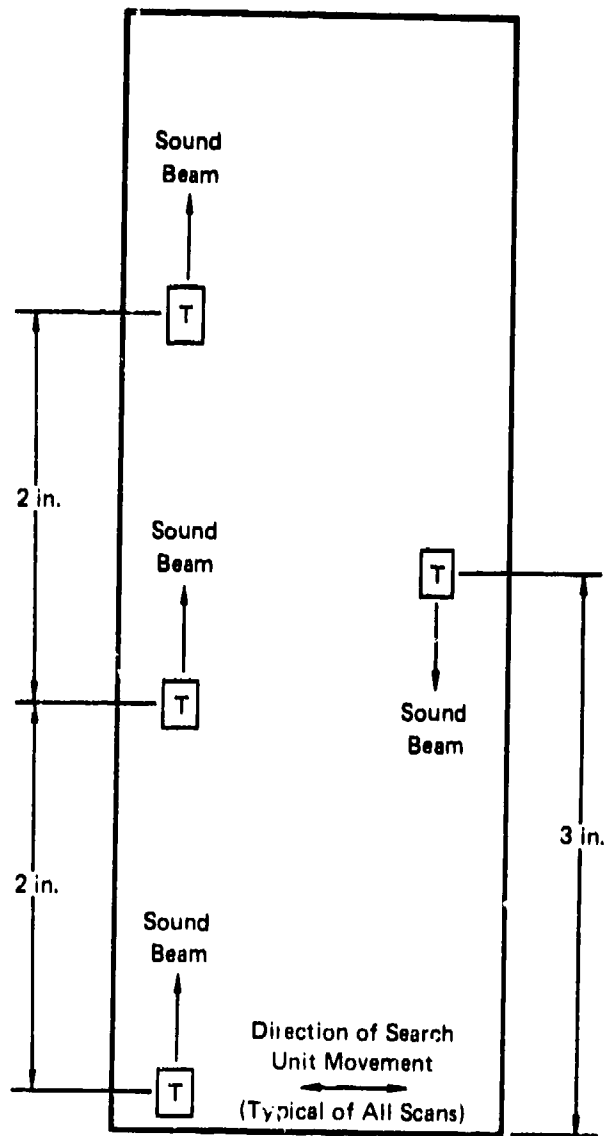


**FIGURE 91**  
**SURFACE WAVE SCANNING**

OP74-0117-13

curves were constructed (see Figure 92). Two of the curves are for the same technician (designated B). As can be seen, the variation between technicians (designated A, B, and C) can become significant at the larger metal travels. In addition, there is a significant variation between the two curves for the same technician (designated B).

Obviously, with such variations it would be difficult to accurately determine the size of a discontinuity in a test part. This was of no consequence for the surface wave testing performed on the cracked specimens since the objective was only to detect the cracks and not to evaluate their size.

The results of the production surface wave testing are shown in Table 63. A notation such as 3/3 indicates that 3 cracks were detected

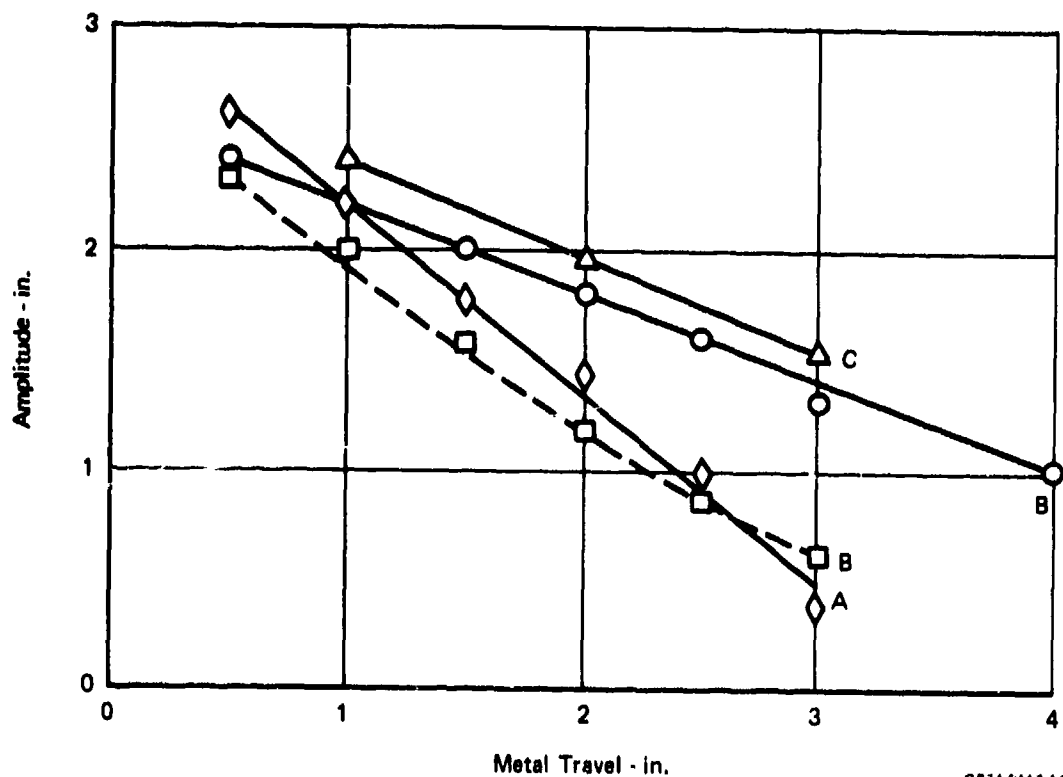


**FIGURE 92**  
**DISTANCE AMPLITUDE CORRECTION (DAC) CURVES FOR THREE REPRESENTATIVE TECHNICIANS**

**TABLE 63**  
**RESULTS OF PRODUCTION SURFACE WAVE ULTRASONIC INSPECTIONS**

Crack Length Range (in.)	Crack Location	Specimen No.	Production Surface Wave Ultrasonics Inspector					Total	Probability of Detection $\Delta$
			A	B	C	D	E		
Less Than 0.025	C	35	0/1	0/1	--	0/1	0/7	3 of 66	At least 1%
	A	53	--	--	--	0/1 (2)	0/2 (3)		
	A	54	--	--	--	0/1	0/2		
	A	55	--	--	--	0/1	1/6 (2)		
	A	63	--	--	--	0/1	0/5		
	C	63	--	--	--	0/1	0/5		
	B	65	1/1 (3)	0/1	--	0/1	0/7 (1)		
	A	70	1/1	--	--	0/1	0/7		
	A	76	--	--	--	0/1 (2)	0/5 (3)		
A	77	--	--	--	0/1	0/5 (1)			
0.025-0.050	A	33	--	--	--	1/1	1/2 (2)	15 of 62	At least 18%
	B	33	--	--	--	0/1 (2)	0/2		
	A	36	1/1	0/1	--	0/1	0/5		
	A	39	1/1	2/2	1/1	--	2/2		
	A	46	--	--	--	--	0/5 (2)		
	B	57	3/3 (7)	2/3	--	--	0/5		
	A	65	0/1	0/1	--	0/1	0/7		
	B	70	1/1	0/1	--	0/1 (3)	0/5		
A	75	--	--	--	--	0/5			
A	81	--	--	--	0/1	0/2 (4)			
0.50-0.10	A	29	3/3 (4)	2/3 (4)	--	--	1/2	40 of 77	At least 47%
	A	34	2/2 (7)	3/3	--	--	1/3		
	A	38	3/3 (10)	2/3 (4)	0/1	--	--		
	B	39	0/1	2/2	1/1	--	0/2		
	A	47	0/2	0/3	0/1	--	--		
	A	49	3/3 (4)	0/3	--	--	0/2		
	B	56	3/3 (5)	0/3 (3)	--	--	0/1		
	B	57	1/3 (1)	0/3 (1)	--	--	2/5		
	A	59	3/3	2/3	--	--	4/4 (1)		
A	73	2/2 (3)	0/3	0/1	--	--			
0.10-0.25	A	3	1/2 (6)	1/3	--	--	0/2	55 of 68	At least 74%
	A	9	2/2 (5)	2/2	--	--	1/1		
	B	9	1/2	2/2	--	--	1/1		
	A	11	3/3 (14)	2/2	--	--	1/1		
	A	15	2/2 (3)	2/2	1/1	--	--		
	A	25	2/2 (5)	2/2	0/1	--	0/4		
	A	56	3/3 (4)	3/3	--	--	1/1		
	A	64	3/3 (12)	2/2	1/1 (2)	--	4/4 (1)		
	A	66	1/1	2/2	1/1 (2)	--	4/5		
A	72	1/1	2/2	1/1	--	0/1			
0.25-0.50	A	8	--	--	--	--	--	54 of 59	At least 84%
	A	12	--	--	--	--	4/4 (5)		
	A	21	--	--	--	0/1	3/5 (1)		
	A	22	1/1	1/1 (1)	--	1/1 (1)	5/5 (2)		
	A	23	--	--	--	0/1	6/6 (3)		
	A	28	1/1 (4)	1/1	--	1/1	5/5		
	C	29	3/3	3/3	--	--	3/3		
	A	30	1/1	1/1	--	1/1	1/1		
	B	30	1/1 (2)	1/1	--	1/1	1/1		
A	31	1/1 (3)	1/1 (2)	--	0/1 (2)	6/6 (4)			

Note: Number of false indications are noted in circles

$\Delta$  95 percent confidence level

out of 3 crack present. A comparison of these results with the production penetrant results would seem to indicate that the penetrant method is more reliable for detecting surface cracks (see Table 64).

From these results; it would appear that the surface wave method is not very effective. It should be pointed out, however, that as discussed below, the surface wave has an effective depth of penetration which allows subsurface cracks to be detected. Consequently, an effective NDT plan for machined parts might include a penetrant inspection to detect surface cracks and a surface wave inspection to detect both surface and subsurface cracks.

A comparison of the capability of the various inspectors is shown in Table 65.

**TABLE 64**  
**COMPARISON OF PENETRANT AND SURFACE WAVE TEST RESULTS**

Crack Length (in.)	Number Cracks Detected		Probability of Detection	
	Penetrant	Surface Wave	Penetrant	Surface Wave 
Less Than 0.025	37 of 95	3 of 66	At least 34%	At least 1%
0.025-0.050	45 of 68	15 of 62	At least 59%	At least 18%
0.050-0.10	110 of 119	40 of 77	At least 88%	At least 47%
0.10-0.25	101 of 103	55 of 58	At least 94%	At least 74%
0.25-0.50	87 of 89	54 of 59	At least 93%	At least 84%

 95 percent confidence level.

OP 74-0117 231

As in the case of the production penetrant tests, there appears to be a significant variation in inspector capability. For the surface wave tests, however, this variation extends to the larger crack sizes. For example, for cracks .10 to .25 inch long, Operator A detected 19 of 21 cracks whereas Operator E detected only 12 of 20. If the results from Operator E were not considered, the overall detection capability for cracks .10 to .25 inch long would increase to 43 of 48 from 55 of 68.

A number of the larger cracks were detected from both sides of the specimens during the surface wave inspection as shown in Table 66. An estimate of the depth of penetration of the surface wave can be determined by considering the actual depth of the cracks. Several of these cracks were intentionally fractured to measure the actual depth of the crack. An estimate of the depth of penetration of the surface wave in the 3/8 inch thick specimens appears below.

Specimen No.	Crack Length (Inches)	Crack Depth (Inches)	Estimated Depth of Penetration of Surface Wave (Inches)
38	.070	.025	.350
56(B)	.080	.020	.355
59	.090	.030	.345
11	.070	.070	.305
15	.200	.070	.305
25	.15	.020	.355
56(A)	.125	.035	.340
30(A)	.48	.18	.195

**TABLE 85  
SUMMARY OF CRACK DETECTION CAPABILITY  
OF SURFACE WAVE ULTRASONICS BY OPERATOR**

Crack Length (in.)	Operator				
	A	B	C	D	E
Less than 0.025	2/3	0/2	-	0/10	1/51
0.025 - 0.050	6/7	4/8	1/1	1/6	3/40
0.050 - 0.100	20/25	11/29	1/4	-	8/19
0.100 - 0.250	19/21	20/22	4/5	-	12/20
0.250 - 0.500	8/8	8/8	-	4/7	34/36

GP74-0117-18

**TABLE 68**  
**CRACKS DETECTED FROM BOTH SIDES OF SPECIMEN BY SURFACE**  
**WAVE ULTRASONICS (SUMMATION OF 5 OPERATORS)**

Crack Length (in.)	Specimen No.	Number of Times Crack Detected from Both Sides
0.050 - 0.10	29	1 of 3
	38	1 of 3
	49	1 of 3
	56	1 of 3
	59	1 of 3
0.100 - 0.25	9(A)	1 of 2
	9(B)	1 of 2
	11	2 of 3
	15	1 of 2
	25	1 of 2
0.250 - 0.50	56	1 of 3
	12	1 of 1
	22	2 of 2
	23	3 of 6
	29	4 of 7
	29	8 of 10
	30(A)	4 of 5
	30(B)	2 of 2
31	2 of 7	

GP74-0117-1W

From these results, it can be concluded that the ultrasonic surface wave from a 1/4 x 1/4 inch, 2 1/4 MHz lead metaniobate search unit penetrates to a depth of at least .355 inch in Ti-6Al-4V. This information may prove useful in deciding if it is necessary to inspect a part from 2 sides or one side.

A tabulation of the false indications recorded by each inspector during the surface wave inspections as a function of the number of pieces examined, including uncracked dummies, is shown in Table 67.

**TABLE 67**  
**SUMMARY OF FALSE INDICATIONS – ULTRASONIC SURFACE WAVE**

Inspector	Number of Specimens Examined	Number of False Indications
A	62	116
B	70	22
C	15	4
D	27	13
E	190	41

GP74-0117-20

Again, a false indication was defined as an indication in a location where a crack was not intentionally grown. As in the case of the penetrant inspections, the number of false indications per pieces inspected varied considerably from one inspector to another. The overall ratio of false indications per piece inspected was 0.54 for surface wave and 0.65 for penetrant. It should be mentioned that several of the false indications that were recorded during the surface wave inspections were surface anomalies such as scratches or nicks.

(2) Laboratory Inspection

For comparison purposes, a laboratory test program was conducted on the specimens. The search unit, equipment, and procedure used were the same as for the production surface wave inspection. However, for the laboratory tests, the amplitude of all responses was noted, even if they were less than the corresponding distance-amplitude response. The results are shown in Table 68. As might be expected, the laboratory results are somewhat better than the production results, even though neither the production nor the laboratory inspectors knew the locations of the cracks and the inspection time was approximately the same for both. Several of the cracks detected in the laboratory, however, exhibited responses of approximately 50 percent of the DAC curve. These responses would not have been recorded in the production inspection since only

**TABLE 68  
RESULTS OF LABORATORY SURFACE WAVE INSPECTION**

Crack Length (in.)	Specimen Number	Number of Cracks Detected	Total
0.025 – 0.050	57	2/2	2/2
0.050 – 0.10	29	0/1	10/17
	34	1/2	
	38	2/2 	
	47	1/2 	
	49	2/2	
	56	0/2	
	57	1/2	
	59	2/2 	
73	1/2 		
0.10 – 0.25	3	1/1	11/11
	9	1/1	
	9	1/1	
	11	1/1	
	15	1/1	
	25	1/1	
	56	2/2	
	64	1/1	
66	1/1		
72	1/1		
0.25 – 0.50	29	2/2	2/2

 One of the cracks detected had a response amplitude of 50 percent of the DAC curve amplitude.

QP74-0117-21

responses equal to or greater than the DAC curve were to be considered rejectable. For cracks .050 to .10 inch long, the proportion of cracks detected is approximately the same for the laboratory and production inspections, if the 50 percent amplitude cracks were considered to be undetected in the laboratory inspection. For the larger crack sizes (.10 to .25 inch long), the laboratory results are clearly superior to the production results.

It should be pointed out that while calibrating at a level equivalent to a  $1/64$  inch diameter flat bottom hole the gain level on the Sperry UM 721 was within 10 dB of the maximum gain. Hence, it does not appear possible to increase the detection capability simply by increasing the scanning gain. Also, increasing the scanning gain would increase the noise level which was approximately 15 percent of saturation during the inspections.

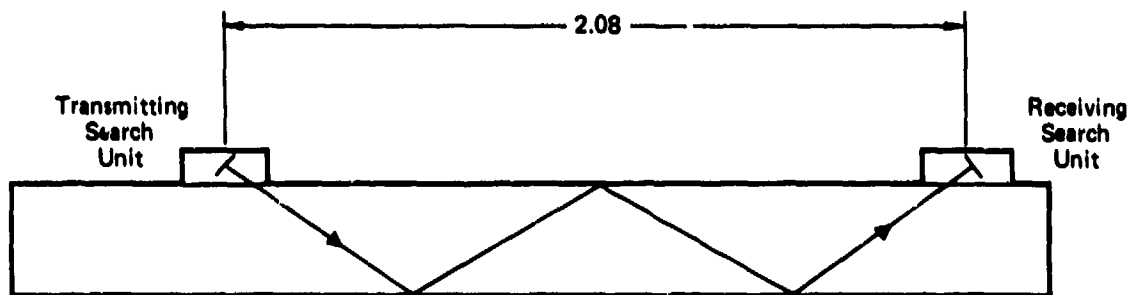
#### d. Ultrasonic Contact Angle Beam Testing

##### (1) Production Inspection

Several of the test specimens were inspected using the contact angle beam method. A  $1/4 \times 1/4$  inch, 5MHz, 60 degree (in steel) shear wave search unit was used in conjunction with a Sperry UM-721 ultrasonic instrument and a 10S dB pulser/receiver. The couplant was 20W oil. The reference standard (No. 95) was a machined piece of Ti-6Al-4V, .312 inch thick, with end-drilled flat bottom holes as artificial reflectors (see Figure 49).

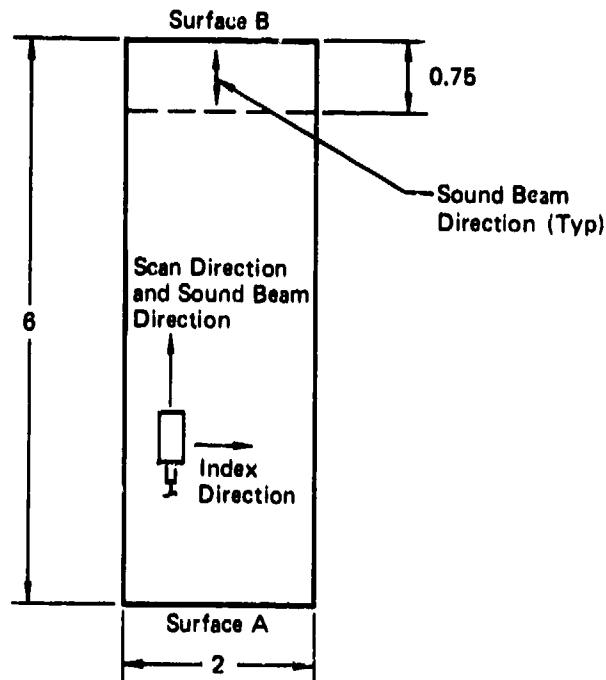
The difference in sound transmission characteristics between the reference standard and the test specimens was measured using 2 search units as shown in Figure 93. The transmitter was the search unit to be used for the actual inspections and the receiver was a  $1/4 \times 1/4$  inch, 5MHz, 60 degree lead metaniobate search unit (S/N BH 0731). With the instrument in the through-transmission mode, the search units were aligned to maximize the signal through the reference standard. The signal amplitude was adjusted to 80 percent of saturation and the dB setting was recorded. Next, the search units were moved to the test specimens, and, using the same distance between search units, the operation was repeated. It was found that the average difference between the reference standard and the test specimens was 2 dB.

A distance-amplitude correction (DAC) curve was constructed with the  $3/64$  inch diameter end drilled flat bottom hole in the reference standard. With the search unit at position 1 (see Figure 94), the hole response was adjusted to 80 percent of saturation and marked on the cathode ray tube screen. Next, the search unit was moved to Positions 2 and 3 without changing the gain control and the signal amplitude was marked on the cathode ray tube screen. A smooth curve was drawn through the points on the CRT.



GP74-0117-2B2

**FIGURE 93**  
**TEST SETUP USED TO MEASURE SOUND TRANSMISSION DIFFERENCE**



GP74-0117-104

**FIGURE 95**  
**SCAN PLAN FOR CONTACT ANGLE BEAM TESTING**

**TABLE 69**  
**RESULTS OF PRODUCTION CONTACT ANGLE BEAM INSPECTION**

Crack Length Range (in.)	Specimen No.	Contact Angle Beam Ultrasonic Inspector		Total	Probability of Detection 
		A	B		
0.025-0.050	57	9/9	1/4	10/13	—
0.050-0.100	57 29 34 49	8/8 6/7 7/7 6/3	2/4 3/4 2/5 2/5	36/46	At least 69%
0.10-0.25	72 9 9 64	4/5 5/5 5/5 5/5	4/5 3/5 5/5 5/5	36/40	At least 80%
0.25-0.50	29	7/7	4/4	11/11	—

 95 percent confidence level

GP74 0117 281

3/64 in. Diameter  
Flat Bottom Hole

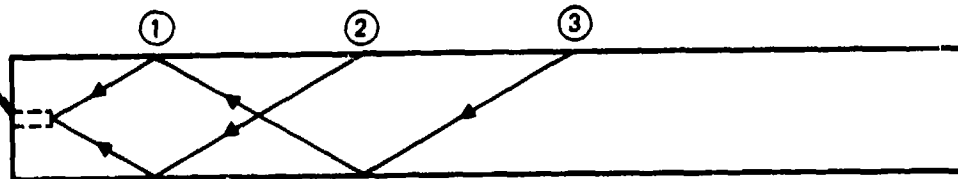


FIGURE 94

GP74-0117-106

PROCEDURE FOR DISTANCE AMPLITUDE CORRECTION CURVE

At this point 2 dB was removed to adjust for differences in sound transmission between the test pieces and the reference standards and another 6 dB was removed to increase the scanning gain.

Each test piece was hand scanned as shown in Figure 95. During each scan the search unit was swiveled within an included angle of 60 degrees to ensure 100 percent inspection coverage. Within 0.75 inch of surfaces A and B, the pieces were scanned in 2 directions at 180 degrees to each other.

Each discontinuity whose amplitude equalled or exceeded the DAC curve, after the 6 dB had been added back in, was marked on the specimen surface. The results are shown in Table 69. In Table 69, an entry such as 3/5 indicates that 3 cracks out of 5 were detected. It appears from the data that the detection capability of Inspector A was greater than Inspector B even though both people have qualified to the same procedure (SNT-TC-1A, Supplement C, Level II).

As shown in Table 70, on several occasions a crack was detected from both sides of the specimen. However, it is important to note that often a crack was not detected from both which indicates that actual parts to be inspected should be inspected from both sides to increase the detection probability.

**TABLE 70**  
**CRACKS DETECTED FROM BOTH SIDES OF SPECIMEN BY**  
**CONTACT ANGLE BEAM ULTRASONICS**  
 Summation of 2 Inspectors

Crack Length (in.)	Specimen No.	Number of Times Detected from Both Sides
0.025-0.050	57 (A)	6 of 13
0.050-0.10	57 (B)	6 of 12
	29 (A)	6 of 11
	34 (A)	8 of 13
	49 (A)	5 of 12
0.10-0.25	72 (A)	5 of 11
	9 (A)	8 of 11
	9 (B)	10 of 11
	64 (A)	9 of 12
0.25-0.50	29 (C)	11 of 11

QP 74-0117-232

e. Overall Production NDT Capability

The surface crack detection capability of individual NDT methods (penetrant, surface wave ultrasonics, and contact angle beam ultrasonics) has been discussed in the previous paragraphs. In a production NDT operation, an individual production part might be inspected several times with various NDT methods to ensure the detection of harmful discontinuities. In these cases, the detection capability for the part is related to the combined detection capabilities of the individual NDT methods. An example of such an NDT plan would be to penetrant inspect the entire surface of a finished part to detect surface cracks. Next, the detected cracks would be removed by rework operations. Following the penetrant inspection and rework operations, selected areas on the part which will experience high stress levels and where a flaw of critical size has a reasonable probability of occurring might be further inspected using surface wave ultrasonics to detect remaining surface cracks and cracks lying slightly below the surface. Finally, these high stress thicker areas might be inspected with contact angle beam ultrasonics to again detect surface cracks and cracks lying to a greater depth below the surface.

If such an NDT plan were used, the overall NDT capability for the detection of surface cracks could be determined from the capabilities of the individual methods (penetrant, surface wave ultrasonics, and contact angle beam ultrasonics). The capability data discussed previously was analyzed to arrive at an overall capability figure for an NDT plan which consists of a penetrant inspection followed by a surface wave and, in some cases, contact angle beam ultrasonic inspection. For example, the detection probability of a production inspection was found to be 88 percent at a 95 percent confidence level for cracks with lengths of 0.050 to 0.10 inch. Then, in a given sample, 12 percent of the existing cracks may go undetected. If, then, the penetrant inspection was followed by an ultrasonic surface wave inspection, at least 47 percent of the cracks missed by the penetrant inspection (or 6 percent of the total cracks present originally) would be detected by the ultrasonic surface wave inspection. Based on these calculations, the detection probability for the combined inspections would be 88 percent plus 6 percent or 94 percent at a 95 percent confidence level. The overall NDT capability for surface cracks is shown below as a function of crack length.

Crack Length (in.)	Probability of Detection 	
	Penetrant Followed by Surface Wave	Penetrant Followed by Surface Wave Followed by Angle Beam
Less Than 0.025	At Least 35%	
0.025-0.050	At Least 66%	
0.050-0.10	At Least 94%	At Least 98%
0.10-0.25	At Least 98%	At Least 99%
0.25-0.50	At Least 99%	

 95% Confidence Level.  
 Data was Not Developed for Contact Angle Beam Inspection at This Crack Size.

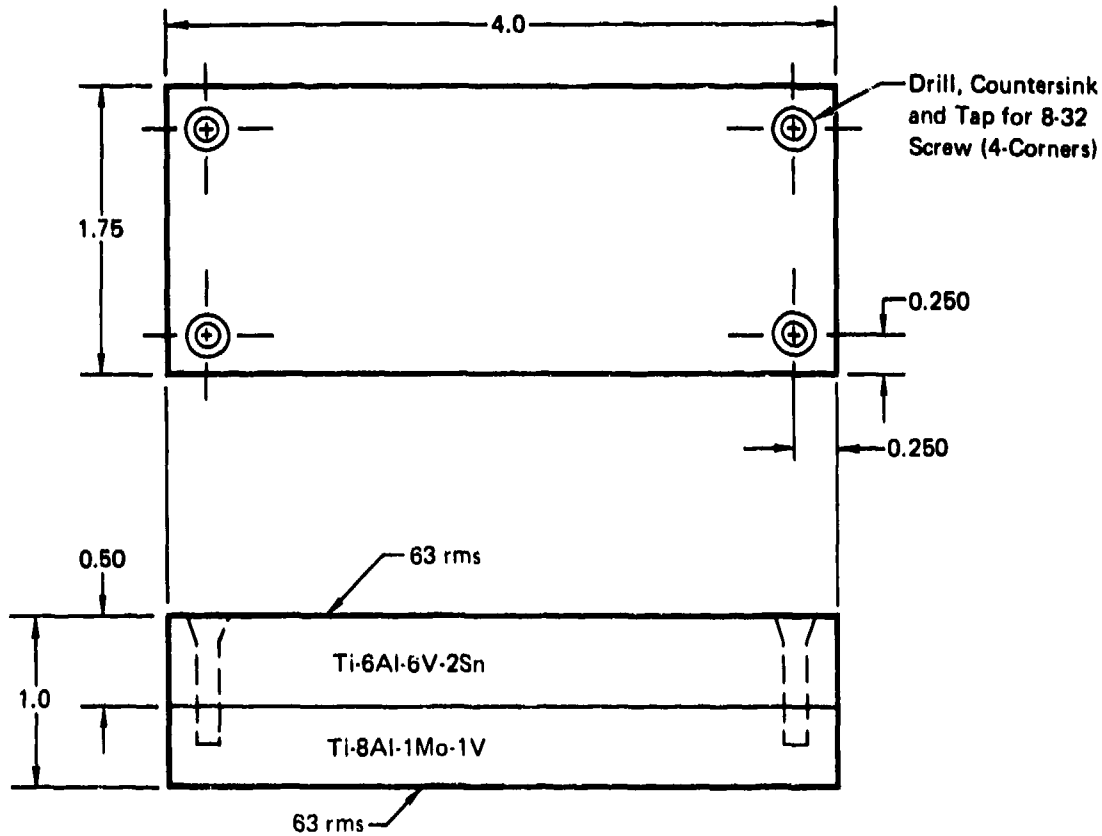
This data indicates that at least 98 percent of all surface cracks with lengths of .050 to .10 inches would be detected with the specified NDT plan.

All the NDT capability data discussed to this point has been on the basis of a 95 percent confidence level. Obviously, the specified detection probability changes as the confidence level changes.

The NDT capability data presented in this report should be used as guidelines as to what can be reasonably expected in production inspections. The actual capability values are somewhat unique to the specific inspection parameters used. The capability values might change significantly when other inspection personnel, penetrant systems, calibration techniques, calibration standards, etc. are used.

#### f. Laboratory Eddy Current Testing

A selected number of the surface cracked specimens were chosen for several eddy current tests. In all, four separate laboratory eddy current tests were performed. The first test, designated Test A, was performed using a Nortec NDT-3 eddy current instrument with an absolute probe at 500 KHz. The absolute probe was an Ideal Specialty P/N 6100 - 1/4 SP probe with a .050 inch diameter ferrite core and 150 turns of No. 40 wire. Liftoff compensation was .003 inch and was accomplished by adjusting the "X" and "R" controls to obtain the same meter indication with and without a .003 inch paper shim between the probe and the test surface. The operating point was chosen using the sensitivity standard shown in Figure 96. The conductivity of the Ti-6Al-6V-2Sn is 1.10% IACS



Notes:

1. All dimensions are in inches.
2. Tolerances are  $\pm 0.010$  in.
3. Surface finish is 125 rms unless otherwise noted.
4. Material is in the annealed condition.
5. Install 8-32 screws in four corners when complete.

FIGURE 96  
TITANIUM EDDY CURRENT SENSITIVITY STANDARD

GP74-0117-223

and the conductivity of the Ti-8Al-1Mo-1V is 0.87% IACS. A previous program indicated that, for titanium, the operating point along the lift-off compensation locus should be chosen relatively far away from the material point in the complex impedance plane to give the maximum response (478 microamps per 1% IACS) to the conductivity difference between the two halves of the sensitivity standard. Crack indications were read as meter deflections and the chosen scan index of 1/16 inch was maintained without a fixture.

A second test, Test B, was performed in the same manner except that crack indications were recorded on a Mosely 680 strip chart recorder and a fixture was used to maintain the 1/16 inch scan index.

Test C was performed using a Magnaflux ED 520 eddy current instrument with an absolute probe. This particular instrument uses continuously variable frequencies (from 55 to 200 KHz) which are fixed by the probe coil and the liftoff compensation chosen. No liftoff compensation was used. The absolute probe was the same as before. Again a strip chart recorder was used as an aid for crack detection and a scan index fixture was used for the 1/16 inch scan index. The sensitivities of the instruments were set to yield a 110 microamp difference between the Ti-6Al-6V-2Sn and Ti-8Al-1Mo-1V halves of the sensitivity standard in tests A, B, and C.

Testing was performed in cooperation with and through the courtesy of NDT Instruments, Inc. These results are designated Test D.

An NDT Instruments Vector III was used along with a 3 MHz probe having a 1/16 inch diameter ferrite sensor. This probe possessed an estimated .015 inch deep x .062 inch wide sensing zone in the titanium. The instrument was adjusted for approximately .002 inch liftoff compensation. The receiver sensitivity control was adjusted to 25% of the maximum. Crack indications were measured as meter deflections. No calibration, such as previously described, was performed. Prior to actual inspection a preliminary test was performed with the Vector III to compare the responses at 500 KHz and 3 MHz. A Ti-6Al-4V reference standard with narrow 3 inch long V-notches having depths of .005 inch, .010 inch, and .015 inch was used. The results indicated that testing at 3 MHz produced about 5 times the meter deflection obtained at 500 KHz (see below). The data indicates that the sensitivity is increased at higher frequencies. The crack vector has a greater separation angle from the lift-off vector at 3 MHz.

Notch Depth (Inches)	Units of Meter Deflection	
	500 KHz	3 MHz
.015	40	100+
.010	12	70
.005	7	35

The results of the four tests are shown in Table 71. A summary appears in Table 72. As can be seen, the detection capability was enhanced by using a scan index and a strip chart recorder. The testing performed at 3 MHz seemed to be more effective than the lower frequency tests, although the small data base does not allow a definite conclusion. Examples are shown below.

**TABLE 71  
EDDY CURRENT TEST RESULTS**

Target Crack Length (in.)	Specimen No.	Actual Crack Length x Depth (in.) 	Test A	Test C	Test B	Test D	
						No. Cracks Detected	Meter Deflection
Less Than 0.025	53	-	0/1	0/1	0/1	-	-
	54	-	0/1	0/1	0/1	-	-
	65	-	0/1	0/1	0/1	-	-
	70(A)	-	0/1	0/1	0/1	-	-
	76	-	0/1	0/1	0/1	-	-
	77	-	0/1	0/1	0/1	-	-
0.025-0.050	39	0.040 x 0.015	1/1	1/1	0/1	1/1	25
	45	0.010 x 0.005	0/1	1/1	1/1	1/1 	41
	65	-	0/1	0/1	0/1	-	-
	70(B)	-	0/1	0/1	0/1	-	-
	75	0.060 x 0.015	0/1	0/1	0/1	0/1 	0
	81	-	0/1	0/1	0/1	0/1	0
0.050-0.10	38	0.070 x 0.025	0/1	1/1	0/1	1/1 	74
	39	0.060 x 0.040	0/1	0/1	0/1	1/1	> 80
	47	-	0/1	1/1	1/1	1/1	> 80
	49	-	0/1	0/1	0/1	-	-
	59	0.090 x 0.030	0/1	1/1	1/1	1/1 	45
	73	-	0/1	0/1	0/1	-	-
0.10-0.25	3	0.119 x 0.019	0/1	0/1	0/1	1/1	15
	11	0.20 x 0.70	1/1	1/1	1/1	1/1 	> 80
	15	0.20 x 0.70	1/1	1/1	1/1	1/1 	> 80
	64	-	1/1	1/1	1/1	-	-
	66	0.105 x 0.030	1/1	1/1	1/1	1/1	36
	72	-	0/1	1/1	1/1	-	-
0.25-0.50	8	0.43 x 0.16	1/1	1/1	1/1	-	-
	12	-	1/1	1/1	1/1	-	-
	21	0.41 x 0.17	1/1	1/1	1/1	-	-
	22	-	1/1	1/1	1/1	-	-
	23	-	1/1	1/1	1/1	-	-
	31	-	1/1	1/1	1/1	-	-

 The location of the crack was known in order to setup the test.  
 Actual crack dimensions were determined by fracturing the specimen and examining the fracture surface.

QP74-0117-98

**TABLE 72  
SUMMARY OF CRACK DETECTION CAPABILITY-  
LABORATORY EDDY CURRENT**

Crack Length (in.)	Test A	Test B	Test C	Test D
Less Than 0.025	0 of 6	0 of 6	0 of 6	-
0.025-0.050	1 of 6	1 of 6	2 of 6	2 of 4
0.050-0.10	0 of 6	2 of 6	3 of 6	4 of 4
0.10-0.25	4 of 6	5 of 6	5 of 6	4 of 4
0.25-0.50	6 of 6	6 of 6	6 of 6	-

QP74-0117 97

<u>Crack Length (Inches)</u>	<u>Specimen No.</u>	<u>Test A</u>	<u>Test B</u>	<u>Test C</u>	<u>Test D</u>
.025 - .050	39	1/1	0/1	1/1	1/1
.050 - .10	38	0/1	0/1	1/1	1/1
.050 - .10	39	0/1	0/1	0/1	1/1
.10 - .25	3	0/1	0/1	0/1	1/1

Following the eddy current testing, several of the cracks were intentionally fractured and the site of the crack was measured from the fracture surface. The actual size of those cracks are shown in Table 71. An examination of crack depth or crack area did not reveal any correlation with meter deflection. The smallest crack detected during the eddy current inspection had an actual length of .010 inch and a depth of .005 inch.

g. Radiographic Inspection of Surface Cracks

Twelve specimens, 3/8 inch thick, containing fatigue cracks were radiographically inspected. These specimens had been fabricated in the manner previously described in Paragraph 1-a of the NDT Capability section of this report. The inspection was performed in a production radiographic inspection facility using production radiographic inspection personnel who had been qualified to SNT-TC-1A, Supplement A, Level II. The cracks examined had lengths which varied from 0.10 to 1.50 inches. The two 1.50 inch long cracks had extended through the thickness of the panel. The radiographic parameters used were as follows.

Kilovoltage	75 KVP (with a 3 mm. focal spot) Faxitron
Focal Spot - To - film Distance	24 Inches
Film	Gaveart D4 (ASTM Class 1)
Screens	No front screen 0.010 inch thick lead back screen
Cassette	Cardboard

The exposure was adjusted to obtain an overall film density of 1.7 to 2.3 H and D density units. A 2 percent thickness titanium MEE-3FD-453 penetrometer was used as an image quality indicator and the IT hole was visible on all the radiographs resulting in an equivalent sensitivity of 1.4 percent.

Three independent production radiographic interpreters were used to interpret the films. Only two of the cracks were detected; these were the 1.50 long cracks and all 3 interpreters detected them. No other cracks were detected even though there were some which had extended through the full section thickness. Subsequently, the films were examined again,

only this time, the crack locations were known by the interpreter. Again, only the two 1.50 inch long cracks were detected. These results emphasize the difficulty in detection cracks with radiographic techniques.

#### h. Bending Fatigue Specimen Fabrication

A second set of surface connected crack specimens were fabricated for use in airframe, engine, and AFML inspections. The specimens were made using 1 X 2 X 5 inch pieces of Ti-6Al-4V with an EDM slot in each as a crack initiator (see Figure 97). The specimens were fatigued in 3 point bending using the parameters shown in Table 73. The crack lengths were

**TABLE 73**  
**PARAMETERS FOR SURFACE CONNECTED CRACKS**  
**MADE BY BENDING FATIGUE **

Specimen No.	EDM Length x Depth (in.)	No. Cycles	Final Crack Length (in.)
R5	0.020 x 0.008	23,090	0.035
B2	0.030 x 0.010	30,700	0.055
B13	0.080 x 0.025	10,000	0.129
B8	0.10 x 0.030	12,790	0.238
B10	0.10 x 0.030	17,500	0.363
B15	0.10 x 0.030	54,990	0.496

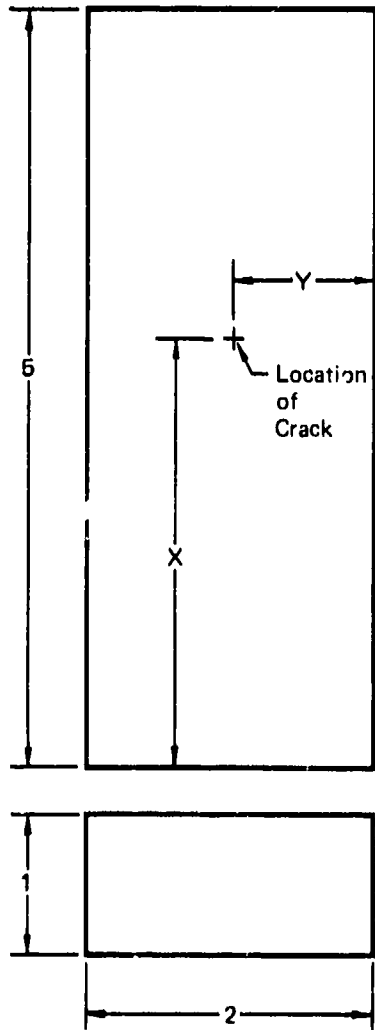
 Specimens were fatigued in 3 point bending with a load of 30,000 lb maximum (67.5 ksi stress) and a frequency of 5 Hz.

GP74 0117 102

optically monitored during the fatiguing process. After the cracks were grown, the EDM slot was removed by a grinding operation. The grinding operation was intentionally light in order to avoid metal flow at the surface.

#### i. Liquid Penetrant Testing of Bending Fatigue Specimens

The set of 6 cracked specimens and three uncracked "dummy" specimens were penetrant inspected in an airframe and jet engine inspection environment as well as at the AFML for comparative purposes. Initially, the surface fatigue specimens were penetrant inspected in the laboratory at the jet engine manufacturer's installation. Three post-emulsifiable Magnaflux penetrants were used for comparative purposes (ZL-2A, ZL-22A, and ZL-30A). In addition, both Magnaflux ZP-4 dry powder developer and Tracer-Tech D499C nonaqueous wet developer were used. All the penetrant systems used were MIL-I-25135, Group VI sensitivity systems. The 9 test specimens (6 cracked



Specimen No.	Crack Length (in.)	X	Y
B5	0.035	3	3/4
B2	0.055	2-1/4	1-1/2
B13	0.129	2-3/4	1-1/8
B8	0.238	2	1
B10	0.363	2-1/2	3/4
B15	0.496	2-1/2	1-1/4

01 74 0117 103

**FIGURE 97**  
**CONFIGURATION OF BENDING FATIGUE SURFACE**  
**CRACKED SPECIMENS**

and 3 uncracked) were initially trichlorethylene vapor degreased and etched very lightly for 3 seconds with a 2% hydrofluoric acid solution prior to application of the penetrant. The penetrant dwell time was 30 minutes in each case. Excess penetrant was removed using Magnaflux ZE-4A for 30 seconds followed by a water spray at 40 psi with 70°F water. Next, the specimens were dried at 150°F in a recirculating hot air oven and developer was applied. A bleed-out time of 5 minutes was used. Finally, the specimens were examined in a darkened booth with 7,400 microwatts per cm<sup>2</sup> of ultraviolet light at the specimen surface as measured with a Weston 703-60 light meter. The white light intensity in the booth was not measured. The laboratory tests were performed by two inspectors. The length of each penetrant indication was measured and recorded.

The results of the laboratory inspections are shown in Table 74. There were no false indications recorded.

As can be seen from the Table 74, each inspector detected all the cracks when nonaqueous wet developer was used. However, several of the smaller cracks went undetected when a dry powder developer was used, even with the higher sensitivity penetrant. It appeared that the dry powder did not adhere well to the ground surfaces.

Next, the specimens, including the uncracked dummies, were penetrant inspected at the engine manufacturer's production penetrant inspection facilities. For comparison purposes, three separate penetrant systems were used. These were (a) Magnaflux ZL-22A fluorescent post-emulsifiable penetrant, ZE-4A emulsifier, and ZP-4A dry powder developer, (b) ZL-22A penetrant, ZE-4A emulsifier, and Tracer-Tech D499C nonaqueous wet developer, and (c) Turco P-40B fluorescent post-emulsifiable, E-4 emulsifier, and DD-2 dry powder developer. All the systems were MIL-I-25135, Group VI sensitivity systems.

The production inspection parameters were a 30 minute penetrant dwell time, a 30 second emulsification time, a 5 minute development time, a 140 to 160°F drying temperature, and a viewing light intensity of 7,400 microwatts per cm<sup>2</sup>. The viewing light intensity was measured with a Weston 703-60 light meter. Each piece was trichlorethylene vapor degreased between inspections. For each penetrant system, independent production penetrant inspectors were used. The length of each crack indication detected was recorded.

**TABLE 74**  
**RESULTS OF ENGINE LABORATORY PENETRANT TESTING OF**  
**SURFACE CRACKED SPECIMENS**  
 (Results for Inspector B Shown in Parenthesis)

Actual Crack Length (in.)	Measured Indication Length					
	ZL-2A (MIL-I-25135, Group V)		ZL-22A (MIL-I-25135, Group VI)		ZL-30A (MIL-I-25135, Group VI++)	
	Dry Developer	Nonaqueous Wet Developer	Dry Developer	Nonaqueous Wet Developer	Dry Developer	Nonaqueous Wet Developer
No Crack	NCF (NCF)	NCF (NCF)	NCF (NCF)	NCF (NCF)	NCF (NCF)	NCF (NCF)
No Crack	NCF (NCF)	NCF (NCF)	NCF (NCF)	NCF (NCF)	NCF (NCF)	NCF (NCF)
No Crack	NCF (NCF)	NCF (NCF)	NCF (NCF)	NCF (NCF)	NCF (NCF)	NCF (NCF)
0.035	NCF (NCF)	0.040 (0.040)	NCF (NCF)	0.040 (0.040)	0.040 (0.040)	0.040 (0.040)
0.055	NCF (NCF)	0.010 (0.010)	NCF (NCF)	0.040 (0.040)	NCF (NCF)	0.045 (0.045)
0.129	NCF (NCF)	0.120 (0.120)	NCF (NCF)	0.120 (0.120)	NCF (NCF)	0.120 (0.120)
0.238	0.060 (0.090)	0.060 (0.090)	0.060 (0.090)	0.060 (0.060)	0.060 (0.160)	0.090 (0.160)
0.363	0.150 (0.090)	0.150 (0.090)	0.120 (0.120)	0.120 (0.120)	0.090 (0.150)	0.090 (0.150)
0.496	0.500 (0.500)	0.500 (0.500)	0.500 (0.500)	0.500 (0.500)	0.500 (0.500)	0.500 (0.500)

NCF - No Crack Found

GP74-0117 101

**TABLE 75**  
**RESULTS OF ENGINE PRODUCTION PENETRANT INSPECTION OF**  
**SURFACE CRACKED SPECIMENS**

Actual Crack Length (in.)	Measured Indication Length							
	ZL-22A with Dry Developer (ZP-4A)			P40-B with Dry Developer (DD-2)			ZL-22A with Nonaqueous Wet Developer (D499C)	
	Inspector							
	A	B	C	A	B	C	A	B
No Crack	0	0	0	0	0	0	0	0
No Crack	0	0	0	0	0	0	0	0
No Crack	0	0	0	0	0	0	0	0
0.035	0	0	0	0	0	0	0.030	0.030
0.055	0	0	0	0	0	0	0.100	0.100
0.129	0	0	0	0	0	0	0.100	0.100
0.238	0	0.250	0.250	0	0	0	0.150	0.150
0.363	0	0	0	0	0	0	0.125	0.125
0.496	0	0	0.350	0	0	0	0.200	0.200

GP74 0117 100

The results are shown in Table 75. No false indications were recorded. As can be seen, the most effective system was the ZL-22A penetrant/D499C nonaqueous wet developer system. The dry powder developer did not work effectively as it did not adhere well to the smoothly ground surface of the specimens.

Next, the test specimens, including the uncracked dummies, were penetrant inspected at the airframe manufacturer's production penetrant facility using Tracer-Tech P-133A fluorescent water washable penetrant, and D499C nonaqueous wet developer. The inspection parameters were the same as for the previous inspection of the surface cracks described in Section IV, Para. 1-p. The inspector was instructed to mark all linear indications. The length of the cracks were not measured during these tests.

Each piece was inspected 3 times by the same man. The test results are shown in Table 76. There were no false indications recorded.

Finally, the specimens, including the uncracked dummies, were penetrant inspected at the AFML. For these tests, the penetrant system was ZL-22A penetrant, ZE-3 emulsifier, and Sherwin D-100 nonaqueous wet developer. The penetrant dwell time was 30 minutes, the emulsification time was 30 seconds, and the drying conditions were 5 minutes at 180°F in a recirculating hot air oven. The specimens containing the .035 and .055 inch long cracks were inspected independently 10 times. The remaining specimens were inspected independently 7 times. Two inspectors participated in the testing. Prior to each inspection, the specimens were cleaned in a trichlorethylene degreaser for 1 hour.

The results of the inspections are shown in Table 77. As can be seen, all the cracks were detected during each inspection. There were no false indications recorded.

#### j. Radioactive Penetrant Testing

The surface cracked test specimens were subjected to a laboratory inspection by Industrial Nucleonics Corporation, using their proprietary radioactive penetrant method. The test specimens were placed in a vacuum chamber which then was evacuated. Next, a mixture of Krypton 84 and radioactive Krypton 85 was back-filled into the chamber. Finally, the Krypton mixture was transferred to a storage container, the vacuum chamber was restored to room atmosphere, and the test specimens were removed. In order to record the crack indications, film was placed on the specimen surface and exposed by the residual radiation. A typical exposure time was 2 hours. After the above technique was used, a second technique was employed to detect the cracks. This technique was identical to the first technique except that a .001 inch thick coating of plastic was placed on the surface of the specimen prior to placing the film on the part.

**TABLE 76**  
**RESULTS OF AIRFRAME PRODUCTION PENETRANT INSPECTION OF GENERAL**  
**ELECTRIC SURFACE CRACKED SPECIMENS**

Specimen No.	Crack Length (in.)	No. of Cracks Detected
B5	0.035	2 of 3
B2	0.055	3 of 3
B13	0.129	3 of 3
B8	0.238	3 of 3
B10	0.363	3 of 3
B15	0.496	3 of 3

GP74 011 / 90

**TABLE 77**  
**RESULTS OF AFML LABORATORY PENETRANT INSPECTION OF**  
**BENDING FATIGUE SURFACE CRACKED SPECIMENS**

Actual Crack Length (in.)	Measured Indication Length (in.)									
	Inspector									
	A	B	C	D	E	F	G	H	I	J
0.035	0.046	0.046	0.046	0.046	0.046	0.046	0.046	0.046	0.046	0.046
0.055	0.062	0.062	0.062	0.062	0.062	0.062	0.062	0.062	0.062	0.062
0.129	0.125	0.125	0.125	0.125	0.125	0.125	0.125	—	—	—
0.238	0.250	0.250	0.250	0.250	0.250	0.250	0.250	—	—	—
0.363	0.375	0.375	0.375	0.375	0.375	0.375	0.375	—	—	—
0.496	0.500	0.500	0.500	0.500	0.500	0.500	0.500	—	—	—

GP74-0117 98

A comparison of the actual crack length with the indication length is shown below.

**TABLE 78**  
**RESULTS OF RADIOACTIVE PENETRANT TESTING**

Actual Length (in.)	Indication Length	
	Process No. 1	Process No. 2
0.035	0.023	0.021
0.055	0.043	0.046
0.129	0	0.106
0.238	0.279	0.236
0.363	0.359	0.366
0.496	0.516	0.508

GP74 0528 1

k. Eddy Current Inspection of Fastener Holes

Eddy current inspection techniques have been used primarily to detect surface connected cracks in components and assemblies where the penetrant method would be impossible or impractical to use effectively. Of particular importance are the fastener hole surfaces. A test program was conducted to determine the detection capability for fatigue cracks in unfilled fastener holes.

The test specimens used for the eddy current study were dogbone fatigue specimens which had undergone fatigue testing under another program. Schematics of the three specimen types are shown in Figures 98, 99, and 100. Prior to any eddy current testing, the fatigue specimens were tested at room temperature to failure. The specimens containing 0.250 and 0.375 inch diameter holes were tested in axial loading on a 10,000 pound Sonntag SP-10 fatigue machine having a 5:1 load intensifying fixture mounted on a table top. The Sonntag machine provided a cyclic rate of 30 cycles per second. The specimens containing 0.750 inch diameter holes were tested on a Weston hydraulic fatigue machine which provided a cyclic rate of 5 cycles per second. The stress ratio for all the tests was +0.1. Each specimen was tested until fracture occurred through one of the two holes.

A total of 230 fractured specimens were initially eddy current tested to select holes containing secondary cracks (see Figure 101). The intact hole in each specimen was scanned with a Nortec NDT-3 eddy current instrument capable of several discrete frequencies between 10 KHz and 2 MHz. The instrument features an adjustable operating point within the complex impedance plane for each of the 7 available frequencies. Ideal Specialty Co. absolute type hole probes of the appropriate size were used. These probes were a single coil and used a ferrite core of .050 inch nominal diameter from .130 to .160 inch long wound with 150 turns of #40 wire.

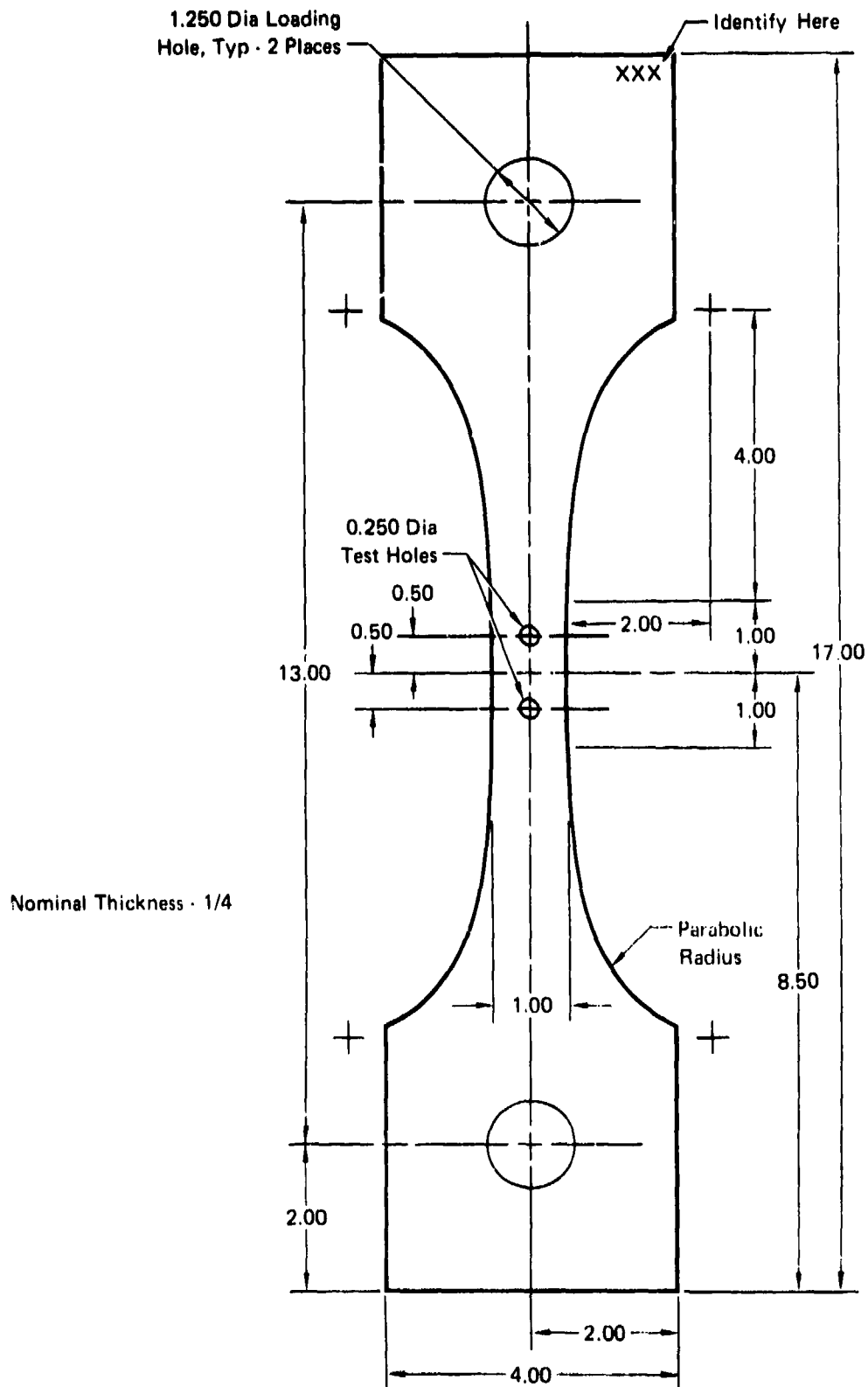


**FIGURE 98**  
**SPECIMENS FOR 0.250 INCH DIAMETER HOLES**

GP 74 0117 22b

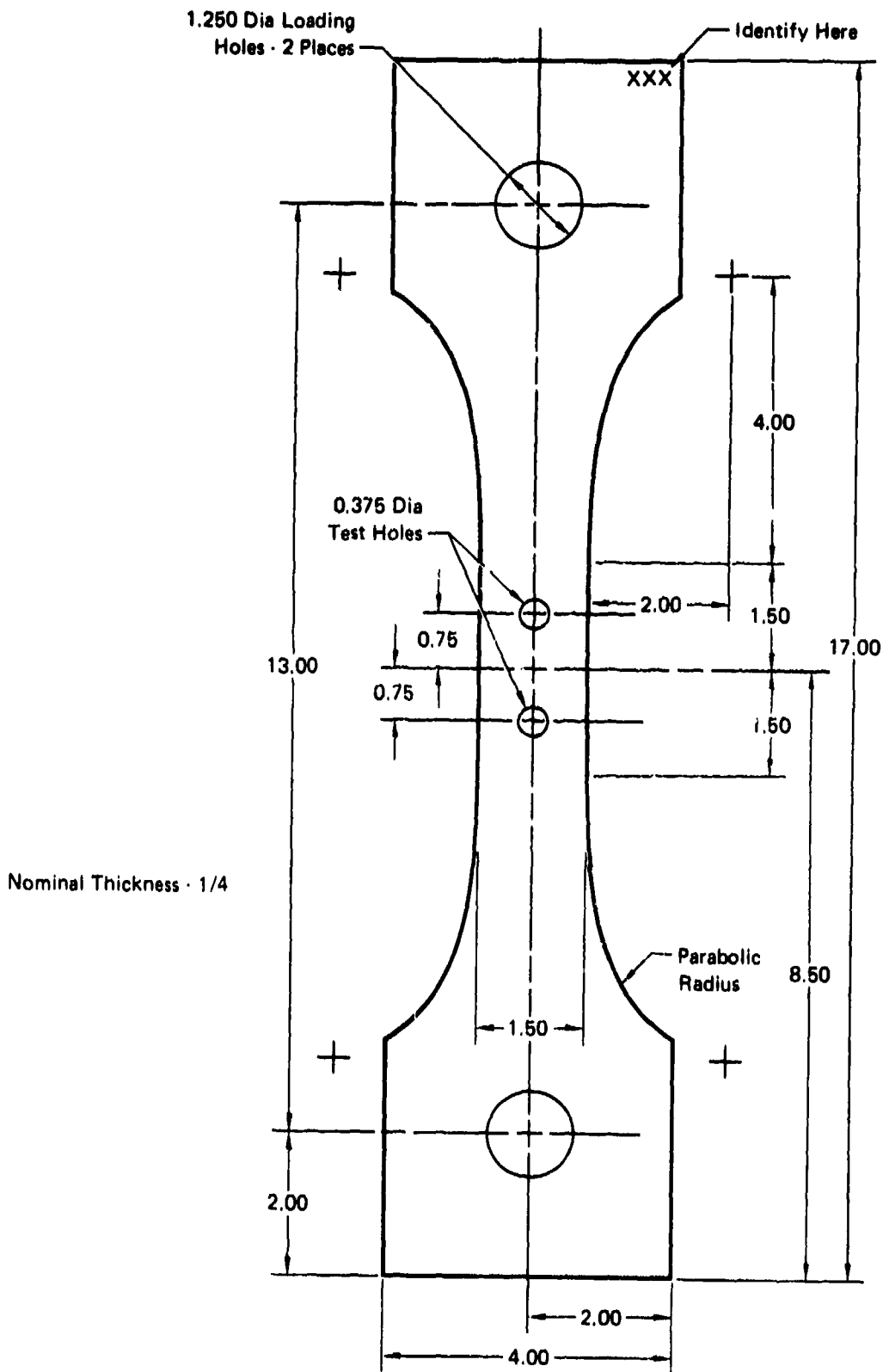


**FIGURE 99**  
**SPECIMEN FOR 0.375 INCH DIAMETER HOLES**

GF 74-0117-226

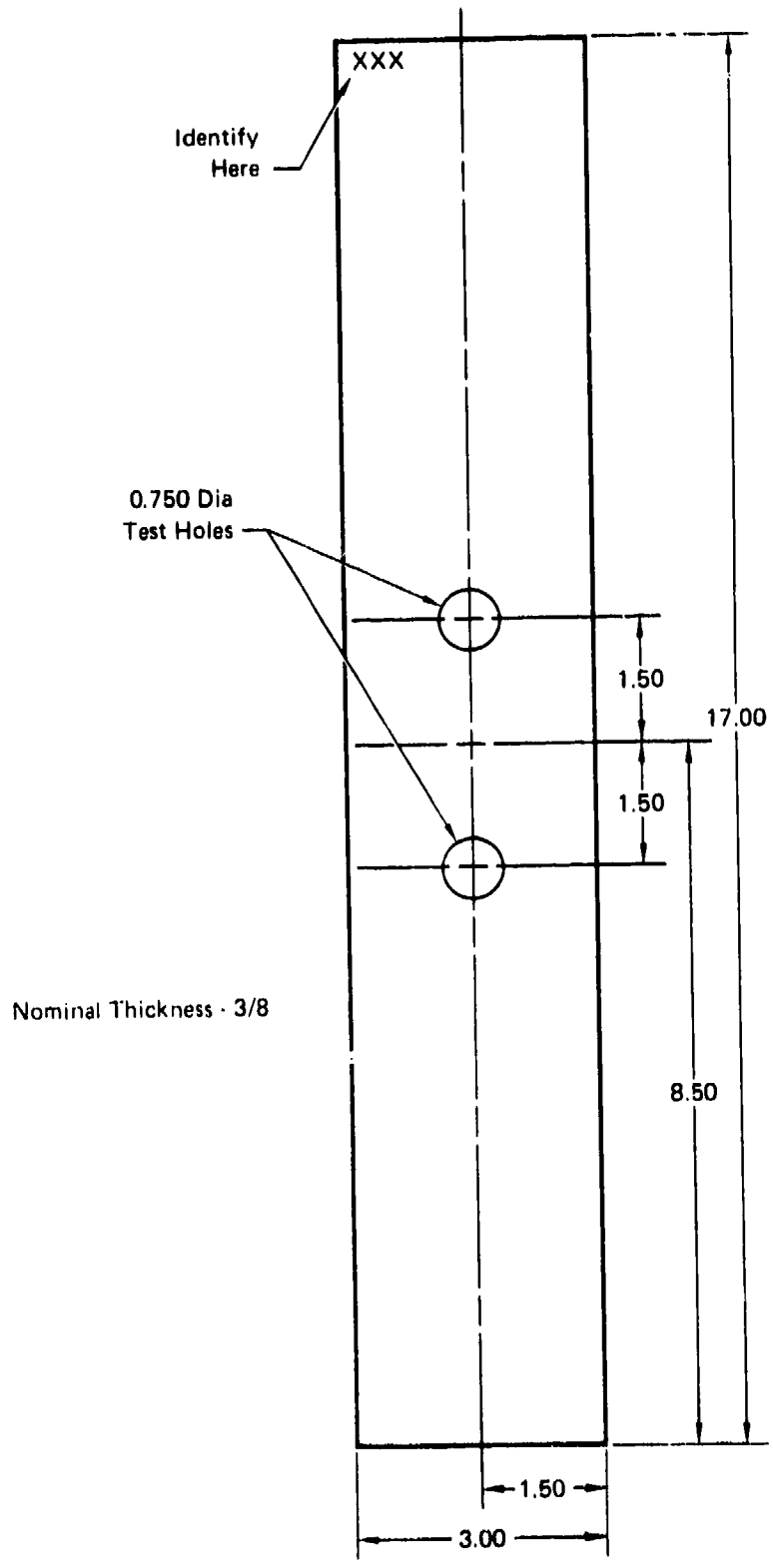


**FIGURE 100**  
**SPECIMEN FOR 0.750 INCH DIAMETER HOLES**

GP 14-011 / 227

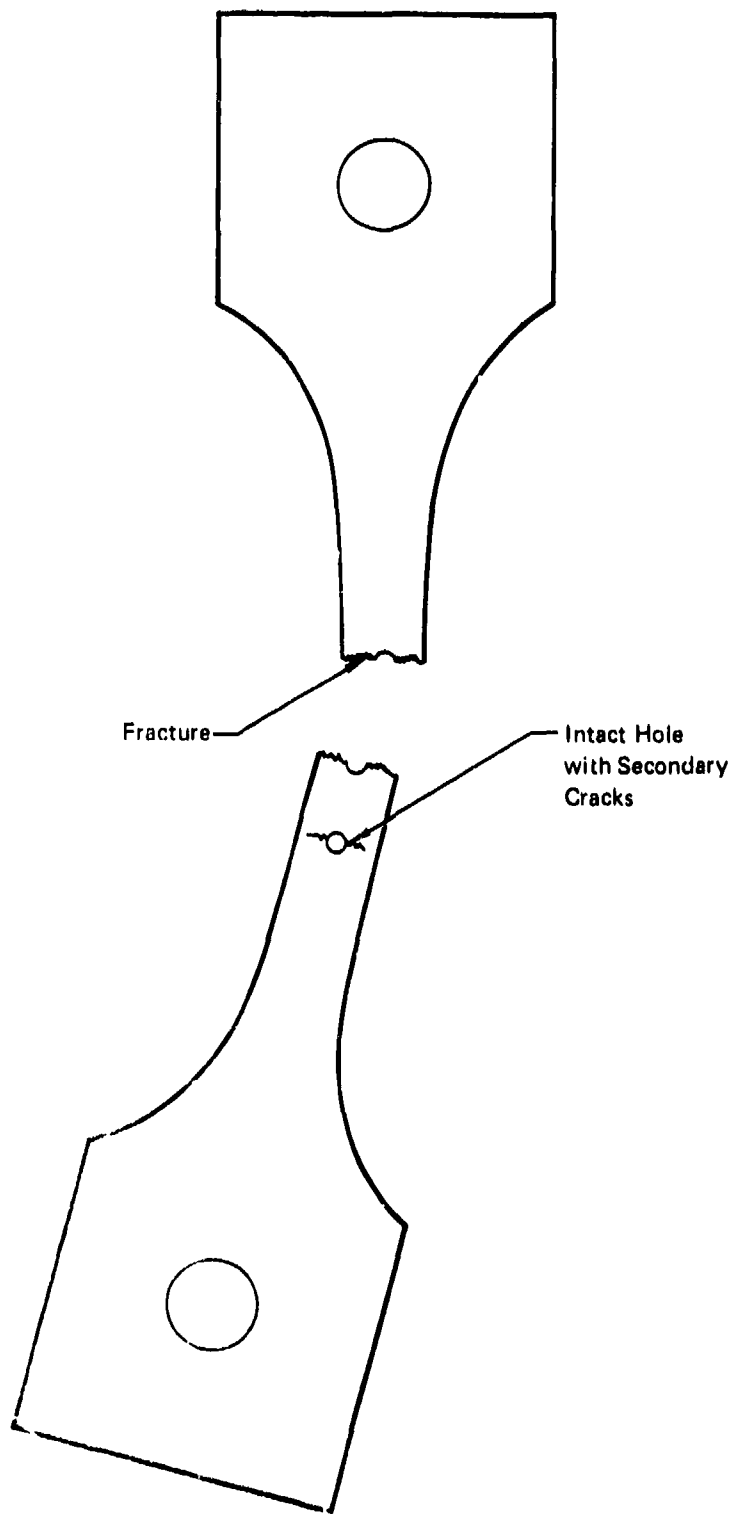


**FIGURE 101**  
**SECONDARY CRACKS IN FASTENER HOLE**

QP74 0117-222

Lift-off compensation was 0.003 inch and the test frequency was a nominal 500 KHz (464 KHz actual). The actual frequency was determined by monitoring the oscilloscope wave form of the signal supplied to the eddy current probe during actual operation. Lift-off compensation was accomplished by adjusting the "X" and "R" controls to obtain the same meter indication with and without a .003 inch paper shim between the probe and hole surface.

The operating point was chosen using the sensitivity standard shown in Figure 102. The conductivity of the Ti-6Al-6V-2Sn is 1.10% IACS and the conductivity of the Ti-8Al-1Mo-1V is 0.87% IACS. A previous program indicated that, for titanium, the operating point along the lift-off compensation locus should be chosen relatively far away from the material point in the complex impedance plane to give the maximum response (478 microamps per 1% IACS) to the conductivity difference between the two halves of the sensitivity standard. The eddy current instrument had been modified internally to permit recording of the signals on a Moseley 680 strip chart recorder which has a response of 100 Hz. Previous experience has shown the strip chart recorder to be a great aid in detecting cracks because a meter deflection doesn't have to be constantly monitored. Also, the strip chart recorder responds to a crack much more quickly than does a meter deflection. The scan index used was as shown in Figure 103. The scan index was chosen to provide for overlap of the inspection areas. The response from each crack was measured in microamps. Of the 230 holes inspected, a total of 39 holes contained indications.

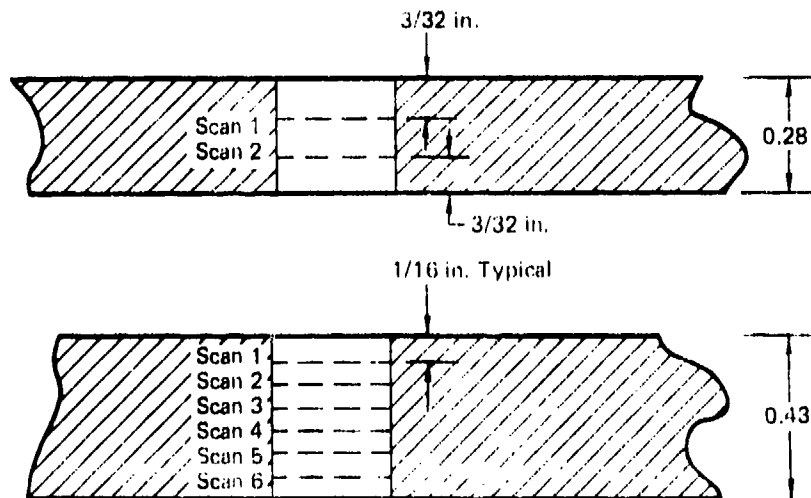
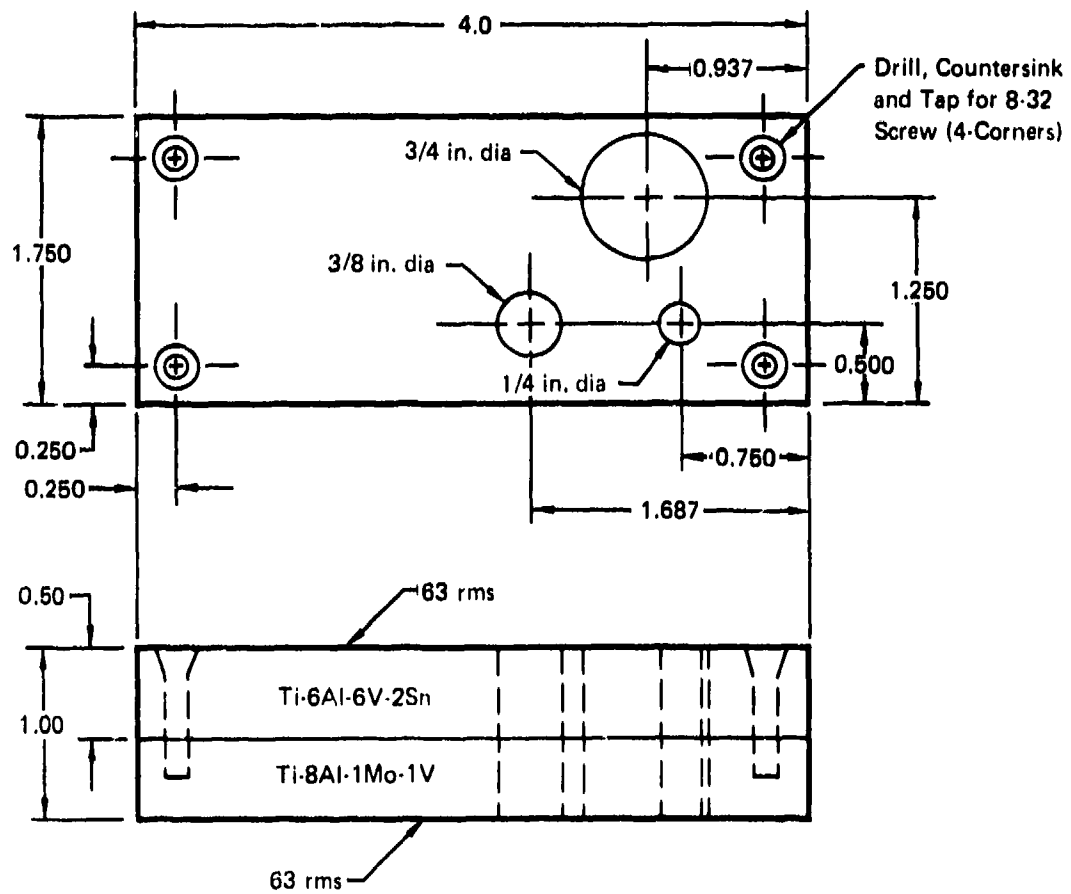


FIGURE 103  
SCAN INDEX USED DURING EDDY CURRENT INSPECTION

Next, the 39 holes with indications were eddy current inspected using the NDT-3 and the same inspection parameters except that a nominal frequency of 100 KHz (104 KHz actual) was used. For this test, negative lift-off compensation was used and the operating point was selected for maximum response to the conductivity difference in the sensitivity standard.



**Notes:**

1. All dimensions are in inches.
2. Tolerances are  $\pm 0.010$  in.
3. Surface finish is 125 rms unless otherwise noted.
4. Material is in the annealed condition.
5. Install 8-32 screws in four corners when complete.

(P74 0117 317)

**FIGURE 102**  
**TITANIUM EDDY CURRENT SENSITIVITY STANDARD**

A third test was performed upon the 39 holes using another eddy current instrument, the Magnaflux ED-520. This particular instrument used continuously variable frequencies (from 55 to 200 KHz) which are fixed by the probe coil and lift-off compensation chosen. Again, appropriately sized Ideal Specialty absolute hole probes were used. Lift-off compensation was negative and the test frequency was 135 KHz. The operating point was selected to give the maximum response to the difference in conductivity in the sensitivity standard. A fourth test was performed using the second eddy current instrument with negative lift-off compensation and a test frequency of 129 KHz. The operating point was changed slightly from that used in the third test because preliminary testing had suggested a superior signal-to-noise ratio might be realized.

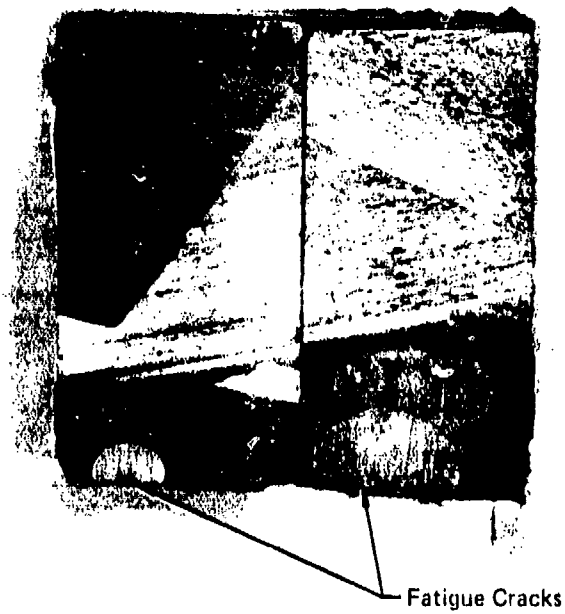
Finally, a fifth test was performed using the first eddy current instrument and Nortec differential hole probes. The nominal test frequency was 500 KHz (464 KHz measured). The instrument operating point was chosen to give the maximum signal-to-noise ratio by locating the null balance point in the impedance plane and measuring the signal-to-noise ratio for several operating points near the null balance point.

After all the eddy current tests were complete, 14 of the cracks were intentionally fractured and the actual size of the crack was measured. A photograph of two of the fracture surfaces is shown in Figure 104. The results of the eddy current tests are shown in Tables 79 and 80. It should be mentioned that, during the testing, each instrument sensitivity was adjusted to yield 22 percent of full scale for the conductivity difference in the reference standard. The ED-520 has a 500 microamp full scale and the NDT-3 has a 100 microamp full scale. Consequently, in order to normalize the data, the NDT-3 responses were multiplied by a factor of 5. The normalized data is shown in Table 79. As can be seen from Table 79, the eddy current response from the smaller cracks was greatest with the low frequency methods using negative lift-off compensation.

Based upon these tests with the equipment used, it appears that the best eddy current method for inspection of unfilled holes in titanium is to use an absolute hole probe, negative lift-off compensation, and a low frequency of approximately 100 to 150 KHz. The smallest crack detected by eddy current during these tests had a maximum depth of .024 inch. It is not known if smaller cracks exist in the fastener holes since the crack growth was not controlled. Consequently, it is not possible to determine the size of a minimum detectable crack from these results. It can be stated, however, that the eddy current method can detect cracks with depths of at least .024 inch.

The results of the previous program prompted further testing. Additional specimens were selected from the same collection as were the Figures 98 through 100 specimens. Several eddy current inspections, described below, were conducted on them.

The test, designated as "NDT-3 500 KHz Comp" in Table 81, was performed using a Nortec NDT-3 eddy current instrument with an absolute probe at 500 KHz. The absolute probe was an Ideal Specialty P/N 64101-1/4 SP probe



UP74 0117 221

**FIGURE 104**  
**PHOTOGRAPH OF TYPICAL FRACTURE SURFACES**

**TABLE 79**  
**RESULTS OF EDDY CURRENT INSPECTION OF FASTENER HOLES**

Specimen No.	Alloy	Hole Dia (in.)	Material Thickness (in.)	Maximum Stress (ksi)	Fatigue Cycles	Absolute Probe Responses (microamps)				Differential Probe 464 KHz	Maximum Crack Depth (in.)					
						Lift Off Compensated		Negatively Compensated								
						464 kHz	134 kHz	128 kHz	104 kHz							
152	Ti-6Al-4V (Annealed)	0.25	0.28	55	78,000	20	40	△	△	△	None Found					
145				55	138,000	20	50	40	△							
148 △				55	74,000	240	280	260	270							
139				55	490,000	200	325	275	290							
112				80	21,000	275	310	285	290							
162				60	69,000	320	435	365	425							
166				55	67,000	550	455	590	475							
181				65	56,000	310	460	320	410							
148 △				55	74,000	510	500	570	495							
355				Ti-6Al-4V (STA)			55	100,000	240			185	225	170	△	△
343							55	206,000	85			185	95	90	△	0.030
380							55	99,000	225			350	260	300	△	0.037
351							55	110,000	475			420	450	420	△	0.104
347							60	89,000	525			545	510	500	△	△
356	55	76,000	870				960	1110	980	△	△					
354	55	139,000	950				1040	1070	930	△	0.179					
358	Ti-6Al-4V (STOA)						55	117,000	1610	1600	1870	1600	△	△		
332							55	85,000	855	1040	930	890	△	△		
219	Ti-6Al-4V (Annealed)	0.75	0.43				55	104,800	80	70	25	△	△	△		
197				55	63,900	310	280	190	△							
198				55	66,000	500	325	260	△							
182	Ti-6Al-4V (Annealed)	0.375	0.28	55	218,000	40	90	△	110	70	△					
193				55	87,000	75	125	90	85			105	0.030			
187				55	64,000	95	190	165	170			190	△			
180				55	72,000	210	380	335	365			310	△			
186				55	72,000	520	660	585	660			555	△			
194				55	78,000	750	830	750	910			810	△			
292	Ti-6Al-6V-2Sn (Annealed)	0.375	0.28	55	36,000	40	50	40	65	△	△					
287				55	106,000	80	270	210	220	220	0.056					
294				55	65,000	300	440	430	450	460	0.097					
205				55	38,000	350	690	610	730	580	0.087					
291				55	36,000	40	30	60	60	△	None Found					
380	Ti-6Al-2Sn (STOA)	0.25	0.28	65	1,308,000	30	30	△	△	△	None Found					
379				55	3,447,000	20	45	△	△							
275	Ti-6Al-6V-2Sn (Annealed)	0.25	0.28	55	77,000	25	40	△	△		None Found					
258				55	26,000	20	50	50	60			0.024				
276				55	53,000	25	40	35	15			△				
280				55	82,000	95	240	225	235			△				
391	Ti-6Al-6V-2Sn (STA)	0.25	0.28	55	32,000	45	80	75	65		0.034					
303				55	23,000	145	175	170	160			△				

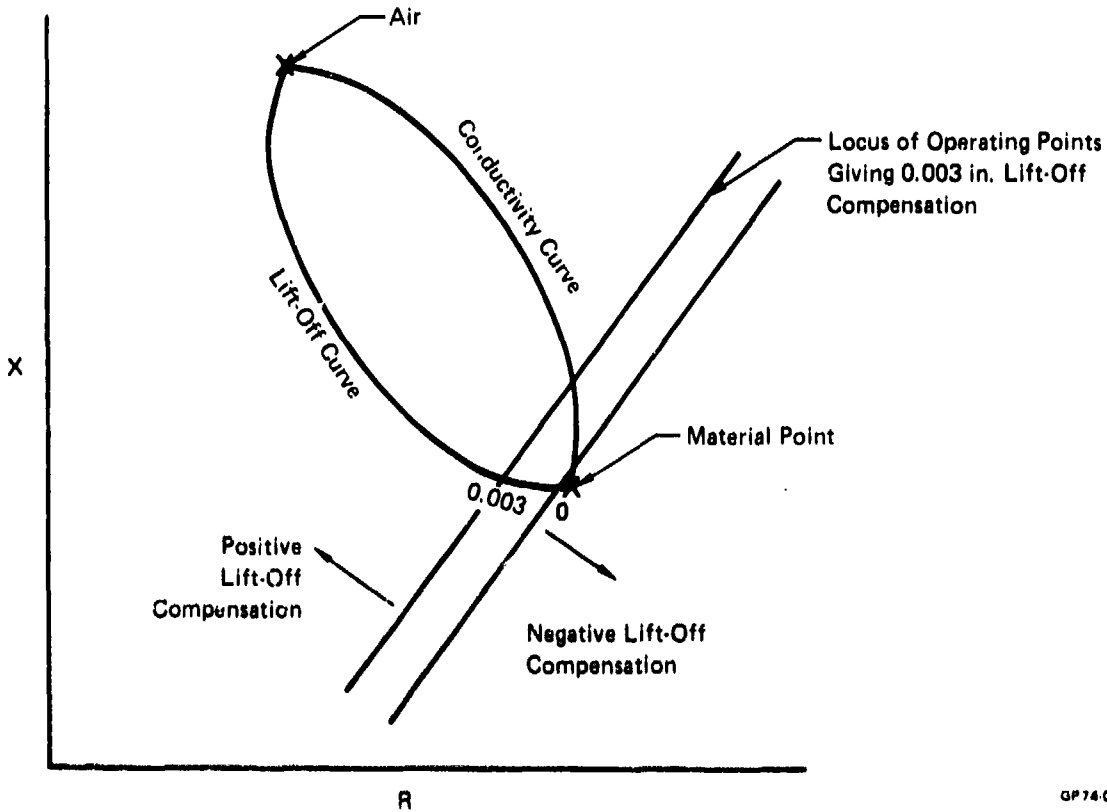
△ Testers from both sides  
 △ No crack detected  
 △ Not tested  
 △ Specimen was not intentionally fractured

GP 74-0117-228

**TABLE 80**  
**SUMMARY OF EDDY CURRENT RESPONSE vs MAXIMUM CRACK DEPTH**

Specimen No	Alloy	Hole Dia. (in.)	Absolute Probe Response ( $\mu$ - amps)				Differential Probe	Maximum Crack Depth (in.)
			Lift Off Compensated	Negatively Compensated				
			464 KHz	134 KHz	129 KHz	104 KHz	464 KHz	
148	Ti-6Al-4V	0.25	240	280	260	270	Not Tested	0.063
139	↓	↓	200	325	275	290		0.037
162	↓	↓	320	435	365	425		0.062
148	↓	↓	510	500	570	495		0.133
343	↓	↓	85	185	95	90		0.030
360	↓	↓	225	350	260	300		0.037
351	↓	↓	475	420	450	420		0.104
354	↓	↓	950	1040	1070	930		0.179
193	Ti-6Al-4V	0.375	75	125	90	85	105	0.030
287	Ti-6Al-6V-2Sn	0.375	80	270	210	220	220	0.056
294	↓	↓	300	440	430	450	460	0.095
295	↓	↓	350	690	610	730	580	0.087
258	Ti-6Al-6V-2Sn	0.25	20	50	50	60	Not Tested	0.024
391	↓	↓	45	80	75	65		0.034

Typical Complex Impedance Plane



GP 74-0117-220

with a .050 inch diameter ferrite core and 150 turns of No. 40 wire. Lift-off compensation was .003 inch and was accomplished by adjusting the "X" and "R" controls to obtain the same meter indication with and without a .003 inch paper shim between the probe and the test surface. The operating point was chosen using the sensitivity standard shown in Figure 102. The conductivity of the Ti-6Al-6V-2Sn is 1.10% IACS and the conductivity of the Ti-8Al-1Mo-1V is 0.87% IACS. A previous program indicated that, for titanium, the operating point along the lift-off compensation locus should be chosen relatively far away from the material point in the complex impedance plane to give the maximum response to the conductivity difference between the two halves of the sensitivity standard (478 microamps per 1% IACS). Crack indications were recorded on a Moseley 680 strip chart recorder and a fixture was used to maintain the 1/16 inch scan index.

The test identified as NDT-6 1.0MHz Comp. was performed identically to that described above except that the frequency was 1.0 MHz. Although a 2.0 MHz module was available for use in the NDT-3, insufficient gain was obtained with this module to warrant any further testing. Discussions with Nortec on this subject led to the use of the prototype NDT-11 instrument.

The Nortec NDT-11, designated as "NDT-11 1.5 MHz Comp" in Table 81 has more gain at the higher operating frequencies than the NDT-3 or NDT-6. A 2MHz differential probe supplied by Nortec and an experimental absolute probe supplied by the Ideal Specialty Co. were used to measure the capability of the NDT-11 prototype instrument. Both probes were hand rotated and indexed 1/16 inch between scans. A fixture was used to maintain constant probe depth during each scan. The calibration methods were the same as was performed using the NDT-6. Medium size fatigue cracks, selected from the previous results, were used in the calibration of the differential probe so that the comparisons found in Table 81 could be made. The Nortec differential probe was found to be no improvement over the previously evaluated NDT-3 and NDT-6 with an absolute probe. The results reported in Table 81 were obtained using the experimental Ideal Specialty absolute probe operating at 1.5 MHz. It consisted of a radial axis .050 inch diameter ferrite core wound with 50 turns of #40 wire. The test designated as "Circograph" in Table 81 was performed with a Forster Circograph 6.230 using a 400 KHz stainless steel differential probe rotating at 3,000 RPM. The instrument read-out is a cathode ray tube (CRT) whose display is synchronized with the rotation of the probe coils such that a flaw's location is readily determined. The method of calibration previously used with the NDT-3 and an absolute probe was not applicable to this method since both coils of the probe see the same bulk material conductivity simultaneously. For this reason, a medium size crack detected by the previously described methods (Specimen 393), was used for calibrating. The instrument was calibrated by adjusting the phase and the gain controls until the signal-to-noise ratio was minimized (about 10 to 1) for this particular crack. Once initially adjusted, the gain was changed only slightly to maintain the noise at a level of less than 20% of the CRT height in the individual holes; the phase position was not altered. The rotating probe was moved slowly in and

**TABLE 81  
EDDY CURRENT CRACK RESPONSE**

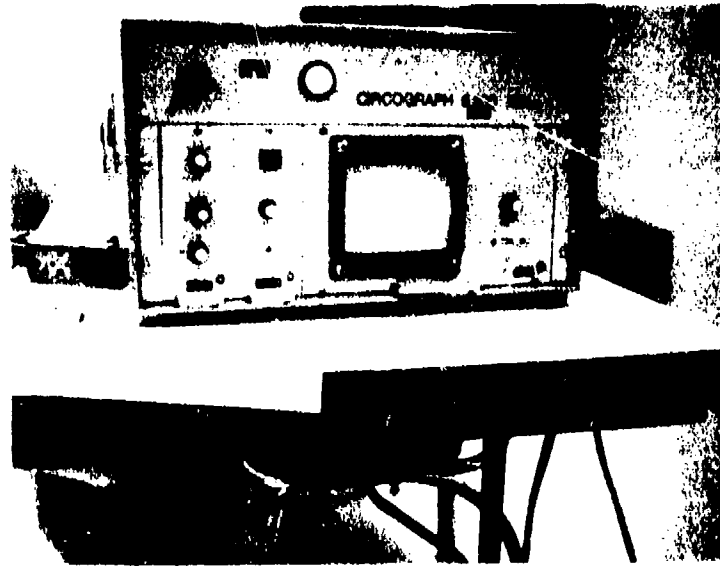
Specimen No.	Material	Maximum Stress (ksi)	Fatigue Cycles	% Full Screen Height	Microamp Response			
					Circograph	NDT-11 1.5 MHz, Comp.	ED 520 Uncomp.	NDT-3 500 KHz, Comp.
276	Ti-6Al-6V- 2Sn, Annealed	55	53,000	-	-	50	-	-
280		55	82,000	75	210	160	160	170
393	Ti-6Al-6V- 2Sn, Annealed	55	23,000	45	130	180	150	210
536	Ti-6Al-4V, Annealed	55	50,000	100 <sup>+</sup>	920	1100	1100	500 <sup>+</sup>
540		55	53,000	-	-	640	528	500 <sup>+</sup>
544		55	23,000	20	40	210	80	110
545		55	39,000	80	230	220	125	230
547		55	71,000	45	-	80	-	-
551		55	92,000	100	540	720	484	500 <sup>+</sup>
552		55	64,000	35	-	-	-	-
553		55	61,000	80	40	-	-	-
554		55	71,000	65	180	-	110	-
555		55	61,000	30	50	-	-	-
559		55	52,000	80	320	350	200	350
560		55	54,000	100	680	-	170	300
562		55	75,000	40	120	-	100	180
576		55	108,000	20	-	100	-	-
579		55	116,000	15	-	-	-	-
580		55	63,000	75	400	638	440	500
589	55	163,000	-	-	-	-	-	
646	80	23,000	85	180	-	150	190	
740	Ti-6Al-6V- 2Sn, Annealed	55	43,000	70	370	264	200	170
754		55	46,000	85	650	374	280	230
758		55	72,000	38	100	143	110	140
816		55	31,000	-	-	-	-	-
187		55	32,000	-	-	-	-	-

GP74 0117 J10

out of the holes. Each hole was scanned along its entire depth at least 4 times. A typical crack response is illustrated in Figure 105. Sinusoidal-type CRT displays were found to be indicative of irregular surface contour in the holes attributable to the flutes of the reamers used. It was noted, however, that after the holes had been tested by five different operators that the holes appeared to be burnished and a stainless steel coating remained in the holes. No significant wear on the probe was noticed; however, before any further tests with an absolute probe, the holes had to be chemically cleaned due to the changes in apparent conductivity of the hole surfaces. Testing of the holes was approximately 10 times faster with the Circograph as with the other systems investigated.

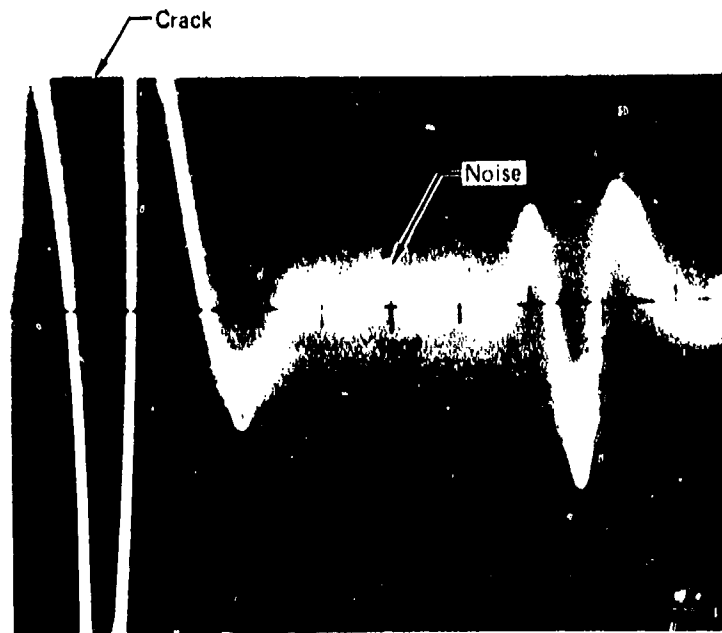
The test labeled "ED 520-Uncomp" was performed using a Magnaflux ED 520 eddy current instrument with an absolute probe. This particular instrument uses continuously variable frequencies (from 55 to 200 KHz) which are fixed by the probe coil and the lift-off compensation. Lift-off compensation was negative and the test frequency was 134 KHz. The operating point was selected to give the maximum response to the difference in conductivity from the two pieces of titanium in the reference standard. The absolute probe was the same as before. The sensitivity of the instrument was set to yield a 110 microamp difference between the piece of Ti-6Al-6V-2Sn and Ti-8Al-1Mo-1V in the sensitivity standard. Again a Moseley 680 strip chart recorder was used as an aid for crack detection and a scan index fixture was used for the 1/16 inch scan index.

More indications were obtained using the Circograph than with the other instruments. Since none of the cracks were fractured to confirm their existence, it is not known how many of the indications were from discontinuities other than cracks. It also appeared that, among the other methods, the methods using absolute hole probes were less sensitive to cracks occurring near the edges of the holes than was the method employing the differential probe. In comparison, the Circograph was the most sensitive method for cracks occurring near the edges of the holes since it was easy to maintain probe normality and there was virtually no edge effect. Also, the high probe rpm allows inspections at very small index values with little loss in test time.



CP 74 0117 108

FORSTER CIRCOGRAPH 6.23



CP 74 0117 309

FIGURE 105  
CATHODE RAY TUBE PRESENTATION OF CRACK RESPONSE

## 1. Verification of Surface Crack Size

Several of the tension-tension fatigue and bending fatigue surface connected cracks used in the program were intentionally exposed in order to measure their actual length and depth. Sawcuts were made adjacent to the crack and the specimen was intentionally failed by overload. The fracture surfaces of the original fatigue cracks were examined and the actual length and depth of each were measured. The actual crack dimensions are listed in Table 82 and photographs of typical fracture surfaces are shown in Figure 106.

Several of the specimens were examined intact at a magnification of 400x in order to measure the width of the cracks. The average crack width was .0005 inch.

## 2. POROSITY

Several hand forged billets (Ti-6Al-6V-2Sn) containing porosity have been collected during past internal programs. The billets sections were 4-1/2 x 4-1/2 inches, 4-1/2 x 6 inches, and 4-1/2 x 5-3/4 x varying lengths. The porosity in each of the billets is positioned as shown in Figure 107. A program was conducted using these pieces to measure the diameter of typical pores which are detectable during a penetrant inspection.

### a. Ultrasonic Method

The billets had been certified as ultrasonically acceptable at a Class A level (similar to class A described in MIL-I-8950B - Inspection, Ultrasonic, Wrought Metal, Process for). Subsequently these same billets were submitted to mechanical properties testing and failed at a level below minimum allowable limits for tensile strength and ductility. As a result of the failure, a section of the failed billet was submitted to a metallographic evaluation. An unacceptable porous condition was found within the billet, with the heaviest concentration of stringer type porosity lying near the outside of the billet. Figure 107 illustrated the distribution of porosity in a typical billet.

With the discovery of the porosity, ultrasonic reinspection of the billets was undertaken. The following setup was used:

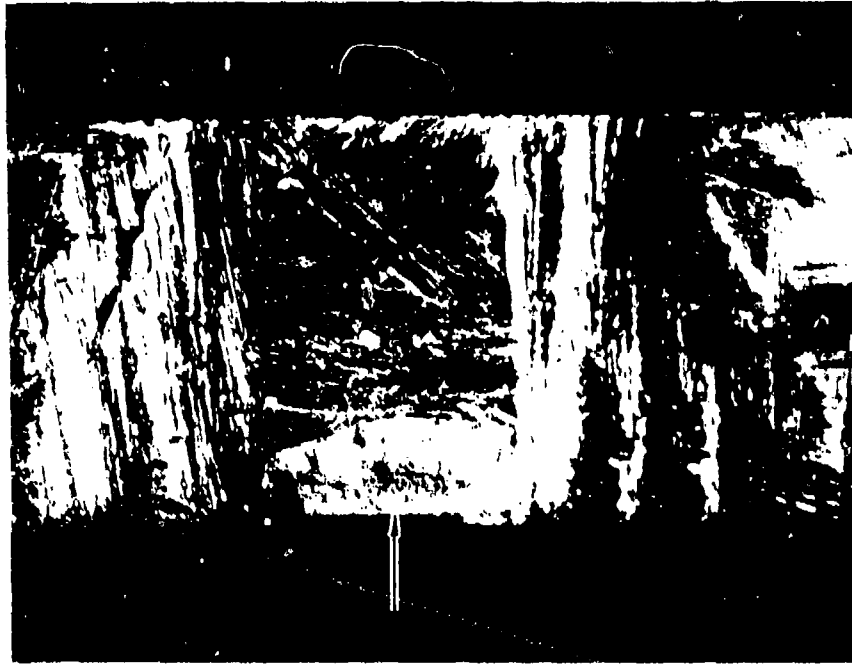
- (1) Parts were immersed and a 2 1/2 inch water path was used.
- (2) A 5.0 MHz flat 3/4" lithium sulphate transducer with a UM721 with a 105 pulser was used for scanning.
- (3) A "distance-amplitude correction" curve based on 3/64" diameter flat bottom holes with metal travels of 1.25, 2.25, 3.25, and 4.75 inches was established by plotting it on the face of the cathode ray tube.

With this test setup, a great deal of noise appeared on the cathode ray tube wherever the billet was examined. This noise fell below the 3/64 inch "distance amplitude correction" curve in all cases except for one or two small areas where individual indications appeared above it. These were not rejectable indications for Class A. Concurrent with these indications, it was noted that there was a 50% or more loss of back reflection in the areas of the billet where the indications were the greatest. This latter observation is a normal rejectable condition. It was noted that the back reflection is normally in saturation when a "DAC" curve is established by using the proper

**TABLE 82  
ACTUAL SIZE OF SURFACE CRACKS**

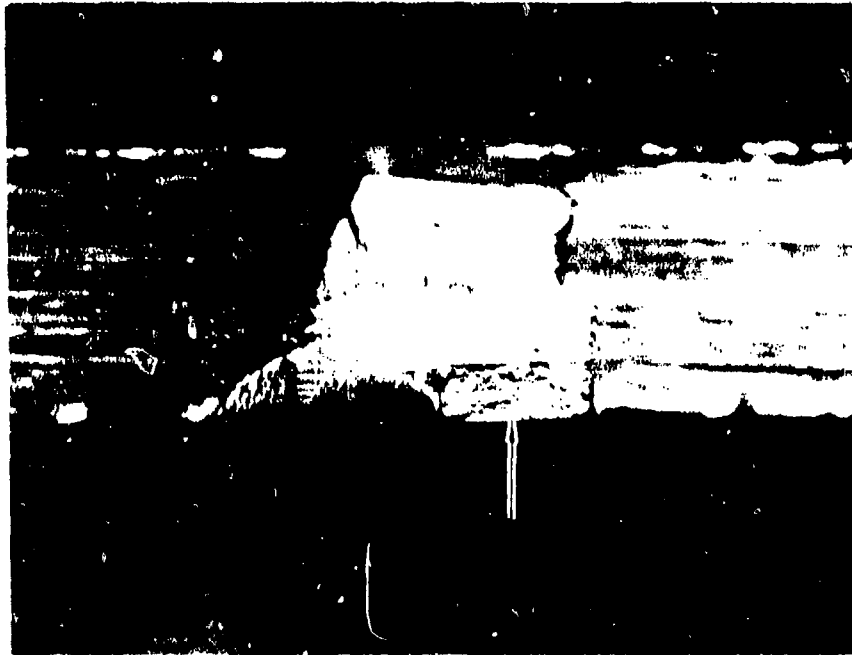
<b>Specimen No.</b>	<b>Target Crack Length (in.)</b>	<b>Actual Crack Length (in.)</b>	<b>Actual Crack Depth (in.)</b>
33	0.025 - 0.050	0.074	0.014
49		0.040	0.015
45		0.010	0.005
75		0.060	0.015
38	0.050 - 0.100	0.070	0.025
82		0.059	0.013
39		0.060	0.040
56		0.080	0.020
59		0.090	0.030
3	0.100 - 0.250	0.119	0.019
11		0.200	0.070
15		0.200	0.070
25		0.150	0.020
56		0.125	0.035
66		0.105	0.030
8	0.250 - 0.500	0.430	0.160
21		0.410	0.170
30		0.480	0.180

GP74-0117 22



Specimen 33  
0.070 In. Long x 0.014 In. Deep

6X



Specimen 3  
0.119 In. Long x 0.019 In. Deep

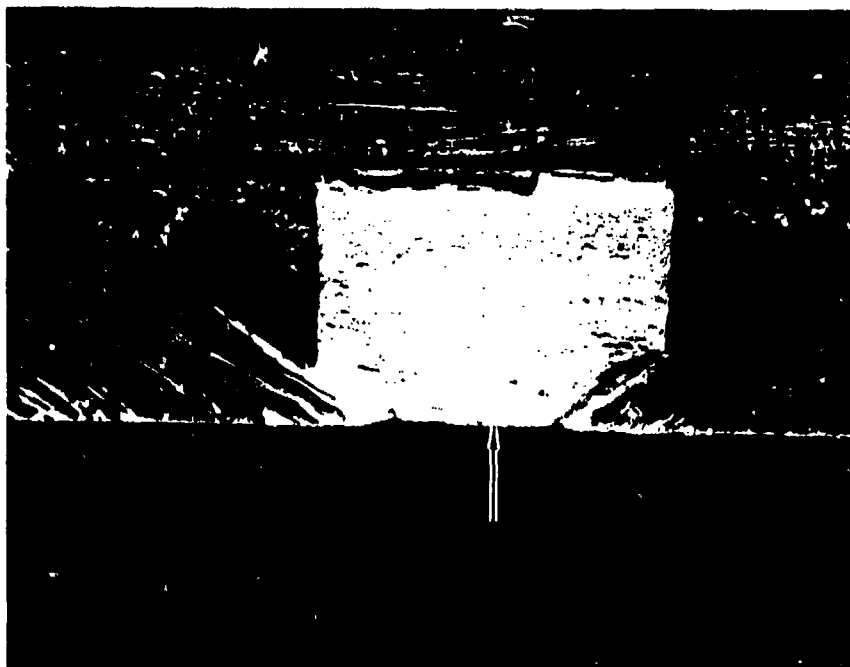
4X

SP-4-0112-0-1

**FIGURE 106**  
**PHOTOGRAPHS OF FRACTURE SURFACE OF SURFACE CRACKS**



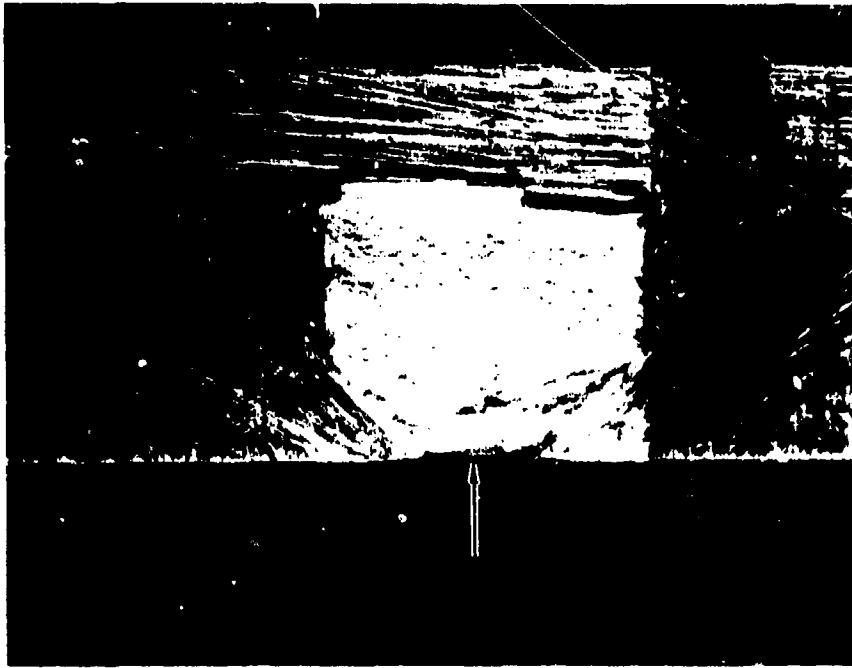
Specimen 30 4X  
0.48 In. Long x 0.18 In. Deep



Specimen 59 6X  
0.090 In. Long x 0.030 In. Deep

GP74 0117 04

**FIGURE 106 (Continued)**  
**PHOTOGRAPHS OF FRACTURE SURFACE OF SURFACE CRACKS**



6X

GP74-0117-65

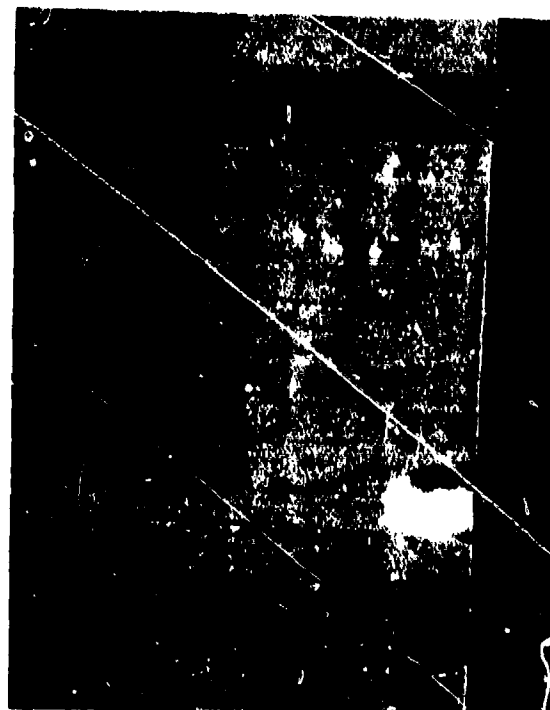
Specimen 39  
0.040 In. Long x 0.015 In. Deep

**FIGURE 106 (Continued)**  
**PHOTOGRAPHS OF FRACTURE SURFACE OF SURFACE CRACKS**



View A

Mag. 8X



View B

Mag. 9X

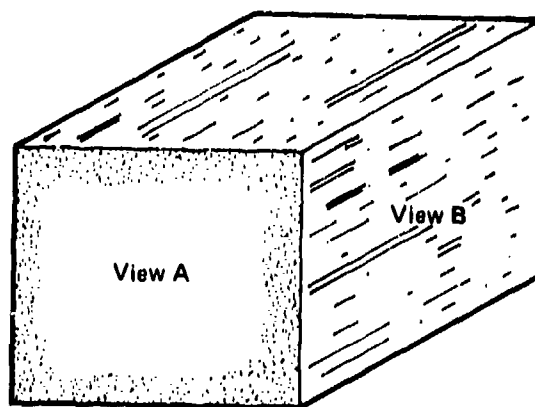


FIGURE 107  
TYPICAL POROSITY IN HAND FORGED BILLETS

GP 74 0117 217

test blocks. With this circumstance, it is impossible to judge a true 50% loss of back reflection unless one of the back surface multiples that is not in saturation is observed. Observation of a multiple back reflection requires compression of the scope picture, which in itself is undesirable, or taking into account the geometric progression of loss on the multiples of the first back reflection is a possibility. Another method for eliminating the problem of the saturated back reflection is to make a separate back reflection test scan of the part. At least part of the industry feels a 50% loss of back reflection is significant only when related to a 50% reduction in height of the observed back reflection on the cathode ray tube for a setup which has been made on the proper ASTM reference blocks. Since, in this case, the back reflection is normally in saturation, the observed 50% loss will amount to an actual 80%, 90%, or more, loss of back reflection. Surface conditions of the billet influence the loss of back reflection to a great extent and a slight shift of the part will often eliminate what appeared to a large loss of back reflection. The fact casts doubt on the ability to correctly evaluate potential porous conditions in parts with non-parallel surfaces. Significant losses in back reflection, at least for a porous condition, must always be accompanied by an increase in the noise level between the front and back surface.

An additional 10 Ti6Al-6V-2Sn billets were ultrasonically inspected using the same method of calibration and equipment as used for the first lot, except that additional ASTM type reference standards having metal travels of 1/4, 1/2 and 3/4 inch were also use to establish the DAC. The sound entry and back surfaces of the billets had surface finishes from 125 to 350 RHR. **Special** attention was given to any loss of back reflection and also significant indications between the front and back surface indications. One billet of the 10, in particular, appeared to have rejectable indications 1/2" to 1" below the front surface. These indications were thought to be too far from the front surface to be due to surface condition, and visually the surface seemed satisfactory for an ultrasonic test. Nevertheless, it was decided that a test should be made to definitely establish that the indications were not due to surface imperfections. The following test was made:

- (1) The billet with the greatest rejectable indications between front and back surface was selected. The areas in question on the billet were pinpointed by marking the billet with a steel stamp.
- (2) The surface of the billet was machined (without entirely removing the steel stamping) to a 32 RHR surface finish.
- (3) The billet was retested ultrasonically and the original rejectable indications between the front and back surface had disappeared.

As a result of this special test, all billets of the lot of 10 billets were routed to the machine shop for clean-up of the surface to a finish of 32 to 63 RHR. After surface improvement, the billets were again tested ultrasonically and found to be acceptable if the back reflection was monitored in saturation, but were rejectable if a second test for back reflection measurement only was performed with the back reflection **at a reduced level. In the second test, the back reflection in the center** of the billets was set at 90 to 95% of full CRT height; and as the search

unit removed toward the edge of the billets, the back surface response dropped to below 45% of full CRT height. No single indications were rejectable. Because porosity had previously escaped detection by ultrasonics, it was decided to send one billet from the lot of 10 to the chemical milling department for a ten second surface etch. (On the previous lot of billets, surface etching had been used to expose porosity). This etch did bring out a porous condition in the billet; and this condition was considered unacceptable.

A subsequent study of the amount of etching required resulted in the following conclusions. If visual methods were to be employed in evaluation, an etch removing about 0.010 inches optimum. If a fluorescent dye penetrant evaluation is to be performed, then a 0.002 inch metal removal is satisfactory for detecting the porosity.

#### b. Radiographic Method

Radiographic techniques using ASTM Class I film and low kilovoltage/high contrast techniques were also used to try and detect the porosity in selected 4 1/2 inch thick billets. It was assumed that since the porosity was concentrated along the edges of the billets, the part's radiographic image would indicate an area of greater part density in the center of the billets. No measurable film density difference was obtained, however, in the resulting radiographs. Image quality of 2-1T was insufficient for detecting individual pores. Note that for a 4 1/2 inch thick section, a 2% contrast only implies a resolution of a 0.090 inch thickness change. The pores were less than 0.020 inches diameter. The evaluation of a 2 inch billet section containing porosity also did not reveal any radiographic indication of changes in density or presence of pores.

#### c. Penetrant Method

Each section from the three billets was etched to remove .010 inch from each surface to ensure removal of any disturbed surface metal resulting from the sawcutting operation. Next, the sections were trichlorethylene vapor degreased for 16 hours and penetrant inspected in the laboratory using Tracer-Tech P-133 fluorescent water washable penetrant and Tracer-Tech D499C nonaqueous wet developer. This penetrant system is equivalent in sensitivity to a MIL-I-25135, Group VI System. A penetrant dwell time of 10 minutes was used. Excess penetrant was removed using a hand held Tri-Con 400501 water spray nozzle with the spray directed normal to the surface; the wash water temperature was approximately 70°F and the wash water pressure was approximately 40 psi. The specimens were washed until clean under 200 microwatts/cm<sup>2</sup> of ultraviolet light. Next, the specimens were dried for 20 minutes in a circulating air oven at 170°F. After a bleed-out time of 5 minutes, the penetrant indications were photographed (see Figure 111) using the following parameters: approximately 1000 microwatts per cm<sup>2</sup> of ultraviolet light, 25 second exposure at f9, Royal Pan Film, Tiffin Yellow No. 2 filter. Next, several of the porosity indications were examined at 200X under a light microscope (Unitron TMD 3370) and the diameters of the pores were measured. The measured diameters are listed in Table 83. The diameter of those pores which were detectable by penetrant inspection varied from 0.0025 to 0.016 inch. As can be seen in View B of Figure 107, several of the pores had considerable depth. At a magnification of 200X, the depth was measured to vary from 0.033 to 0.106 inch long.

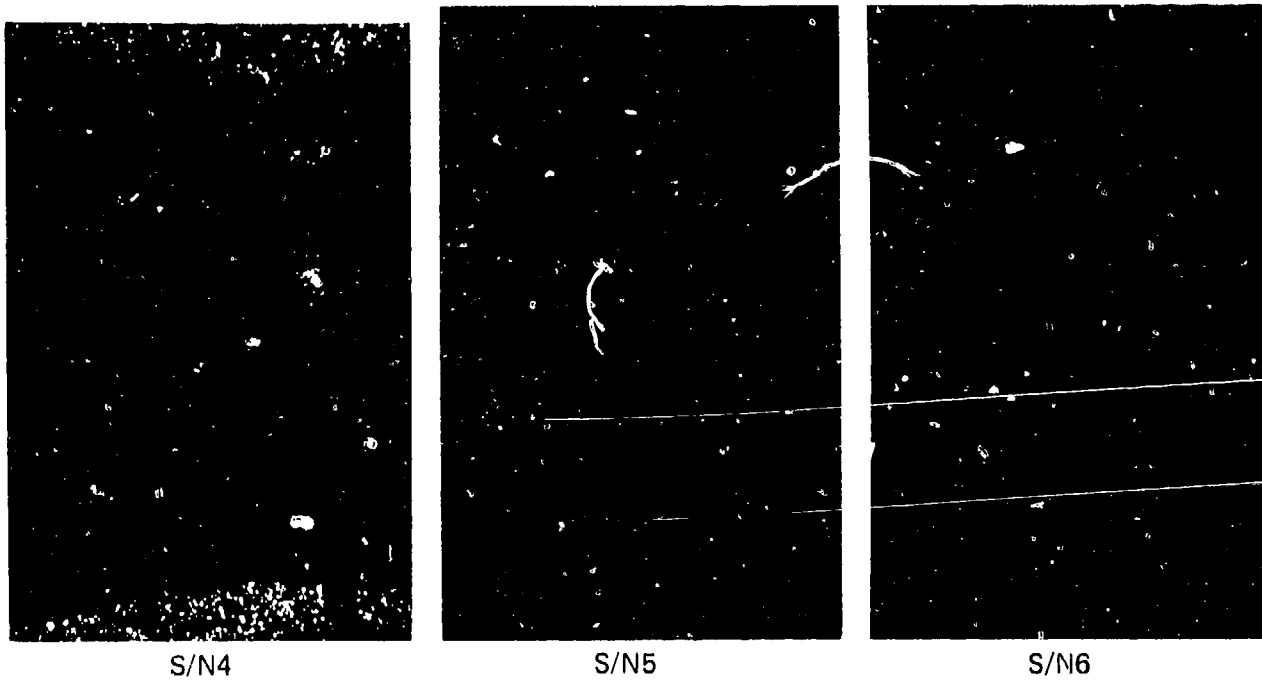


FIGURE 108  
PENETRANT INDICATIONS OF POROSITY

GP74 0117 230

TABLE 83  
POROSITY DIAMETERS

Specimen	Porosity Diameter (in.)	Specimen	Porosity Diameter (in.)	Specimen	Porosity Diameter (in.)
S/N4	0.0025	S/N5	0.0045	S/N6	0.0025
	0.003		0.005		0.0043
	0.005		0.005		0.0045
	0.006		0.005		0.0045
	0.006		0.006		0.0045
	0.0065		0.007		0.0045
	0.012		0.009		0.008
	0.013				0.008
	0.016				0.009
			0.009		

GP74 0117 218

### 3. INTERNAL CRACKS

#### a. Specimen Fabrication

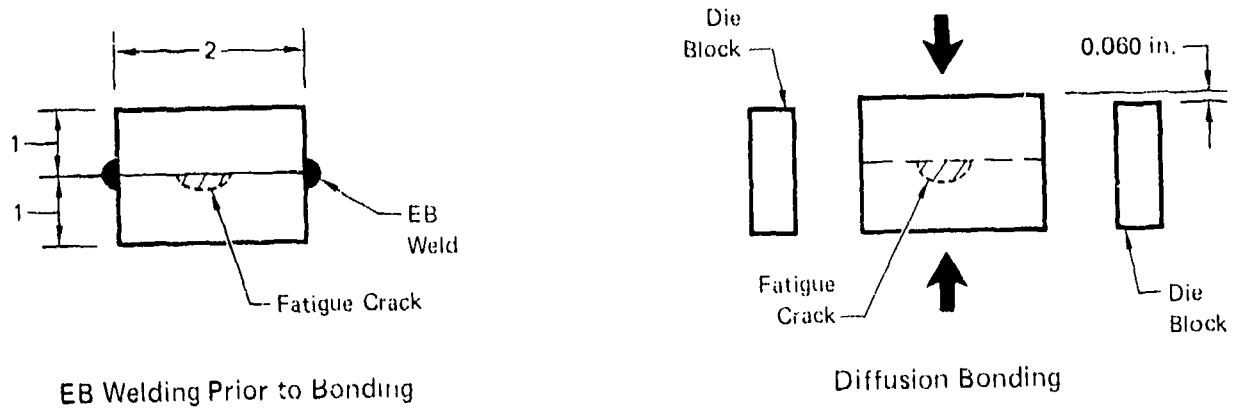
Each specimen was fabricated by initially cutting 2 x 5 inch blanks from 1 inch thick Ti-6Al-4V plate and grinding the 2 x 5 inch face on each to a 16 rms finish. Rectangular EDM slots were then located on the ground 2 x 5 inch faces with the long dimension of the slot parallel to the 2 inch dimension. The slots serve as crack initiation sites and varied from .005 deep x .015 long to .010 deep x .100 long depending upon the size of the crack desired. A fatigue crack was generated from each EDM slot by fatiguing in 3 point bending with 67,000 psi stress at the block surface. The crack growth was monitored optically and was controlled to the desired length. Next, the EDM slot was removed by grinding, leaving only the fatigue crack. The length of the fatigue crack was again measured at high magnification. A cap, 1 x 2 x 5 inches, was mated to the cracked specimen and the two were diffusion bonded together (see Figure 109). Prior to diffusion bonding, the ground face of each block was etched to clean the mating surfaces in preparation for bonding. The two blocks were initially joined by electron beam welding in a vacuum as shown in Figure 109. The cracked block and the cap were diffusion bonded together in a vacuum at 1710-174 F for approximately 1 hour under a load that was slowly increased from zero to approximately 2.5 tons. Die blocks were used to restrict the reduction in thickness to .060 inch.

A list of the specimens with the crack lengths prior to bonding is presented in Table 84.

**TABLE 84**  
**CRACK LENGTHS BEFORE BONDING IN INTERNALLY**  
**CRACKED SPECIMENS**

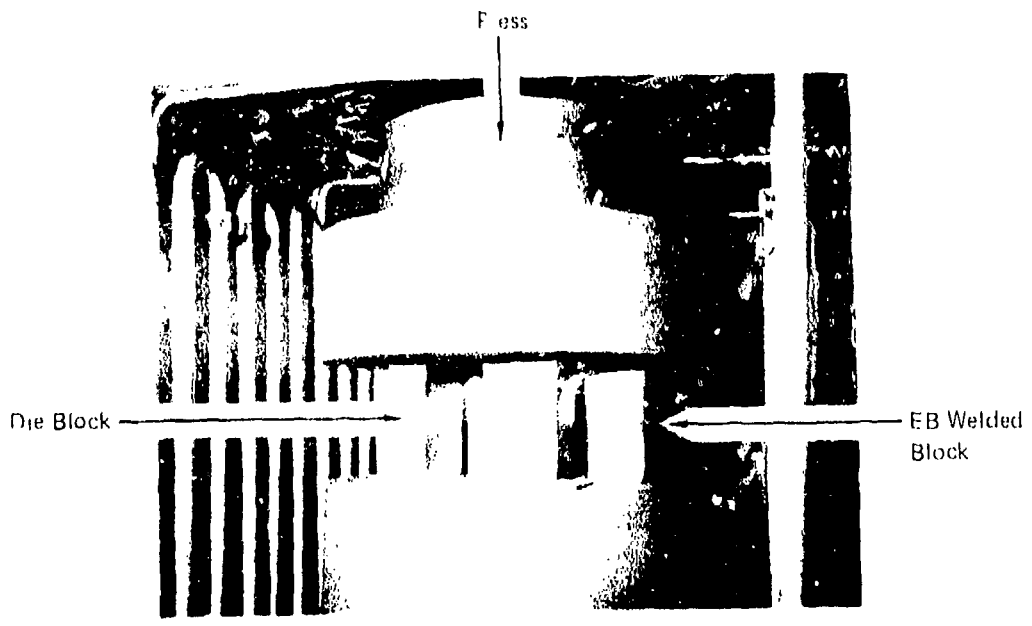
Specimen	Elox Size (in.)	Crack Length (in.)	Specimen	Elox Size (in.)	Crack Length (in.)
A1	0.030 Deep x 0.100 Long	0.231	12	0.010 Deep x 0.060 Long	0.124
A4	0.010 x 0.030	0.059	14	0.010 x 0.060	0.114
A6	0.008 x 0.020	0.032	28	0.010 x 0.060	0.108
A8	0.025 x 0.080	0.123	16	0.010 x 0.100	0.286
A11	0.030 x 0.100	0.505	17	0.010 x 0.100	0.281
A14	0.030 x 0.100	0.368	18	0.010 x 0.100	0.269
26	0.005 x 0.015	0.020	29	0.010 x 0.100	0.268
27	0.010 x 0.030	0.048	20	0.010 x 0.100	0.285
7	0.010 x 0.030	0.054	21	0.010 x 0.100	0.536
8	0.010 x 0.030	0.050	22	0.010 x 0.100	0.561
10	0.010 x 0.030	0.055	24	0.010 x 0.100	0.632
11	0.010 x 0.060	0.104	25	0.010 x 0.100	0.598
13	0.010 x 0.060	0.124			

GP 74 0117 40



EB Welding Prior to Bonding

Diffusion Bonding



Photograph of Diffusion Bonding Set-Up

FIGURE 109  
DIFFUSION BONDING OF INTERNALLY CRACKED SPECIMENS

GP 77 0117 215

## b. Ultrasonic Testing

The specimens containing internal cracks were subjected to the test program summarized in Table 85. Initially, Specimen Numbers A1, A4, A6, A8, A11, and A14 were along with 3 uncracked dummy specimens immersion angle beam and immersion straight beam inspected by General Electric in their laboratory. A 3/4 inch diameter focused lithium sulfate 15 MHz search unit with a focal length of approximately 7 inches in water was used. A Branson 600 ultrasonic instrument was used to pulse the search unit at a frequency of 5 MHz. The water path was 6 inches and the scan index was 1/8 inch. For the angle beam inspection a sound beam angle of 45 degrees in the metal was used. The scanning was manual using a scan index of .090 inch.

An evaluation was made of the difference in sound transmission characteristics between the reference standard and a representative test specimen by monitoring back surface reflections. Since the gain setting at a particular amplitude in the reference standard was within 30 percent of the same amplitude back reflection in the test specimen, no correction was made during the actual testing.

The first series of tests were performed at a scanning gain established with the Ti-6Al-4V reference standard shown in Figure 110. The search unit was adjusted such that the responses from the side drilled holes at 3/8 and 1-1/2 inch metal travels were equal. Next, these responses were adjusted to 80 percent of saturation and the test specimens were scanned at that gain level. The amplitude of all discontinuities at that scanning gain were recorded. The sound beam angles for the various tests at that scanning gain are shown in Figure 111.

A second series of tests were performed by adding 12 dB of gain to the original gain level. For each discontinuity found, the search unit was manipulated to maximize the response and the signal amplitude was recorded. The results of the testing is shown in Table 86. Only Angle Beam Test No. 1 was successful among the angle beam tests in detecting cracks. This probably indicates, that, for the other tests, the cracks were not oriented favorably with respect to the sound beam such that the sound was not reflected back to the receiving search unit.

In addition, the straight beam testing was successful in detecting three of the cracks. The response from several of the cracks was relatively small. For example, the amplitude of the response from the .123 inch long crack was 15 percent of saturation with the straight beam test. Such small responses may result in acceptability of production parts, depending upon the acceptance criteria used. One explanation for the small response from such a relatively large crack is that, during the fabrication of the specimens, partial healing of the crack may have occurred during diffusion bonding and the actual crack length may be less than the expected crack length. There were no false indications recorded during the inspections. It should be pointed out that the small amplitudes recorded in Table 86 are approximations since it is not possible to accurately measure such small amplitudes from the CRT screen.

**TABLE 85**  
**SUMMARY OF ULTRASONIC TESTING OF INTERNALLY**  
**CRACKED SPECIMENS**

Testing Group	Test Method
Jet Engine	Lab - Straight Beam Immersion Lab - Angle Beam Immersion Production - Straight Beam Immersion Production - Angle Beam Immersion
Air Force Materials Laboratory	Lab - Angle Beam Immersion
Airframe	Lab - Straight Beam Immersion Lab - Straight Beam Contact

GP74 0117 50

**TABLE 36**  
**ENGINE ULTRASONIC INSPECTION (LABORATORY) RESULTS FOR**  
**INTERNAL CRACKS**

Specimen No.	Crack Length (in.) ④	Amplitude of Response (% of Saturation)			
		Straight Beam Test No. 1		Angle Beam Test No. 1	
		①	②	①	②
A1	0.231	No Response	No Response	No Response	③
A4	0.059	No Response	No Response	No Response	No Response
A6	0.032	No Response	No Response	No Response	No Response
A8	0.123	15%	60%	③	21%
A11	0.505	23%	100%	40%	100%
A14	0.368	45%	100%	65%	100%

① Scanning gain was established by setting the minimum response to 80% of full saturation.

② Scanning gain was established as above except 12 dB was added.

③ Response was too small to be measured.

④ Actual crack length may be less than shown due to partial healing during diffusion bonding.

GP74 0117 53

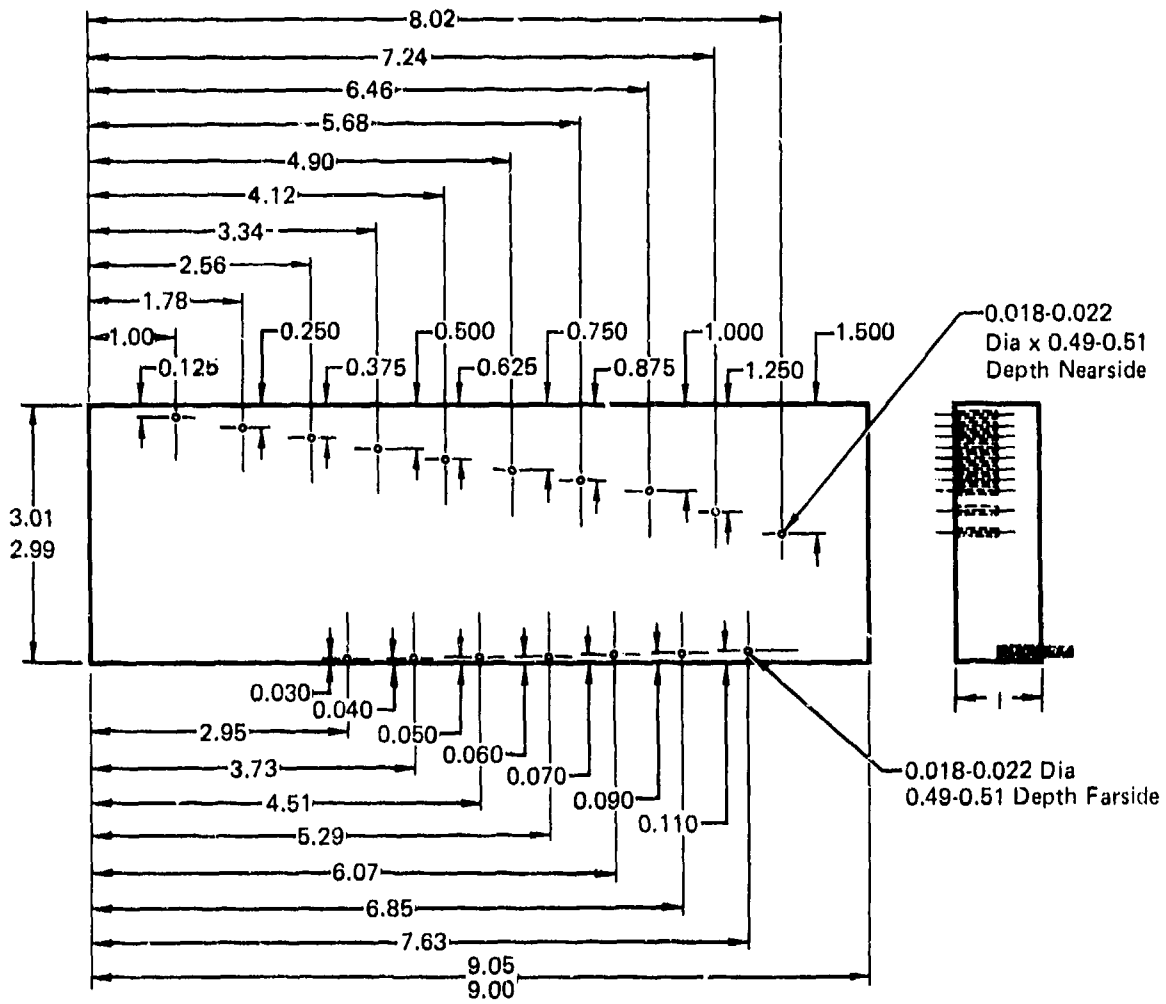
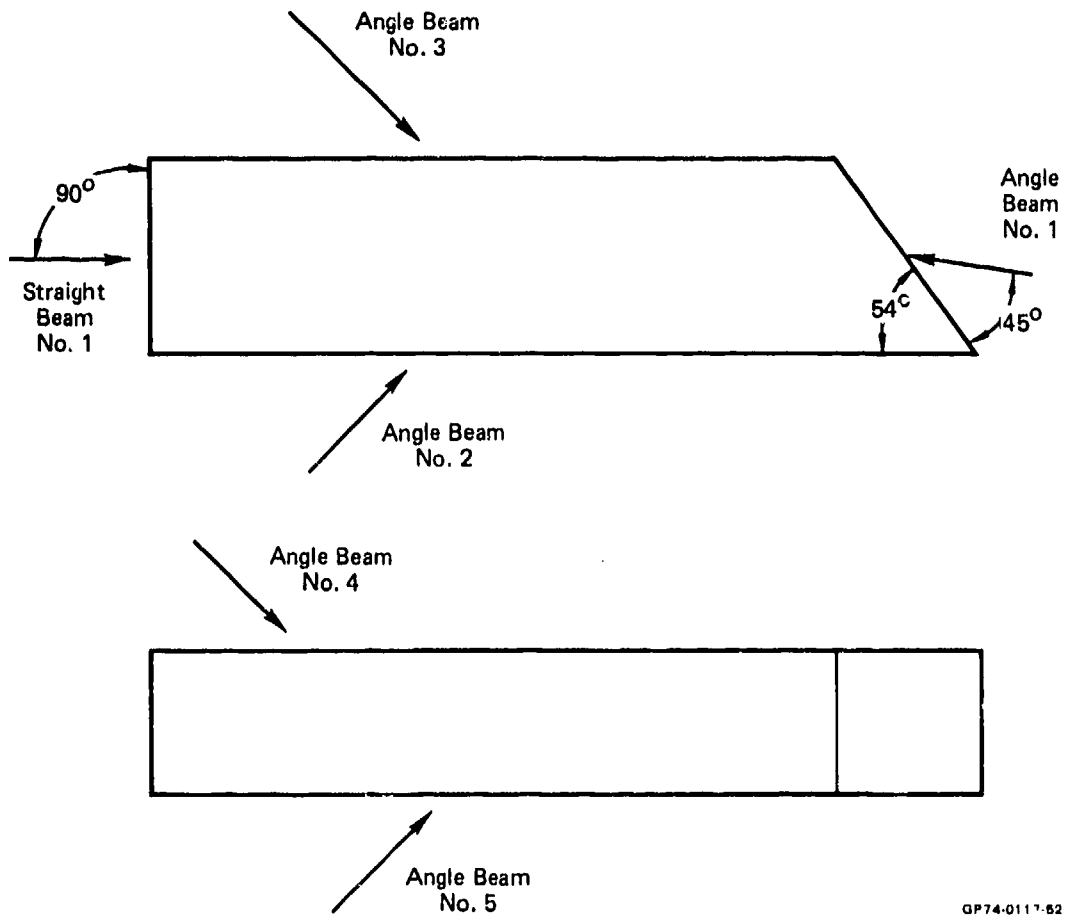


FIGURE 110  
REFERENCE STANDARD

GP74-0117-01



GP74-0117-52

**FIGURE 111**  
**SOUND BEAM ANGLE FOR GE LABORATORY INSPECTION**  
**OF INTERNAL CRACKS**

Following the laboratory inspection of the internal cracks, production ultrasonic inspections were made on the 6 cracked specimens and the 3 uncracked specimens using the normal production inspection facilities and personnel. The sound beam directions were the same as for the laboratory inspections. Each specimen was inspected 3 times by each of 3 inspectors. The results of the testing was shown in Tables 87 and 88. Of the angle beam tests, only Angle Beam No. 1 was successful.

In some cases, there was a large variation in response amplitude as recorded from one test to another for the same inspector. For example, for specimen A14 which has an original crack length of .368 inch. Inspector A recorded response amplitudes of 12%, 78% and 100% of saturation in 3 tests. In other cases, however, the 3 response amplitudes were approximately the same. As with the laboratory inspections, there were no false indications recorded.

For comparison purposes, the 6 cracked specimens and the 3 uncracked dummy specimens were ultrasonically inspected at the Air Force Materials Laboratory. A 1/2 inch diameter, lead zirconate titanate, 7 MHz search unit was used. This search unit was focused and had a focal length in water of approximately 6 to 9 inches. The test frequency was 5 MHz and a Branson 600 ultrasonic instrument was used. The water path was 2-1/2 inches and the scan index was 0.020 - 0.040 inches. The inspection procedure and reference standard was the same as used by the engine manufacturer. Two independent inspectors were used. A summary of the results is in Table 89. Of the angle beam tests, only Angle Beam No. 1 was successful.

**TABLE 87**  
**RESULTS OF ENGINE PRODUCTION STRAIGHT BEAM IMMERSION TESTS** <sup>1</sup>

Specimen	Crack Length (in.)	Response Amplitude (% of Saturation)								
		Inspector A			Inspector B			Inspector C		
		1	2	3	1	2	3	1	2	3
A6	0.032	—	—	—	—	—	—	—	—	—
A4	0.059	—	—	—	—	—	—	—	—	—
A8	0.123	15	12	8	8	5	8	12	12	10
A1	0.231	—	—	—	—	—	—	—	—	—
A14	0.368	12	Sat.	78	Sat.	18	50	35	30	32
A11	0.505	18	40	60	8	15	23	25	35	35

<sup>1</sup> Scanning gain was established by setting the minimum response to 80% of saturation.

GP74-0117-54

Specimen	Crack Length (in.)	Response Amplitude (% of Saturation)								
		Inspector A			Inspector B			Inspector C		
		1	2	3	1	2	3	1	2	3
A6	0.032									
A4	0.059									
A8	0.123	65	65	35	48	43	45	60	65	60
A1	0.231									
A14	0.368	59	Sat.	Sat.	Sat.	80	Sat.	Sat.	Sat.	95
A11	0.505	75	Sat.	Sat.	37	70	Sat.	90	Sat.	Sat.

<sup>1</sup> Scanning gain was established by setting the minimum response to 80% of saturation and subtracting 12 dB of attenuation.

GP74-0117-55

**TABLE 88**  
**RESULTS OF ENGINE IMMERSION ANGLE BEAM TESTS** 

Specimen	Crack Length (in.)	Response Amplitude (% of Saturation)								
		Inspector A			Inspector B			Inspector C		
		1	2	3	1	2	3	1	2	3
A6	0.032									
A4	0.059									
A8	0.123	10	10	12	5	9	5	5	12	13
A1	0.231									
A14	0.368	61	46	60	57	62	10	Sat.	Sat.	Sat.
A11	0.505	25	30	30	33	47	60	72	70	75

 Scanning gain was established by adjusting the minimum response to 80% of saturation.

GP74-0117 56

Specimen	Crack Length (in.)	Response Amplitude (% of Saturation)								
		Inspector A			Inspector B			Inspector C		
		1	2	3	1	2	3	1	2	3
A6	0.032									
A4	0.059									
A8	0.123	47	55	62	35	50	28	30	65	65
A1	0.231									
A14	0.368	Sat.	Sat.	Sat.	Sat.	Sat.	40	Sat.	Sat.	Sat.
A11	0.505	Sat.	Sat.	Sat.	Sat.	Sat.	Sat.	Sat.	Sat.	Sat.

 Scanning gain was established by adjusting the minimum response to 80% of saturation and subtracting 12 dB of attenuation.

GP74 01:7 57

**TABLE 89  
RESULTS OF AFML LABORATORY ULTRASONIC INSPECTIONS**

Specimen	Crack Length (in.)	Response Amplitude (% of Saturation)			
		Angle Beam			
		Inspector 1		Inspector 2	
		△1	△2	△1	△2
A6	0.032	0	0	0	0
A4	0.059	0	0	0	0
A8	0.123	0	50	0	70
A1	0.231	0	0	0	0
A14	0.368	63	Saturation	32	Saturation
A11	0.505	48	Saturation	20	80

△1 Scanning gain was established by setting the minimum response to 80% of saturation.

△2 Scanning gain was established by setting the minimum response to 80% of saturation and subtracting 12 dB of attenuation.

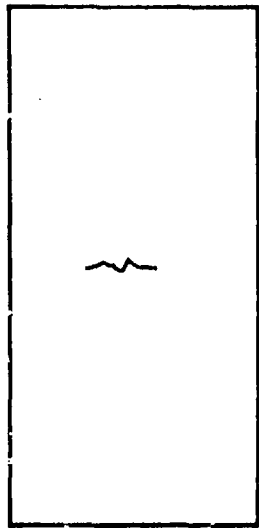
GP/4 0117 58

All the specimens listed in Table 84 were straight beam immersion inspected in the laboratory at the airframe manufacturer. A flat 3/4 inch diameter, 5 MHz SIZ search unit (S/N 21269) was used in conjunction with a Branson 600 ultrasonic instrument and a 623Ts pulse/receiver. A 3 inch water path was used and this water path was maintained to  $\pm 1/8$  inch between the reference standards and the test parts, the reference standards used were typical ASTM-type standards with 3/64 inch diameter flat bottom holes as reflectors. The reference standard material was Ti-6Al-4V. An adjustment was made for the difference in sound transmission characteristics between the reference standard and the test piece by comparing the dB difference in back reflection through the 5 inches of metal in the test specimen and through the 5 inch metal travel reference standard. It was found that the difference was 1 dB per inch of metal travel. Next, the metal travel of each reference standard was multiplied by 1 dB per inch in order to arrive at the required correction factors. Next, the 3/64 inch diameter flat bottom hole in the reference standard exhibiting the maximum response in the set was adjusted to 80% of saturation. The responses from the other reference standards were mathematically adjusted using the correction factors and marked on the CRT screen to form a DAC curve. For scanning purposes, an additional 6 dB of attenuation was subtracted for greater sensitivity.

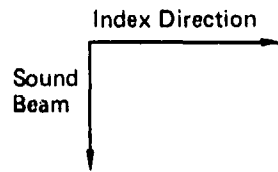
The scan index used was 0.25 inch. The scan index was checked on the reference standard to determine that at the extreme ends of the scan index, the response was greater than 50 percent of the maximum response from the 3/64 inch diameter flat bottom hole in the reference standard at a 3 inch metal travel. Each test part was manually scanned as shown in Figure 112. For all discontinuities with amplitude greater than 50% of the DAC, the search unit was manipulated to maximize the response, the scanning gain was reduced by 6 dB and the amplitude was recorded as a percentage of the DAC curve height. In a normal production inspection, only those discontinuities whose amplitude equalled or exceeded the DAC curve would be rejected.

The results of the laboratory inspection is shown in Table 90. Photographs of typical cathode ray tube presentations are shown in Figure 113. As had occurred in some of the previous testing, there were cases where the ultrasonic response versus crack length before bonding did not follow the expected pattern. For example, in Specimen 9 the response was 50% of the DAC and in Specimen 12 the response was 20% of the DAC, even though the crack length prior to bonding was twice that in Specimen 9. This could occur if partial healing of the cracks took place during diffusion bonding. Subsequent destructive analysis of the cracks in Specimen Numbers 11, A1, and A4 failed to reveal any evidence that the cracks survived the diffusion bonding operation. The smallest crack detected during the testing had a crack length prior to bonding of .048 inch (Specimen 27).

Following the straight beam immersion tests, a laboratory straight beam contact test was performed upon each specimen. A 3/4 inch diameter, 5 MHz, SFZ search unit (S/N 11356) was used along with a Branson 600 instrument. The specimens were checked for difference in sound transmission characteristics from the reference standards as before. The difference was small enough to ignore. The specimens were scanned with the



Type A Specimen



Type B Specimen

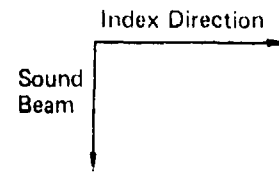


**FIGURE 112**  
**SETUP FOR STRAIGHT BEAM IMMERSION TESTING OF**  
**INTERNALLY CRACKED SPECIMENS**

GP/4 0117-59

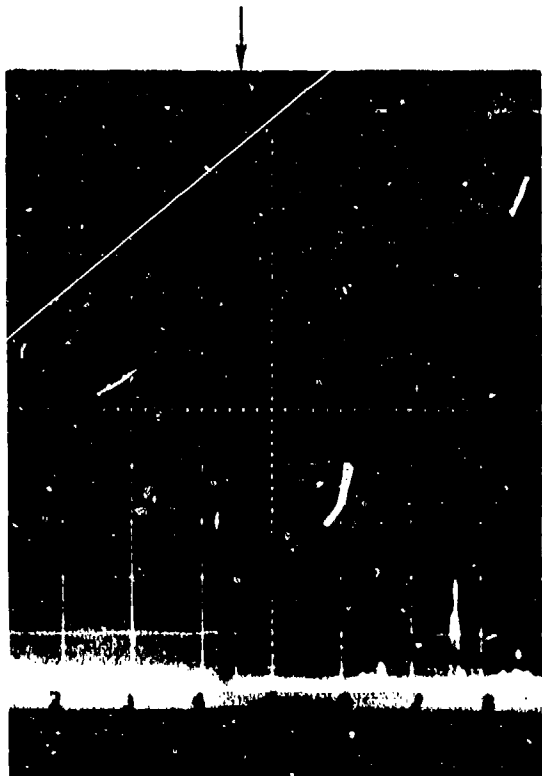
**TABLE 90**  
**ULTRASONIC INSPECTION RESULTS (AIRFRAME) FOR INTERNAL CRACKS**

Crack Length Before Bonding (in.) <sup>2</sup>	Specimen No.	Ultrasonic Response (%DAC)	
		Straight Beam Immersion	Contact Straight Beam
0.020	26	No Response	No Response
0.032	A6	No Response	No Response
0.048	27	30%	No Response
0.050	8	30%	No Response
0.052	9	50%	No Response
0.055	10	No Response	No Response
0.059	A4	No Response	No Response
0.104	11	60%	Saturated <sup>1</sup>
0.108	28	30%	100% <sup>1</sup>
0.114	14	40%	No Response
0.123	A8	Saturated <sup>1</sup>	80%
0.124	12	20%	No Response
0.124	13	30%	No Response
0.231	A1	25%	No Response
0.268	29	100% <sup>1</sup>	No Response
0.269	18	25%	No Response
0.281	17	20%	No Response
0.285	20	40%	100% <sup>1</sup>
0.286	16	30%	No Response
0.368	A14	Saturated <sup>1</sup>	Saturated <sup>1</sup>
0.505	A11	Saturated <sup>1</sup>	Saturated <sup>1</sup>
0.536	21	160% <sup>1</sup>	Saturated <sup>1</sup>
0.561	22	100% <sup>1</sup>	Saturated <sup>1</sup>
0.598	25	100% <sup>1</sup>	-
0.632	24	50%	100% <sup>1</sup>
Uncracked	23	No Response	No Response
Dummies	33	No Response	No Response
	38	No Response	No Response
	39	No Response	No Response

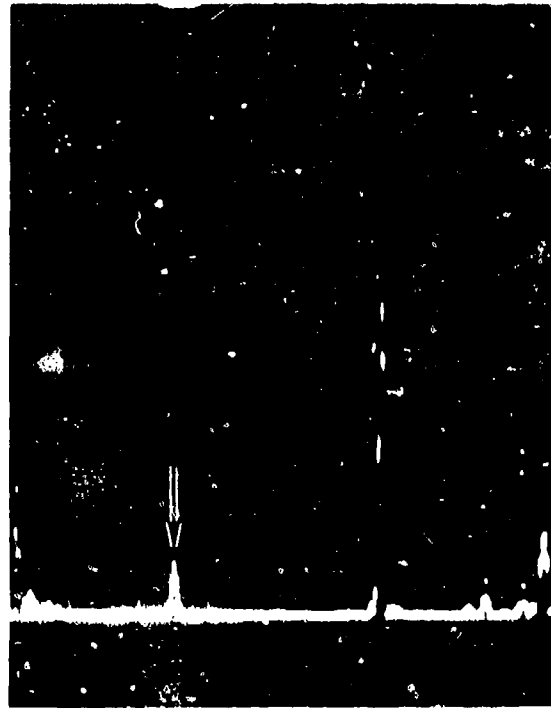
<sup>1</sup> If the rejection criteria would be to reject all parts with cracks whose response was equal to or greater than the DAC curve, these parts would be rejected.

<sup>2</sup> Actual crack may be less than the shown length because of partial healing during bonding.

QP74-0117-80



Saturated Signal from 0.505 In. Long Crack  
(Specimen A11)



Signal from 0.23 In. Long Crack in Specimen A1  
(Signal is 25% of DAC Curve)

GP/4-0117-81

**FIGURE 113**  
**TYPICAL RESPONSES FROM INTERNAL CRACKS DURING STRAIGHT**  
**BEAM IMMERSION TESTS**

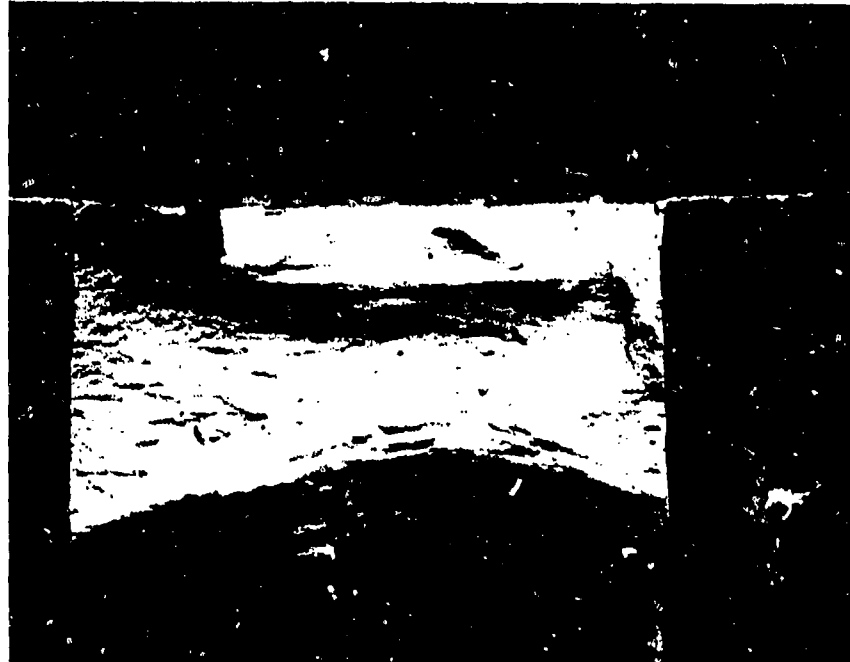
sound beam direction the same as in the immersion tests. The couplant was "Lubriplate" grease. The results of the testing is shown in Table 90. As can be seen, the contact tests were not as effective as the immersion tests for detecting the cracks. Eleven cracks detected by the immersion method were not detected by the contact method. These cracks ranged in length (prior to diffusion bonding) from .048 to .286 inches. Of course, the present length of these cracks may be less than the length prior to bonding.

c. Verification of Internal Crack Size

Two of the internal cracks used in the program were intentionally exposed in order to measure their actual size. Saw cuts were made adjacent to the cracks and the specimens were intentionally failed by overload. The fracture surfaces were examined and the actual length and depth of each fatigue crack was measured. The measured crack dimensions are recorded below and representative photographs appear in Figure 114.

<u>Specimen No.</u>	<u>Target Crack Length (Inches)</u>	<u>Actual Length (Inches)</u>	<u>Actual Depth (Inches)</u>
20	.285	.37	.075
21	.536	.56	.140

Three other specimens containing internal cracks were cross sectioned and examined metallographically to locate the cracks. These specimens, Numbers 12, A1, and A4, were selected because the ultrasonic response from the cracks were quite low or zero and it was desired to determine if partial healing of the cracks had occurred during diffusion bonding. Each cross section was polished several times and there was no evidence of cracks in any of the cross sections. Based on this, it appears that these cracks either partially or totally healed during diffusion bonding which explains the lack of significant ultrasonic response from these specimens.



Specimen 20  
0.37 In. Long x 0.075 In. Deep

4X



Specimen 21  
0.56 In. Long x 0.140 In. Deep

4X

CP74 0117 62

FIGURE 114  
PHOTOGRAPHS OF FRACTURE SURFACE OF INTERNAL CRACKS

#### 4. SEGREGATES - JET ENGINE DISK FORGINGS

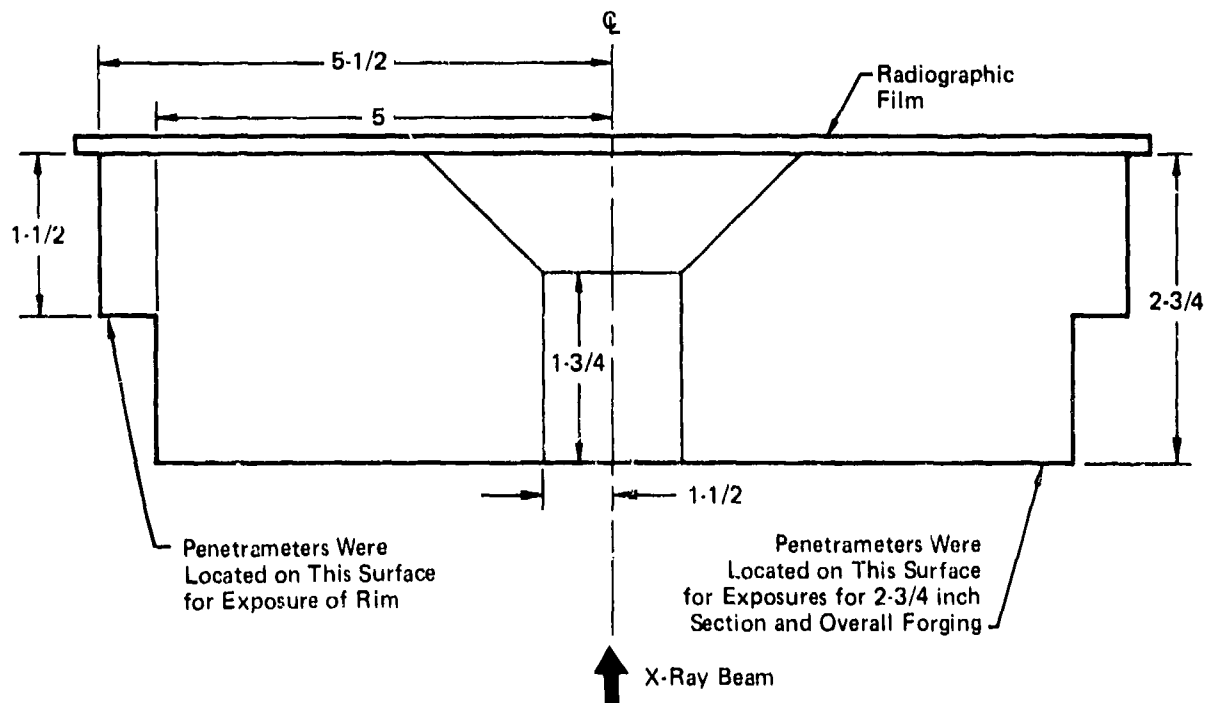
##### a. Radiographic Inspection

Disk forging No's 4, 5, and 6 from the ingot bottom and No's 7, 8, and 9 from the ingot top were inspected radiographically by the engine manufacturer. Production X-ray interpreters, qualified to MIL-STD-453, were used to interpret the films. The forgings had been machined to a 125 rms or better finish. First, two exposures were made of each forging with a G.E. OX-250 X-ray machine to examine the 2 3/4 inch thick area. The parameters shown in Table 91 were used. MIL-STD-453 2 percent thickness titanium penetrameters were used as image quality indicators and were placed on the source side of the forgings (see Figure 115). Each exposure was made with the X-ray beam centered at the forging center. The film was processed manually. The geometric unsharpness was .385 mm. Examination of the GAF 400 film indicated that the 1T hole in the 1 1/2 inch penetrameter was visible resulting in an equivalent sensitivity of 1.4 percent. When the GAF 100 and GAF 400 films were placed together and examined, the 1T hole was visible in the 1 1/2 inch penetrameter. The overall film density was 2.4 to 2.6 H and D when the two films were viewed together and 1.9 to 2.1 H and D where the GAF 400 film was viewed separately. For the NDT 55 film, the overall density was 2.3 to 2.5 H and D and the 1T hole was visible. When these films were examined for evidence of discontinuities, the rim section was not examined. Two additional exposures were made to examine the rim section and the thin section in the center of the forging. (see Table 91). Again a G.E. OX-250 X-ray machine was used. One inch titanium penetrameters were placed on the rim for Exposure 1. Exposure 2, made at a separate facility, was made with a 3 inch titanium penetrameter since a 1 inch penetrameter was not available. The overall film density ranged from 1.5 H and D at the rim to 3.2 in the center section for the GAF 400 film and 1.9 in the rim section for the NDT 55 film. The 2T penetrameter hole was visible on the GAF 400 film and the 1T hole was visible on the NDT 55 film resulting in an equivalent sensitivity of 1.4 percent.

Finally, an exposure was made of the entire forging using a Vandergraf in order to examine the entire forging on one radiograph. The overall film density varied from 2.8 to 3.1 H and D and the geometric unsharpness was 0.155 mm.

There was no evidence of segregates discernible in any of the films.

Following the radiographic inspections, forging No's 4, 5, 8, and 9 were sent to the Air Force Materials Laboratory for radiographic inspection. One exposure was made of each forging with a Norelco PC-300 X-ray machine. A kilovoltage of 280 KVP and a 10 m.a./6 minute exposure were used. The film was Kodak M and a .010 inch thick lead front screen was used along with a .010 inch thick lead back screen. The source-to-film distance was 43 inches and the geometric unsharpness was .011 inch. Three inch titanium MIL-STD-453 penetrameters were placed on the source side of the forging during each exposure. Each



GP74 0117 260

**FIGURE 115**  
**RADIOGRAPHY OF DISK FORGINGS**

**TABLE 91**  
**JET ENGINE MANUFACTURER LABORATORY DISK X-RAY INSPECTION PARAMETERS**

	2-3/4 in. Section		Rim Section		Entire Forging
	Exposure 1	Exposure 2	Exposure 1	Exposure 2	
KVP.....	250	250	250	250	1500
MA.....	10	10	10	10	10
Time (min).....	8	6	3	2-1/6	2-5/11
Film.....	GAF 100 and 400	NDT 55	GAF 400	NDT 55	NDT 55
Screens (Lead) Front (min).....	0.005 in.	0.010 in.	0.005 in.	0.010 in.	0.010 in.
Back (min).....	0.010 in.	0.010 in.	0.010 in.	0.010 in.	0.010 in.
Source-to-Film Distance.....	36 in.	38 in.	36 in.	48 in.	42 in.
Developing (min).....	8	5	8	5	7

GP74 2117 249

film was processed manually and examined by an interpreter qualified to MIL-STD-453. The overall film density was approximately 2.0 H and D density units and the 1T hole was visible in the penetrometer image or through the 2 3/4 inch thickness resulting in an equivalent sensitivity of 1.53 percent.

As in the case of the investigation by the engine manufacturer, there was no evidence of any segregates discernible.

#### b. Penetrant Inspection

A laboratory fluorescent penetrant inspection was carried out on the 6 disk forgings at the engine manufacturer. The specimens were swabbed with alcohol as a cleaning method prior to application of the penetrant. The penetrant, Magnaflux ZL-22A which is a MIL-I-25.35, Group VI post-emulsifiable penetrant, was allowed to dwell on the forgings for 30 minutes. Excess penetrant was washed from the forgings by a water spray at 45 psi and the water temperature varied from 78°F to 85°F and the washing time varied from 55 seconds to 105 seconds. Next, the forgings were oven dried at 136°F - 168°F for 10 minutes prior to application of the Magnaflux ZP-4A dry powder developer. A minimum of 5 minutes was allowed for development. The forgings were examined in a darkened booth with 1,100 microwatts per cm<sup>2</sup> of ultraviolet light intensity at the forging surface.

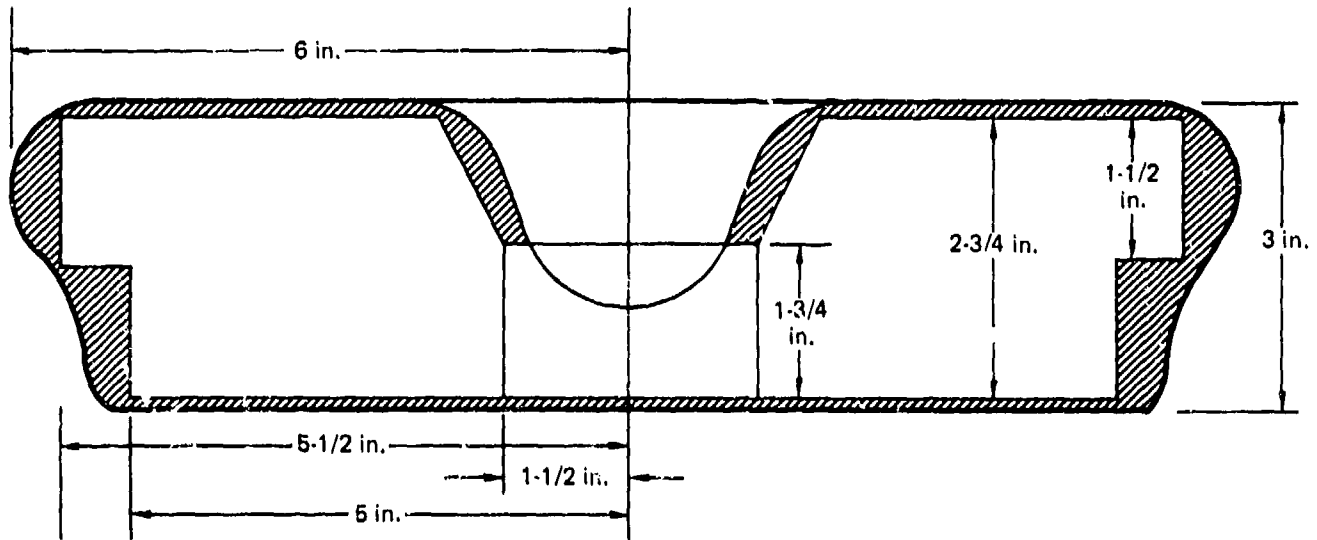
A second penetrant inspection was performed on the forgings with Magnaflux ZL-30A post emulsifiable penetrant. Prior to the second inspection, the forgings were again cleaned by swabbing with alcohol. A penetrant dwell time of 30 minutes was used prior to emulsification with Magnaflux ZE-4A for 1 minute. Excess penetrant was removed by spray washing at 50 psi and a water temperature of 70°F - 91°F. The washing time was 10 seconds. After washing, the forgings were oven dried at 140°F - 150°F for 10 minutes before application of the Magnaflux ZP-4A dry powder developer. A minimum of 5 minutes was allowed for development. The forgings were examined in a darkened booth with 1,100 microwatts per cm<sup>2</sup> of ultraviolet light intensity at the inspection surface.

There were no relevant penetrant indications detected during the two inspections. The only indication was from burrs and machine tears.

Next, the forgings were sent to the Air Force Materials Laboratory for penetrant inspection. The forgings were cleaned by trichloroethylene degreasing for 1 hour prior to immersion in Magnaflux ZL-22A fluorescent penetrant for 30 minutes. Emulsification with ZE-3 was performed for 30 seconds. After excess penetrant was washed from the surfaces, the forgings were dried for 5 minutes at 180°F. Next, Sherwin D-100 nonaqueous wet developer was applied for a minimal 5 minutes. As in the case of the engine inspections, there were no relevant penetrant indications.

#### c. Ultrasonic Inspection

Prior to ultrasonic inspection, the disk forgings were machined to a 125 rms or better surface finish as shown in Figure 11.5. After



GP74 0117 247

**FIGURE 116**  
**AREAS MACHINED ON DISK FORGING**

the machining operation, the forgings were subjected to ultrasonic inspections at the engine manufacturer and also at the Air Force Materials Laboratory (see Table 92).

Production inspection of the forgings at the engine manufacturer consisted of several straight and angle beam immersion inspections. A 1.5MHz 3/4 inch diameter lithium sulfate focused search unit with a focal length of 6 to 9 inches in water was used. The search unit was pulsed at 5MHz using a Branson 600 ultrasonic instrument. A waterpath of 6 inches was used for both the straight beam and angle beam inspections and a 1/8 inch scan index was chosen as a typical production inspection scan index. The indexing was automatic while the scanning was manual. The refracted sound beam angle in the metal was 45 degrees for the angle beam inspections.

#### Production Angle Beam Immersion Inspection

The search unit position with respect to the reference standard was adjusted so that the sound beam angle was 45 degrees in the metal. Next, the water path was adjusted to 6 inches to bring the focal point of the sound beam to the .020 inch diameter hole with the greatest metal travel. During calibration, the gain was adjusted to bring the hole response to 80 percent of saturation, 12 dB of attenuation was removed and the gain setting was recorded. Then, the search unit was moved to obtain responses from each of the other holes and their response was adjusted to 80 percent of saturation, 12 dB of attenuation was removed, and the gain setting was recorded. The scanning gain for the inspection of the test specimens was the highest recorded gain setting plus an additional 12 dB.

During the scanning of the test parts, all discontinuities with amplitudes greater than 40 percent of the corresponding reference standard response at the same metal travel distance were evaluated further by manipulating the search unit. If the response, at the "plus 12 dB" gain, exceeded 60 percent of the corresponding reference response, the discontinuity was recorded.

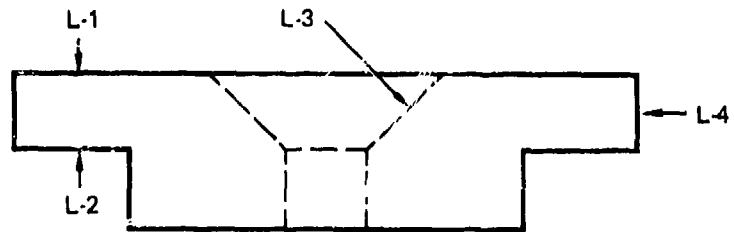
The reference standard used had similar sound transmission characteristics as compared to the forgings. The gain setting at a particular back reflection amplitude in the reference standard was within 30 percent of the same amplitude back reflection in the forging at the same metal travel.

The sound beam angles used in the angle beam inspection are shown in Figures 117 and 118. As can be seen, circumferential, axial, and radial shear were used. If, during initial calibration, it was found that it was not possible to inspect through the entire thickness of the forging, inspections were performed from opposite surfaces to ensure 100 percent inspection.

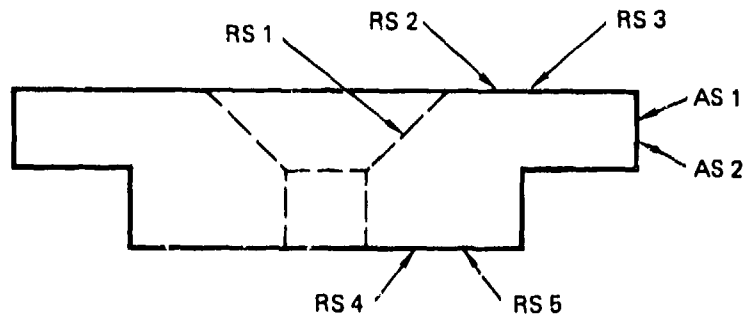
**TABLE 92**  
**SUMMARY OF ULTRASONIC INSPECTIONS OF DISK FORGINGS**

Forging No.	Location in Original Ingot	GE Production Inspection		AFML Inspection	
		A	B	A	B
4	Bottom	X	X		
5		X	X	X	X
6		X	X		
7	Top	X	X		
8		X	X		
9		X	X	X	X

GP74-0117-248



Straight Beam Inspection



Radial and Axial Shear Inspections

GP74 0117 242

**FIGURE 117**  
**SOUND BEAM DIRECTIONS FOR DISK FORGING INSPECTIONS**

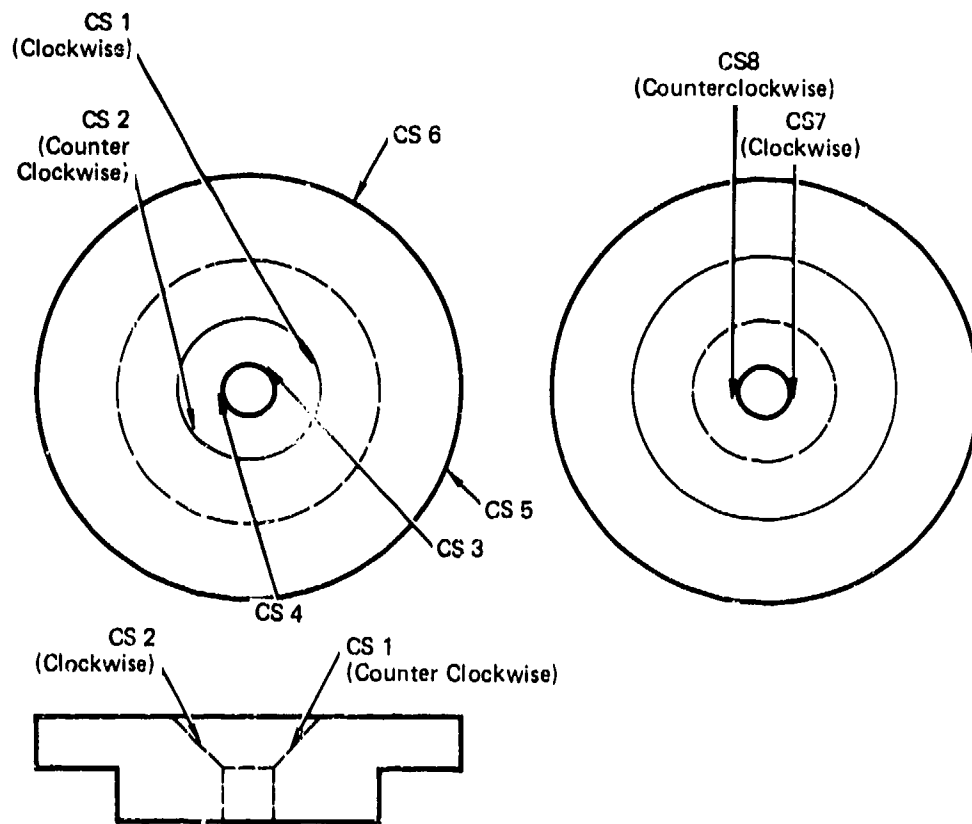


**FIGURE 118**  
**CIRCUMFERENTIAL SHEAR INSPECTION**

GP74 0526 12

### Production Straight Beam Immersion

Initially, the search unit was manipulated to maximize the response from the .020 inch diameter hole at a metal travel of 1/8 inch in the reference standard. Next, the water path was adjusted in order to produce an approximately equal response from the .020 inch diameter holes at 3/8 and 1 1/4 metal travels. The gain control was adjusted to bring the two responses to 80 percent of saturation, 12 dB of attenuation was removed, and the gain setting was recorded. The search unit was positioned over the remaining holes in the reference standard and the response was adjusted to 80 percent of saturation. Next, 12 dB of attenuation was removed and the gain setting was recorded. Finally, the scanning gain was obtained by adjusting the smallest hole response to 80 percent of saturation and removing an additional 12 dB of attenuation.

During the scanning of the test parts all discontinuities with amplitudes greater than 40 percent of the corresponding amplitude of the reference hole at the same metal travel were evaluated further by manipulating the search unit for maximum response. If the response, at the "plus 12 dB" gain, exceeded 60 percent of the corresponding reference response, the discontinuity was recorded.

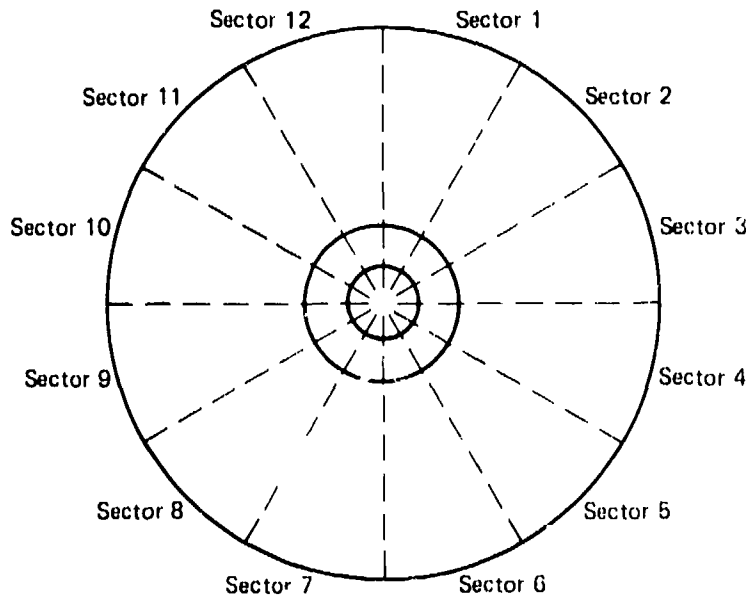
The results of the inspections are shown in Figures 119 and 120. A combined total for each inspector is presented in Figure 121.

As can be seen, there were only 2 indications as a result of the longitudinal wave inspection but many indications as a result of the shear wave inspections. This is true for both inspectors. This is similar to the results of the ultrasonic inspection of the ingot and 9 inch diameter billet where several indications were found using a shear wave that was not found using a longitudinal wave. These results may stem from the orientation of the discontinuities within the forgings. Also, since the wave length of shear waves is less than that of longitudinal waves (for a constant frequency), the resolution capability of shear waves is probably greater than with longitudinal waves. An examination of the data indicates that many more indications were located using radial shear than were located with axial or circumferential shear.

A comparison of the results for each inspector is shown in Figure 121. In each disk forging, Inspector B located more ultrasonic indications than did Inspector A. For example, for Disk Forging No 5, Inspector A located a total of 32 indications whereas Inspector B located a total of 183. It should be pointed out, however, that all 6 disk forgings would have been rejected by both inspectors according to the G.E. production acceptance criteria since rejection is not based on the quantity of discontinuities.

### AFML Inspection

Disks No 5 and 9 were straight beam immersion and angle beam immersion inspected at the Air Force Materials Laboratory using AFML personnel and equipment. For these inspections, a 1/2 inch diameter, Branson lead zirconate titanate 7 MHz search unit was used. This search



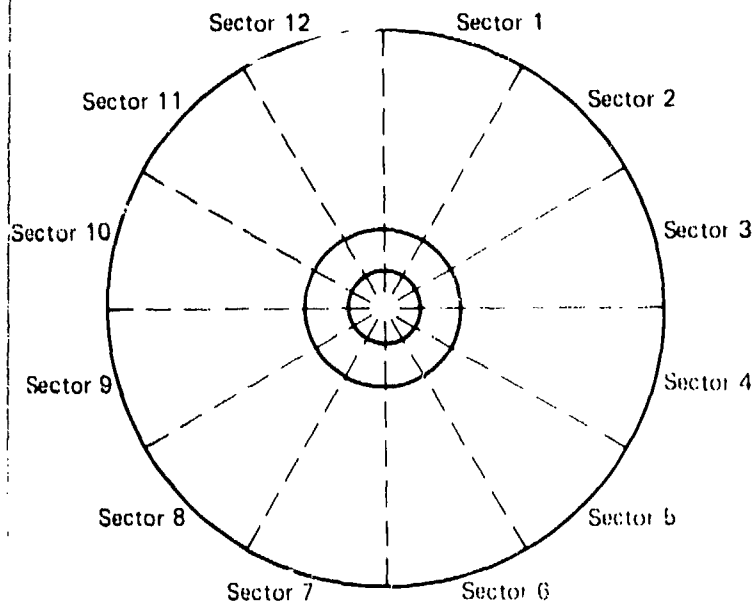
Forging No.	Total Longitudinal (L-1, L-2, L-3, and L-4)												
	Sector	1	2	3	4	5	6	7	8	9	10	11	12
4	0	0	0	2	0	0	0	0	0	0	0	0	0
5	0	0	0	0	0	0	0	0	0	0	0	0	0
6	0	0	0	0	0	0	0	0	0	0	0	0	0
7	0	0	0	0	0	0	0	0	0	0	0	0	0
8	0	0	0	0	0	0	0	0	0	0	0	0	0
9	0	0	0	0	0	0	0	0	0	0	0	0	0

Forging No.	Total Radial Shear (RS 1, RS 3 and RS 5)												Total Radial Shear (RS 2 and RS 4)												
	Sector	1	2	3	4	5	6	7	8	9	10	11	12	1	2	3	4	5	6	7	8	9	10	11	12
4	0	0	2	2	1	0	0	0	4	1	1	0	0	0	0	0	0	0	0	0	1	0	0	0	0
5	1	2	0	0	5	2	0	4	11	0	0	4	0	0	0	0	0	0	0	0	0	0	0	0	0
6	15	8	3	9	8	3	23	11	8	7	9	6	0	0	0	0	0	0	0	0	0	0	0	0	0
7	1	1	1	0	2	0	7	2	13	0	4	13	0	0	0	0	0	0	0	0	0	0	0	0	0
8	6	4	3	6	2	0	0	5	7	8	11	10	0	0	0	0	0	1	0	0	0	0	0	0	0
9	0	1	0	0	0	0	0	0	1	0	0	0	0	0	0	0	0	0	0	0	0	0	0	0	0

Forging No.	Total Circumferential Shear (CS 1, CS 2, CS 3, CS 4, CS 5, and CS 6)												Total Axial Shear (AS 1 and AS 2)												
	Sector	1	2	3	4	5	6	7	8	9	10	11	12	1	2	3	4	5	6	7	8	9	10	11	12
4	0	0	0	0	0	0	0	2	1	0	0	0	1	0	1	0	0	1	0	0	0	1	0	0	0
5	2	0	0	0	0	0	0	0	0	0	0	0	1	0	0	0	0	0	0	0	0	0	0	0	0
6	0	0	0	0	0	0	0	0	0	0	0	0	2	0	0	0	0	0	1	0	1	0	0	0	0
7	0	2	0	0	0	0	0	0	0	0	0	0	0	0	0	0	0	0	0	0	0	0	0	0	0
8	0	0	0	0	0	0	0	0	0	0	0	0	0	0	0	0	1	1	0	0	0	0	0	0	0
9	0	2	0	2	0	0	1	1	1	0	0	1	0	0	0	0	0	0	0	0	0	0	0	0	0

**FIGURE 119**  
**DEFECT LOCATION SUMMARY FOR ENGINE INSPECTOR A**

GP74 0117 245



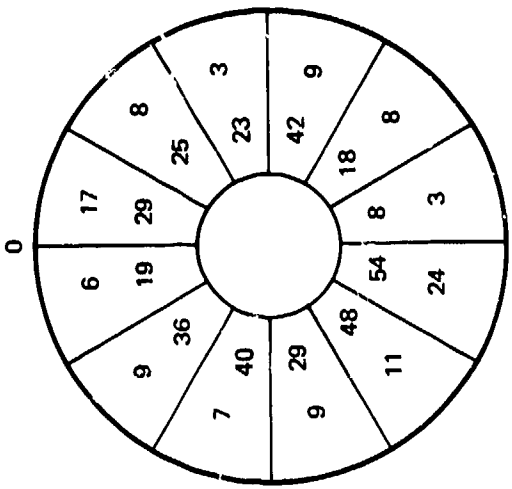
Forging No.	Total Longitudinal (L-1, L-2, L-3, and L-4)												
	Sector	1	2	3	4	5	6	7	8	9	10	11	12
4	0	0	0	0	0	0	0	0	0	0	0	0	0
5	0	0	0	0	0	0	0	0	0	0	0	0	0
6	0	0	0	0	0	0	0	0	0	0	0	0	0
7	0	0	0	0	0	0	0	0	0	0	0	0	0
8	0	0	0	0	0	0	0	0	0	0	0	0	0
9	0	0	0	0	0	0	0	0	0	0	0	0	0

Forging No.	Total Radial Shear (RS 1, RS 3 and RS 5)												Total Radial Shear (RS 2 and RS 4)												
	Sector	1	2	3	4	5	6	7	8	9	10	11	12	1	2	3	4	5	6	7	8	9	10	11	12
4	8	0	7	3	4	10	2	4	19	20	5	2	0	0	0	0	0	0	0	0	0	0	0	0	0
5	3	12	3	8	19	5	4	26	50	12	35	6	0	0	0	0	0	0	0	0	0	0	0	0	0
6	29	24	23	42	18	8	52	47	29	40	36	19	0	1	0	0	0	0	2	1	0	0	0	0	0
7	0	6	5	1	4	21	1	25	39	2	6	20	0	0	0	0	0	0	0	0	0	0	0	0	0
8	11	10	16	4	3	4	3	6	18	23	36	16	0	0	0	0	0	0	0	0	0	0	0	0	0
9	10	32	4	1	27	5	15	22	23	12	24	11	0	0	0	0	0	0	0	0	0	0	1	1	0

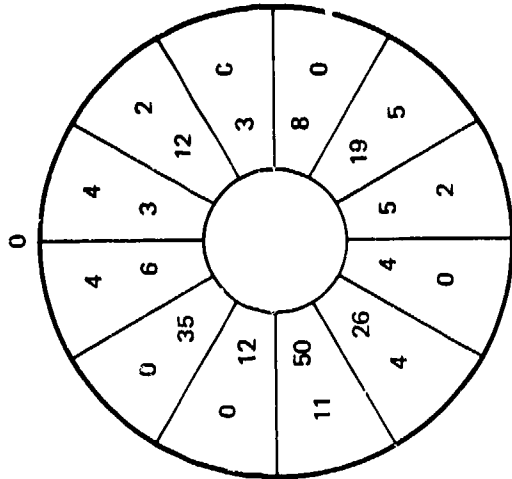
Forging No.	Total Circumferential Shear (CS 1, CS 2, CS 3, CS 4, CS 5, and CS 6)												Total Axial Shear (AS 1 and AS 2)												
	Sector	1	2	3	4	5	6	7	8	9	10	11	12	1	2	3	4	5	6	7	8	9	10	11	12
4	0	0	0	0	0	0	0	0	0	0	0	0	0	0	0	0	0	0	0	0	0	0	0	0	0
5	0	0	0	0	0	0	0	0	0	0	0	0	0	0	0	0	0	0	0	0	0	0	0	0	0
6	0	0	0	0	0	0	0	0	0	0	0	0	0	0	0	0	0	0	0	0	0	0	0	0	0
7	0	0	0	0	0	0	0	0	0	0	0	0	0	0	2	1	0	1	0	1	2	2	0	0	0
8	0	0	0	0	0	0	0	0	0	0	0	0	0	0	0	0	0	0	0	0	0	0	0	0	0
9	0	0	0	0	0	0	0	0	0	0	0	0	0	0	0	0	0	0	0	0	0	0	0	0	0

GP 74 0117 246

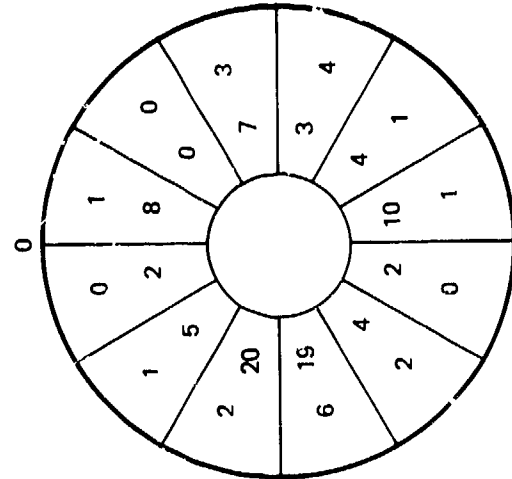
FIGURE 120  
DEFECT LOCATION SUMMARY FOR ENGINE INSPECTOR B



Disk No. 4

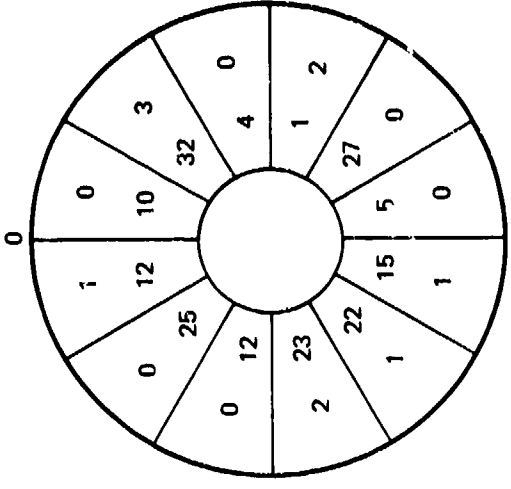


Disk No. 5

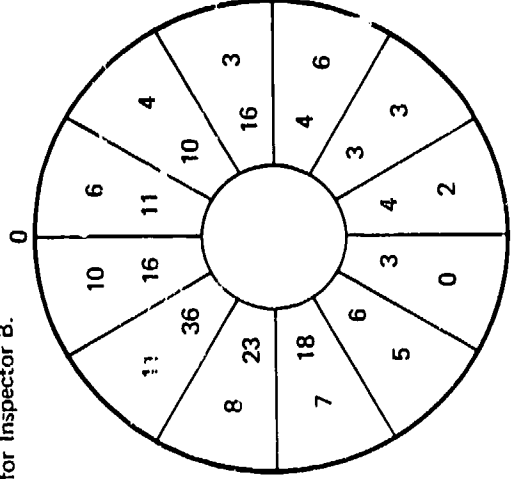


Disk No. 6

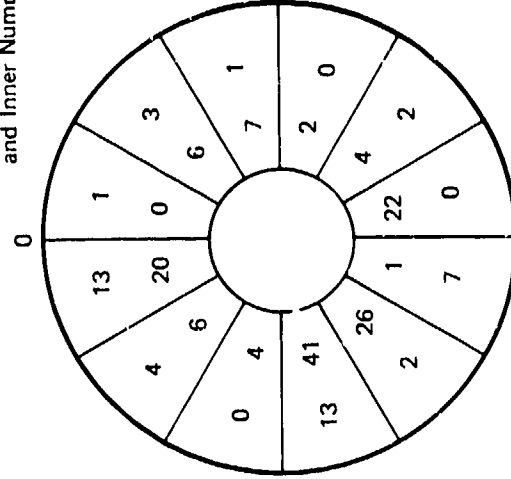
Outer Results are for Inspector A  
and Inner Numbers are for Inspector B.



Disk No. 7



Disk No. 8



Disk No. 9

FIGURE 121  
TOTAL ULTRASONIC INDICATIONS FROM GE PRODUCTION  
INSPECTIONS OF DISK FORGING

unit was focused and had a focal length in water of approximately 5 inches. The test frequency was 5 MHz and Branson 600 ultrasonic instrument was used. During the inspections, the disks were located on a turntable and C-scan recordings were made of the indications. The scan rate was 17 revolutions per minute. For the angle beam inspections, the refracted sound beam angle in the metal was 45 degrees.

The General Electric reference standard, used by G.E. in their disk forging inspection, was also used in the AFML inspections. The search unit was positioned over the reference standard in order to adjust the sound beam angle in the metal to 45 degrees for the angle beam inspection. The water path established during the straight beam calibration was used. Then, gain settings were obtained for an 80% response from each hole in the reference standard. Next, the response from the .020 inch diameter reference hole at a 1.25 inch metal travel was adjusted to 80 percent of saturation. The scanning gain was increased by removing an additional 12 dB of attenuation and the C-scan was set to print-out any discontinuities whose amplitude exceeded 60 percent of saturation. It was found, however, that it was not always possible to interpret the results at this high gain since there was a myriad of indications printed out on the C-scan. This can be explained by the fact that very small discontinuities near the sound entry surface were being inspected at an effective sensitivity level in excess of the "plus 12 dB" level by virtue of their short metal travels. In order to evaluate the disk forgings, then, separate scans were made of each at lower gain levels of "plus 5 dB" and "plus 8 dB"; as a result, approximate distance - amplitude corrections were obtained for discontinuities at the shorter metal travels. The C-scans were used to locate the discontinuities. Each discontinuity was then evaluated by direct comparison of their response with the response from the reference hole at the same metal travel. If the discontinuity response at the "plus 12 dB" gain exceeded 60 percent of the corresponding reference response, the discontinuity was documented.

The straight beam immersion tests were set-up by adjusting the water path (2 11/16 inches) until the response from the 3/8 and 1 1/4 inch deep reference holes were identical. Next, the responses were adjusted to 80 percent of saturation, and the sensitivity was increased to 12 dB. No indications were recorded on the C-scans.

Two independent AFML technicians were used and the Figures 117 and 118 scan plans were reproduced by Inspector A whereas, for Inspector B, L-3, L-4, C.S.3, C.S.4, C.S.5, and C.S.6 were omitted.

A summary of the test results appear in Figure 122. Listed are those indications whose amplitude equalled or exceeded 60 percent of the reference hole response at the "plus 12 dB" level. A comparison of the inspection results from G.E. and AFML for disk forging No's 5 and 9 are shown in Table 93.

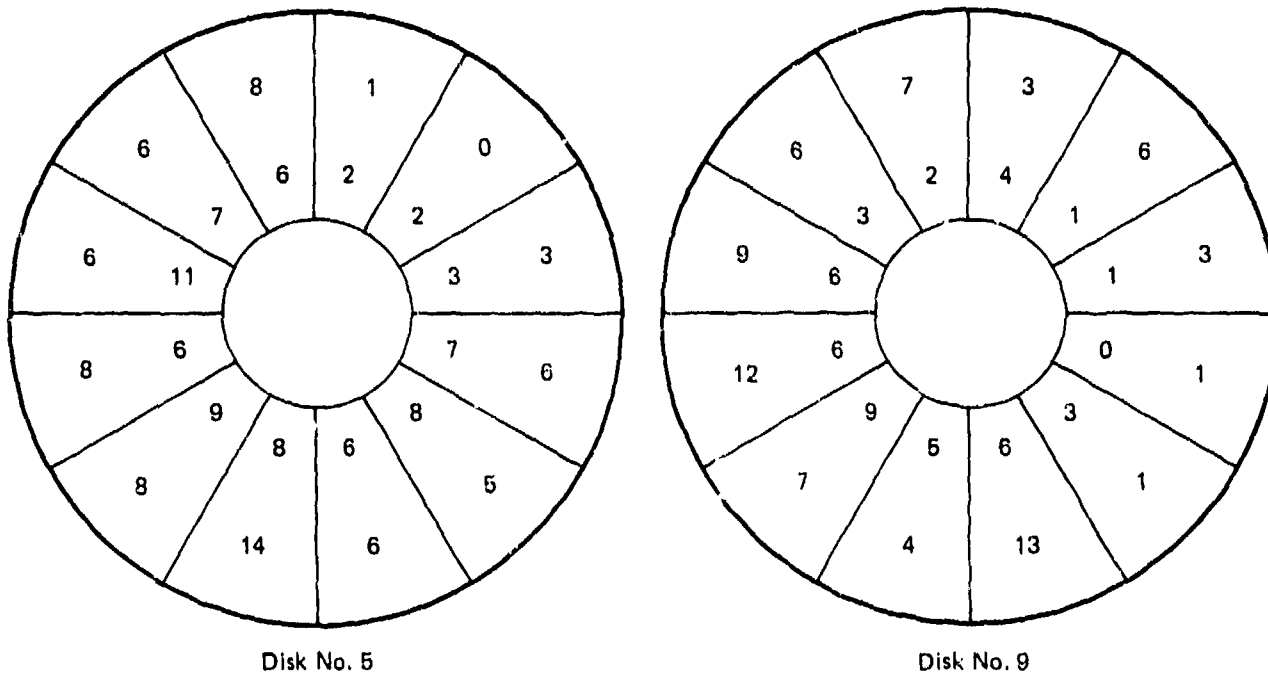
**TABLE 93  
COMPARISON OF TOTAL GE ULTRASONIC INDICATIONS WITH TOTAL  
AFML ULTRASONIC INDICATIONS**

Inspector	Sector (in degrees)												Total
	0	30	60	90	120	150	180	210	240	270	300	330	
Disk No. 5													
GE A	4	2	0	0	5	2	0	4	11	0	0	4	32
GE B	3	12	3	8	19	5	4	26	50	12	35	6	183
AFML A	1	0	3	6	5	6	14	8	8	6	6	8	*71
AFML B	2	2	3	7	8	6	8	9	6	11	7	6	*75
Disk No. 9													
GE A	1	3	0	2	0	0	1	1	2	0	0	1	11
GE B	10	32	4	1	27	5	15	22	23	12	25	11	187
AFML A	3	6	3	1	1	13	4	7	12	9	6	7	**72
AFML B	4	1	1	0	3	6	5	9	6	6	3	2	**46

\* 5 indications found by AFML Inspector A on testing not completed by AFML Inspector B.  
 \*\*10 indications found by AFML Inspector A on testing not completed by AFML Inspector B.

(IP74 0117 241)

Outer Results are for Inspector A  
and Inner Results are for Inspector B



GP74 0117 240

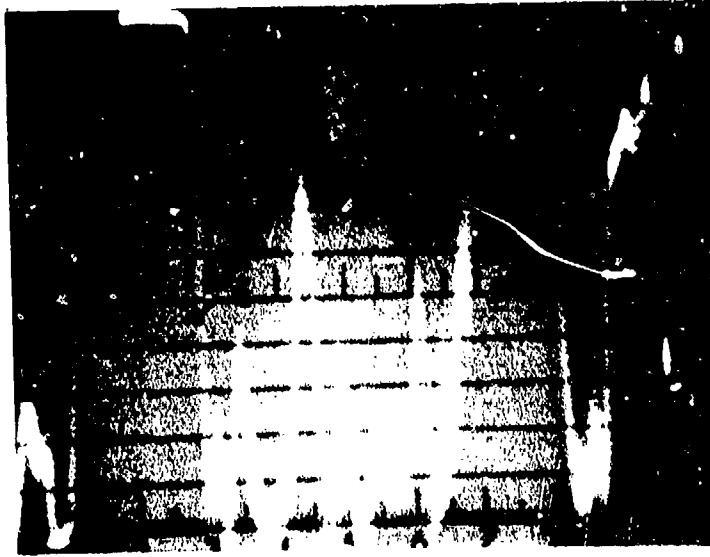
**FIGURE 12?**  
**TOTAL ULTRASONIC INDICATIONS FROM AFML INSPECTIONS OF DISK FORGINGS**

## 5. PLATE

### a. Ultrasonic Inspection

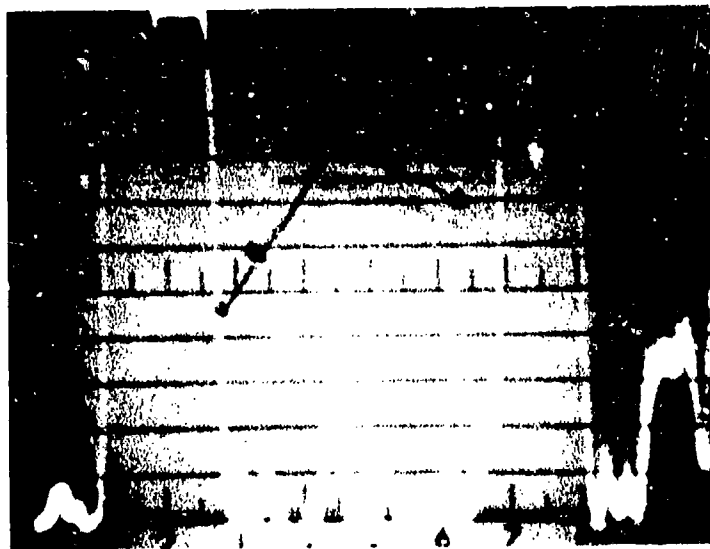
The production ultrasonic inspection was carried out on the plate using the straight beam immersion method. A 3/4 inch diameter, 5 MHz SIZ flat search unit (S/N 18650) was used along with a Sperry UM771 (S/N 66720) and a 10S dB pulser/receiver (S/N 66727). The vertical and horizontal linearity of the electronic system had been checked within 4 months of the inspection according to the procedures given in ASTM E317-68. A 3 inch water path was chosen for the inspections. This water path was maintained constant for the reference standards and the plate to  $\pm 1/8$  inch.

Ti-6Al-4V reference standards with 3/64 inch diameter flat bottom holes at metal travels of 3/8, 1/2, 3/4, 1, and 1-1/4 inches were used for calibration. These reference standards were commercially purchased Ti-6Al-4V ASTM-type straight beam reference standards. Initially, a distance-amplitude curve (DAC) was constructed by positioning the search unit for maximum response from that 3/64 inch diameter flat bottom reference hole which exhibited the largest amplitude signal. The signal amplitude then was adjusted to 80 percent of saturation on the cathode ray tube (CRT). Without changing the gain control, the search unit was positioned over the remaining reference standards and the amplitudes were marked on the CRT screen. The points were joined by a smooth curve. In order to increase the test sensitivity, an attempt was made to inspect the plate at a higher scanning gain. First, 19 dB of attenuation was removed which is approximately equivalent to calibrating with a 1/64 inch diameter flat bottom. However, at this gain level, the ultrasonic noise in the plate was so high (exceeded 25% of the DAC curve) as to prevent effective inspection (see Figure 123). Next, a total of 7 dB was subtracted (equivalent to a 2/64 inch diameter hole calibration) but again the noise in the plate exceeded 25% of the DAC curve was too high (see Figure 124). Finally, the gain was reset for the original 80% of saturation from the highest amplitude reference standard. The rationale of increasing sensitivity by a specific amount rather than attempting to drill and use exceedingly small reference standard holes is valid within certain limits and should be mentioned at this time. On a previous internal program using aluminum ASTM type blocks, it was found that the relationship between the search unit diameter and frequency effects the response from the holes. Both contact and immersion type search units were used. Frequencies and diameters of the active areas were varied and the responses were measured from several holes. The table following lists the average results obtained.



GP74 0117-23

**FIGURE 123**  
**HIGH NOISE LEVEL IN PLATE AFTER SUBTRACTION OF 19 dB**



GP74 0117-210

**FIGURE 124**  
**HIGH NOISE LEVEL IN PLATE AFTER SUBTRACTION OF 7 dB**

		Response Variations, (dB)					
Frequency, MHz		2-1/4		5		10	
Hole Dia. (Inches)		5 to 3	5 to 8	5 to 3	5 to 8	5 to 3	5 to 8
Dia. (inches)	1/4"	-10	+8	-14	+18	-12	+19
	1/2"	- 7	+6	-10	+ 8	-12	+10
	3/4"	- 8	+7	- 9	+ 9	-10	+ 7

It is obvious that at the normal test conditions using 5 MHz 3/4 inch diameter search units, the ratio of hole areas between a 3/64 inch, a 5/64 inch, and an 8/64 inch diameter flat bottom hole varies directly with the dB gain or loss required to obtain identical CRT response amplitude. (i.e. If the ratio of areas between an 8/64 and a 3/64 is 64/9 or 7.1, then the dB ratio should be about 17 dB if area/amplitude is the only variable.) However, as the frequency is increased or the search unit diameter is reduced, the area/amplitude relationship no longer holds as can be seen in the values obtained using a 10 MHz 1/4 inch diameter search unit. This can be explained using the hole diameter to wave length ratio and the reradiation concept discussed in the Nondestructive Testing Handbook by McMaster (**Reference 5**).

In addition, the responses from standard drilled holes (no flat bottom) were compared to ASTM type holes described above and the results listed in the following table were obtained.

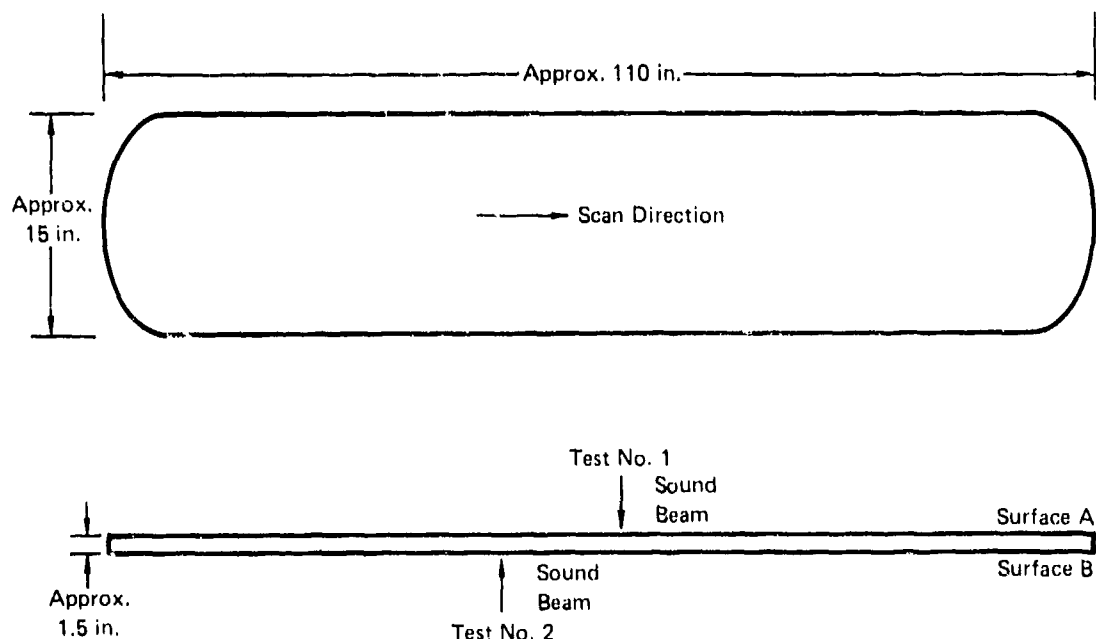
		Response Variations (dB)		
Frequency, MHz		2-1/4	5	10
Hole Size (64ths)	#3	-1	-5	-12
	#5	-2	-14	-18
	#8	-8	-18	-28

Variations in hole bottom flatness had less effect as the frequency and hole size were reduced. The behavior of this data also can be described by the hole diameter to wavelength ratio. Plotting the  $\text{Log } D/\lambda$  ratio versus the difference in dB from one hole diameter to the next (in the range of  $3/64$  to  $8/64$  diameter) proved that a straight line relationship exists and showed that the flat bottom hole response will equal the response from any surface of the same diameter when the  $D/\lambda$  ratio is equal to or less than 0.5.

This data, although performed on aluminum, should be directly applicable to titanium since the contour surface block results as well as the transmission data discussed in this section demonstrates the transferability of results from one material to the other. Note, however, whether material transmission characteristics or surface orientation (both front and back surfaces) or both resulted in differences in back reflection responses of at least 16 dB from one area of the bar to another.

A check was made for the difference in sound transmission characteristics between the reference standards and the 1-1/2 inch thick plate. At the gain established as described above, the decibel (dB) difference was noted between the back surface response in the plate and in a reference standard with the same metal travel. It was found in the case of the two plates that there was no dB difference between the plate and reference standard so that no correction was necessary.

As shown in Figure 125, the plate was scanned manually from two sides. In each case, the scan index was 0.25 inch. This was chosen using the scanning gain by determining the total traversing distance across the reference standards through which no less than 50% of the DAC curve is obtained.



GP74 0117-24

**FIGURE 125**  
**SCAN PLAN FOR PLATE**

All discontinuities with amplitude greater than 50% of the DAC curve were evaluated for acceptance or rejection. Each discontinuity response was directly compared to the flat bottom hole response in a reference standard of appropriate metal travel. The location and size of each rejectable discontinuity was marked on the plate and, upon completion of the inspection, the information was transferred to mylar overlays. Finally, all the markings were removed from the plate.

Upon completion of the 5 MHz straight beam immersion testing, the plates were reinspected using a 10 MHz, 1/2 inch diameter, lead zirconate titanate search unit (S/N 15384). The remaining equipment, production inspector, and procedure was as for the 5 MHz inspection.

A typical CRT photograph of a discontinuity in the plate is shown in Figure 126.

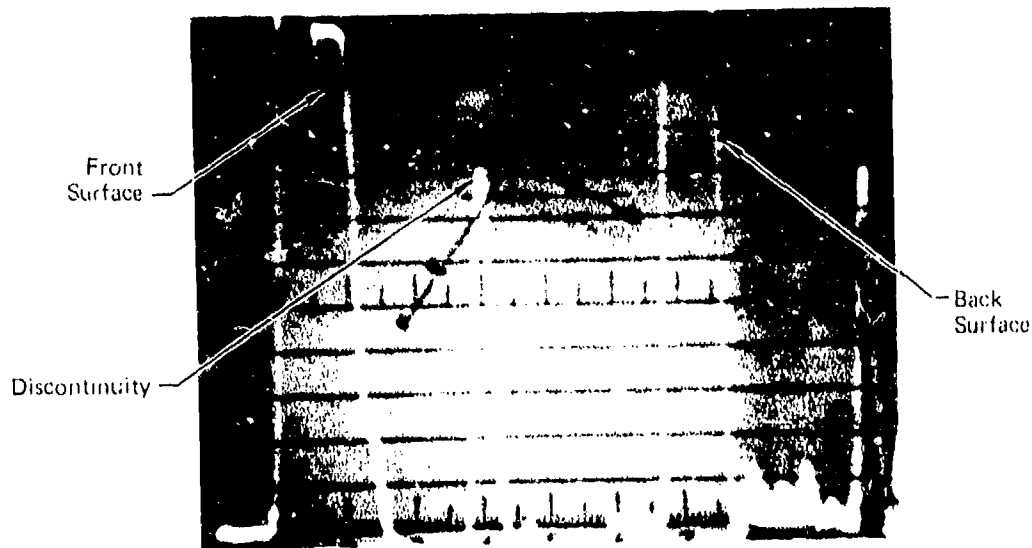


FIGURE 126  
TYPICAL RESPONSE FROM DISCONTINUITY IN PLATE

The results of the two straight beam inspection is shown in Tables 94 and 95. The approximate location of each discontinuity is shown in the sketch in Figure 127. Several discontinuities were found in the plate which originated from the bottom of the original ingot. There were no rejectable discontinuities detected in the plate which originated from the top of the original ingot. Type II alpha segregates were expected in this material from the ingot top.

**TABLE 94**  
**SUMMARY OF STRAIGHT BEAM TESTING OF PLATE FROM INGOT**  
**BOTTOM (SURFACE "A" WAS THE SOUND ENTRY SURFACE)**

Defect No.	Approximate Length		Approximate Depth		Response Amplitude	
	5 MHz	10 MHz	5 MHz	10 MHz	5 MHz	10 MHz
1	△1	0.5	0.6	0.6	No. 3	< No. 2
2	5.0	5.5	0.7	0.6	> No. 5	> No. 5
3	△1	0.5	0.6	0.6	> No. 5	> No. 3
4	1.6	1.6	0.9	0.9	> No. 5	No. 5
5	0.5	0.75	0.75	0.8	> No. 5	> No. 3
6	△1	△1	0.9	0.8	< No. 3	> No. 2
7	△1	△1	0.8	0.8	No. 3	< No. 2
8	3.25	3.75	0.6	0.8	> No. 5	> No. 5
9	△2	△2	△2	△2	△2	△2
10	△1	△1	0.6	0.6	No. 3	> No. 2
11	△1	0.75	0.4	0.9	> No. 3	> No. 2
12	△1	△1	0.9	0.8	No. 2	< No. 2
13	0.75	0.75	0.5	0.5	> No. 3	No. 2
14	1.0	0.5	0.6	0.6	> No. 3	> No. 2
15	△1	△1	0.6	0.6	> No. 3	< No. 2
16	△2	△2	△2	△2	△2	△2

△1 Indication was not linear  
 △2 Indication was not detected

GP74-0117 2B

**TABLE 95**  
**SUMMARY OF STRAIGHT BEAM TESTING OF PLATE FROM INGOT**  
**BOTTOM (SURFACE "B" WAS THE SOUND ENTRY SURFACE)**

Defect No.	Approximate Length		Approximate Depth		Response Amplitude	
	5 MHz	10 MHz	5 MHz	10 MHz	5 MHz	10 MHz
1	0.4	0.75	0.9	0.9	No. 3	> No. 2
2	5.5	5.5	0.8	0.8	> No. 5	> No. 5
3	0.5	0.75	0.9	0.9	No. 3	No. 3
4	1.75	1.6	0.6	0.6	> No. 5	> No. 5
5	0.75	0.75	0.8	0.8	> No. 5	> No. 3
6	△	△	0.8	0.5	> No. 3	No. 2
7	△	△	0.6	0.7	> No. 3	> No. 2
8	3.5	3.5	0.9	0.9	> No. 5	> No. 5
9	△	△	1.2	△	No. 3	△
10	△	△	0.9	0.9	No. 3	> No. 2
11	0.5	△	1.2	0.6	No. 3	> No. 2
12	△	△	0.6	0.8	< No. 3	> No. 2
13	0.75	0.5	1.0	1.2	> No. 3	> No. 2
14	0.75	0.5	0.9	0.9	No. 3	< No. 2
15	△	0.75	0.9	1.0	No. 3	> No. 3
16	△	△	1.2	1.1	> No. 3	< No. 2

△ Indication was not linear  
 △ Indication was not detected

QP74-0117 26

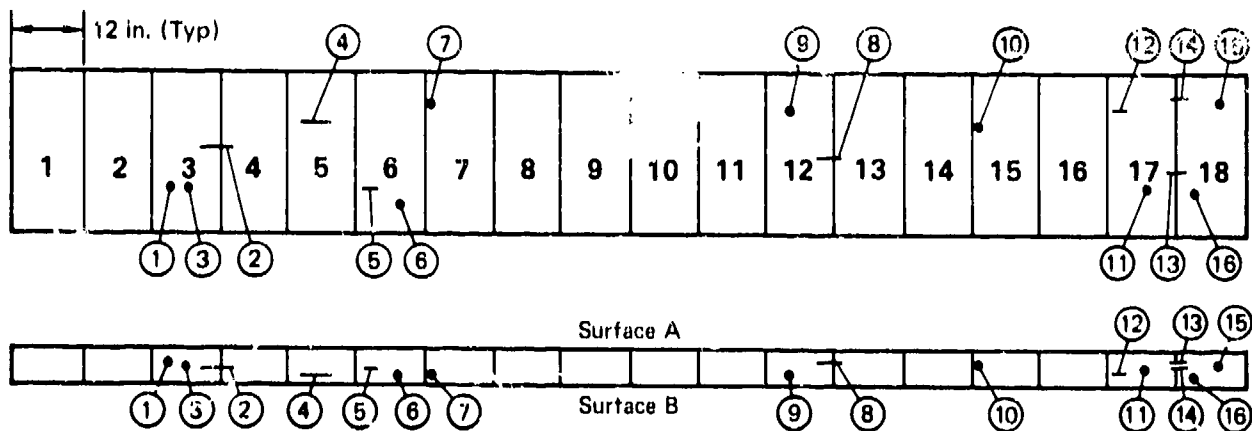


**FIGURE 127**  
**LOCATION OF DEFECTS IN PLATE A**

QP74-0117 27

The discontinuities found in the plate from the ingot bottom varied in length from zero (non-linear) to 5.5 inches. The amplitude response varied from less than a 2/64 inch diameter flat bottom hole to greater than a 5/64 inch diameter flat bottom hole.

The test results indicate that greater resolution was achieved with the 10 MHz frequency than the 5 MHz frequency. For example, several of the discontinuities which appeared to be non-linear using 5 MHz were found to have length when tested with 10 MHz (see Table 94).

#### b. Radiographic Inspection

The plate material was radiographically inspected using production radiographic facilities. The exposures were made with a Siefert Isovolt 400 X-ray machine having a 4.0 mm focal spot. The exposures were made at 150 KV and 10 millamperes for 15 minutes. A MIL-STD-453 - 3 penetrometer was used as an image quality indicator and was placed on the source side of the plate. The front screen was .005 inch thick lead and the back screen was .010 inch thick lead. Cardboard cassettes were used with 14 x 17 inch Geveart D4 film (ASTM Type I) and a 1/8 inch thick lead sheet was used to back up the film cassette. The focal spot-to-film distance was 45 inches and the direction of the central beam was aligned to be perpendicular to the film surface. Twelve inch wide areas were exposed using the 14 x 17 inch film to provide for overlapping of exposures. The exposed film was processed in a Kodak Model B X-Omat automatic processor using Geveart G135N developer and G334N fixer. The density of each radiograph was between 2.0 and 2.5 H and D.

None of the segregates which were detected ultrasonically were observed on the radiographs. A second examination of the films was made in the area of ultrasonic indications but, again, there was no evidence of discontinuities on the films. From this, it can be concluded that the Type I stabilized alpha detects in plate are more easily detected using ultrasonic techniques than radiography.

## 6. BAR

### a. Ultrasonic Inspection

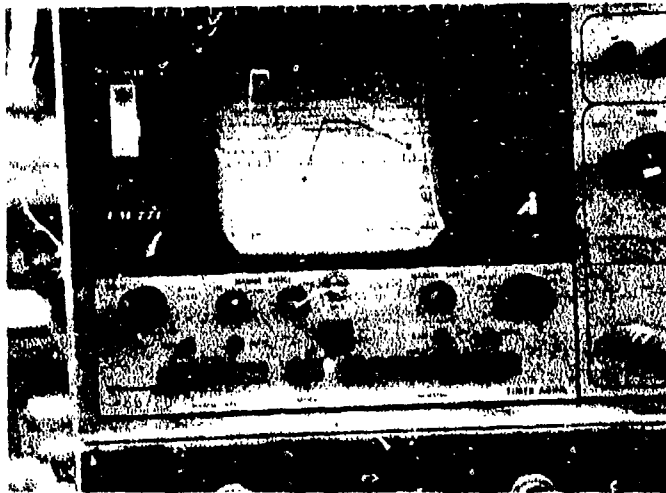
The initial production straight beam inspection of the bar was performed using the same 5 MHz search unit as was used for the plate inspection. All the equipment for the bar inspection was the same as for the plate inspection. Ti-6Al-4V reference standards with 3/64 inch diameter flat bottom holes at 1/2, 3/4, 1, 1-1/4, and 1-3/4 inch metal travels were used to establish the DAC curve as described for the plate inspection. As with the plate inspection, an attempt was made to increase the scanning gain by subtracting 19 dB and then 7 dB but again the ultrasonic noise level was greater than 25% at the DAC curve level (see Figure 128). As in the case of the plate inspection, the gain was reset at the original DAC curve level. The scan index was .25 inch.

Correction was made for the difference in sound transmission characteristics between the reference standards and the bar using the same procedure as for the plate inspection. It was found that there was a wide variation in the sound transmission characteristics along each bar. Consequently, each bar was divided into 12 inch segments and correction was made for the average attenuation within each segment. The variation in average dB difference between each segment of the bar and the reference standards is shown in Table 96. As can be seen the variation was as great as zero to 13 dB within a single bar. A portion of the dB difference may be due to surface irregularities.

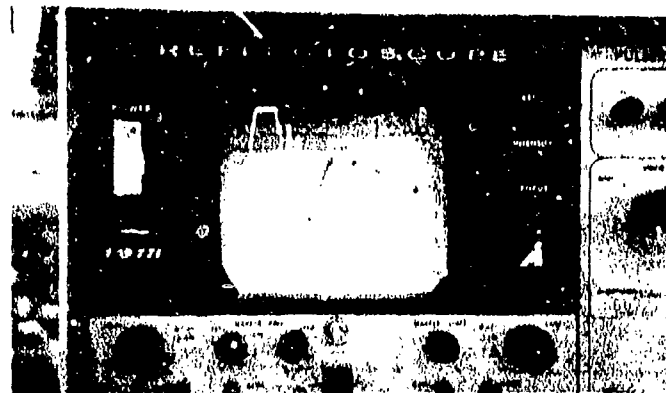
**TABLE 96**  
**VARIATION IN AVERAGE SOUND TRANSMISSION CHARACTERISTICS**  
**BETWEEN BAR AND REFERENCE STANDARDS FOR 5 MHz STRAIGHT**  
**BEAM TESTING**

Bar No.	Variation in Average dB Difference Between Bar and Reference Standard
1-2A2A	0 to 13 dB
1-2A2B	0 to 6 dB
1-2A2C	3 to 12 dB
1-2A2D	0 to 7 dB
1-2A2E	1 to 10 dB
1-1A2A	0 to 7 dB
1-1A2B	0 to 8 dB
1-1A2C	2 to 9 dB
1-1A2D	3 to 8 dB
1-1A2E	0 to 7 dB

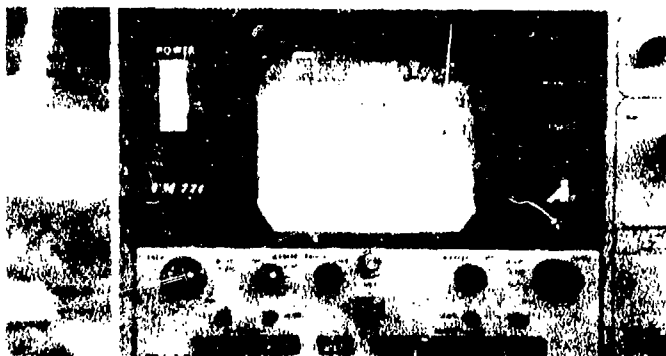
GP24 0117 31



Actual Scanning Gain Used for Inspection of Bar



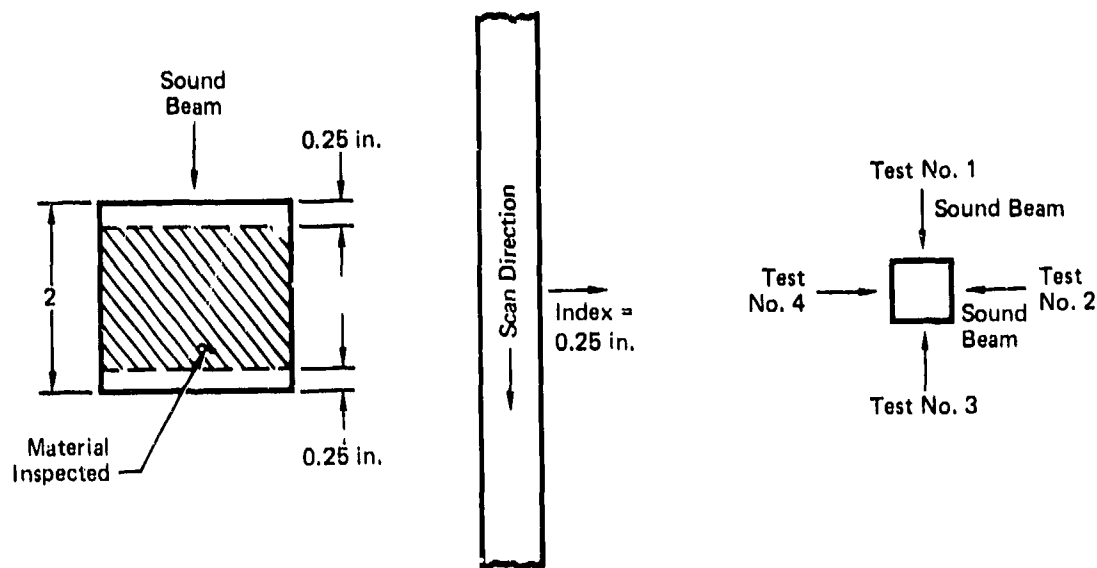
19 dB Subtracted (Equivalent to a 1/64 Flat Bottom Hole Response)



7 dB Subtracted (Equivalent to a 2/64 Flat Bottom Hole Response)

**FIGURE 128**  
**PHOTOGRAPHS OF CATHODE RAY TUBE PRESENTATION**  
**OF BACK SURFACE RESPONSE AND NOISE IN BAR AT**  
**SEVERAL GAIN LEVELS**

As with the plate inspection, the waterpath was 3 inches  $\pm$  1/8 inch. Many of the bars were warped and twisted. Consequently, it was not possible to scan them automatically and still maintain a  $\pm$  1/8 inch water path. Therefore, the scanning bridge was moved by hand by the operator. The bars were scanned as shown in Figure 129.



GP/4-0117-32

FIGURE 129  
SCAN PLAN FOR BAR

Each bar was inspected in 4 mutually perpendicular directions to overcome detection difficulties that might arise from the orientation of discontinuities.

As with the plate, all discontinuities with amplitude greater than 50% of the DAC on the cathode ray tube were evaluated further to determine acceptance or rejection. Each discontinuity was evaluated by manipulating the search unit to maximize the response from the discontinuity.

The location and size of each discontinuity whose response exceeded the DAC curve was marked on the bar surface. After completion of the inspection, the information was transferred to mylar overlays and the markings were removed from the surface of the bar.

For comparative purposes, a second straight beam immersion inspection was performed using a 10 MHz, 1/2 inch diameter, lead zirconate titanate search unit (S/N 15384). The remaining equipment, production inspector, and procedure was as for the 5 MHz inspection.

Figure 130 is used to explain the results of the straight beam immersion tests and Figure 131 is a schematic showing the section layout. The inspection data is presented in Figure 132.

As can be seen, several discontinuities are present in the bars which originated from the bottom of the original ingot. There were no rejectable discontinuities detected in the bars which originated from the top of the original ingot. Type II alpha segregates were expected in this material from the ingot top. It is not known if these segregates **exist in the bar at this point or if the** ultrasonic inspections were not successful in detecting them.

The discontinuities found in the bars from the ingot bottom varied in length from zero (non-linear) to 9.3 inches. The amplitude response varied from less than a  $2/64$  inch diameter flat bottom hole to greater than a  $5/64$  inch diameter flat bottom hole.

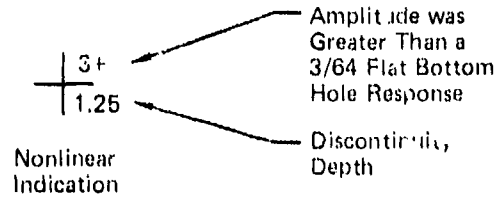
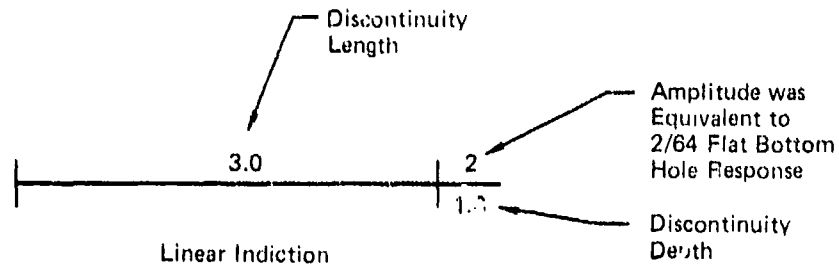
The test results indicate that greater resolution was achieved with the 10 MHz frequency than the 5 MHz frequency. For example, the 5 MHz inspection of Bar 1-2A2A, Section 7 indicated the presence of 2 separate discontinuities, where as, the 10 MHz inspection revealed one continuous discontinuity. In addition, there were a few point discontinuities detected at 10 MHz which were not detected at 5 MHz.

The importance of correcting for differences in sound transmission characteristics between the bar and the reference standard, can be seen from the test results. For example, in one area of Bar 1-2A2A, a difference of 13dB was encountered. Without correction, the response amplitude would be reduced to approximately 25 percent of its amplitude after correction and it is doubtful that discontinuities equivalent to a  $2/64$  inch diameter flat bottom hole would have been detected.

Following the straight beam inspections, several of the bars were inspected using angle beam immersion techniques. The following bars were inspected:

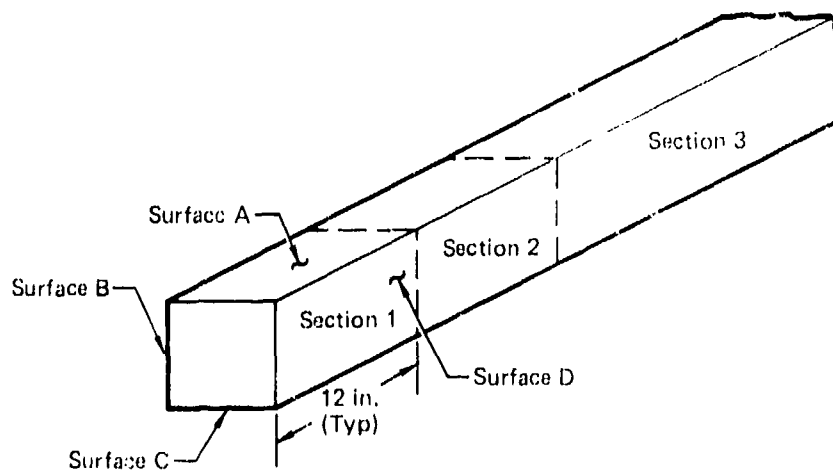
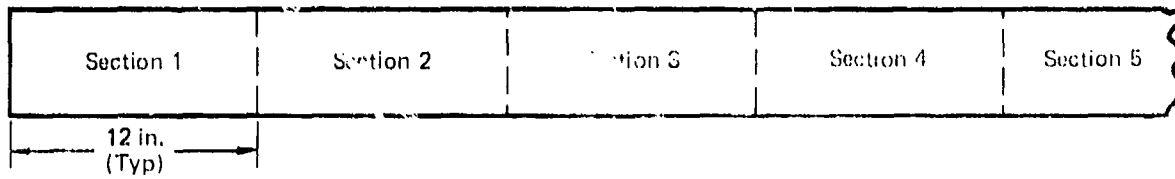
1-2A2A, 1-2A2B, 1-2A2D, 1-1A2A, 1-1A2B, 1-2A2C

Each bar was inspected using a  $3/4$  inch diameter, 5 MHz, flat Aerotech Gamma search unit (S/N 112322) and a Sperry UM 771 Ultrasonic instrument with a 10S dB pulser/receiver. The reference standard was a 2 inch thick as-rolled plate, machined to the configuration previously described in Figure 48. The difference in sound transmission between the bar and the reference standard was measured using the straight beam immersion method. A  $1/2$  inch diameter, 10MHz, Aerotech Gamma search unit was used. A frequency of 10 MHz was chosen to keep the wave length the same as with for 5 MHz shear mode sound beam. The search unit was positioned over the reference standard and the back reflection through the 2 inches of metal was adjusted to 30 percent of saturation. Next, without changing the gain control, the search unit was positioned over the 2 inch thick bar. The search unit was moved to several positions on each bar and, in this manner, an average dB difference between the bar and reference standard was arrived at.



GP74 0117 34

**FIGURE 130**  
**DATA PRESENTATION**



GP74 0117 31

**FIGURE 131**  
**LAYOUT OF BARS FOR ULTRASONIC INSPECTION**

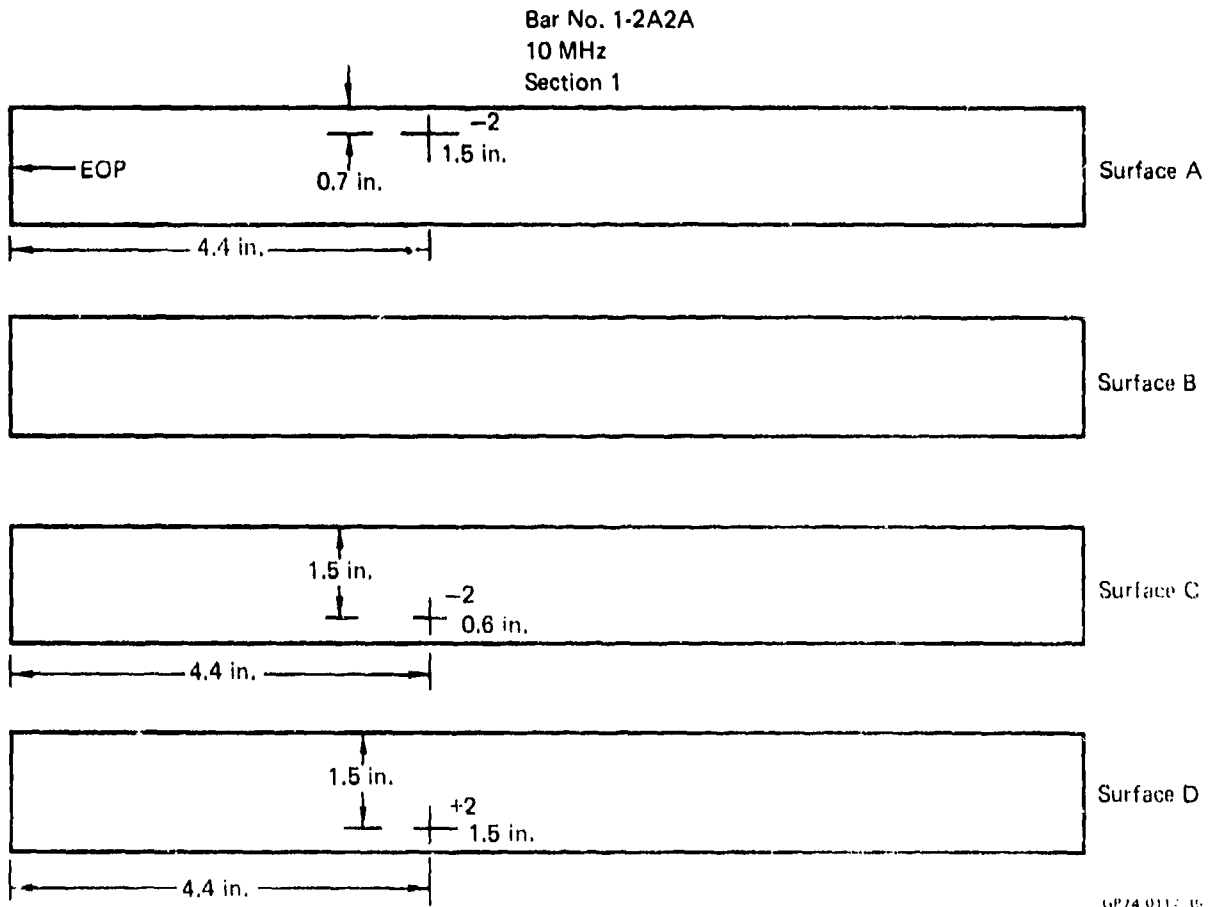


**FIGURE 132**  
**LOCATION OF DEFECTS IN BAR**

Bar No. 1-2A2A  
 5 MHz  
 Section 7

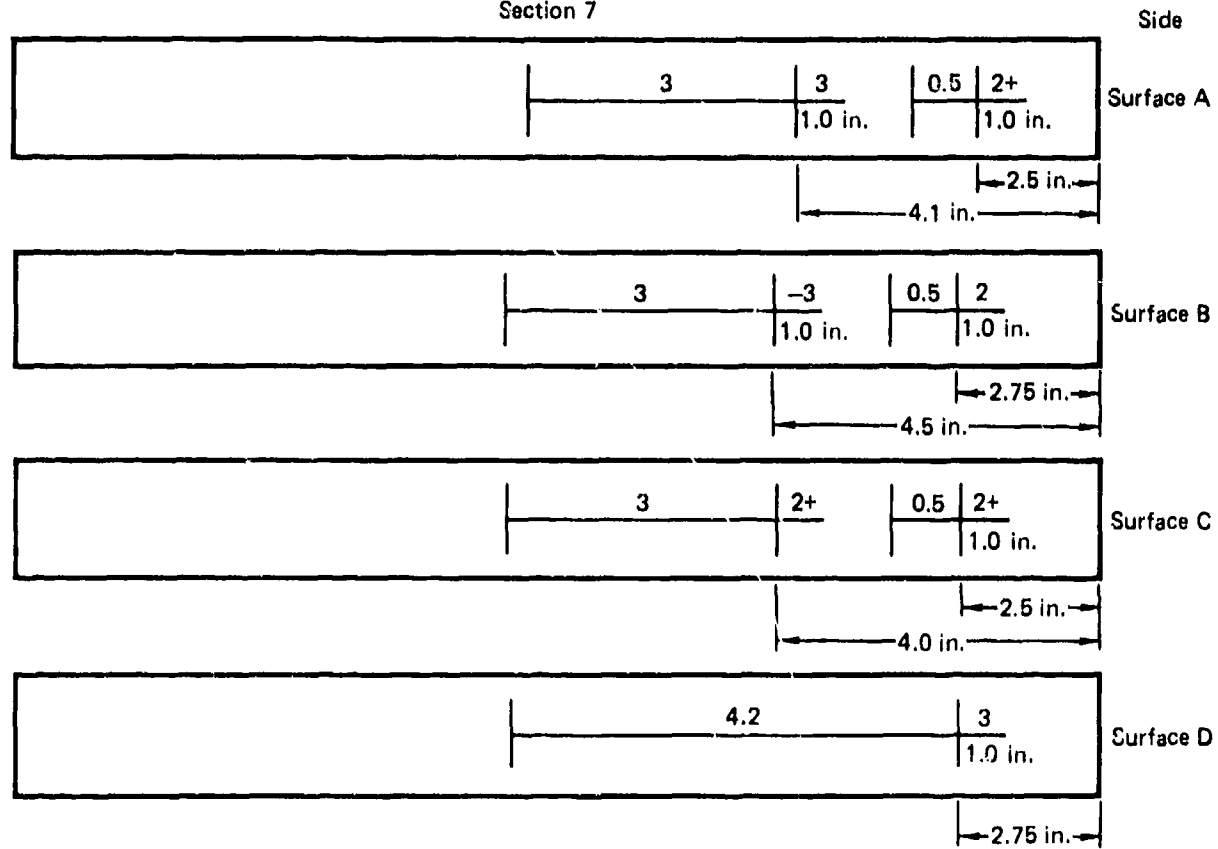
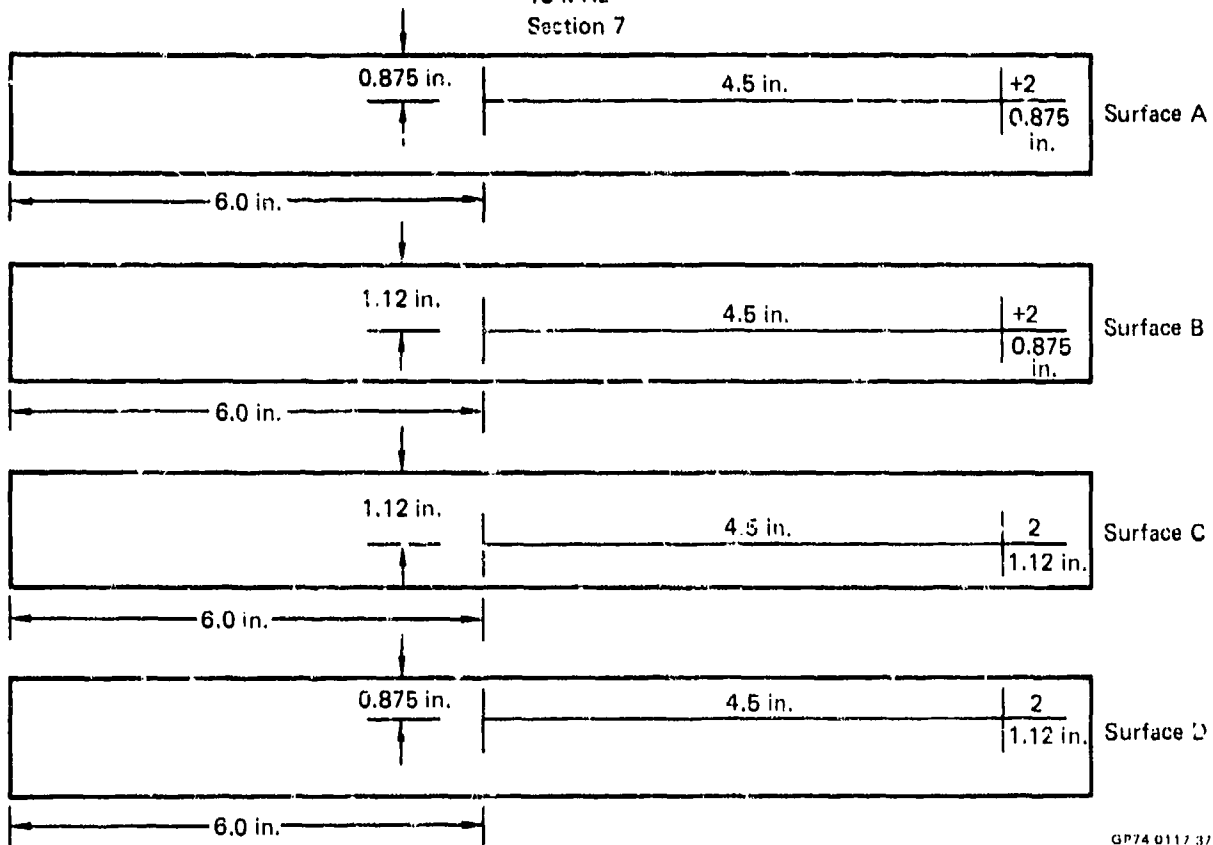


FIGURE 132 (Continued)  
 LOCATION OF DEFECTS IN BAR

QP 74-0117-36

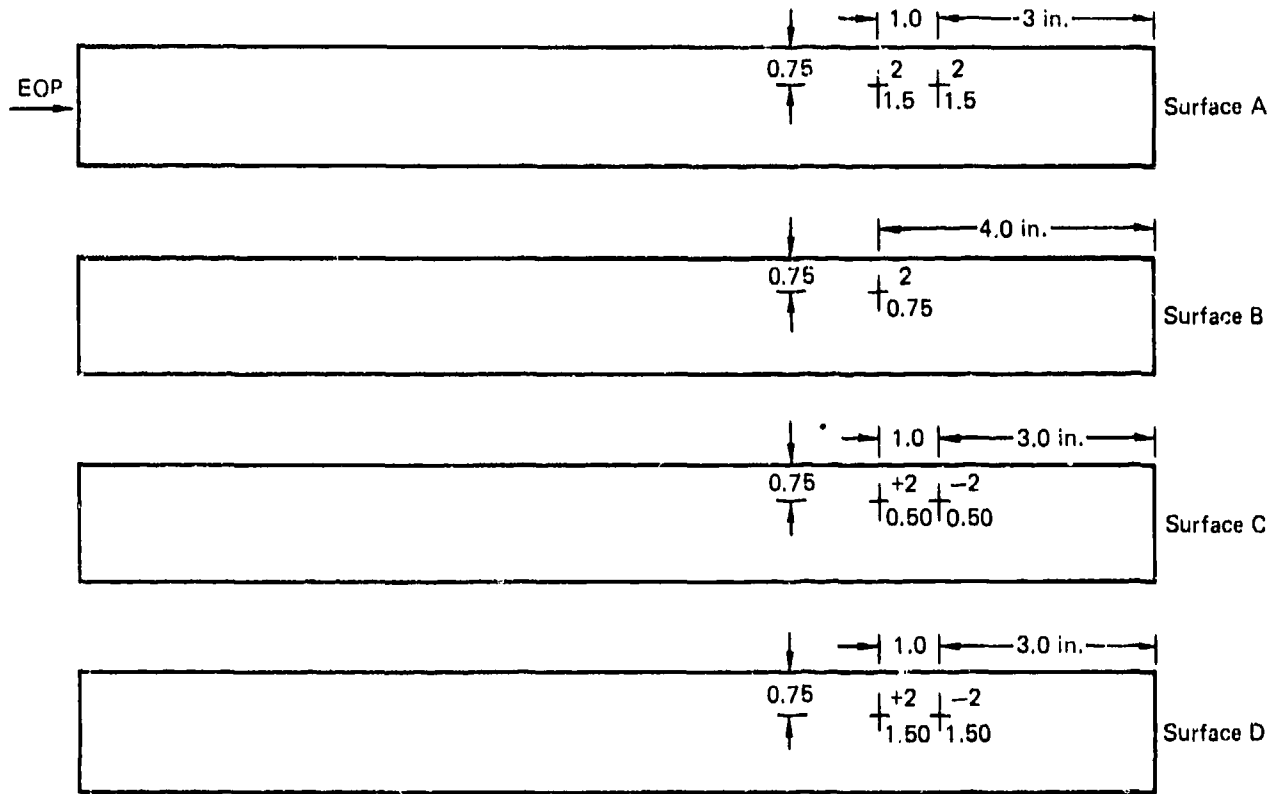
Bar No. 1-2A2A  
 10 MHz  
 Section 7



GP74 0117 37

FIGURE 132 (Continued)  
 LOCATION OF DEFECTS IN BAR

Bar No. 1-2A2B  
 5 MHz  
 Section 1



GP74 0117-38

FIGURE 132 (Continued)  
 LOCATION OF DEFECTS IN BAR

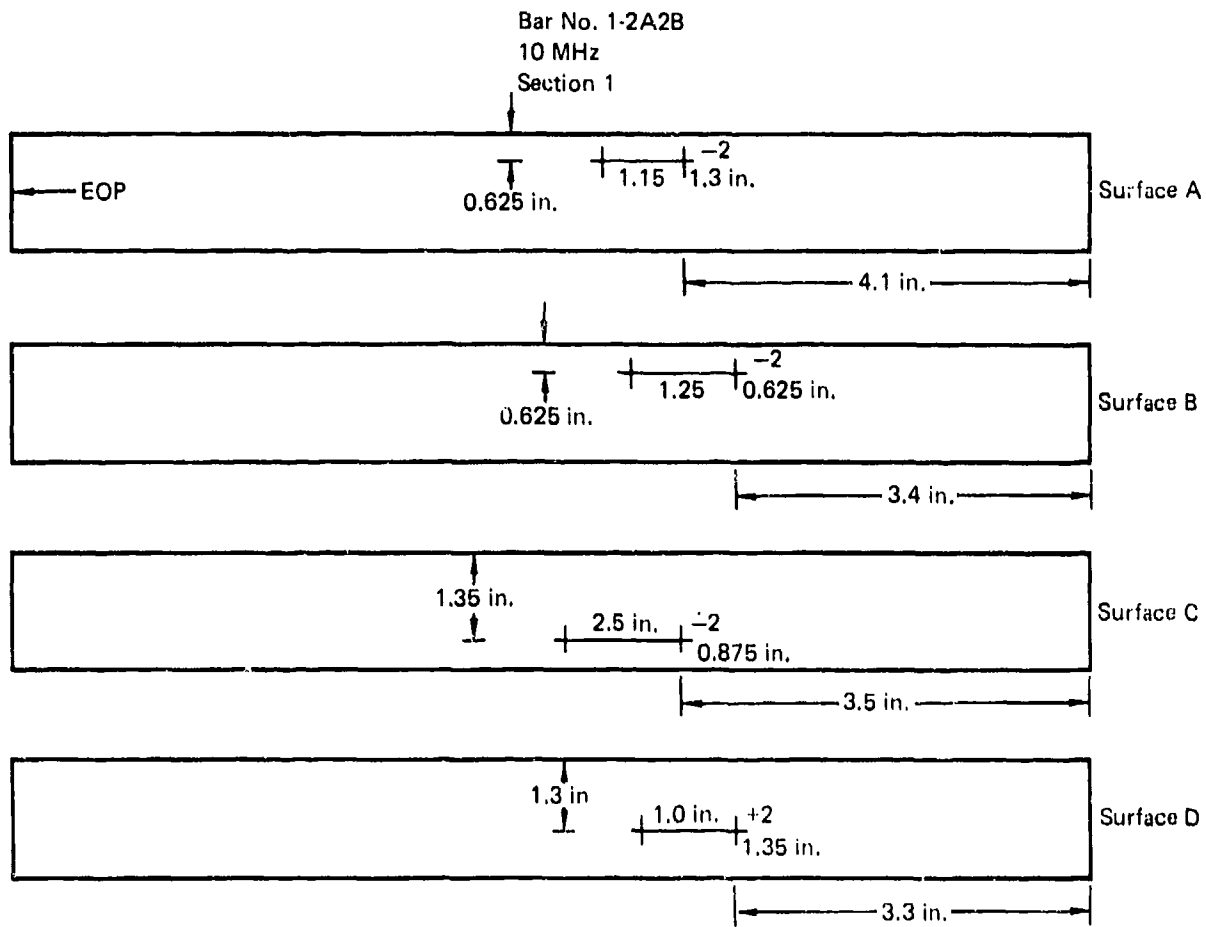
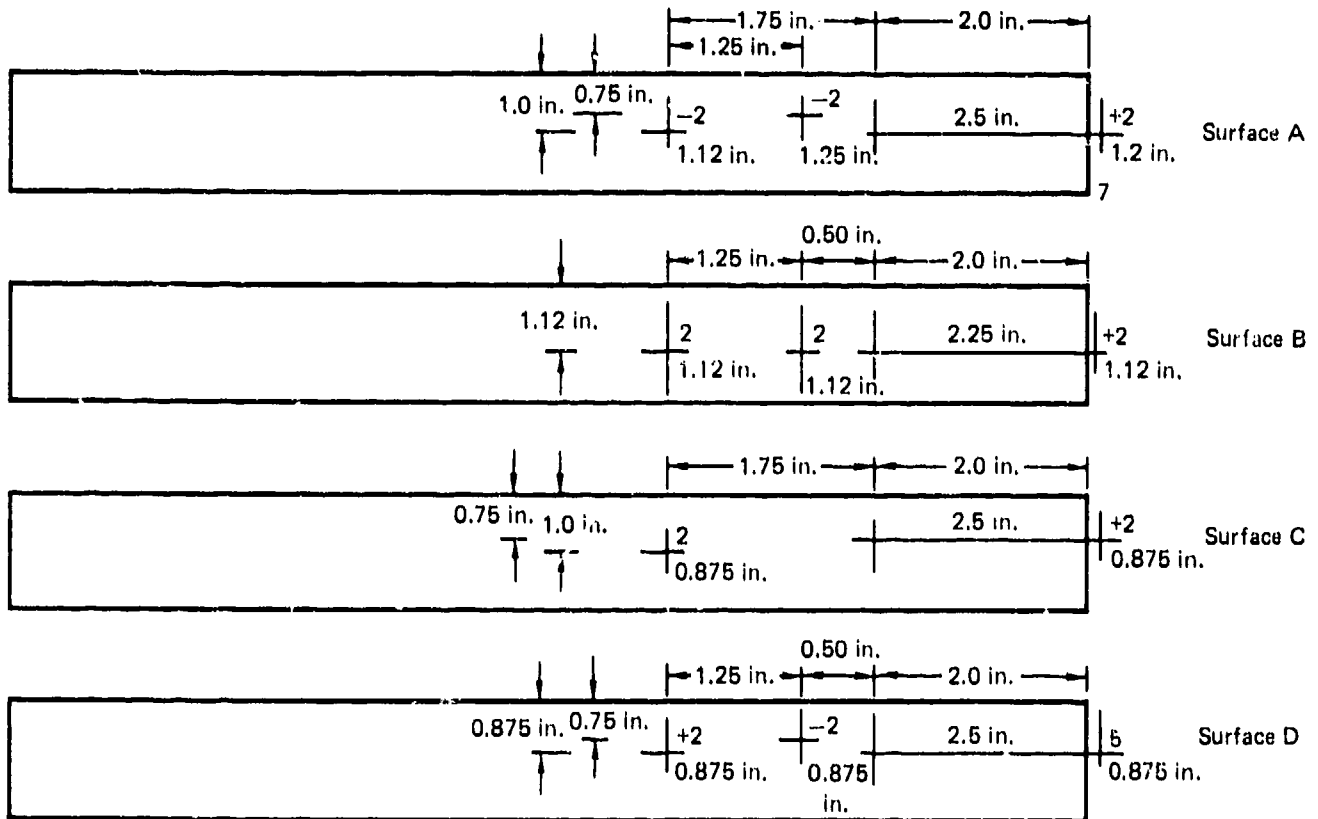


**FIGURE 132 (Continued)**  
**LOCATION OF DEFECTS IN BAR**

GP74 0117 39

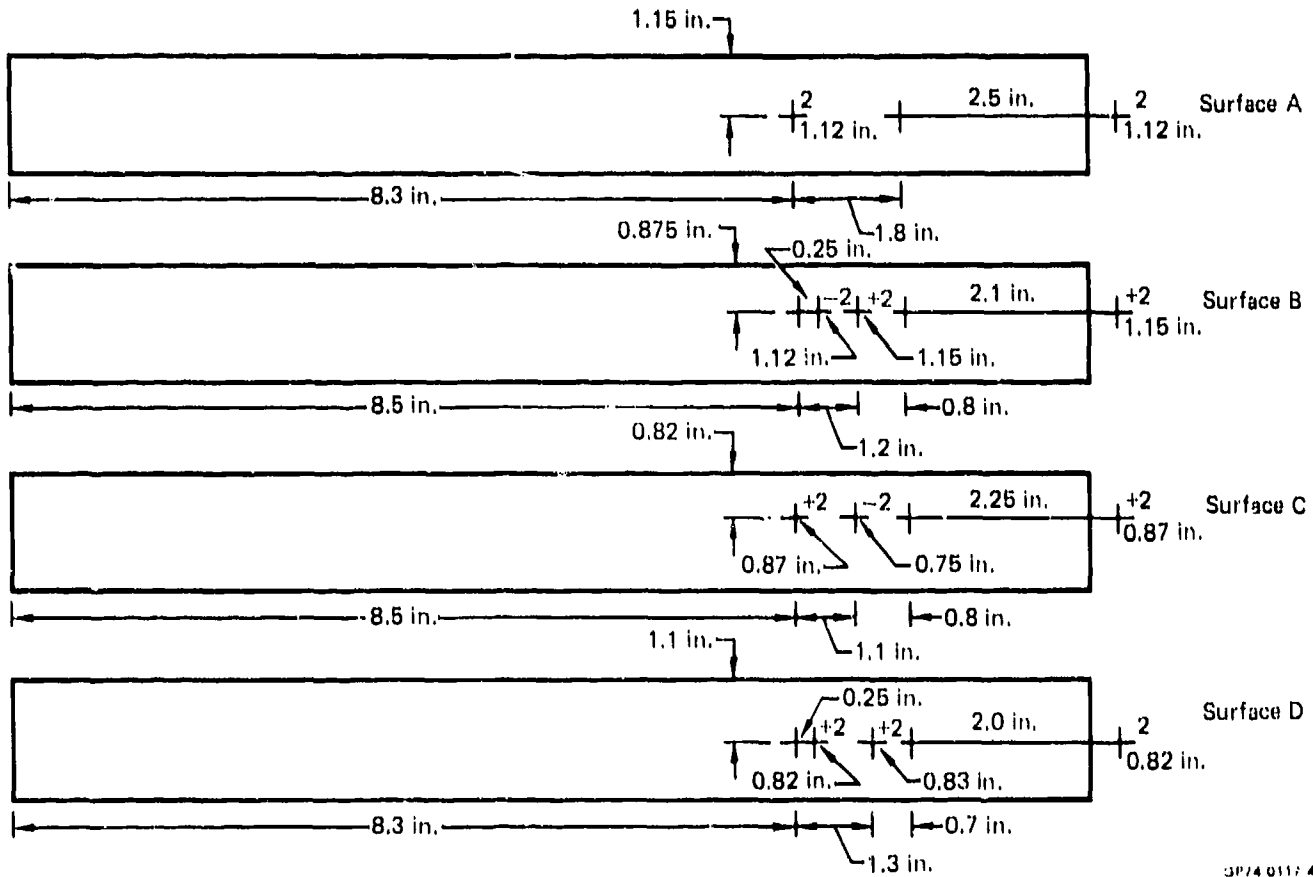
Bar No. 1-2A2B  
 5 MHz  
 Section 6



QP74-0117 40

FIGURE 132 (Continued)  
 LOCATION OF DEFECTS IN BAR

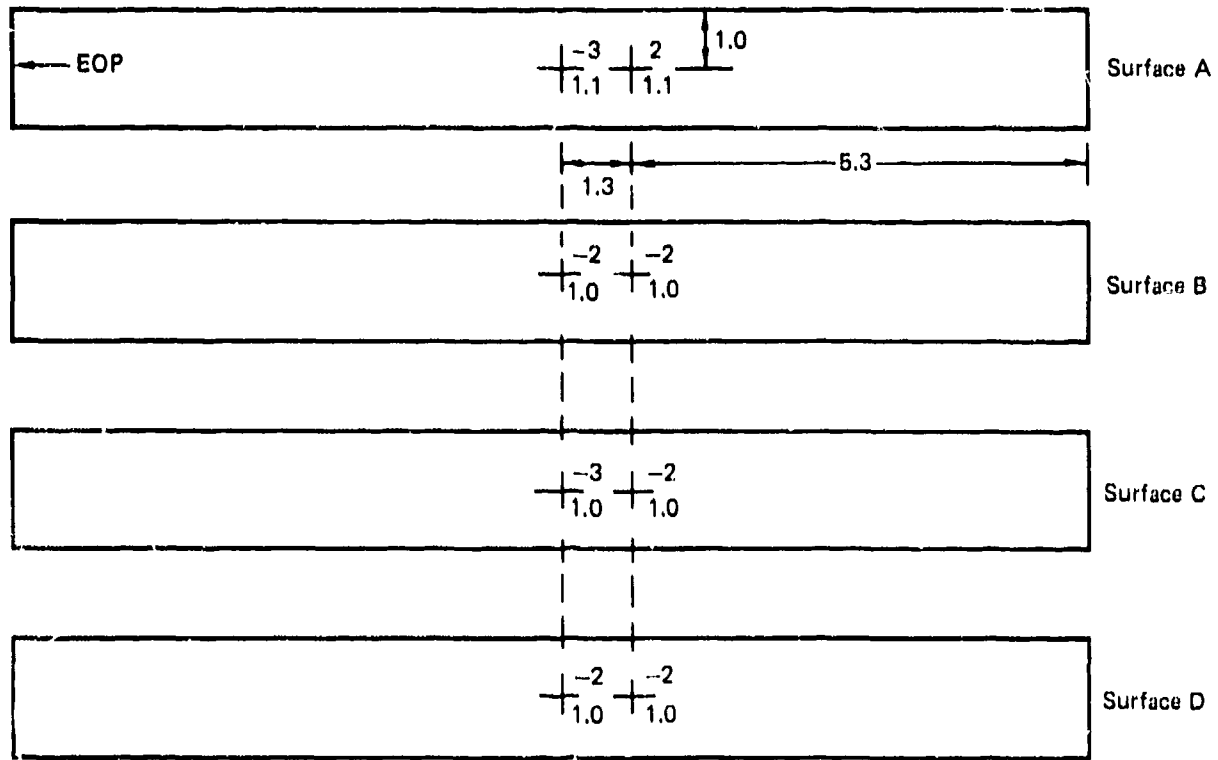
Bar No. 1-2A2B  
 10 MHz  
 Section 6



3P74 0117 41

FIGURE 132 (Continued)  
 LOCATION OF DEFECTS IN BAR

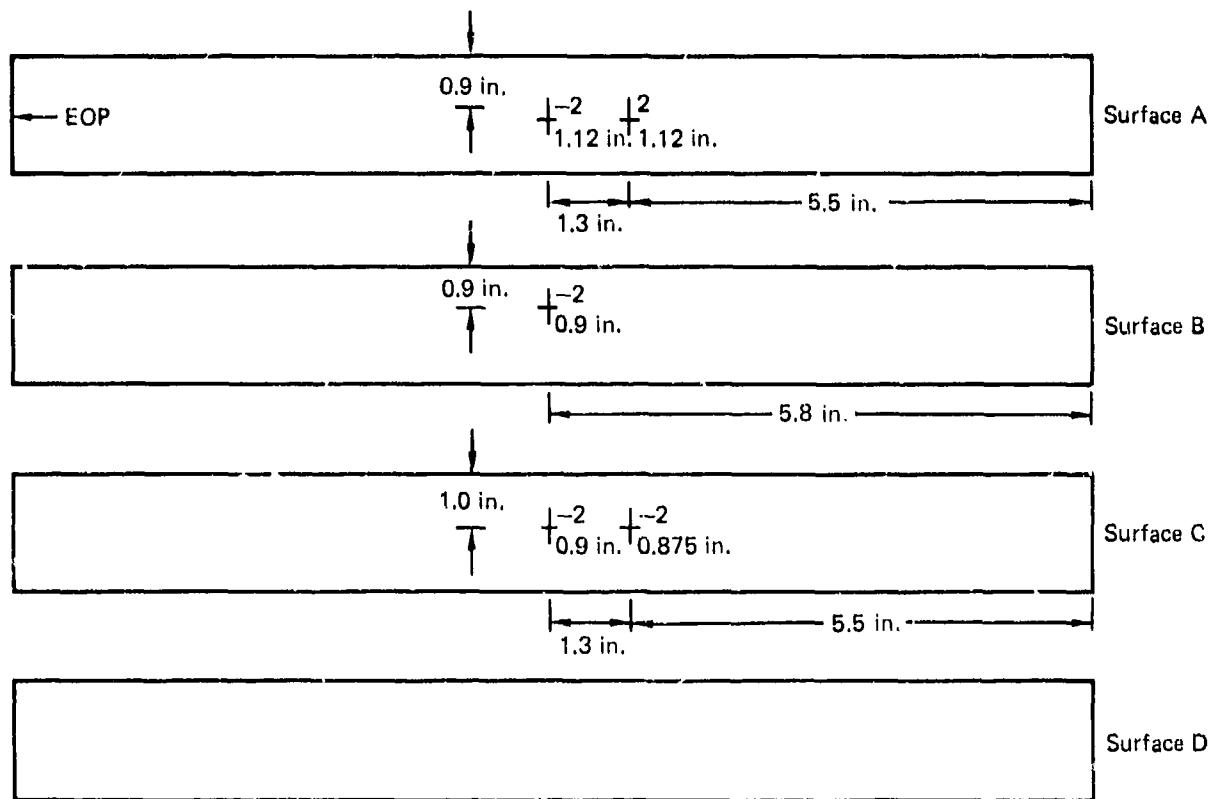
Bar No. 1-2A2D  
5 MHz  
Section 1



GP74-0117-42

FIGURE 132 (Continued)  
LOCATION OF DEFECTS IN BAR

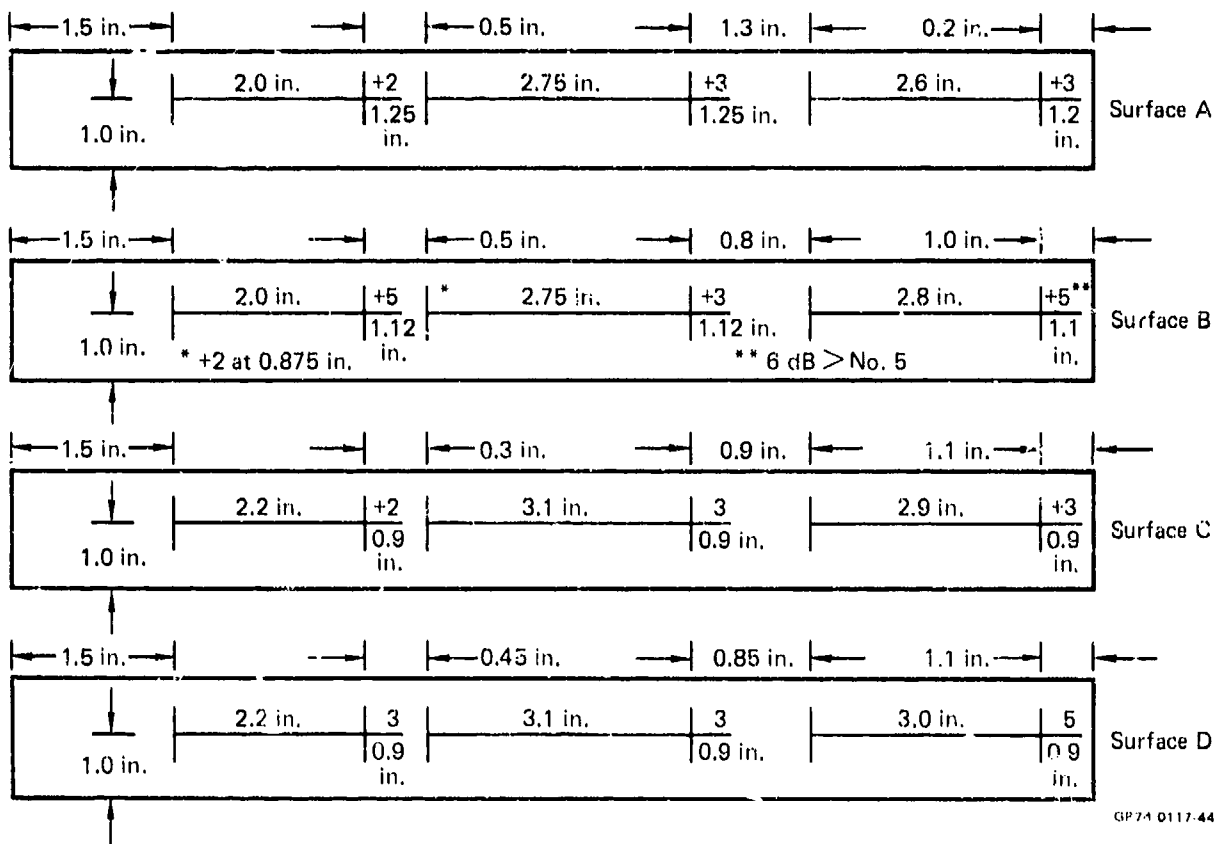
Bar No. 1-2A2D  
10 MHz  
Section 1



GP74 0117 43

FIGURE 132 (Continued)  
LOCATION OF DEFECTS IN BAR

Bar No. 1-2A2E  
 5 MHz  
 Section 4



GP74 0117-44

FIGURE 132 (Continued)  
 LOCATION OF DEFECTS IN BAR

Bar No. 1-2A2E  
 10 MHz  
 Section 4

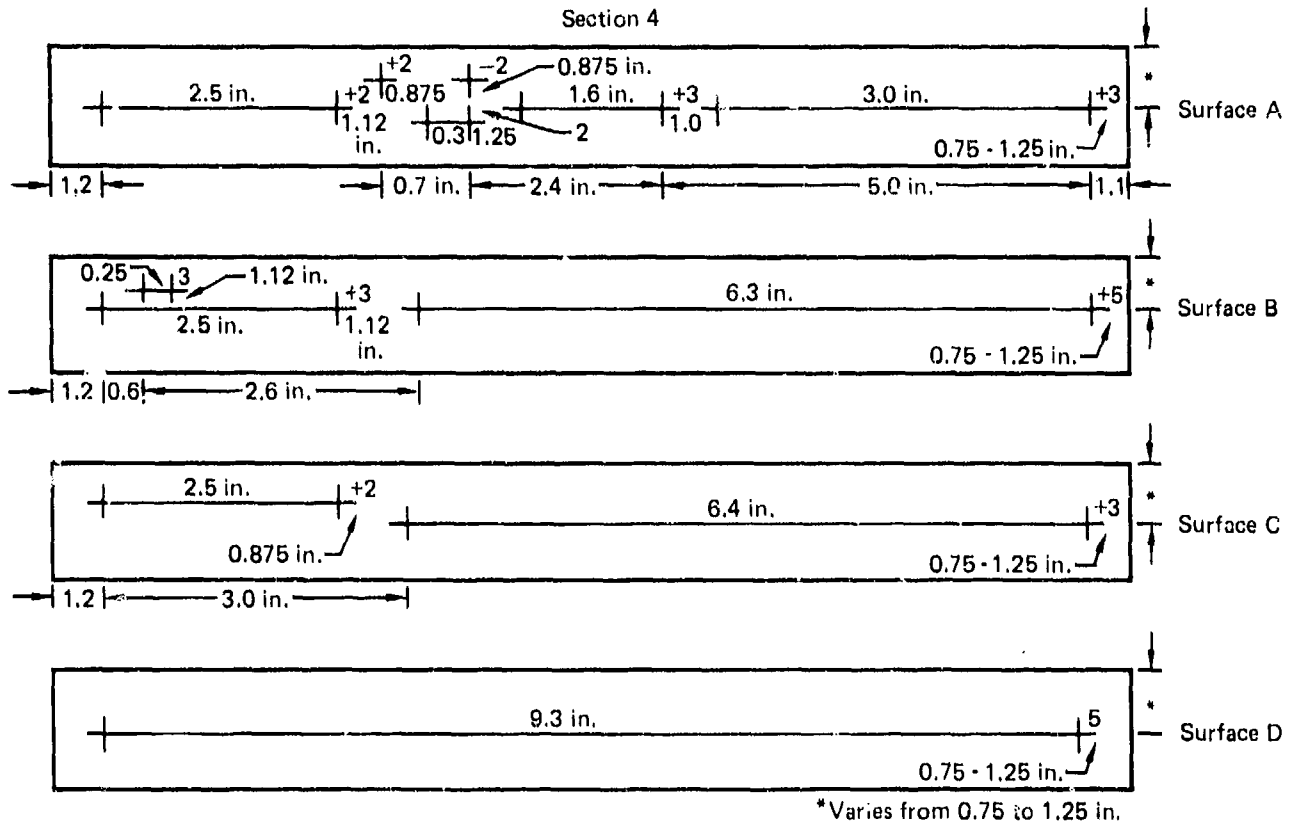
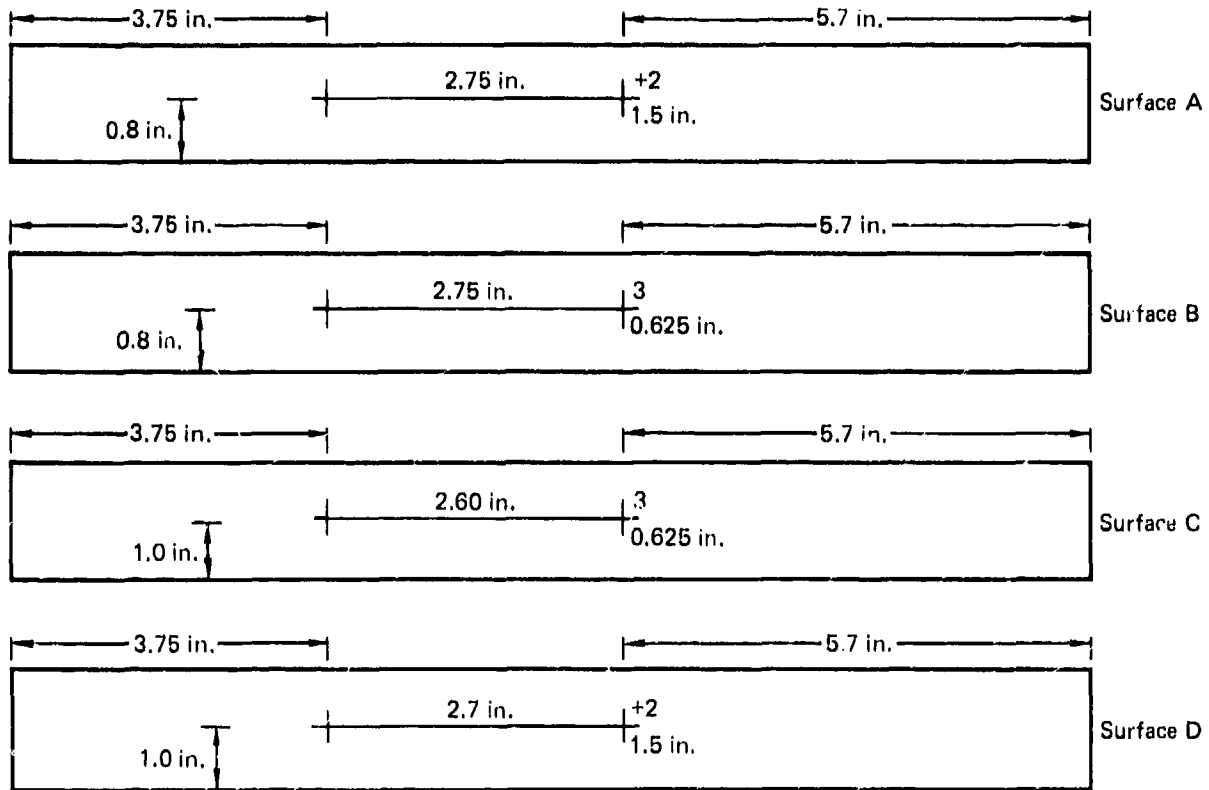


FIGURE 132 (Continued)  
 LOCATION OF DEFECTS IN BAR

GP74 0117 4B

Bar No. 1-2A2E  
5 MHz  
Section 5



GP74-0117 46

FIGURE 132 (Continued)  
LOCATION OF DEFECTS IN BAR

Bar No. 1-2A2E  
10 MHz  
Section 5

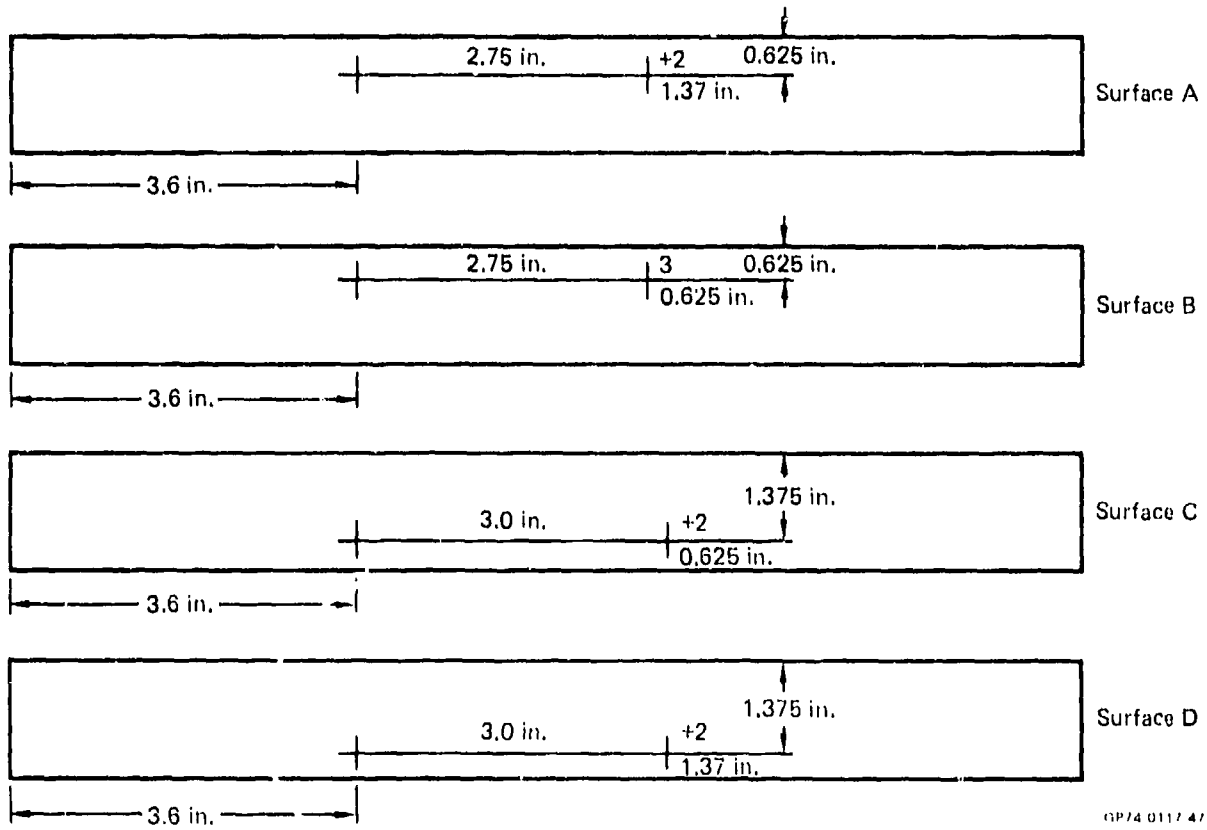


FIGURE 132 (Continued)  
LOCATION OF DEFECTS IN BAR

Next, the 5 MHz search unit was attached and adjusted for a 3 inch water path and a refracted sound beam angle in the bar of  $45$  degrees  $\pm 5$  degrees. A distance - amplitude correction (DAC) curve was developed using the side-drilled  $5/64$  inch diameter holes in the reference standard. The search unit was located for sound entry points 1, 2, 3, 4, and 5 shown in Figure 133. The signal amplitude was adjusted to 80 percent of saturation at whichever point gave the highest amplitude signal. Without changing the gain control, the search unit was positioned at the other points, the signal amplitudes were marked on the cathode ray tube (CRT), and the points were joined by a smooth curve. Then, the search unit was located at Position 6 and the instrument gain was adjusted to bring the response from the  $2/64$  inch diameter hole to coincide with Point 2 on the DAC curve.

The scan index was .25 inch. This index was chosen using the scanning gain by determining the total traversing distance across the reference standard through which no less than 50 percent of the DAC curve response is obtained. Each bar was scanned using Surface A as the sound entry surface. The scanning direction was parallel to the 7 foot length of each bar. All discontinuities whose amplitude exceeded 50 percent of the DAC curve were evaluated further for reject or accept status.

None of the bars exhibited ultrasonic responses which exceeded 50 percent of the DAC curve, however. This was true even for those areas where discontinuities were detected previously by straight beam testing. Subsequent metallographic examination of the discontinuities detected by the straight beam tests indicated that most of the segregates were somewhat planar and oriented parallel to the sound entry surface. Such an orientation would favor detection by straight beam techniques but, apparently, would be unfavorable for an angle beam test.

## 6. RADIOGRAPHIC INSPECTION

The bar was radiographically inspected using the production radiographic facilities. The procedure was the same as for the plate except the exposures were made at 210 KV and 10 milliamps for 15 minutes.

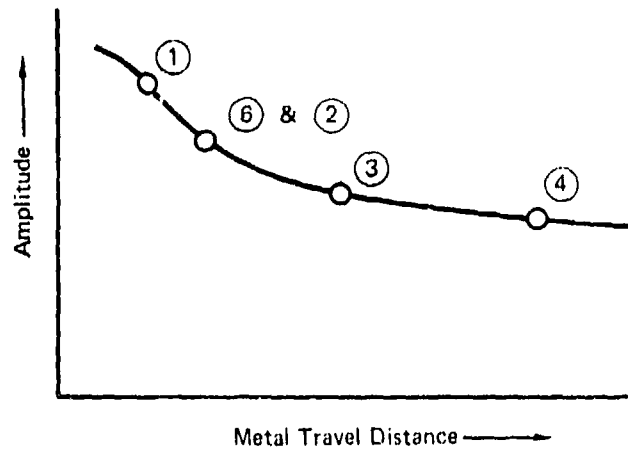
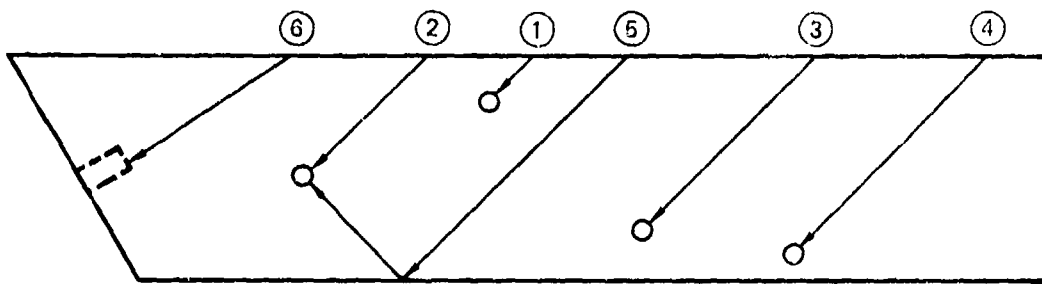
As with the plate, none of the Type I alpha segregates detected ultrasonically were observed on the radiographs.

## 7. SEGREGATES - AIRFRAME FORGINGS

### a. Ultrasonic Inspection

Each of the airframe forgings were inspected using the straight beam immersion method. A  $3/8$  inch diameter, 10 MHz lithium sulfate search unit (S/N 15384) was used with a Sperry UM721 ultrasonic instrument and a 10S dB pulser/receiver. The water path was 3 inches  $\pm 1/8$  inch.

Commercially produced Ti-6Al-4V reference standards with  $3/64$  inch diameter flat bottom holes at metal travels of  $1/8$ ,  $1/4$ ,  $1/2$ ,  $3/4$ , 1,  $1-1/4$ , and  $1-3/4$  inches were used for calibration. These reference standards were ASTM - type straight beam reference standards.



1074 0117 213

**FIGURE 133**  
**SOUND ENTRY POINTS USED TO ESTABLISH THE DAC CURVE**

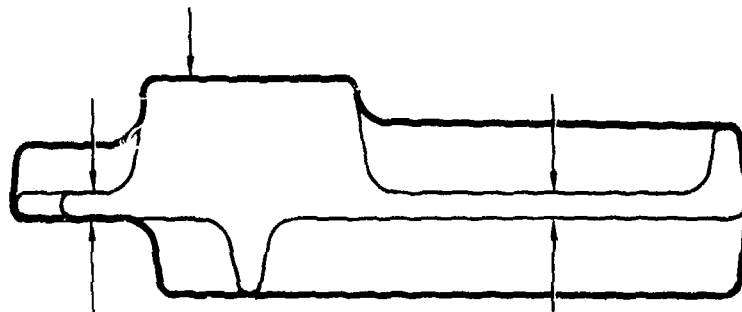
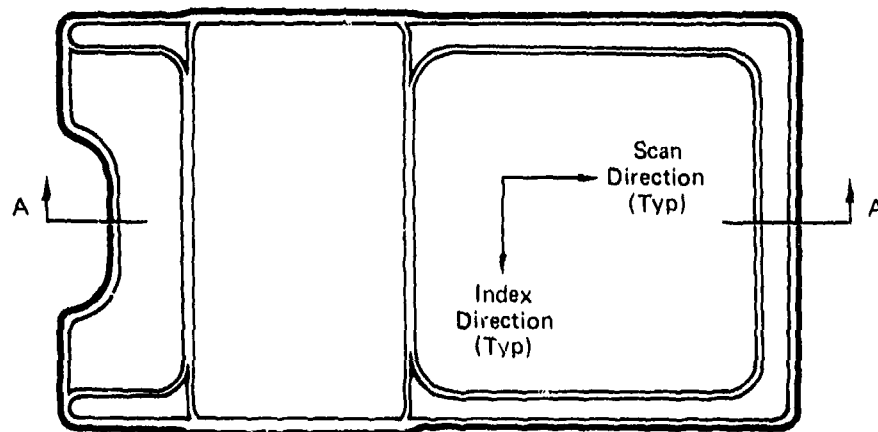
Initially, a distance-amplitude correction (DAC) curve was constructed by positioning the search unit for maximum response from the 3/64 inch diameter flat bottom hole which exhibited the largest amplitude signal. The signal amplitude was adjusted to 80 percent of saturation on the cathode ray tube (CRT). Without changing the gain control, the search unit was positioned over the remaining reference standards and the amplitudes were marked on the CRT screen. The points were joined by a smooth curve.

In order to increase the test sensitivity, an attempt was made to inspect the forgings at a higher scanning gain. A total of 7 dB of attenuation was removed which is equivalent to calibrating with a 2/64 inch diameter flat bottom hole. At this gain level, the ultrasonic noise in the forgings was less than 25 percent of the DAC curve.

A check was made for the difference in sound transmission characteristics between the reference standards and the forgings. At the gain level established above, the decibel (dB) difference was noted between the back surface response in the forging and in a reference standard with the same metal travel. This was done at approximately 10 locations in each of 4 of the forgings. The average dB difference was 2 dB. It was decided that this difference was insignificant and no corrections were made for it.

The scan index was 0.25 inch. This was chosen using the scanning gain by determining the total traversing distance across the reference standards through which no less than 50 percent of the DAC curve is obtained.

The scan plan for the forgings is shown in Figure 134. As can be seen the thin sections were scanned from opposite sides to improve the inspectability near the sound entry surface. Each discontinuity whose amplitude exceeded 50 percent of the DAC curve was evaluated further. The search unit was manipulated to maximize the response from the discontinuity and, if the maximized response equalled or exceeded the DAC curve, the location of the discontinuity was marked on the surface of the forging. A summary of the results is shown in Figure 135. As can be seen, ultrasonic indications were found in Forging No. 1 which is from the bottom of the original ingot and Forging No's 5 and 7 from the top of the original ingot.

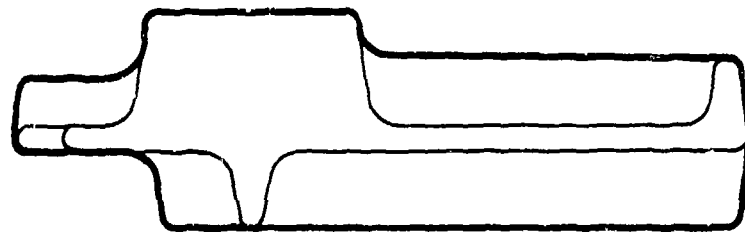
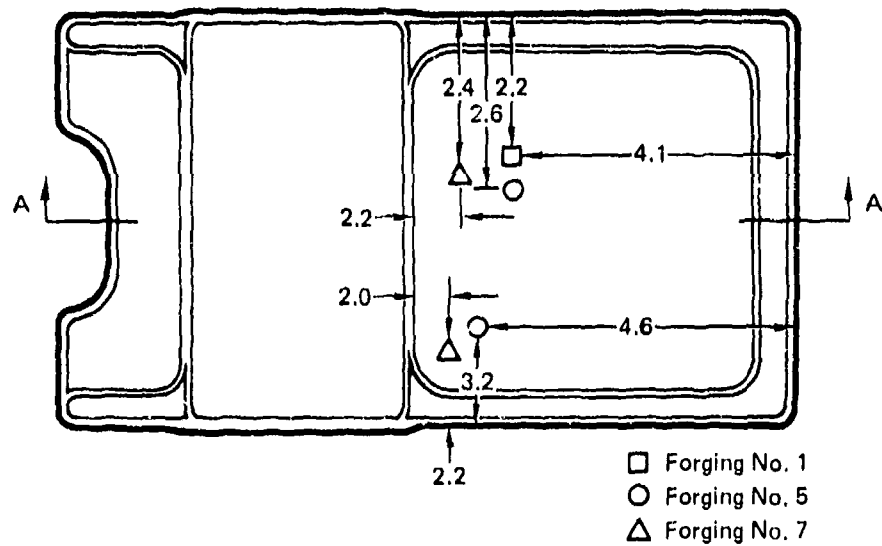


Section A-A

**FIGURE 134**

**SCAN PLAN FOR AIRFRAME FORGINGS**

GP74 0117 235



Section A-A

GP 74 0117 234

**FIGURE 135**  
**ULTRASONIC INDICATIONS IN AIRFRAME FORGINGS**

### 8. METALLOGRAPHIC EXAMINATION OF SEGREGATES IN BAR, PLATE, AND FORGINGS

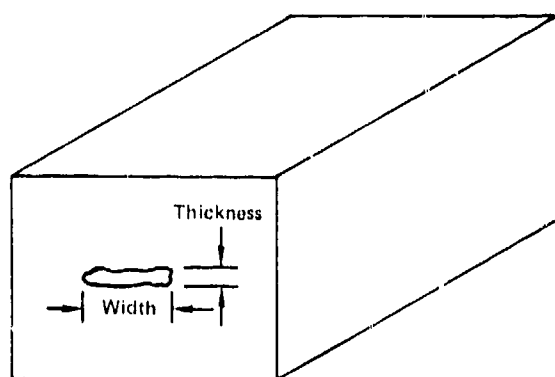
Several discontinuities which were detected during the ultrasonic inspections were sectioned and examined metallographically. Those discontinuities which were examined are listed below.

<u>Part No</u>	<u>Ultrasonic Response</u> $\triangle$	<u>Length (Inches)</u>	<u>Depth (Inches)</u>
Bar 1-2A2B Section 1	Less than No 2 flat bottom hole	1.15	1.30
Bar 1-2A2B Section 6	No 2 flat bottom hole	2.50	1.12
Bar 1-2A2E Section 4	Greater than No 5 flat bottom hole	9.3	0.75
Bar 1-2A2E Section 5	Greater than No 2 flat bottom hole	3.0	1.37
Plate A - Skction 3	Greater than No 5 flat bottom hole	5.0	0.63
Plate A - Section 17	No 2 flat bottom hole	0.75	0.50
Plate A - Skction 18	No 2 flat bottom hole	0.50	0.63
Airframe Forging No 7	Greater than No 2 flat bottom hole		
Airframe Forging No 4	-	-	-
Engine Disk Forging No 4	-	-	-
Engine Disk Forging No 6	-	-	-
Engine Disk Forging No 7	-	-	-

$\triangle$  Results of 10 MHz straight beam immersion test

Photomicrographs of the discontinuities found metallographically in the bar and plate are shown in Figures 136 through 142. A summary of the size of each is documented in Table 97.

**TABLE 97**  
**DIMENSIONS OF TYPE I ALPHA STABILIZED DEFECTS**



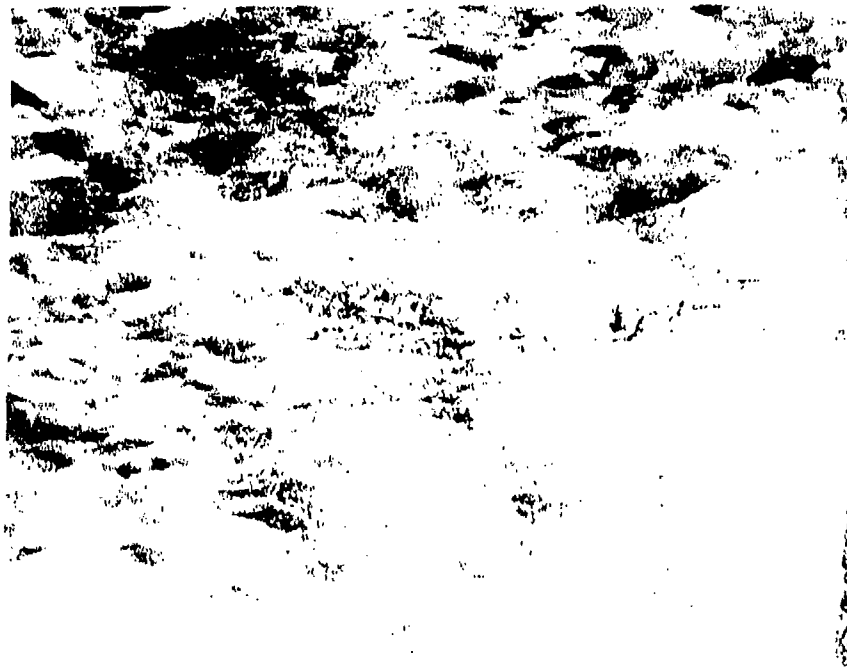
Location of Segregate	Width (in.)	Thickness (in.)
Bar 1-2A2B Section 1	0.20	0.03
Bar 1-2A2B Section 6	0.02	0.01
Bar 1-2A2E Section 4	0.09	0.02
Bar 1-2A2E Section 5	0.18	0.03
Plate A - Section 3	0.28	0.006
Plate A - Section 17	0.23	0.05
Plate A - Section 18	0.21	0.03

GP74 0117 4B

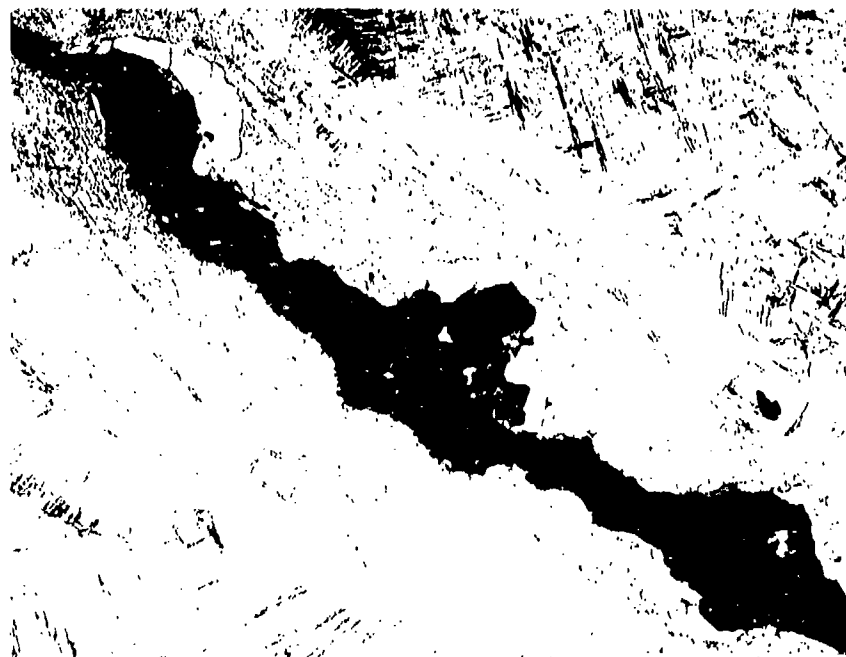
The discontinuities in the bar and plate all were from material which originated from the bottom of the ingot. This area had been seeded with nitrided sponge to induce Type I alpha stabilized defects. The detected discontinuities all had the characteristics of Type I segregates as described in "Characterization of Alpha Segregation Defects In Titanium 6Al-4V Alloy" by E. M. Grala in AFML TR 68-304. In each, there was evidence of cracks and/or voids associated with alpha stabilized phase.

The cross sections taken through Airframe Forging No 7 were taken through both of the ultrasonic indications. The cross sections taken through Airframe Forging No 4 were taken through two random areas since there were no ultrasonic indications in this forging.

There was no evidence of segregates or cracks and voids in the cross sections through Airframe Forging No 7. At this point, it is not known if the ultrasonic indications were false indications or if the segregates were present but not detected during the metallographic examination. Since there were no ultrasonic indications in the forgings from the top of the ingot, two random cross sections were taken through Airframe Forging No 4 to determine if there were Type II segregates present which were not detected ultrasonically. There was no evidence of Type II segregates and, therefore, the testing was inconclusive. A typical photomicrograph of the airframe forging microstructure is shown in Figure 143.



8X

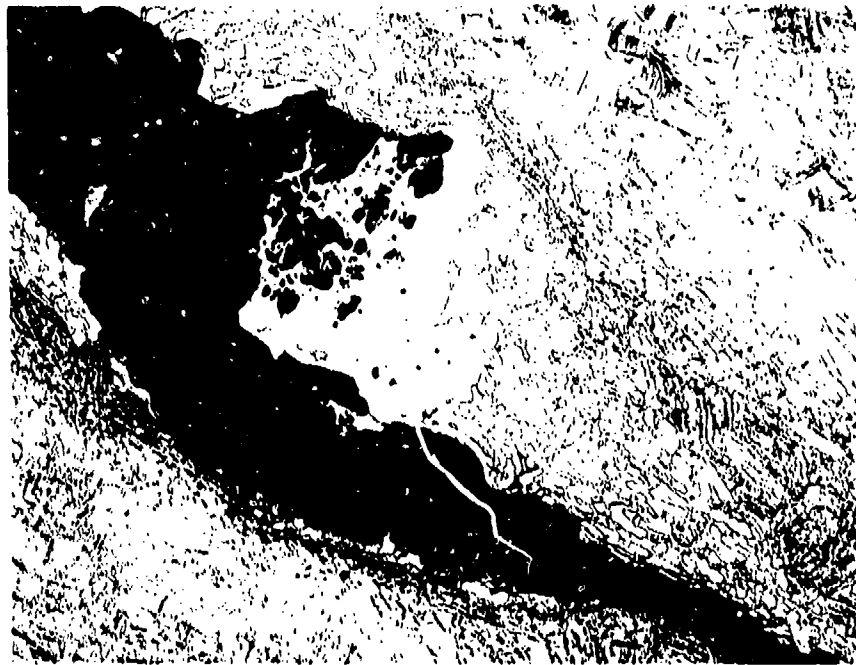


Kroll's

100X

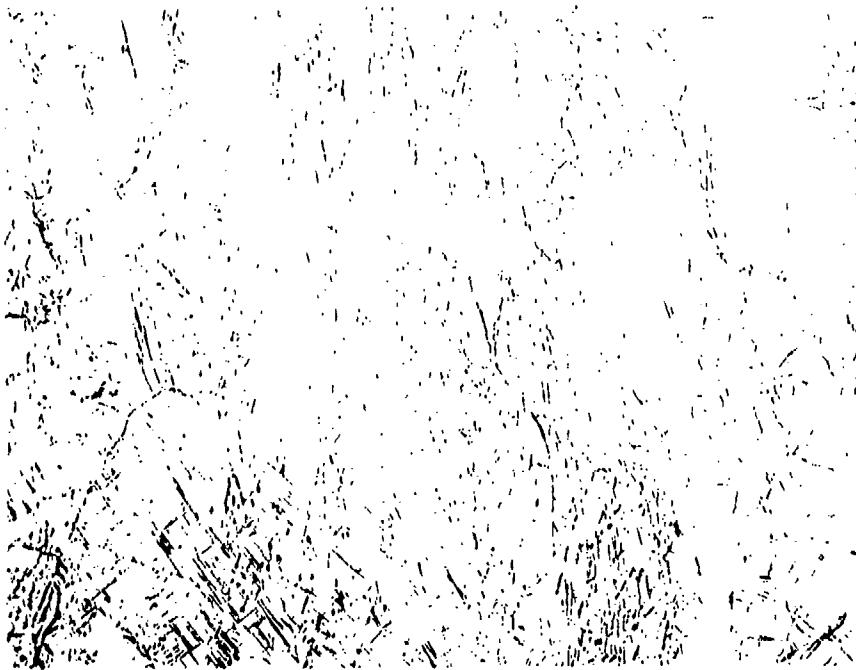
6-74-0117-66

**FIGURE 136**  
**PHOTOMICROGRAPHS OF SEGREGATE IN PLATE A, SECTION 3 (RESPONSE WAS**  
**GREATER THAN NO. 5 FLAT BOTTOM HOLE)**



Kroll's

100X



Kroll's

100X

Matrix

GP740117.07

**FIGURE 136 (Continued)**  
**PHOTOMICROGRAPHS OF SEGREGATE IN PLATE A, SECTION 3 (RESPONSE WAS**  
**GREATER THAN NO. 5 FLAT BOTTOM HOLE)**



50X

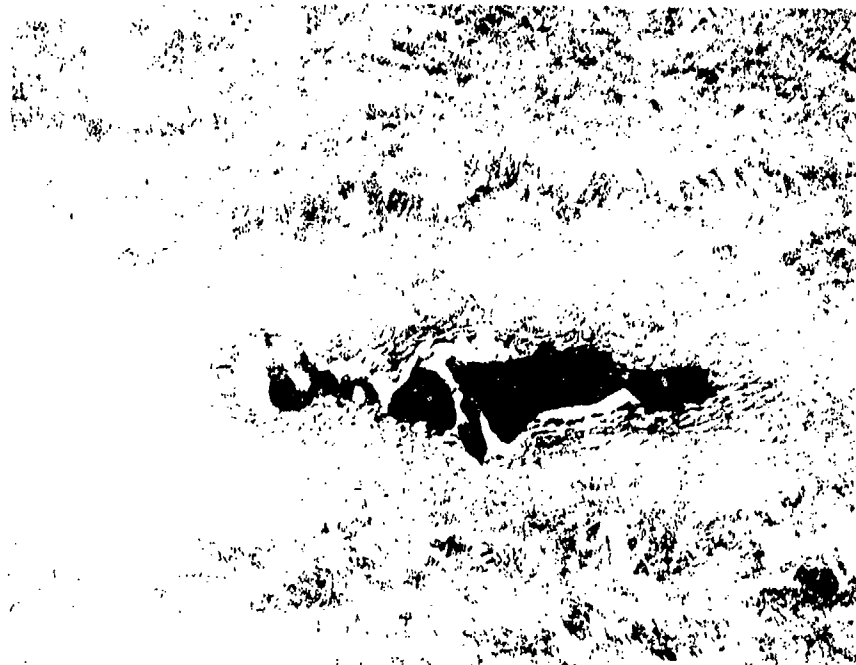


100X

FIGURE 137  
PHOTOMICROGRAPHS OF SEGREGATE IN PLATE A, SECTION 17 (RESPONSE WAS  
EQUAL TO NO. 2 FLAT BOTTOM HOLE)



50X



50X

GP74 0117 04

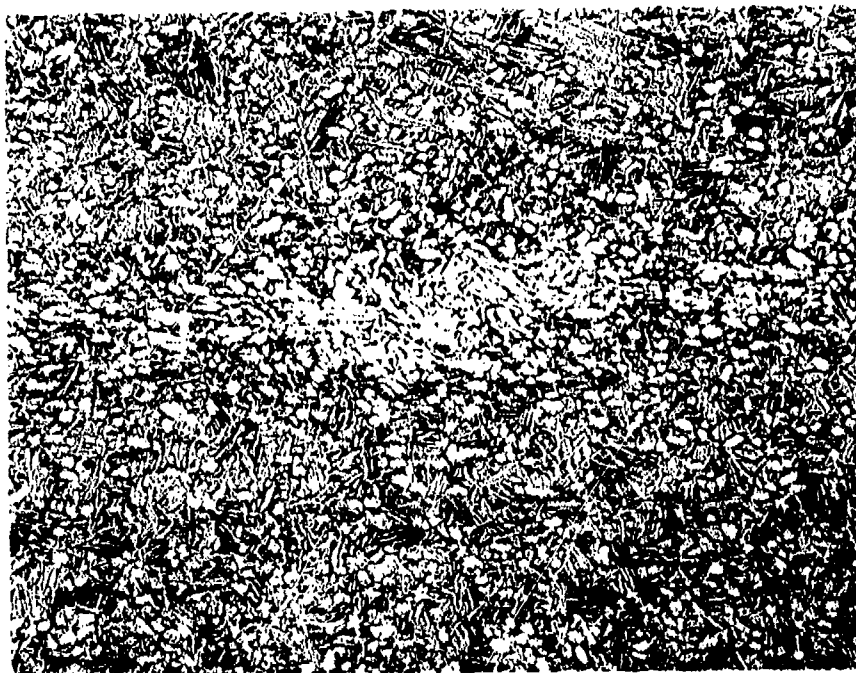
FIGURE 138  
PHOTOMICROGRAPHS OF SEGREGATES IN PLATE A, SECTION 18 (RESPONSE WAS  
EQUAL TO A NO. 2 FLAT BOTTOM HOLE)



100X

GP74-0117-70

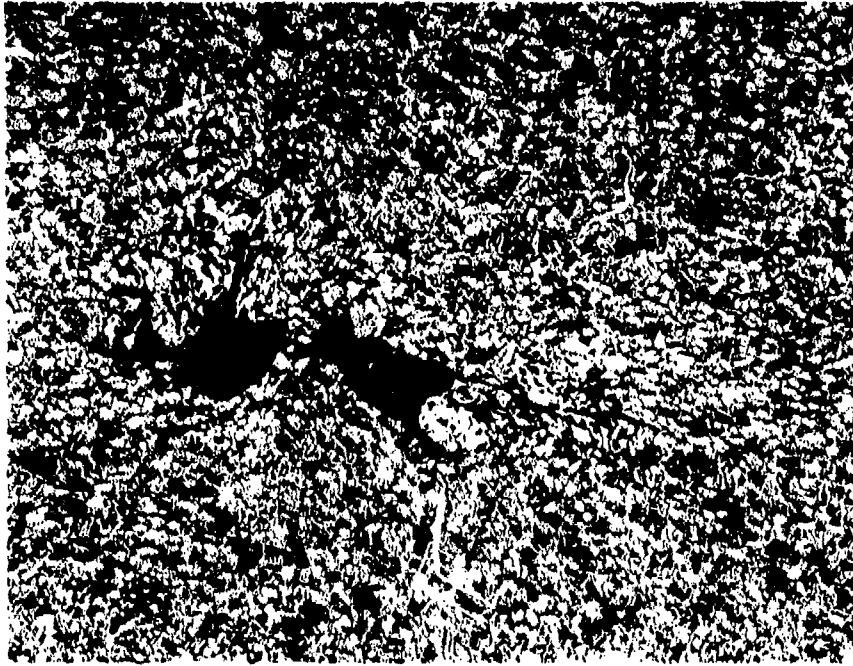
**FIGURE 138 (Continued)**  
**PHOTOMICROGRAPHS OF SEGREGATES IN PLATE A, SECTION 18 (RESPONSE WAS**  
**EQUAL TO A NO. 2 (FLAT BOTTOM HOLE))**



200X

GP74-0117 74

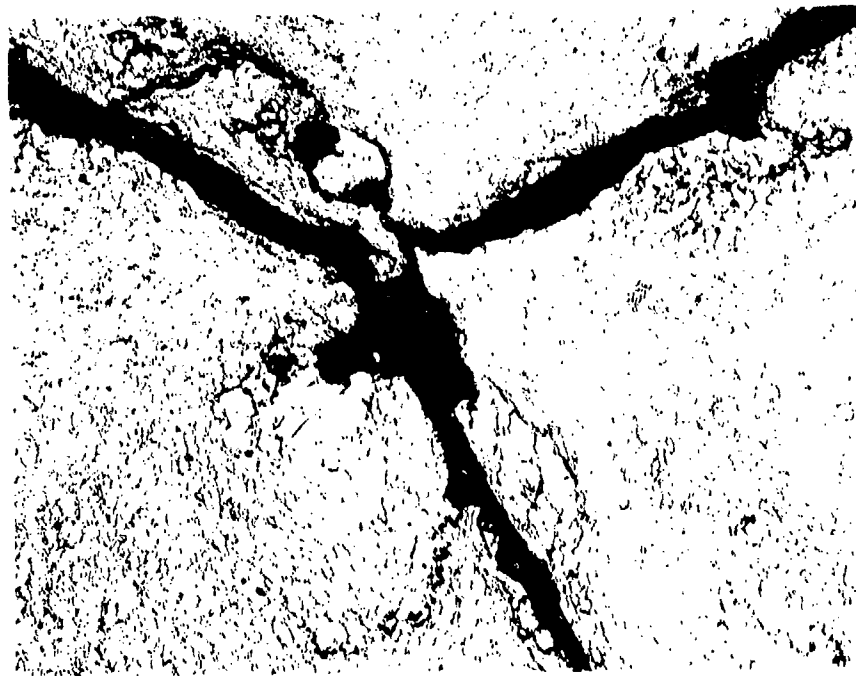
**FIGURE 139**  
**PHOTOMICROGRAPHS OF SEGREGATE IN BAR 1-2A2B, SECTION 1 (RESPONSE**  
**WAS LESS THAN NO. 2 FLAT BOTTOM HOLE)**



150X

GP74-0117-73

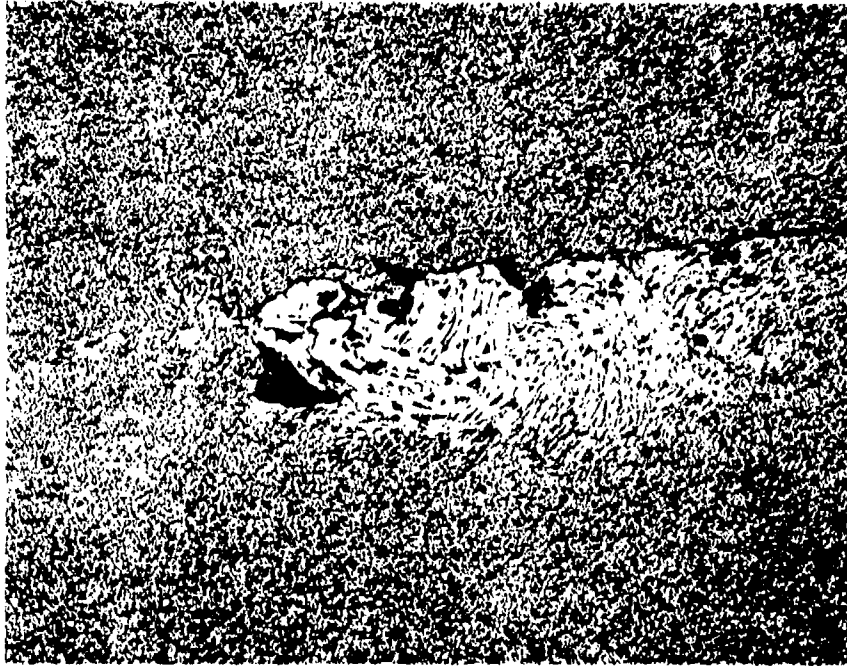
**FIGURE 140**  
**PHOTOMICROGRAPHS OF SEGREGATE IN BAR 1-2A2B, SECTION 6 (RESPONSE**  
**WAS EQUAL TO NO. 2 FLAT BOTTOM HOLE)**



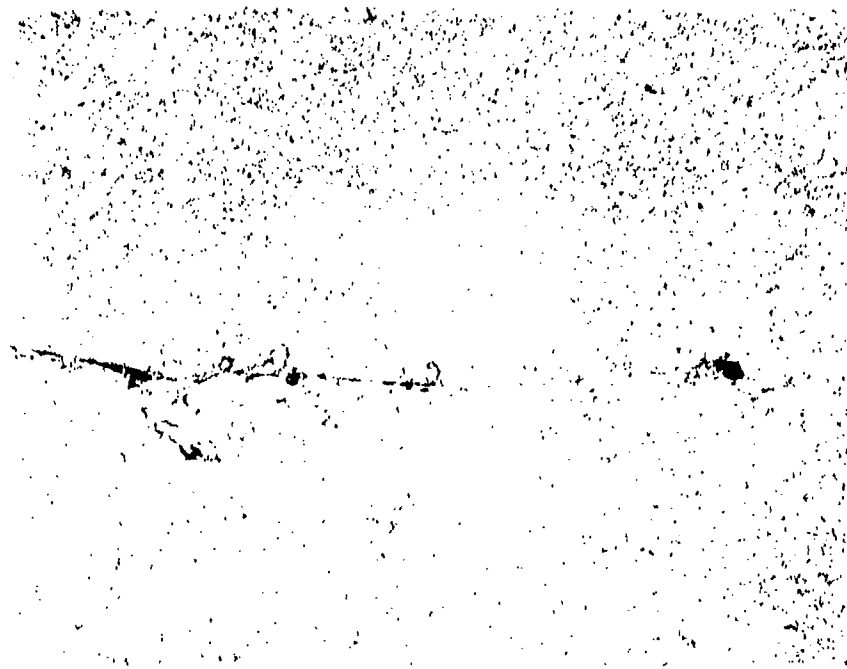
200X

GP74-0117-71

**FIGURE 141**  
**PHOTOMICROGRAPHS OF SEGREGATE IN BAR 1-2A2E, SECTION 4 (RESPONSE**  
**WAS GREATER THAN NO. 5 FLAT BOTTOM HOLE)**



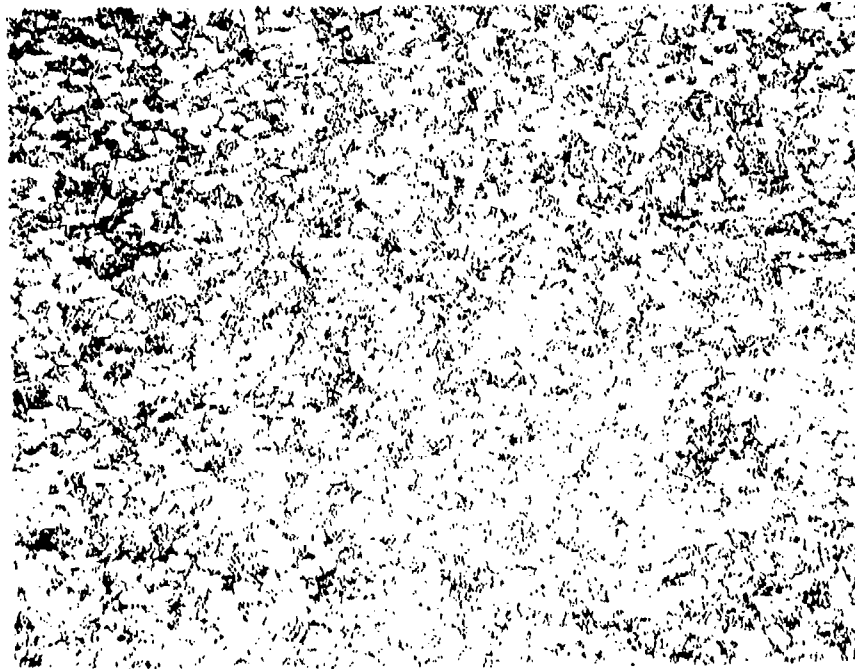
50X



50X

GP74 0117 22

**FIGURE 142**  
**PHOTOMICROGRAPHS OF SEGREGATE IN BAR 1-2A2E, SECTION 5 (RESPONSE**  
**WAS GREATER THAN NO. 2 FLAT BOTTOM HOLE)**



200X

Forging No. 7

**FIGURE 143**

GP74-0117 212

**TYPICAL AIRFRAME FORGING MICROSTRUCTURE**

Prior to sectioning Disk Forging No's 4, 6, and 7, an immersion angle beam laboratory ultrasonic inspection was performed to precisely locate several discontinuities detected during the production inspections. A 3/4 inch diameter long focused lithium sulfate search unit was used along with an Immerscope R1 pulser/receiver. The test frequency was 15 MHz. A water path of 5 inches was used and the sound beam angle in the forgings was 45 degrees. The scan index was .050 inch and the scan rate was 2.25 revolutions per minute. Calibration was performed in the same manner as for the production ultrasonic inspection of the forgings described previously. An X-Y recording was prepared for all the scans used in the production ultrasonic inspection from an analog signal provided by the ultrasonic equipment. The locations of the subsequent sections for metallographic purposes were based on these results.

Finally, a manual scan inspection was performed using the same equipment except for a Sperry HFN pulser/receiver. An additional 12 dB of attenuation was used for this inspection.

A comparison of the results of the original C-scan, analog-scan, and manual scan Disk Forgings No 6 and 7 is shown in Tables 98 and 99. As can be seen, there is a high degree of reproducibility among these three methods.

The locations of the sections taken through the disk forgings are shown in Figure 144. Each section was polished and then macroetched with a 5 percent HF-95 percent water solution for 5 to 10 minutes. Following this, selected areas were prepared metallographically and examined at high magnification. The etchant used was 10 percent HF-90 percent water for a few seconds. Photomicrographs of the discontinuities in the disk forgings are presented in Figures 145 and 146.

The discontinuity in Disk Forging No 4 appears to be a Type I alpha stabilized defect in appearance. This defect was detected by both shear wave and longitudinal wave ultrasonic inspection during the General Electric production ultrasonic inspection. During that inspection, the ultrasonic amplitude response was 25 percent of saturation in the longitudinal wave inspection and 40 percent of saturation in the radial and circumferential shear wave inspections.

The defect was examined with a Cambridge Steroscan Model Mark IIA scanning electron microscope and an aluminum analysis was made in several areas. The aluminum content was 3.9 percent adjacent to the void and 6.0 percent in the matrix away from the void. The aluminum content in an alpha phase area was 1.5 percent. These compositional differences compare favorably with the previous results reported in "Characterization of Alpha Segregation Defects in Titanium 6Al-4V Alloy" by E. M. Grata in AFML TR 68-304 for Type I alpha stabilized defects.

**TABLE 98**  
**COMPARISON OF THREE METHODS USED IN FINDING**  
**DEFECTS FOR EVALUATION (DISK NO. 6)**  
**Top Circumferential Shear O.D. to I.D.**

Defect	Type Scan	Angular Position* (deg)	Depth (in.)	Amplitude (%)
A	C-Scan	40	0.625	NA
	Analog-Scan	40	0.687	77
	Manual-Scan	40	0.600	44
B	C-Scan	320	0.750	NA
	Analog-Scan	320	0.687	62-75
	Manual-Scan	320	0.850	30
C	C-Scan	300	1.000	NA
	Analog-Scan	298	0.750	68
	Manual-Scan	300	0.900	20
H	C-Scan	170	0.750	NA
	Analog-Scan	168	0.875	60
	Manual-Scan	170	0.800	30
I	C-Scan	355	1.000	NA
	Analog-Scan	355	NA	50
	Manual-Scan	355	0.700	50
J	C-Scan	255-258	0.250	NA
	Analog-Scan	255-258	0.312	88
	Manual-Scan	255	0.300	40-45
J <sub>2</sub>	C-Scan	262-266	0.250	NA
	Analog-Scan	265	0.250	80
	Manual-Scan	265	0.300	65

\* Entering point of beam given - circumferential mode

Note: Depth given for C-scan is the gate center depth - actual depth can be  $\pm 1/16$  - also, the amplitude cannot be given as a reference; gray-scale was not made at the time of the scan.

N.A. -- Not Applicable

GP 74 0117 212

**TABLE 98 (Continued)**  
**COMPARISON OF THREE METHODS USED IN FINDING**  
**DEFECTS FOR EVALUATION (DISK NO. 6)**  
 Bottom Radial Shear OD to ID

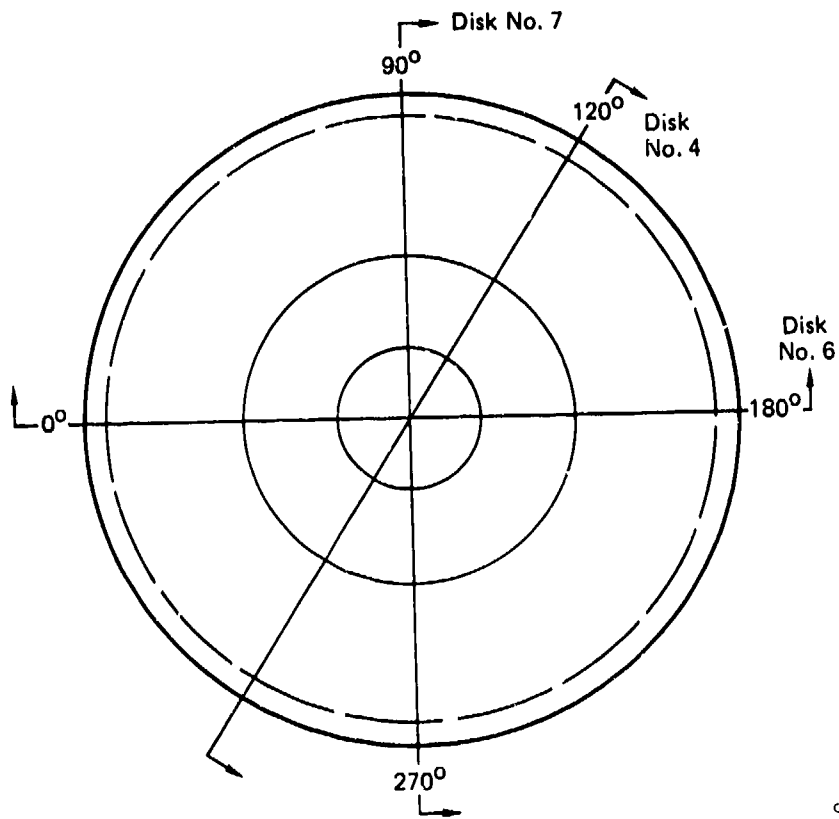
Defect	Type Scan	Angular Position (deg)	Depth (in.)	Amplitude (%)
E	C-Scan	15	1.000	NA
	Analog-Scan	14-16	0.937	79-90
	Manual-Scan	15	1.000	70
F	C-Scan	200	1.000	NA
	Analog-Scan	204-206	1.000	90
	Manual-Scan	200	1.000	80
G	C-Scan	313-315	1.000	NA
	Analog-Scan	306-308	1.062	85
	Manual-Scan	315	0.950	60
G <sub>2</sub>	C-Scan	330	1.250	NA
	Analog-Scan	342	0.812	75
	Manual-Scan	330	1.100	60
D	C-Scan	155	1.250	NA
	Analog-Scan	155	0.937	85
	Manual-Scan	155	0.950	50

GP74 0117 23B

**TABLE 99  
COMPARISON MANUAL AND ANALOG SCANS FOR DISK NO. 7**

Indic.	Type Scan	Angular Position (deg)	Distance from CD (in.)	Depth (in.)
<b>Bottom Radial Shear In</b>				
A	Analog	176	0.9-1.2	1
A	Manual	176	0.9	1.1
B	Analog	224	0.4-0.5	1-1.1
B	Manual	224	0.4-0.5	1.1
C	Analog	240	0.8-0.9	0.95-1.0
C	Manual	240	0.8-0.9	0.95
D	Analog	192	1.35-1.45	0.85-1.0
D	Manual	192	1.4	0.9
F	Analog	350-355	1.45-1.6	1.02-1.1
E	Manual	350-355	1.5	1.05
F	Analog	250	1.9-1.95	0.3
F	Manual	250	1.9	0.3
G	Analog	98-100	1.25-1.25	1.15-1.17
G	Manual	100	1.25-1.3	1.15
H	Analog	22	0.9-1.0	1.15
H	Manual	22	1.0	1.15
N	Analog	84-86	2.250	0.4
N	Manual	85	2.250	0.4
<b>Top Radial Shear In</b>				
I	Analog	124-126	0.25-0.3	0.7-0.75
I	Manual	124	0.3	0.75
J	Analog	98-102	0.85-0.95	0.8-0.9
J	Manual	100	0.850	0.9
K	Analog	278	0.45-0.5	0.7-0.75
K	Manual	278	0.5	0.7-0.75
L	Analog	140-144	2.1-2.2	1+
L	Manual	140	2.15	1+
M	Analog	92	1.3-1.35	0.95
M	Manual	82	1.3	0.95

GP74 0117 23H



GP74 0117 239

**FIGURE 144**  
**LOCATION OF METALLOGRAPHIC CROSS SECTIONS IN DISK FORGINGS**



Disk Center ↓

100X

Disk Forging No. 4



Disk Forging No. 6

100X

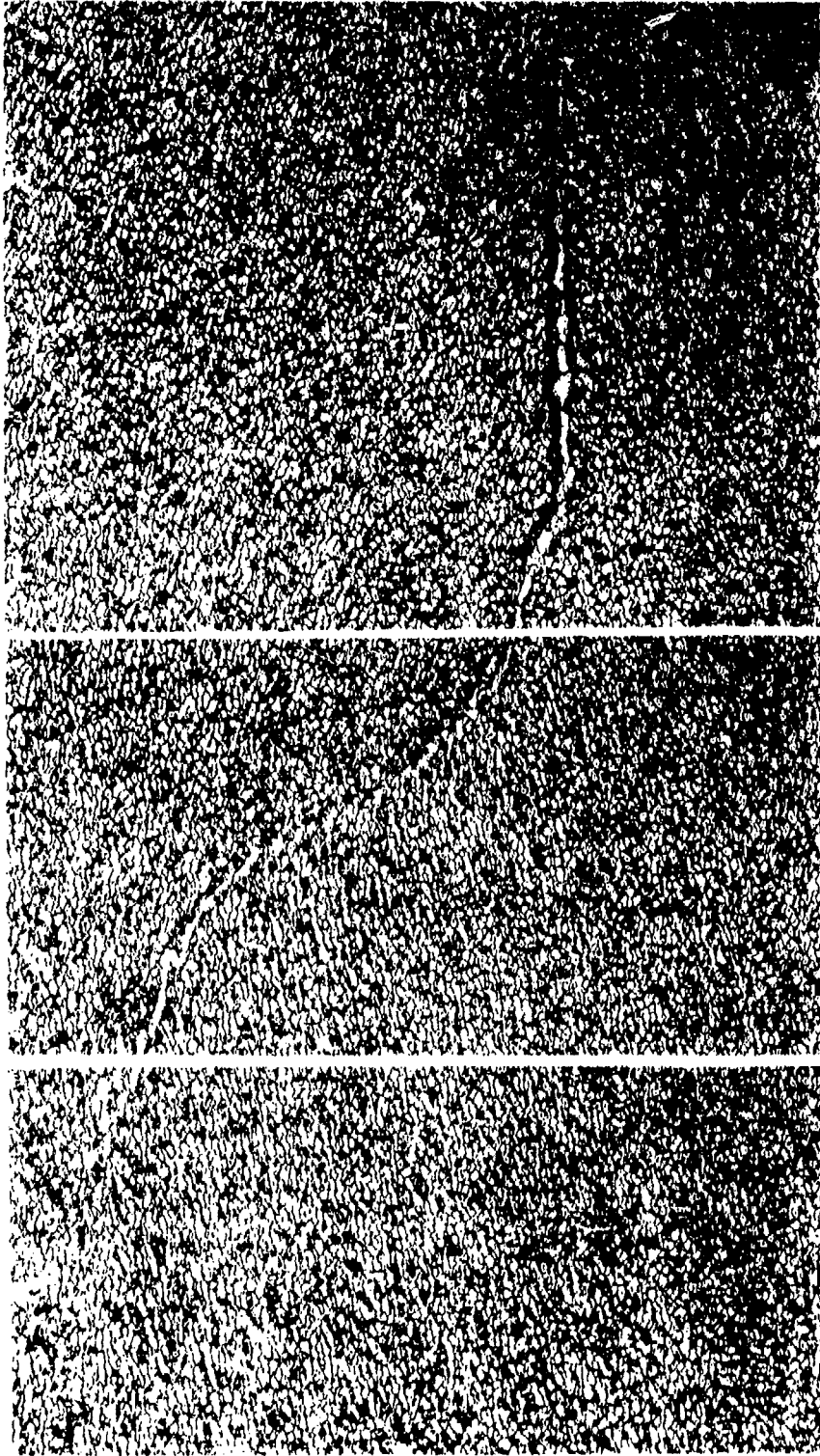


Disk Forging No. 7

100X

GP74-0117 213

**FIGURE 145  
DISCONTINUITIES IN DISK FORGINGS**



100X

FIGURE 146  
PHOTOMICROGRAPH OF DISCONTINUITY M IN DISK FORGING NUMBER 7 (SEE TABLE 99)

## SECTION VI

### CONCLUSIONS

The following conclusions may be drawn from the results reported here:

- (1) To most effectively detect a wide variety of crack and porosity sizes with a production penetrant inspection, several parameters must be carefully controlled. These parameters include the penetrant dwell and bleed-out times, the emulsification time, the temperature and pressure of the water used to remove the excess penetrant, the type of developer used, and the ultraviolet/white light intensity in the inspection. Some manufacturing operations performed prior to penetrant inspection, such as glass bead peening and shot peening, can reduce the effectiveness of subsequent penetrant inspection. Removal of material by chemical etching prior to the penetrant inspection can improve the effectiveness of the penetrant inspection.
- (2) Surface connected cracks with lengths of approximately .050 to .10 inch can be detected with a high probability at a 95 percent confidence level in a production penetrant inspection. Smaller cracks can also be detected, but with a lower probability of detection. The overall capability for crack detection in a particular production part is related to the chosen NDT plan. For example, a penetrant inspection followed by a surface wave and angle beam ultrasonic inspection will substantially increase the probability of crack detection.
- (3) The effectiveness of ultrasonic inspection of titanium ingot, billet, and forgings can be increased by using the shear wave mode as well as the longitudinal wave mode.
- (4) Macroetching and anodic etching of the random billet sections are ineffective techniques for establishing the existence of Type I stabilized areas.
- (5) Ultrasonic inspection of titanium ingot and billet material could be significantly improved by implementation of such developed inspection techniques as the use of proper reference standards, proper preparation of the billet surfaces, and compensation for sound transmission differences.
- (6) A significant difference in sound transmission characteristics can exist between the part to be inspected and the reference used when inspecting titanium bar, plate, and forgings. When these differences are large, compensation must be made to conduct an effective ultrasonic inspection.
- (7) Contour sound entry surfaces can significantly effect the results of a straight beam immersion ultrasonic inspection and compensation should be made for this effect. The amount of compensation required varies as a function of radius of curvature, metal travel distance and search unit. Aluminum contour reference standards can be used for inspecting titanium if adjustments are made for differences in sound transmission characteristics. One contour reference standard can be used to inspect a contour surface with a range of radii.

(8) The effectiveness of immersion angle beam inspection of internal cracks in machined thick section titanium is highly dependent upon the orientation of the crack with respect to the sound beam. Crack detection capability is very poor with the sound beam at 45 degrees to the crack surface.

(9) Discontinuities, which are oriented perpendicular to the sound entry surface, are more easily detected in thin section parts than thick section parts when using angle beam ultrasonics. Discontinuities, which are oriented parallel to the sound entry surface, can be detected in thin section parts using straight beam ultrasonics.

(10) A multiple inspection NDT approach, such as a penetrant inspection followed by both a surface wave and contact angle beam ultrasonic inspection, is highly effective in detecting surface cracks. At least 98 percent (95 percent confidence level) of all cracks with lengths .050 to 0.10 inch can be detected with such an inspection approach.

(11) The radiographic method does not appear to be an effective method for the detection of Type I or Type II alpha stabilized defects in titanium bar, plate, and forgings, whereas the ultrasonic method can be effective in detecting Type I alpha stabilized defects in titanium ingot and billet as well as bar, plate, and forgings.

(12) Eddy current methods potentially can detect fatigue cracks with depths of approximately .025 inch in unfilled fastener holes. Higher frequency eddy current inspection may be capable of detecting smaller cracks.

## Section VII

### Recommendations

The following recommendations are made based on the results reported here:

- (1) The processing parameters for other penetrant systems need to be investigated to establish the variations to be expected from one system to another.
- (2) The crack detection capability of other penetrant systems need to be measured to determine the variation within one MIL-I-25135 group.
- (3) The quantitative effect of various mechanical processes upon penetrant crack detection capability needs further definition.
- (4) Further work should be done in the area of ultrasonic inspection of contour surfaces to determine at which radius the contour effect becomes negligible.
- (5) The crack detection capability of surface wave ultrasonics should be measured for subsurface cracks at various depths below the surface.
- (6) Several aspects of ultrasonic inspection of titanium ingot and billet, such as controlling search unit characteristics and using proper reference standards, need to be implemented by the titanium producers.
- (7) Several aspects of radiographic inspection need to be improved. Improvements in the plaque-type image quality indicators are necessary to achieve reproducible radiography. Image quality indicators are needed for material thicknesses of 1/4 inch or less. A need exists for low KV, high milliamperage X-ray equipment to improve subject contrast while maintaining reasonable exposure time. A method is needed to measure the actual KV of an X-ray machine.
- (8) The minimum detectable crack depth in titanium fastener holes with high frequency eddy current needs to be determined.
- (9) The effect of the alpha segregates, detected in this program, upon the mechanical properties of Ti-6Al-4V needs to be established.
- (10) Military nondestructive testing specifications should be revised to include data developed during this program such as penetrant dwell times for high sensitivity water washable penetrants and ultrasonic inspection procedures for contour surfaces.

## VIII. REFERENCES

- (1) N. S. Abbott, "Effect of Mechanical Processing Upon Penetrant Inspection Sensitivity", TIS Number CPO2OGF012.20, Report MDC A1181, McDonnell Aircraft Company, 24 June 1971.
- (2) Sattler, F. J. and Matay, I. M., "Advanced Nondestructive Testing Techniques for Titanium Billets and Ingots", AFML TR-70-118, June 1970.
- (3) E. M. Grala, "Characterization of Alpha Segregation Defects in Titanium 6Al-4V Alloy", AFML TR-68-304.
- (4) F. W. Wood, "Improvement of Titanium Alloy Ingot Consolidation", AFML-TR-72-46, May 1972.
- (5) R. C. McMaster, Ed., Nondestructive Testing Handbook, Vol. 2, Society for Nondestructive Testing, Ronald Press, 1963.